THE STRENGTH OF REINFORCED AND PRESTRESSED CONCRETE BEAMS SUBJECTED TO COMBINED BENDING, TORSION AND SHEAR

A thesis

Presented for the Degree

of

Doctor of Philosophy

by

SAIB PUTROUS YOUSIF M.Sc., Dp., Adv. Stud. Eng.

Department of Civil Engineering

The City University, London

December, 1974

PAGE NUMBERING AS ORIGINAL

SYNOPSIS

This thesis presents a rational and unified approach for determining the strength of reinforced and prestressed concrete rectangular beams subjected to combined bending, torsion and shear. In this study failures have been classified into three broad categories:

1) yield modes (3 cases)
2) partial yield modes (6 cases)
3) over-reinforced modes (3 cases)

The effect of dowel action, aggregate interlock, uncracked concrete and spacing of stirrups on the resistance of applied torque have been examined.

The predictions of the proposed theories have been compared with more than a thousand test results available in literature. In general the agreement is good.

A method for predicting cracking strength for reinforced and prestressed concrete beams subjected to bending, torsion and shear is given.

The results of tests on 25 thin-walled prestressed concrete box-beams subjected to torsion, bending and shear are presented.

Experimental and theoretical investigations on the behaviour and strength of dowels in concrete are given.

TABLE OF CONTENTS

ACKNOWLEDGEMENTS

The tests reported in Chapter 6 were carried out in the Structural Engineering Laboratory of the Department of The Civil Engineering at the City University. The author wishes to thank Professor J.E. Gibson for providing the facilities for this work.

The work was carried out under the supervision of Dr. M.Smolira, to whom the author wishes to express his gratitude for the guidance and encouragement provided during the course of this research.

The tests reported in Chapter 7 were carried out in the Concrete Laboratory of the Department of Civil and Structural Engineering at the Polytechnic of the South Bank. The author would like to thank Mr. C. Anderson, deputy head department, for providing the facilities and for his constant help and encouragement during the course of this investigation.

The author is also indebted to the Concrete Laboratory Staffs of the City University and the Polytechnic of South Bank for their assistance with the experimental work.

The figures have been traced by Mr. S. Patel. The thesis has been typed with unfailing care by Miss J. Hallett.

The author also wishes to thank his wife for her assistance and support throughout this research work.

The author wishes to express his sincere gratitude for all help and encouragement he has received.

To My Wife

BIOGRAPHICAL NOTE

The author obtained his college diploma in Structural Engineering at Brixton School of Building in April 1966. During this course the author worked with Holland, Hannen and Cubitts for a period of one year on a sea defence project and construction of highway bridges. The author also worked with Freeman Fox and Partners for a period of six months on design and detailing of reinforced concrete structures. In October 1966, the author was registered as a diploma student in Structures in the Civil Engineering Department, University of Manchester and obtained the Diploma of Advanced Studies in Structures in December 1967. In October of the same year, he was registered as an M.Sc student at the Department of Civil Engineering, University of Surrey and was awarded the M.Sc. degree in Bridge Engineering in October 1968.

In October of the same year, he worked for the Civil Engineering Division of Unilever Ltd. for a period of one year on design of multi storey structures.

In October 1969, he was registered in the Civil Engineering Department, The City University, as a part-time student to read for the degree of Ph.D for which this thesis is submitted.

Since November, 1969, the author joined the Department of Civil and Structural Engineering at the Polytechnic of South Bank, where he is teaching Theory of Structures, Stress Analysis and Structural Design.

LIST OF SYMBOLS

A_1	area enclosed by the centre line of the transverse reinforcement
A	area of cross-section
A_{sl}	area of longitudinal corner bars located at the bottom of the beam
A'_{sl}	area of longitudinal corner bars located at the top of the beam
A_{sv}	area of one stirrup used as a shear or torsion reinforcement - one leg
A_{sl}	total area of longitudinal reinforcement located at the bottom of the beam
A'_{sl}	total area of longitudinal reinforcement located at the top of the beam
a	shear span
b	width of beam or width of specimens in dowel tests
b_e	effective width of beam or effective width of specimens in dowel tests
b_l	limiting width of dowel specimens
b_w	width of web
c_b	bottom cover to a dowel in dowel test specimens
c_d	cover to the longitudinal reinforcement measured from its centroid
c_{s1} & c_{s2}	side cover to a dowel in dowel test specimens
d	effective depth of main tension reinforcement
d'	effective depth from extreme compressed fibre to compression reinforcement
E_c	modulus of elasticity of concrete
E_s	modulus of elasticity of steel
e	eccentricity
F	force
F_e	force in a longitudinal corner bar

F_{du}	dowel strength of dowel category 2
F_{ld}	dowel force induced by longitudinal reinforcement
F_{ldx} & F_{ldy}	components of F_{ld}
F_{ldu}	dowel strength of longitudinal bar
F_d	dowel force
F_s	axial force in stirrups per unit length
F_{sx} & F_{sy}	axial forces in the short and long stirrup leg per unit length
F_{sd}	dowel forces induced in the stirrups per unit length
F_{sdu}	dowel strength of stirrups
f	strength in terms of stress
f_{cb}	bearing strength of concrete
f'_c	ultimate strength of concrete in compression-cylinder test
f_{cu}	ultimate strength of concrete in compression-cube test
f_{co}	uniaxial compressive strength of concrete
f_r	modulus of rupture of concrete
f_c	stress in concrete
f_p	stresses in beam due to prestressing force
f_{sv}	stresses in the stirrups
f_{sx} & f_{sy}	stresses in the shorter and longer legs of the stirrups respectively
f_{sl}	stresses in longitudinal reinforcement
f_t	tensile strength of concrete
f_y	yield or proof stress of steel
f_{yl}	yield or proof stress of longitudinal reinforcement
f_{yv}	yield or proof stress
G_c	shear modulus of concrete
h	overall depth of section
h_f	depth of compression zone

I	second moment of area
K, k_i	coefficients
L	span of beam or length of beam
L_d	length of a dowel
M	external bending moment
M_{cr}	cracking moment
M_u	moment of resistance of a section in simple flexure
M_{sc}	resistant moment as limited by resistance of concrete in compression under combined forces
M_{ub}	balanced moment of resistance of a section in simple flexure
M_p	plastic moment of resistance of a bar
m	ratio of volume of longitudinal bars to volume of stirrups
m'	ratio of yield force of longitudinal bars for beams subjected to torsion
m'_b	ratio of yield force of longitudinal bars for beams subjected to torsion and bending
P	prestressing force
P_e	effective prestressing force after losses
p	parameter of stirrups
q	shear flow in box-beam
q_a	shear flow resisted by aggregate interlock
q_t	shear flow due to torsion
q_d	shear flow resisted by dowel action
q_v	shear flow due to apply shear force
R_y	ratio of A'_{sl} A_{sl}
r	parameter relating transverse to longitudinal reinforcement
S_v	spacing of stirrups
T	external torsional moment
T_{cr}	resistance to torsional cracking
T_a	torsional resistance due to aggregate interlock

T_{du}	torsion required to produce dowel failure
T_l	torsion producing yielding of longitudinal failure
T_{si}	torsion producing yielding of stirrups failure
T_s	$2 \frac{A_{sv} f_{yv}}{S_v} X_1 Y_1$
T_u	ultimate torsional resistance
T_{sc}	torsional strength as limited by strength of concrete
T_y	torsion required to produce yielding of reinforcement
V	external shear force
V_o	shear force required to produce yielding of reinforcement
V_u	shear strength of the beam in simple flexure
v	shear resistance per unit area
w	crack width or deflection
x	length along x-axis
X	depth of neutral axis
X_1	smaller centre line dimension of stirrups
X_{11}	smaller centre to centre dimension between longitudinal corner bars of rectangular section
y	length along y-axis
Y_1	larger centre line dimension of stirrups of rectangular section
Y_{11}	larger centre to centre dimension between longitudinal corner bars of rectangular section
z	section modulus
z_t	torsional modulus
z	lever arm between tension in main tension reinforcement and compression in concrete compressive zone

α	coefficient
α_e	modular ratio
ϵ	strain
ϵ_{cu}	limiting (ultimate) compressive strain of concrete
ϵ'_{cu}	limiting (ultimate) compressive strain of concrete in the presence of shear stresses
ϵ_{sl}	strain in main tension reinforcement
ϵ'_{sl}	strain in compression reinforcement
ϵ_{pe}	strain in prestressing reinforcement after losses
ε_c	Vb/T
ε_y	VX_1/T
γ	shear strain in concrete
λ	$\frac{1}{1+\left(\frac{2\tau_x}{f_x}\right)^2}$
τ	shear stress
τ_t	shear stress due to torsion
τ_v	shear stress due to transverse shear
ϕ	diameter of reinforcement
$\theta, \theta_1, \theta_2, \theta_3$	inclination of the initial cracking with respect of longitudinal axis
θ_{min}	minimum inclination of compressive stress field
	bending to torque ratio

CHAPTER 1

INTRODUCTION

1.1 Structural Concrete Members Subjected to Combined Torsion, Bending and Shear

In the past two decades considerable development has taken place in the fields of Structural analysis, construction techniques and properties of building materials due to which it is now possible to create forms of greater structural efficiency and beauty. This development has resulted in many structural forms where torsion can no longer be ignored.

The importance or otherwise of any particular force system on the behaviour of structures or structural components depends on the structural form, type of applied loads, physical properties, boundary conditions and modes of connection. In most traditional framing systems, the arrangement of the members minimises torsional effects, but the range of structures in which torsional forces are significant is growing. The following are examples of such structures:

1. Spine box-beam bridges.
2. Other bridge-deck constructions
3. Bow girders.
4. Spiral and free standing staircases.
5. Multi-storey core structures.

Spine box-beam bridges have gained increasing popularity and constitute by far the largest group of structures where torsion is important. A detailed examination has been made by Swann (1.1) of the characteristics of 173 bridges built in the

last 15 years reflecting the recent trend in the use of box beams.

The period has also witnessed a shift in design philosophy from allowable stress methods towards the limit state design concept which recognises the need to provide a safe and serviceable structure at economic cost. Therefore, the designer must be able to predict the performance of these structures under various loading stages. It is generally recognised that these structures behave reasonably elastic up to cracking and hence available elastic methods of analysis are adequate for assessing the response of these structures under service loads. The validity of the elastic methods diminish as the ultimate load is approached - hence these methods are inadequate in assessing the ultimate strength of these structures.

No general method of analysis presently available, is valid for all stages of loading, therefore attention is concentrated on the study of the behaviour of these structures at two essential types of loading:

A. Service loads.

B. Ultimate loads.

1.2 Elastic Behaviour

The 1960s saw intensive research primarily on the study of elastic response of structures where it is possible to analyse with the aid of computers, varieties of complex structural systems that were hitherto impossible to analyse.

It has become clear that structural members exhibit two ways of resisting torsion in the elastic range. The first way denotes pure torsion or St. Venant torsion resulting in a shear stress field in the section while the second way denotes warping torsion producing longitudinal stresses. Depending on the type of cross-sectional shape of the member, span, mode of support and boundary conditions, the resistance to torsion may range from the pure St. Venant torsion to warping torsion. The relative importance of these two ways of resisting torsion is demonstrated by reference to the three cases of simply supported beams with rigid cross-section shown in Fig. 1.1.

It is seen that the magnitudes of the warping moment M_w at the centre of span are directly dependant on the parameter χ which in turn is a function of the span, St. Venant torsional rigidity (GJ) and the warping torsional regidity (I_w). If χ is small, the warping torsion predominates as in the case of a thin-walled cross-sectional beam such as cold formed steel profiles where the St. Venant torsion can be ignored. However, if J is large, St. Venant torsion predominates as in the case of the solid section where the warping torsion can be ignored. The exact theory of torsion for the case of prismatic members which are free to warp was first presented in 1886 by St. Venant. The theory was then extended by Vlasov (1.2) to cover the general case of restrained thin-walled beams.

Structural concrete members can be classified into two main groups according to their behaviour in torsion. The first group comprises box-beams

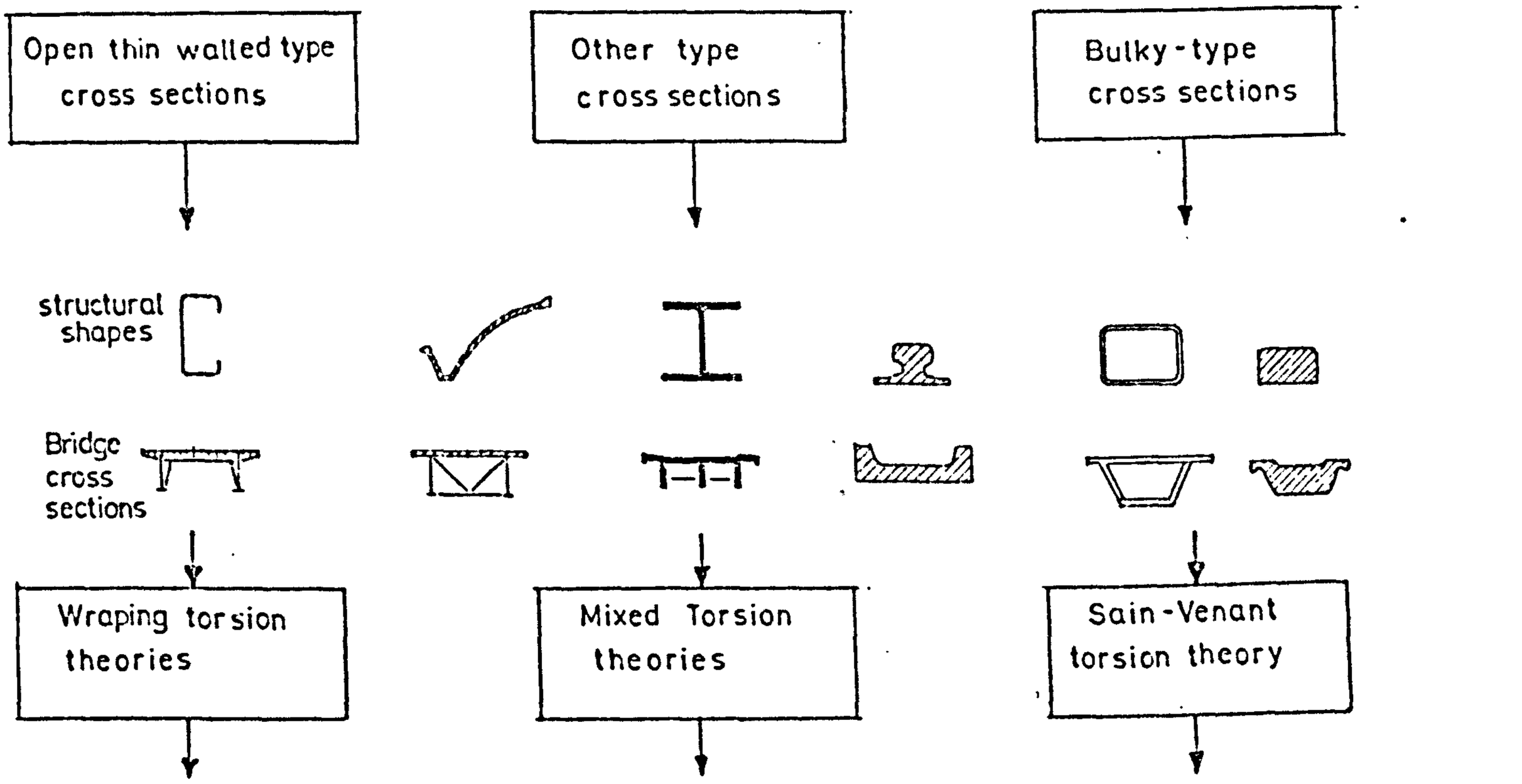

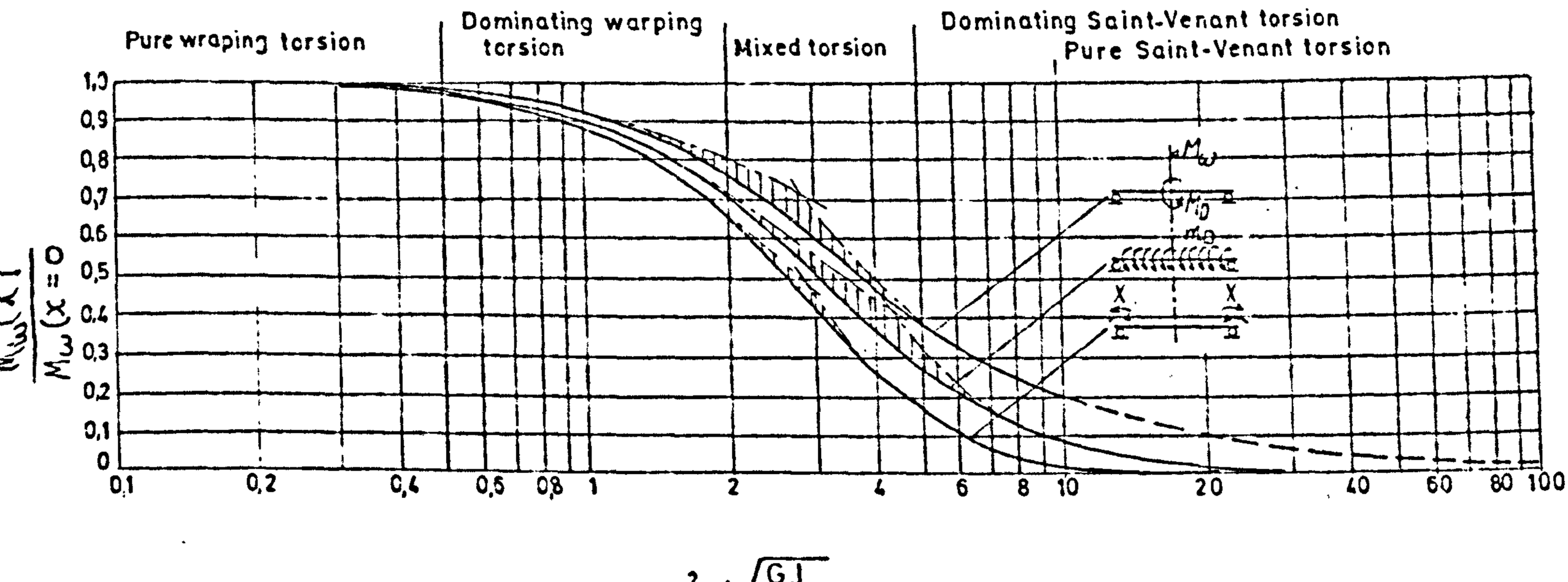

$$\chi^2 = L\sqrt{\frac{GJ}{EI_w}}$$

FIG. 1.1 Classification of torsional resistance of structural members according to Kollbrunner and Basler.

with thick-walled rigid cross-section in which the profile's cross-section does not change under load. The second group comprises thin-walled box-beams with deformable cross-sections.

The torsional deformation of a thin-walled box-beam will result in further warping stresses arising from in-plane displacement of the walls of the beam and transverse flexural distorsional moment arising from the out of plane displacement of the walls. Various analytical techniques have been developed in the past decade which consider the cross-sectional deformation of a thin-walled beam. These may be classified as follows:

a. Beam methods.
b. Folded plate methods.
c. Finite segment methods.
d. Finite strip methods.
e. Finite element methods.
f. Equivalent gridwork methods.

A review giving the advantages, disadvantages, adequacy and limitation of these methods has been published by Maisel (1.3). The validity of some of these theories has been tested against the behaviour of concrete model box-beams by Mitwally (1.4). It is clear from the available analytical and experimental evidence that the torsional and distorsional response must be considered in the design of thin-walled box-beams.

1.3 Ultimate Strength

At the inception of this research programme it was recognised that although considerable progress has been made in the field of elastic

analysis, knowledge of the ultimate strength of thick and thin-walled box members subjected to combined torsion, bending and shear was almost non-existant. The scarcity of research information on the ultimate strength of these members has delayed the development of a rational design method for box-beam bridges. Collapse of various important steel box-beam bridges highlighted the need for and gave impetus to research workers to study the ultimate strength of steel box-beams.

Study of the ultimate strength of reinforced and prestressed concrete beams under bending and shear has been so extensive that its logical outcome has now been incorporated in the code of practice of many countries including the U.K.; whereas study of these beams under combined torsion, bending and shear has been lacking. Furthermore, considerable disagreement exists among researchers on how torsion is resisted at ultimate load even for the simple loading case of reinforced concrete beams subjected to pure torsion.

The earliest contribution to the study of ultimate strength of concrete members subjected to torsion is due to Morsch (1.5) in 1903. Another important early contributor is Rausch (1.6) who in 1929 studied the strength of reinforced concrete beams under pure torsion. Nylander (1.7) in 1945 was the first to publish test results of the strength of reinforced concrete beams under combined torsion, bending and shear. Between 1950.1955, Cowan (1.8) developed an elastic approach to the design of reinforced concrete beams under combined loading systems.

The most important theoretical and experimental contribution in the study of reinforced concrete beams under combined torsion, bending and shear was made by Lessig (1.9) and Colleagues in Russia. In this work, a new approach based on the equilibrium conditions of an observed failure mechanism was presented.

In 1966, the American Concrete Institute organised a symposium on this subject at which 18 papers were presented (1.10). These papers illustrate the extent of disagreement that existed among the authors on how torsion is resisted in reinforced concrete members.

Lampert and Thurlimann (1.11) have proposed the space truss analogy for the case of combined bending and torsion. The validity of the Lessig and Lampert theories is restricted by the yielding of reinforcement. To satisfy this requirement various empirical limits on certain parameters have been suggested by these authors.

Lessig's theory was extended by Goode and Helmy (1.12) and Collins et al (1.13) to include the case for yielding of longitudinal bars located on the top of the beam. In addition Goode and Helmy considered other modes of failure of reinforced concrete beams subjected to bending and torsion in which the transverse and/or the longitudinal steel do not yield. Collins et al also suggested semi empirical formulae to predict the ultimate strength of members subjected to combined torsion, bending and shear. Alternative skew bending approach was developed in 1965 by Evans and Sarkar (1.14) for the case of reinforced concrete beams under combined bending and torsion. Another paper was published

by Evans and Khalil (1.15) for the case of pre-stressed concrete beamsunder bending and torsion.

In 1970 Zia (1.16) published a short state of the art review on the subject of torsion in concrete members. In this paper Zia pointed out that there was no general theory for predicting the strength of concrete members under combined torsion, bending and shear. He also pointed out the need for further research on prestressed concrete beams under torsion bending and shear.

In 1972 Lampert and Collins (1.17) attempted to clarify the confusion that had been created by the large number of contradictory papers about torsion in reinforced concrete beams subjected to bending and torsion.

1.3.2 Comments on Ultimate Strength Methods

From the above brief review the following comments can be made:

a. Confusion still exists with regard to the mechanism of transfer of torsion in reinforced and prestressed concrete beams.

b. Research information on the strength of reinforced and prestressed concrete beams under the combined action of torsion, bending and shear is scarce.

c. The effect of warping and transverse moments due to distorsion of the cross section on ultimate strength has not been investigated.

(a) may be attributed to the fact that shear or torsion can be resisted by one or more of the following:

1. Uncracked concrete.
2. By interlocking of aggregate in cracked concrete.
3. Reinforcement acting as a dowel.
4. Reinforcement in the form of longitudinal and transverse reinforcement.

This confusion may be due to the failure of reinforced and prestressed concrete beams under combined torsion, bending and shear produced by failure of one or more of the four possible shear paths. Therefore, the following twelve modes of failure are envisaged for rectangular beams:

i Three modes characterised by yielding of longitudinal and transverse reinforcement.

ii Three modes characterised by yielding of longitudinal reinforcement and the failure of aggregate interlock or failure due to dowel forces.

iii Three modes characterised by yielding of transverse reinforcement and failure of aggregate interlock or failure due to dowel forces.

iv Three modes characterised by failure of concrete prior to yielding of reinforcement.

There is no one general theoretical treatment to all of the above modes of failure neither is there any information on the mechanism of transfer of torsion for the various modes of failure.

1.4 Object and Scope

From the above short review it is evident that although considerable progress has been made for the case of elastic behaviour, relatively small volume of research has been published on ultimate strength of reinforced and prestressed concrete members under combined torsion and shear.

The object of this research is:

1. To propound a rational approach for predicting cracking and ultimate strength of reinforced and prestressed concrete members subjected to combined torsion, bending and shear.
2. To investigate mechanisms of transfer of torsion for reinforced concrete beams under pure torsion.
3. To present test results on the behaviour and strength of thin-walled prestressed concrete box-beams under the action of in-plane forces generated by torsion, bending and shear.

It has been the aim throughout the development of this work that the proposed theories should not only be rational but also simple and accurate so that they could be of direct use to the practicing structural engineer. In order to achieve this objective, the effect of various parameters which are known to influence the strength of reinforced and prestressed concrete members under torsion, bending and shear were examined. Parameters found to have secondary contributionswere eliminated.

A method for predicting the cracking strength for reinforced and prestressed concrete beams subjected to torsion bending and shear is given in Chapter 2. Chapter 3 presents a theoretical study of the mecahnism of transfer of torsion and the strength of reinforced and prestressed concrete members under pure torsion.

In Chapter 4, theoretical expressions for predicting the ultimate strength of reinforced and prestressed concrete membersare given for three yield modes of failure for beams subjected to torsion, bending and shear. In Chapter 5, theoretical expressions for predicting the ultimate strength of reinforced and prestressed concrete members under torsion, bending and shear are given for modes other than yield failure.

In Chapters 2-5, the proposed theories have been compared with a large number of test results reported in literature.

The test results from 25 thin-walled prestressed concrete beams subjected to pure torsion, torsion and bending, torsion bending and shear are given in Chapter 6. Chapter 7 contains a theoretical and experimental study of the behaviour of dowels. Chapter 8 contains the summary of conclusions of this thesis.

CHAPTER 2

CRACKING STRENGTH OF PLAIN AND PRESTRESSED CONCRETE MEMBERS SUBJECTED TO BENDING TORSION AND SHEAR

Summary

The existing methods for calculating cracking strength are reviewed. A lower bound method for calculating the cracking resistance for beams subjected to bending, torsion and shear is presented which is based on an acceptable elastic stress field, maximum stress failure criterion and modified tensile strength for concrete.

The predictions of the theory are compared with about 400 test results available in literature. In general the agreement is good.

2.1 Introduction

All available research information on the behaviour of structural concrete members subjected to torsion, indicate that there are fundamental changes in the response of these members after the formation of the first crack such as a drastic drop in the torsional stiffness which in some cases may lead to immediate failure. Hence since cracking affects the serviceability and strength of these structural members, it is essential that the cracking torque be accurately predicted by simple and rational theory.

Although a number of theories are now available for predicting the cracking torque, they all lack the necessary consistency when compared with test results. This discrepancy could be attributed to one or more of the following reasons:

a) The stress distribution across the section is incorrectly assumed.
b) The use of incorrect failure criterion.
c) Wrong assessment of tensile strength of concrete.

It is therefore, the object of this chapter to review these theories, to examine their accuracy and limitations and to develop a rational approach to this problem which will yield a better correlation with available test results. This subject will be dealt with according to the manner of loading i.e. pure torsion, combined bending and torsion, combined bending, torsion and shear.

2.2 Pure Torsion

A summary of the cracking torque theories for

concrete beams under pure torsion is given in Table 2.1.

2.2.1 Stress Distribution Prior To Cracking

It is not surprising to find the first cracking strength theories utilizing the St. Venant elastic theory for pure torsion, this theory assumes that the concrete is homogeneous and obeys Hook's law up to the point of cracking. Bach (1), for example, utilized this theory and assumed that cracks occur when the maximum principal tensile stress in the section reaches the uniaxial tensile strength of concrete. Experimental evidence indicates that the torque-rotation relationship for concrete remains almost linear up to cracking and for unreinforced concrete beams, failure usually occurs suddenly in a brittle manner hence, confirming the validity of the assumptions made in this theory. On the other hand this approach usually underestimates the cracking torque of test results by almost 50%. Further criticism of this approach is the difficulty encountered in solving the St. Venant equation for any practical problems.

To account for these discrepancies between predicted and test results, Marshall (8, 9) and others utilized the Nadia plastic theory of torsion. In this theory the materials are assumed to undergo infinite plastic deformation and cracking is assumed to occur when the maximum principal tensile stress reaches the uniaxial tensile strength of concrete. This theory was selected on the basis of its ability to predict the results in the tests they carried out.

TABLE 2.1 Summary of cracking strength theories forbeams under pure torsion

Investigator	Reference	Year	Stress Distribution	Failure criterion	Concrete Strength	Application
Graf and Bach	1		St. Venant	Max. Pr Stress	f_t	P
Cowan	2,3	1950	St. Venant and Nadia	Max. Pr Stress	f_t	RC & P.S.C
Humphreys	4	1957	St. Venant	Max. Pr Stress	f_t	P & P.S.C.
Zia	5	1961	St. Venant	Simplified Mohrs Internal friction	f_t	P & P.S.C.
Evans & Khalil	6	1970	Adjusted St. Venant	Max. Pr Stress	f_t	P.S.C.
Collins M.P. et al	7	1968	Nadia	Max. Pr Stress	f_t	R.C
Gausel E.	8	1970	Nadia	Max. Pr Stress	f_t	P.S.C.
Marshall W.T.	10,11	1944 1974	Nadia	Max. Pr Stress	f_t	R.C.
Navaratnarajah	12	1968	St. Venant and Nadia	Max. Pr Stress	E_c	R.C.
Hsu. T.C.	13,14, 15	1966 1968	Skew bending	Mohrs Internal friction	f_r	P. & P.S.C.
Martin L.H.	17	1971	Skew bending	Max. Pr Stress	f_r	P.
Martin L.H. & Wainwright P.J.	18	1973	Skew bending	Max. Pr Stress	f_r	P.S.C.

P = Plain Concrete beams

R.C. = Reinforced Concrete beams

P.S.C. = Prestressed Concrete beams

Max.Pr = Maximum Principal

f_t = Tensile Strength of Concrete

f_r = Modulus of rupture of concrete

E_c = Young's Modulus for concrete

These authors justified the use of their theory by reference to the non-linear relationship obtained between torque and strains. In general this non-linearity is insignificant and does not justify the use of the plastic theory. In addition this method appears to overestimate the cracking torque particularly for the larger size members encountered in practice.

In 1966 Hsu (11, 12) introduced a new elastic approach for predicting the cracking torque for rectangular solid sections. He argued that torsional cracking occurs as a result of bending about skewed axes. Failure was assumed to occur when the maximum bending stress on this section reached the modulus of rupture of the concrete. Hsu verified his approach by the use of high speed photography and by comparison with his test results.

It can be shown that this method usually yields an upper bound prediction to the cracking strength since it is based on an assumed fracture plane i.e. it is always possible that a lower value for cracking can be obtained by considering other fracture planes. Although this approach was successfully applied to solid rectangular beams by Hsu and was further refined and extended to solid circular sections by Martin (17), it is doubtful whether this approach could accurately be applied to other sections which are commonly encountered in practice such as , T or box sections. These limitations may be illustrated by considering a square hollow section beam shown in Fig. 2.1. Using first the Skew bending theory as proposed by Hsu and taking moments of forces about the neutral axis on the Skew failure plane as shown in Fig. 2.1:

$$T_{cr} \cos \theta = \frac{Z f_t}{\sin \theta}$$

where Z is the section modulus of the cross section.

Re-arranging this equation we get:

$$T_{cr} = \frac{Z f_t}{\cos \theta \sin \theta} \qquad 2.1$$

It can be shown that T_{cr} has a minimum value when $\theta = 45^{o}$. Substituting this value of θ into equation 2.1

$$T_{cr} = 2 Z f_t \qquad 2.2$$

For $t \ll h$, $Z = \frac{4}{3} t h^2$ and the cracking torque becomes

$$T_{cr} = \frac{8}{3} t h^2 f_t$$

It is interesting to note that this expression over estimates the cracking torque by 33% when compared with the Bret Batho theory.

An alternative solution to this problem may be found by considering the helical mode of failure and the stress distribution prior to failure as shown in Fig. 2.2.

Taking moments of the forces about the longitudinal axis, we get:

$$T_{cr} = \frac{4 h t f_t}{\sin \theta} \cos \theta \frac{h}{2}$$

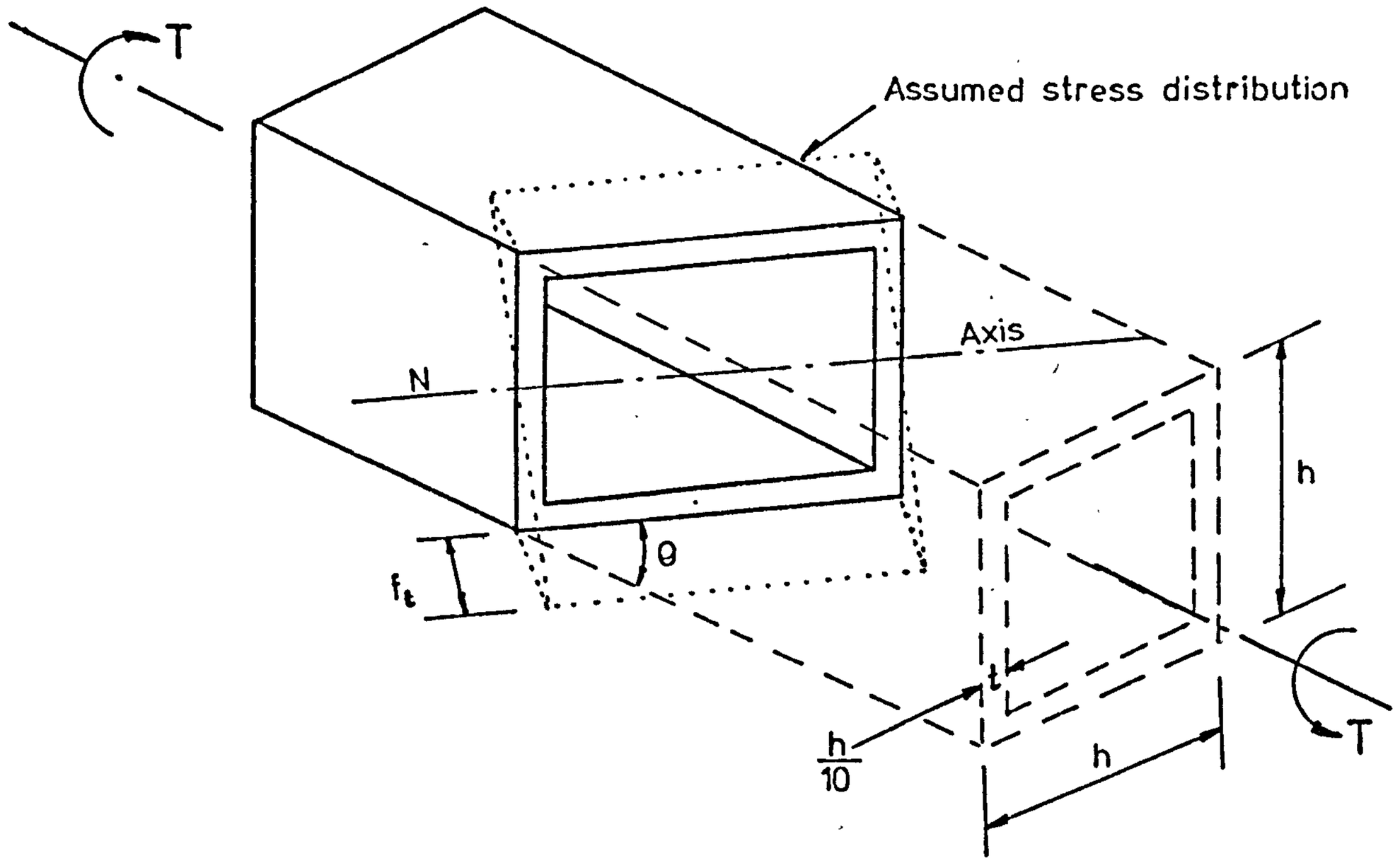

Fig. 2.1. Assumed failure plane of a box-beam under pure torque (due to Hsu)

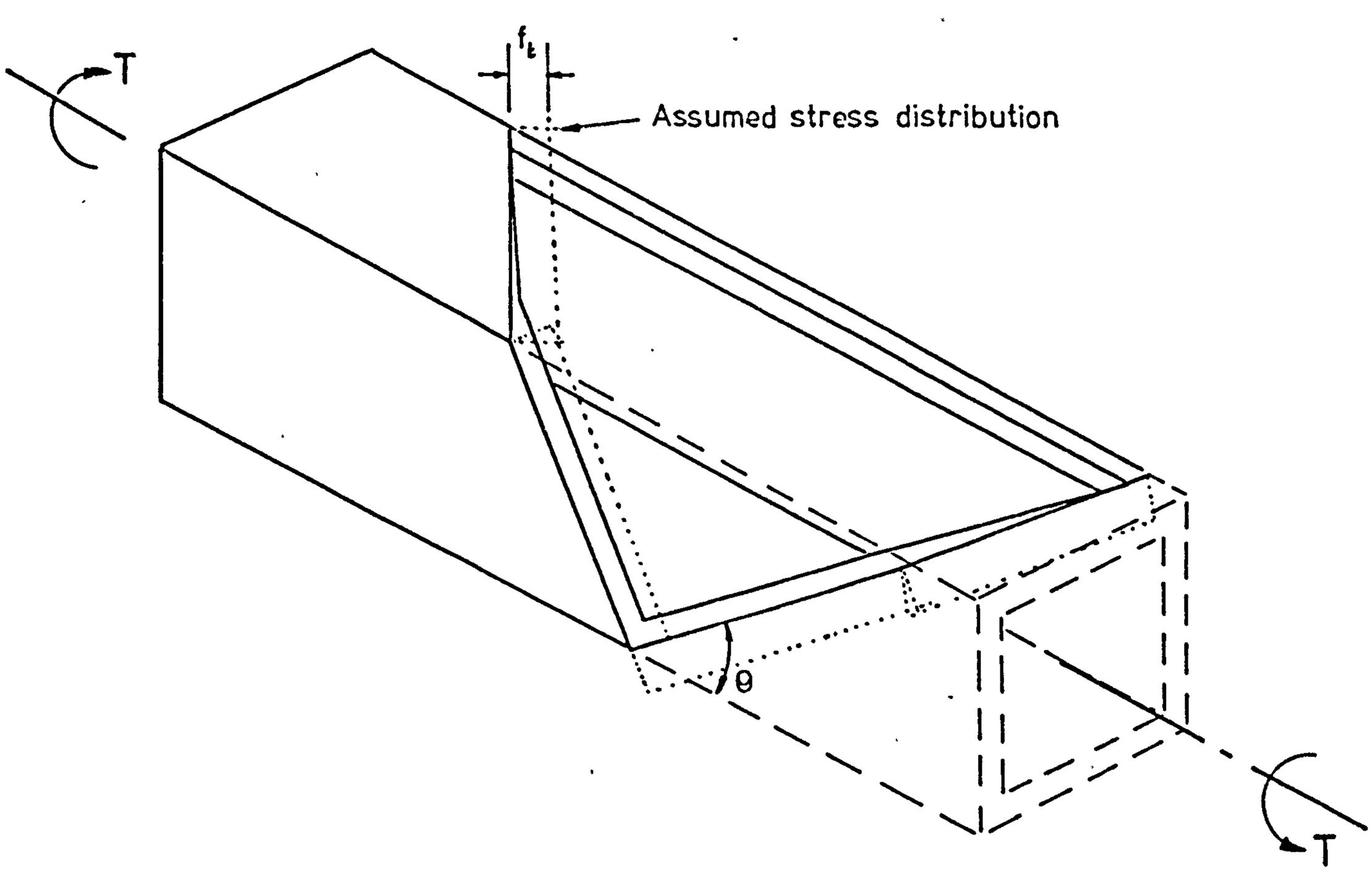

Fig. 2.2. Alternative failure plane of a box-beam under pure torque

$$T_{cr} = 2\ t\ h^2\ f_t\ \cot\theta \qquad 2.3$$

T_{cr} may be shown to have a minimum value when $\theta = 45^{o}$ when equation 2.3 becomes:

$$T_{cr} = 2\ t\ h^2\ f_t \qquad 2.4$$

This equation is identical to the Bret Batho expression.

If a longitudinal crack is introduced in this beam, the response of this member to pure torque will be drastically altered and the cracking torque using the St. Venant theory for this open section is:

$$T_{cr} = \frac{4}{3}\ h\ t^{2} f_t$$

and the ratio of the cracking torque for the closed and the open sections is

$$\frac{T_{cr}\ \text{Closed}}{T_{cr}\ \text{Open}} = \frac{3}{2}\ \frac{h}{t}, \text{ and for } \frac{h}{t} = 10, \quad \text{This ratio} = 15.$$

Although the St. Venant torsion theory deals with these problems accurately, it is doubtful whether the open section can be solved satisfactorily and rationally by the Skew bending theory. In addition to these limitations to the Skew bending theory, experimental evidence indicates that the cracks usually take a helical form in contrast to what has been assumed by Hsu. The measurements of longitudinal strains in beams also does not support the stress distribution assumed in Hsu's theory, hence this concept is inferior to the St. Venant theory of torsion.

2.2.2 Failure Criterion

As stated earlier, all the experimental evidence

on the cracking of plain and prestressed concrete beams (where $\frac{fp}{f_t} > 0.5$) indicates that failure of these beams occurs immediately after cracking with a cleavage made of fracture being exhibited. Hence the universal use of the maximum principal stress failure criterion is fully justified.

2.2.3 Tensile Strength of Concrete

All available research data on the tensile strength of concrete indicates that it varies considerably with the testing technique. For example the direct tensile strength and the strength obtained from the modulus of rupture test may differ by more than 100% for the same concrete. Consequently the accuracy of prediction of cracking in any given situation depends on the appropriate selection of the tensile strength of the concrete, for instance in the case of a thin-walled box section subjected to bending a direct tensile strength may be more appropriate whereas for cracking resistance of a solid section in bending it may be preferable to utilize the flexural tensile strength.

Similarly the flexural tensile strength is more appropriate for the prediction of cracking for beams with rectangular solid sections subjected to pure torque. For example, for rectangular beams with high aspect ratio, the principal stresses due to pure torsion follow closely the stress distribution due to bending, except at the ends of the shorter sides of the cross section as shown in Fig. 2.4. On the other hand for thin-walled beams subjected to pure torque the principal stresses are almost uniformly distributed across the thickness of the wall and along the walls of the beam. Hence, in this situation the direct tensile strength is

more appropriate.

It is interesting to point out in passing that the agreement obtained by Hsu between his test results and theory is due to the appropriate selection of tensile strength of concrete rather than the use of his new skew bending theory.

The variation between the modulus of rupture as a measure of tensile strength and the direct tensile strength has been attributed (21) to the following:

a) The volume of concrete subjected to maximum stress is small, being limited to the extreme fibres, and therefore, the probability of a flaw being present at the critical location is smaller in the flexural test than the direct test.

b) Due to some plastic deformations occuring as failure is approached.

Since the flexural test similates the type of stress system imposed on a rectangular solid section subjected to bending and or torsion, it is the most useful test to apply if cracking is to be predicted under these conditions.

Experimental investigations (12) aimed at measuring direct tensile strength and modulus of rupture show that the modulus of rupture for the same concrete decreases with increase in depth of beam. Hsu attributed this effect to the variation in the strain gradient and he argued that when the size of the modulus of rupture beam becomes very large the strain gradient diminishes and the modulus of rupture, fr, approaches the tensile strength, f_t.

The experimental results obtained by Hsu are

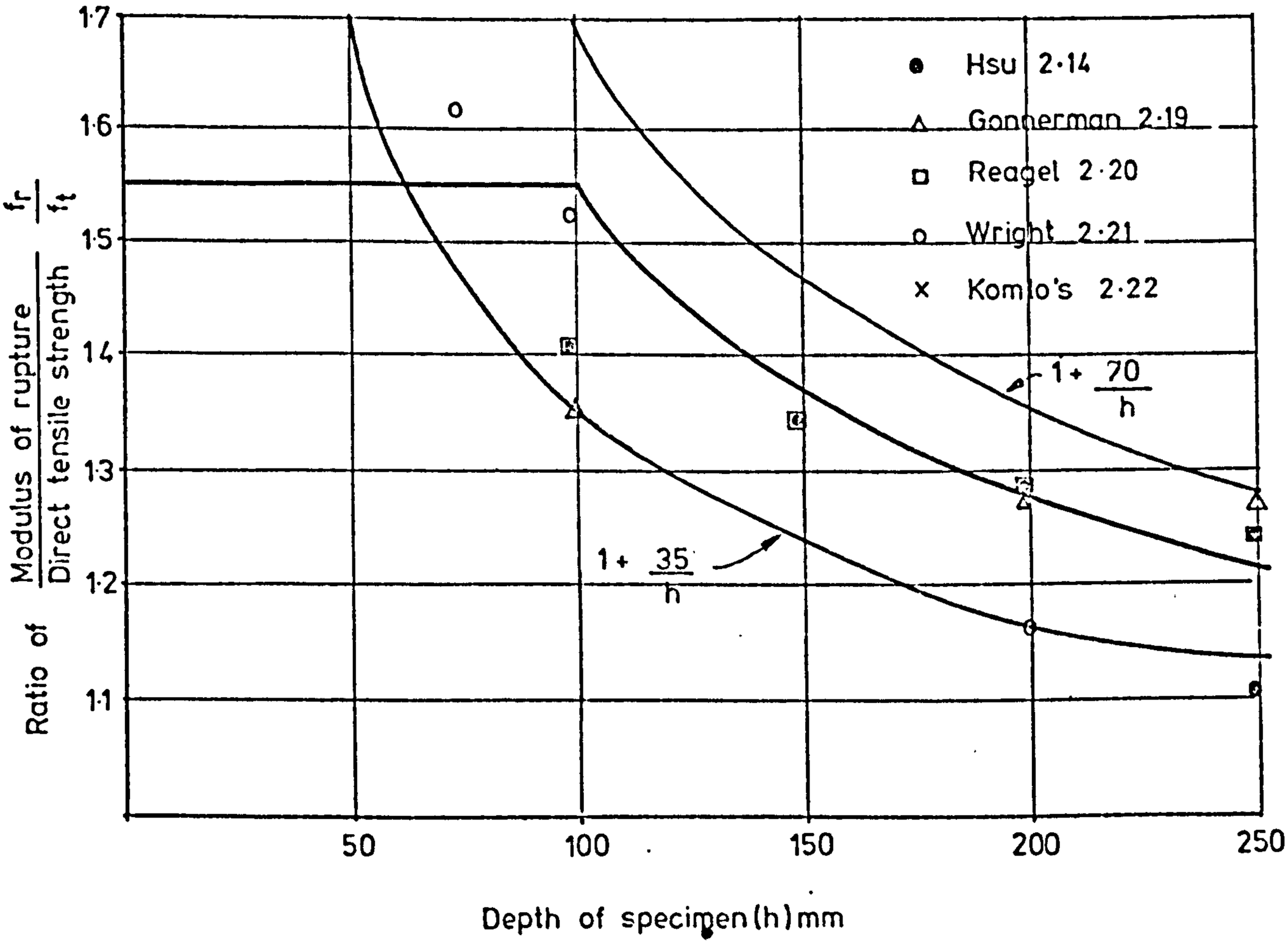

Fig.2.3. Relationship between the ratio of $\frac{f_r}{f_t}$ and depth of flexural beam

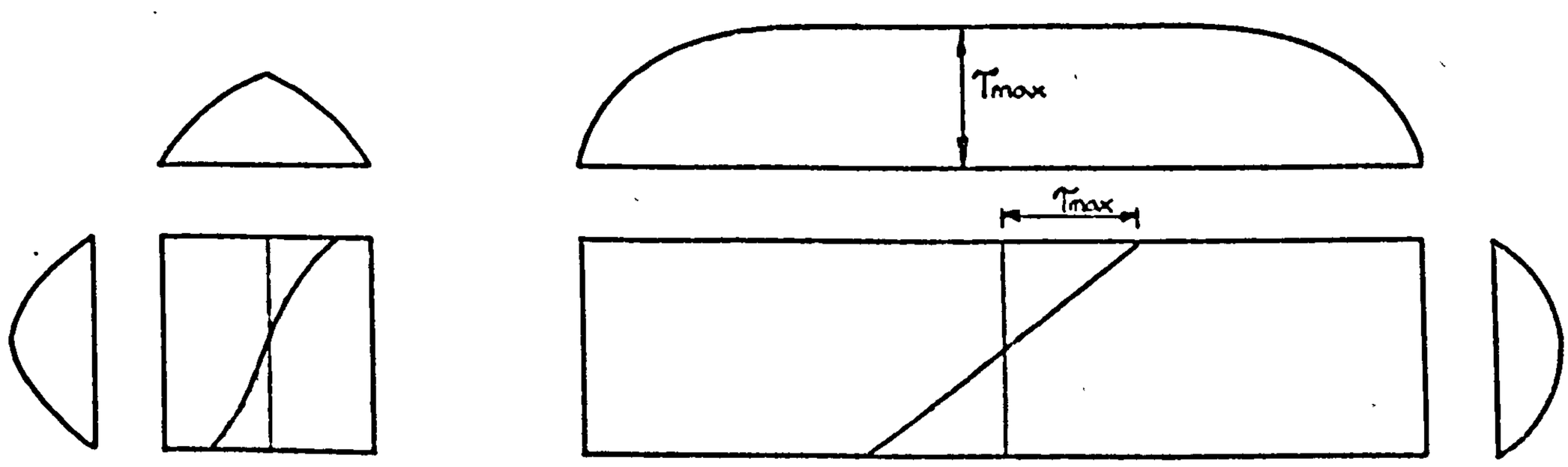

Fig.2.4. Sheer stress distribution in square and rectangular sections according to st.Venant theory.

plotted in Fig. 2.3 as a ratio of f_r/f_t against depth h mm together with data obtained by Gonnermant (19), Reagel (20, Wright (21), and Komlas (22). Some of these investigations did not report the tensile strength, f_t and their data are plotted using Hsu's f_r/f_t value of 1.34 for the 150 mm beam size as a reference.

It is seen that the experimental relationship between f_r/f_t and h varies between the limits

$$1 + \frac{35}{h} < \frac{f_r}{f_t} < 1 + \frac{70}{h}$$

Hence the following average relationship between $\frac{f_r}{f_t}$ and h is recommended

$$\frac{f_r}{f_t} = 1 + \frac{55}{h}, \text{ but not greater than } 1.55 \text{ ---- } 2.5$$

a similar expression has been suggested by Hsu (13).

In general only the cylinder compressive strength, f'_c, or the cube strength, fcu, are measured, hence, the relationship between the compressive strength and tensile strength is needed. Among the many empirical expressions relating the tensile strength to the compressive strength of concrete which are available, the following expression has received wide recognition and it has been included in CP 110.

$$f_t = 0.36 \sqrt{f_{cu}} \qquad 2.6$$

This expression is compared with test results in Fig. 2.6 where it is seen that it provides a safe limit for the test results and bence, a safe prediction of cracking strength is expected when this relationship is used.

The scatter in the test results has been

attributed by Johnston (23) to the many parameters that usually influence this relationship. Therefore, a similar scatter in the ratio of experimental to theoretical cracking strength of a concrete member is expected if this expression is used.

In cases where the cylinder strength f'_c is given, the relationship $f'_c = 0.8\ f_{cu}$ is used.

If the bending stress distribution occuring just before cracking for the rectangular beam shown in Fig. 2.4 is compared with the stress distribution due to pure torsion occuring just before cracking, then it will be seen that the surface area on the wide face of this beam which is under maximum stress is smaller for the torsional case than for bending and this discrepancy increases with a decrease in the aspect ratio of the section. This discrepancy has a maximum value for a square section and is negligible for rectangular beams with $\frac{h}{b} > 10$. Therefore, the cracking torque for rectangular beams having $\frac{h}{b} > 10$ would be predicted accurately if the modulus of rupture is used as a measure of tensile strength. On the other hand the use of modulus of rupture is expected to underestimate the cracking torque for rectangular beams having $\frac{h}{b} < 10$.

In order to obtain accurate prediction of cracking torque for rectangular beams, a correct estimate of the tensile strength is essential and under this condition the tensile strength of concrete appeared to be a function of $\frac{b}{h}$. This can be shown by plotting all experimental results available in literature on plain rectangular

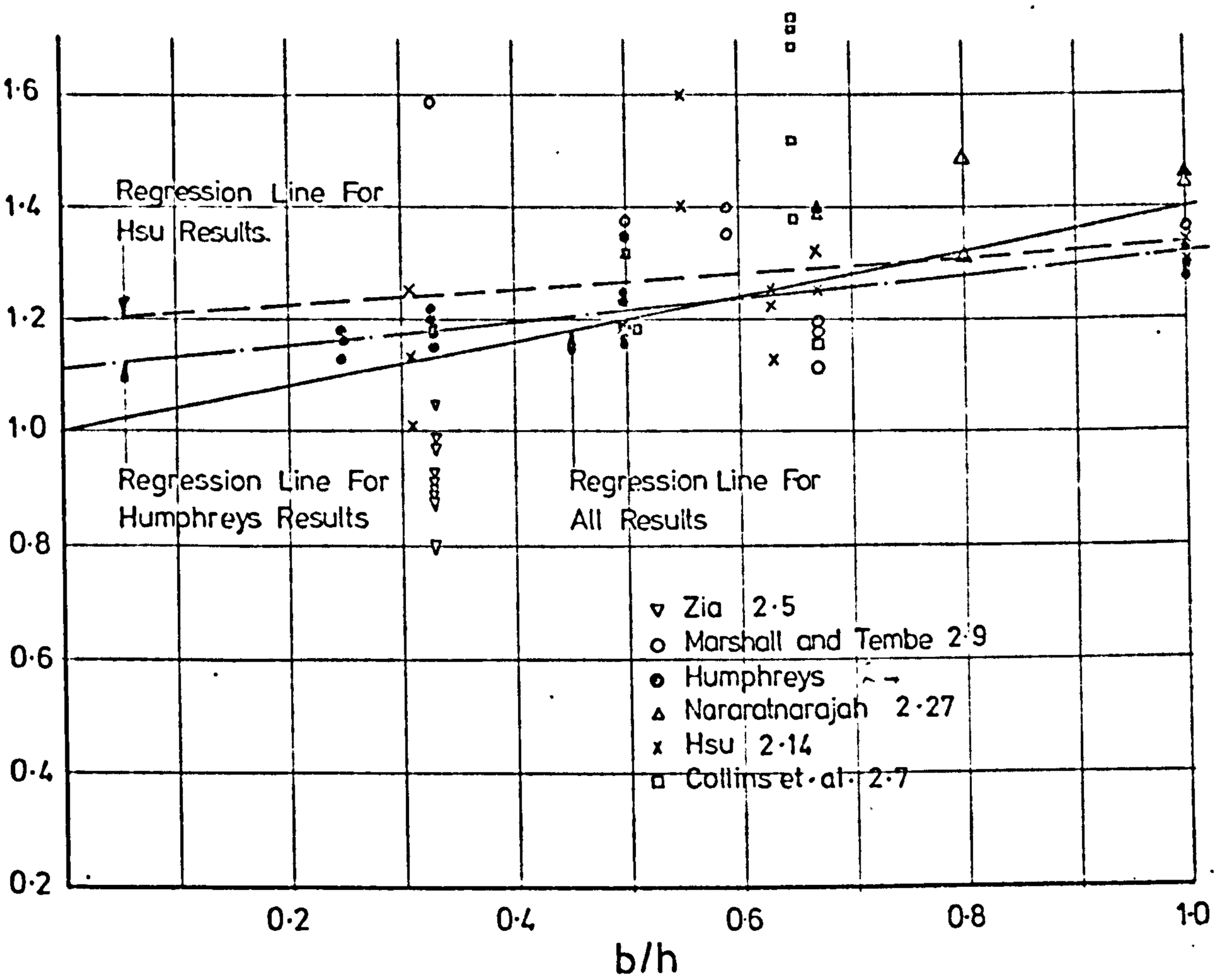

FIG 25. Influence of the b/h ratio upon the tensile strength of concrete in rectangular solid beams subjected to pure torque.

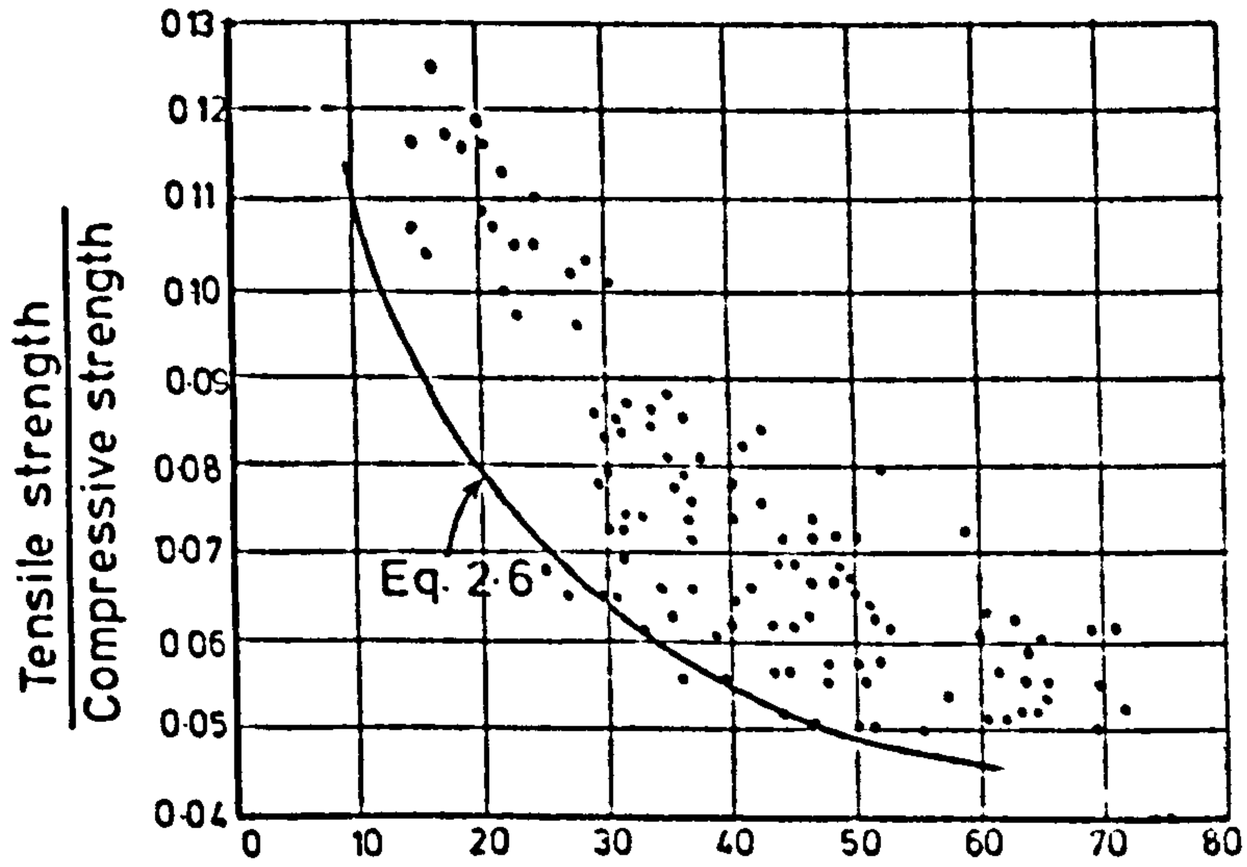

Fig. 2·6 Relationship between Cube strength and the ratio of tensile & compressive strength

(For sources of test results see ref 21)

concrete beams subjected to pure torque as a ratio of maximum St. Venant stress (f_{t2}) occuring at cracking to the modulus of rupture of concrete (fr) against the aspect ratio of the section $\frac{b}{h}$ as shown in Fig. 2.5. Regression analysis for these results indicates that the ratio f_{t2}/f_r tend to unity as $\frac{b}{h}$ approaches zero. Regression lines for the test results of Hsu and Humphreys are also obtained as follows:

$$\frac{f_{t2}}{f_r} = 1.01 + 0.4\,\frac{b}{h} \qquad \text{for all the test results}$$

$$= 1.2 + 0.15\,\frac{b}{h} \qquad \text{for Hsu results}$$

$$= 1.1 + 0.22\,\frac{b}{h} \qquad \text{for Humphreys results}$$

From this analysis and the test results shown in Fig. 2.5, it appears that accurate assessment of the influence of the aspect ratio $\frac{b}{h}$ on the value of $\frac{f_{t2}}{f_r}$ may take the following form:

$$\frac{f_{t2}}{f_r} = 1 + \frac{b}{4h} \qquad 2.7$$

2.3 Rectangular Concrete Beams Subjected to Bending Torsion and Shear

Some of the research work summarized in Table 2.1 contains theories for predicting the cracking torque for beams subjected to bending and torsion.

Cowan (3) derived an expression for predicting cracking strength for rectangular beams subjected to bending and torsion by assuming an elastic-plastic stress distribution in bending (i.e. he assumed a linear stress distribution in the compression zone and a second degree parabolic

variation of the tensile stresses), together with a plastic shear stress distribution due to torsion. The cracking strength was then obtained by equating the maximum principal tensile stress to the uni-axial tensile strength of concrete.

This approach was adopted by Evans and Sarker (24) and Fairbairn (25) for calculating the inclination of the cracks for rectangular reinforced concrete beams subjected to torsion and bending which was necessary for their ultimate strength theories.

Martin's skew bending theory which was mentioned earlier has been developed for the case of combined bending and torsion. A linear stress distribution across the skew plane was assumed. This theory has been extended recently by Wainwright to prestressed concrete beams subjected to bending and torsion.

These theories, however, have the same limitations and inaccuracies of their pure torsion counterpart. In addition no published theoretical work is at present available for predicting the cracking torque for beams subjected to the combined action of bending, torsion and shear.

All research evidence on the behaviour of concrete beams subjected to bending, torsion and shear indicates that this behaviour is reasonably elastic up to cracking. Hence if this behaviour is assumed and cracking is taken to be governed by the criterion of maximum stress then cracking would occur when the maximum principal stress reaches the appropriate tensile strength of concrete. For expediency, cracking is taken to be initiated

only at three possible critical points on the cross section. These points are located at the centre line of the bottom face, web and top face of the cross section of the beam. These possible modes of cracking will be referred to in the following as mode 1, mode 2 and mode 3 as shown in Fig. 2.6.

2.3.1 Mode 1

If the equilibrium of forces acting on element 1 shown in Fig. 2.6 are considered just prior to cracking, then:

From vertical equilibrium we obtain

$$\tau = \frac{f_{t1}}{\sin \theta_1} \cos \theta_1 = f_{t1} \cot \theta_1 \qquad 2.8$$

From horizontal equilibrium we obtain

$$\tau \cot \theta_1 = f_{t1} \cdot (f_{z1} - f_{p1}) \qquad 2.9$$

eleminating θ_1 between these two equations and rearranging we obtain:

$$\frac{\tau^2}{f_{t1}^2} + \frac{f_{z1}}{f_{t1}} = 1 + \frac{f_{p1}}{f_{t1}} \qquad 2.10$$

Now using the following relationship between applied moments and stresses:

$$\tau = \frac{T_{cr}}{Z_{t1}} \quad \text{and} \quad f_z = \frac{M_{cr}}{Z_1}$$

where Z_1 and Z'_1 are the section modulus and St. Venant modulus for point 1 respectively. Substituting these expressions into equation 2.10 and rearranging into a non dimensional interaction form:

$$\left(\frac{T_{cr}}{T_{cr1}}\right)^2 + \left(\frac{M_{cr}}{M_{cr_1}}\right) = 1 \qquad 2.11$$

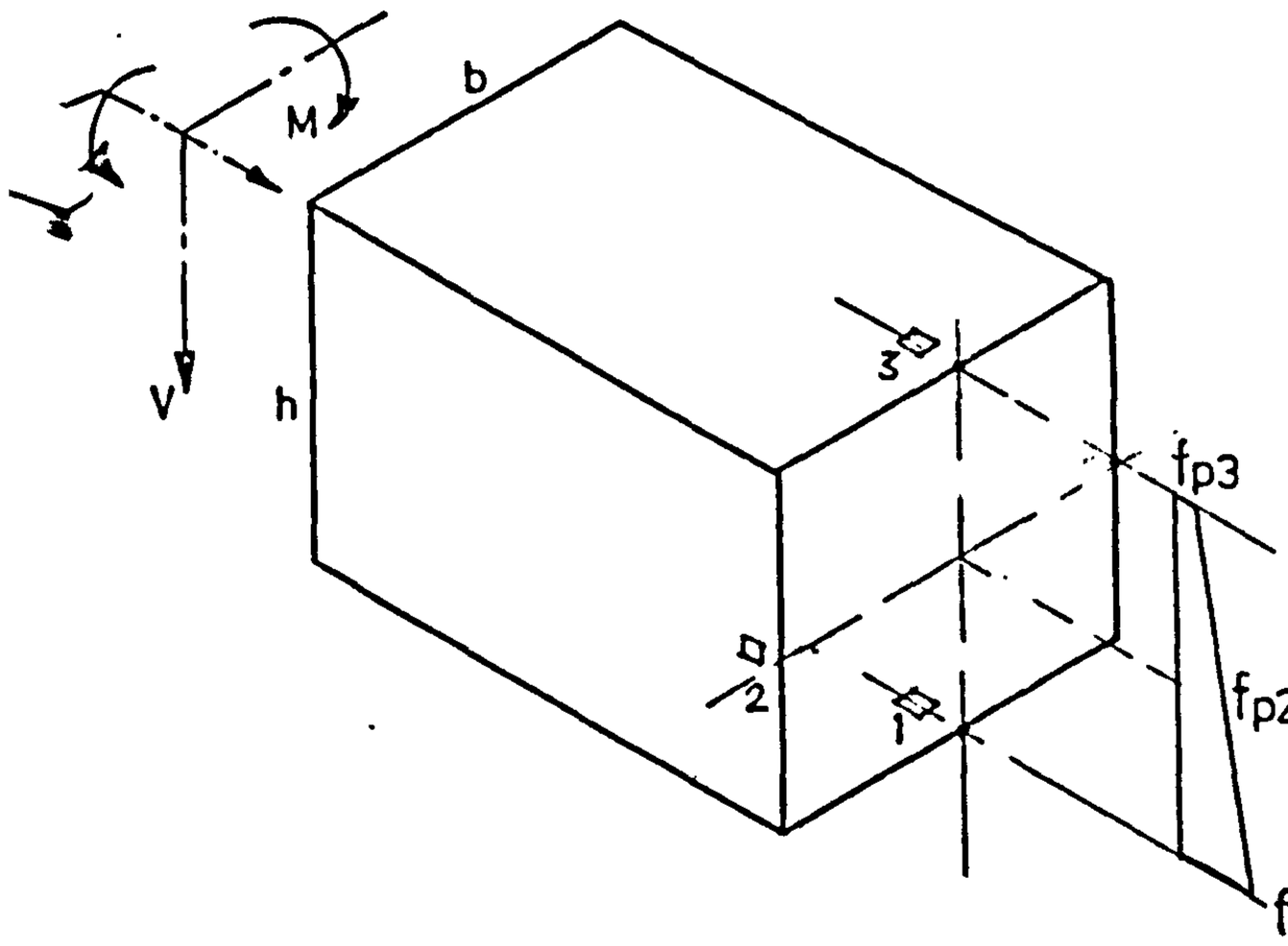

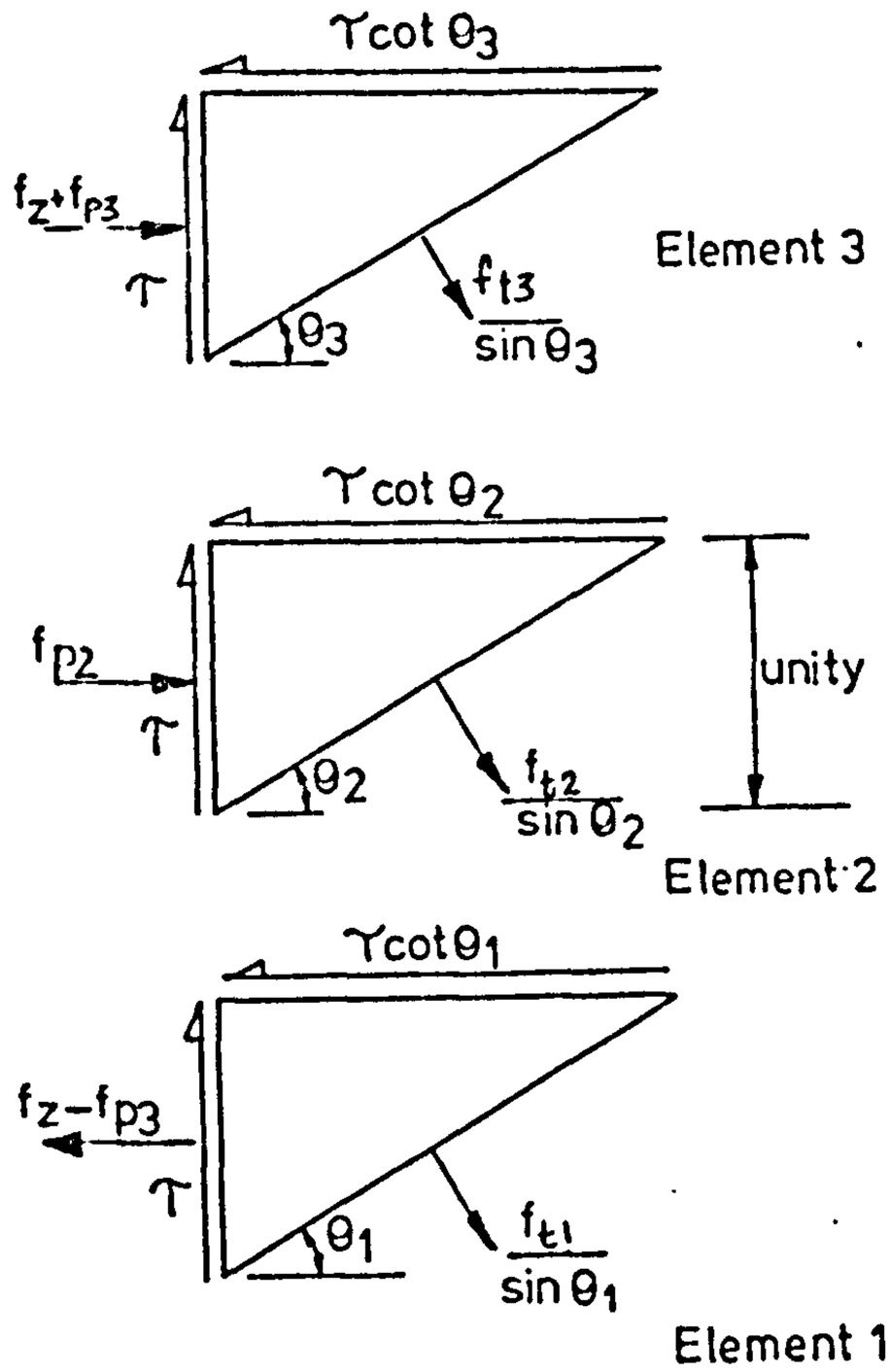

Fig 2.7. Forces acting on rectangular elements just prior to cracking for beam subject to bending, torsion & shear.

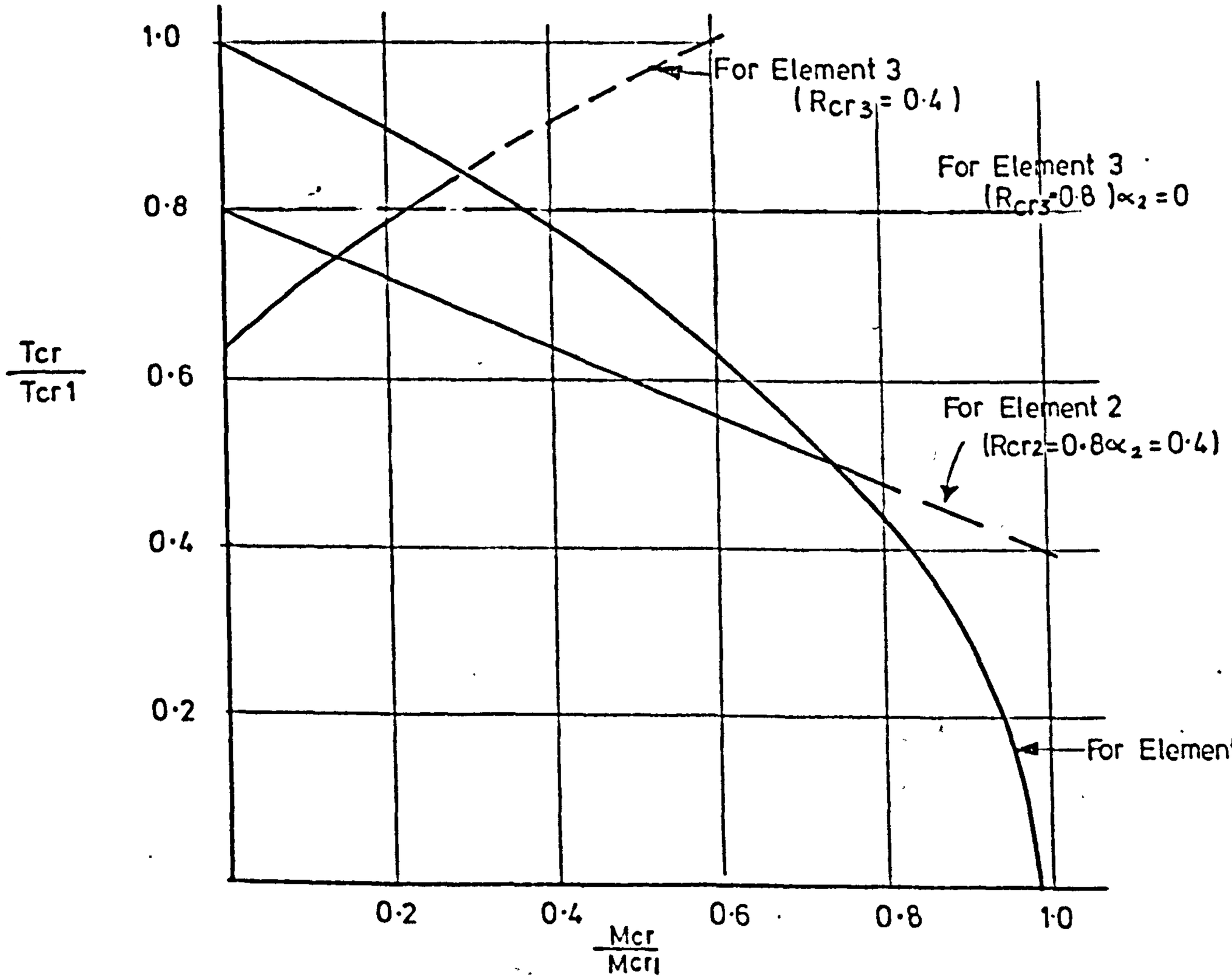

FIG 2.8 Theoretical relationship between modes of cracking.

where

$$T_{crl} = Z_{tl} \; f_{tl} \sqrt{1 + \frac{f_{pl}}{f_{tl}}} \qquad 2.12$$

which is the cracking torque of element 1 under pure torsion and

$$M_{crl} = Z_{l} \; f_{tl} \left(1 + \frac{f_{pl}}{f_{tl}}\right) \qquad 2.13$$

which is the cracking moment of element 1 under pure bending.

If the torque and moment are applied simultaneously according to a predetermined ratio $\psi_{cr} = \frac{M_{cr}}{T_{cr}}$. Then the cracking torque may be found by solving equation 2.11

$$\frac{T_{cr}}{T_{crl}} = \sqrt{1 + \left(\alpha \psi_{cr}\right)^2} - \alpha \psi_{cr} \qquad 2.14$$

where $\alpha = \frac{Z_{tl}}{2Z_{l} \sqrt{1 + \frac{f_{pl}}{f_{tl}}}}$

The angle of this crack from the longitudinal axis of the beam (θ_1) may be found by combining equation 2.8 and 2.14 as follows:

$$\cot \theta_1 = \sqrt{1 + \frac{f_{pl}}{f_{tl}} + \left(\frac{Z_{tl}}{2Z_{l}} \psi_{cr}\right)^2} - \frac{Z_{tl}}{2Z_{l}} \psi_{cr} \qquad 2.15$$

For a rectangular solid section subjected to bending and torsion and where fp = zero, then equation 2.15 may be shown to approximate to the following: expression:

$$\cot \theta_1 \simeq \frac{1}{1 + \psi_{cr}} \qquad 2.16$$

2.3.2 Mode 2

If we consider the vertical and horizontal equilibrium of forces acting on the element 2 shown in Fig. 2.6 we get

$$\tau = f_{t2} \cot \theta_2 \qquad 2.17$$

$$\tau \cot \theta_2 = f_{t2} + f_{p2}$$

combining these two equations and rearranging we obtain:

$$\tau = f_{t2} \sqrt{1 + \frac{f_{p2}}{f_{t2}}} \qquad 2.18$$

Substituting in this equation in terms of the applied torque and shear force:

$$\tau = \frac{T_{cr}}{z_{t2}} + \frac{V_{cr}}{S_2} \qquad 2.19$$

where z_{t2} is the St. Venant torsional modulus for Point 2 and S_2 is the "Shear Area" of the section we obtain

$$\frac{T_{cr}}{T_{cr_2}} = \frac{1}{1 + \frac{z_2}{S_2} \frac{V_{cr}}{T_{cr}}} \qquad 2.20$$

or

$$\frac{T_{cr}}{T_{cr_1}} = \frac{R_{cr2}}{1 + \frac{z_2}{S_2} \frac{V_{cr}}{Tcr}} \qquad 2.21$$

where

$$\frac{T_{cr2}}{T_{cr1}} = R_{cr2} = \frac{z_{t2}\, f_{t2}}{z_{t1}\, f_{t1}} \sqrt{\frac{1 + \frac{f_{p2}}{f_{t2}}}{1 + \frac{fp1}{f_{t1}}}}$$

and for the case of a beam subjected to a single point load Vcr can be written:

$$V_{cr} = \frac{M_{cr}}{a}$$ where a is the shear span hence

equation 2.21 may be written as follows:

$$\frac{T_{cr}}{T_{cr1}} = R_{cr2} - \alpha_{cr} \frac{M_{cr}}{M_{cr1}} \qquad 2.22$$

where $$\alpha_{cr} = \frac{z_{t2}}{s_2} \frac{1}{a} \frac{M_{cr2}}{T_{cr2}}$$

The crack angle θ_2 may be found from equation 2.17 and 2.18 as follows:

$$\cot \theta_2 = \sqrt{1 + \frac{f_{p2}}{f_{t2}}} \qquad 2.23$$

2.3.3 Mode 3

The torque causing cracking at element 3 in fig. 2.6 may be found by considering the change in direction of the bending stresses from that of mode 1. This will lead to the following general non interaction equation

$$\left(\frac{T_{cr}}{T_{cr3}}\right)^2 - \frac{M_{cr}}{M_{cr3}} = 1 \qquad 2.24$$

and for a doubly symmetrical section we have

$$\frac{M_{cr3}}{M_{cr1}} = \frac{1 + \frac{f_{p3}}{f_{t3}}}{1 + \frac{f_{p1}}{f_{t1}}} = R_{cr3}$$

and

$$\frac{T_{cr3}}{T_{cr1}} = \sqrt{\frac{1 + \frac{f_{p3}}{f_{t3}}}{1 + \frac{f_{p1}}{f_{t1}}}}$$

Hence, equation 2.24 may be written as follows

$$\left(\frac{T_{cr}}{T_{crl}}\right)^2 - \frac{M_{cr}}{M_{crl}} = R_{cr_3} \qquad 2.25$$

This equation may be solved for the cracking torque as follows:

$$\frac{T_{cr}}{T_{crl}} = \sqrt{R_{cr_3} + \left(\alpha \psi_{cr}\right)^2} + \alpha \psi_{cr} \qquad 2.26$$

and

$$\cot \theta_3 = \sqrt{1 + \frac{f_{p3}}{f_{t3}} + \left(\frac{z_{t3}\, \psi_{cr}}{2z_3}\right)^2} + \frac{z_{t3}\, \psi_{cr}}{2z_3} \qquad 2.27$$

The relationships between these modes of cracking are shown in Fig. 2.8 on which it can be seen that the shape of the interaction diagram will depend on the values of Rcr and that for reinforced and prestressed concrete beams which are uniformly stressed, $R_{cr_3} = 1$. This means that mode 3 cracking will not occur for these beams. Mode 3 cracking would only occur in an eccentrically prestressed beam and only when the prestress at the top of the beam is low.

The effect of shear is seen to extend mode 2 cracking over a wider range of the load combinations.

2.4 Application of Proposed Method to Rectangular Concrete Beams

2.4.1 Box Beam

For thin-walled box beams, the cracking

resistance may be simply obtained by substituting the appropriate section properties in equations 2.14, 2.22 and 2.26. The St. Venant modulus may be obtained from the Bret-Batho expression given in equation 2.4. The tensile strength for the concrete may be taken as the uniaxial tensile strength given in expression 2.6 for all these three critical points.

2.4.2 Rectangular Solid Section Beam

The prediction of cracking strength for these members has given rise to many controversies and disagreements between research workers in this field. As mentioned earlier, the correct assessment of cracking strength depends on the method of calculating the sectional properties and the selection of the appropriate tensile strength of concrete. Among the required sectional properties the calculation of the St. Venant modulus is very difficult to obtain without the aid of a computer. However, for rectangular sections the St. Venant modulus may be written as:

$$Z_t = k\, b^2\, h$$

where k is coefficient which depends on the $\frac{b}{h}$ ratio and the position of the point under consideration.

Many simplified expressions have been suggested for evaluation of k for a point located on the middle of the wider face of the rectangular beam. For example Bach (1) suggested the following expression:

$$k_2 = \frac{1}{3 + \dfrac{2.6}{\dfrac{h}{b} + 0.45}}$$

This expression is found to give a good correlation with the exact solution. No such simplified expressions are available however in literature for other points of the section so the following expression is suggested for the determination of a point located at the middle of the shorter side of a rectangular beam:

$$k_1 = \frac{1}{2.24 + \dfrac{1.65}{\dfrac{h}{b} - 0.35}}$$

This expression can be shown to give good correlation with exact values.

The second required parameter for the calculation of cracking strength is the correct assessment value of the tensile strength of concrete. For a point located on the middle of the beam, the tensile strength may be obtained from equations 2.5, 2.6 and 2.7 as follows:

$$f_{t2} = 0.36 \sqrt{f_{cu}} \left[1 + \frac{55}{b}\right] \left[1 + \frac{1}{4}\frac{b}{h}\right] \qquad 2.28$$

Similarly the tensile strength for a point located at the middle of the shorter face of the rectangular beams will depend on the strain gradients across the section due to bending and torsion. In the case when the section is subjected to bending only, the tensile strength may be taken as the modulus of rupture as given by expression 2.5 and 2.6. On

the other hand when the beam is subjected to a pure torque, the strain gradient will be equivalent to the case of that of a square beam cross section and the tensile strength may be found from expression 2.28 by putting $\frac{b}{h}$ = unity. When the section is under combined torsion and bending the tensile strength is expected to lie between these limits and is a function of the $\frac{M}{T}$ ratio. Hence the following expression is suggested:

$$f_{tl} = 0.36 \sqrt{f_{cu}} \left[1 + \frac{55}{h}\right] \left[1 + \frac{0.25}{1 + \frac{\Psi}{10}}\right] \qquad 2.29$$

2.5 Correlation of Proposed Method With Test Results

The cracking strength equations developed in this chapter are compared with published data listed in Tables 2.2 to 2.5 and shown in Fig. 2.9 to Fig. 2.12.

2.5.1 Plain Concrete Beams Subjected to Pure Torque

Table 2.2 compares the theoretical and experimental results of 70 rectangular plain concrete beams having different aspect ratios, sizes and concrete strength subjected to pure torque. The mean value of T_{cr} (exp)/T_{cr} (th) is 1.08 with a coefficient of variation of 14.62 percent. The accuracy of prediction obtained from this theory may be compared with values obtained from other theories. For example Martin found the ratio T (exp)/T (th) = 1.04 with a coefficient of variation of 21 percent for these test results. Hence the proposed method gives a better coefficient of variation than the Skew bending theory. The reason for the shift in the ratio of T (exp)/T (th) from unity can be attributed to the safe predictions of the

TABLE 2.2 Correlation of Theory to Experimental Results For Rectangular Plain Concrete Beams Subjected to Pure Torsion

Investigator	Ref	Number of Beams	Mean $\frac{T_{cr\ (exp)}}{Tcr\ (th)}$	Coefficient of Variation %
Humphreys	4	20	1.08	3.71
Zia	5	9	0.85	7.4
Evans & Khalil	6	2	0.93	-
Collins et al	7	8	1.23	20
Marshall & Tembe	9	12	1 13	11.9
Hsu	12	10	1.13	9.53
Iyenar & Rangan	26	3	1.04	4.34
Navaratnarajah	27	6	1.17	4.23
Total		70	1.08	14.62

tensile strength as obtained from equation 2.6 and illustrated in Fig. 2.6.

2.5.2 Reinforced Concrete Beams Without Web Reinforcement Subjected to Pure Torque

Table 2.3 compares the theoretical and experimental results of 49 rectangular beams with longitudinal reinforcement only subjected to pure torsion. The mean value of $T_{cr}(exp)/T_{cr}$ (th) is 1.12 with a coefficient of variation of 7.6 percent. These results indicate that the presence of longitudinal reinforcement has little effect on the cracking resistance of the beam. The cracking strength of these beams also correspond to their ultimate strength.

Fig. 2.9 shows that the ratio of the experimental cracking torque to the predicted values is independent of the aspect ratio of the beam cross section. This is unlike the ratios of T_{cr} (exp)/T_{cr} (th) obtained from all other theories which can be shown to be influenced by the aspect ratio of the beam.

2.5.3 Reinforced Concrete Beams With Web Reinforcement Subjected to Pure Torque

Table 2.3 also gives a comparison between the theoretical and experimental results for 61 reinforced concrete beams containing varying amounts of reinforcement and having different concrete strengths, aspect ratios and sizes. The mean value of T_{cr} (exp)/T_{cr} (th) is 1.2 and the coefficient of variations is 10.08 percent. These results indicate that the web reinforcement increases the cracking torque by an average value of 12 percent. This increase in cracking resistance due to the

TABLE 2.3 Correlation of Theory to Experimental Results For Rectangular Reinforced Concrete Beams Subjected to Pure Torsion

Investigator	Ref	Number of Beams	Mean $\frac{T_{cr\ (exp)}}{T_{cr\ (th)}}$	Coefficient of Variation %	Details of Beams
Humphreys	4	17	1.11	5.1	Without Web reinf.
Marshall and Tembe	9	6	1.14	4.8	" "
Iyengar and Rangan	26	24	1.14	5.7	" "
Goode and Helmey	27	2	0.96	-	" "
Total		49	1.12	7.26	
Hsu	16	49	1.23	8.6	With Web reinf.
Okada	29	12	1.06	9.33	" "
Total		61	1.2	10.08	
Mitchell et al	30	9	0.75	8.9	Box Beams With Web reinf.
Lampert and Thurlimann	31	3	0.89	6.34	
Total		12	0.78	11.05	

presence of reinforcement has been reported by Hsu (16) who found that the cracking resistance increased with increase in the volume of reinforcement in the beam.

Table 2.3 also contains the results of 12 reinforced concrete box beams. The mean value of T_{cr} (exp)/T_{cr} (th) is 0.78 and the coefficient of variation is 11.05 percent. It is interesting to note that the cracking strength of these beams were consistantly lower than the predicted values. This may be due to the additional stresses occuring as a result of shrinkage restraint developing as a result of the method of fabrication which was adopted for these specimens. The wall-thickness of these boxes may well have been smaller in certain parts of the beams than the design wall-thickness of these specimens. However, these results deserve further investigation to find the actual reason for this reduction in the cracking strength.

2.5.4 Prestressed Concrete Beams Without Web Reinforcement Subjected to Pure Torsion - Torsion and Bending.

Table 2.4 compares theoretical and experimental results for 101 available tests. The mean ratio of T_{cr} (exp)/T_{cr} (th) = 1.07 with coefficient of variation 12.06 percent.

The ratio of T_{cr} (exp)/T_{cr} (th) for the beams subjected to pure torsion has been plotted in Fig. 2.10 against the ratio of fp/f_{cu}. It can be seen that the increase in the compressive principal stresses as a result of increase in prestress has no effect on the $\frac{T_{cr\ exp}}{T_{cr\ th}}$ ratio up to a limiting value of $fp/f_{cu} = 0.7$, therefore, the assumption made regarding the use of maximum stress failure

criterion is fully justified and since for all practical prestressed concrete beams, fp/f_{cu} is unlikely to exceed 0.5, the use of this comparatively simple failure criterion will lead to a simple method for predicting cracking strength. For a ratio fp/f_{cu} exceeding 0.7 the maximum stress criterion is seen to overestimate the cracking resistance of prestressed concrete beams. For this reason an upper limit on this ratio of 0.7 is suggested.

Mode 2 cracking for prestressed concrete beams always leads to immediate failure.

The ratio of T_{cr} (exp)/T_{cr} (th) is plotted in Fig. 2.11 against moment/torque for beams subjected to bending and torsion for all cracking modes. It is seen that the ratio M/T has no significant influence on the correlations between the theoretical predictions and the experimental cracking torque.

For beams cracking according to mode 1, cracking usually did not precipitate failure and they continued to sustain a further increase in torque as a result of redistribution of stresses in the beams. Beams cracking in mode 3 continued to take further increase in torque up to the occurrence of mode 2 cracking.

Using the skew bending concept, Wainwright found that for the beams given in Table 2.4 which cracked according to mode 2, the ratio T (exp)/T (th) = 1.01 and the coefficient of variation was 14 percent. Therefore, the proposed approach has a narrower band width for the scatter in the T_{cr} (exp)/T_{cr} (th) values than other theories, hence confirming the soundness of this approach. The reason for the

TABLE 2.4 Correlation of Theory to Experimental Results For Rectangular Prestressed Concrete Beams - Without Web Reinforcement - Subjected to Pure Torsion, Bending and Torsion.

Investigator	Ref	Mode of Cracking	Number of Beams	Mean $\frac{T_{cr\ (exp)}}{T_{cr\ (th)}}$	Coefficient of Variation %
Humphreys	4	2	56	1.05	10.51
		3	4	1.30	8.70
Zia	5	2	3	0.79	2.8
		3	6	1.2	8.59
Evans and Khalil	6	1	18	1.1	8.75
		2	2	1.06	
		3	1	1.29	
Okada	29	1	4	1.1	11.85
		2	4	0.96	8.10
Nylander	32	2	3	1.19	4.10
Total		1	22	1.09	9.34
		2	68	1.03	11.75
		3	11	1.26	8.60
		1,2& 3	101	1.07	13.06

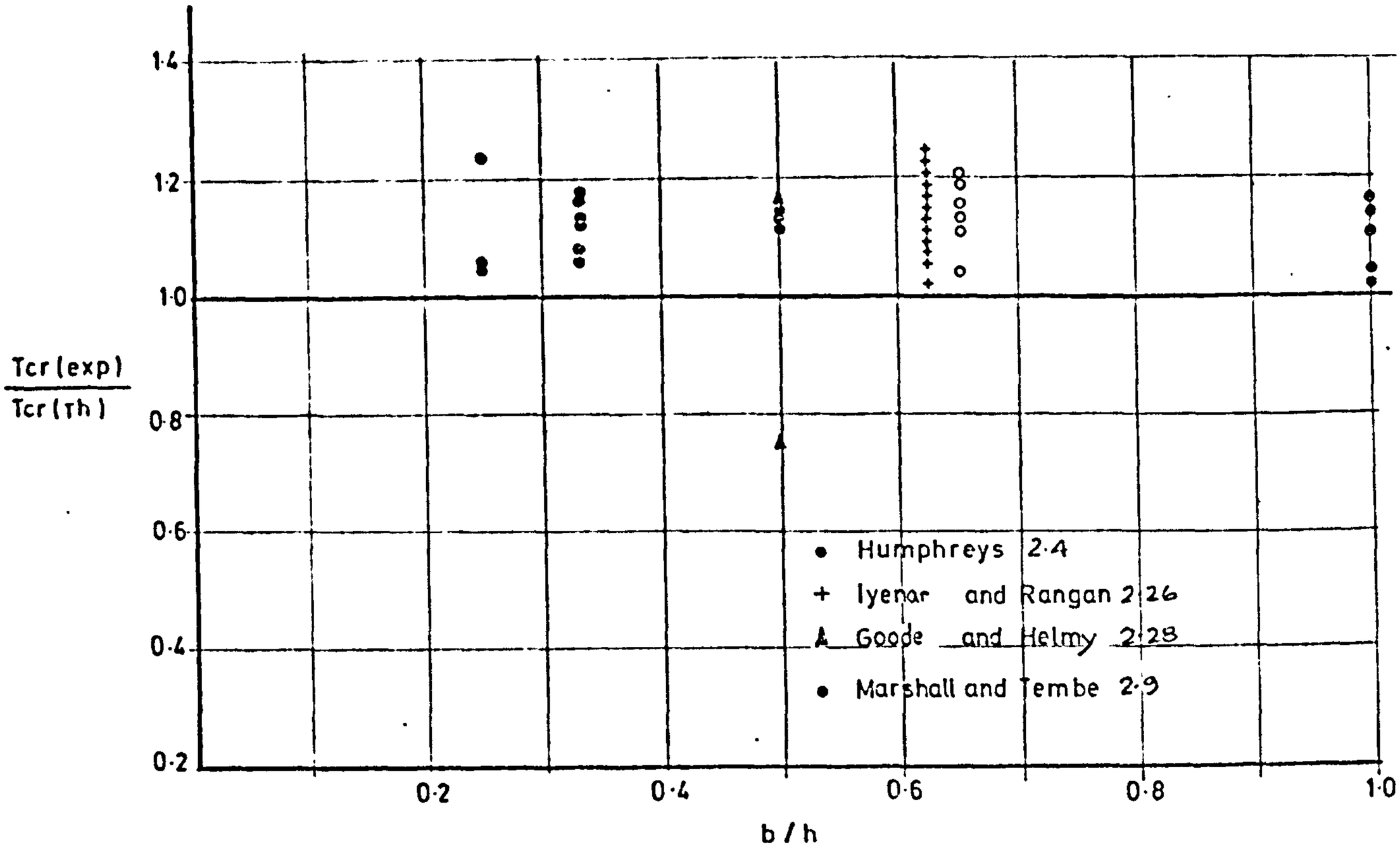

FIG 2·9 COMPARISON OF THE THEORETICAL PREDICTIONS WITH TEST RESULTS FOR REINFORCED CONCRETE RECTANGULAR BEAMS WITHOUT WEB REINFORCEMENT. (PURE TORQUE)

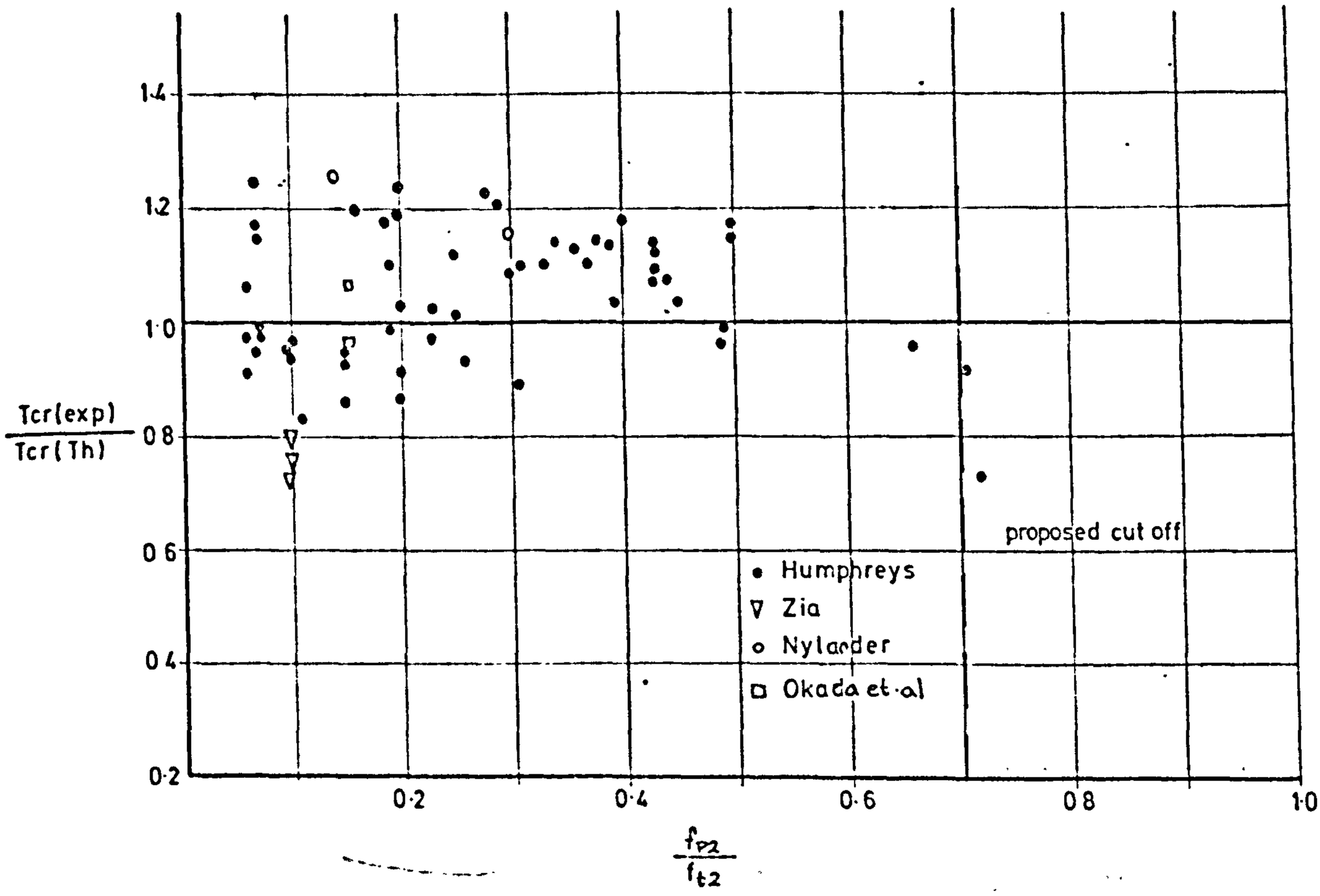

FIG 2·10 COMPERISON OF THE THEORETICAL PREDICTIONS WITH TEST RESULTS FOR UNIFORMLY - PRESTRESSED CONCRETE RECTANGULAR BEAMS WITHOUT WEB REINFORCEMENT (PURE TORQUE)

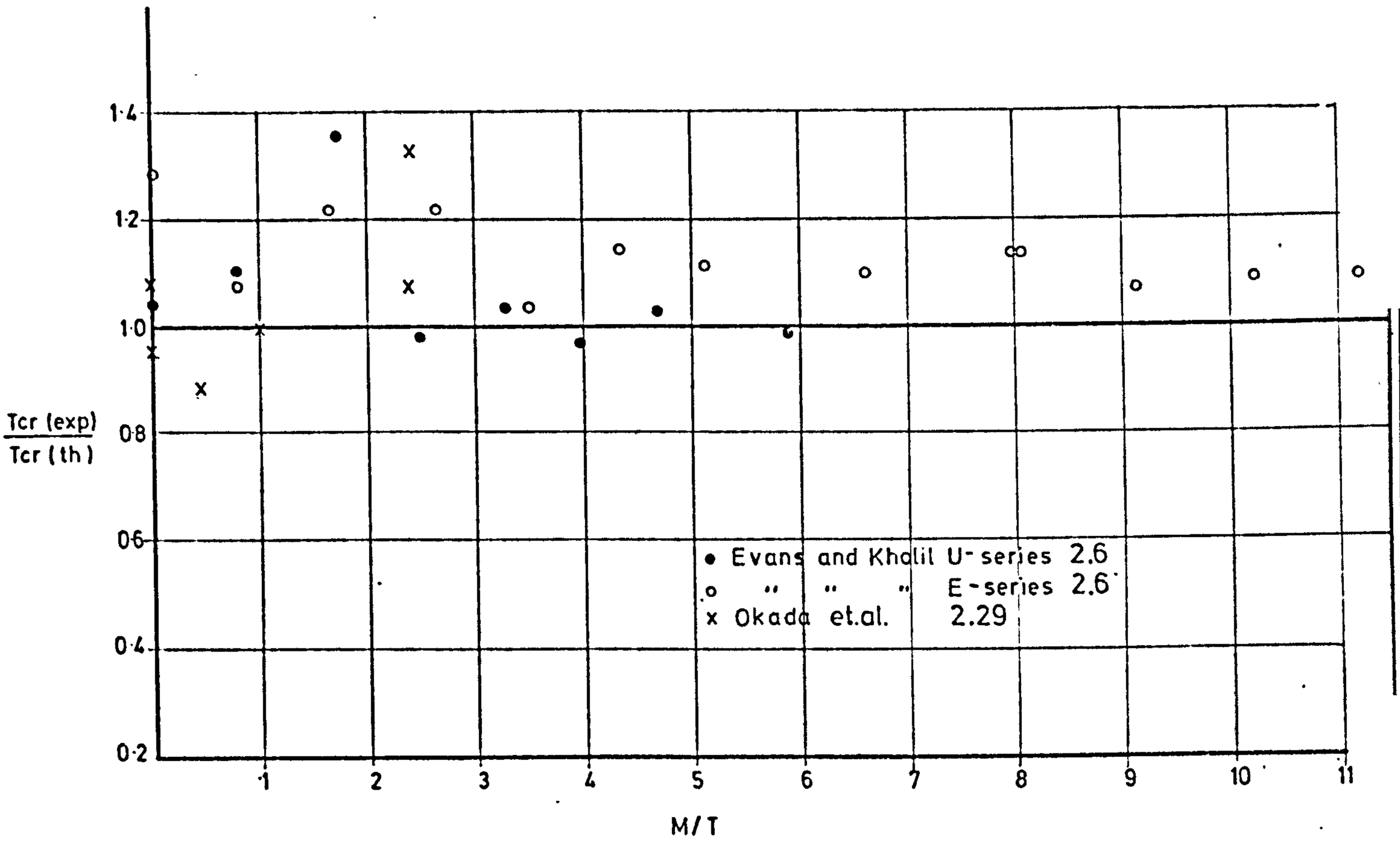

FIG. 2·11 Tcr(exp)/Tcr(th) – M/T FOR PRESTRESSED CONCRETE BEAMS WITHOUT WEB REINFORCE MENT - SUBJECTED TO BENDING AND TORSION.

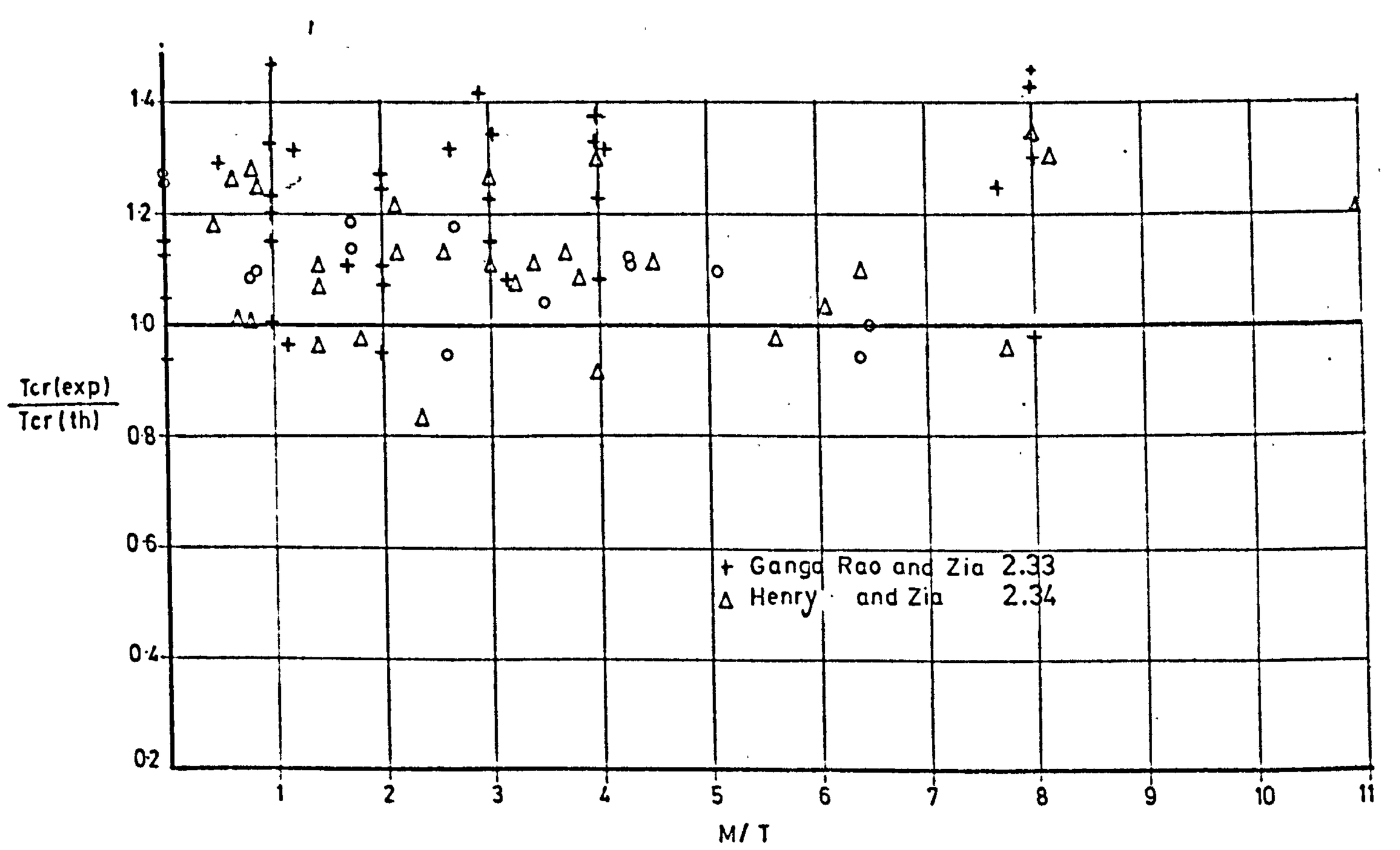

FIG 2·12 Tcr(exp)/Tcr(th)– M/T FOR PRESTRESSED CONCRETE BEAMS WITH WEB REINFORCEMENT - SUBJECTED TO BENDING, TORSION AND SHEAR

TABLE 2.5 Correlation of Theory to Experimental Results For Rectangular Prestressed Concrete Beams with Web reinforcement Subjected to Bending, Torsion and Shear

Investigator	Ref	Mode of Cracking	Number of Beams	Mean $\frac{T_{cr\ (exp)}}{T_{cr\ (th)}}$	Coefficient of Variation	Loading
Evans and Khalil	6	1	10	1.08	8.0	
		2	2	1.10	-	B & T
		3	2	1.26	-	
Okada	29	1	4	1.32	13.80	B & T
		2	4	1.15	2.60	
Ranga Rao and Zia	33	1	30	1.24	12.23	B & T
		2	10	1.12	10.40	
Henry and Zia	34	1	24	1.11	13.13	B, T & Shear
		2	7	1.17	10.40	
Total		1	68	1.18	14.03	
		2	24	1.14	9.5	
		1,2 & 3	94	1.17	13.06	

high value of T_{cr} (exp)/T_{cr} (th) has already been explained.

2.5.5 Prestressed Concrete Beams With Web Reinforcement - Subjected to Bending and Torsion, and Bending, Torsion and Shear.

Table 2.5 contains the results of 94 rectangular prestressed concrete beams with web reinforcement and subjected to bending and torsion. The details of the beams reported by Henry and Zia are similar in detail to the beams tested by Ranga Rao and Zia, but subjected to bending, torsion and shear. The mean ratio of T_{cr} (exp)/T_{cr} (th) = 1.17 and the coefficient of variation is 13.06 percent for all the experimental results. The ratio of T_{cr} (exp)/ T_{cr} (th) has been plotted against the M/T ratio. These results appear to reflect the same picture as in the case of beams without reinforcement with the exception that beams with web reinforcement appear to have higher cracking strengths than beams without web reinforcement.

Henry and Zia describe the mode of cracking of their beams. It can be shown that the proposed theory predicts these cracking modes satisfactorily.

2.6 Conclusions

From this study of the cracking strength of reinforced and prestressed concrete beams which are subjected to bending, torsion and shear, the following conclusions are drawn:

1. Elastic theories accurately predict the stress distribution in the beam up to cracking.

2. The maximum stress failure criterion gives a simple and accurate prediction of the cracking strength.

3. Cracking strength for concrete and pre-stressed beams under combined bending, torsion and shear can be accurately predicted with the use of elastic stress field, maximum stress failure criterion and a modified tensile strength.

4. Of the various methods of specifying the tensile strength of concrete, the modulus of rupture was found to be the most appropriate for predictions of cracking of rectangular solid sections.

5. The modifications for modulus of rupture proposed in this study are based on the influence of the strain gradient on the tensile strength which has been found to be a function of the height, $\frac{b}{h}$ and $\frac{M}{T}$ ratios.

6. Computation of the cracking resistance based on an assumed plane of fracture (Hsu and Martin theory) has been shown to give an upper bound solution to the problem. In contrast the proposed method of calculating the cracking resistance based on assumed elastic stress field would produce a good lower bound solution.

7. The cracking torque may be increased substantially by prestressing. This increase in torsional resistance has an upper value at $\frac{fp}{f_t} = 0.7$.

8. For reinforced and plain concrete beams, cracking according to mode 2 leads to immediate failure.

9. The presence of longitudinal reinforcement has little effect on cracking resistance.

10. The addition of web reinforcement may increase the crack resistance by 12 percent.

11. The proposed method has been compared with the results of 387 tests reported in literature. In general the agreement is good.

CHAPTER 3

ULTIMATE STRENGTH OF REINFORCED AND PRESTRESSED CONCRETE BEAMS WITH TRANSVERSE REINFORCEMENT SUBJECTED TO PURE TORSION.

Summary

Theoretical studies of the behaviour and strength of reinforced and prestressed concrete beams having web reinforcement and subjected to pure torsion are presented in this chapter.

The effect of

a) spacing of stirrups,
b) dowel forces,
c) resistance of concrete and
d) aggregate interlock

have been examined.

Rational theories for predicting various modes of failure have been developed and these have been compared with test results of about two hundred reinforced and prestressed concrete beams published in technical literature.

3.1 Introduction

Since the pioneering work of Marsch (3.1) in 1904 it has been known that the addition of transverse reinforcement to a reinforced or prestressed concrete beam subjected to pure torsion improves their behaviour and can increase their strength beyond cracking.

In 1929 Rausch (3.2) suggested the space truss analogy as a way of calculating the ultimate strength of beams under pure torque.

The research study on the behaviour of concrete beams subjected to pure torsion has been sporadic during the first half of this century and it is only in the last decade that research activities on this subject have been intensified.

In 1970, Zia (3.3) published a short "state of the art" review examining all important published data on the subject. In this paper, Zia stated that no generally accepted theory has yet been developed for the prediction of the ultimate torque carrying capacity of reinforced concrete beams (let alone prestressed concrete beams); although many approaches have been suggested in the published literature. This maybe attributed to the large number of factors that are known to affect the ultimate torque capacity, leading to a variety of modes of failure. In 1966 Hsu (3.5) identified the following modes of failure:

1. Under-reinforced failure (U.R)

   This mode of failure is said to occur when both the longitudinal and transverse reinforcement reach their full axial yield

strength at failure.

2. Partially over-reinforced failure (POR)
When only the longitudinal or the transverse reinforcement reaches its full axial yield strength at failure. This mode of failure will be designated in the following as POR.

3. Over-reinforced failure (OR)
When both the longitudinal and transverse reinforcement do not reach their full axial yield strength at failure. This mode of failure will be designated as OR.

4. Inadequate reinforcement failure
In this mode, failure occurs immediately after cracking due to an inadequate volume of reinforcement.

The object of this chapter is to examine in detail these modes of failure and the existing methods that are used for calculating the ultimate torque carrying capacity of reinforced and prestressed concrete beams, to study the importance or otherwise of some phenomena that have been observed in tests which could not be explained by existing theories, and finally to develop rational theories for these modes of failures.

3.2 Under-reinforced Failure

All existing experimental evidence on this subject suggests that this mode of failure is usually gradual and the member exhibits considerable ductility and is therefore desirable in practical situations. Many methods for calculating the ultimate torque of reinforced concrete beams for this mode of failure can be found in literature and these maybe classified into three main categories as follows:

1. Empirical approaches
2. Semi-rational methods
3. Yield or equilibrium theories.

This classification may indicate the range of the opinions which exist among investigators on how torque is resisted by reinforced concrete beams after cracking has occurred. This disagreement between the theories and the inability of any of them to predict satisfactorily the ultimate torque carrying capacity for beams within a practical range of variable maybe attributed to either wrong assumptions, erroneous interpretation of test results or lack of experimental evidence. The following discussion traces the broad development of these methods and examines the validity and limitations of the various assumptions which have been made in their development.

3.2.1 Empirical Approaches

Among the pioneers who conducted experimental investigation on this subject are Turner and Davis (3.8), Marshall and Tembe (3.9) who provided valuable research data on this subject. In recent years extensive tests programmes have been carried out by Hsu (3.5) at the Portland Cement Association

in America. Further experimental data has been published by Rangan (3.10) and Pandit (3.11). All these investigators have suggested an empirical expression for predicting the ultimate torsional strength for reinforced concrete beams which take the following form:

$$T_u = \alpha_1 T_{cr} + \alpha_2 T_s \qquad 3.1$$

where T_u is the ultimate torque

$\alpha_1 T_{cr}$ represent the torque resisted by concrete which was taken as the cracking torque (except in Hsu's method)

$\alpha_2 T_s$ is the torque resisted by the web reinforcement and α_1 and α_2 are factors which were determined empirically.

A summary of all the methods used for calculating the ultimate torque for reinforced and pre-stressed concrete beams are given in Table 3.1. It must be pointed out that although these expressions were intended for beams failing in this mode only, the experimental techniques used to ascertain the occurrence of this mode were either suspect or did not exist. For example readings from E.R.S gauges attached to one side of the reinforcement do not necessarily indicate that the reinforcement reached its full axial yield strength.

TABLE 3.1 Summary of Ultimate Strength Theories for Reinforced and Prestressed Concrete Beam with Web Reinforcement Subjected to Pure Torque

Investigator	Ref	Year	Contribution of Concrete	Contribution of reinforcement	Application
Rausch	3.2	1929	0	T_s	R.C.
Anderson	3.12	1937	T_{cr}	0.67 T_s	R.C
Cowan	3.13	1953	T_{cr}	0.8 T_s	R.C.
Lessig	3.14	1958	0	$\simeq T_s \sqrt{m'}$	R.C.
Hsu	3.5	1966	$2.4 \frac{b^2h}{\sqrt{b}} \sqrt{f'_c}$ *	$(0.66m + 0.33 \frac{Y_1}{X_1}) \frac{T_s}{2}$	R.C.
Mattock	3.16	1966	$\frac{2.4 \sqrt{f'_c}}{2} (1 - \frac{1}{3} \frac{b}{h})$ *	$(0.66m + 0.33 \frac{Y_1}{X_1}) \frac{T_s}{2}$	R.C.
Hsu and Mattock	3.7	1969	$\frac{2}{3}.4\ b^2h \sqrt{f'_c}$ *	$(0.66 + 0.33 \frac{Y_1}{X_1}) \frac{T_s}{2}$	R.C.
Pandit	3.11	1970	$2\ b^2h \sqrt{f'_c}$ *	$(1 - \frac{Sv}{h}) (2 \frac{P'1}{Pv} \frac{f_{yl}}{f_{ys}}) T_s \sqrt{m'}$	R.C.
Lampert	3.17	1971	0	0.8 T_s	R.C.
Swann	3.23		0	0.5 T_s	R.C.
Iyengar and Rangan	3.10		T_{cr}	$(1-k)\left[0.2m - \sqrt{m} (0.45 \frac{Y_1}{X_1} - \frac{Sv}{X_1+Y_1})\right]$	R.C.
Victor and Mathakrishnan	3.25		$\frac{5}{3} b^2h \sqrt{f'_c}$ *	0.8 T_s	P.S.C.
Zia	3.4		T_{cr} (E)	$(0.33m + 0.16 \frac{Y_1}{X_1}) \frac{T_s}{2}$	P.S.C.
Gausel	3.26		T_{cr} (P)	0.8 T_s	P.S C.
Bishara	3.27		T_{cr} (P)	$(0.66 + 0.33 \frac{Y_1}{X_1}) \frac{T_s}{2}$	P.S.C.
Hsu and Mattock	3.7		$\frac{2.4}{3} b^2h \sqrt{f'_c} \left[2.5 \sqrt{1 + 10 \frac{fp}{f_c}} - 1.5\right]$ *		P.S.C.

$T_s = 2 \frac{Asv\ fyv}{Sv} X_1 Y_1$

T_{cr} = Torque causing cracking

R.C. = Reinforced Concrete Beam

P.S.C. = Prestressed Concrete Beam

* For Imperial Units

E=Cracking torque based on elastic stress distribution

P=Cracking torque based on plastic stress distribution

P'_l = Percentage of the top or bottom reinforcement whichever is the lower.

P'_v = Percentage of stirrup reinforcement.

3.2.2 Semi-Rational Methods:

The methods suggested by Anderson (3.12), Cowan (3.13) and Hsu (3.5) can be classified under this heading. These methods require an equal volume of longitudinal and transverse reinforcement and consider the torsional resistance of a reinforced concrete member as the sum of the resistance of the concrete member and the contribution of the reinforcement. These theories can be expressed for rectangular sections as follows:

$$T_u = T_c + \alpha\left(2\,\frac{A_{sv}\,f_{yv}}{S_v}\,X_1\,Y_1\right) \qquad 3.2$$

where

T_c = the torque resisted by the concrete alone.

A_{sv} = the cross sectional area of one leg of the stirrups.

f_{yv} = the yield stress for the stirrups

Sv = the pitch of the stirrups

X_1 and Y_1 = the smaller and larger centre-line dimension of the closed stirrups

α = efficiency factor for the reinforcement.

Anderson and Cowan further assumed that the shear stress distribution after cracking varies according to the St. Venant theory of the uncracked section, therefore, the tensile stresses in the reinforcement were assumed to vary along each face of the rectangular sections, with a maximum stress occuring at the centre of the wider face and zero at the corners of the section, hence, obtaining an efficiency factor α for the contribution of the reinforcement. Anderson gave this factor as a function of the volume of the reinforcement and the height to width ratio of

the cross section whereas, Cowan found that this factor is a function of the height to width ratio only. For practical applications Anderson suggested that α be taken as 0.67, whereas, Cowan suggested α should be 0.8.

The validity of these theories has been contested by Marshall and Tombe (3.9) on the basis that these theories overestimated their test results. Swann (3.24) pointed out that the inclusion of the concrete contribution in these methods was introduced arbitrarily and did not appear in their mathematical analysis. Hsu (3.6) listed the following test observations that were in disagreement with the basic assumptions of these theories.

i) At cracking, a reinforced concrete beam continues to twist under a constant torque until the reinforcement is brought into action. This indicates a transition from the St. Venant equilibrium condition to a new one.

ii) After cracking, the stresses in the reinforcement do not follow the St. Venant stress distribution. For example, the strain in the stirrups yield both at the centre and at the cornersas the ultimate torque is approached. This indicates that there is a considerable stress redistribution after cracking.

iii) After cracking the distribution of principal compressive strains in the concrete do not follow the St. Venant theory and maybe

several times greater than those predicted by the St. Venant theory.

iv) Solid and hollow beams having indentical reinforcement are found to have an identical ultimate torsional strength. Therefore, the concrete core of a reinforced concrete beam failing in this mode does not contribute to the resistance of the beam which is contrary to the assumptions made in the above theories.

This evidence therefore, suggests without any doubt that the assumptions made in these theories are incorrect.

In 1968 Hsu (3.6) obtained an expression for ultimate torque by assuming that failure would occur as a result of bending about skew axes as shown in Fig. 3.1. The ultimate torque was obtained from the equilibrium of forces acting on this skew plane which was taken at 45^{o} to the longitudinal axis of the beam. In this theory Hsu assumed that the forces in the shorter side of the stirrups are negligible and may be ignored but that the contribution of the dowel action of longitudinal reinforcement was to be considered. Swann (3.24) argued that this theory does not correctly satisfy equilibrium. This theory appears to have been developed so that the final solution corresponds to an empirical expression which had been previously obtained by the same author. As mentioned earlier, the method used for identifying under-reinforced failure in this investigation is open to question and the empirical expression could well cover the partially over-

reinforced mode of failure. It can also be shown that the magnitude of the dowel forces which were assumed in this method cannot develop, therefore, the validity of the assumptions made in this theory are suspect.

3.2.3 Yield or Equilibrium Theories

These theories are the most rational of all the methods that have been developed up to now. Many seemingly different yield theories have been published under different names but in general they are all based on the following assumptions:

a. All the reinforcement reaches full axial tensile yield strength before failure.

b. Dowel forces of reinforcement are ignored.

c. The aggregate interlock action between cracks is neglected.

d. The tensile strength of concrete is neglected

e. The concrete does not resist any torsion.

f. There is no "kinking" of reinforcement.

g. The beam is prismatic.

h. No warping or longitudinal restraint is allowed for.

i. The internal forces are in equilibrium with the applied torque.

j. No secondary failure will occur due to improper detailing of the reinforcement.

k. The only disputed assumption among the advocates of the yield theory is that of the inclination of the failure surface or the direction of the diagonal compressive field. There are two school of thoughts regarding this assumption:

i) The angle of the failure surface on the direction of the compressive stress field is equal to the angle of cracking which is 45^{o} for reinforced concrete beams.

ii) This angle is a function of the ratio of the volume of the longitudinal to the transverse reinforcement.

Not all of these assumptions were clearly stated by the various authors but the remainder of the assumptions is implicit in their analysis therefore, it is not surprising if these methods produce the same results.

The only variation that exists between the various yield theories is the way in which the equilibrium equations have been manipulated. Two methods have been suggested in the past for the solution of this problem:

1. The space truss analogy
2. The skew bending theory.

1. Space truss analogy

This anology was first suggested in 1929 by Rausch (3.2) who devised a mathematical model which consists of a network of bars to represent the action of a reinforced concrete member resisting pure torque. In this model, the concrete is represented by compression struts and the reinforcement by tension bars. The struts are assumed to be inclined at 45^{o} and from consideration of equilibrium condition, he obtained the following formula for a rectangular section:

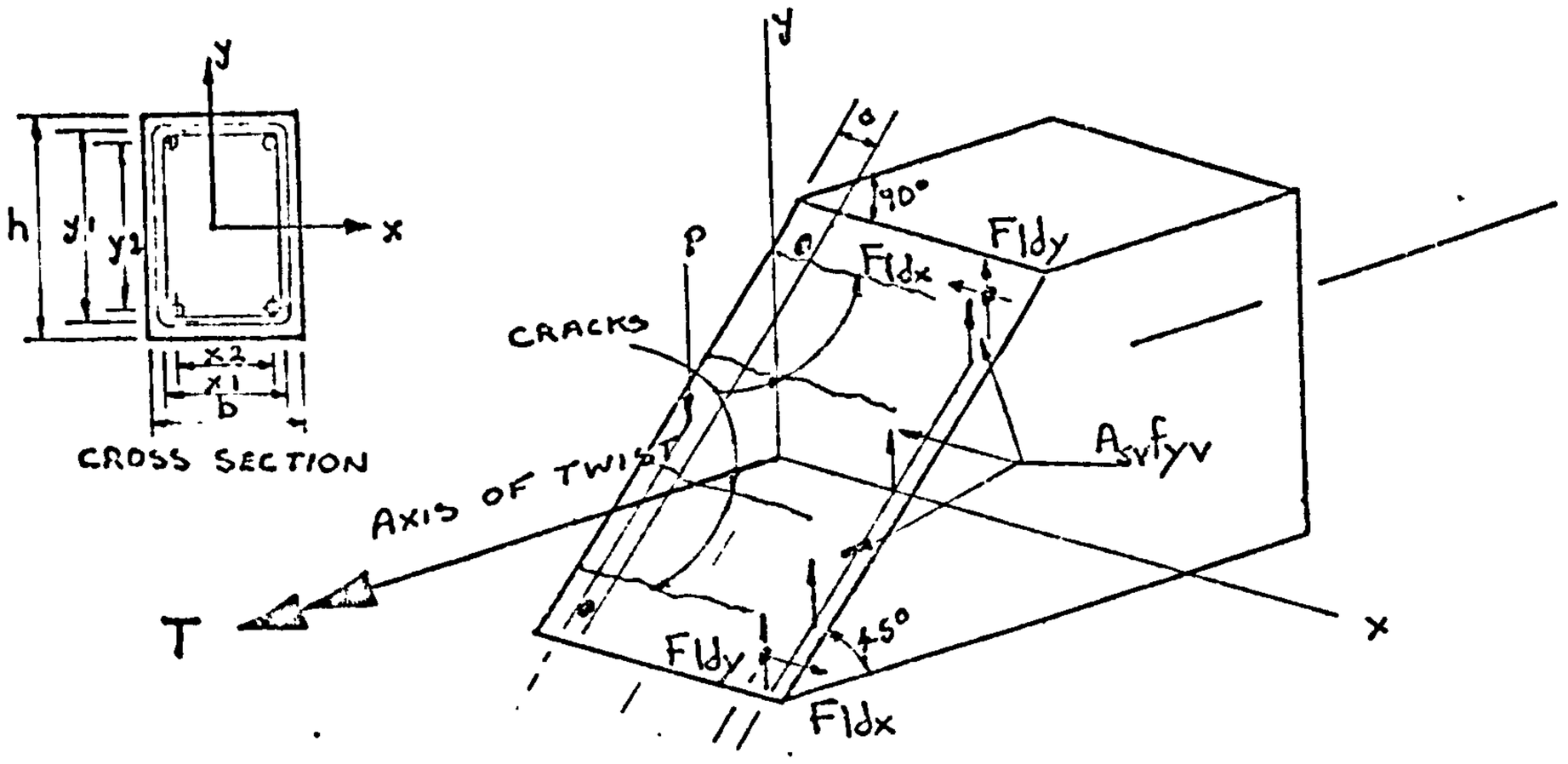

FIG 3·1 FAILURE SURFACE OF FREE BODY ACCORDING TO HSU

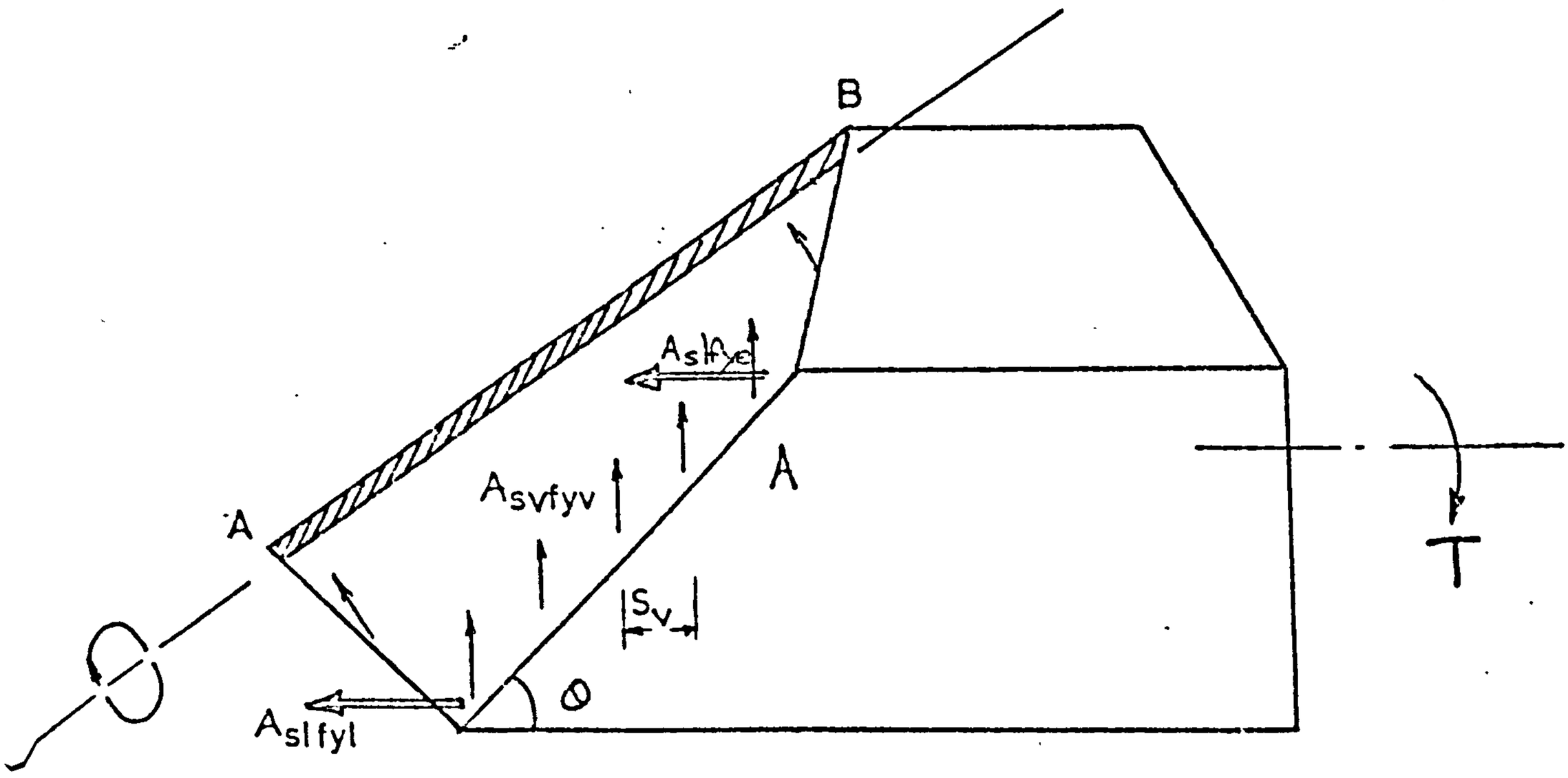

FIG 3·2 FAILURE SURFACE OF FREE BODY ACCORDING TO LESSIG

$$T_y = \frac{2A_{sv}\ f_{yv}}{Sv}\ X_1\ Y_1 \qquad 3.3$$

Despite the ability of this method to explain the behaviour of a reinforced concrete beam containing an equal volume of longitudinal and transverse reinforcement, it was not found to fit test results obtained from beams that contained different ratios of volume of longitudinal to transverse reinforcement.

The concept of the space truss analogy has been generalized quite recently by many European research workers such as Lampert and Thurlimann (3.18) of Switzerland, Kuyt (3.28) of Holland, Inge Karlsson (3.29) and Elfgren of Sweden (3.30). These investigators assumed that the angle of the concrete struts or the diagonal compressive stress field depend on the ratio of the volume of the longitudinal to the transverse reinforcement. They have also extended this theory to beams having any cross sectional shape. From consideration of equilibrium of forces the following expression was obtained:

$$T_y = \frac{2A_{sv}\ f_{yv}}{Sv}\ A_1 \sqrt{\frac{\sum A_{sl}\ f_{yl}}{P}\ \frac{S_v}{A_{sv}\ f_{yv}}} \qquad 3.4$$

where A_1 is the area of the cross-section within the stirrups and for rectangular section = $X_1\ Y_1$

$\sum A_{sl}\ f_{yl}$ is the yield force of the longitudinal reinforcement.

P is the perimeter of the cross-section and for rectangular section = $2\ (X_1 + Y_1)$

It can be shown that equation 3.3 is a particular case of this general equation 3.4.

Lampert and Thurlimann have also applied the limit theorum of plastic collapse and obtained an upper bound solution to the problem by considering the kinematic approach for an assumed mechanism of failure and a lower bound solution by considering the static approach in deriving equation 3.4.

2. The Skew Bending Theory

The present intensive research activities on torsional resistance of reinforced concrete beams started in 1958 following the publication of a new approach to the problem by Lessig (3.14). Lessig chose the failure surface shown in Fig. 3.2 formed by a continuous diagonal crack on three faces of a rectangular beam and a straight line AB on the fourth face. The region close to AB is considered to be in compression and the steel in this region is ignored. Lessig formulated two equilibrium equations for the forces acting on this failure surface: (1) equilibrium of moments about the neutral axis x - x, and the equilibrium of foreces along an axis perpendicular to the compression zone. By minimizing the moment equilibrium equation, she found that the theoretical minimum torsional resistance occurs when the neutral axis x - x is parallel to the wider face of the rectangular section.

In 1962 Yudin (3.31) simplified Lessig's theory by assuming the diagonal crack to be inclined at 45^{o} to the longitudinal axis. From consideration of the equilibrium of forces he obtained an expression identical to equation 3.3.

Lessig's approach has been modified and used during the last decade by Collins et al (3.32) and Kuyt (3.28) who demonstrated that the skew bending approach would yield an identical expression to that given in equation 3.4.

It is worth noting in passing that these two methods of formulation of equilibrium equations correspond to the two wellknown methods of statics used in simple truss analysis. These methods are the method of joint resolution and the method of sections.

3.2.4 Alternative Methods for Determining the Yield Equation

It is evident from the previous review that the yield theory is receiving more recognition by research workers than other methods, hence in order to provide a better understanding to this problem, it will be shown that it is possible to obtain the yield equation by other treatments as follows:

Method A

The torsional resistance of a prismatic rectangular thin-walled box beam will be considered in this method. The beam is reinforced with close stirrups equally spaced with four equal longitudinal bars each located in one corner of the beam as shown in Fig. 3.3.

When the applied torque exceeds the cracking torque, diagonal cracks will appear at an angle to the longitudinal axis. These cracks will spiral around all four sides from one end of the beam to the other.

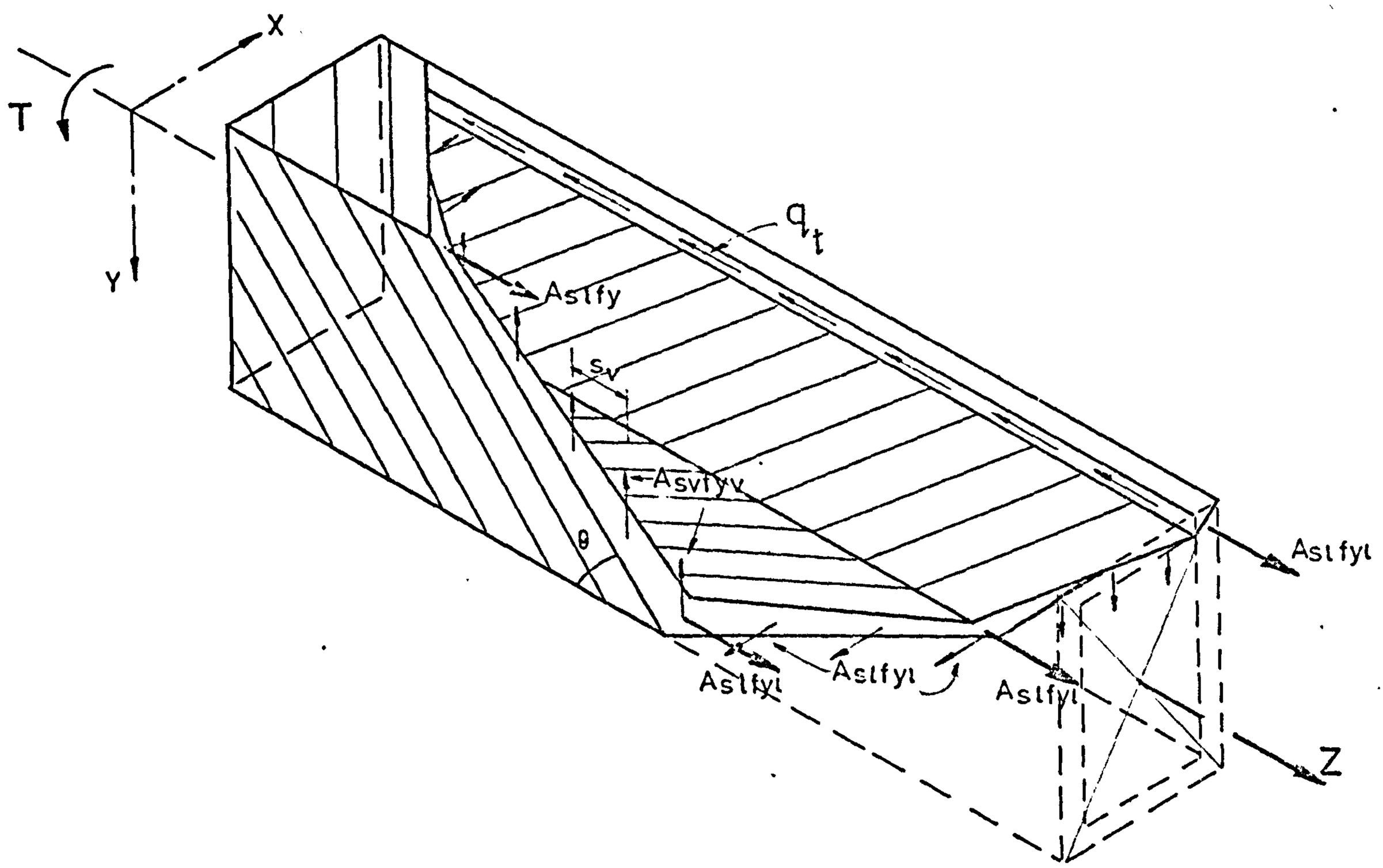

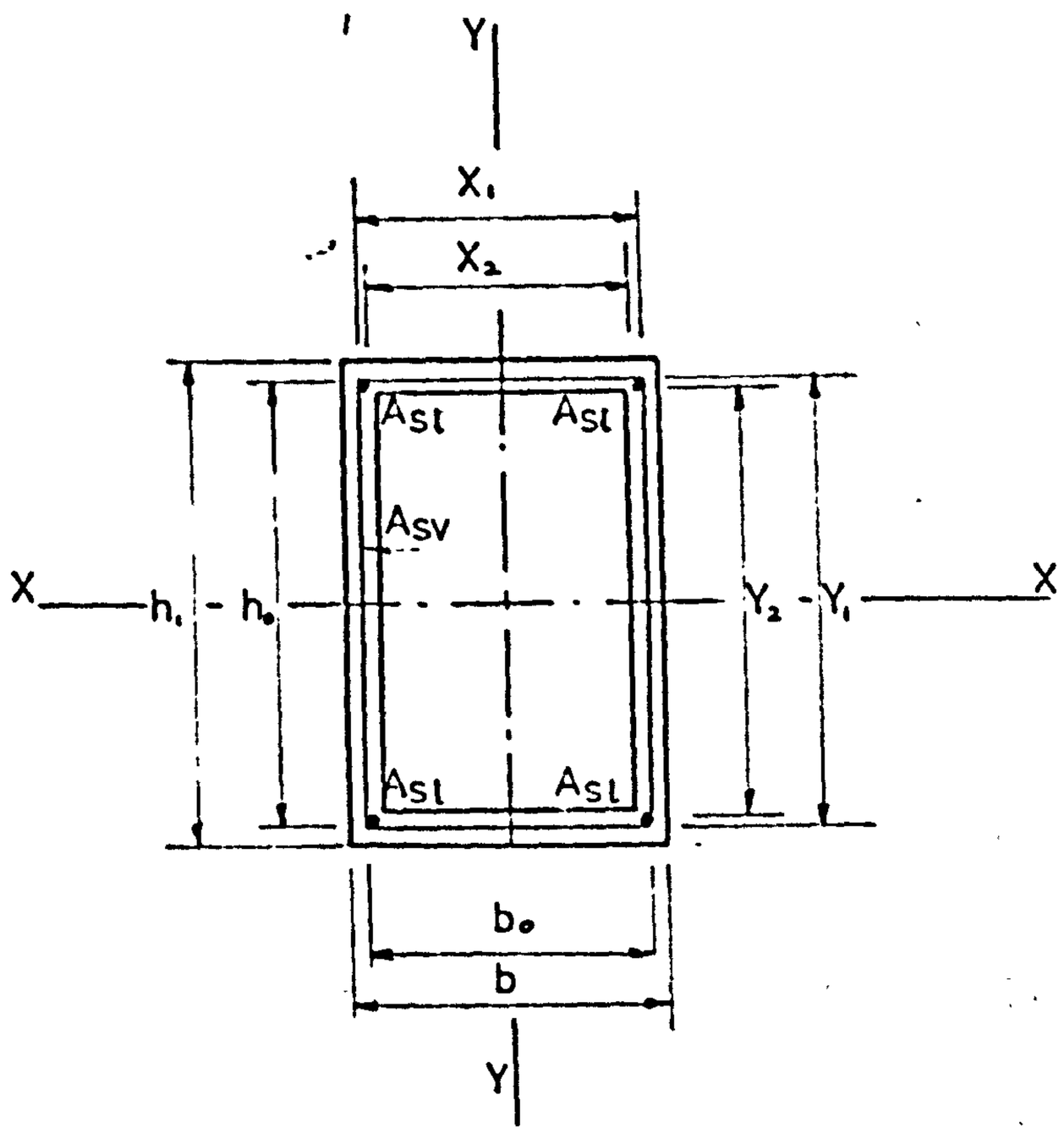

FIG 3.3 PROPOSED FAILURE SURFACE (METHOD A)

If we consider the failure surface shown in Fig. 3.3 which is formed by a continuous crack on four faces then the ends of the spiral crack are linked by a longitudinal shear compression zone running parallel to the longitudinal axis of the beam and located at one of the corners. The internal forces acting on this failure surface are also shown in Fig. 3.3. Adopting the assumptions made for the yield theory given in section 3.23, and from consideration of equilibrium of forces, the ultimate torque resistance of this section can be determined.

From equilibrium of the direct forces along the x - axis, the direct force per unit length (q_d) acting on the shear compression zone may be obtained:

$$2\ q_d\ (X_1 + Y_1)\ \cot\theta = \frac{A_{sv}\ f_{yv}}{S_v}\ 2(X_1 + Y_1)\ \cot\theta$$

$$\therefore\ q_d = \frac{A_{sv}\ f_{yv}}{S_v} \qquad 3.5$$

From the equilibrium of the direct forces acting along the Z - axis, the following equation may be obtained:

$$q_t\ 2\ (X_1 + Y_1)\ \cot\theta = 4\ A_{sl}\ f_{yl}$$

$$\therefore\ q_t = \frac{2\ A_{sl}\ f_{yl}}{(X_1 + Y_1)\ \cot\theta} \qquad 3.6$$

where q_t is the shear flow acting on the shear compression zone.

From moment equilibrium about the x - axis we get:

$$q_t \; 2(X_1 + Y_1) \cot\theta \frac{Y_1}{2} = \frac{A_{sv} f_{yv}}{S_v} Y_1 \cot\theta (X_1 + Y_1) \cot\theta$$

$$\therefore \quad q_t = \frac{A_{sv} f_{yv}}{S_v} \cot\theta \qquad 3.7$$

From moment equilibrium about y - axis we get:

$$q_t \; 2 (X_1 + Y_1) \cot\theta \frac{X_1}{2} = \frac{A_{sv} f_{yv}}{S_v} X_1 \cot\theta (X_1 + Y_1) \cot\theta$$

$$\text{or} \quad q_t = \frac{A_{sv} f_{yv}}{S_v} \cot\theta \qquad 3.8$$

Taking moment about the Z - axis we get:

$$T_y = \frac{2 A_{sv} f_{yv}}{S_v} X_1 Y_1 \cot\theta \qquad 3.9$$

From equations 3.7, 3.8 and 3.9 we get:

$$q_t = \frac{T_y}{2 X_1 Y_1} \qquad 3.10$$

This equation is identical to the relationship between applied torque and internal shear flow obtained in the previous chapter for thin-walled uncracked beams (Bredt Batho formula).

From equations 3.6 and 3.7 the angle of inclination of cracks may be determined as follows:

$$\cot^2\theta = \frac{2 A_{sl} f_{yl}}{(X_1 + Y_1)} \frac{S_v}{A_{sv} f_{yv}} = m' \qquad 3.11$$

$$\text{or} \quad \cot\theta = \sqrt{m'}$$

Hence equation 3.9 becomes:

$$T_y = \frac{2 A_{sv} f_{yv}}{S_v} X_1 Y_1 \sqrt{m'} \qquad 3.12$$

This equation is identical to equation 3.4 which was obtained from the space truss theory.

Method B

For this method, the prismatic thin walled beam of polygonal cross-section shown in Fig. 3.4a is considered. The walls of the beam are orthogonaly reinforced with longitudinal reinforcement equal to $\frac{\sum A_{sl} f_{yl}}{P}$ uniformly distributed around the circumference of the equally spaced closed stirrups.

Consider a small rectangular element in the cracked wall of this beam as shown in Fig. 3.4. The element has a unit length measured along the circumference of the beam and a width equal to $\cot\theta$, where θ is the angle of inclination of the cracks.

It is assumed that the applied torque on the beam is replaced by an equivalent force system which consists of a constant shear flow q_t uniformly distributed around the circumference where

$q_t = T/2A_l$.

It is also assumed that the behaviour of the cracked element is equivalent to the behaviour of the single truss panel shown in Fig. 3.4c and the concrete in this element is assumed to be concentrated around the diagonal BD which acts as a strut. The longitudinal reinforcement is divided equally into two bands which are concentrated at the top and bottom of the element, representing the booms of the truss. Transverse reinforcement is also equally divided into two bands which are concentrated and placed on both sides of the element representing the vertical component of the truss.

In order to find the relationship between the applied shear force and the internal forces, it is necessary to replace the shear flow which is acting on this element by an equivalent force system which consists of concentrated forces applied at the modes of the truss system as shown in Fig. 3.4c.

From the equilibrium of forces at joint A of the truss we get:

$$\frac{q_t}{2} \cot \theta = \sum \frac{A_{s1} f_{y1}}{2p} \qquad 3.13$$

$$\text{and} \quad \frac{q_t}{2} = \frac{A_{sv} f_{yv}}{2S} \cot \theta \qquad 3.14$$

Equating these two equations and eliminating $\cot \theta$ we get:

$$q_t = \frac{A_{sv} f_{yv}}{S_v} \sqrt{\sum \frac{A_{s1} f_{y1}}{P} \frac{S_v}{A_{sv} f_{yv}}} \qquad 3.15$$

Using the Brett-Batho expressions we get:

$$Ty = 2 \frac{A_{sv} f_{yv}}{S_v} A_1 \sqrt{m'} \qquad 3.16$$

where $m' = \cot \theta$ as shown earlier.

This equation is identical to equation 3.4.

From the equilibrium of joint B we may obtain the diagonal compressive force (Fc) as follows:

$$F_c = \frac{q_t}{2 \sin \theta} = \frac{T}{4A_1 \sin \theta} \qquad 3.17$$

taking B as the width of the strut, tw is the thickness of the wall and fc as the diagonal

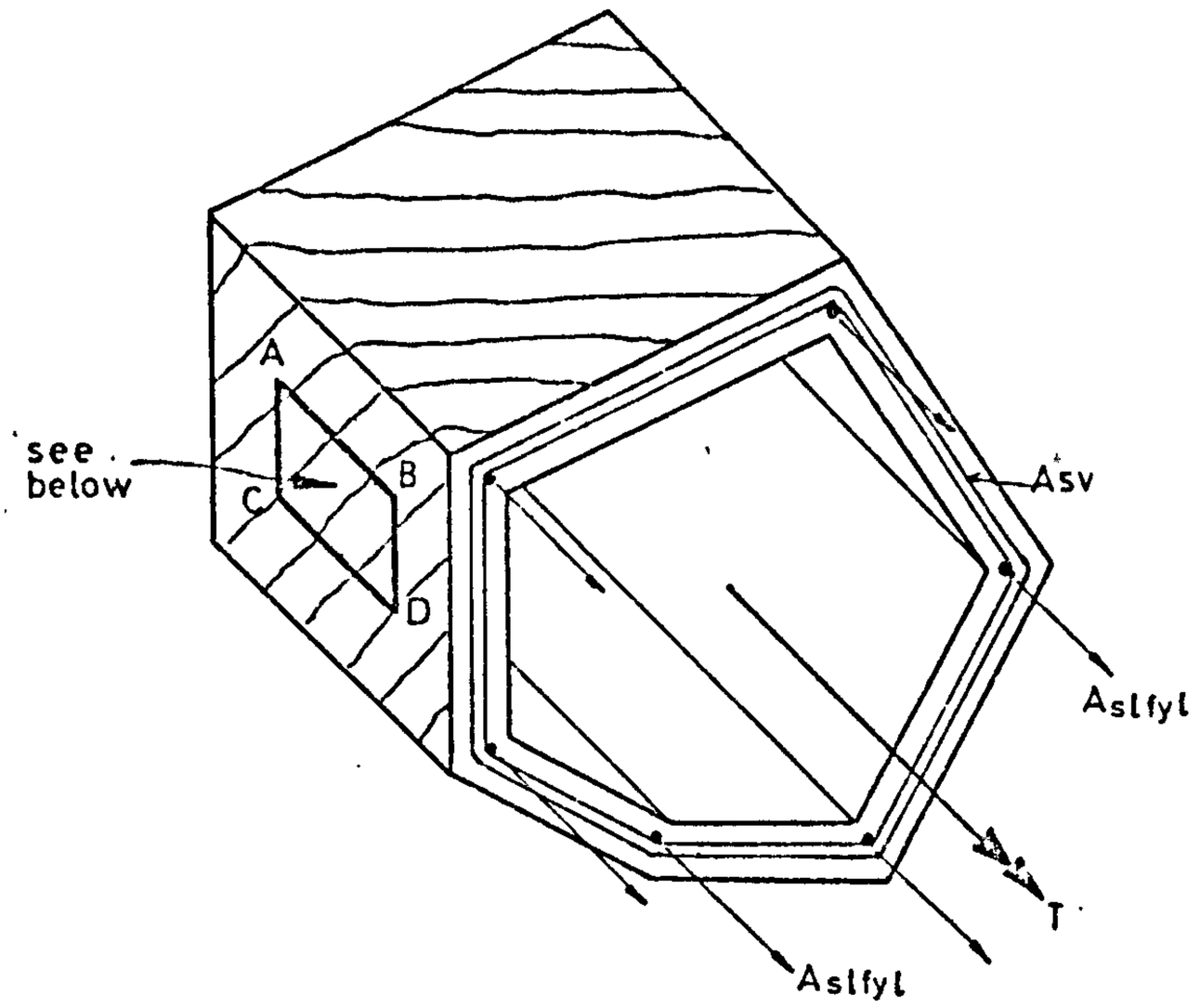

3·4a THIN WALLED ORTHOTROPICALLY REINFORCED BEAM WITH POLYGONAL CROSS - SECTION.

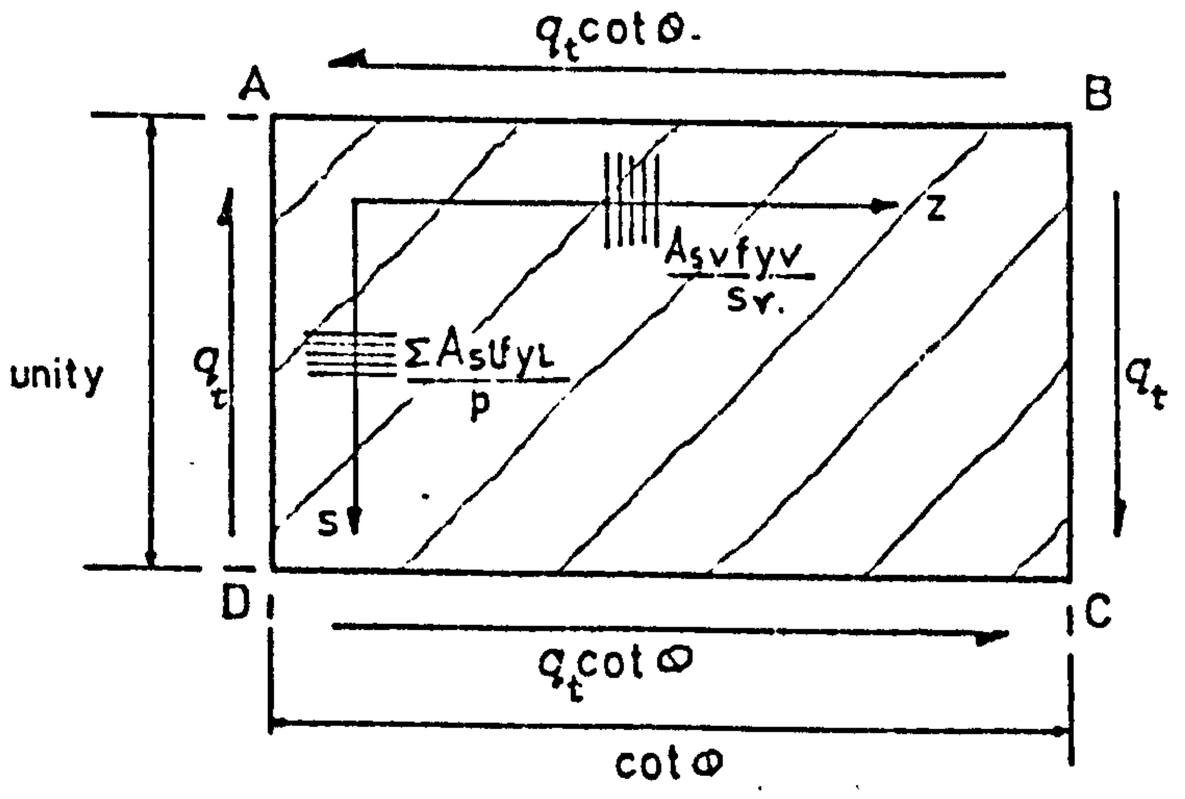

FIG 3·4b ORTHOTROPICALLY REINFORCED RECTANGULAR ELEMENT CUTOFF· THE BEAM SHOWN ABOVE.

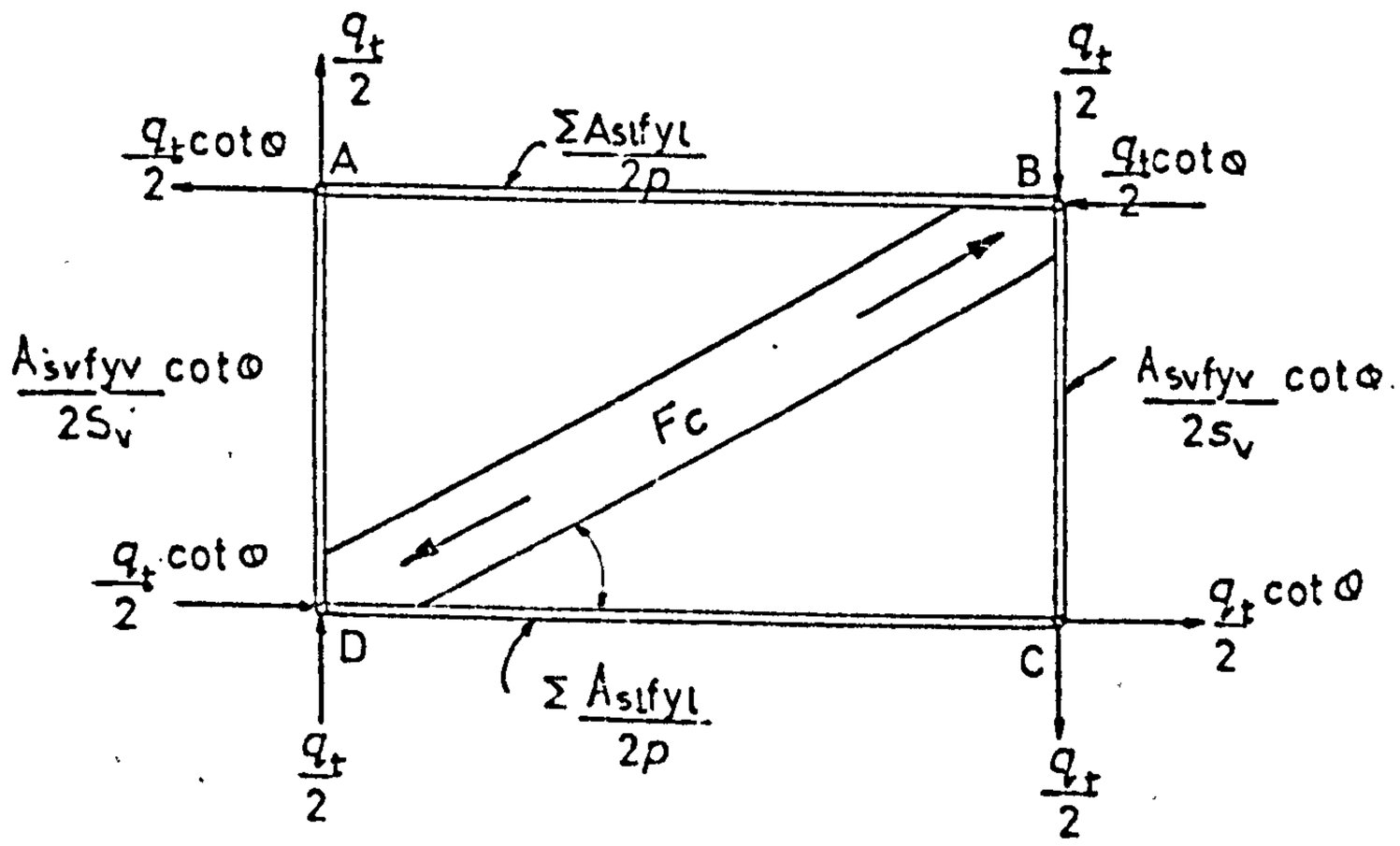

FIG 3·4c TRUSS IDEALIZATION FOR THE FORCES ACTING ON A RECTANGULAR ELEMENT USED IN METHOD B

compressive stresses in the beam, equation 3.17 becomes:

$$f_c = \frac{T}{A_1 \, t \quad \text{Sin } 2\theta} \qquad 3.18$$

3.2.5 Examination of the Assumptions of the Yield Theory

Although the general yield theory provides a better explanation of test results than the elastic theory proposed by Cowan (3.13), it does not explain the following observed phenomena:

a. The general yield theory usually overestimates the torsional resistance of most of the reinforced concrete beams tested up to now under pure torsion. For this reason some of the advocates of this theory (2.23 and 2.32) suggest the use of a reduction or efficiency factor α = 0.8.

b. Hsu (3.5) found that the tensile stresses in the shorter legs of the stirrups are usually smaller than the tensile stresses in the larger legs of rectangular beams. These stresses in the shorter legs of the stirrups do not reach yield stress at failure. Whereas in the yield theory these stresses are assumed to reach their yield value at failure.

c. The concrete on both sides of a crack undergo relative shear displacement indicating the possibility of development of dowel forces in the longitudinal reinforcement. The presence of these dowel forces was confirmed by the bending stress measured by Hsu (3.5)

from diametrically opposite ERS gauges attached to a longitudinal corner bar.

d. In general, crack width measurements and rotations of a symmetrically reinforced rectangular beam indicates that the beam rotates about an axis located at the centre of the beam and not as assumed by Lassig's theory.

e. The balance ratio of m' where yielding takes place simultaneously for all the reinforcement is shown by Hsu to be 1.2 in contrast to what had been assumed by the Rausch yield theory.

f. The yield theory requires the concrete strut to be a function of m'. However, tests show thatthe inclination of cracks under pure torsion is consistantly close to 45^{o} for reinforced concrete beams and is a function of the level of prestressing force for prestressed concrete beams and is independent of the ratio m'. Therefore, if the diagonal compressive stress field in a beam differs from the angle of cracking, shear transfer across the crack must develop. These stresses can only be transfered by aggregate interlock.

g. Tests indicate that for beam with equal volume of reinforcement (m = 1) the measure strain of the longitudinal reinforcement are always greater than the strains measured on the stirrups. This discrepancy between these strains was found to increase as $\frac{X_1}{Y_1}$ approached unity.

h. The stresses in the longitudinal reinforcement do not reach the yield value at failure for beams with m' $>$ 2.

It is possible that some of these phenomena may have little effect on the general behaviour of concrete beams subjected to pure torsion whereas others may have more serious consequences causing premature secondary modes of failure and hence restricting the general application of the yield theory. The importance or otherwise of each of these observed phenomena and their influence to the resistance and strength of concrete structural members has not been studied adequately therefore, it is intended to examine their effects in more detail as follows. These discrepancies between the observed and the assumed behaviour maybe attributed to one or more of the following factors:

1. The discreet nature of the reinforcement
2. The occurrence of the dowel forces
3. The development of stresses in the remaining uncracked part of the concrete beam
4. The development of the aggregate interlock.

3.3 Factors Influencing Torsional Behaviour of Concrete Members

3.3.1 Effect of Stirrup Spacing

Several research workers, (3.5, 3.11, 3.33, 3.34) have found that the torsional capacity of similar beams with equal volumes of reinforcement, decreases with increase in the stirrup spacing.

No rational assessment, however, of this effect has yet been produced, although some researchers have suggested arbitrary reduction, factors and rules on detailing reinforcement to minimize the effect of this factor. For example Lampert and Thurlimann (3.18) have suggested that the maximum spacing of the stirrups should be limited to half the smaller dimension of the stirrups or 200 mm later Mitchell et al (3.33) proposed the following:

$$Sv \leqslant 300 \text{ mm}$$

$$\frac{P}{Sv} \geqslant 8$$

$$\frac{\sum A_{s\ell}}{A_{sl}} \quad \frac{S_v}{\phi s\ell} \quad \frac{S_v}{P} \leqslant 25 \text{ or } \frac{S_v}{\phi . s\ell} \leqslant 16$$

where $\phi s\ell$ is the diameter of the corner bar and the other symbols are as previously defined.

Pandit (11) suggested an empirical reduction factor: $\alpha s = 1 - \frac{S_v}{Y_1}$ for the contribution of the steel in his empirical torsional strength equation. It has also been reported by these investigators that where failure occurs as a result of excessive spacing, the stresses in the stirrup reinforcement does not reach the yield value.

If we assume for the purpose of this study that the torque is resisted primarily by truss action and consider the rectangular hollow beam shown in Fig. 3.3 with equal volumes of reinforcement i.e. m' = 1 and $\theta = 45^{o}$. If fs is taken as the tensile stress in the stirrups at failure, then equation 3.6, 3.7 and 3.12 becomes:

$$q_t = \frac{\alpha_s \; 2 \; A_s \; f_y}{(X_1 + Y_1)}$$

$$q_t = \frac{A_{sv} \; f_s}{S_v}$$

$$T_u = \frac{2 \; A_{sv} \; f_{s1}}{S_v} \; X_1 \; Y_1 \qquad 3.19$$

where α_s is a factor which represents the effect of the spacing of the stirrups which is determined as follows.

If we assume that the diagonal compressive forces to be resisted mainly by the usual space truss action and partly by the longitudinal reinforcement acting as a continuous beam which is supported by the stirrups, the maximum bending moment induced in the longitudinal reinforcement at failure due to this action maybe taken as:

$$M = \frac{n \; Sv^2}{16} \qquad 3.20$$

where n is the average lateral force acting on the longitudinal reinforcement per linear length. Therefore, α_s may be taken as a factor which represents the effect of reduction in the axial yield strength of the longitudinal bar due to these secondary moments.

From equations 3.19 and 3.16 we get

$$\alpha_s = \frac{f_{s1}}{f_{y1}} \; m \quad \text{where } m = \frac{2 \; A_s}{(X_1 + Y_1)} \; \frac{S_v}{A_{sv}}$$

and for $f_{y_1} = f_{yv} = f_y$ and $m = 1$

we get $\frac{T_u}{T_y} = \alpha_s \qquad 3.21$

It can be shown that for a bar subjected to a combined action of moment (M) and axial force (F), the ultimate strength is given by the following interaction equation

$$\left(\frac{F}{F_p}\right)^2 + \frac{M}{M_p} = 1 \qquad 3.22$$

where Fp and Mp are the full axial tensile yield strength and the full plastic moment of the bar respectively. Combining equations 3.21 and 3.22 we get:

$$\frac{T_u}{T_y} = \sqrt{1 - \frac{M}{M_p}} \qquad 3.23$$

The lateral force acting on the longitudinal reinforcement (n) in equation 3.20 maybe written as follows:

$$n = \beta q_t = \beta \frac{T_u}{2 A_1}$$

where β is a factor which represents the percentage of shear flow that is sustained by the longitudinal reinforcement spanning as a beam between the stirrups.

The maximum moment induced in the longitudinal reinforcement becomes:

$$M = \frac{\beta S_v}{32} \frac{T_u}{A_1} \qquad 3.24$$

Also the full plastic moment of resistance of the bar is

$$M_p = \frac{\phi_{sl}^3 f_{yl}}{6}$$

Hence, $$\frac{M}{M_p} = \frac{3}{64} \frac{\beta S_v^2}{A_{sl} f_y \phi_{sl}} \frac{T}{A_1} \qquad 3.25$$

This equation maybe written as:

$$\frac{M}{M_p} = \frac{3\pi\beta}{32} \frac{A_{sv}}{A_{sl}} \frac{S_v}{\phi s\ell} \frac{T_u}{T_y}$$

using the relationship $m = \frac{\sum A_{sl}}{P} \frac{S_v}{A_{sl}} = 1$

This equation maybe written as follows:

$$\frac{M}{M_p} = k_1 k_s \frac{T_u}{T_y} \qquad 3.26$$

where $k_1 = \frac{3\pi}{32\beta}$ and $k_s = \sum \frac{A_{sl}}{A_{sl}} \frac{S_v}{P} \frac{S_v}{\phi s\ell}$

substituting equation 3.26 into equation 3.23 we get:

$$\frac{T_u}{T_y} = 1 - k_1 k_s \frac{T_u}{T_y}$$

solving this equation we obtain:

$$\frac{T_u}{T_y} = \sqrt{1 + \left(\frac{k_1 k_s}{2}\right)^2} - \frac{k_1 k_s}{2} = s$$

In this equation $k_1 k_s$ is usually small, hence, the second term under the square root is very small compared with unity, therefore, this equation maybe simplified to the following:

$$T_u = \left(1 - \frac{k_1 k_s}{2}\right) T_y \qquad 3.27$$

This equation shows the effect of stirrups spacing on the ultimate strength of the beam relative to its torsional strength predicted by the yield theory. Therefore, the reduction in the torsional capacity of the beam due to stirrup spacing is a function of β and ks, β may also be influenced by the crack spacing the strength

of concrete, etc. A value for $\frac{k_1}{2}$ of $\frac{1}{250}$ maybe taken for practical purposes as shown on Fig. 3.5.

Although the proposed theory allows for variations in the value of Ks it is suggested that for practical purposes α_s may be taken as a constant with a value of 0.9, it is further recommended that the maximum stirrup spacing Sv should be limited to $\frac{p}{8}$. These recommended values are shown on Fig. 3.5.

3.3.2 Effects on Dowel Forces

The dowel forces which are known to develop across longitudinal bars when they intersect cracks have been either completely ignored, as in the yield theory or considered to play a major role in resisting torque according to Hsu (3.6), Gresund et al (3.35, 3.36) and Martin (3.37 and 3.38). These forces must have certain effects on the strength and behaviour of the beam and the opposing extreme views on the contribution of dowel forces illustrate the lack of understanding on this subject and the unreliability of the assumption associated with dowel forces made in all existing torsional strength theory for concrete members. Hence, in the following a detailed study of this subject has been carried out.

Consider the internal forces in the rectangular concrete box beam shown in Fig. 3.6, where $\frac{Fsx}{Sv}$, $\frac{Fsy}{Sv}$ are the axial forces per unit length measured along the beam axis of the stirrups which are intersecting the crack in the smaller and larger dimension of the box beam

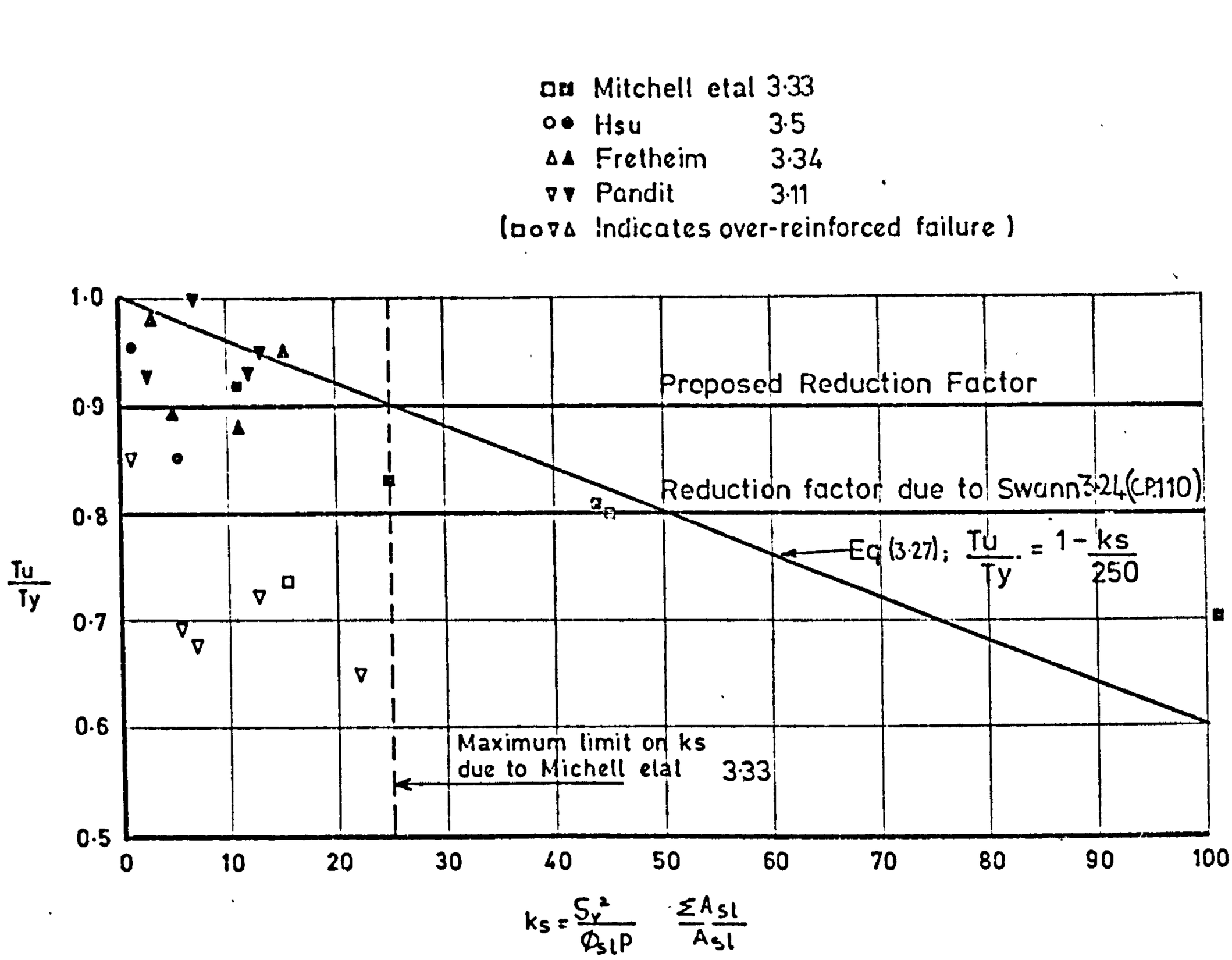

FIG. 3·5 EFFECT OF STIRRUP SPACING

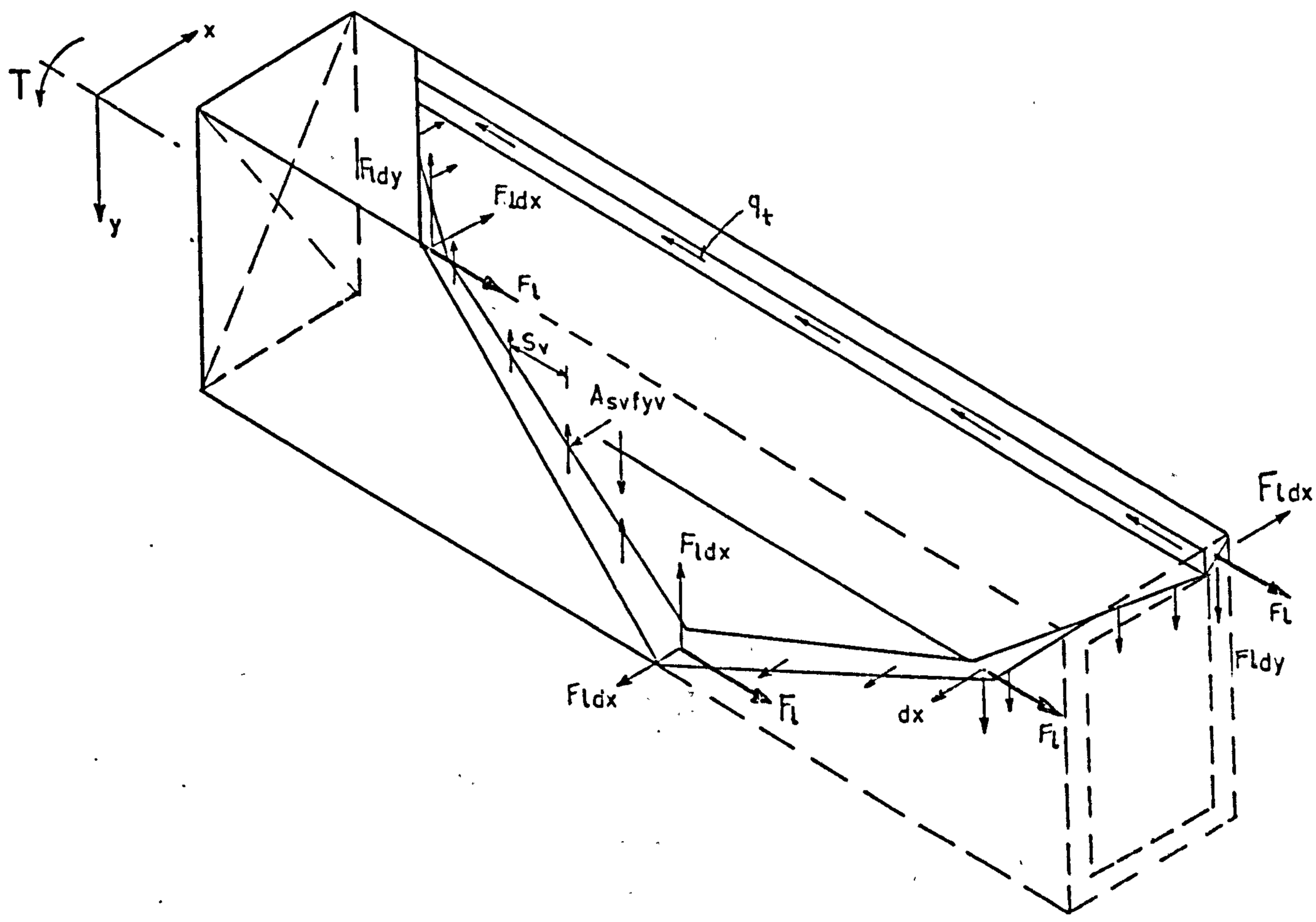

FIG. 3·6 FAILURE SURFACE WITH DOWEL FORCES.

cross-section respectively. F_{sd} is the dowel force per unit length resisted by the stirrups. F_l is the axial force in each of the longitudinal corner bars. F_{dx} and F_{dy} are the components of the dowel force induced in each longitudinal bar in the X_1 and Y_1 direction respectively. The stirrup forces are assumed to be uniformly distributed along each side of the box beam. The sectional properties of the beam as defined earlier in Fig. 3.3. Assuming that $X_1 = X_2$ and $Y_1 = Y_2$.

From equilibrium of forces along the Z axis we get:

$$q_t \; 2 \; (X_1 + Y_1) \cot \theta = 4 F_l + \frac{F_{sd}}{S_v} 2 \; (X_1 + Y_1) \cot \theta$$

$$q_t = \frac{2F_l}{(X_1 + Y_1) \cot \theta} + \frac{F_{sd}}{S_v} \qquad 3.28$$

From moment equilibrium about the x - axis we get:

$$q_t = (X_1 + Y_1) \cot \theta \; \frac{Y_1}{2} = \frac{F_{sd}}{S_v} (X_1 + Y_1) \cot\theta \, Y_1 \cot \theta$$

$$+ 2 F_{ldy} (X_1 + Y_1) \cot \theta$$

$$\text{or} \quad q_t = \frac{F_{sd}}{S_v} \cot \theta + 2 \frac{F_{ldy}}{Y_1} \qquad 3.29$$

From moment equilibrium about the Y - axis we get:

$$q_t \; 2 \; (X_1 + Y_1) \cot \theta \; \frac{X_1}{2} = \frac{F_{sx}}{S_v} (X_1 + Y_1) \cot\theta \, X_1 \cot \theta$$

$$+ 2 F_{dx} (X_1 + Y_1) \cot \theta$$

$$\text{or } q_t = \frac{F_{sx}}{S_v} \cot \theta + 2 \frac{F_{dx}}{X_1} \qquad 3.30$$

taking moment about the Z - axis we obtain:

$$T = \frac{F_{sy}}{S_v} X_1 Y_1 \cot\theta + \frac{F_{sx}}{S_v} X_1 Y_1 \cot\theta + F_{1dx} Y_1 + 2F_{1dy} X_1$$

or

$$\frac{T}{A_1} = \frac{F_{sy}}{S_v} \cot\theta + \frac{F_{sx}}{S_v} \cot\theta + 2\frac{F_{1dx}}{X_1} + \frac{F_{1dy}}{Y_1} \qquad 3.31$$

Equating equations 3.29, 3.30 and 3.31 we obtain:

$$q_t = \frac{T}{2A_1}$$

Hence this relationship is invariable.

If the materials are assumed to behave elastically and the displacement (crack width) along any typical crack is to be uniform, the relationship between the axial and dowel forces may be obtained from the compatibility of displacement condition occuring at a typical crack. This displacement may be resolved into a longitudinal displacement W_ℓ and tangential displacement Ws. The ratio W_ℓ / Ws will depend on the stiffness of the reinforcement which intersects the crack and resists the vertical and horizontal components of the shear flow.

For vertical displacement Ws, the following relationship applies:

$$W_s = \frac{\eta_1 \Delta}{E_s A_s} F_s = \delta s F_s \qquad 3.32$$

where F_s is the force in any stirrup,

A_s is the area of stirrup

E_s is the elastic modulus for steel

Δ is the effective length of the stirrup which

η_1 is contributing to this displacement

η_1 is a factor introduced to account for the bond action between the stirrups and the concrete.

δ_s is the flexibility coefficient

Similarly the relationship between this displacement and the dowel forces F_{1d} maybe obtained from the result of investigations into this subject which are given in Chapter 7.

$$\left.\begin{aligned} \frac{W_s}{2} &= \frac{40}{E_c \ \phi_\ell^{7/4}} F_{1d} \\ \text{or } W_s &= \delta_d F_{1d} \end{aligned}\right) \qquad 3.33$$

where $\delta_d = \dfrac{80}{E_c \ \phi_\ell^{7/4}}$

where E_c is the elastic modulus for concrete and ϕ_ℓ is the diameter of the longitudinal reinforcement. From these two equations the following relationships are obtained:

$$\left.\begin{aligned} &\frac{F_{sx}}{F_{1dx}} = \frac{\delta_d}{\delta_s} = k_1 k_d \\ &\text{where } k_1 = \frac{80}{\eta \Delta} \frac{E_s}{E_c} \text{ and } k_d = \frac{A_s}{\phi_\ell^{7/4}} \\ &k_1 \doteq \alpha_e \quad \text{where } \alpha_e \text{ is modular ratio} \\ &\text{similarly } \frac{F_{sy}}{F_{1dy}} = k_1 k_d \\ &\text{and } \frac{F_1}{F_{sd}} = \frac{k_1}{k_d} \end{aligned}\right) \qquad 3.34$$

Now combining equations 3.28 to 3.34 we obtain the following relationship:

$$q_t = \frac{F_{sd}}{Sv}\left[1 + \frac{2}{(X_1 + Y_1)\cot\theta}\frac{S_v}{}\frac{k_1}{k_d}\right] \qquad 3.35a$$

$$q_t = \frac{2F_{\ell}}{(X_1 + Y_1)}\left[\frac{1}{\cot\theta} + \frac{(X_1 + Y_1)}{2\,\varepsilon_v}\frac{k_d}{k_1}\right] \qquad 3.35b$$

$$q_t = \frac{F_{sy}}{S_v}\left[\cot\theta + 2\,\frac{S_v}{Y_1 \cdot k_1 k_d}\right] \qquad 3.35c$$

$$q_t = \frac{2F_{1dy}}{Y_1}\left[1 + \frac{Y_1}{2\,Sv} \cdot k_1\, k_d\, \cot\theta\right] \qquad 3.35d$$

$$q_t = \frac{F_{sx}}{S_v}\left[\cot\theta + 2\,\frac{S_v}{X_1\ k_1 k_d}\right] \qquad 3.35e$$

$$q_t = 2\,\frac{F_{1dx}}{X_1}\left[1 + \frac{X_1}{2\,S_v}\,k_1\, k_d \cot\theta\right] \qquad 3.35f$$

Now equating equation 3.35c and 3.35e we get

$$\frac{F_{sx}}{F_{sy}} = \frac{\left[\cot\theta + 2\,\frac{S_v}{Y_1\ k_1\ k_d}\right]}{\left[\cot\theta + 2\,\frac{S_v}{X_1\ k_1\ k_d}\right]} = \frac{f_{sx}}{f_{sy}}$$

and equating equation 3.35b and 3.35c and re-arranging:

$$\frac{f_{sl}}{f_{sv}} \times \frac{1}{m} = \frac{\left[\cot\theta + 2\,\frac{S_v}{Y_1\ k_1\ k_d}\right]}{\left[\frac{1}{\cot\theta} + \frac{(X_1 + Y_1)}{2\,S_v}\,\frac{k_d}{k_1}\right]}$$

where f_{sl} and f_{sv} are the stresses in the longitudinal reinforcement and the stirrup respectively.

and $m = \frac{2 A_{sl}}{(X_1 + Y_1)} \frac{S_v}{A_{sv}}$

for reinforced concrete beams having $Y_1 = 2 X_1$ $= 45^o$, and m = 1 and for $k_1 = 7$, these equations give

$$\frac{f_{sx}}{fsy} \simeq 0.9$$

and $$\frac{f_{sl}}{f_{sv}} \simeq 1.2$$

Therefore these results explain the reason why the measured strains in the shorter leg of the stirrup are always greater than the strains in the longer leg of the stirrups and why the measured strain in the longitudinal reinforcement are always larger than the strains in the stirrups. However, all the observed discrepancies between measured strains in the reinforcement and those predicted by the simple truss theory reported by Hsu and others investigators for beams with equal volumes of reinforcement can be adequately explained by the above truss-dowel theory.

The contribution of the dowel forces developing in the longitudinal reinforcement relative to the forces resisted by the stirrups maybe found by comparing the second term inside the bracket of equation 3.35c with Cot θ . An average value for the contribution of dowel forces to the resistance of torque can be taken as 10% in the elastic range, however, these dowel forces would decrease appreciably as the stresses in the longitudinal reinforcement reach their yield value. Therefore the assumption made by the

yield theory that the stirrups attain their yield stress on both legs appear to be acceptable since the neglect of the dowel forces will compensate for the additional forces which are assumed to be developing in the shorter leg of the stirrup.

3.3.3 The Effect of the Uncracked Concrete in the Beam

When a reinforced concrete beam subjected to torsion is cracked, the concrete between two adjacent cracks will form a continuous helical spring extending from one end of the beam to the other. Hence the beam will be transformed into a number of concrete springs held together by the stirrups. Although this concrete is resisting primarily compressive forces due to the truss action, they may also resist applied torque. This phenomena has not been investigated previously. The elastic behaviour of helical springs has been studied by many stress analysts and the results maybe found in text books on theory of elasticity. Timoshenko (3.39) derived the following relationship between torque applied to the ends of a cylindrical spring and the longitudinal extension of the spring:

$$\Delta_t = S_R \sin\theta \cos\theta \left[\frac{1}{GJ} - \frac{1}{EI}\right] T$$

and the longitudinal extension of a cylindrical spring due to direct longitudinal force P is:

$$\Delta_P = SR^2 \left[\frac{\cos^2\theta}{GJ} + \frac{\sin^2\theta}{EI}\right] P$$

where R is the radius of the cylindrical helix, θ is the angle between the helix and its longitudinal axis. GJ and EI are the torsional and flexural rigidity respectively and Z is the length of the

helix.

For the case where $\theta = 45^{\circ}$, EI $\gg$ GJ then $Z = L\sqrt{2}$ where L is the length of the helix. The above equations may be simplified as follows:

$$\Delta_t = \delta_t \, T \qquad 3.36a$$

$$\Delta_p = \delta_p \, P \qquad 3.36b$$

where δ_t and δ_p are the flexibilities of the spring under pure torque and longitudinal force respectively. For this case

$$\delta_t = \frac{RL}{\sqrt{2}\,GJ} \quad \text{and} \quad \delta_p = \frac{R^2 L}{\sqrt{2}\,GJ}$$

In a reinforced concrete beam under pure torsion this longitudinal extension will be elastically restrained by the longitudinal reinforcement, therefore, the contribution of the spring action will depend on the ratio of the stiffness of the spring to the stiffness of the longitudinal reinforcement. This problem may be analysed as a statically indeterminate structure with a force in the longitudinal reinforcement being the redundency. Introducing a cut in the longitudinal reinforcement and then establishing compatibility of deformation and equilibrium we obtain:

$$\delta_t \, T - \delta_p \sum P = \delta_\ell \sum F_\ell$$

and $$\sum P - \sum F = 0$$

where δ_ℓ is the flexibility of the longitudinal reinforcement $= \dfrac{L}{E_s \sum A_{sl}}$

substituting for the flexibilities in the above

equations and rearranging we obtain:

$$\sum F_e = \frac{T}{R\ (1 + k_c)} \qquad 3.37$$

where $k_c = \frac{\delta e}{R\delta t} = \frac{\sqrt{2}\ GJ}{R^2\ E_s \sum A_{sl}}$

The value of k_c when compared with unity represents the significance of the springs contribution to the resistance to torque. For a wide range of practical box beam parameters k_c was found to have a value of less than 2%, therefore, this effect may be ignored.

Although the contribution of the concrete acting as a spring and the dowel forces were found to be insignificant, the secondary stresses developed due to these actions may result in local failures of concrete which in turn may lead to other premature modes of failure. The importance of these secondary stresses will be examined further when considering these other modes of failure.

3.4 New Yield Theory

One of the objections to the present yield theory is the use of a large number of simplifying assumptions which cause a considerable scatter in the prediction of test results. Therefore, the following yield theory considers the crack inclination to be a function of the direction of the principal stresses prior to cracking rather than a function of the ratio of the volume of the longitudinal to the transverse reinforcement (m') which was made in the yield theories previously reviewed.

If we examine the forces acting on an element cut from the wall of the beam shown in Fig. 3.4 and if we assume that a single crack passes through its diagonal BD and the stress in all the reinforcement intersecting this crack reach their tensile yield strength at failure then an examination of the forces acting on any segment of this element suggest that shear stresses must develop along the crack if equilibrium of forces is to be maintained. If we ignore the dowel forces and assume that these shear stresses can be resisted by the aggregate interlock action, then from equilibrium of the horizontal forces acting on the segment shown below we obtain:

$$q_t \cot\theta = \frac{\sum A_{sl} f_{yl}}{p} - q_a \cot\theta \qquad 3.38$$

From vertical equilibrium of forces we get:

$$q_t = \frac{A_{sv} f_{ys}}{S_v} \cot\theta + q_a . \qquad 3.39$$

where q_a is the shear force per unit length resisted by aggregate interlock

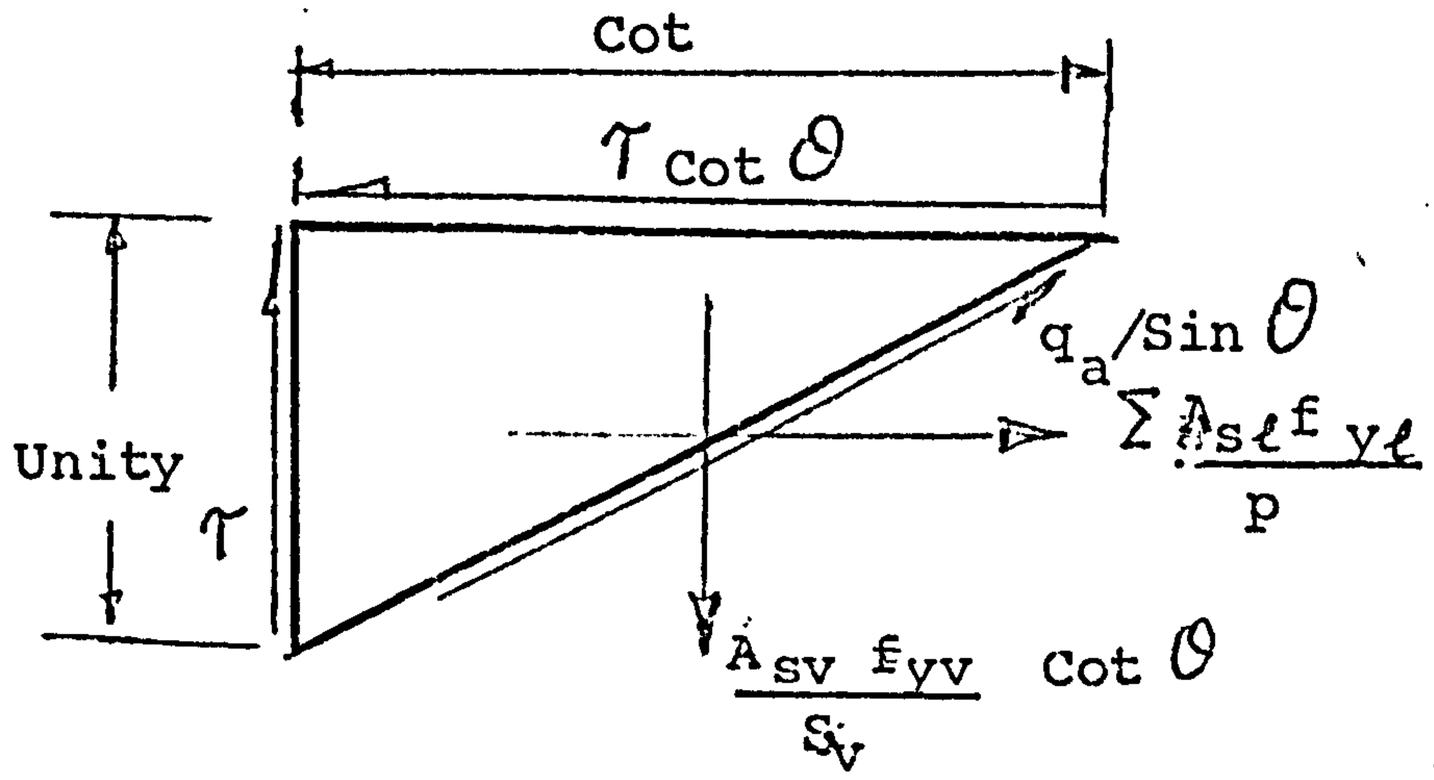

Combining equations 3.38 and 3.39 and eliminating q_a and rearranging:

$$q_t = \frac{A_{sv}\, f_{ys}}{S_v} \left[\frac{\cot^2\theta + m'}{2 \cot\theta} \right]$$

Substituting for q_t in the above equation using the Bredt-Batho expression we get:

$$Ty = 2 \frac{A_{sv}\, f_{ys}}{S_v} A_1 \left[\frac{\cot^2\theta + m'}{2 \cot\theta} \right] \qquad 3.40$$

where $\cot\theta$ can be taken as $\sqrt{1 + f_p/f_t}$

From equilibrium of forces along the crack, the shear flow resisted by aggregate interlock at failure can be obtained as follows:

$$q_a = (1 - m') \left[\frac{A_{sv}\, f_{yv}}{S_v} \cot\theta + (1 - \cot^2\theta) \frac{T}{2A_1} \right] \sin^2\theta$$

3.41

equation 3.40 can also be obtained using the failure surface shown in Fig 3.3.

Yield failure will occur as long as the shear stresses developing along the crack are smaller than the aggregate interlock strength. However, if the angle of cracking is not governed by the direction of the principal stresses prior to cracking then may be determined by differentiating equation 3.40 with respect to θ which gives

$$\cot\theta = \sqrt{m'}$$

and the solution will be identical to those obtained previously.

3.5 Partially Over-Reinforced Failures

The prediction of ultimate strength for beams failing in this mode is essential for determining the limits of under-reinforced mode of failure. It has also been suggested that the limits which have been proposed on m' by the advocates of the yield theory are unnecessarily restrictive and usually difficult to satisfy in practical situations. Unlike the under-reinforced failure, no theory is presently available for beams failing in this mode, although several empirical expressions have been suggested (3.25, 3.40) which can be expressed as equation 3.2.

It can be seen from equation 3.38 and 3.39 that failure may occur as a result of yielding of either the longitudinal or the transverse reinforcement when the aggregate interlock strength is reached, consequently equations 3.38 and 3.39 may be written as:

$$T_{ys} = Ta + \frac{2 A_{sv} f_{ys}}{S_v} A_1 \qquad 3.42$$

$$\text{and} \quad T_{yl} = Ta + \frac{2 A_{sv} f_{ys}}{S_y} A_1 \, m' \qquad 3.43$$

where Tys is the ultimate torque of a beam failing by yielding of stirrups only.

T_{yl} is the ultimate torque of a beam failing by yielding of the longitudinal reinforcement only.

Ta is the maximum torque resisted by the aggregate interlock.

It must be kept in mind that for these modes of failures, dowel action could also be contributing to the resistance of the applied torque. Although failure is initiated by yielding of the longitudinal or transverse reinforcement, the maximum torque would correspond to the failure of aggregate in resisting shear or dowel failure. Therefore the maximum dowel strength and shear resistance by aggregate interlock must be known in order to assess the ultimate strength of these beams. The problem of dowel behaviour and strengths is given in chapter 7 whereas a summary of test results on aggregate interlock found in literature is given in the following section.

3.5.1 Aggregate Interlock Action

Research by Fenwick (3.41) and Taylor (3.42) on the mechanism of shear force transfer across reinforced concrete beams failing by diagonal tension indicate that aggregate interlock may account for the resistance of approximately half the total shear force sustained after cracking of reinforced concrete beams without shear reinforcement. Fenwick carried out a series of tests on specially designed concrete specimens in which the aggregate interlock forces were assessed. The effect of crack widths and concrete strength on aggregate interlock were investigated. It was found that the aggregate interlock increased with increase in concrete strength and decreased with a decrease in the crack width. The ultimate shear stress resisted by this action may be approximated to 0.9 f_t for crack widths equal to 0.06 mm decreasing linearly to 0.5 f_t for crack

widths equal to 0.4 mm. In these tests the crack widths were maintained throughout each test.

Taylor (3.42) pointed out that in reinforced concrete beams failing in shear, the movements at the cracks occurred normally and parallel to the cracks simultaneously, hence arguing that the test results obtained by Fenwick tend to overestimate the effect of aggregate interlock. He also conducted a series of tests on the effect of aggregate interlock where the size and type of aggregate, the strength of concrete and the ratio of the vertical to the shear displacement across the crack were investigated. The ultimate shear stress resisted by aggregate interlock obtained from these tests may be approximated to $0.55\ f_t$ for $\frac{W_n}{W_t} = 0$, decreasing linearly to zero for $\frac{W_n}{W_t} = 3$ where W_n is displacement normal to the crack, W_t is shear displacement across the crack and f_t, is the tensile strength of the concrete. These results also indicate that the attainment of maximum aggregate interlock is accompanied by a sudden drop in the shear resistance, hence, exhibiting brittle characteristics.

Unfortunately, no such data is available for beams subjected to torsion, i.e. the stress distribution and displacement pattern has not been examined.

For reinforced concrete beams subjected to pure torsion, the displacement pattern at diagonal cracks is expected to be a function of the relative stiffness of the longitudinal to transverse reinforcement. For beams with equal volumes of longitudinal and transverse reinforcement i.e. (m = 1) it is reasonable to assume that only a normal displacement

across the crack will take place and the shear displacement is expected to be zero. On the other hand for beams containing longitudinal reinforcement only or for beams where the transverse reinforcement has reached its yield value, then a shear and normal displacement would be expected and the ratio of these displacements may be tentatively taken as unity.

The contribution of aggregate interlock in beams failing in this mode may be determined by assuming that the maximum shear stress resisted by aggregate interlock is equal to half the tensile strength of the concrete and that the distribution of these stresses would approximate to the plastic stress distribution, hence Ta becomes:

$$T_a = \frac{1}{2} b^2 h \left(1 - \frac{b}{3h}\right) \frac{f_t}{2} \qquad 3.44$$

The contribution of dowel forces to the resistance to torque of beams failing in this mode may be included by considering the dowel forces occuring just prior to yielding of the reinforcement, hence equations 3.42 and 3.43 may be modified by substituting equations 3.35 for the term representing the contribution of steel reinforcement as follows:

$$T_{ys} = T_a + \frac{2 A_{sv} f_{ys}}{S_v} A_1 \left[\cot \vartheta + \frac{S_v}{Y_1} \frac{1}{k_1 k_d}\right] \qquad 3.45$$

and

$$T_{yl} = T_a + \frac{2 A_{sv}}{S_v} A_1 m \left[\frac{1}{\cot} + \frac{X_1 + Y_1}{2 S_v} \frac{k_d}{k_1}\right] \qquad 3.46$$

3.6 Comparison Between Various Yield Theories and Their Limits

Fig. 3.7 shows a comparison between the Rausch-Yudin theory, the general yield theory given in equation 3.4 and the proposed yield theory given in equation 3.40 for reinforced concrete members with varying m'. In addition the partial yield equations 3.42 and 3.43 are plotted for the case of $\frac{T_s}{T_{cr}} = 2$. It can be seen that for beams having $0.5 < m' < 1.75$ the beams will fail in under-reinforced mode and for beams having m' outside these limits, failure will occur in a partially reinforced mode. These limits to the yield theory may be compared with the following empirically obtained limits:

1.	Hsu (3.5)	$0.7 < m < 1.5$
2.	Kuyt (2.28)	$\sqrt{\frac{2}{2}} < m' < \sqrt{2}$
3.	Navaratnarjah (3.43)	$\frac{1}{2} < m' < 2$
4.	Lampert (3.17), Collins (3.32)	$\frac{1}{4} < m' < 4$

It can be concluded that the limits suggested by Lampert and Collins are relatively high and that the Rausch-Yudin theory on the other hand provides a conservative estimate of torsional strength. It is interesting to note that the proposed yield theory produces almost identical results to those obtained by equation 3.4 over the range of m' for which the proposed yield theory is applicable.

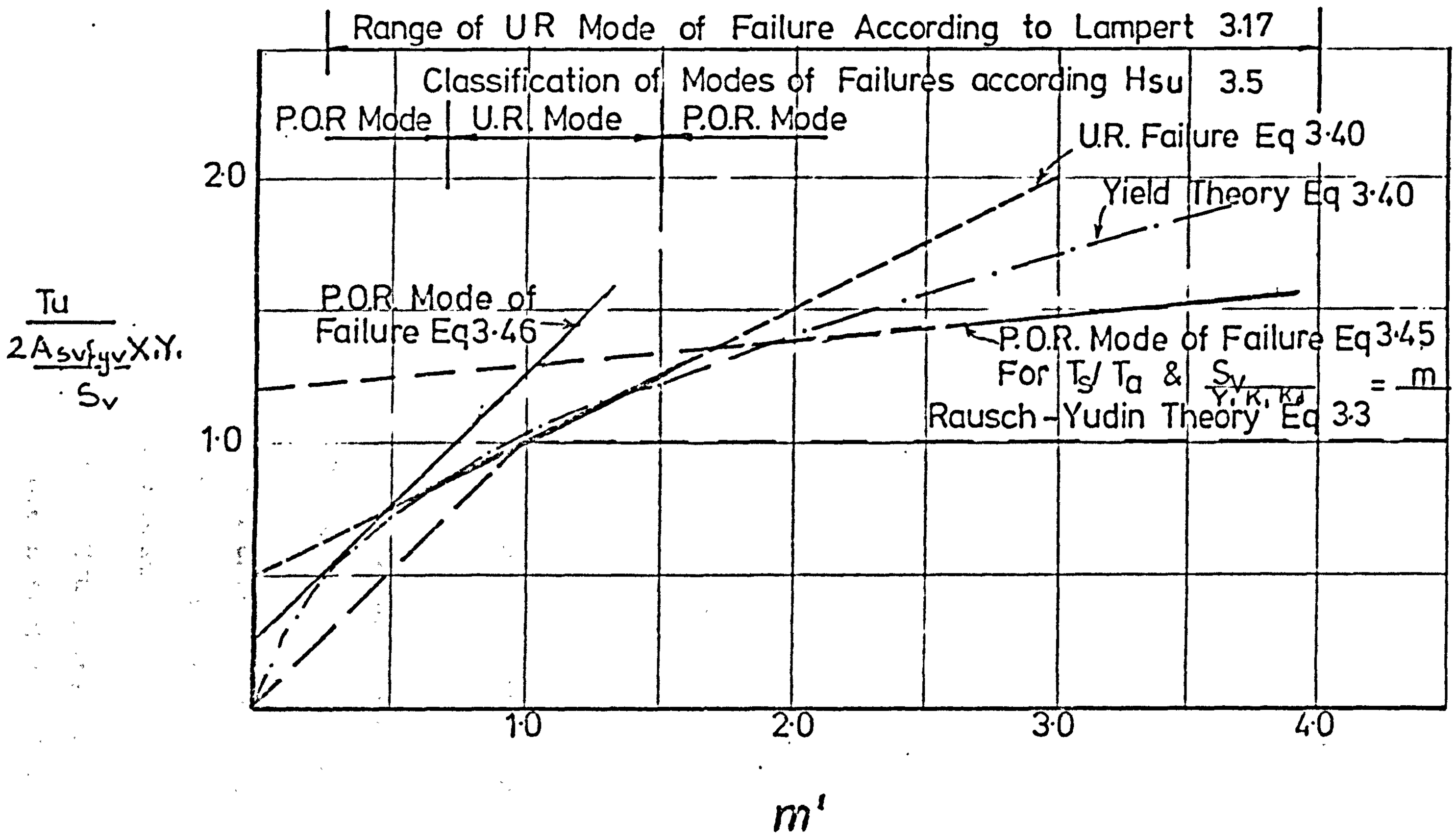

Fig3.7 COMPARISON OF PROPOSED THEORY WITH YIELD THEORY

3.7 Over-Reinforced Mode of Failure

As stated before this mode of failure occurs prior to yielding of reinforcement and consequently it should be avoided since the materials are inefficiently used. Unfortunately very little research information is available on this mode of failure and no rational theory is presently available for predicting the torsional strength of over-reinforced members. A summary of the available torsional equations for prediction of over-reinforced failure is given in Table 3.2. This table shows that the torsional resistance of over-reinforced concrete beams is approximately equal to three times the torque which produces initial cracking. In contrast, for beams tested in bending and shear, the shear at which diagonal compression failure occurs is equal to four to five times the shear force causing diagonal tension cracking. This discrepancy was attributed by Lampert and Thurlimann (3.18) to the presence of additional compressive stresses due to warping of the concrete, on the other hand, Swann attributed this discrepancy to corner spalling at failure.

The following examination of test phenomena may provide an explanation of this mode of failure:

1. Swann (3.24) noticed that longitudinal cracks always occur prior to failure particularly near the corners of the beam.
2. Visual inspection by Hsu (3.6) of the crack pattern over the cross section of a beam at the location of failure after being cut by

TABLE 3.2 Summary of Available Empirical Expression Used For Calculating the Torsional Strength for Beams Subjected to Pure Torsion - Over-reinforced Mode of Failure

Investigator	Ref	Original Expression	Converted Expression in metric in term of f_{cu}
Lessig	3.16	$\alpha_d\ b^2h\ f_{cu}$ where α_d	varies from 0.07 to 0.12
Collins et al	3.23	$5\ b^2h\ \sqrt{f'_c}$	$0.4\ b^2h\ \sqrt{f_{cu}}$
Hsu	3.5	$p_{tb} < 2400\ \frac{\sqrt{f'_c}}{f_{yv}}$	
Hsu and Kemp	3.7	$\frac{b^2h}{3}\ 14\ \sqrt{f'_c}$	$0.47\ b^2h\ \sqrt{f_{cu}}$
Pandit	3.11	$6\ b^2h\ \sqrt{f'_c}$	$0.48\ b^2h\ \sqrt{f_{cu}}$
Swann	3.23	$\left(1-\frac{b}{3h}\right)\frac{b^2h}{2}\ 0.92\ \sqrt{f_{cu}}\ \alpha$ where $\alpha = \frac{Y}{250}$ but $\not> 1$	$0.48\ \alpha\ (1-\frac{b}{3h})\ b^2h\ \sqrt{f_{cu}}$
Martin	3.37	$6\ (1.5 - \frac{b}{h})\ b^2h\ \sqrt{f_{cu}}$	$0.48\ (1.5-\frac{b}{h})\ b^2h\ \sqrt{f_{cu}}$

p_{tb} = total volume percentage of reinforcement
f'_c = cylinder compressive strength of concrete
f_{cu} = cube strength of concrete

a diamond saw confirmed that dowel forces developing in the longitudinal reinforcement are the cause of corner spalling.

3. The crack patterns at this diamond cut section of the beam also indicate that the concrete surrounding the reinforcement cage tends to separate from the beam core forming an external shell. This could only be due to the development of dowel forces in the stirrups.

4. Swann (3.24) found that the yield stress of the reinforcement has no effect on this mode of failure, he also found that the ultimate torsional strength of beams failing in this mode increases with increase in the percentage of the total reinforcement.

5. Surface strain/torque relationships obtained by Swann for beams failing in this mode indicate a marked stress redistribution as ultimate torque is reached. Also the principal compressive strain measurements suggest that aggregate interlock must occur.

6. Tests by Stewart (3.43) on reinforced and prestressed concrete beams show that these failures are of cleavage type and this mode of failure continues to occur even when the dowel forces are eliminated.

This summary suggests that over-reinforced failure could occur as a result of the following:

a) Dowel forces in the longitudinal reinforcement
b) Dowel forces developing in the transverse reinforcement
c) Stresses in the concrete due to the extension of the beam (concrete spring action). This possible mode of failure will be dealt with in

3.7.1 Over-Reinforced Failure Due to Dowel Forces Developing In the Longitudinal Reinforcement.

Although the resistance of the dowel forces to the applied torque have been found to be very small, the stresses caused in the surrounding concrete due to these forces could lead to corner spalling prior to the yielding of reinforcement.

The torque at which corner spalling occurs may by found for rectangular beams with four equal bars from equations 3.35 and the Bredt-Batho equations as follows:

$$T_{1d} = 4\, X_1\, F_{1d} \left[1 + \frac{Y_1}{2S_v}\, k_1\, k_d\, \cot\theta\right] \qquad 3.47a$$

or

$$T_{1d} = 4\, Y_1\, F_{1du} \left[1 + \frac{X_1}{2S_v}\, k_1\, k_d\, \cot\theta\right] \qquad 3.47b$$

where F_{1du} is the dowel force that causes corner spalling. This force can be determined from the following expression which is developed in chapter 7:

$$F_{1du} = 3.4\, C_\ell \sqrt{f_{cu}\, C_\ell} \left[1 + 0.4 \left(\frac{\phi_\ell}{C_\ell}\right)^2\right]$$

where C_ℓ is the cover to the longitudinal corner reinforcement taken from its centre.

The contribution of aggregate interlock may also be added to equation 3.47, but since the reinforcement is stressed within the elastic range at this stage the contribution of aggregate interlock would be a function of the ratio of the

stiffness of the longitudinal reinforcement to the stiffness of the transverse reinforcement. This may be taken tentatively as follows:

$$T_{ao} = T_a \left(1 - \frac{1}{m}\right) \quad \text{for } m > 1$$

$$T_{ao} = T_a \; m \quad \text{for } m < 1$$

where T_a is as defined in equation 3.44.

3.7.2 Over-Reinforced Failure Due to Dowel Forces Developing In The transverse Reinforcement

The torque which may cause this mode of dowel failure may be obtained from equation 3.35a as follows:

$$T_{sd} = 2 \frac{F_{sdu}}{S_v} X_1 Y_1 \left[1 + \frac{2 S_v}{(X_1 + Y_1) \cot\theta} \frac{k_1}{k_d}\right]$$

where F_{sdu} is the maximum dowel force which can be resisted by the transverse reinforcement. This dowel strength will be shown in chapter 7 as:

$$F_{sdu} = 15 \; \phi_s^{7/4} \sqrt{f_{cu} \frac{C_s}{\phi_s}}$$

where C_s is the cover to the transverse reinforcement measured from its centre line.

It may be shown that this mode of failure is only possible when high strength reinforcement such as prestressing strands are used as longitudinal reinforcement in a reinforced concrete beam and hence it may be ignored.

3.8 Partial Yield-Over-reinforced Failures

The expressions for ultimate strength which were obtained previously were based on either full tensile yield strength being attained at failure in either the longitudinal or the transverse reinforcement or the stress remaining in the elastic range at failure. However, a transition mode of failure would occur as a result of some partial yielding of the reinforcements. Development of a rational theory for prediction of these modes of failure would be difficult and the use of a single expression for predicting partially over-reinforced and over-reinforced failures would be preferable. For this reason, the following semi-rational approach is suggested, equation 3.39 may be written as follows:

$$q_v = q_a + \frac{A_{sv}\, f_{sv}}{S_v} \cot \theta$$

where f_{sv} is the stress in the stirrups when corner spalling takes place. This stress may be taken to include the effect of dowel forces. Hence the ultimate torque for reinforced concrete rectangular beam becomes:

$$T_{du} = \alpha_1 \left(1 - \frac{b}{3h}\right) b^2 h\, f_t + \alpha_2 \frac{A_{sv}}{S_v} X_1\, Y_1\, f_{sv} \cot \theta$$

If we assume the stress f_{sv} in the stirrups at corner spalling to be proportional to the tensile strength of concrete and the cover to the longitudinal reinforcement (C_ℓ). It is evident that the dowel stiffness of the longitudinal reinforcement is proportional to its diameter and the dowel forces

would be inversely proportional to the diameter of the bar. Therefore, the above equation may be written after further simplifications as follows:

$$T_{du} = X_1 Y_1 \left[\alpha_1 \left(1-\frac{X_1}{3Y_1}\right) X_1 + \alpha_2 \frac{A_{sv}}{S_v} \frac{c_\ell}{\phi_\ell} \cot\theta \right] \sqrt{f_{cu}}$$

where α_1 and α_2 are coefficients which have been determined from all available test results for beams failing as partially over-reinforced and over-reinforced modes. These coefficients are:

α_1 = 0.15 for rectangular solid section beams
= 0.08 for box beams
α_2 = 22

These modes of failure were found to be influenced by the ratio of the volume of longitudinal to transverse reinforcement (m). Experimental results suggest that this equation would become:

$$T_{du} = X_1 Y_1 \left[\alpha_1 \left(1-\frac{X_1}{3Y_1}\right) X_1 + \alpha_2 \frac{A_{sv}}{S_v} \frac{c_\ell}{\phi_\ell} m^{0.6} \cot\theta \right] \sqrt{f_{cu}} \quad 3.49$$

3.9 Verification of Proposed Theory With Test Results

Tables 3.3 to 3.35 and Fig. 3.8 to Fig. 3.12 compare the theoretical predictions with experimental results for about 200 tests on reinforced and prestressed concrete beams subjected to pure torsion. These results cover a wide range of variables such as size, proportions, cross sectional shape, materials strength, m, and m'. Fig. 3.8 gives a comparison of the theoretical predictions with test results from beams where the lower predicted strength was obtained from the

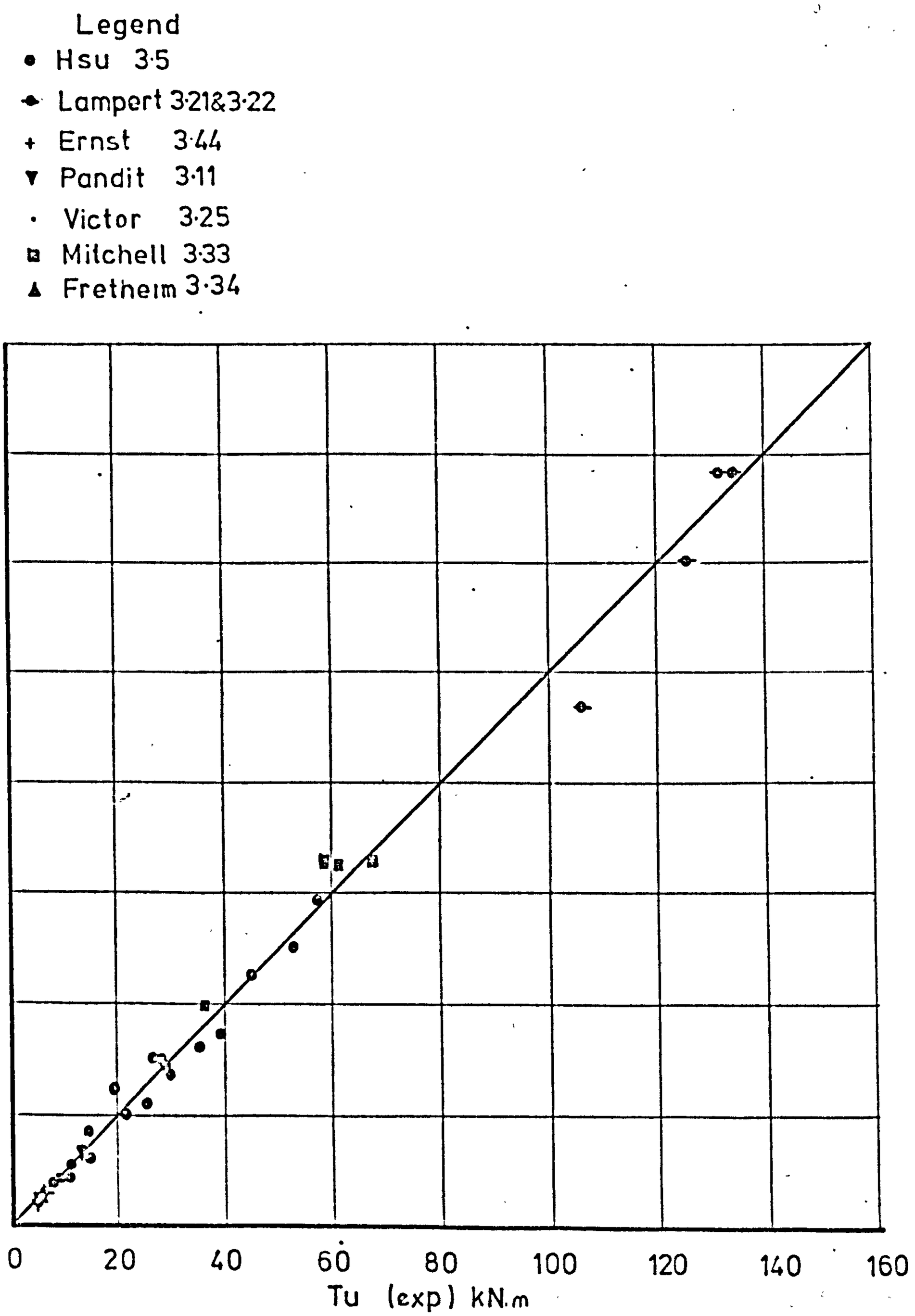

Fig 3.8 COMPARISON OF THEORETICAL PREDICTION WITH TEST RESULTS FOR BEAMS UNDER PURE TORSION (UNDER-REINFORCED FAILURE)

proposed yield theory (equation 3.40 modified by a factor $\alpha_s = 0.9$ to allow for the effect of spacing of the stirrups). Similarly Fig. 3.9 indicates that the torsional strength of under-reinforced failure with equal volume of reinforcement is directly proportional to the parameter $\frac{A_{sv}\, f_{yv}}{s_v} X_1 Y_1$, and the proposed reduction factor of 0.9 appears to be justified.

Table 3.3 gives correlation of the proposed yield theory with experimental results. The mean ratio of Ty (exp)/Ty(th) = 1.04 with coefficient of variation of 9.7 percent. This compares with the conventional yield theory where the mean ratio of Ty (exp)/Ty(th) = 0.99 and the coefficient of variation is 12.6 percent.

For beams containing different volumes of longitudinal reinforcement at the top and the bottom the smaller volume was used for the calculation of yield torque. The mean ratio of 1.09 with a coefficient of variation of 12 percent was obtained for these beams. The proportion of test beams which failed by yielding of all the reinforcement is approximately 30 percent.

Similarly Table 3.4 gives a correlation between yield theory and test results of prestressed concrete beams.

Fig. 3.10 shows correlation between experimental results for beams predicted by equation 3.45 and 3.46 to fail as partially over-reinforced. Fig. 3.11 shows a comparison between test results and theoretical predictions obtained from equation 3.47 which yielded the lowest torsional strength.

Table 3.5 gives a correlation between predicted and test results for beams where equation 3.49 produced the lowest torsional strength. The mean ratio of Tu (exp)/Tdu was 1.0 with a coefficient of variations of 14.3 percent for this mode of failure. The proportion of the test beams which were predicted to fail in this mode is approximately 60 percent.

Fig. 3.12 shows a plot of ultimate torque against reinforcement parameter $\frac{A_s f_{ys}}{Sv} X_1 Y_1$ for beams tested by Hsu (3.5) which also shows the theoretical prediction as obtained from the yield theory and the over-reinforced failure theory. These results indicate that there is a change inthe mode of failure from yield to over-reinforced at a certain value of the reinforcement parameter which is influenced by the strength of the concrete. These results illustrate that the empirical expression obtained by Hsu covers these two modes of failures although Hsu suggests that these beams are all classified as under-reinforced.

TABLE 3.3 Correlation of Yield Theories With Experimental Results For Reinforced Concrete Beams Subjected to Pure Torsion

$$T_{cr} < T_y < T_{du}$$

Investigator	Ref	Proposed Theory			Existing Theory		
		No. of Beams	Mean $\frac{Ty\ (exp)}{Ty\ (th)}$	Coefficient of Variation	No. of Beams	Mean $\frac{Ty\ (exp)}{Ty\ (th)}$	Coefficient of Variation
Hsu	3.5	16	1.1	9.10	11	1.04	4.2
Lampert and Thurlimann	3.18 3.21	7	1.03	6.80	7	0.93	7.5
Ernst	3.42	4	0.99	5.15	4	0.94	2.3
Victor	3.25	3	0.95	3.5	5	1.13	15.4
Mitchell et al	3.33	4	0.94	5.9	4	0.84	5.8
Total		34	1.04	9.7	31	0.99	12.6
Beam with unequal top and bottom longitudinal reinforcement							
Pandit	3.11	3	0.94	5.90	3	0.99	4.80
Iyenger and Rangan	3.10	10	1.14	10.14	10	1.12	10.14
McMullen and Warwaruk	3.45	2	1.02	-	2	1.09	-
Collins et al	3.32	1	1.21	-	1	1.22	-
Total		16	1.09	12	12	1.11	10.7

TABLE 3.4 Correlation of Yield Theories with Experimental Results for Prestressed Concrete Beams Subjected to Pure Torsion

$$T_{cr} < T_y < T_{du}$$

Investigator	Ref	Proposed Theory			Existing Theory		
		No. of Beams	Mean $\frac{Ty\ (exp)}{Ty\ (th)}$	Coefficient of Variation	No. of Beams	Mean $\frac{Ty\ (exp)}{Ty\ (th)}$	Coefficient of Variation
Mukherjee and Warwarak	3.47	1	0.83	-	1	0.84	-
Gangarao and Zia	3.48	5	0.83	18.64	6	0.95	14.64
Evans and Khalil	3.49	2	1.27	-	2	1.18	-
Okado et al	3.50	2	0.91	-	2	1.31	-
Superfesky	3.51	6	0.96	4.5	8	1.0	5.4
Total		17	0.93	17.8	20	1.02	15.1

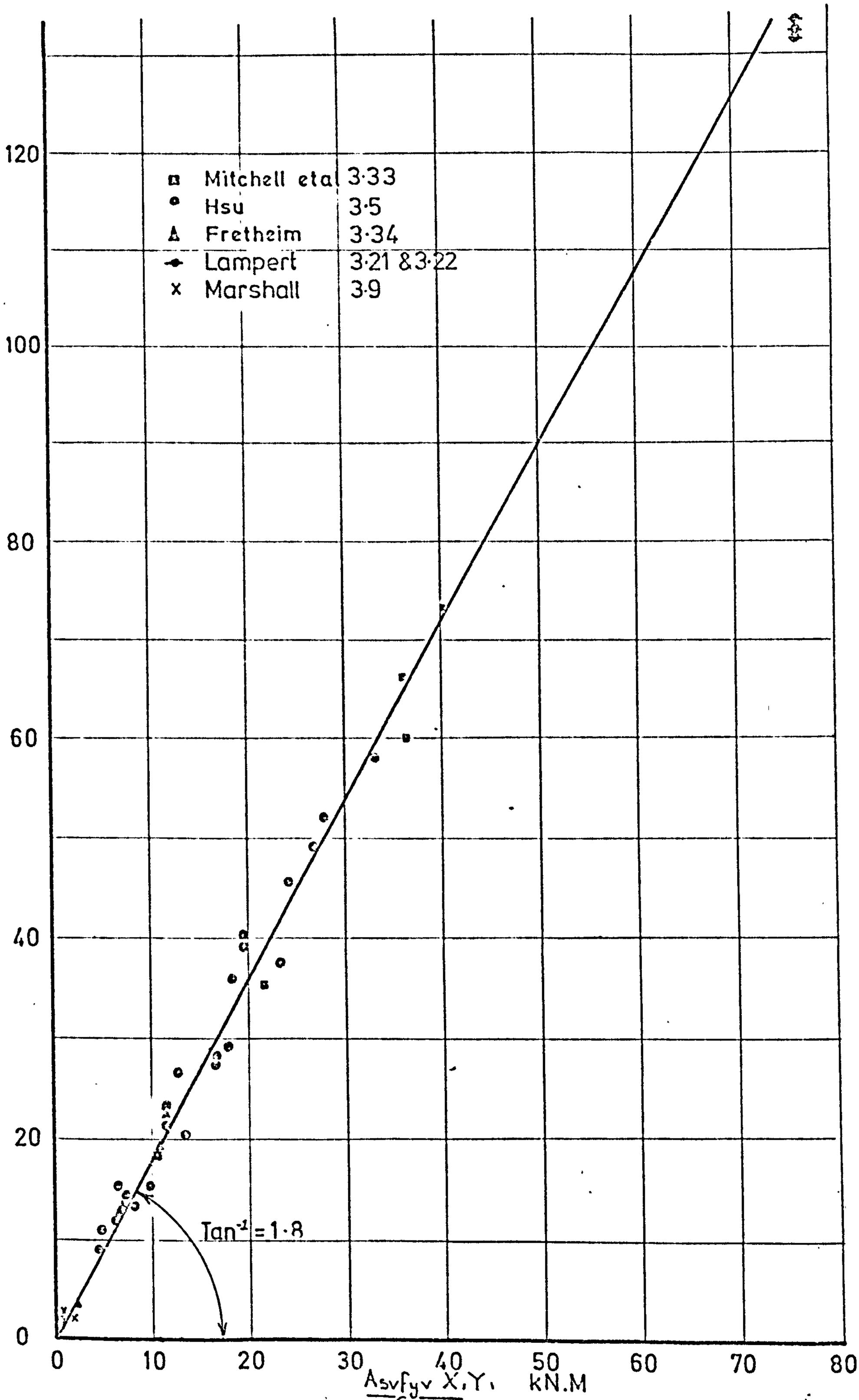

FIG.3.9 TORSIONAL CAPACITIES OF UNDER-REINFORCED BEAMS WITH $m = m' = 1$

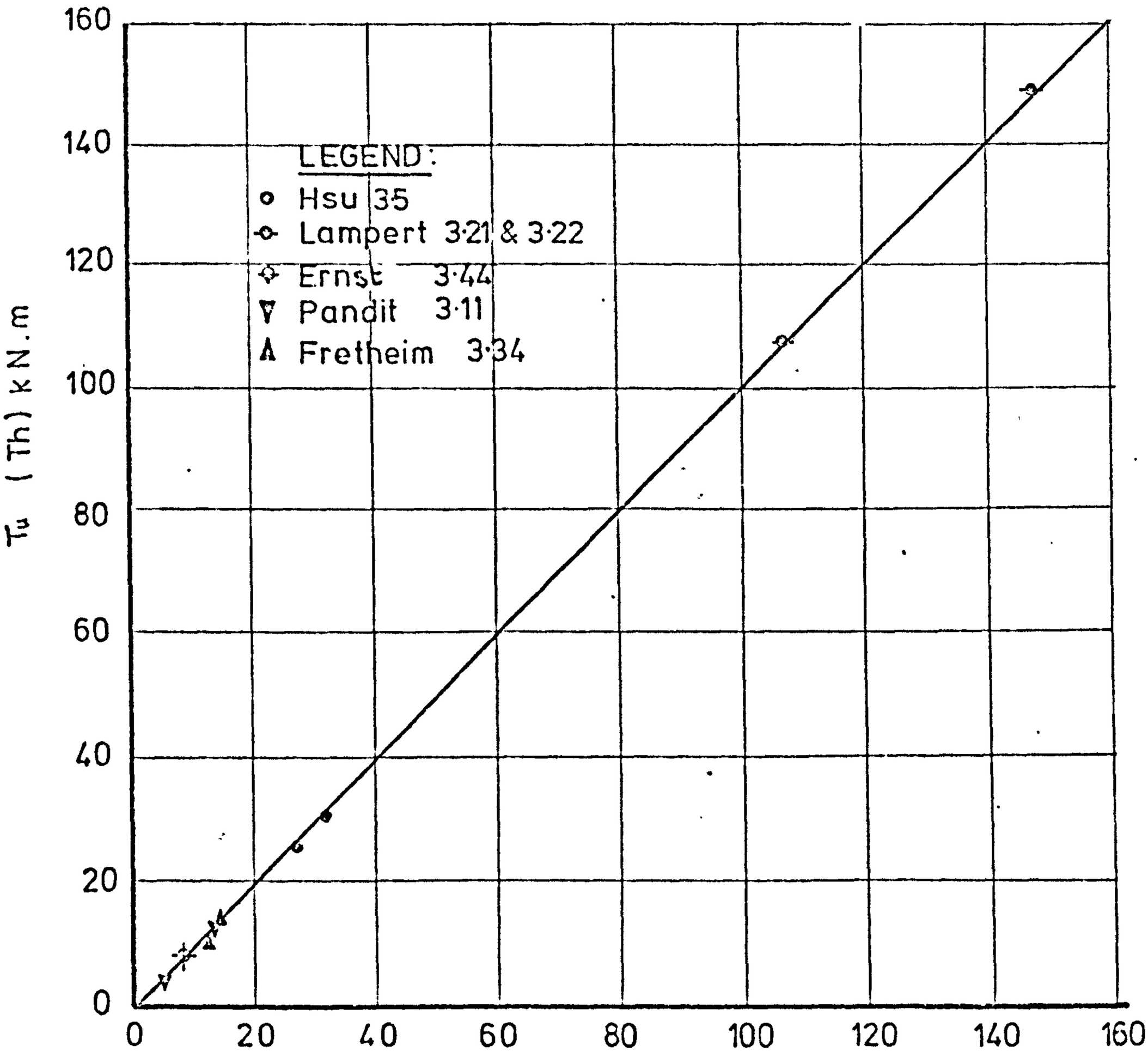

FIG 3.10 COMPARISON OF THEORETICAL PREDICTION WITH TEST RESULTS FOR BEAMS UNDER PURE TORSION (PARTIALLY-OVER REINFORCED FAILURE.)

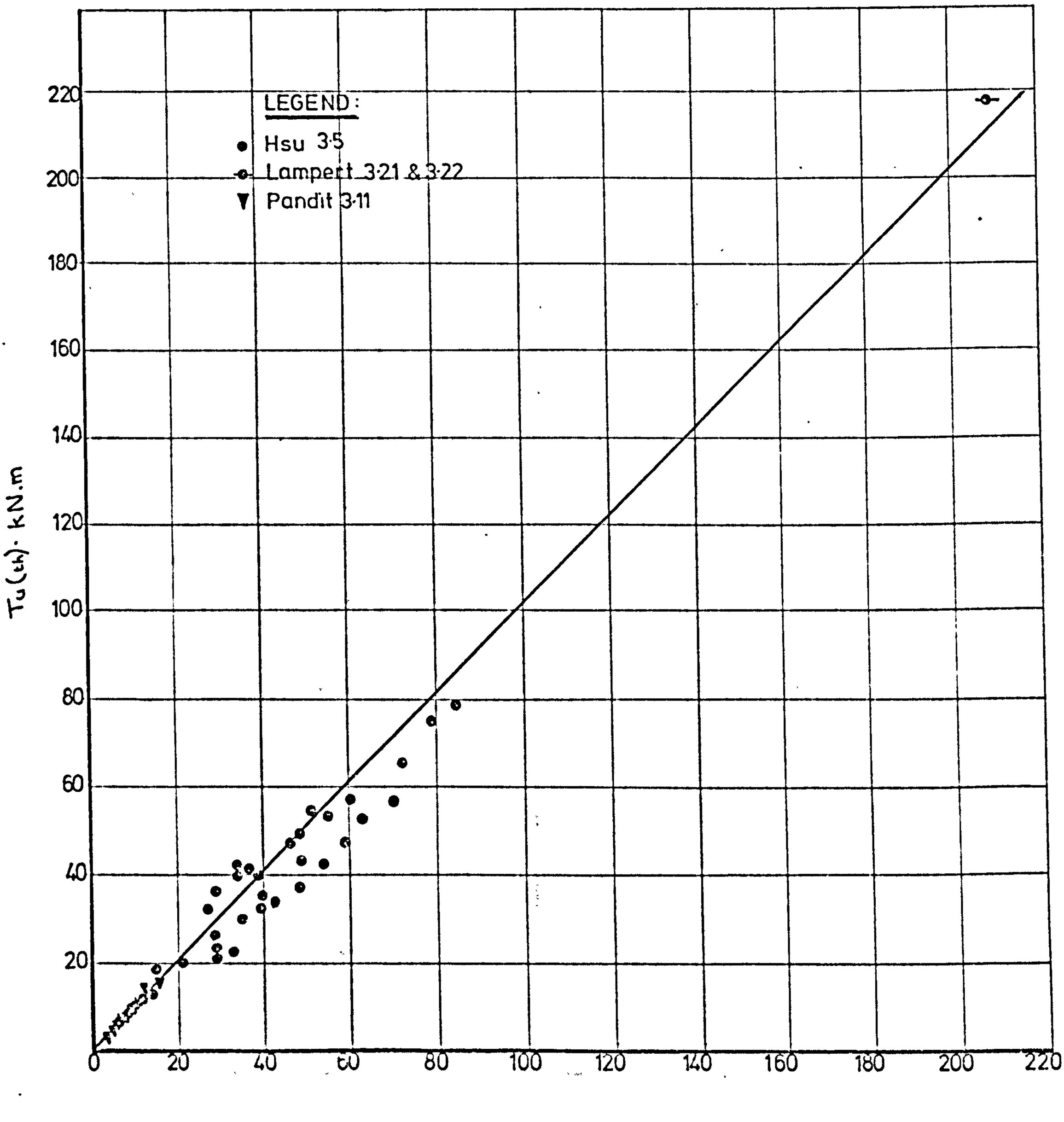

FIG 3.11 COMPARISON OF THEORETICAL PREDICTION WITH TEST RESULTS FOR BEAMS UNDER PURE TORSION (OVER-REINFORCED FAILURE)

TABLE 3.5 Correlation of Theory to Experimental Results For Reinforced Concrete Beams For Beams Subjected to Pure Torsion

$$T_{du} < T_y$$

Investigator	Ref	Number of beams	Mean $\frac{T_{u\ exp}}{T_{u\ th}}$	Coefficient of Variation %
Hsu	3.5	37	1.1	9.9
Lampert	3.18 3.23	1	0.96	-
Ernst	3.44	5	0.89	3.4
Pandit	3.11	6	1.07	8.8
Victor	3.25	3	1.25	2.3
Mitchell et al	3.33	1	1.22	-
Swann	3.23	14	0.87	7.14
Iyenger and Rangan	3.10	6	0.84	8
Evans and Sarkar	3.46	3	0.89	8.7
McMullen and Warwaruk	3.45	1	1.17	-
Collins et al	3.32	2	0.86	-
Okada et al	3.50	12	0.99	8.7
Total		97	1.00	14.3

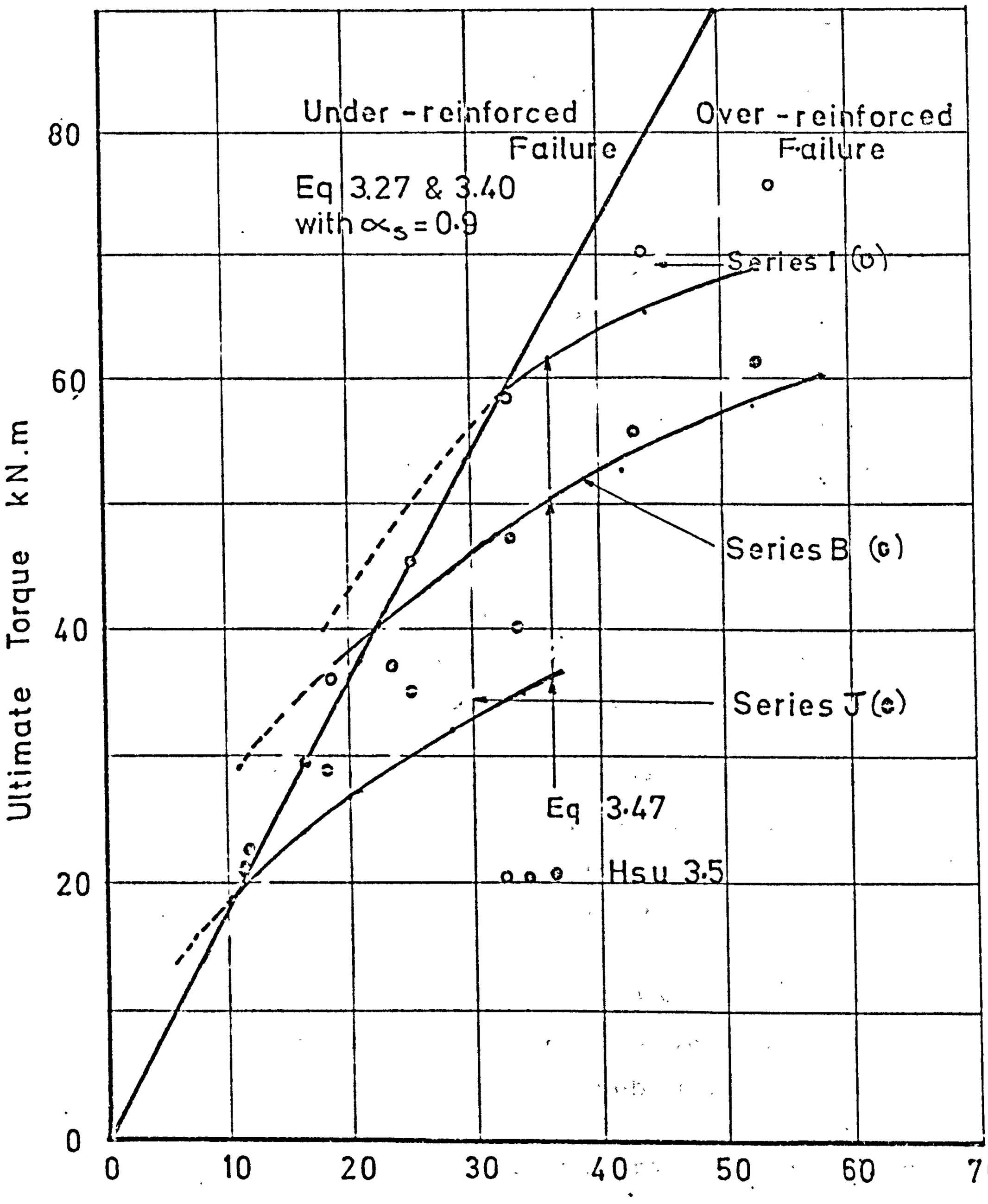

FIG 3.12 TORSIONAL STRENGTH OF BEAMS HAVING $m = m' = 1$

3.10 Conclusions

1. The existing torsional theories have been briefly reviewed and their assumptions were found not to be in agreement with test data.

2. The torsional behaviour of reinforced and prestressed concrete beams may be influenced by the spacing of the stirrups, dowel forces and aggregate interlock.

3. The torsional strength is found to decrease with increase of spacing of the stirrups.

4. It has been found that the contribution of dowel action of the longitudinal reinforcement to the resistance to torque is small compared with the truss action, hence the assumption made by Hsu (3.6), Martin (3.7) and (3.8) and Gesund (3.5) and (3.6) with regard to the contribution of dowel action is incorrect.

5. For reinforced and prestressed concrete beams failing by yielding of the reinforcement, the concrete strength and dowel actions have little influence on the resistance to torque.

6. The torsional strength of reinforced and prestressed concrete beams can be enhanced by the addition of web reinforcement.

7. For beams failing by partial yielding of the reinforcement both aggregate interlock and dowel action contribute to the resistance to the applied torque.

8. Over-reinforced failure may develop as a result of either stress induced by dowel forces or the stresses induced in the concrete due to the elongation of the beam.

9. Good agreement was found between predictions based on the proposed strength equations and experimental results.

CHAPTER 4

ULTIMATE STRENGTH OF REINFORCED AND PRESTRESSED CONCRETE MEMBERS SUBJECTED TO BENDING, TORSION AND SHEAR.

YIELD FAILURE

Summary

A theoretical analysis of the ultimate strength of reinforced and prestressed concrete beams subjected to combined bending, torsion and shear is presented. This analysis is based on the assumptions that all reinforcement crossing a critical section or failure surface reaches full axial tensile yield strength.

The effect of the angle of cracking and the length of the moment lever arm on yield failure have been examined.

Simple rules to ensure the validity of the yield theory are suggested. The proposed theory is compared with 574 reinforced and prestressed concrete beam results reported in technical literature.

4.1 Introduction

Available test data on reinforced and pre-stressed concrete beams subjected to bending, torsion and shear indicate that failure may be classified as:

1. Under-reinforced or yield failure - This denotes the failure of beams when all the reinforcement intercepting the failure zone attains its full tensile yield strength.

2. Partially over-reinforced or partial yield failure - This defines the failure of beams when either the longitudinal reinforcement or the lateral reinforcement attains its full tensile yield strength.

3. Over-reinforced failure - Failure which occurs prior to yielding of all reinforcement of the beam.

This chapter deals exclusively with the yield mode of failure and the other modes will be the subject of Chapter 5.

In 1959, Lessig (4.1 to 4.4) developed a rational ultimate strength theory for reinforced concrete beams subjected to bending, torsion and shear. In this theory, failure was considered as a result of bending about a skew neutral axis. She derived expressions for predicting the ultimate strength for two possible modes of failure. She denoted failure with the neutral axis located near and parallel to the top face of a rectangular beam as mode 1 and failure with the neutral axis located near and parallel to one side of the beam as mode 2.

Collins et al (4.5) suggested an additional mode of failure with neutral axis located near and parallel to the soffit of the beam and was denoted as mode 3.

From consideration of equilibrium and other simplifying assumptions, Lessig obtained the following expressions for determination of torsional strength for mode 1.

$$T_{y1} = A_{sl}\, f_{yl} \left[\left(d - \frac{x}{2}\right) + m\, k_2 \left(\frac{c_1}{b}\right)^2 \right]$$

$$k_2 = k_1 \left(h - c - \frac{x}{2}\right) + \frac{b}{4}\left(1 - k_1\right)\left(1 - k_1 - \frac{4c}{b}\right)$$

$$k_1 = \frac{b}{2h + b} \qquad r = \frac{A_{sv}\, f_{yv}}{S_v} \quad \frac{b}{A_{sl}\, f_{yl}}$$

$$\frac{x}{d} = \left(\frac{x}{d}\right)_o \left[\frac{1 + k_1\, r \left(\frac{c_1}{b}\right)^2}{1 + \left(\frac{c_1}{b}\right)} \right]$$

where $\left(\frac{x}{d}\right)_o$ is the depth of the compression zone/ effective depth for the case of pure bending.

$$\frac{c_1}{b} = \phi + \sqrt{\phi^2 + \frac{\left(b - \frac{x}{2}\right)}{r\, k_2}}; \quad \text{where } \phi = \frac{M}{T}$$

it can be seen that these equations are coupled and can only be solved by a trial and error process.

Since the publication of this theory, other yield theories have been developed for reinforced concrete beams subjected to bending, torsion and shear. These theories are summarised under the name of their developers in Table 4.1. It must be pointed out that all these theories have the

following common assumptions:

1. The beam has a constant cross-section.

2. The reinforcement intersecting the failure plane attains full tensile strength at failure.

3. The stirrups within the failure zone are equally spaced.

4. The reinforcement in the compression zone is neglected.

5. The concrete outside the compression zone is cracked and carries no tension.

6. The torsional resistance of the compression zone is ignored.

7. Dowel forces are neglected.

8. Aggregate interlock stresses are neglected.

9. The ratio of $\frac{M}{T}$ remains constant within the failure zone.

10. No local loads are present within the length of the failure zone.

The major differences in these theories are:

i. Definition of the shape of the failure surface and the direction of the axis about which the beam rotates.

ii. The strength of the compression zone or the assessment of the lever arm for the longitudinal tensile reinforcement at failure.

iii. The formation of the equilibrium equations.

The treatment used for each of the available yield theories regarding these three problems are

summarized in Table 4.1 together with the loading condition which was assumed, the applicability of the theory and the modes of failure which were considered.

4.1.1 Definition of the shape of the failure surface

The following definitions refer to the angles of cracking θ assumed by various authors as listed in Table 4.1.

θ_1 - Lessig assumed the failure surface was composed of three straight lines spirally around the beam at a constant angle. This angle was obtained from consideration of equilibrium of forces at failure. The beam was assumed to bend about a neutral axis joining the ends of this crack. The inclination of the cracks obtained from this method does not agree generally with the angles of cracks measured in experimental work.

θ_2 - Yudin (4.6) suggested later that this angle be taken as constant on each surface at 45^o to the beam axis. This assumption was found to produce a considerable simplification in the solution of the problem at the expense of accuracy of prediction of test results which indicate that it is a conservative assumption.

θ_3 - Gesund et al (4.7) assumed that the failure surface is composed of a crack at an angle of 45^o on the side of the beam and at variable angles on the soffit of the beam. From experimental data an angle of 90^o was suggested for beams subjected to $\frac{T}{M}$ less than 0.25 and 63.5^o if $\frac{T}{M}$ is greater than 0.25. These assumptions would lead to a discontinuity

in the strength equations at $\frac{T}{M} = 0.25$. The beam was assumed to rotate at failure about an axis parallel to the longitudinal axis and lying on the top face of the beam.

θ_4 - Evans and Sarker (4.8) developed another yield theory which also considered the basic mechanism of a spiral tension crack on the three sides of the beam and neutral axis near the fourth face. The shape of the tension spiral was determined from the direction of the principal tensile stresses on the soffit of the beam prior to cracking. This crack was assumed to propagate from the soffit of the beam at a constant angle of inclination and to extend to almost half the depth. The remaining part of this tension crack was then taken at 45^{o}. Failure was assumed to occur above the neutral axis inclined at 45^{o} to the beam axis. These assumptions and those made earlier by Yudin and Gresund are not in agreement with actual crack inclinations measured in experiments, particularly in cases where the loading on the beam approaches the pure bending case.

θ_5 - Fairbairn and Davis (4.10) presented an improved and simplified version of Evans' theory. In this theory the tension cracks defining the failure surface on the three sides of the beam are composed of three straight lines spiralling around the beam at a constant angle up to the neutral axis of the beam. This angle was governed by the principal stress at the soffit of the beam prior to cracking. The line connecting the ends of this crack was taken as the neutral axis of the beam. Hence, for the case of pure bending the

crack was vertical and the direction of the neutral axis was in agreement with the position of the pure bending theory case. They have also suggested simple expressions to define the angle and inclination of the crack.

4.1.2 The Strength of The Compression Zone

Z1 - Lessig obtained the depth of the compression zone by equating the compressive forces perpendicular to the failure surface, to the components of the tensile forces in the steel. The effect of shear stresses on the strength of the compression zone have been ignored in this approach. Later Lessig suggested the following empirical expression for the depth of the compression zone in order to simplify the calculation of the torsional strength of the beam.

$$\frac{x}{d} = \frac{\sum A_{sl}\, f_{yl} - \sum A'_{sl}\, f'_{yl}}{f'_c\, bd} \qquad (1 + \frac{5}{\psi})$$

Z2 and Z3 - Many research workers suggested a constant lever arm factor for the determination of the torsional strength of beams subjected to bending and torsion. Lampert et al (4.11) considered the distance between the top and bottom longitudinal reinforcement as the lever arm whereas Gesund (4.7) considered the lever arm to be the distance between the tension reinforcement and the extreme compression fibre of the beam.

Z4 - Collins et al (4.5) succeeded in simplifying Lessig's theory by assuming the depth of the compression zone to be that of the pure bending case. They based their assumptions on the statement that considerable variations of the value of $\frac{x}{d}$ will have

little effect upon the ultimate torsional strength of the beam. Hence they were able to eliminate the calculations for the depth of the compression zone which were necessary in Lessig's theory.

Z5 - In 1973, Martin developed a theory similar to that of Collins et al (4.19) but considered the effect of shear stresses due to torsion on the strength of the compression zone. This theory may be criticised for its complexity, the use of an incomplete failure criterion and incorrect assumptions regarding the distribution of the shear stresses due to torsion.

4.1.3 Formation of Equilibrium Equations

In deriving the ultimate torsional strength equations for reinforced concrete beams subjected to bending and torsion the following techniques have been used:

E1 - Lessig formulated one quilibrium equation by equating moments of forces about an axis perpendicular to the neutral axis and optimising the torsional strength equation with respect to the length of the compression zone.

E2 - Yudin (4.6) derived his torsional strength equation by taking moments of external and internal forces along both the longitudinal and transverse axis passing through the centroid of the skew compression zone.

E3 - Gesund and his co-authors considered the equilibrium of moments about the longitudinal axis of rotation which is parallel to the axis of the beam and an axis perpendicular to it.

TABLE 4.1 Comparison Between Yield Theories For Reinforced and Prestressed Concrete Members Subjected to Combined Bending and Torsion, Bending torsion and shear.

Investigator	Ref	Year	Mode of Failure	Inclination of Failure crack θ	Lever arm z	Equilibrium Method Used E	Loading case	Application
Lessig	4.1	1959	1 & 2	1	Z1	E3	B & T B,T & S	R.C.
Yudin	4.6	1962	1	2	Z2	E2	B & T	R.C.
Gesund et al	4.7	1964	1	3	Z3	E3	B & T B,T & S	R.C.
Evans & Sarkar	4.8	1965	1	4	Z1	E2	B & T	R.C.
Collins et al	4.5	1966	1,2 & 3	1	Z4	E4	B & T B,T & S	R.C.
Fairbairn & Davies	4.10	1969	1	5	Z1	E2	B & T	R.C.
Lampert & Thurlimann	4.11	1969 1971	1,2 & 3	1	Z2	E3	B & T	R.C. & P.S.C.
Elfgreen	4.15	1971	1,2 & 3	1	Z2	E5	B & T B,T & S	R.C.
Kuyt	4.16	1971	1,2 & 3	1	Z2	E3	B,T & S	R.C.
Martin	4.14	1972	1,2 & 3	1	Z5	E4	B & T	R.C.
Hall et al	4.17	1973	1,2 & 3	1	Z4	E4	B,T & S	P.S.C.

R.C. = Reinforced Concrete P.S.C. = Prestressed Concrete Beam

B & T = Beams subjected to Bending and Torsion

B,T & S = Beams subjected to Bending, Torsion and Shear

E4 - Collins and his co-workers obtained their torsional strength equations from one equilibrium moment equation taken about the skew neutral axis. This equation involved an angle of failure plane as a variable. The torsional resistance was then obtained by optimising this equation.

E5 - Lampert and Thurlimann (4.11) have extended their space truss analogy to the case of bending and torsion.

4.1.4 Comments on Existing Yield Theories

From this brief review the following comments can be made:

1. Unlike the rational theories for prediction of ultimate strength under pure bending, these theories exclude the condition of compatibility of deformation, therefore the steel strain at failure cannot be determined analytically and for this reason some authors have empirical expressions in their theories to ensure their validity.

2. Due to the large number of assumptions made for these theories, considerable restrictions have been imposed by their developers, hence making them less attractive for practical applications.

3. No comparative studies are available in the relatively new yield theories although an attempt has been made (4.18) to compare the earlier yield theories.

4. Some yield theories such as those suggested by Lessig and Martin (4.14) are cumbersome for use in practical situations and hence no conclusive

work is available to show the effect of simplifications made by other theories on the accuracy of prediction of test results.

5. Recent test evidence (4.19) indicates that there are considerable differences between the axis of rotation assumed for the skew bending theory and the experimental values. Similarly the angles of cracking assumed by Lessig, Collins, Lampert, Martin etc. differ from those measured experimentally.

6. Table 4.1, indicates that most of the existing yield theories do not cover the case of beams subjected to bending, torsion and shear which is the most important loading case that would be encountered in practice. Similarly most of these theories have been developed for the case of reinforced concrete beams and only recently has the problem of prestressed concrete beams been studied.

Therefore, the aims of this Chapter are as follows:

a. To propound a rational yield theory based on more acceptable assumptions.

b. To consider the effect of various assumptions with regard to the angle of cracking on the torsional strength.

c. To examine the effect of various simplifications regarding the depth of the compression zone.

d. To determine rationally the boundary conditions for yield failure.

4.2 Proposed Yield Theory

General Assumption

Reported test evidence on the behaviour of reinforced concrete and prestressed beams subjected to bending and torsion suggest that the position of the shear centre varies at different stages of the beam loading. It's position is influenced by cracking and inelasticity, for example, for beams failing according to mode 1 of Lessig's classification, the shear centre is known to lie in the compression zone and for mode 2 the position of the shear centre is known to move to one side of the beam and for mode 3 it is found to lie near the soffit of the beam. Also these test results indicate that the assumption of planes before bending remaining plane after bending is reasonably valid for this general case of loading.

Therefore, it is expedient to classify the modes of failure as follows:

Mode 1.

This mode of failure is defined as occuring when the stirrups and the longitudinal reinforcement located near the soffit of the beam reach their full tensile strength at the critical section of the beam. For this mode of failure, the shear centre is assumed to coincide with the point ofintersection of the centre line of the stirrups at the top of the beam with the vertical axis of symmetry of the beam as shown in Fig. 4.1. The angle of inclination of the cracks is assumed to be governed by the direction of the principal stresses at the soffit of the beam prior to cracking.

Mode 2

This mode of failure is defined as the case where both the stirrups and the longitudinal reinforcement located along one face of the beam reach their full tensile yield strength. This mode usually occurs at low values of applied moment. Consequently the neutral axis may be assumed to remain unchanged after cracking since all four sides of the beam would be cracked. The point of intersection of this neutral axis with the centre line of the stirrup leg contains the unyielded longitudinal reinforcement and may be taken as the shear centre.

Mode 3

This mode is assumed to occur as a result of the stirrups and the top longitudinal reinforcement reaching their full tensile yield strength. Since this failure will occur for beams with smaller top longitudinal reinforcement and under approximately pure torque loading condition, then the position of the neutral axis may be taken as that for mode 2 and the position of the shear centre may be taken as the point of intersection of the stirrup leg on the tensile face of the beam with the vertical axis of symmetry of the beam.

It must be noted that the position of the shear centre would not influence the derivation of the following torsional strength equations.

Since the reinforcement has been assumed to develop its full tensile strength, the dowel forces may be neglected.

4.2.1 Analysis of Mode 1

The strength of the rectangular box beam shown in Fig. 4.1 will be studied. The failure of an element cut from the bottom flange assumed in this analysis to correspond to the failure of the beam.

From the equilibrium of the horizontal forces acting on this element we have:

$$F_z + q_t \cot \theta_1 = m'_b \frac{A_{sv} f_{yv}}{Sv} - q_a \cot \theta_1 \qquad 4.1$$

where F is the direct force acting on this element due to bending and, q_s is the shear flow due to the applied torque acting on the beam at failure

$$m'_b = \frac{\sum Asl\ fyl}{(X_1 + Y_1)} \quad \frac{S_v}{A_{sv} f_{yv}}$$

q_a is the shear flow resisted by aggregate interlock
A_{sv} area of stirrups, S_v spacing of stirrups and
f_{yv} is the yield stress for the stirrups.

From the equilibrium of vertical forces acting on this element we have:

$$q_t = \frac{A_{sv} f_{yv}}{S_v} \cot \theta_1 + q_a \qquad 4.2$$

Eliminating q_a between equation 4.1 and 4.2 and rearranging

$$F_z + 2q_t \cot \theta_1 = \frac{Asv\ fyv}{S_v} \left[\cot^2 \theta_1 + m'_{b1} \right] \qquad 4.3$$

but

$$q_t = \propto \frac{T_{y1}}{2X_1\ Y_1}, \quad F_z = \frac{M}{(X_1 + Y_1)\ Z} \quad \text{and } \psi = \frac{M}{T}$$

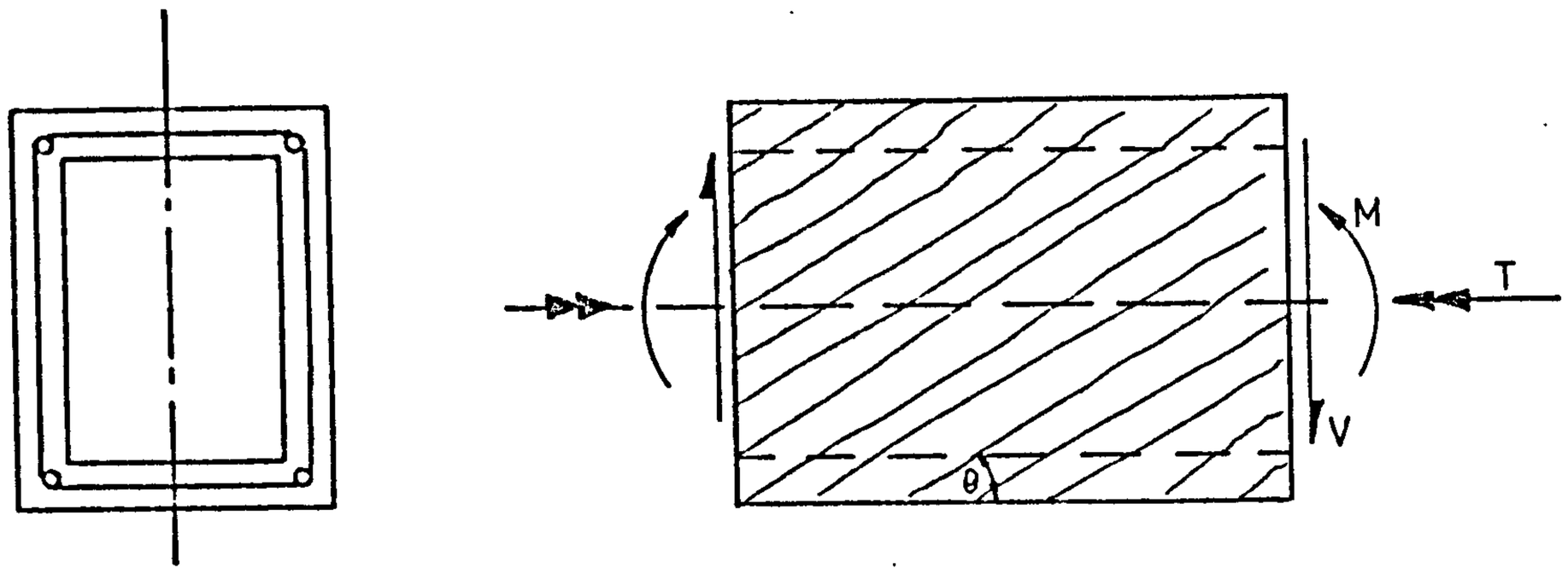

FIG 4.1. Forces Acting on Rectangulor Element at Failure For Beam Subjected to Bending — Torsion and Shear.

where z is a lever arm for longitudinal reinforcement and α is a factor representing the fraction of the applied torque being resisted by the reinforcement and $(1 - \alpha)$ represents the fraction of the applied torque being resisted by the compression zone.

Substituting these values into equation 4.3 and rearranging we obtain:

$$\frac{T_{y1}}{T_s} = \frac{k_z}{2}\left[\frac{\cot^2\theta_1 \; 1 + m_b'}{\frac{\alpha}{k_z}\cot\theta_1 + \frac{\psi}{\left(1 + \frac{Y_1}{X_1}\right)}}\right] \qquad 4.4$$

where $k_z = \frac{z}{Y_1}$ and

$$T_s = \frac{2\, A_{sv}\, f_{yv}}{S_v} \quad X_1\, Y_1$$

it is evident that an increase in the percentage of the reinforcement for any given beam will result in a decrease in the values of k_z and α. Therefore, for simplicity $\frac{\alpha}{k_z}$ may be taken as a constant and can be approximated to unity, then

$$\frac{T_{y1}}{T_s} = \frac{k_z}{2}\left[\frac{\cot^2\theta_1 + m_b'}{\cot\theta_1 + \frac{\psi}{\left(1 + \frac{Y_1}{X_1}\right)}}\right] \qquad 4.5$$

where $\cot\theta_1 = \sqrt{1 + \frac{f_{pl}}{f_{tl}} + \left(\frac{Z_{tl}}{2Z_1}\right)^2} - \left(\frac{Z_{tl}}{2Z_1}\right)$

equation 4.5 may be written in interaction form as follows:

$$\frac{T_{y1}}{T_s}\cot\theta_1 + \frac{M}{M_u}\frac{k_z\, m_b'}{2} = \frac{k_z}{2}\left(\cot^2\theta_1 + m_b'\right) \qquad 4.6$$

where M_u is the flexural strength of the beam under

pure moment condition.

If the angle of cracking is to be taken as equal to the angle of inclination of the compressive field at failure as asssumed by Lessig, Collins etc. then the inclination of θ_1 may be found by determining the lowest failure torque from equation 4.5. This means that:

$$\frac{d\,Ty_1}{d\,\theta_1} = 0$$

therefore,

$$\left(\cot\theta_1 + \frac{\psi}{(1 + \frac{Y_1}{X_1})}\right) \frac{d}{d\theta_1} \left(\cot^2\theta_1 + m_b'\right) - \left(\cot^2\theta_1 + m_b'\right)$$

$$\frac{d}{d\theta_1}(\cot\theta_1) = 0$$

This leads to

$$\cot\theta_{min} = \sqrt{m_b' + \left(\frac{\psi}{1 + \frac{Y_1}{X_1}}\right)^2} - \frac{\psi}{1 + \frac{Y_1}{X_1}} \qquad 4.7$$

when this value of Cot is substituted into equation 4.5 we get:

$$\frac{T}{T_s} = k_z \left[\sqrt{m_b' + \left(\frac{\psi}{1 + \frac{Y_1}{X_1}}\right)^2} - \frac{\psi}{1 + \frac{Y_1}{X_1}}\right] \qquad 4.8$$

This form of equation has been produced previously by Collins et al using the skew bending approach Equation 4.8 can be written in a general interaction form as follows:

$$\frac{1}{m_b'} \left(\frac{T_{y1}}{T_s\, k_z}\right)^2 + \frac{M}{M_u} = 1 \qquad 4.9$$

If θ_1 is taken equal to 45^o as assumed by Yudin, then

equation 4.4 becomes:

$$\frac{T_{y1}}{T_s} = \frac{k_z}{2}\left[\frac{1 + m'_b}{1 + \frac{\psi}{1 + \frac{Y_1}{X_1}}}\right] \qquad 4.10$$

From longitudinal equilibrium of forces acting on the section under consideration, then

$$\sum \left(A_{sl}\, f_{yl} - A'_{sl}\, f'_{yl}\right) = k_{sc}\, k_1\, f_{cu}\, bx \qquad 4.11$$

where k_{sc} is a reduction factor representing the effect of shear stresses on the compression zone and k_1 is a ratio of the average compressive stresses in the compressive zone of the beam at flexural failure to the cube strength.

The expression for the lever arm is:

$z = d - k_2 x$, where k_2 is the distan e from the extreme compressive fibre to the compressive force resultant. From this relationship and equation 4.11 we may obtain:

$$k_z = \frac{d}{Y_1}\left[1 - \frac{k_2}{k_1\, k_{sc}}\left(P\,\frac{f'_{yl}}{f_{cu}} - P'\,\frac{f'_{yl}}{f_{cu}}\right)\right] \qquad 4.12$$

where $P = \frac{A_{sl}}{bd}$ and $P' = \frac{A'_{sl}}{bd}$

It can be shown that $\frac{k_2}{k_1}$ is constant for a wide range of concrete strengths and has a value of $\frac{3}{4}$, if the rectangular parabolic stress block suggested in CP 110 is used, then equation 4.12 becomes

$$k_z = \frac{d}{Y_1}\left[1 - \frac{3}{4k_{sc}}\left(P\,\frac{f_{yl}}{f_{cu}} - P'\,\frac{f'_{yl}}{f_{cu}}\right)\right]$$

The value k_{sc} depends on the distribution of shear and direct stresses in the compression zone as well as the strength of concrete under combined shear compression. Collins et al (4.5) found that the torsional strength can be predicted accurately by putting k_{sc} = unity.

Yielding of the compression reinforcement can be ascertained from the compatibility condition used in the analysis of strength under pure bending.

4.2.2 Analysis of Mode 2

From equilibrium of the horizontal forces acting on an element cut from the side of the beam shown in Fig. 4.1

$$q.\,\mathrm{Cot}\,\theta_2 = m_b' \frac{A_{sv}\, f_{yv}}{S_v} \left(\frac{R_y + 1}{2}\right) - q_a\,\mathrm{Cot}\,\theta_2 \qquad 4.13$$

where $R_y = \dfrac{\sum A'_{sl}\, f'_{yl}}{\sum A_{sl}\, f_{yl}}$

From equilibrium of the vertical forces acting on this element we obtain:

$$q = \frac{A_{sv}\, f_{yv}}{S_v}\,\mathrm{Cot}\,\theta_2 + q_a \qquad 4.14$$

Eliminating q_a between equation 4.13 and 4.14 and rearranging:

$$q = \frac{A_{sv}\, f_{yv}}{S_v}\left[\frac{\mathrm{Cot}^2\ 2 + m_b'\ \left(\frac{Ry + 1}{2}\right)}{2\,\mathrm{Cot}\,\theta_2}\right] \qquad 4.15$$

where q is the shear flow due to torque and the applied shear force acting on this element.

As a result of the yielding of reinforcement on one side of the beam, the shear stiffness of this side would become zero, consequently the applied shear force will be resisted by the other side. Also as a result of this yielding and the shift of the shear centre to one side of the beam, the applied shear force will give rise to an additional torque on the section equal to $\frac{VX_1}{2}$. Therefore, the total torque acting on this section becomes:

$$T_t = T + \frac{VX_1}{2} = T \left(1 + \frac{\delta y}{2}\right) \qquad 4.16$$

where $\delta_y = \frac{VX_1}{T}$

Now the total shear flow acting on this element becomes:

$$q = \frac{T_t}{2X_1 Y_1} = \frac{T}{2X_1 Y_1} \left(1 + \frac{\delta_y}{2}\right)$$

Substituting this expression into equation 4.15 and rearranging we have:

$$\frac{T_{y2}}{T_s} = \left[\frac{\cot^2\theta_2 + m_b' \left(\frac{R_y + 1}{2}\right)}{2 \cot\theta_2 \left(1 + \frac{\delta y}{2}\right)}\right] \qquad 4.17$$

where $\cot\theta_2 = \sqrt{1 + \frac{f_{p2}}{f_{t2}}}$ which for reinforced concrete is equal to unity.

However, if the angle of cracking is taken as equal to the angle of inclination of the compressive field at failure, then θ_2 is obtained by equating $dT/d\theta_1$ to zero as follows:

$$\cot\theta_2 = \sqrt{m_b' \left(\frac{R_y + 1}{2}\right)}$$

when this value is substituted into equation 4.17 the failure torque for this mode is obtained as

$$\frac{T_{y2}}{T_s} = \frac{1}{(1 + \frac{\delta y}{2})} \sqrt{m_b' \quad \frac{(R_y + 1)}{2}} \qquad 4.18$$

Alternatively the shear flow acting on this element may be considered as the sum of the shear flow due to torsion and shear force:

$$q = q_t + q_v$$

$$q = \frac{T}{2X_1 Y_1} + \alpha \frac{V}{2Y_1} = \frac{T}{2X_1 Y_1} (1 + \alpha \delta y_1) \qquad 4.19$$

where α represents the fraction of the shear force being resisted by the reinforcement. It is evident from above that α has a value lying between ½ and 1.

4.2.3 Analysis of Mode 3

From equilibrium of horizontal and vertical forces acting on an element of the compression flange shown in Fig. 4.1 we have after combining and rearranging:

$$- F_z + 2q_t \cot\theta_3 = \frac{A_{sv} f_{yv}}{S_v} \left(\cot^2\theta_3 + m_b' \quad R_y\right) \qquad 4.20$$

$$\text{but } q_t = \frac{T_{y3}}{2X_1 Y_1} \quad \text{and } F_z = \frac{M}{(Y_1 + X_1) Y_1}$$

equation 4.20 becomes after rearranging:

$$\frac{T_{y3}}{T_s} = \frac{1}{2} \left[\frac{\cot^2\theta_3 + m_b' \quad R_y}{\cot\theta_3 - \frac{\psi}{1 + \frac{Y1}{X_1}}} \right] \qquad 4.21$$

Since cracking of beams failing in this mode will usually be initiated at the side of the beam and

propagate to the top and bottom of the beam, $\cot\theta_3$ may be taken as $\sqrt{1+\frac{fp2}{ft2}}$ and for reinforced concrete beams may be taken as 1.

However, if the angle of cracking is taken as equal to the angle of inclination of the compression field at failure, then θ_3 is obtained by equating $dT/d\theta_3$ to zero and the failure torque for this mode becomes:

$$\frac{T_{y3}}{T_s} = \sqrt{m'_b \; R_y + \left(\frac{\psi}{1+\frac{Y_1}{X_1}}\right)^2} + \frac{\psi}{1+\frac{Y_1}{X_1}} \qquad 4.22$$

An examination of equation 4.22 reveals that the minimum torsional strength will correspond to the lowest value of ψ. This would occur at the cross section subjected to the minimum bending moment e.g. near the support of simply supported beam. Since this mode of failure usually takes place over a finite length of the beam after considerable stress redistribution, the critical section at which failure occurs may be taken as $(X_1 + Y_1)\cot\theta_2$ from the support, therefore ψ_{max} may be reduced by the ratio of $\frac{(X_1 + Y_1)\cot\theta_2}{a}$ where a is the shear span measured from the support to the first point load. Consequently ψ max is calculated from the bending moment at the first point load.

This equation may be written in the following simple dimensionless form:

$$\frac{1}{m'_b}\left(\frac{T}{T_s}\right)^2 - k_z \frac{M}{M_u} = R_y \qquad 4.23$$

4.3 Alternative Yield Theory

The strength equations for the three modes of failure can also be obtained by a study of the equilibrium conditions of equilibrium for the free body diagram for the box beam shown in Fig. 4.2. If it is assumed as before, that $\theta_a = \theta_b = \theta_c = \theta$ The beam to be studied has the same notations and geometrical properties as the beams studied in the preceding section.

Taking moments about the z axis at point O;

$$T = 2\frac{A_{sv}\ f_{yv}}{S_v}\ X_1\ Y_1\ \cot\theta + 2\ q_a\ X_1\ Y_1 \qquad 4.24$$

Now, taking moment about the x axis:

$$M = 2\ A_{sl}\ f_{yl}\ z - \frac{A_{sv}\ f_{yv}}{S_v}\ (X_1 + Y_1)\ \cot^2\theta - 2q_a Y_1 (X_1+Y_1)\ \cot\theta \qquad 4.25$$

To simplify the analysis it is further assumed that $z = Y_1$, and eliminating q_a between these two equations we have:

$$\frac{M}{\left(1 + \frac{Y1}{X_1}\right.} + T\ \cot = \frac{2\ A_{sl}\ f_{ylY_1}}{1 + \frac{Y_1}{X_1}} + \frac{A_{sv}\ f_{yv}}{S_v}\ X_1\ Y_1\ \cot^2\theta$$

rearranging this equation we get:

$$\frac{T}{T_s} = \frac{1}{2}\left[\frac{m'_b + \cot^2\theta}{\cot\theta + \frac{\psi}{1 + \frac{Y_1}{X_1}}}\right] \qquad 4.26$$

This equation is the same as equation 4.10.

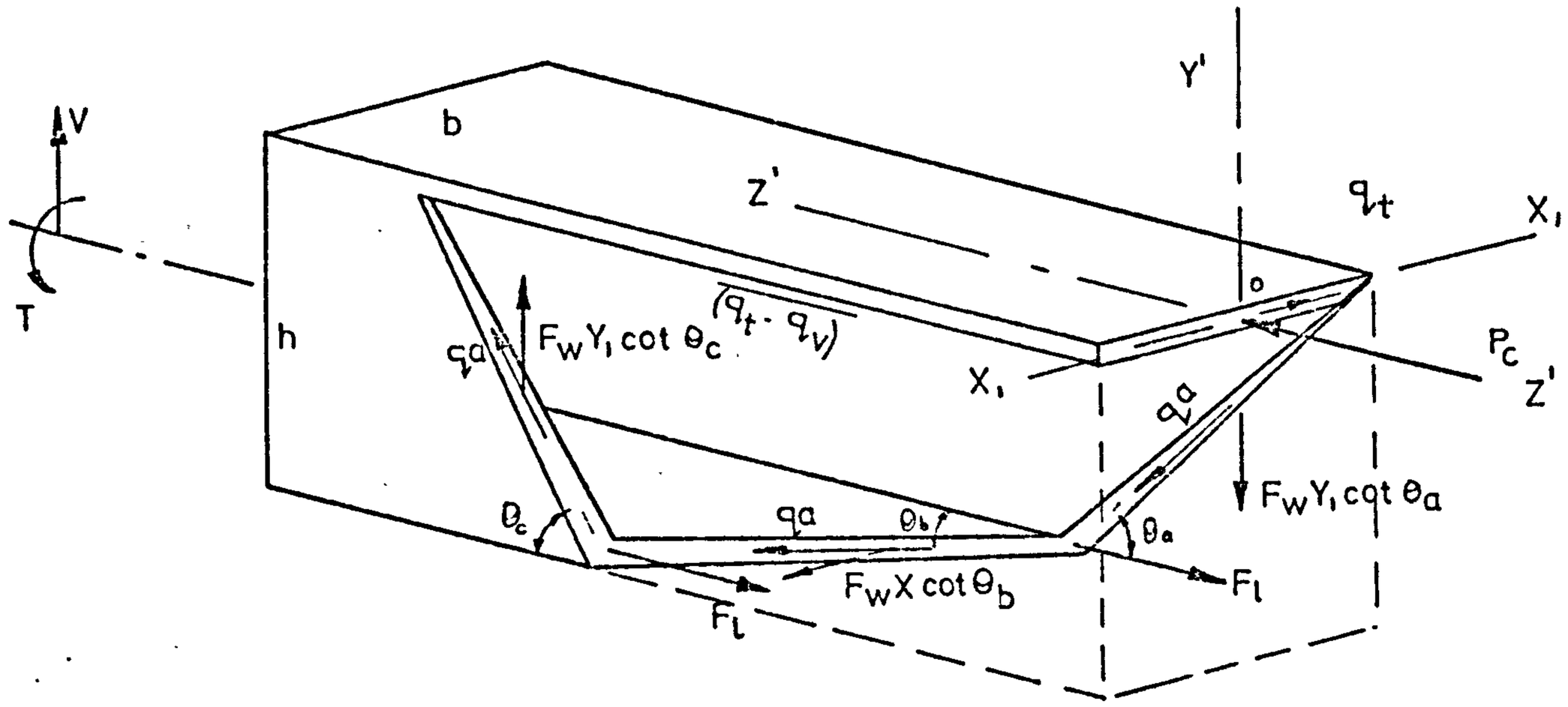

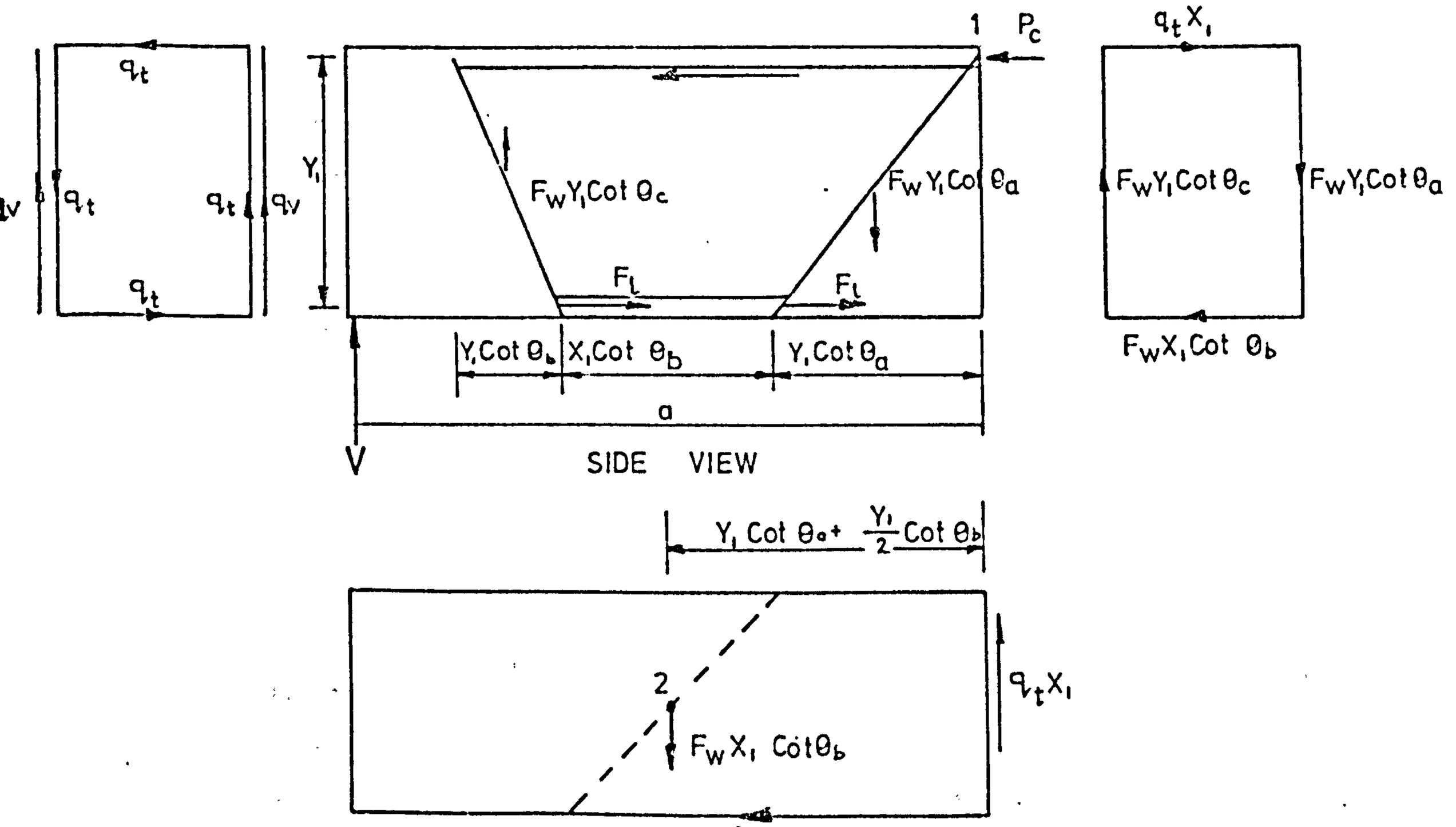

FIG 4.2 Failure Surface For Beam Subjected to Bending, Torsion and Shear according to Mode 1

In deriving equation 4.5, 4.8, 4.17, 4.18 and 4.21, it was assumed that failure occurs at one cross section of a beam whereas equation 4.25 considers failure to occur over a finite length of a beam. Hence, for beams having a varying bending moment over its length, the second method of analysis may over estimate its torsional strength.

Examination of the forces acting on the free body diagram shown in Fig. 4.2 reveals that the vertical forces acting in the z - y plane do not satisfy the condition of equilibrium unless different crack angles are considered for the analysis of mode 1 type of failure. Hence, the assumption of constant crack inclination that has been made by most previous investigators cannot be justified for this reason when the beam is subjected to bending, torsion and shear.

In order to examine this problem the crack angles on the side of the bottom of the beam are assumed to have different values and may be written as follows:

$$a = \cot\theta_a$$
$$b = \cot\theta_b$$
$$c = \cot\theta_c$$

To simplify the analysis, the stresses due to aggregate interlock are ignored. From vertical equilibrium of forces acting on the free body diagram shown in Fig. 4.2:

$$V = Y_1 \frac{A_{sv}\, f_{yv}}{S_v} (a - c)$$

this may be written as

$$\frac{V}{2Y_1} = q_v = \frac{A_{sv}\, f_{yv}}{S_v} (a - c) \qquad 4.27$$

From the consideration of equilibrium of forces acting in the x - Z plane and in the direction of x, we obtain:

$$q_t X_1 = \frac{A_{sv} f_{yv}}{Sv} X_1 b$$

$$q_t = \frac{A_{sv} f_{yv}}{Sv} b \qquad 4.28$$

Taking moments about the Z axis at point O we get:

$$T = \frac{A_{sv} f_{yv}}{Sv} \left(\frac{a}{2} + b + \frac{c}{2} \right) X_1 Y_1 \text{ , or}$$

$$q_t = \frac{A_{sv} f_{yv}}{Sv} \left(\frac{a}{4} + \frac{b}{2} + \frac{c}{4} \right) \qquad 4.29$$

From equations 4.27, 4.28 and 4.29 the following relationship can be obtained:

$$q_t + q_v = \frac{A_{sv} f_{yv}}{Sv} a$$

and 4.30

$$q_t - q_v = \frac{A_{sv} f_{yv}}{Sv} c$$

Taking moments about the Y axis at point O

$$(q_t - q_v)\left[Y_1 a + X_1 b + Y_1 c\right]\frac{X_1}{2} = \frac{A_{sv} f_{yv}}{Sv} X_1 a (Y_1 a + X_1 \frac{b}{2})$$

Substituting for a, b and c from the equation 4.30 we obtain:

$$q_t q_v \left(2 + \frac{X_1}{Y_1} \right) = q_v q_t - q_v^2 \qquad 4.31$$

Now taking moment about the x axis thus:

$$M = {}^{2A}_{sl} f_{yl} Y_1 + \frac{A_{sv} f_{yv}}{Sv} \frac{a^2}{2} Y_1^2 - \frac{A_{sv} f_{yv}}{Sv} c Y_1 \left(Y_1 a + X_1 b + Y_1 \frac{c}{2}\right)$$

Substituting for a, b, c and expression 4.31 in the above equation we obtain:

$$\frac{M}{Y_1} = A_{sl}\, f_{yl} - \frac{Sv}{A_{sv}\, f_{yl}}\, q_t^{\,2}(X_1 + Y_1) + q_t q_v\, Y_1$$

Using $q_t = \frac{T}{2X_1Y_1}$, $q_v = \frac{V}{2\,Y_1}$ above and rearranging, in the following dimensionless form

$$\frac{M}{Mo} + \left(\frac{T}{To}\right)^2 + \left(\frac{T\,V}{T1\;Vo}\right)\frac{Y_1}{(X_1 + Y_1)Y_1} = 1 \qquad 4.32$$

where

$Mo = 2\, A_{sl}\, f_{yl}\, Y_1$ (pure bending strength)

$$To = 2\,\frac{A_{sv}\, f_{yv}}{Sv}\, X_1\, Y_1 \sqrt{2\,\frac{A_{sl}\, f_{yl}}{(X_1+Y_1)}\,\frac{Sv}{A_{sv}\, f_{yv}}}$$

$$Vo = 2\,\frac{A_{sv}\, f_{yv}}{Sv}\, Y_1 \sqrt{2\,\frac{A_{sl}\, f_{yl}}{Y_1}\,\frac{Sv}{A_{sv}\, f_{yv}}}$$

Similar analysis can be performed for other modes of failure. For modes 2 and 3, test evidence on reinforced concrete beams (4.21) indicate that the crack inclination is almost constant, at 45^{o}, hence a simpler solution may be obtained from equation 4.17, 4.18, 4.21 and 4.22.

Equation 4.32 may be written as:

$$\frac{T_y}{T_s} = \frac{1}{\left(1 + \dfrac{\delta_y}{1 + \dfrac{X_1}{Y_1}}\right)}\left[\sqrt{\left(1 + \frac{\delta_y}{1 + \dfrac{X_1}{Y_1}}\right)m_b' + \left(\frac{\psi}{1 + \dfrac{Y_1}{X_1}}\right)^2} - \frac{\psi}{1 + \dfrac{Y_1}{X_1}}\right] \qquad 4.33$$

It may be noticed that equation 4.8 becomes a particular case of this general equation 4.33.

4.4 Relationship Between Various Proposed Yield Theories

Fig. 4.3 compares various theoretical predictions of strength for reinforced concrete rectangular beams subjected to bending and torsion in a form of a non dimensional interaction diagram. It can be seen that the choice of the angle of the crack has an appreciable influence on the strength prediction particularly for beams with high values of m'. In general the theories which have been obtained by minimizing the torsional strength with respect to the angle of cracking gave the lowest prediction of strength and the theories utilizing the angle of the direction of principal stresses gave the highest strength and an intermediate value is usually obtained by taking $\theta = 45^{o}$. The validity or otherwise of any of these theories can only be tested against experimental results as will be examined later in this chapter.

It is evident from Fig. 4.3 that for beams with smaller volumes of longitudinal reinforcement placed in the compression zone than the reinforcement provided in the bottom of a beam (Ry $<$ 1) failure may occur according to mode 1, 2 or 3. For beams subjected to $\frac{M}{Mu} < 0.1$, failure is governed by mode 3 and it can be seen that an increase in the bending moment will result in an increase in the torsional strength as was shown by Collins et al. Where $0.1 < \frac{M}{Mu} < 0.25$, failure would be according to mode 2 where the applied moment has no effect on the torsional strength of the beam. For the case where $0.25 < \frac{M}{Mu}$ failure will be in accordance with mode 1 when the torsional resistance of the beam decreases with increase in

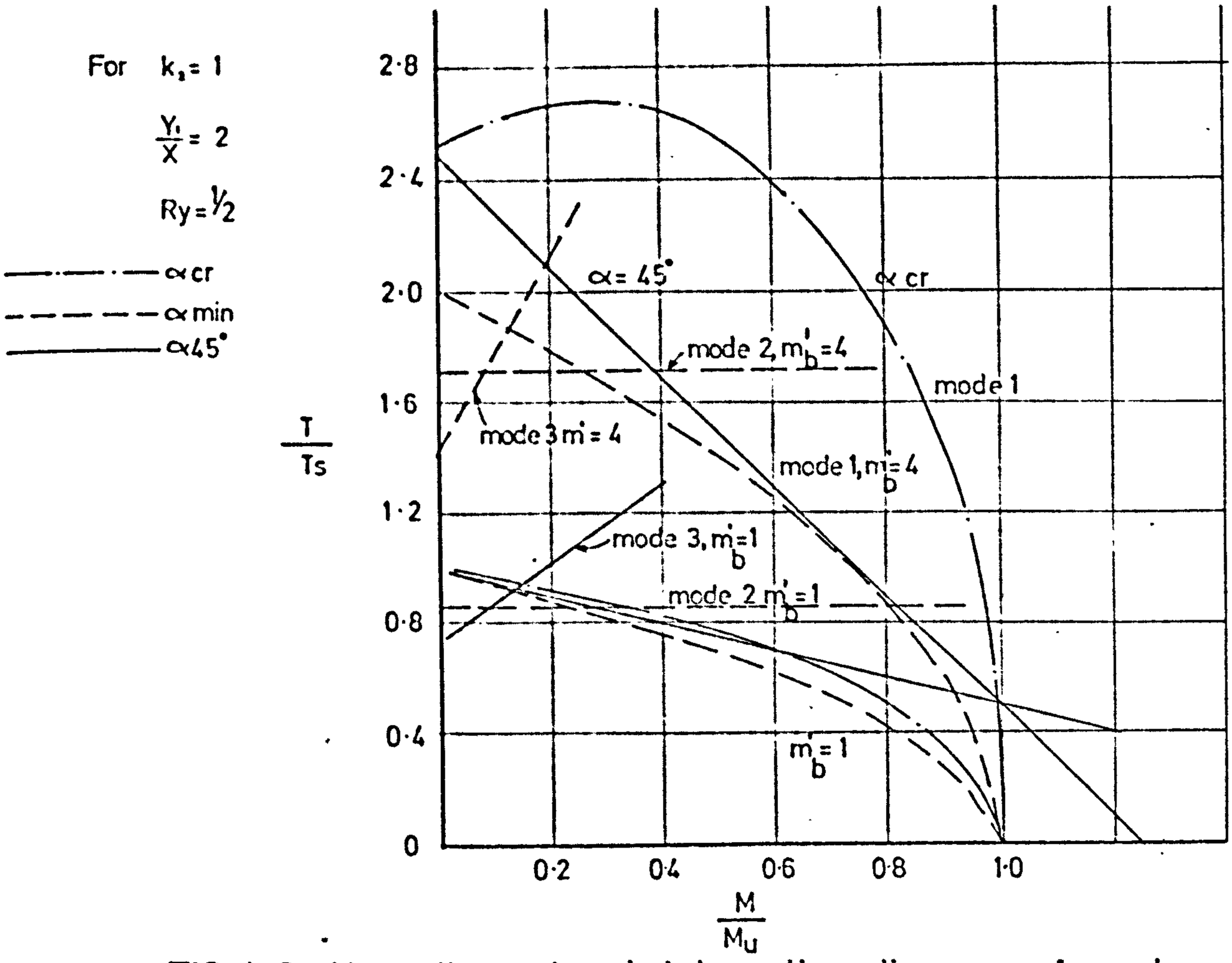

FIG 4·3 Non-dimensional interaction diagrams for a beam loaded in combined bending & torsion for varying ratio m' and angle of cracking.

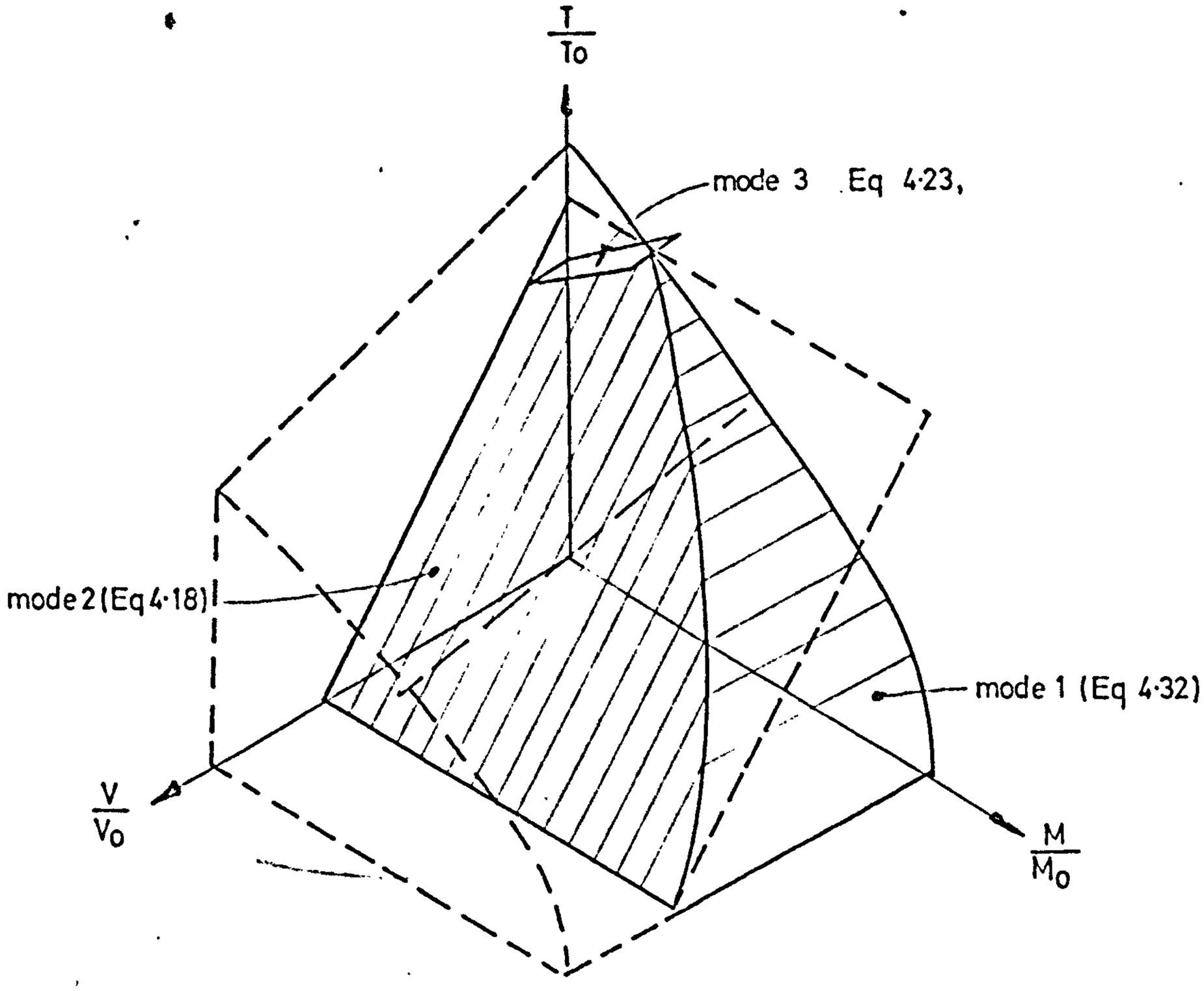

FIG 4·4 Non-dimensional interaction surface for beam loaded in combined bending, torsion and shear for $\frac{Y_1}{X_1} = 2$ and $Ry = \frac{1}{2}$

the applied bending moment.

For beams with Ry = 1, failure will always be governed by mode 1 only.

For beams subjected to combined action of bending, torsion and shear, failure can be represented in the form of interaction surfaces as shown in Fig. 4.4, for a reinforced concrete beam with $\frac{Y_1}{X_1} = 2$ and $Ry = \frac{1}{2}$. It is seen that mode 1 failure is associated with high values of applied moment and mode 2 failure is associated with high shear. Mode 3 failures occur as the pure torque loading condition is approached.

A disadvantage of the theories which consider the angle of cracks at failure to be governed by the direction of the principal stresses just prior to cracking is the need for determining this angle. In order to simplify the calculation of torsional strength of reinforced concrete beams Fairbairn and Davis (4.10) suggested the following simple expressions for this angle.

$$\psi < 2, \quad \cot\theta = \frac{0.6}{\sqrt{\psi}}$$

$$2 < \psi < 8, \quad \cot\theta = \frac{0.8}{\psi}$$

$$\psi > 8, \quad \cot\theta = 0.1$$

These values are plotted in Fig. 4.5 together with the method suggested by Evans and Sarkar (4.8) and the elastic theory suggested in Chapter 2. It is seen that this angle may be approximated to $\cot\theta = \frac{1}{1+\psi}$.

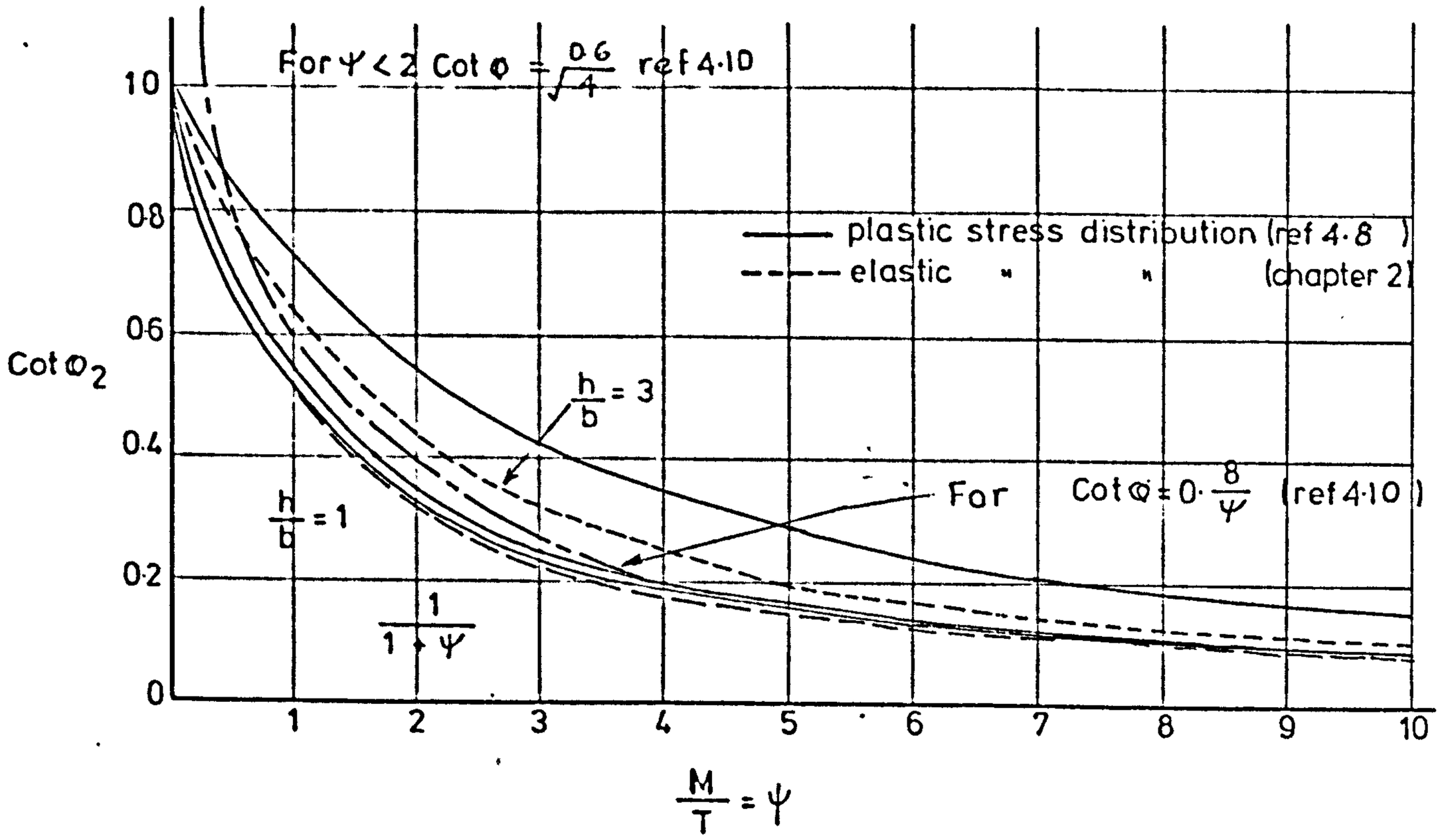

FIG 4.5 Effect of M/T on angle of cracks of a reinforced concrete beam subjected to bending and torsion

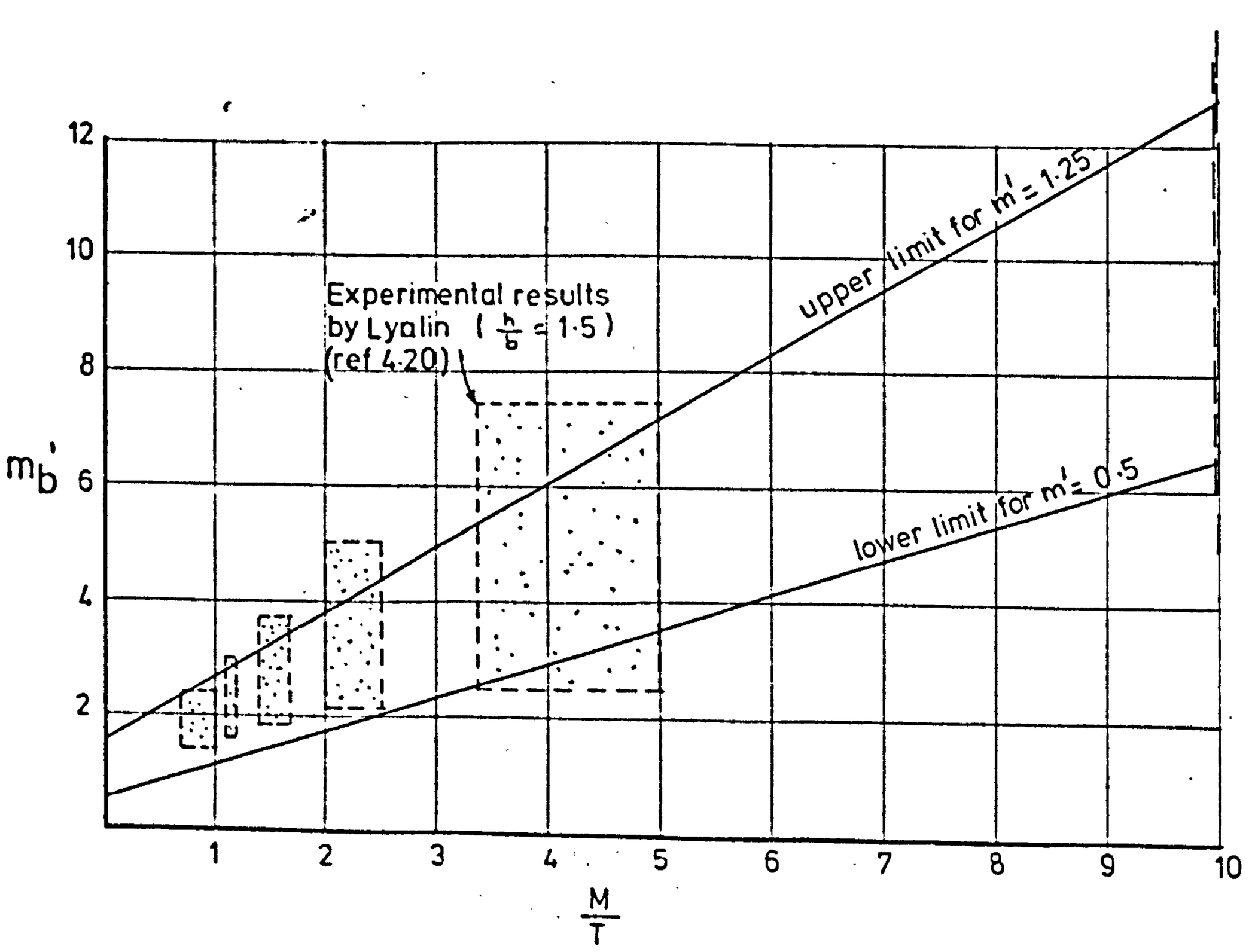

FIG 4.6 Limits on m_b' for yeild failure $\frac{y_1}{x_1} = 1.5$

4.5 Limitations on The Yield Theory

In the derivation of the yield theory, it was assumed that the reinforcement crossing a failure surface reaches full tensile yield strength. Measured strains on reinforcement indicate however that this assumption is not valid for a large number of the beam tests reported in literature. Failure with yielding of only one of the categories of reinforcement (stirrups or longitudinal reinforcement) or without yielding of reinforcement may occur as a result of the following:

a. Large value of m'_b
b. Large volume of longitudinal reinforcement
c. Large volume of transverse reinforcement
d. Beams subjected to high shear force.

The boundary conditions of the yield theory can be obtained by the following methods:

1. Theoretical prediction of beam strength failing by other possible modes of failure i.e. partial yield or over-reinforced failure.
2. By empirical methods, where the range of certain parameters are determined experimentally and a simple rule provided to ensure the validity of the yield theory.

The first method will be fully discussed in Chapter 5, and the second method will be examined in the following.

4.5.1 Ratio Between Longitudinal and Transverse Reinforcement

Tests on reinforced concrete beams subjected

to bending, torsion and shear (4.20) indicate that full yielding does not occur for beams with m_b' outside certain limits, and the range of m_b' usually depends on and the $\frac{h}{b}$ ratio.

Lessig (4.1) gave the following empirical limits to the ratio of transverse longitudinal reinforcement by which it is hoped to ensure yielding of both categories of reinforcement:

$$0.5 \leqslant 0.8 \quad r \left(1 + 2 \quad \frac{b}{2b + h}\right) \leqslant \quad 1.5$$

Later Collins et al (4.5) suggested the following limits on this ratio:

$$r \quad 4 + \frac{4}{1 + \frac{2h}{b}} \leqslant 0.9$$

Recently Martin (4.14) suggested the following limit

$$r \left(1 + \frac{h}{b} + 2\psi \right) \leqslant 1$$

In deriving these expressions, Lessig, Collins and Martin obtained a ratio of r by minimizing the volume or internal forces required to resist the applied loads which result in a single value of r for any given value of ψ . Realising the restricted nature of these results they employed test data in order to obtain a range of r for any given value of ψ

In the following a method is proposed whereby the limits on m_b' are obtained from the knowledge of the valid range of m_b' under pure torsion condition which was obtained in Chapter 3.

Equating equation 3.4and equation 4.8 we obtain:

$$\frac{T}{Ts} = \sqrt{m'} = \left[\sqrt{m_b' + \left(\frac{\psi}{1+\frac{Y_1}{X_1}}\right)^2} - \left(\frac{\psi}{1+\frac{Y_1}{X_1}}\right)\right] k_z$$

putting $k_z = 1$ and rearranging we get:

$$m_b' = m' + 2\sqrt{m'}\,\frac{\psi}{1+\frac{Y_1}{X_1}} \qquad 4.34$$

This equation indicates that the range of m_b' for the yield condition increases with increase in ψ as shown in Fig. 4.6. These results can be seen to compare favourably with the experimental results obtained by Lyalin (4.20).

4.5.2 Maximum Percentage of Longitudinal Reinforcement

Ifthe percentage of longitudinal reinforcement exceeds a certain amount, failure will occur prior to yielding of the reinforcement. To avoid this situation, Lessig proposed the following empirical limit on the depth of the compression zone for her yield theory that is:

$$\frac{x}{d} \rangle\ 0.55 - 0.7\sqrt{\frac{T}{M}}$$

In contrast Collins et al (4.5) suggested the following empirical rule in order to prevent over-reinforcement. $\frac{(A_{11} f_{11} - A_{11}' f_{y1}')}{bd f_c'}$ 0.4

4.5.3 Maximum Shear Force

When a beam is subjected to a load combination that will give rise to shear failure by yielding of

stirrups only, then the yield theory is expected to over estimate the strength. It is interesting to note that there is no simple rule in the published literature on the shear force that could be applied if the yield theory is to remain valid.

4.5.4 Proposed simplified Boundary Conditions for the Yield Failure

From this brief review and from the comparison of yield theory predictions with test results to be given in the next section of the chapter, the following conditions are proposed in order to ensure yielding of reinforcement.

1. The beam is under-reinforced in flexure. This condition can be determined from the ccmpatibility rule and maximum compressive strain used in the theory of the ultimate flexural strength for reinforced and pre-stressed concrete beams as given in CP 110 in order to prevent shear compression failure.

2. The theoretical torsional yield strength for beams under combined bending, torsion and shear is equal or smaller than T_{du} (equation 3.49) in order to prevent partial and over-reinforced torsional failure.

3. For beams subjected to bending, torsion and shear, δy is equal to or smaller than unity in order to prevent shear torsion failure.

4.6 Comparison of The Proposed Yield Theories With Experimental Results

The theoretical studies presented in this chapter show that the prediction of ultimate strength of reinforced and concrete beams is influenced by the choice of the angle of cracking of the failure surface, also in order to produce a simple theoretical expression for prediction of strength of these beams, various simplifying assumptions are needed. These problems can best be examined by comparing the predicted strength with available test results. For this purpose, the experiments which have been carried out at 24 different research centres or universities in U.S.A., U.S.S.R., U.K., Canada, Australia, Japan, Sweden and India are used. These results consist of 574 reinforced and prestressed concrete beams with web reinforcement covering a wide range of variables such as size of specimen, $\frac{Y_1}{X_1}$, percentage of reinforcement, ψ, δ_y, m_b', materials strength and level of prestress.

The method used for this comparison is to compare the maximum experimental torque for any test with the ultimate torque predicted by the yield theories e.g. $\frac{T(exp)}{T(th)}$. The theoretical ultimate torque has been calculated for mode 1, 2 and 3 and the smallest predicted value was considered as the governing failure torque.

A summary of this comprehensive comparison is given in Tables 41 to 48 and Figs. 4.7 to 4.11.

4.6.1 Reinforced Concrete Beams Subjected to Bending and Torsion

The available test results in this category of beam represent almost half the total of 574 test results studied.

Table 4.2 gives the number of beams which have failed according to mode 1, the mean ratio $\frac{T(exp)}{T(th)}$ and coefficient of variation for each set of results. These beams satisfy the boundary conditions stated earlier. The theoretical calculation has been obtained using equation 4.5 and 4.8 assuming $k_z = 1$. For the first theoretical method (equation 4.5) the angles of cracking were calculated in accordance with the method given in Chapter 2. For this case, 95 beams out of a total of 240 are classified as a yield failure giving a mean ratio of $\frac{T(exp)}{T(th)} = 0.95$ with a coefficient of variation of 10.2 percent. This compares with a ratio $\frac{T(exp)}{T(th)} = 1.06$ and coefficient of variation of 14 percent when equation 4.8 was used.

It is seen that both equations provided good estimates of the experimental results with equation 4.5 overestimating the torsional strength by an average of 5 percent in contrast to equation 4.8 which underestimates the test results by an average of 6 percent. Equation 4.5 provides a more consistant estimate of the strength of these beams with a narrower band in the scatter of the $\frac{T(exp)}{T(th)}$ about unity than equation, 4.8.

In order to examine the influence of the boundary rules on the predictions of the yield

theory, this comparison has been repeated in Table 4.3 but using T_s as an upper limit to the yield theory as suggested by Martin (4.14). It is seen that T_s gives a more restrictive upper bound to the yield theory than T_{d1} and hence only 79 beams can be classified as failing according to mode 1 if equation 4.5 is used - for prediction of torque with the mean ratio $\frac{T(exp)}{T(th)}$ = 0.96 and a coefficient of variation of 9.9%. This is compared with 96 beams failing according to mode 1 with a mean ratio of $\frac{T(exp)}{T(th)}$ = 1.02 and coefficient of variation of 9.3 percent if equation 4.8 is used for the theoretical prediction. It is interesting to compare these correlations of results with those obtained by Martin's (4.14) yield theory. He compared his yield theory with the first seven sets of the experimental results given in Table 4.3. He found that only 77 beams failed according to mode 1 of his yield theory with a mean ratio $T(exp)/T(th) = 1.05$ and coefficient of variation of 11.6 percent. Therefore, the complications that are induced in a yield theory by considering the effect of shear stresses on the depth of the compression zone as suggested by Martin are not justified.

Fig. 4.7 shows a plot of $T(exp)/T(th)$ using both equation 4.5 and 4.8 against k_z which has been obtained according to equation 4.12. The contribution or otherwise of the longitudinal reinforcement located near the top face of the beam has been checked from the principle of plane section before bending remaining plane after bending and the maximum compressive strain given in CP 110. These results indicate that

TABLE 4.2 Correlation between yield theories (mode 1) and test results For reinforced concrete beams subjected to bending and torsion, $k_z = 1$ and $T_{cr} < T_{yl} < T_{du}$

Investigator	$\theta = \theta_{cr}$				$\theta = \theta_{min}$		
	Ref	Number of beams	Mean $\frac{T(exp)}{T(th)}$	Coefficient of Variation	Number of beams	Mean $\frac{T(exp)}{T(th)}$	Coefficient of Variation %
Gesund et al	4.7	12	0.92	10.9	12	1.01	6.2
Goade & Helmy	4.21	8	0.98	10.9	11	1.1	9.8
Evans & Sarkar	4.8	12	0.92	7.2	12	0.97	7.1
Iyengar & Rangan	4.22 4.23	11	1.0	7.8	13	1.09	6.8
Chinekaov	4.24	2	0.92	-	6	1.08	7.3
Pandit & Warworuk	4.25	6	0.95	11.9	7	1.01	8.9
Jackson & Estanero	4.19	23	0.95	11.9	27	1.01	8.6
Elfgren	4.15	5	1.02	2.94	6	1.14	3.9
McMullen & Warworuk	4.26	0	-	-	10	0.99	-
Collins et al	4.5	10	0.88	11.1	14	0.95	12.1
Okada et al	4.27	6	1.00	1.7	38	1.15	18.5
Total		95	0.95	10.2	147	1.06	14.0

TABLE 4.3 Correlation between yield theories (mode 1) and test results for reinforced concrete beams subjected to bending and torsion $k_z = 1$ and $T_{cr} < T_{yl} < T_s$

Investigator	$\theta = \theta_{cr}$			$\theta = \theta_{min}$		
	Number of beams	Mean $\frac{T(exp)}{T(th)}$	Coefficient of Variation	Number of beams	Mean $\frac{T(exp)}{T(th)}$	Coefficient of Variation %
Gesund et al	9	0.96	8.4	9	1.01	6.6
Goade & Helmy	6	0.98	10.9	9	1.06	8.7
Evans & Sarkar	12	0.92	7.2	12	0.97	7.1
Iyengar & Rangan	12	0.99	7.9	13	1.08	6.8
Chinckaov	3	0.87	6.8	5	0.95	2.6
Pandit & Warwaruk	8	0.94	11.4	8	0.99	9.7
Jackson & Estanero	17	0.99	9.2	21	1.03	8.4
Elfgren	5	1.03	4.2	5	1.15	2.7
McMullen & Warw ruk	3	0.94	2.1	3	0.97	2.7
Collins et al	4	0.9	13.7	10	0.92	8.7
Okada et al	0	-	-	1	1.11	-
Total	79	0.96	9.9	96	1.02	9.3

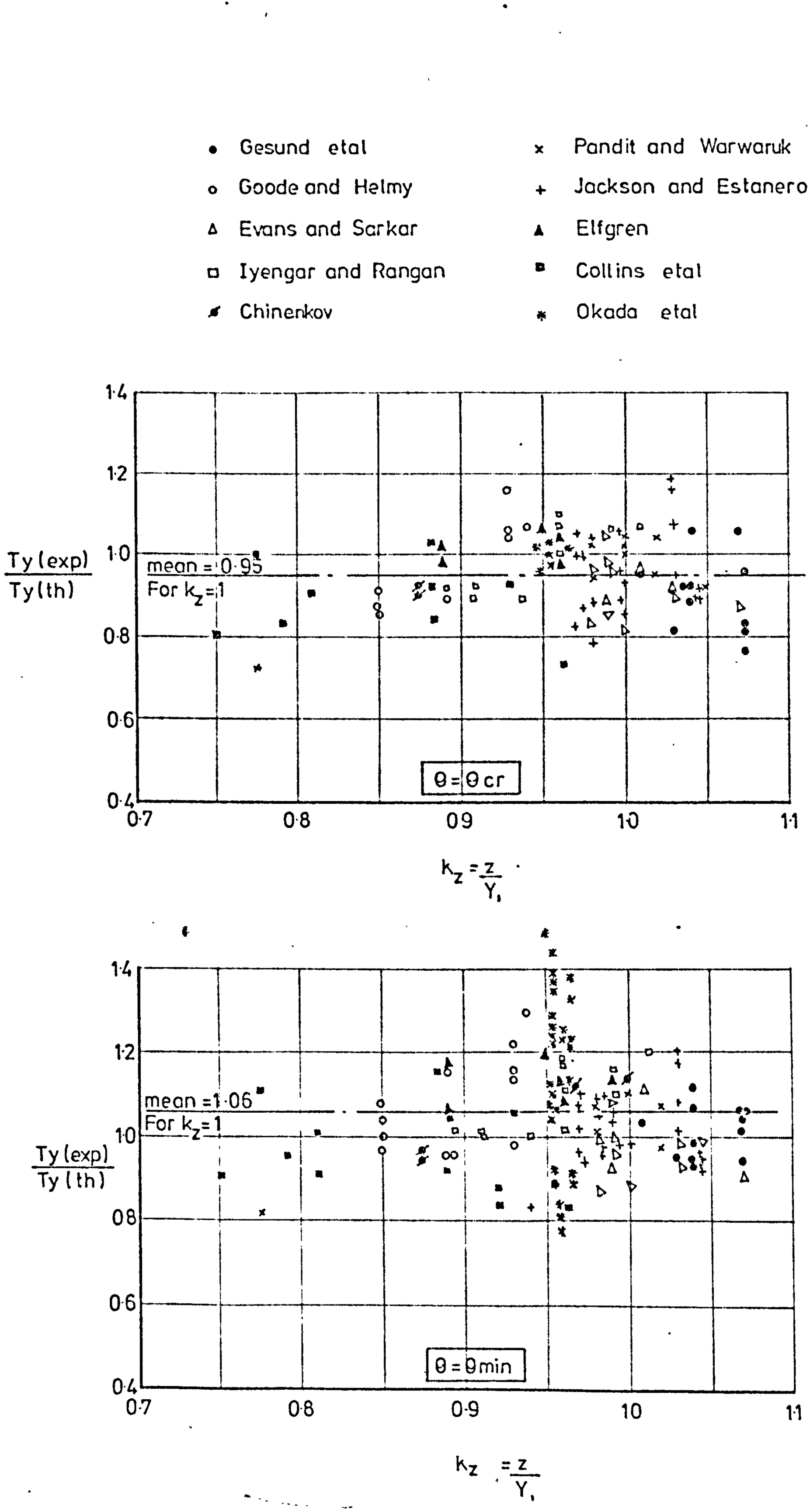

Fig. 4.7 Comparison of experimental and theoretical. ultimate torque for reinforced concrete beams subjected to bending and torsion for mode 1, $K_z = 1$ and $T_{cr} < T_{y1} < T_{du}$

k_z may be taken as unity hence producing a considerable simplification of the theory without loss in accuracy of prediction for these beams. It is also seen from Fig. 4.7 that the assumption $\theta = \theta_{min}$ would result into a larger scatter in the value of T(exp)/T(th) than for the case where θ is taken as the angle of cracking.

Table 4.4 in Fig. 4.8 gives a comparison between these two theoretical predictions with test results for beams failing according to mode 3. This result indicates that mode 3 occurs less frequently than mode 1. It is seen that the correlation between the yield theories and the test results are good but since the number of beams are small, the coefficient of variation is higher than for mode 1. Failure by this mode can be prevented in practice by provision of a sufficient volume of longitudinal reinforcement at the top of the beam. The need or otherwise for top longitudinal reinforcement may be obtained from equation 4.8 and 4.22.

Although the upper limit to the yield theory as suggested by Martin (4.14) appears to be simple and reasonably predicts the change in the mode of failure for reinforced concrete beams subjected to bending and torsion, it can be shown that this rule is far from satisfactory when applied to prestressed concrete beams and for cases of reinforced concrete beams subjected to bending, torsion and shear. In addition this expression does not predict satisfactorily the torsional strength where T_s is $< T_y$. In contrast T_{du} can be used more satisfactorily for prestressed concrete beams and predicts the

TABLE 4.4 Correlation between yield theories (mode 3) and test results for reinforced concrete beams subjected to bending and torsion

For $T_{y3} < T_{du}$

Investigator	Ref	$\theta = \theta_{cr}$ Number of Beams	Mean $\frac{T(exp)}{T(th)}$	Coefficient of Variation	$\theta = \theta_{min}$ Number of Beams	Mean $\frac{T(exp)}{T(th)}$	Coefficient of Variation %
Goode & Helmy	4.21	10	1.09	15.4	12	1.13	15.3
Jackson & Estanero	4.19	1	0.88	-	1	0.99	-
McMullen & Warwaruk	4.26	0	-	-	2	0.97	-
Collins et al	4.5	3	0.81	4.3	3	0.8	2.5
Total		14	1.01	17.6	18	1.07	18.6

For $T_{y3} < T_s$

Goode & Helmy	4.21	4	1.04	9.0	4	1.06	15.6
Jackson & Estanero	4.19	1	0.88	-	1	0.99	-
McMullen & Warwaruk	4.26	2	0.94	2.4	2	0.99	4
Total		7	0.97	11.7	7	1.02	12.7

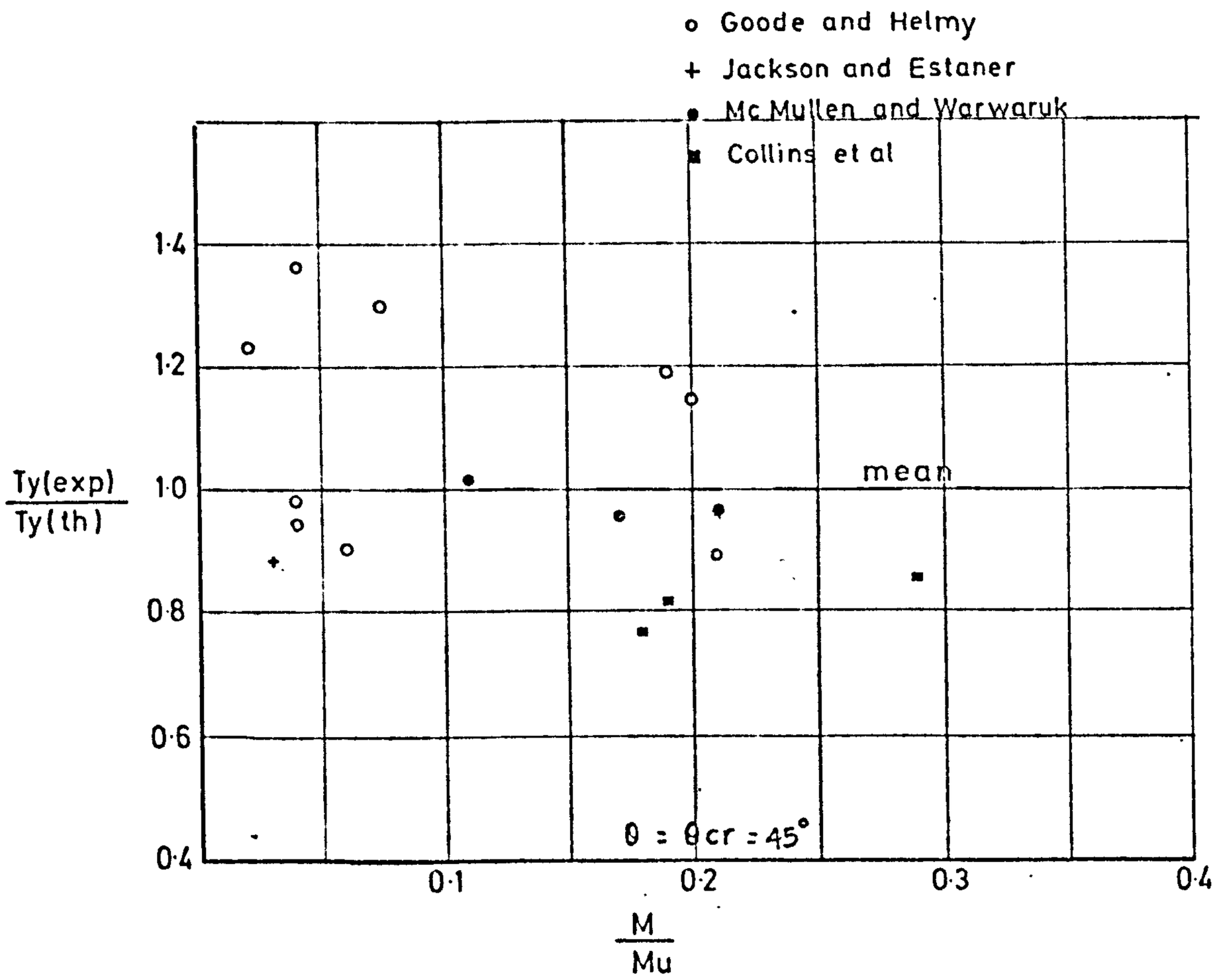

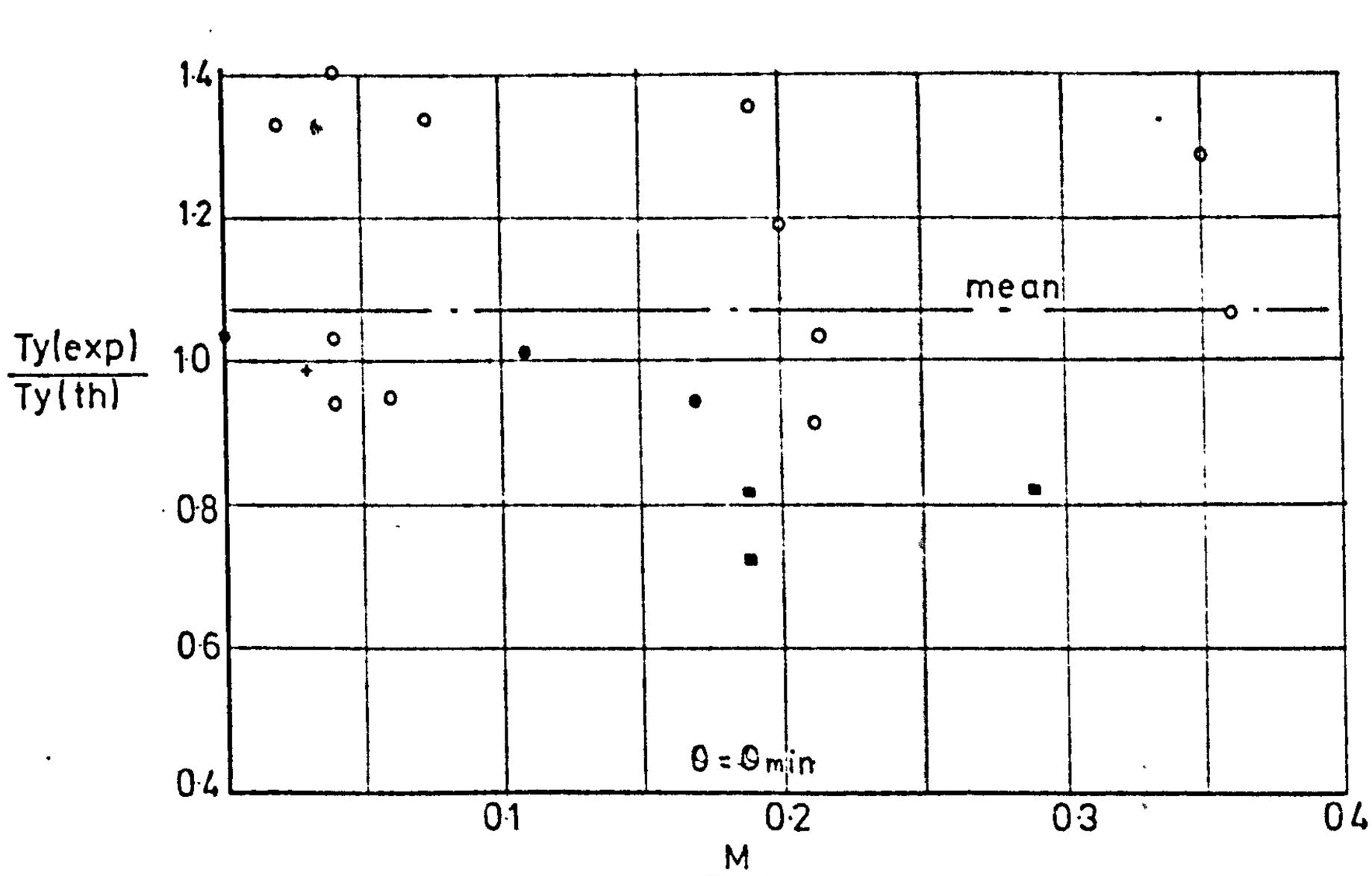

FIG. 4·8 Comparison of experimental and theoretical ultimate torque for reinforced concrete beams subjected to bending and torsion for mode 3 $k_z = 1$ $T_{cr} < T_{y3} < T_{du}$

TABEL 4.5 Correlation between theoretical prediction of torsional strength with test results for reinforced concrete beam subjected to bending and torsion

$$T_{cr} < T_{du} < T_{y1} \text{ or } T_{y3}$$

Investigator	Total Number of Beams tested	Number of beams	Mean $\frac{T(exp)}{T(th)}$	Coefficient of Variation %
Gesund et al	12	-	-	-
Goade & Helmy	32	14	1.0	9.9
Evans & Sarkar	12	3	0.89	8.0
Iyengar & Rangan	23	10	0.97	7.6
Chinekaov	11	8	1.09	6.9
Pandit & Warworuk	11	5	1.06	8.6
Jackson & Estanero	68	43	0.87	8.5
Elfgren	9	4	1.27	22.3
McMullen & Warworuk	5	4	1.16	6.62
Collins et al	17	4	0.77	5.2
Okada et al	42	37	0.9	9.4
Total	242	132	0.94	13.1

55%

torsional strength for beams having T_{du} is T_y.

Table 4.5 gives a summary of the theoretical predictions using T_{du} with the remaining experimental results which have not been accounted for by the yield theory. The mean ratio T(exp)/T(th) = 0.95 and coefficient of variation of 13.1 percent. It is seen that this mode of failure accounts for 55 percent of the total beam tests studied.

4.6.2 Prestressed Concrete Beams Subjected to Bending and Torsion

Table 4.6 gives a summary of the comparison between theoretical predictions for 71 prestressed concrete beams and the combined bending and torsion test results found in literature.

It can be seen that the same observations and conclusions obtained from the previous comparison on reinforced concrete beams apply to prestressed concrete beams. Examination of Table 4.6 for the case when T_{du} was used as an upper limit to the torsional strength shows that equation 4.5 gives a mean ratio of T(exp)/T(th) = 0.84 and coefficient of variations of 11.15 percent, this is compared with a mean ratio of T(exp)/T(th) = 1.05 with coefficient of variation of 15.1 percent if equation 4.8 is used for theoretical predictions.

The remainders of the beams which have not been accounted for in Table 4.6 were either over-reinforced in flexure such as the beam tested by Mukherjee and Warwaruk (4.28) or T_{du} was less than T_y.

TABLE 4.6 Correlation between yield theories and test results for Prestressed Concrete beams subjected to bending and torsion.

Investigator	Ref	Total number of beams tested	Mode of Failure	$T_{cr} < T_y < T_{du}$						$T_{cr} < T_y < T_s\sqrt{1 + f_p/f_t}$					
				$\theta = \theta_{cr}$			$\theta = \theta_{min}$			$\theta = \theta_{cr}$			$\theta = \theta_{min}$		
				Number of beams	Mean $\frac{T(exp)}{T(th)}$	Coefficient of beam	Number of beams	Mean $\frac{T(exp)}{T(th)}$	Coefficient of Variation	Number of Beams	Mean $\frac{T(exp)}{T(th)}$	Coefficient of Variation	Number of Beams	Mean $\frac{T(exp)}{T(th)}$	Coefficient of Variation
Mukherjec & Warwaruk	4.28	20	1	3	0.86	19	5	0.92	15.5	3	0.86	19	3	1.03	1.0
			3	3	0.79	5.6	5	0.82	2.4						
GangaRaos	4.29	33	1	24	0.82	11	29	1.05	14.3	1	0.89	-	5	0.94	11.9
Evans & Khalil	4.9	12	1	8	0.91	6	9	0.97	5.2	6	0.99	9	7	1.01	9.0
			3	2	1.16	-	2	1.17	-						
Okada	4.27	6	1	6	0.78	9.5	6	1.26	6.2	0	-	-	0	-	-
Total		71	Mode 1	41	0.84	11.15	49	1.05	15.1	10	0.97	8	15	0.99	9.7
			Mode 2	5	0.94	20.3	5	0.96	19.1						

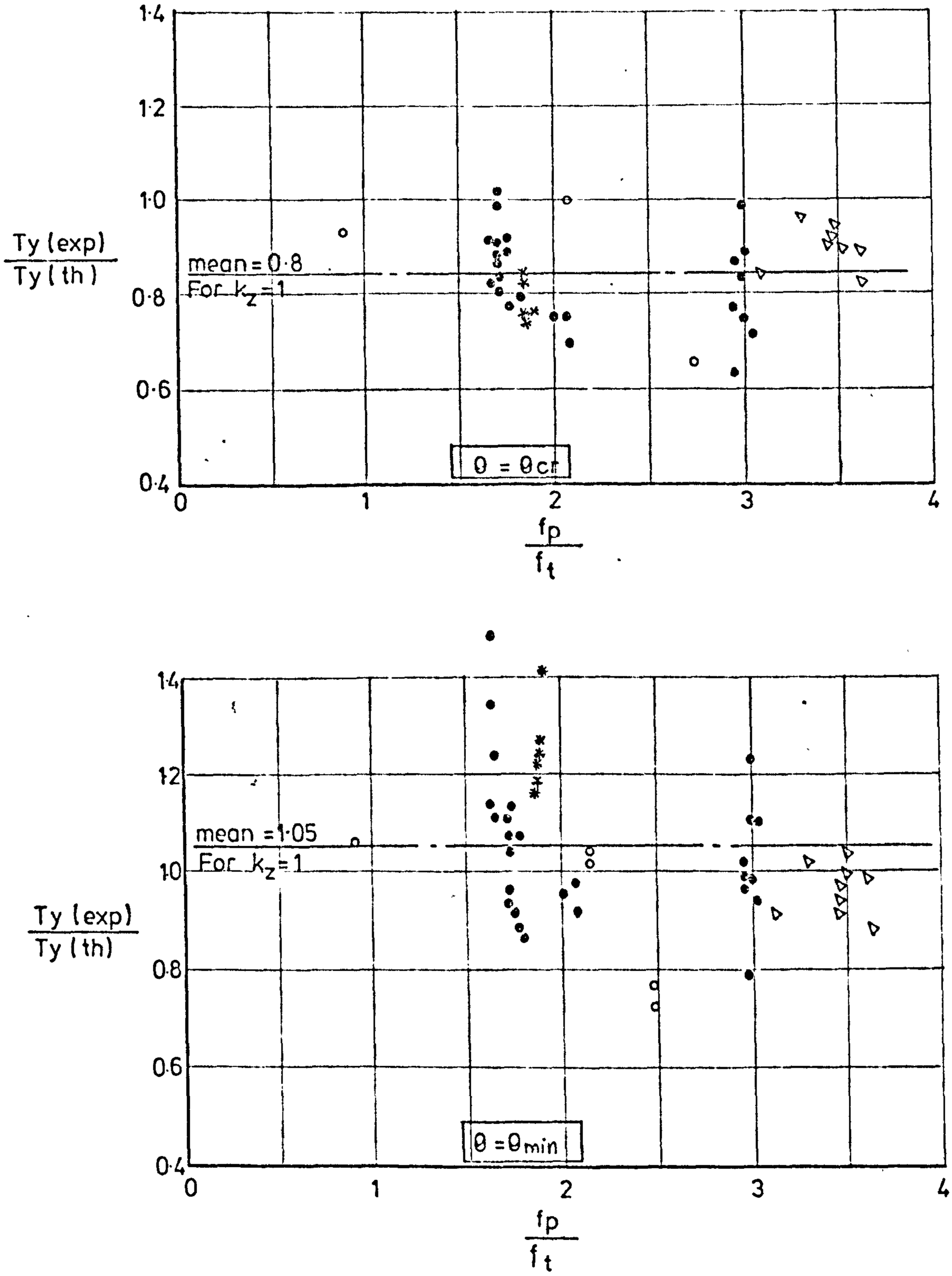

Fig 4.9 Comparison of experimental and theoretical. ultimate torque for prestressed concrete beams subjected to bending and torsion for mode 1, $K_z = 1$ and $T_{cr} < T_y < T_{du}$

It is seen from Table 4.6 that only a quarter of the prestressed concrete beams which were classified as a yield failure will be classified thus if $T_s \cot \theta_2$ is used as an upper limit to the yield theory.

Fig. 4.9, shows that both yield theories (equation 4.5 and 4.8) can be applied for prediction of torsional strength of prestressed beams having a large range of prestress.

4.6.3 Reinforced Concrete Beams Subjected to Bending, Torsion and Shear

Equations 4.18, 4.22 and 4.33 have been used to predict the torsional strength of 190 beams tested under combined bending torsion and shear. These results are summarised in Table 4.7 and 4.10. The ratios T(exp)/T(th) have been plotted on Fig. 4.10 against δ_y for the beam satisfying the limits imposed for beams subjected to bending and torsion. It will be noticed that for high value of δ_y, i.e. $\delta_y > 1$, the yield theory over-estimated the results. This may be due to a change in the mode of failure from a yield to a partial yield mode. This confirms that a further limit should be imposed on the yield theory, that is $\delta_y \leqslant 1$.

Examination of Table 4.7 shows that where θ is taken as θ_{min}, the yield theory predicts the ultimate strength of reinforced concrete members subjected to combined bending torsion and shear with reasonable accuracy.

For this case T(exp)/T(th) has a mean value

TABLE 4.7 Correlation between proposed yield theory and test results for reinforced concrete beams subjected to bending, torsion and shear

$M < M_{ub}$ $T_{cr} < Ty < T_{du}$ and $\delta_y \leqslant 1$

Investigator	Ref	Total number of tested beams	Mode of Failure	Number of beams	Mean $\frac{T(exp)}{T(th)}$	Coefficient of Variation %
Lessig	4.1 to 4.4	34	1	12	1.18	9.6
Lyalin	4.20	34	1	15	1.12	4.8
Yudin	4.6	18	1	15	1.14	17.2
McMullen and Warwaruk	4.26	18	1	3	1.1	9.8
Collins et al	4.5	60	1	14	0.97	11.0
			3	2	0.87	
Elfgreen	4.15	26	1	13	1.1	7.5
Total		190	1	72	1.1	12.7

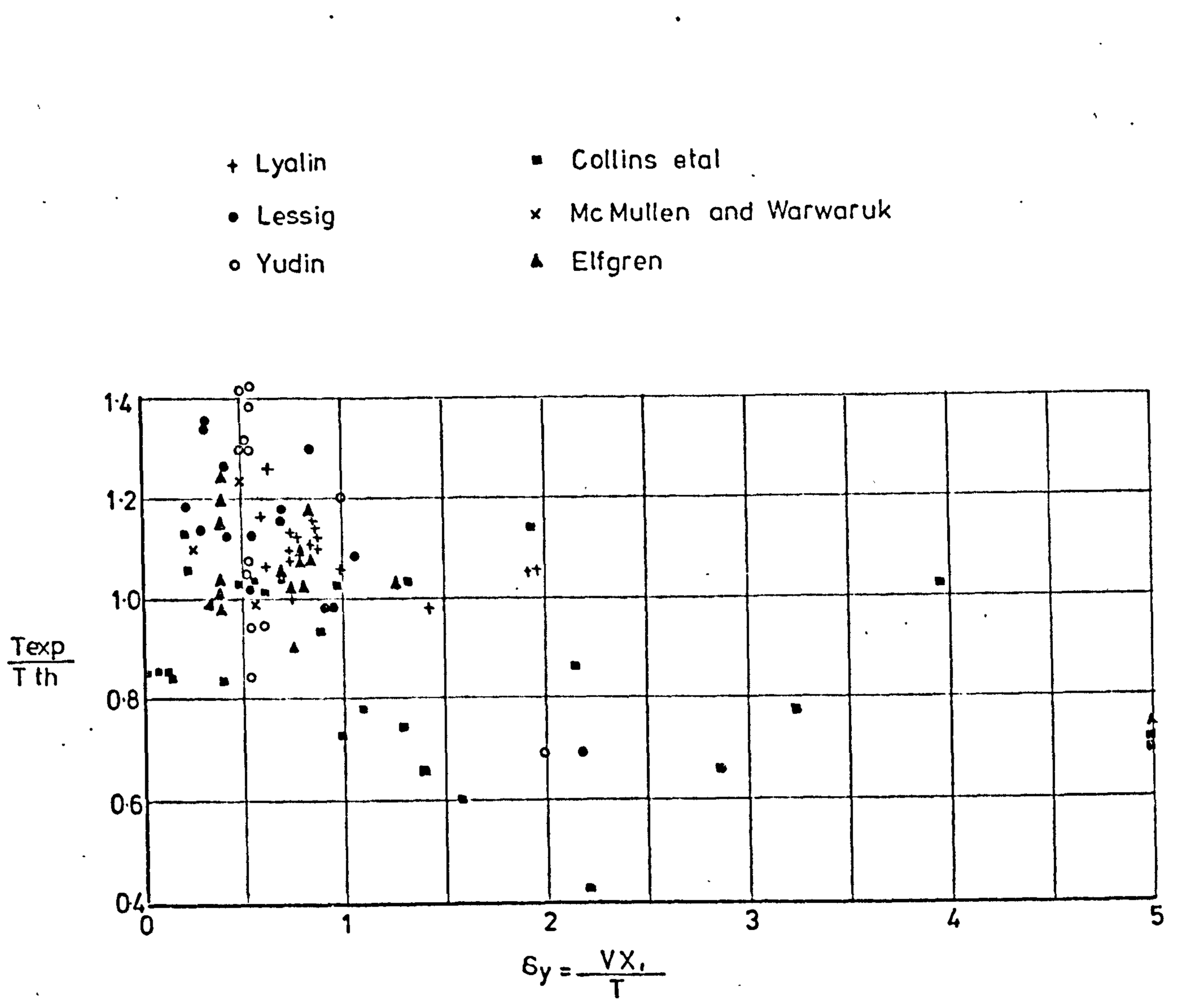

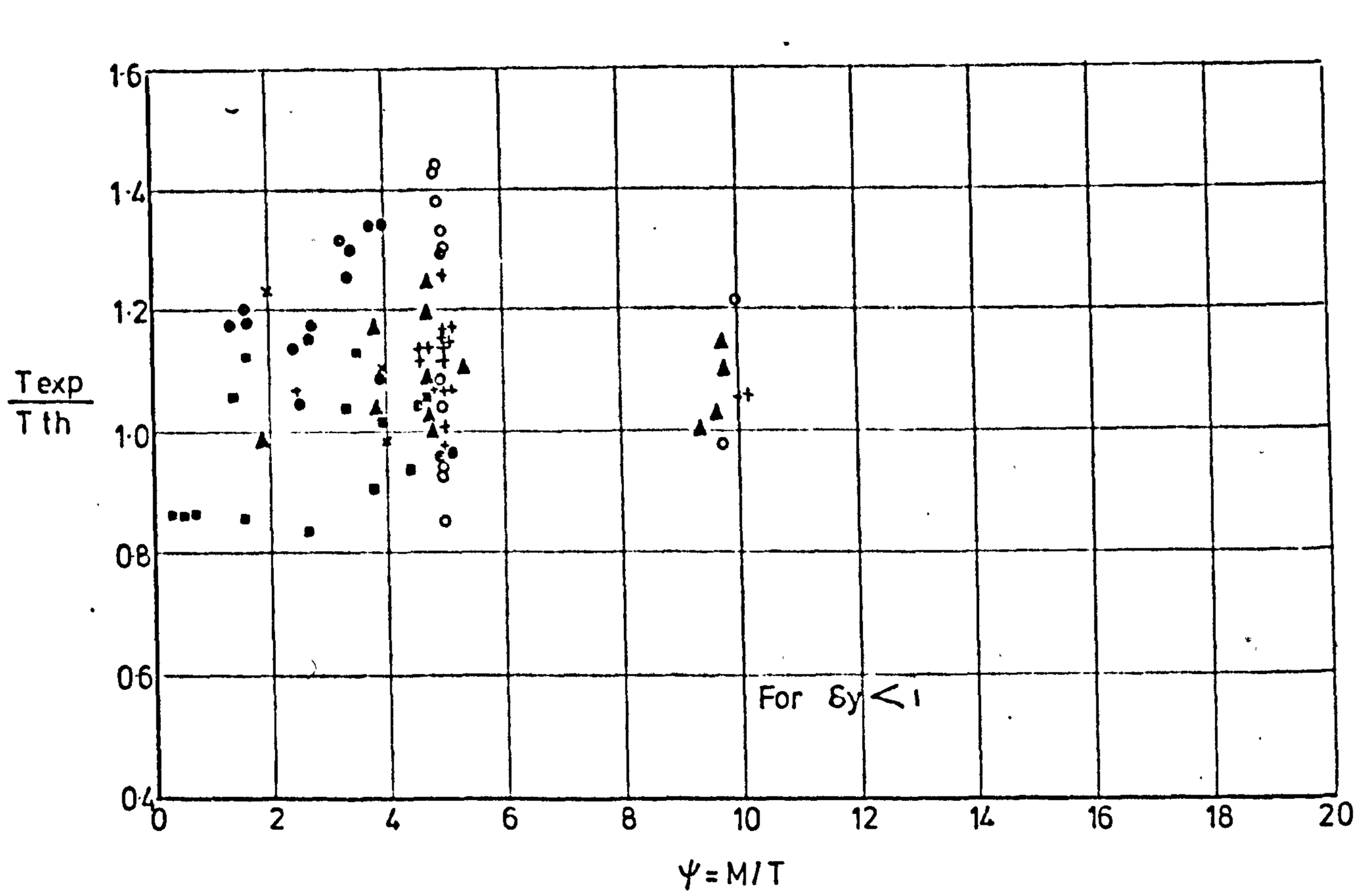

Fig. 4.10 Comparison of experimental ultimate torque for reinforced concrete beams with web reinforcement subjected to bending, torsion and shear

of 1.1 and a coefficient of variation of 12.7 percent.

The ratio T(exp)/T(th) for the beam satisfying all the limits imposed on the yield theory are plotted against ψ. This correlation between theory and experiment is comparable to those obtained for reinforced concrete beams subjected to bending and torsion only.

4.9.4 Prestressed Concrete Beams Subjected to Bending, Torsion and Shear

Table 4.8 gives a summary of comparisons between predicted and experimental results on prestressed concrete beams subjected to bending, torsion and shear. For this case T(exp)/T(th) has a mean value of 1.12 and a coefficient of variation of 12.1 percent. These figures are almost identical to thos obtained for reinforced concrete beams. Fig. 4.11 gives a plot of T(exp)/T(th) against δ_y and ψ which shows the same pattern of results as those obtained earlier.

To sum up this comparison between the theoretical prediction and test results, it can be stated that many simplification of the yield theory would only result in a small and insignificant loss in accuracy of the prediction of strength.

TABLE 4.8 Correlation between proposed yield theory and test results for prestressed concrete beams subjected to bending, torsion and shear

$$M < M_{ub}, \quad Tcr < Ty < T_{du} \text{ and } \delta_y \leqslant 1$$

Investigators	Ref	Total Number of beams tested	Mode of Failure	Number of beams	Mean $\frac{T(Exp)}{T(th)}$	Coefficient of Variation %
Mukherjee and Warwaruk	4.28	22	1	7	0.96	5.6
Henery and Zia	4.30	32	1	31	1.14	9.9
Swann and * Williams	4.31	16	1	12	1.08	12.6
Total		70	1	50	1.12	12.1

* box beams

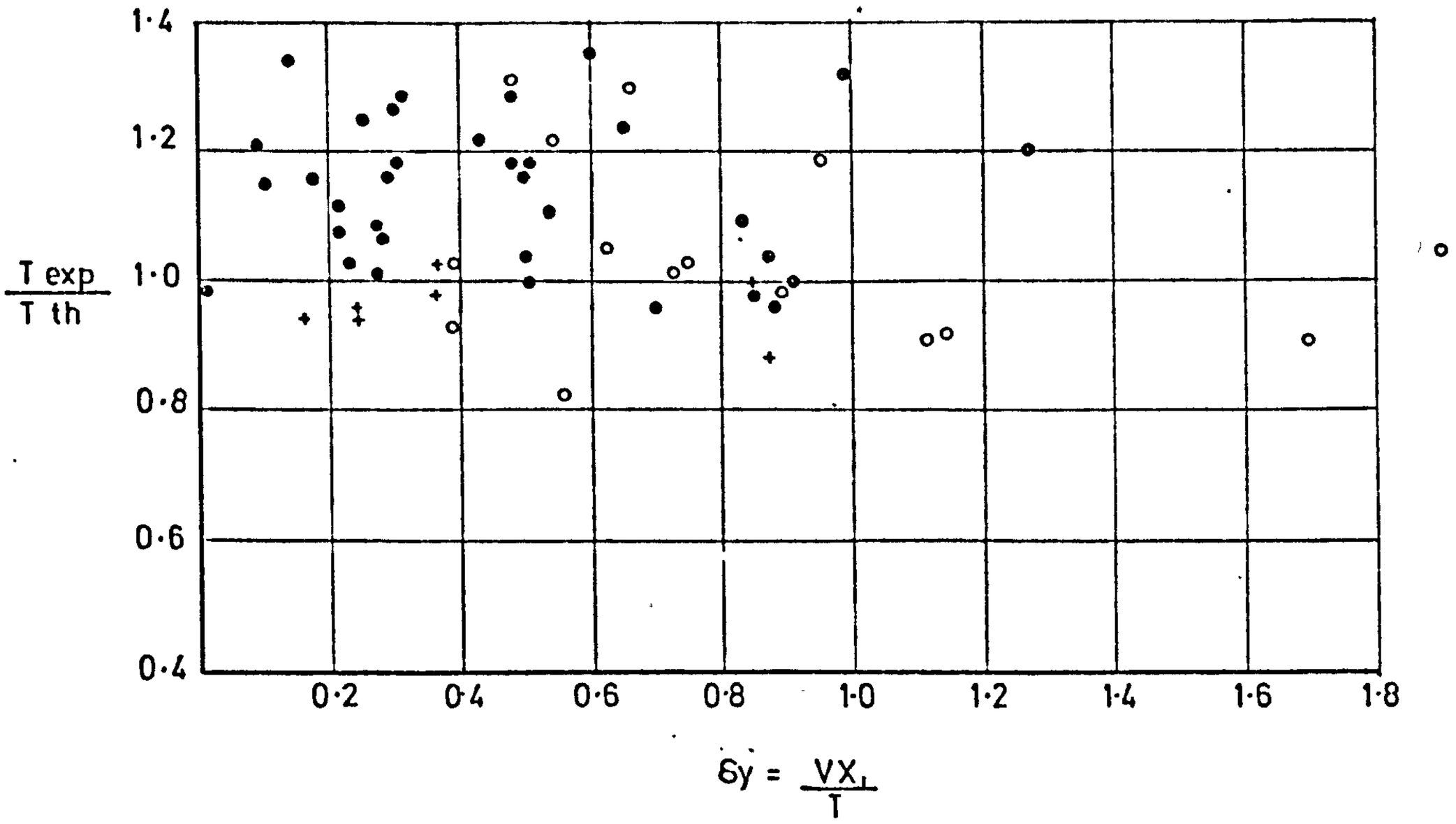

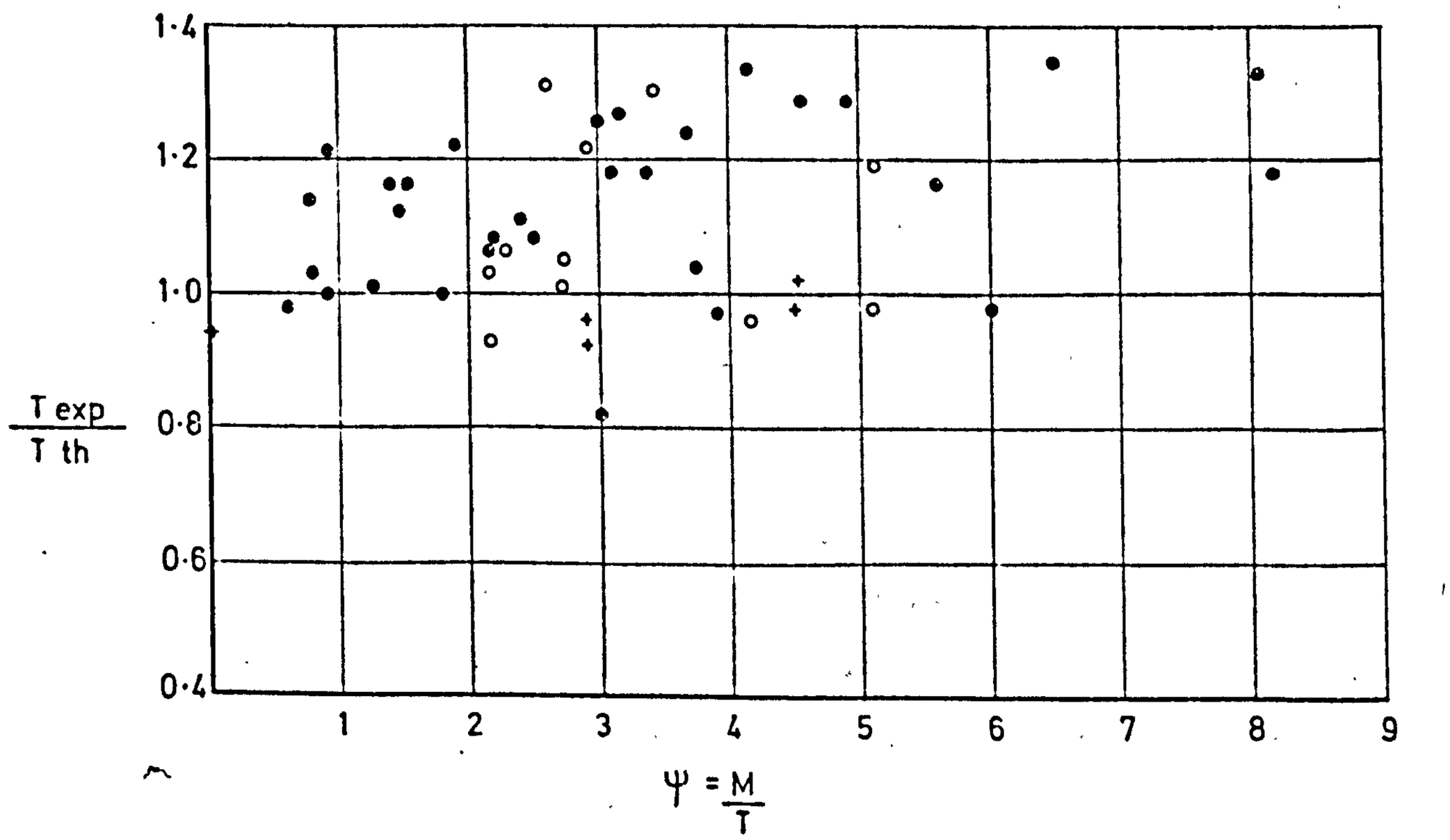

FIG 4 11 Comparison of experimental ultimate torque for prestressed concrete beams with web reinforcement subjected to bending torsion and shear.

4.7 Conclusions

The main conclusions which may be drawn from this investigation are as follows:

1. Yield Failure of reinforced and prestressed concrete beamssubjected to combined bending, torsion and shear may occur by three different modes.

2. In general, failure is governed by mode 1.

3. The addition of longitudinal reinforcement in the top face of the beam does not increase the strength of beams which fail according to mode 1.

4. In practice when modes 2 and 3 are critical they can be prevented by provision of sufficient reinforcement in the compression zone of the beam.

5. The choice of the angle of cracking influences the prediction of ultimate strength. In general, if the yield theory is based on the angle of cracking determined from the direction of the principal stresses, the theory would over-estimate the torsional strength of reinforced and prestressed concrete beams by 5 to 10 percent.

6. The torsional theory which assumes the angle of cracking to be governed by the direction of the compressive field occuring at failure under-estimates the strength of beams by 5 to 10 percent.

7. The effect of the variation of the depth of the compression zone on the prediction of the

strength of the beam is small and may be neglected.

8. The presence of shear stresses in the compression zone has a little effect on yield failures.

9. In general good agreement has been obtained when comparing predictions based on the proposed yield equations with the results of 574 beam tests reported in literature.

10. The range of m_b' increases with ψ where yielding of both reinforcements occurs.

11. The accuracy of prediction of any yield theory depends on the methods of determining the change from yield to other modes of failure.

12. There is no significant loss of accuracy in the prediction of yield strength due to many simplifying assumptions such as $k_z = 1$.

CHAPTER 5

ULTIMATE STRENGTH OF REINFORCED AND PRESTRESSED CONCRETE MEMBERS SUBJECTED TO BENDING, TORSION AND SHEAR

PARTIAL YIELD AND OVER-REINFORCED FAILURES

Summary

Six partial yield modes and two over-reinforced modes occuring in reinforced and prestressed concrete beams have been examined and theoretical expressions for prediction of these modes are given.

Strengths predicted by the proposed theoretical expressions have been compared with available test results.

5. Introduction

As already mentioned in chapter 4, reinforced and prestressed concrete members subjected to bending, torsion and shear may fail after yielding of one category of reinforcement only. These modes of failures will be referred to in the following as a partial yield failure. Failure may also occur prior to yielding of all reinforcements. These modes of failures will be referred to as over-reinforced failures. Partial yield and over-reinforced modes of failures are usually associated with the following conditions:

1. reinforced and prestressed concrete beams with large value of m'_b or without web reinforcement.
2. beam containing large volume of longitudinal reinforcement.
3. Unbonded prestressed concrete beam.

Partial yield failures have been reported by many researchers (5.1-5.4) testing beams under combined bending and shear or bending and torsion or bending, torsion and shear. These modes of failures have been found by Helmy (5.2-5.4) to occur either as a result of yielding of the stirrups or the longitudinal reinforcement. Failures due to yielding of stirrups will be referred to as the S modes whereas failures due to yielding of the longitudinal reinforcement will be referred to as L modes.

Partial yield failures have been attributed to the failure of concrete after partial yielding of the reinforcement (5.6). Some researchers assumed

that this failure occurs as a result of the failure of the uncracked concrete due to the combined action or shear and direct stresses and developed theoretical expressions for these modes of failure. These theories will be referred to as shear-compression theories. Other researchers ignored the effect of the compressive stresses developing in the uncracked concrete zone on the ultimate failure of the beam. These theories will be referred to as shearing failure theories.

The aim of this chapter is to develop various theoretical expressions for the prediction of partial yield and over-reinforced modes of failures.

5.1.1 Shearing Modes of Failures

The most important contribution to the study of partial yield failures occuring in reinforced concrete beams subjected to bending and torsion is that due to Goode and Helmy (5.2 to 5.4). They identified from experimental observations three partial yield modes of failure.

a. failure due to yielding of the top longitudinal reinforcement only.
b. failure due to yielding of bottom longitudinal reinforcement only.
c. yielding of stirrups only.

They also propounded a conservative theoretical approach for prediction of these modes of failure by assuming the angle of cracking = 45^{o} and ignoring the contribution of the uncracked concrete, aggregate interlock and dowel action. This approach can be classified as shearing theory.

A considerable amount of research information is found in technical literature on partial yield failures for reinforced and prestressed concrete beams subjected to bending and shear. This work has been reviewed by the shear study group of the Institution of Structural Engineers (5.1). However, the most recent, thorough and extensive research programme on this subject has been conducted by Regan et al (5.5 to 5.9) Regan proposed the following semi-empirical theory for the ultimate shear resistance of reinforced concrete beams:

$$V_u = \alpha_1 \left((100 \frac{\sum A_{sl}}{bd} f_{cu} \right)^{\alpha_2} bd + \alpha_3 \frac{2A_{sv} f_{yv}}{S_v} \qquad 5.1a$$

for rectangular beams the coefficients α_1 and α_2 were given in reference (5.7) as $\alpha_1 = 0.4 \left(\frac{V_d}{M}\right)^{\alpha_2}$ and $\alpha_2 = \frac{1}{3}$ and in reference (5.8) $\alpha_1 = 0.3$ and $\alpha_2 = 0.4$, α_3 is given as 1.5 in both references.

For T beams the ultimate strength was given as:

$$V_u = \alpha_1 \left(f_{cu} \right)^{\alpha_2} b_s d_s + \alpha_3 \frac{2A_{sv} f_{yv}}{S_v} (d - h_f) \qquad 5.1b$$

The coefficients α_1 and α_2 were given in reference (5.7) as $\alpha_1 = 0.8$ and $\alpha_2 = \frac{1}{3}$ and in reference (5.8) $\alpha_1 = 0.27$ and $\alpha_2 = \frac{2}{3}$. α_3 was given in both reference as 2.

b_s is the effective breadth of the compressive flange with regard to shear and was given as:

$b_s = 150 + b_w$, in reference (5.7) and

$= 1.5\ d_s + b_w$ in reference (5.8)

where b_w is the web breadth and h_f is the flange depth.

From experimental investigations on reinforced concrete beams subjected to combined bending, torsion

and shear, Collins et al (5.5) also identified partial yield failures similar to the shearing failure of reinforced concrete beams occuring under bending and shear. They also suggested the following expression for predicting this mode of failure

$$\frac{V}{V_u} + \frac{1.6\ T}{b\ V_u} = 1$$

where V_u is the shear strength in the absence of torsion. The ACI method was suggested for calculating V_u.

This theory was compared by these authors with test results and they obtained a value for the ratio $V_{exp} / V_{th} = 1.39, \pm 22\%$.

5.1.2 Shear-Compression Theories

Various theoretical expressions have been developed for predicting the strength of reinforced and prestressed concrete beams under combined loading which consider failure of these beams to be governed by the failure of the uncracked concrete. Available shear compression theories either consider the combined action of bending and shear or bending and torsion. Most of the important shear theories for the case of beams subjected to bending and shear have been reviewed by the shear study group of the Institution of Structural Engineers. These theories assume that failure of the beam is caused by the compression failure of the concrete at the head of the diagonal crack. The effect of this diagonal cracking was found to reduce the area of the compression zone as compared to the flexural failure.

In developing shear compression theories, various assumptions are made with regard to the following principles

a Compatibility of strains

b Failure criterion of concrete

c Stress distribution

d Shear transfer

e Maximum compressive strain in extreme fibres

A summary of these assumptions are given in Table 5.1 for all the important shear compression theories.

a) Shear-compression theories for beams subjected to bending and shear.

The ultimate shear-compression moment for rectangular reinforced concrete beams can be given as

$$M_{sc} = \alpha_1 f_{cu} x (1 - \alpha_2 x) bd^2 + \alpha_3 \frac{2A_{sv} f_{yv}}{S_v} d^2$$

where x is the depth of the compression zone at failure and α_1, α_2 and α_3 are unknown parameters. x is determined by considering the equilibrium conditions and the conditions listed in Table 5.1 which are briefly discussed in the following:

a) Compatibility of Strain

All the shear compression theories listed in Table 5.1 reject the assumption that plane sections before bending remain plane during loading (Bernoulli's assumption), a modified form of this assumption is generally used which is based on the total deformation of the portion of the beam which contains the

Table 5.1 Summary of principal used in development of existing shear-compression theories

Investigator	Ref	Compatibility Conditions	Strength of Concrete	Limiting Compressive Strain	Stress distribution due to		Shear transfer	Application
					Bending	Shear		
Walther	5.10	Special	Mohr' Failure criterion	$0.003\lambda^2$	R	R	$V_c + V_s$	R.C & P.S.C. Beam under B & S
Bjuggren	5.11	Modified Bernoulli theorem	N.C.	0.003	P	P	Do	R.C. beams under B & S
Regan	5.6	Do	N.C.	0.0035	P	P	Do	Do
Sheikh et al	5.12	Do	Coulumb's Internal friction theory	$0.000\,6\frac{M}{V_{cd}}$	R	R	$V_c + V_d + V_s$	R.C. & P.S.C. beam under B & S
Pandit and Warwaruk	5.14	Not stated	Cowan internal friction theory	N.C.	N.S	Plastic	$T_c + T_a + T_s + T_d$	R.C. beam under B & T
Iyengar and Regan	5.15	Not stated	Krishnaswamy failure criterion	N.C.	N.S	Plastic	$T_c + T_a + T_s$	Do
Evans & Khalil	5.16	Bernoulli theorem	Max Principal stress criterion	Elastic theory	Triangular	Plastic	$T_c + T_s$	P.S.C. beam under B & T
				$\frac{\epsilon'_c}{\epsilon_{cu}} = (\frac{M}{M_u})^2$	P			
Martin & Wainwright	5.17	Bernoulli theorem on the skew axis	Cowan internal friction theory	Elastic theory	P	Elastic due to diff. bending	T_c	Do

N.C. = This condition has not been considered

N.S. = This condition has not been stated

P = Prabolic stress distribution

R = Uniform stress distribution

V_c, T_c = Shear and torsion resisted by uncracked concrete respectively

T_a = Shear and torsion resisted by cracked concrete

V_s, T_s = Shear and torsion resisted by stirrups

V_d, T_d = Shear and torsion resisted by dowel action of longitudinal reinforcement

diagonal cracks. This compatibility condition is usually expressed as

$$\frac{\Delta_c}{\Delta_s} = \frac{x/d}{1 - x/d}$$

where Δ_c is the total deformation of the extreme compression fibre occuring over the length of the beam containing the shear crack. Δ_s is the elongation of the tensile reinforcement over the same length considered for Δ_c.

b) Failure Criterion of Concrete

Various treatments of this principle have been adopted by the authors of the shear compression theories listed in Table 5.1. Bjuggren and Regan ignored the effect of shear stresses on the strength of the compression zone, whereas Walther and Sheikh's (5.13) theories consider their influence. Walther utilized Mohers criterion of failure and Sheikh used Coulomb's shear friction theory of failure.

c) Stress Distribution in Compression Zone

As for the theories of flexural strength of reinforced and prestressed concrete, various approximations to the distribution of the direct and shear stresses have been adopted by the authors of the shear compression theories. Walther and Sheikh adopted a rectangular stress block for shear and flexural stresses whereas Regan suggested a parabolic stress distribution. It is possible that the choice of the stress block

will have little influence on the shear compression strength of the beam as in the case of the pure bending theory.

d) Shear Transfer

All the shear compression theories except that developed by Sheikh, assume that the shear is resisted by the uncracked concrete zone and the transverse reinforcement only i.e. the contribution of the aggregate interlock and dowel action have been ignored. It is probable that the effect of this conservative assumption is cancelled by the other assumptions which have been made.

e) Maximum Compressive Extreme Fibre Strain (ϵ_{cu})

When considering the concrete strain in the compression zone various treatments have been adopted by the authors of the compression theories. Bjuggren and Regan (5.1) adopted the normal flexural limiting strain $\epsilon_{cu} = 0.003$ (Bjuggren) and 0.005 (Regan), whereas Walther argued that the shear stresses not only effect the strength of the compression zone but also reduce the limiting strain, and he suggested the following expression for parameter.

$$\epsilon'_{cu} = 0.003\,\lambda^2$$

where $$\lambda = \frac{1}{1 + 3.2\left(\frac{V_e d}{M}\right)^2}$$

Sheikh obtained the following expression for this parameter by experiment

$$\epsilon'_{cu} = 0.0006 \frac{M}{V_c d}$$

where V_c is the shear resisted by the compression zone and d is the effective depth of the beam.

b) Shear Compression Theories for Beams Subjected to Bending and Torsion

Table 5.1 also lists the various assumptions which were adopted for the five principles stated above for the development of existing shear compression theories for reinforced and prestressed concrete beams subjected to bending and torsion. The following is a brief review of these theories

a) Pandit and Warwaruk (5.14) proposed a torsional theory which considered the torsion to be resisted by the steel and concrete of reinforced concrete beams subjected to combined bending and torsion, the total torsional resistance of the beam is obtained from

$$T = T_c + T_{s1} + T_{s2}$$

where T_c is the torsional resistance of the concrete, T_{s1} is the torsional strength of the stirrups, T_{s2} is the torsional strength due to dowel action of the longitudinal reinforcement. In this theory the torsional resistance of the concrete is taken to be made of the torsional strength of the cracked and uncracked portion of the beam. The area of the uncracked portion or the

compressive zone was assumed to be one quarter of the cross section and subjected to bi-axial stress due to direct stresses due to bending and the shear stresses (calculated from the plastic theory) due to torsion. These stresses were combined using Cowan (5.20) shear friction failure criterion for the concrete. The shear stresses resisted by the cracked part of the beam were taken as constant at 0.75 of the tensile strength of the concrete.

The stirrups strength was based on the number of stirrups intersecting a critical crack inclined at 45^{o} to the longitudinal axis. The stresses in the stirrups according to this theory depend on the dowel strength of the longitudinal bars. In calculating the dowel strength of the longitudinal reinforcement, the bars were assumed to act as a cantilever with a span equal to the spacing of the stirrups and these bars were assumed to develop their full plastic moment of resistance!

The assumption of the fixed depth of the compression zone and the method used for calculating the dowel strength of the longitudinal bars are all open to criticism and questions.

b) Iyengar and Rangan theory

This theory was based on the assumptions that the member was cracked, the transverse steel yields, the contribution of horizontal

(shorter) legs of the stirrups to the torsional resistance is neglected and the dowel action was also ignored.

In this theory failures have been divided into two modes:

1. torsional
2. flexural

For the torsional mode the theory is based on the assumption that the torque is resisted by the concrete and the stirrups. Failure of the beam was taken to occur as a result of failure of the concrete under the combined action of the compressive and tensile principle stresses due to torsion only. The torsional shear stresses were calculated on the basis of the average values obtained from the elastic and plastic theories. In this theory failure was controlled by the Krishnaswamy failure criterion.

Flexural mode of failure was controlled by the failure of the concrete in the compression zone. Using the same failure criterion for concrete adopted for the torsional mode, the direct stresses due to bending and the shear stresses due to torsion were combined to obtain the strength of the beam. The torsional shear stresses were assumed to be distributed over the whole section in accordance with the plastic theory.

This theory also invites many criticisms such as the assumption made for the distribution of the torsional stresses and the assumption of the tensile force in the stirrups.

c) Evans and Khalil (5.16) published the first rational shear-compression theory for prestressed concrete beams subjected to bending and torsion. In this theory failures have been divided into three main groups depending on the applied moments. For group 1 where the beams are subjected at failure to a moment equal to or less than the pure cracking moment. The strength of these beams were determined from the following semi-rational expression:

$$T = T_{cr} + \zeta T_s$$

where T_{cr} is the torque which caused cracking and ζT_s is the contribution of the stirrup reinforcement.

For group 2 the ultimate torsional strength was taken as the combined torsional resistance of the compression zone and the stirrups. The strength of the uncracked concrete was determined by combining the average direct stresses due to bending and the shear stresses due to torsion. Failure was controlled by the maximum principle tensile stress failure criterion. The direct stresses were determined by the elastic theory of cracked prestressed concrete beams and the shear stresses were

determined from the plastic theory of torsion.

This failure was assumed to occur for beams subjected to a moment greater than the pure flexural cracking moment and a moment less than 80 percent of the pure flexural ultimate strength of the beam.

In group 3, the torsional resistance was also taken as the combined contribution of the uncracked compressive zone and the web reinforcement. The direct stresses were determined assuming a parabolic stress block and the extreme fibre compressive strains were assumed to be reduced by the existance of the torsional shear stresses and the strength of this compressive zone is governed by the shear stress at which failure changes from a cleavage to a shear type in accordance with the Cowan dual failure criterion. The validity of this assumption will be discussed in the next section of this chapter.

c) Martin and Wainwright (5.17) recently developed a shear compression theory for pre-stressed concrete beams subjected to bending and torsion. This theory was developed for the case of beams without shear reinforcement, it is based on the concept of skew bending in which the torque is assumed to be resisted by differential bending of the compression zone with the longitudinal reinforcement acting as a dowel. The direct and shear stresses in the compression zone assumed to vary

parabolically and failure due to these stresses is assumed to be governed by Cowan's failure criterion of concrete. In addition all the materials of the beam are assumed to obey Hookes law up to failure.

This theory requires a trial and error procedure for the determination of the strength of prestressed concrete beams and does not consider the possibility of failure of the dowel action. It can be shown that for the condition assumed in this theory failure will always be governed by the dowel action rather than the concrete in the compression zone, unless the contribution of the aggregate interlockis considered together with the dowel action when failure may be governed by the failure of the concrete in the compression zone.

5.2 Comments on Existing Theories

From this review the following conclusions may be drawn:

1. None of the theoretical shear compression theories deals with the general case of beams subjected to bending, torsion and shear. In addition they are more difficult than the shearing theories.

2. The shear compression theories which have been developed for the case of beams subjected to bending and shear assume that the shear is resisted mainly by the uncracked portion of concrete. This assumption has been vindicated by Fenwick (5.18) and Taylor (5.19) who found that for beams without shear reinforcement and

failing in shear, the compression zone resists only 25 percent of the applied shear.

3. Fenwick and Taylor's work indicated that aggregate interlock resists over 50 percent of the applied shear, therefore, the calculation of the shear strength of the beam in terms of aggregate interlock appears to be more acceptable. The contribution of the shear-resistance of the compression zone and dowel action of the longitudinal reinforcement may be considered indirectly in terms of the strength of the aggregate interlock.

4. Considerable simplification of the method for predicting partial yield failure can be achieved by ignoring the influence of the direct compressive stresses in the compressive zone.

5. For practical purposes the prediction of partial yield failures are given by the following shearing theories.

6. The problems of predicting all possible partial yield failure modes have not been explored.

7. To develop a rational theory for over-reinforced failures it is necessary to consider principles similar to those which have been followed for the development of shear compression theories, therefore, the following discussion would cover the five principles that have been employed in the development of shear compression theories.

a) Compatibility Conditions

Although the method used for the shear-compression theories for beams subjected to

bending and shear is rational, a generalisation of this method to the case of beams subjected to bending, torsion and shear is impracticable. Therefore, the following duel compatibility conditions are more appropriate for this general case of loading.

1. The Bernoulli assumption is suggested for the case of beams subjected to bending and torsion and a low value of shear.

2. Modified Bermoulli's assumption based on a finite length of the beam for the case of beams subjected to bending and shear and a low value of applied torsion.

b) Failure Criterion for Concrete

To test the validity or otherwise of the various failure theories that have been adopted in the development of shear compression theories, the experimental results reported by helmy on a thin-walled cylinder subjected to compression and torsion are plotted in Fig. 5.1. In Fig. 5.1a the ratios of direct compressive stress at failure to the uni-axial compressive strength have been plotted against the ratios of the compressive stress to shear stress. In Fig. 5.1b, the ratio of the shear stresses at failure to the tensile strength of concrete has been plotted against the ratio of the direct compressive stress at failure to the uni-axial strength of concrete. The uni-axial strength for concrete has been taken as $f_{co} = 0.67\ f_{cu}$ and the tensile strength has been taken as $f_t = 0.36\sqrt{f_{cu}}$. On these diagrams the following theoretical failure curves are

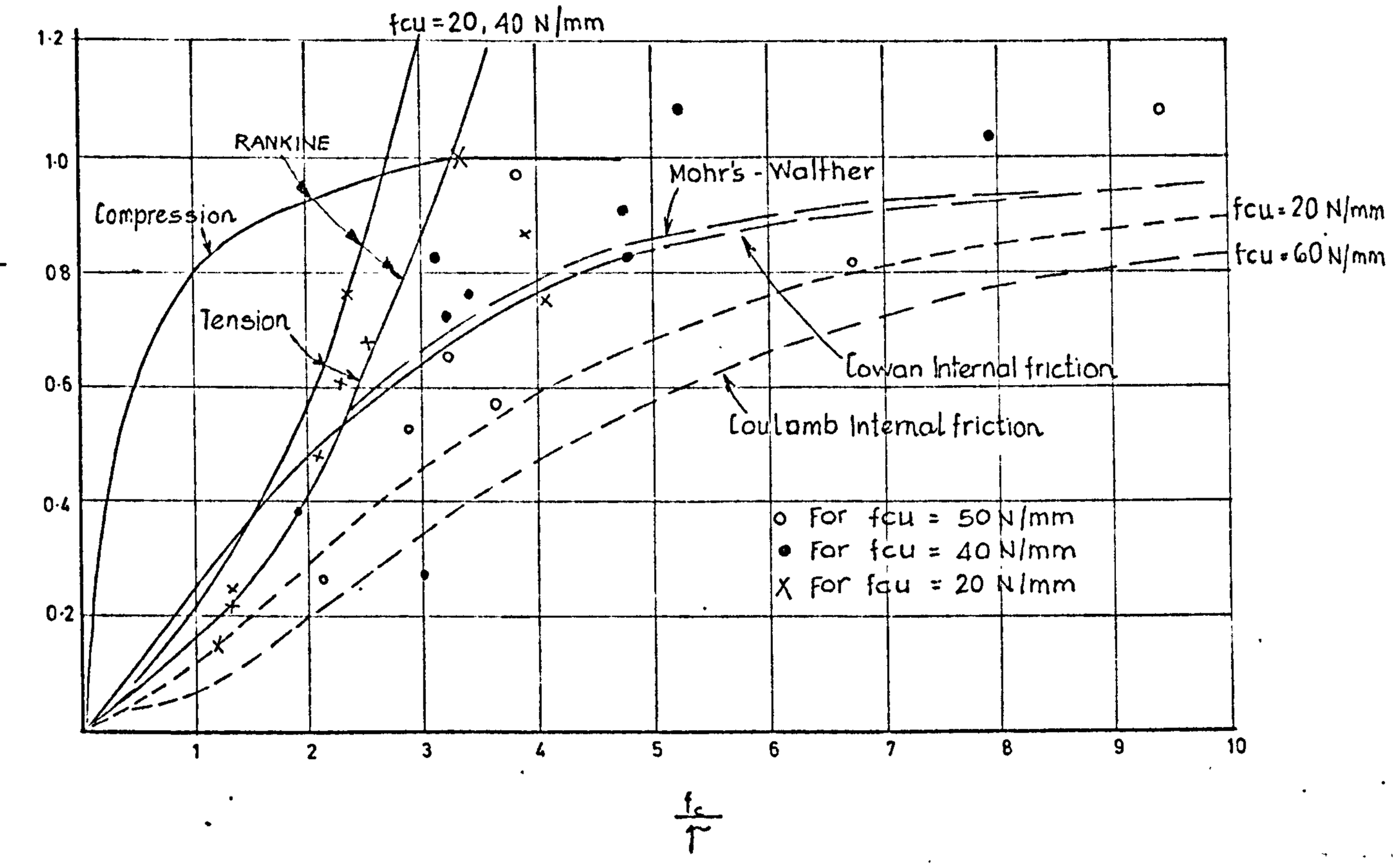

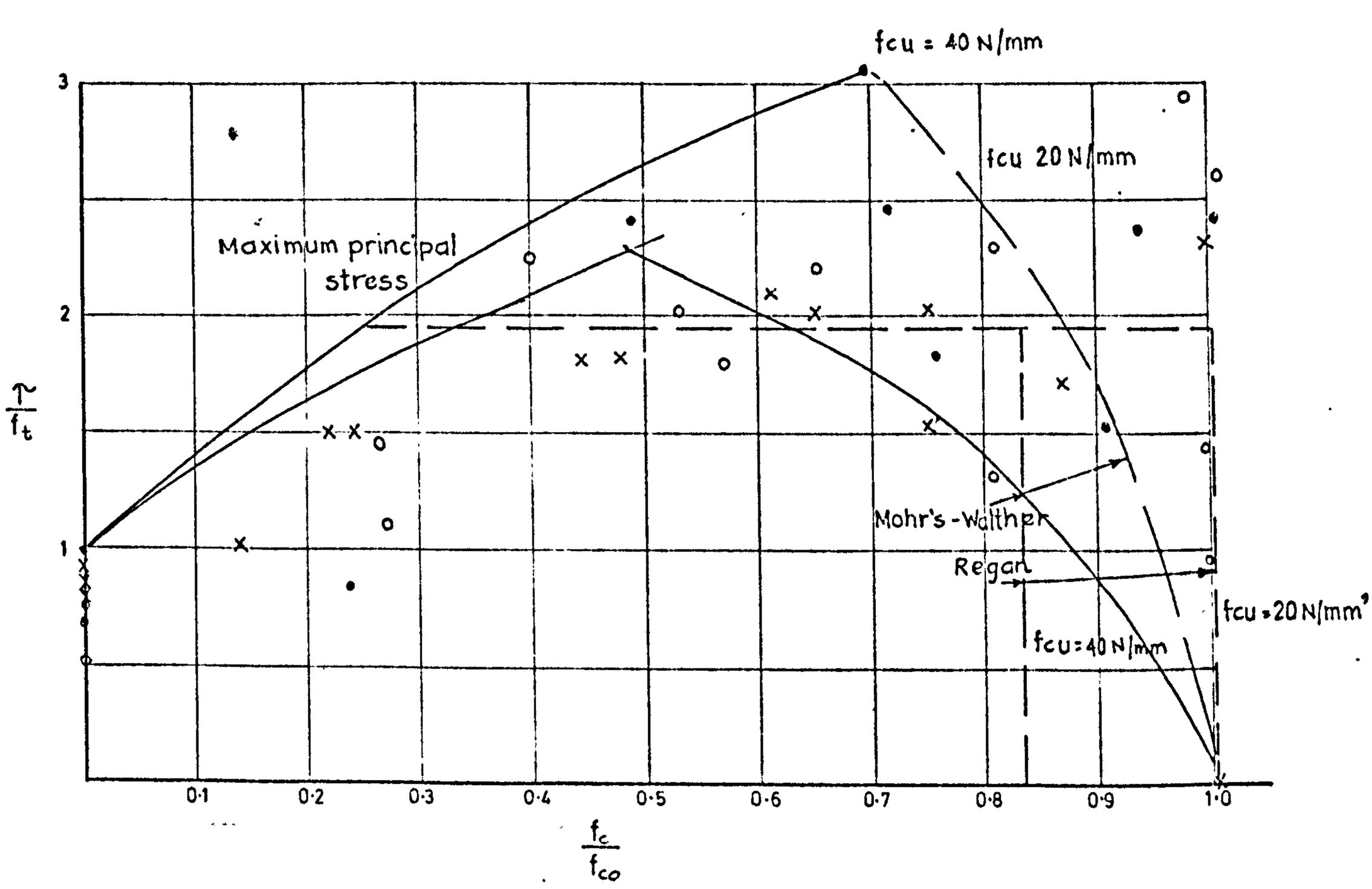

FIG 5·1 COMPARISDN OF VARIOUS THEORIES OF FAILURE FOR CONCRETE UNDER COMBINED COPRESSION & SHEAR STRESSES WITH TEST RESULTS. (Ref 5·4)

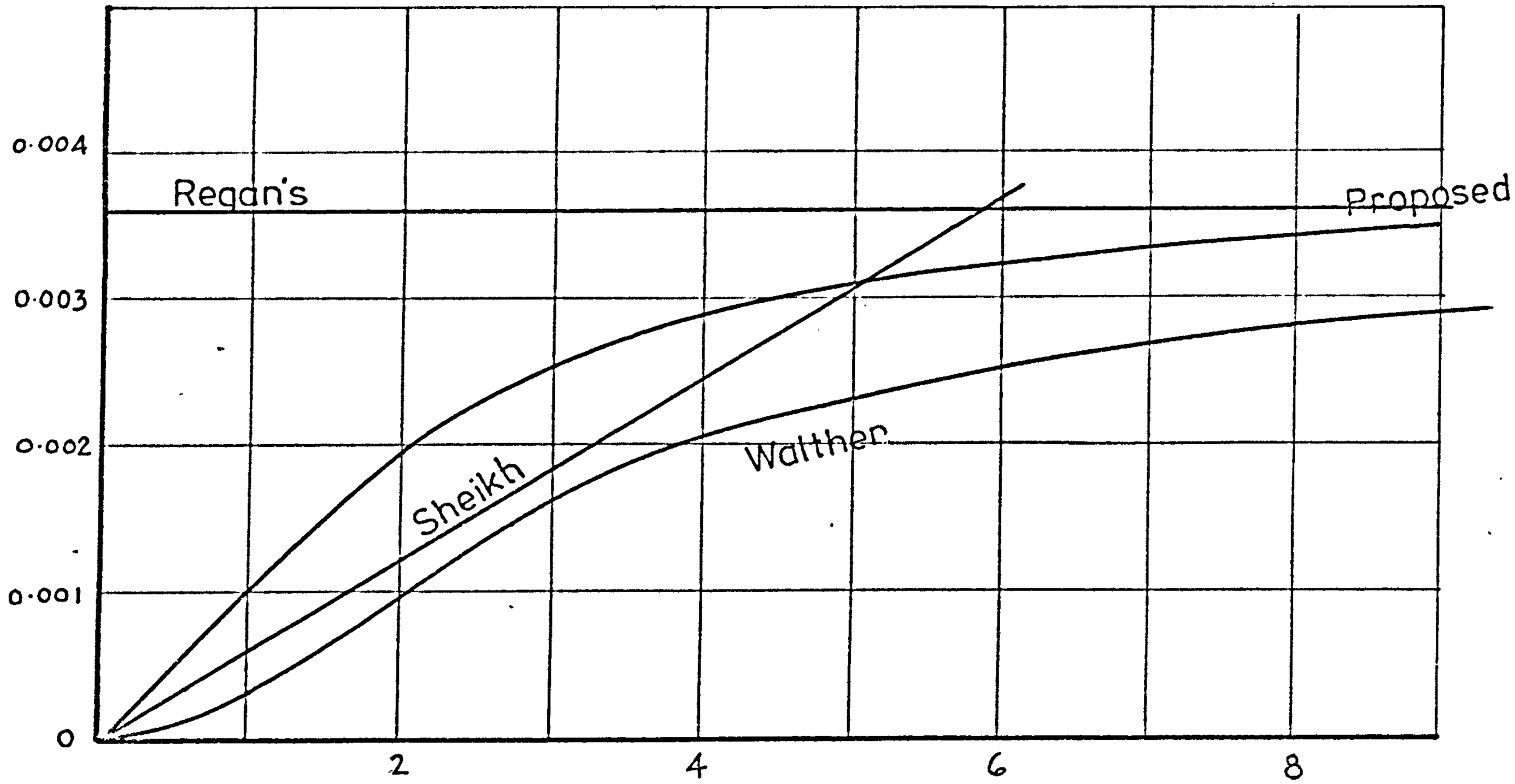

FIG. 5.2 INFLUENCE OF SHEAR STRESS ON THE MAXIMIN COMPRESSIVE STRAIN

plotted:

1. Rankine Principle Stress Theory
2. Mohr's-Walther theory using second degree parabola (5.10).
3. Cowan's shear friction theory (5.20)
4. Coulomb's internal shear friction theory
5. Regan's Failure Criterion (5.9).

From this comparison, it can be concluded that;

1. The Coulomb theory considerably underestimates the strength of concrete under a combined stress system.
2. Walther and Cowan's theories give reasonably the same results and appear to agree with the test results for specimens subjected to $f_x/\tau_x > 2$.
3. The maximum principal stress theory appear to predict the test results for specimens having $f_x/\tau_x < 2$.
4. The maximum principal compressive stress theory appears to overestimate the test results considerably.
5. The assumptions used by Evans and Khalil for the calculation of the strength of beams in group 3 can not be substantiated from this comparison.
6. Regan's criterion, although simple, requires three expressions to cover the whole range of the stress system and may be less accurate.
7. A duel failure criterion as suggested by Cowan appears to offer a reasonable solution to the problem.

8. Since Mohr-Walther's theory is expressed in simpler terms than Cowan's friction theory, it can be used together with the maximum principal stress criterion in order to determine the strength of concrete. This theory may be expressed as follows:

$$\frac{f_x}{f_{co}} = \frac{1}{1 + \left(\frac{2\tau_x}{f_x}\right)^2}$$

c) Stresses Distribution

There is no available test evidence to suggest that the choice of an assumed stress distribution in the compression zone would significantly influence the prediction of the strength of the beam, therefore, the choice of stress distribution should be governed by the degree of simplicity that would be obtained in the analysis

d) Shear Transfer

The shear compression theories due to Pandit and Worwaruk and Iyengar and Rangan both acknowledge indirectly the contribution of aggregate interlock in resisting shear stresses. On the other hand Evans and Khalil acknowledge indirectly the contribution of aggregate interlock for group 1 and ignore it completely in the case of group 2 and 3. This treatment by Evans and Khalil is satisfactory since it is based on the cracking pattern of unbonded prestressed concrete beams therefore, the contribution of aggregate interlock seems to be a function of the bending to torque ratio

and the bond characteristics. A rational theory should consider the contribution of these forces together with the resistance of the uncracked portion of concrete and the dowel action of longitudinal reinforcement.

e) Maximum Compressive Strain in Extreme Fibres

There is considerable disagreement on the choice of this parameter. Fig. 5.2 shows a comparison between the various assumptions made in the shear compression theories together with the test results reported by Sheikh. These results suggest that this maximum strain is influenced by the presence of shear stresses and this parameter may be obtained from the following assumption:

$$\frac{\epsilon'_{cu}}{\epsilon_{cu}} = \frac{f_x}{f_{co}}$$

5.3 Shearing Modes Theories

Shearing modes of failures are assumed in this analysis to occur as a result of failure of aggregate interlock after yielding of one category of reinforcement. These modes can be divided into S and L modes and further subdivided as follows:

L1 Failures which occur when the bottom longitudinal reinforcement reaches the full axial yield strength.

L2 This failure occurs when the longitudinal reinforcement located near the one side of the beam reach their full axial yield strength.

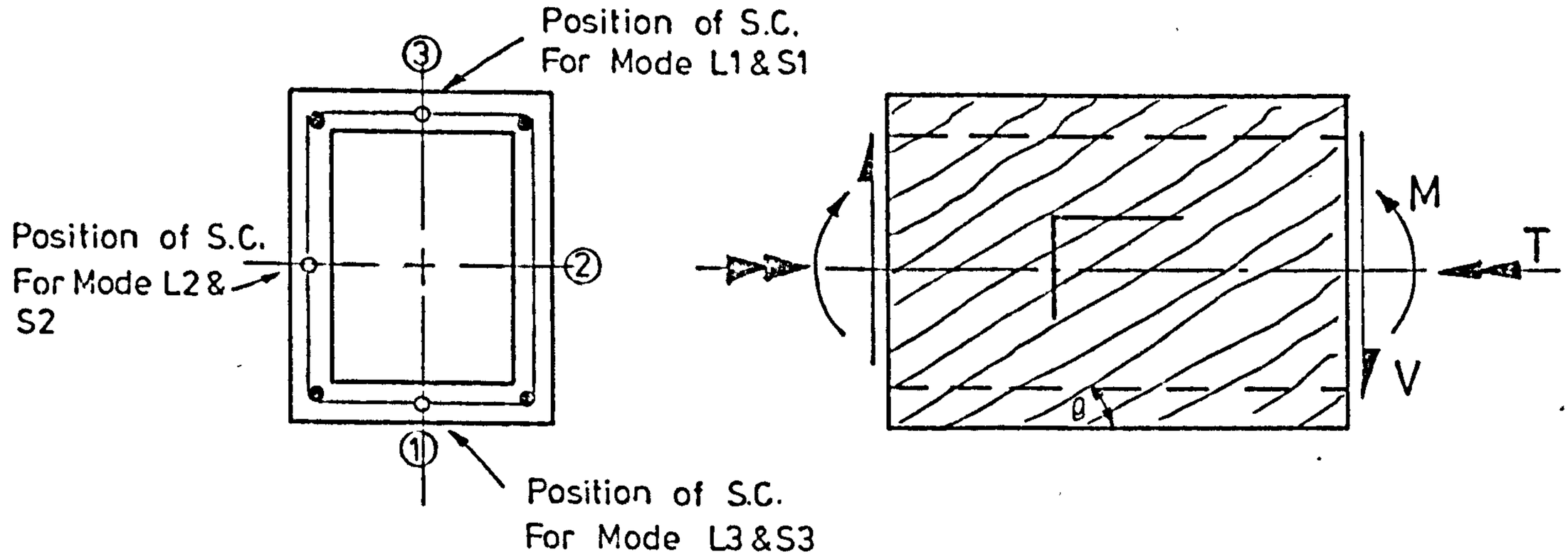

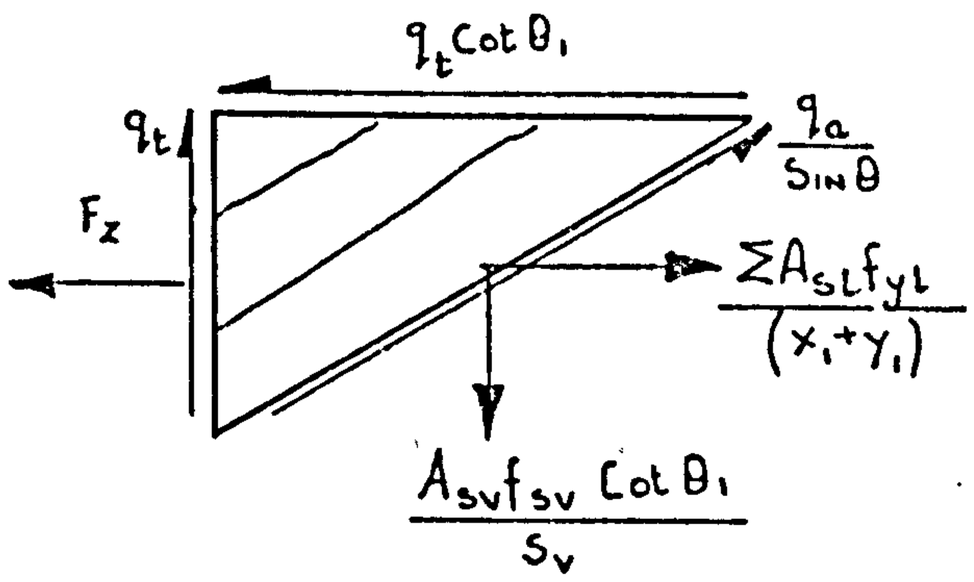

Mode L1

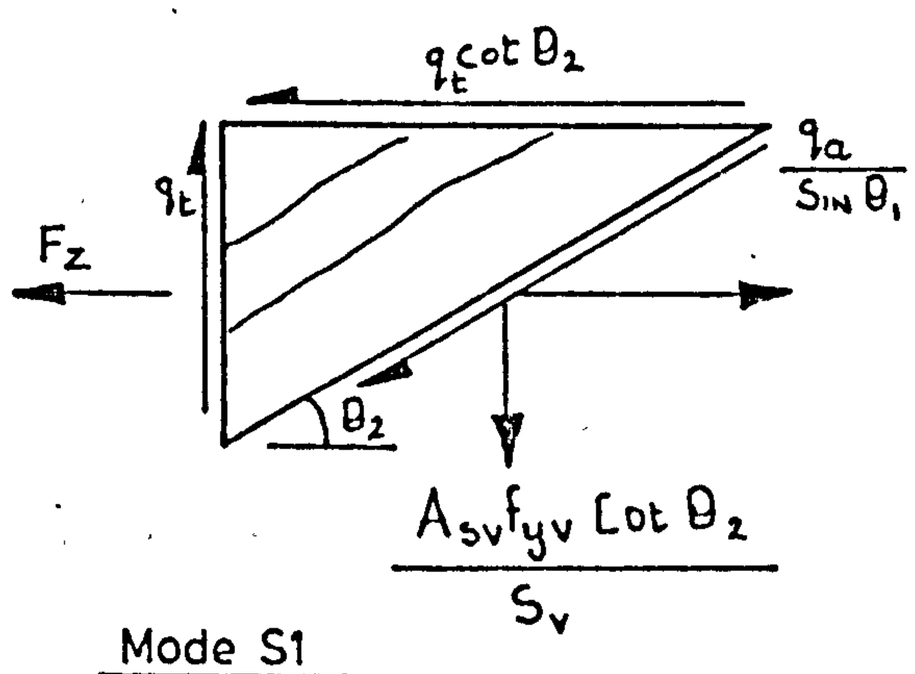

Mode S1

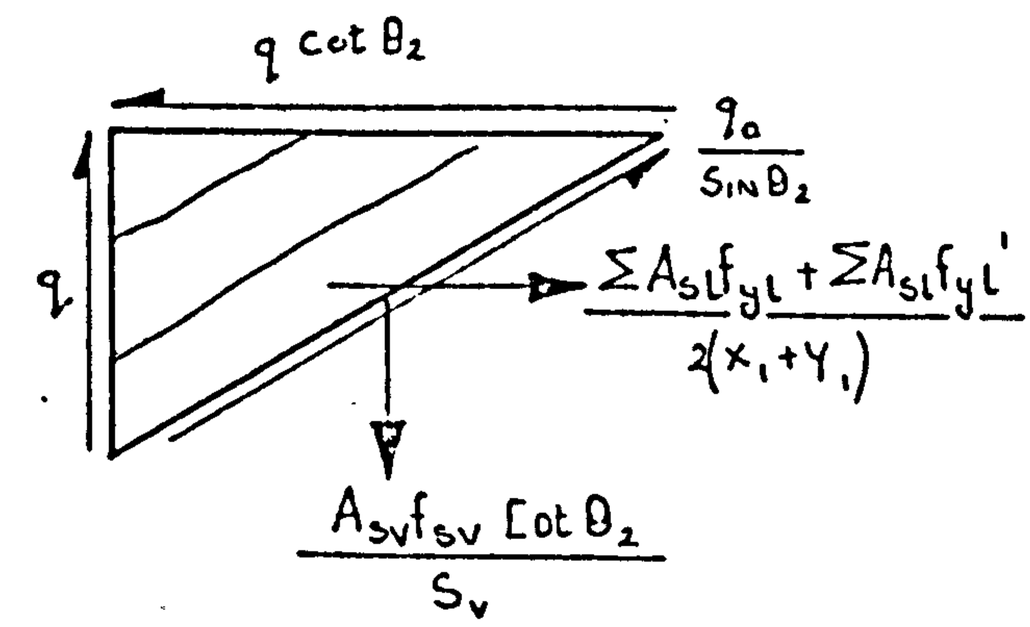

Mode L2

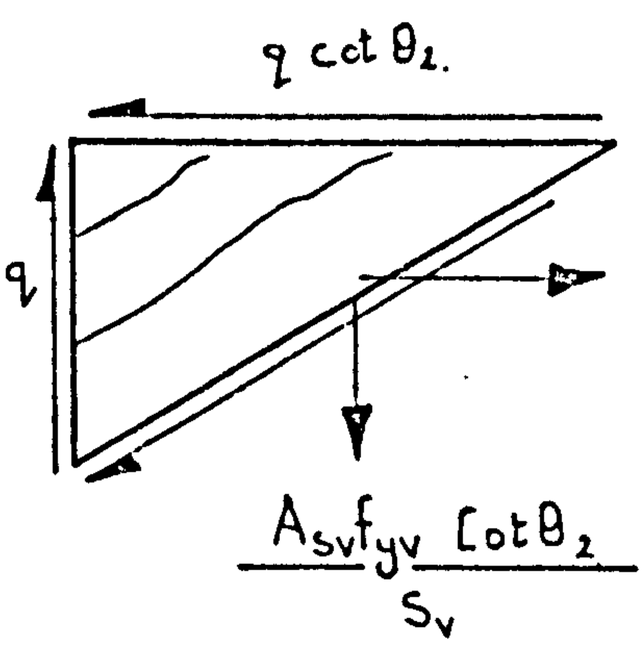

Mode S2

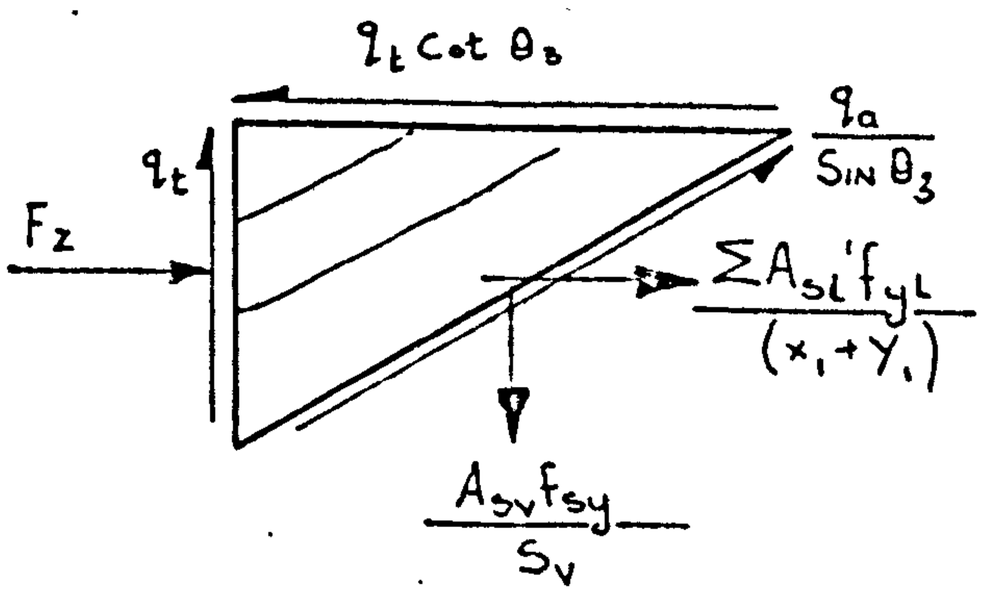

Mode L3

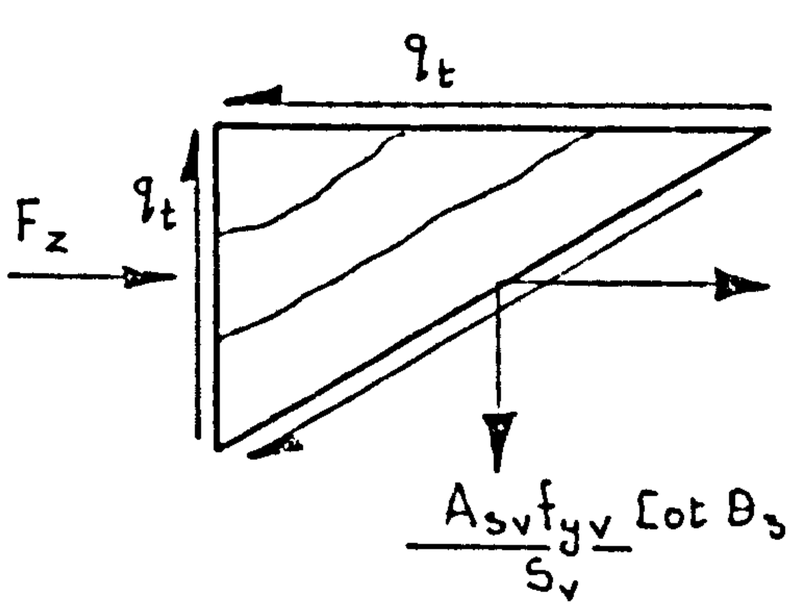

Mode S3

FIG 5.3 Forces acting on rectanguler element of failure for beam subjected to bending—torsion & shear.

L3 Failure which occurs when the top longitudinal reinforcement reaches full axial yield strength.

S1 This failure occurs when both the vertical and the bottom legs of the stirrups reach their full tensile yield strength.

S2 This failure occurs when one vertical leg and the top and bottom legs of the stirrups reach their full tensile yield strength.

S3 This occurs when both vertical legs and the top leg of the stirrups reach their full tensile yield strength.

Mode L1 failure may occur for beams subjected to small torsion and high bending moment where the cracking inclination is almost at 90^{o} to the longitudinal axis of the beam. For this mode and mode S1, the axis of rotation tends to shift towards the compression zone of the beam hence, it is reasonable to assume that the position of shear centre for these modes will correspond to the position of the shear centre assumed for mode 1 of the yield failures. Similarly the position of the shear centre for modes L2 and S2 would correspond to the position assumed for mode 2 of the yield modes and so on.

In the following development of theoretical expressions for the partial yield failure, the rectangular box beam used in the development of the yield theory given in chapter 4 will also be used.

PAGE

MISSING

IN

ORIGINAL

5.3.1 Mode L1

Considering the longitudinal equilibrium of forces acting on an element cut from the bottom flange of this box-beam shown in Fig. 5.3 we get:

$$F_z + q_t \cot \theta_1 = \sum \frac{A_{sl}\ f_{yl}}{(X_1 + Y_1)} + q_a \cot \theta_1 \qquad 5.2$$

substituting for $F_z = \frac{M}{(X_1 + Y_1)\ Y_1}$, $q_t = \frac{T_{\ell 1}}{2\ X_1\ Y_1}$ and

rearranging we get:

$$\frac{T_{\ell 1}}{T_s} \cot \theta_1 + m'_b \frac{M}{M_o} = m'_b + \frac{T_a}{T_s} \cot \theta_1 \qquad 5.3$$

where $M_o = Y_1 \sum A_{sl}\ f_{yl}$, $T_s = \frac{2\ A_{sv}\ f_{yv}}{S_v}\ X_1\ Y_1$,

$m'_b = \frac{A_{sl}\ f_{yl}}{(X_1 + Y_1)} \frac{S_v}{A_{sv}\ f_{yv}}$ and T_a is the torque resisted by aggregate interlock.

5.3.2 Mode L2

Similarly the failure load may be determined from consideration of the longitudinal equilibrium of forces acting on an element from the web of the box beam.

$$q \cot \theta_2 = \frac{\sum (A_{sl}\ f_{yl} + A'_{sl}\ f'_{yl})}{2\ X_1 + Y_1} + q_a \cot \theta_2 \qquad 5.4$$

taking the total torque $= T + \frac{VX_1}{2}$ and,

$$q = \frac{T}{2\ X_1\ Y_1} \text{ and } R_y = \frac{\sum A'_{sl}\ f'_{yl}}{\sum A_{sl}\ f_{yl}}$$

we get:

$$\frac{T_{L2}}{T_s} = \left[\frac{(1 + R_y)\ m'_b}{2\ \text{Cot}\,\theta_2} + \frac{T_a}{T_s} \right] \frac{1}{(1 + \frac{\delta_y}{2})} \qquad 5.5$$

where $\delta_y = \frac{VX_1}{T}$

5.3.3 Mode L3

Similarly from consideration of the longitudinal equilibrium of forces acting on an element from the top flange of the box-beam

$$-F_z + q_t\ \text{Cot}\,\theta_2\ \frac{\sum A'_{sl}\ f'_{yl}}{(X_1 + Y_1)} + q_a\ \text{Cot}\,\theta_2 \qquad 5.6$$

substituting for $F_z = \frac{M}{(X_1 + Y_1)\ Y_1}$ and $q_t = \frac{T_{L3}}{2\ X_1\ Y_1}$

and rearranging we get:

$$\frac{T_{L3}}{T_s}\ \text{Cot}\,\theta_2 - m'_b\ \frac{M}{M_o} = R_y\ m'_b + \frac{T_a}{T_s}\ \text{Cot}\,\theta_2 \qquad 5.7$$

5.3.4 Mode S1

From consideration of the transverse equilibrium of the forces acting on element 2 shown in Fig. 5.3 we get:

$$q = \frac{A_{sv}\ f_{yv}}{S_v}\ \text{Cot}\,\theta_2 + q_a \qquad 5.8$$

substituting for $q = \frac{T}{2\ X_1\ Y_1} + \frac{V}{2\ Y_1}$ and rearranging

we obtain:

$$\frac{T_{sl}}{T_s} = \left[\cot\theta + \frac{T_a}{T_s}\right]\frac{1}{1+\delta_y} \qquad 5.9$$

but this mode is usually associated with a high applied shear force, therefore it is best to express this mode of failure in term of shear. Thus rearranging equation 5.9 we get:

$$V = \frac{\delta_y}{1+\delta_y}\left[2\, q_a\, Y_1 + \frac{2\, A_{sv}\, f_{yv}}{S_v}\, Y_1 \cot\theta\right] \qquad 5.10$$

but $q_a = v_a\, b_w$

where v_a is the average shear stress resisted at failure by aggregate interlock which is known to be influenced by the concrete strength and percentage of longitudinal tensile reinforcement and may be taken as:

$$v_a = 0.4 \sqrt[3]{100\, \frac{\sum A_{sl}}{bd}\, f_{cu}}$$

This term approximate to the value suggested by Regán (5.8) and similar to the values given in CP 110.

For rectangular beam $2\, b_w \rightarrow b$, and taking $Y_1 = d$ equation 5.10 becomes

$$V = \frac{\delta_y}{1+\delta_y}\left[0.4 \sqrt[3]{100\, \frac{\sum A_{sl}}{bd}\, f_{cu}}\; bd + \frac{2A_{sv}\, f_{yv}}{S_v}\, Y_1 \cot\theta\right] \qquad 5.11$$

the term inside the brackets corresponds to equation 5.3 hence, the effect of torsion is to reduce the shear resistance of the beam by the factor $\frac{\delta_y}{1+\delta_y}$

5.3.5 Mode S2

From consideration of the transverse equilibrium acting on an element shown in Fig. 5.3, we get:

$$q = \frac{A_{sv}\ f_{yv}}{S_v} \quad \cot \theta_2 + q_a$$

The total torque about the shear centre $= T + \frac{VX_1}{2}$

and taking $q = \frac{T_t}{2\ X_1\ Y_1}$. Substituting these values and rearranging we obtain:

$$\frac{T_{s2}}{T_s} = \left[\cot \theta_2 + \frac{T_a}{T_s}\right] \frac{1}{1 + \frac{\delta_y}{2}} \qquad 5.12$$

5.3.6 Mode S3

Similarly from consideration of the longitudinal equilibrium of forces acting on an element cut from the top flange of the box-beam we obtain:

$$q_t = \frac{A_{sv}\ f_{yv}}{S_v} \cot \theta_2 + q_a$$

but $q_t = \frac{T_{s3}}{2\ X_1\ Y_1}$ we get:

$$\frac{T_{s3}}{T_s} = \cot \theta_2 + \frac{T_a}{T_s} \qquad 5.13$$

This mode will only occur if the beams contain a large volume of tensile longitudinal reinforcement i.e. $R_y << 1$ where the shear centre will be located near the bottom face of the beam.

5.4 Inter-Relation of Shearing Modes and Yield Modes of Failure

There are a total of nine yield and partial yield modes of failure. The relationship between these modes can best be illustrated by reference to the non-dimensional interaction diagrams shown in Fig. 5.4. These diagrams were constructed for reinforced concrete beams subjected to combined bending and torsion only and having typical values of m_b' and R_y. The inclination of the cracks was taken for simplicity as 45^o except for mode L1 where it has been taken at 90^o.

It is seen that all yield and partial yield modes are possible and the interaction diagram may be composed of two or more lines representing different modes of failure. Interaction diagrams composed of three straight lines representing modes L1, Y1 and S would represent the failure of beams containing an equal volume of longitudinal reinforcement placed on the top and the bottom of the beam i.e. $R_y = 1$. An interaction diagram such as this has previously been obtained empirically by Kemp (5.23), and Zia and Cardenas (5.22).

Although all these modes are possible, mode L1 may be safely ignored if the yield theory proposed in chapter 1 is used with $\theta = \theta_{min}$ as shown in Fig. 5.4.

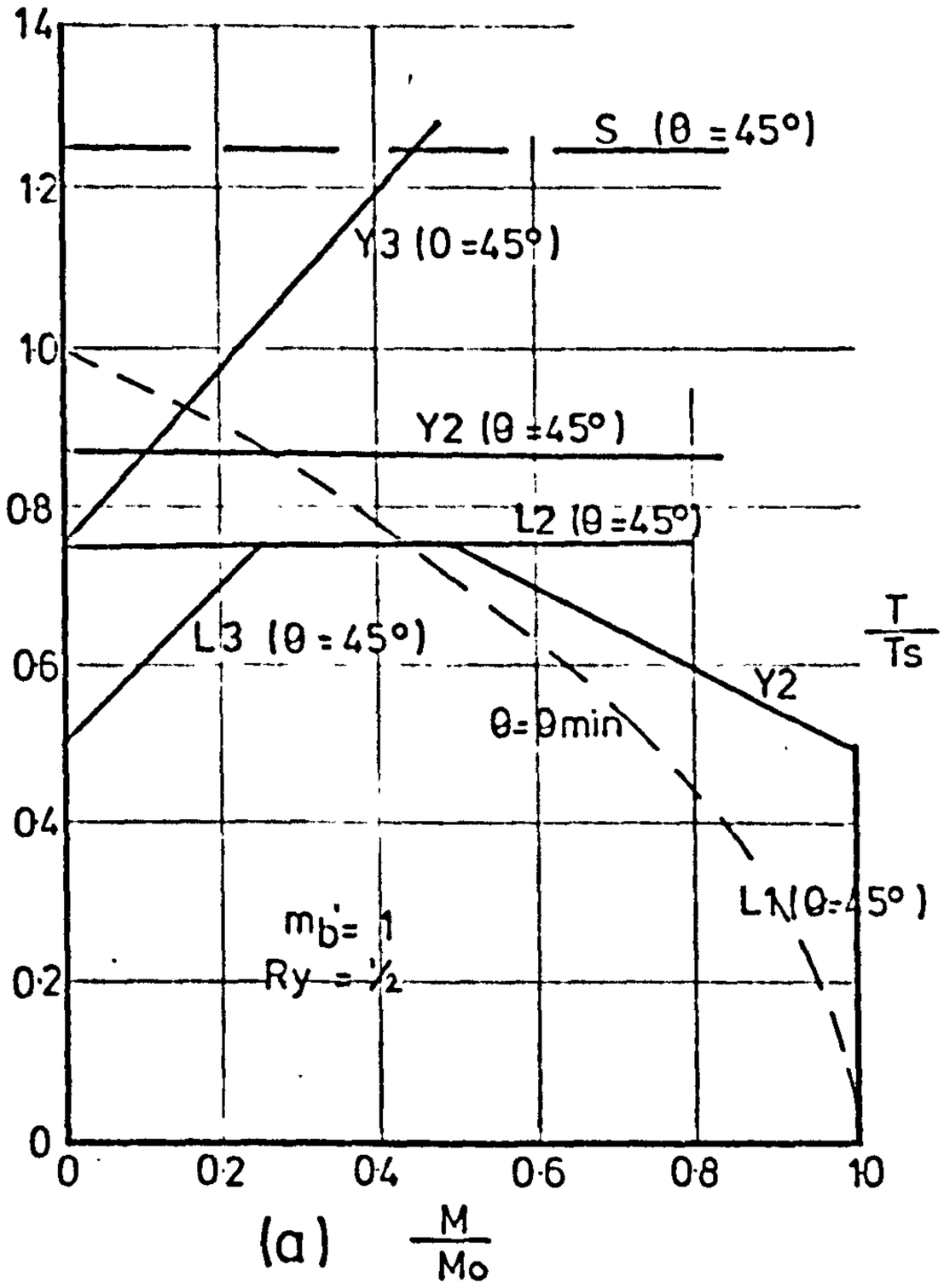

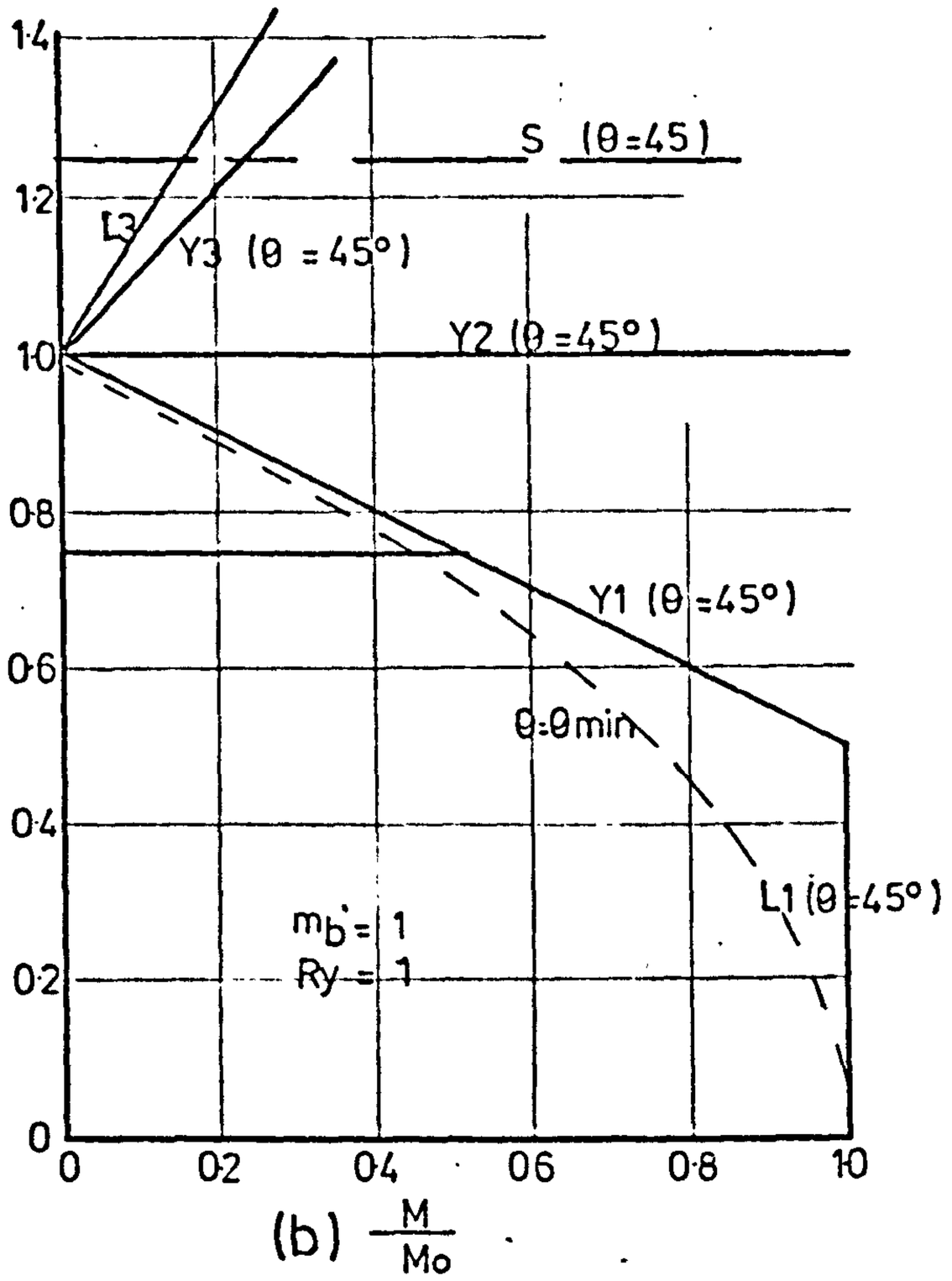

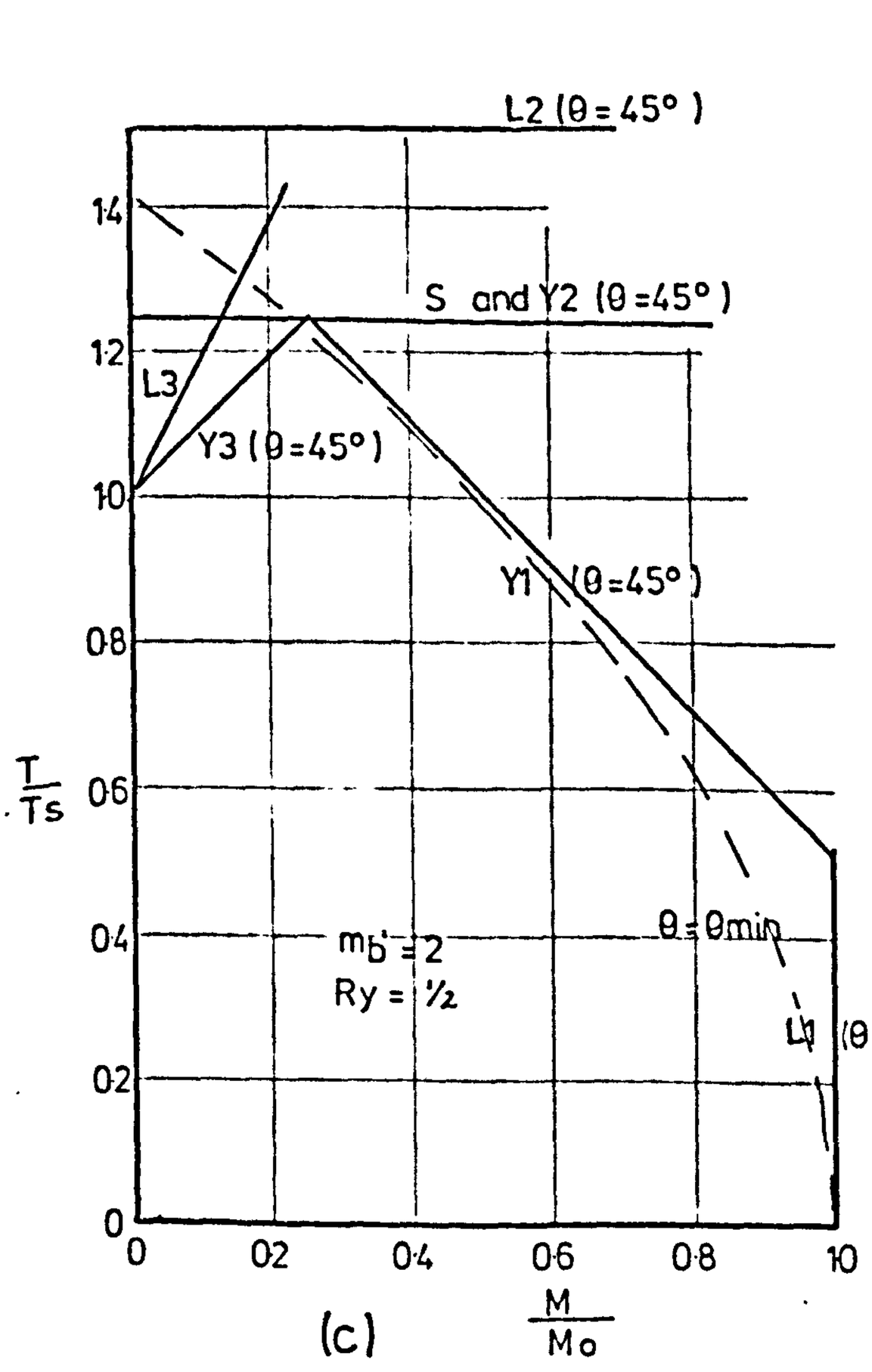

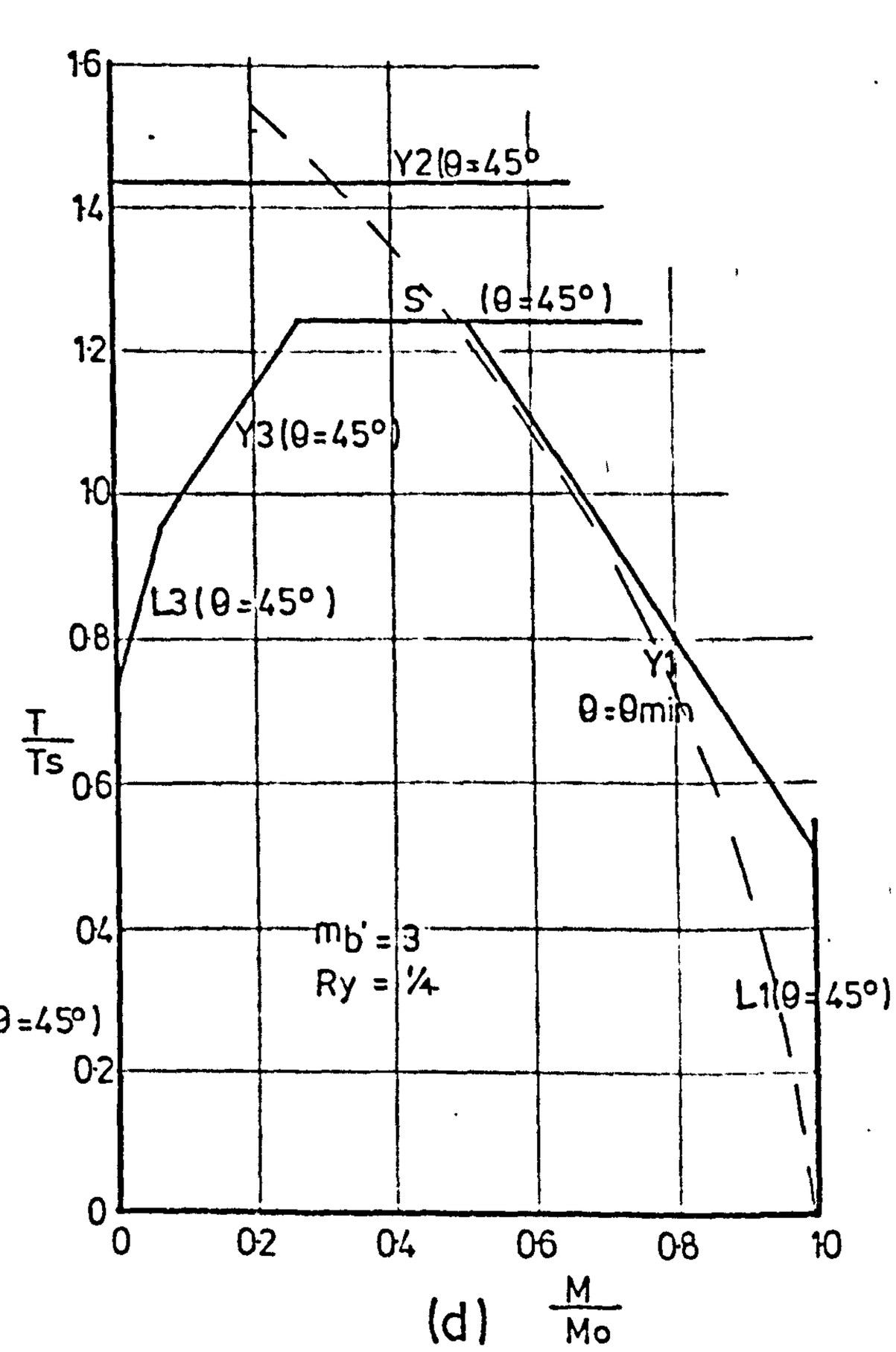

Fig. 5.4. Typical interaction diagrams for $\frac{Ta}{Ts} = 0$ & $\delta y = 0$

5.5 Comparison With Test Results

In order to examine the validity of these simple partial yield expressions, the predictions given by these expressions have been compared with available experimental results. Fig. 5.5 gives in the form of an interaction diagram, the results of tests on reinforced concrete beams subjected to torsion and shear only as reported by Klus (5.24). This diagram also shows the theoretical prediction obtained by using equations 5.11 and 5.12. The theoretical interaction diagram agrees favourably with the empirical interaction diagram obtained by Klus. At very high applied shears $\delta_y > 2$ mode S1 is dominant whereas for the case of high torsion where $\delta_y < 2$ mode S2 becomes critical.

The proposed theories have also been compared in Fig. 5.6 with the test results of 29 reinforced concrete beams tested under combined bending, torsion and shear reported by Collins (5.5). Again the proposed theory predicts satisfactorily the interaction between torsion and shear. The proposed methods predict that almost 55 percent of the beams tested failed in mode S1. For this mode the ratio of V_{exp}/V_{th} is 1.1 and the coefficient of variation is 8.45 percent.

It can also be observed that the limit of $\delta_y < 1$ which was proposed in chapter 4 in order to ensure yield failure is only approximate.

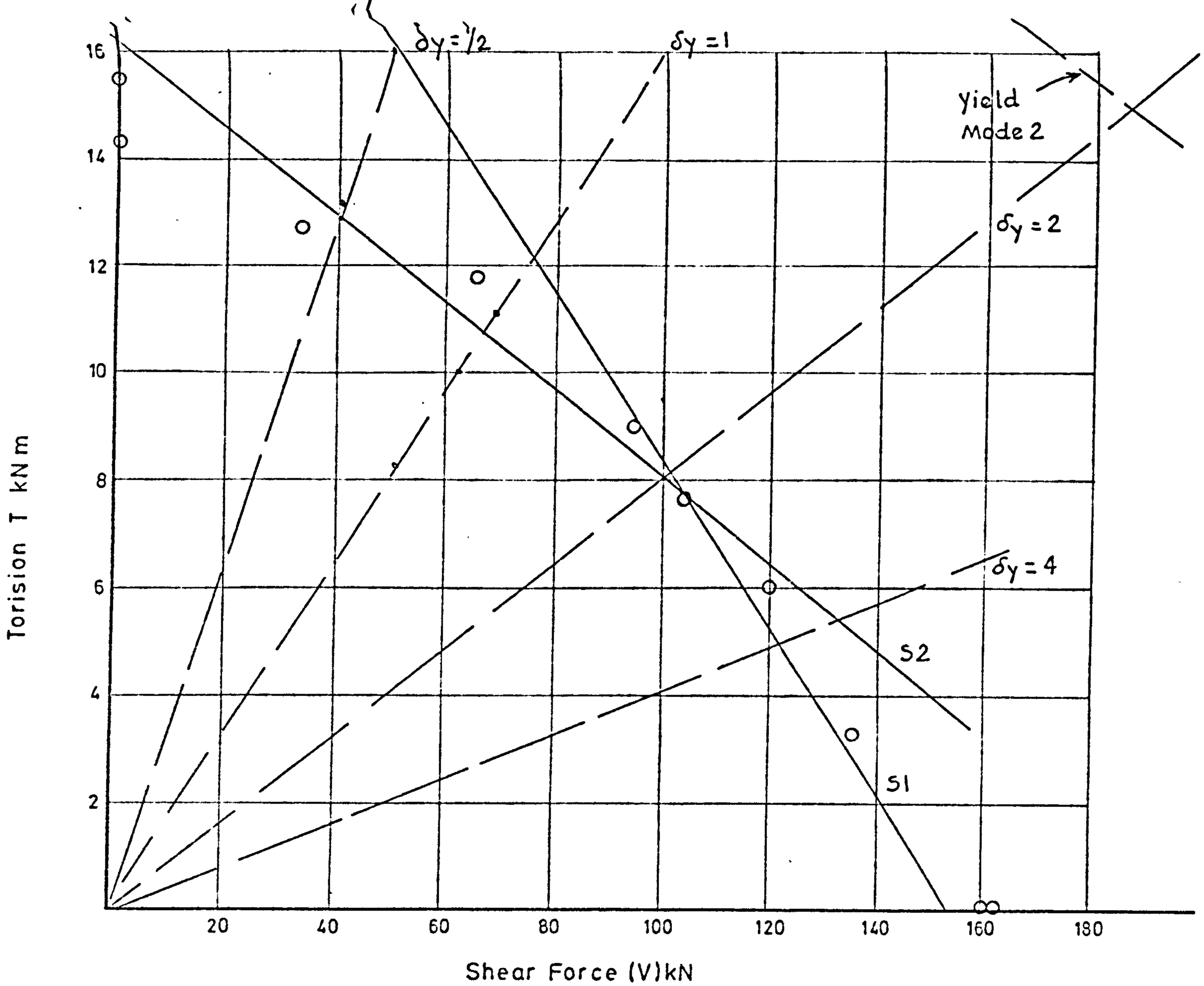

FIG. 5·5 Interaction Diagram for Klus test results (5·24)

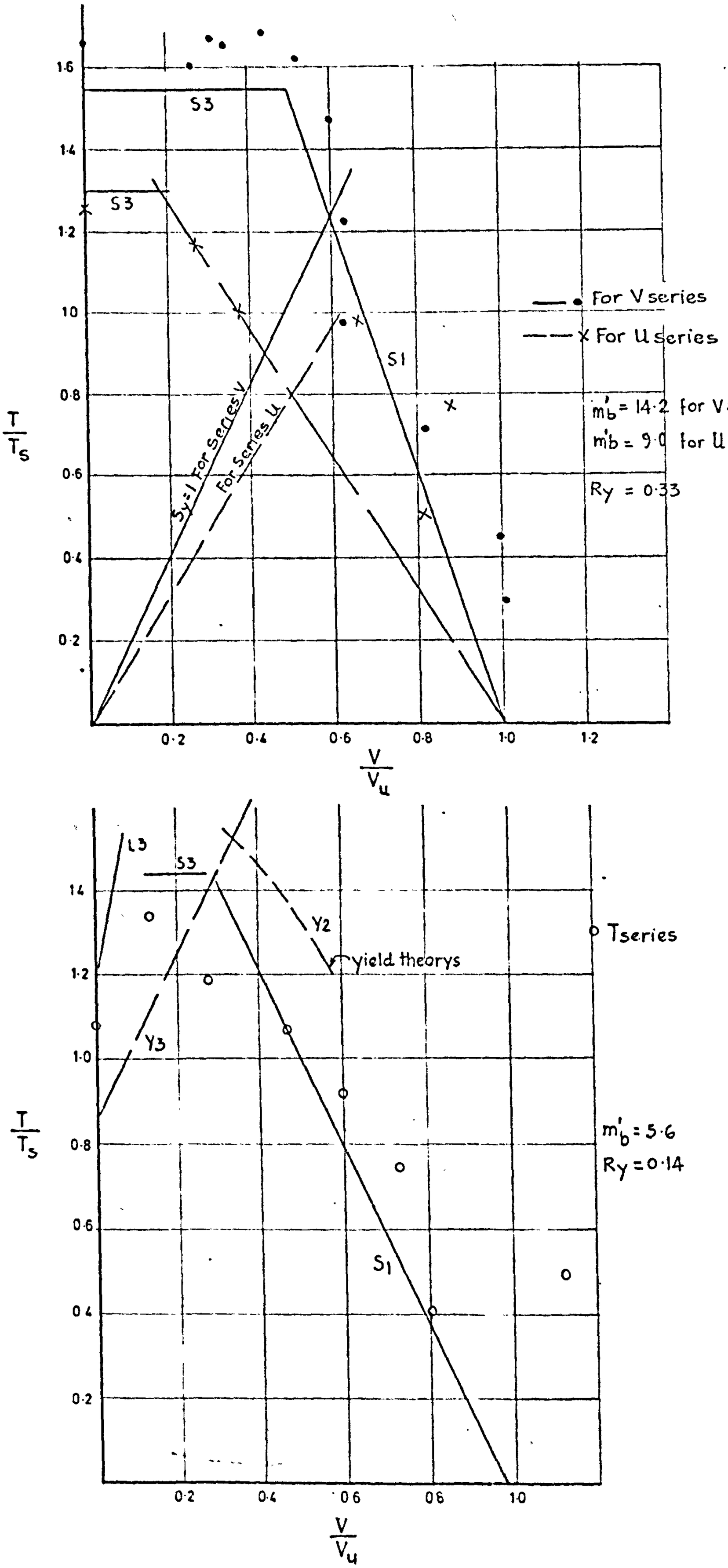

FIG 5·6 INTERACTION DIAGRAMS FOR COLLINS et al .TEST RESULTS (5·5)

5.6 Over-Reinforced Modes of Failure

In the following development of theoretical expressions for the prediction of over-reinforced modes of failure, it is convenient to sub-divide the failure into three cases:

1. Torsional
2. Bending
3. Shear

In each case the beam is assumed to be subjected to combined bending, torsion and shear with one of these forces being more predominant than the other. The shear mode of failure is not considered in this study.

5.6.1 Torsional Failure

As mentioned in chapter 3, reinforced and prestressed concrete beams will be transformed after cracking into a number of concrete springs and the secondary stresses which are induced in them could lead to failure of the beams.

In order to examine the behaviour of one of these springs under the action of longitudinal extension Δ, the square thin-walled reinforced concrete beam shown in Fig (5.7) will be examined. This beam is considered to consist of a series of concrete springs having a square cross-sectional area. The stresses which are developed in any of these springs due to the longitudinal extension may be found indirectly by applying a longitudinal tensile force at the centre of the beam as shown in Fig. (5.7). In the following analysis the effect of dowel action and aggregate

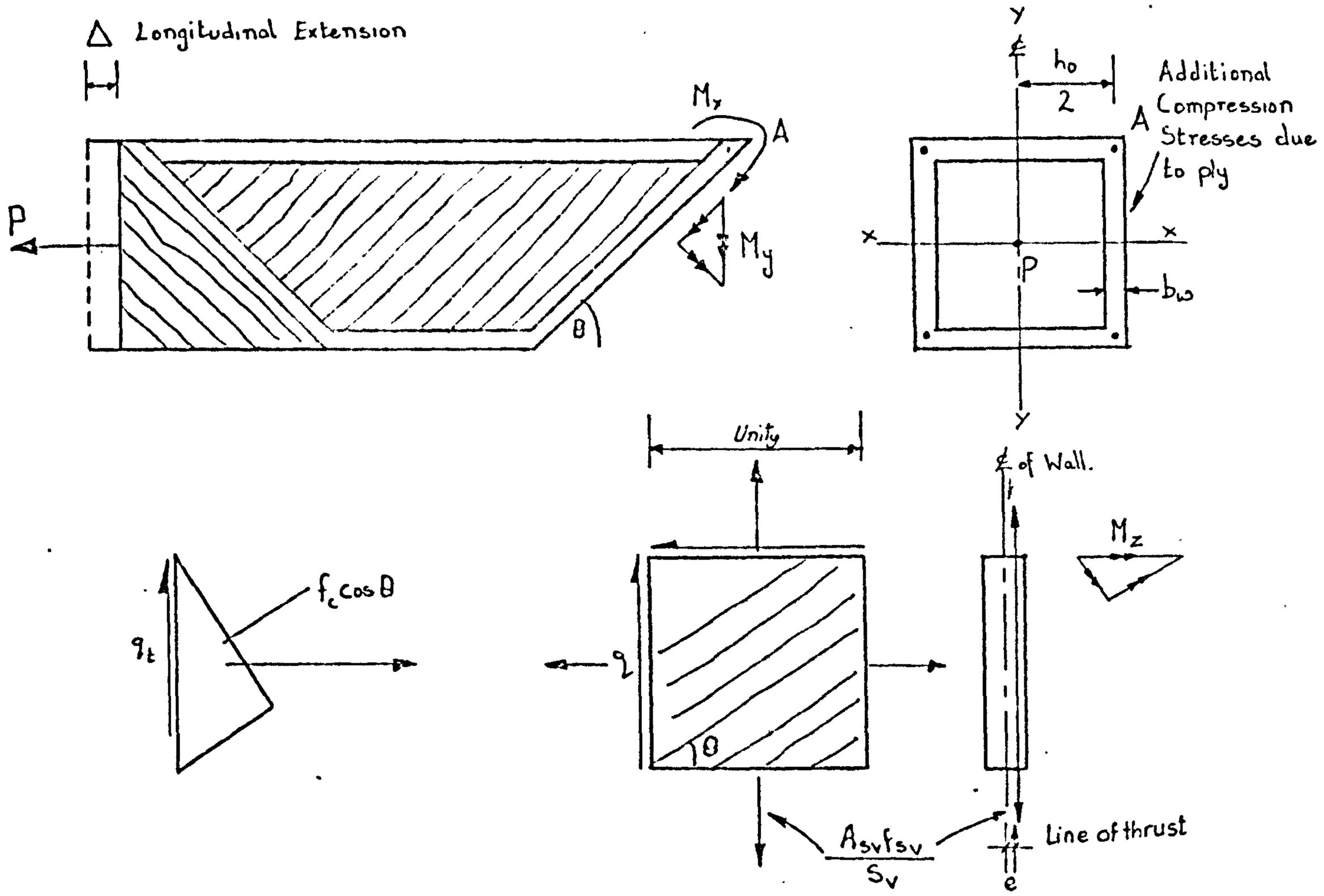

FIG. 5.7 Shows possible secondary stresses in a rectanguler box beam

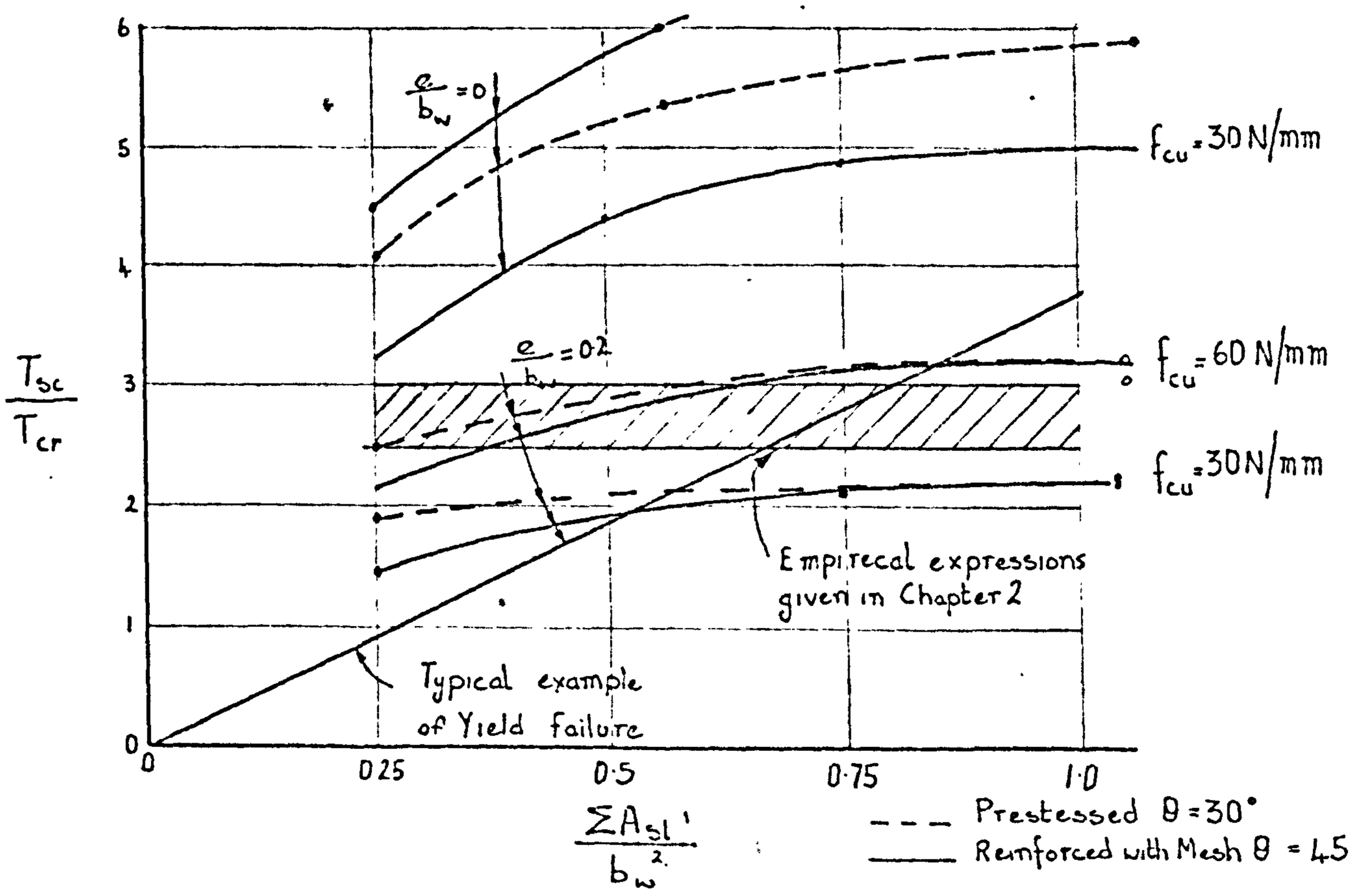

FIG. 5.8 SHOWS THE INFLUENCE OF PERCENTAGE OF LONGITUDINAL REINFORCEMENT, CONCRETE STRENGTH AND ECCENTRICITY OF STIRRUPS ON DIAGONAL COMPRESSIVE FAILURE.

interlock that may develop between two adjacent springs would be ignored and the material assumed to behave elastically.

Taking moment at point A, about the x and y axis we get:

$$M_x = M_y = \frac{P_{ho}}{2}$$

where ho is the width of the beam measured between the centre line of the wall and M_x and M_y are moments resisted by typical springs. The extension of the spring due to M_y acting along the entire length of the spring may be written as:

$$\Delta_y = \frac{h_o^2}{4} \frac{L}{\cos\theta} \left[\frac{\sin^2\theta}{G_c J} + \frac{\cos^2\theta}{E_c I} \right] P \qquad 5.16$$

where L is the length of the beam, GJ and EI are the torsional and flexural rigidities of the concrete spring respectively.

It can be shown that the extension of the spring due to M_x is small compared with $_y$ and hence may be ignored. It it is further assumed that $EI \simeq GJ$ and $\Delta_y = \Delta$ then equation 5.16 may approximate to:

$$\frac{\Delta}{L} \qquad \frac{ho^2 \; P}{3 E_c I \cos\theta} \qquad 5.17$$

This represents the extension of the spring per unit length.

Due to this loading M_x will produce the following maximum bending stress:

$$f_{cx} = \frac{P_{ho}\ b_w}{4\ I} \qquad 5.18a$$

and M_y will produce the following maximum bending and torsional stresses:

$$f_{cyl} = \frac{P_{ho}\ b_w}{4\ I}\ \cos\theta \qquad 5.18b$$

$$\gamma_{cl} = \frac{P_{ho}}{2J}\ \sin\theta \qquad 5.18c$$

Combining equations 5.16 and 5.18 we get:

$$f_{cx} = 0.75\ E_c\ \frac{b_w}{h_o}\ \cos\theta\ \frac{\Delta}{L} \qquad 5.19a$$

$$f_{cyl} = 0.75\ E_c\ \frac{b_w}{h_o}\ \cos^2\theta\ \frac{\Delta}{L} \qquad 5.19b$$

$$\gamma_{cl} = 0.6\ E\ \frac{b_w}{h_n}\ \sin\theta\ \cos\theta\ \frac{\Delta}{L} \qquad 5.19c$$

In addition we can consider the space truss analogy in which the stresses in the longitudinal reinforcement and the direct compressive stress in the concrete strut due to this truss action may be written as:

$$f_{sl} = \frac{2\ T\ \cot}{h_o\ \ A_{sl}} \quad \text{and} \qquad 5.20$$

$$f_c = \frac{T}{A_1\ b_w\ 2\ \sin\theta\ \cos\theta} \qquad 5.21$$

therefore, the strain in the longitudinal reinforcement due to applied torque is:

$$E_{sl} = \frac{\frac{2\ T\ \cos}{h_o\ E_s \sum A_{sl}}}{} \qquad 5.22$$

For compatibility of longitudinal strains in the longitudinal reinforcement and the unit extension

of the concrete spring, the stresses in the concrete spring become:

$$f_{cxl} = \frac{1.5}{\alpha_e} \frac{b_w}{\sum A_{sl}} \frac{T}{A_l} \cos\theta \cot\theta$$

$$f_{cyl} = \frac{1.5}{\alpha_e} \frac{b_w}{\sum A_{sl}} \frac{T}{A_l} \cos^2\theta \cot\theta \qquad 5.23$$

$$\tau_{cl} = \frac{1.2}{\alpha_e} \frac{b_w}{\sum A_{sl}} \frac{T}{A_l} \cos^2\theta \cot\theta$$

where $\alpha_e = \frac{E_s}{E_c}$

the presence of these secondary stresses may explain why diagonal compressive failures obtained in tests occur at loads that are consistantly lower than those predicted by the truss theory (5.25 and 5.26).

In general transverse reinforcement is located eccentrically to the centre line of the wall which induces a further transverse moment. If we consider the square element having unit length as shown in Fig. 5.7 where the transverse reinforcement is located eccentrically to the centre line of the wall, then the transverse moment per linear length of the wall that could develop is equal to

$$M_z = \frac{A_{sv} f_{sv}}{S_v} e \qquad 5.24$$

where e is the distance from the centre line of the wall to the line of thrust. The eccentricity of the line of thrust e depends on the position of the reinforcement in the wall, the geometrical proportion of the cross section of the wall and

the flexibility of the joints between the walls. For beams having m' = 1, equation 5.24 may be written as:

$$M_z = e \frac{T}{2 A_1}$$

This moment may also be resolved into two components one of which will induce a torsional moment into the concrete struts of the beam and the other a transverse moment. These moments will give the following maximum bending and shear stresses in the concrete strut.

$$f_{cyz} = \frac{M_z b_w 2}{2I} = \frac{3 e}{b_w 2} \frac{T}{A_1} \qquad 5.25a$$

$$\tau_{cz} = \frac{M_z b_w \cot \theta}{J} = \frac{2.5 e}{b_w 2} \frac{T}{A_1} \cot \theta \qquad 5.25b$$

Therefore, the maximum direct and shear stresses may be obtained as follows:

$$f_c = \frac{T}{A_1 b_w} \left[\frac{1}{2 \sin \theta \cos \theta} + \frac{1.5}{\alpha_e} \frac{b_w^2}{\sum A_{sl}} \cos^2 \theta \cot \theta + \frac{3 e}{b_w} \right]$$

5.26a

and

$$\tau_x = \frac{T}{A_1 b_w} \left[\frac{1.2}{\alpha_e} \frac{b_w^2}{\sum A_{sl}} \cos^2 \theta + 2.5 \frac{e}{b_w} \cot \theta \right] \qquad 5.26b$$

equation 5.26a explains why the diagonal compressive strains measured in tests on box beam girders reported by Lampert et al (5.25 and 5.26) were appreciably higher than those predicted by the truss theory which is represented by the first term inside the bracket.

A possible mode of failure of the concrete strut would be the failure of concrete under the combined action of direct compressive and shear stresses given in equations 5.26. For reinforced concrete beams may be taken at 45^{o} and if $f_{co} = 0.76\ f_{cu}$, $f_t = 0.36\sqrt{f_{cu}}$, $\alpha_e = 7.5$ and since distribution of stresses would most probably take place prior to failure, then failure would be assumed to occur when the total of the direct stresses due to truss action and half of the maximum direct stresses due to the transverse bending (second and third term of equation 5.26a) equals the limiting strength of the concrete. Using Mohr-Walther's theory of failure of concrete and equations 5.26, the strength of the box beam governed by the failure of the concrete may be obtained as follows:

$$\frac{T_{sc}}{T_{cr}} = \frac{\sqrt{f_{cu}}}{\left[1 + \frac{1}{20}\frac{b_w^2}{\sum A_{sl}} + \frac{1.5\ e}{b_w}\right]\left[1 + \frac{\left(\frac{1}{5}\frac{b_w^2}{\sum A_{sl}} + \frac{5\ e}{b_w}\right)}{\left(\frac{1}{20}\frac{b_w^2}{\sum A_{sl}} + \frac{1.5\ e}{b_w} + 1\right)}\right]} \quad 5.27$$

where T_{cr} is the torque which causes first cracking. This equation has been solved for typical values of concrete strength and e and the results plotted in Fig. 5.8 as $\frac{T_{sc}}{T_{cr}}$ against $\frac{\sum A_{sl}}{b_w}$. It is seen that when $\frac{e}{b_w} = 0.2$ the predicted theoretical values compare favourably with the results obtained from the empirical expressions which are reviewed in chapter 3.

However, other modes of failure involving failure of the concrete are possible particularly the failure of the corner of the beam due to these secondary stresses acting together with the stresses induced by the longitudinal bar. The methods given in chapter 3 would satisfactorily predict this mode of failure.

In order to extend this shear compression failure theory to prestressed concrete beams, the compatibility condition used must be adjusted in order to allow for initial stretching of the longitudinal prestressing wires.

Therefore, the longitudinal strains of the beam may be written as follows:

$$\epsilon_{slp} = \epsilon_{sl} - \epsilon_{se} \qquad 5.28$$

where ϵ_{sl} is the longitudinal strain in the wires due to the applied torque and ϵ_{se} is the strain due to prestressing.

Substituting equation 5.22 into equation 5.28 and equating equation 5.19 and combining with equation 5.24 we get:

$$f_c = \frac{T}{A_1 b_w}\left[\frac{1}{\sin\theta\cos\theta} + \frac{1.5}{\alpha_e}\frac{b_w^2}{\sum A_{sl}}\cos^2\theta\left(\cot\theta - \frac{T_{cr}}{T}\frac{f_p}{f_t}\right) + \frac{3e}{b_w}\right] \qquad 5.29a$$

$$\tau_x = \frac{T}{A_1 b_w}\left[\frac{1.2}{\alpha_e}\frac{b_w^2}{\sum A_{sl}}\sin\theta\cos\theta\left(\cot\theta - \frac{T_{cr}}{T} \times \frac{f_p}{f_t}\right)\frac{2.5e}{b_w}\cot\theta\right] \qquad 5.29b$$

using the same assumption and the failure criterion used for the reinforced concrete beam d noting that $\cot\theta = \sqrt{1 + \frac{f_p}{f_t}}$ the failure torque would become as follows:

$$\frac{T_{sc}}{T_{cr}} = \frac{\sqrt{f_{cu}}}{\left[\frac{1}{2\sin\theta\cos\theta} + \frac{b_w^2}{\sum A_{sl}}\cos^2\theta\left\{\cot\theta - (\cot^2\theta - 1)\frac{T_{cr}}{T_{sc}}\right\} + \frac{1.5e}{b_w}\right]} \times$$

$$\times \frac{1}{\left[1 + \frac{\frac{2.4}{\alpha_e}\frac{b_w^2}{\sum A_{sl}}\sin\theta\cos\theta\left\{\cot\theta - (\cot^2\theta - 1)\frac{T_{cr}}{T_{sc}}\right\} + \frac{5e}{b_w}\cot\theta}{\frac{1}{2\sin\theta\cos\theta} + \frac{1}{20}\frac{b_w^2}{\sum A_{sl}}\cos^2\theta\left\{\cot\theta - (\cot^2\theta - 1)\frac{T_{cr}}{T_{sc}}\right\} + \frac{1.5e}{b_w}}\right]} \quad 5.30$$

equation 5.30 has also been solved for the case where $\theta = 30^\circ$ and the results are shown in Fig. 5.8 which shows that prestressing has little effect on this mode of failure.

5.6.2 Bending Mode

This over-reinforced mode of failure occurs when the $\frac{M}{T}$ ratio is high. It is similar in nature to the over-reinforced failure for beams subjected to pure bending. Therefore, the failure is assessed in terms of the ultimate moment of resistance of the section. For the purpose of this analysis the strength of the thin-walled

prestressed concrete box beam shown in Fig. 5.9 will be examined and the following assumptions made:

1. Plane sections before bending remain plane up to failure.

2. The concrete in the compressive zone is subjected to direct stresses due to bending, moment and prestressing force and shear stresses due to the applied torque.

3. The stress distribution in the compression zone due to bending is assumed to be uniform.

4. The strength of the concrete in the compression zone is governed by the Mohr-Walther failure criterion.

5. The stresses in the steel remain in the elastic range up to failure.

6. The tensile strength of concrete is neglected.

7. At failure the extreme fibre compressive strain would reach a limiting value.

8. The stress in the stirrups has no effect on failure.

From equilibrium of longitudinal forces

$$(A_f + 2\, b_w\, x)\, \lambda \alpha_1\, f_{cu} = P + P' \qquad 5.31$$

where α_1 is the ratio of the average flexural strength of the concrete to the cube strength. T is the parameter which allows for the effect of shear stresses on the strength of the compression zone. P and P' are the forces in the top and bottom layers of prestressing wires respectively.

A_f is the area of the flange.

From the geometry of the strain distribution shown in Fig

$$\epsilon_{su} = \epsilon_{se} + \lambda \epsilon_{cu} k_f \left(\frac{d - x}{x}\right) \qquad 5.32a$$

and

$$\epsilon'_{su} = \epsilon'_{se} + \lambda \epsilon_{cu} k_f \left(\frac{x - d'}{x}\right) \qquad 5.32b$$

where ϵ_{se} and ϵ'_{se} is the strain in the steel due to the effect of prestress in the bottom and top layers respectively. k_f is a bond slip factor. ϵ_{cu} is the normal flexural limiting strain and can be taken as 0.0035. λ is a parameter which allows for the effect of shear stresses on this limiting strain.

Taking E_s as the Young's modulus for the prestressing wires, and multiplying equations 5.32 by the product of E_s and the area of the prestressing wires we get:

$$P = P_e + \lambda \Gamma \sum A_{sl} \left(\frac{d - x}{x}\right) \qquad 5.33a$$

$$P' = P'_e + \lambda \Gamma \sum A'_{sl} \left(\frac{x - d'}{x}\right) \qquad 5.33b$$

where $\Gamma = \epsilon_{cu} k_f E_s$

combining equations 5.31 and 5.33:

$$C_f + C_w x = P_e + P'_e + \left\{ \sum A_{sl} \left(\frac{d-x}{x}\right) - \sum A'_{sl} \left(\frac{x-d'}{x}\right) \right\} \qquad 5.34$$

where $C_f = \lambda \alpha_1 f_{cu} A_f$

$C_w = 2 \lambda \alpha_1 f_{cu} b_w$

rearranging and solving we get:

$$x = \left[\left(P_e + P'_e\right) - \left(\Sigma A_{sl} + \Sigma A'_{sl}\right)\lambda\Gamma - C_f\right]\frac{1}{2C_w} + \sqrt{\frac{\lambda\Gamma}{C_w}\left(d\,\Sigma A_{sl} + d'\,\Sigma A'_{sl}\right) + \left[\left\{\left(P_e+P'_e\right)-\left(\Sigma A_{sl}+\Sigma A'_{sl}\right)\lambda\Gamma - C_f\right\}\frac{1}{2\,C_w}\right]^2} \qquad 5.35$$

Now the moment of resistance of the section can be obtained by taking moments about the centroid of the bottom wire. This will give

$$M_{sc} = C_w x\left(d-\frac{x}{2}\right) + C_f\left(d-\frac{h_f}{2}\right) - \left\{P'_e - \lambda\Gamma\,\Sigma A'_{sl}\left(\frac{x-d'}{x}\right)\right\}(d-d')$$

5.36

For unbonded prestressed concrete beams Barker (5.27) suggested that k_f should be determined experimentally and gave a safe value for k_f as 0.1. Cowan (5.21) later found from tests on unbonded prestressed concrete beams that k_f is directly proportional to the depth of the neutral axis $\frac{x}{d}$. Pannel (5.28) found that this factor is also a function of the length of the beam (L) and his work indicates that k_f is inversely proportional to L therefore, k_f may be written as

$$k_f = k_u\,\frac{x}{L}$$

where k_u is a constant which can be determined experimentally. Available test evidence (5.28) suggests that k_u is equal to 12.

Substituting this expression for k_f and rearranging we get:

$$x = \frac{P_e + P'_e + \left(d\,\Sigma A_{sl} - d'\,\Sigma A'_{sl}\right) - C_f}{C_w + \left(\Sigma A_{sl} + \Sigma A'_{sl}\right)\lambda\,\Gamma_u} \qquad 5.37$$

where $\int_u = \frac{k_u \epsilon_{cu} E_s}{L}$

To test the validity of this approach the theory has been used to predict the strength of the 38 unbonded rectangular prestressed concrete beams reported by Pannel (5.28) and the values are compared with his test results in Fig. 5.10. The ratio of M_{exp}/M_{th} for the 38 specimens is 1.01 and the coefficient of variation is 4.3 percent. For these calculations ϵ_{cu} E_s k_u was taken as 8000 N/mm^2 and $\alpha_1 = 0.6$.

Determination of

This parameter depends primarily on the ratios of the shear to the direct stress occuring in the compressive zone and in turn the shear stress in the compression flange depends on the manner in which torsion is being resisted. For beams with lateral reinforcement and assuming that the shear flow induced by the torque follows the Bret-Patho's theory then

$$\tau_x = \frac{T}{2 S_1 Y_1 h_f}$$

and assuming that the direct stresses can be determined approximately as

$$f_x \simeq \frac{M}{X_1 Y_1 h_f}$$

then, $\lambda = \frac{1}{1 + \left(\frac{2\tau_x}{f_x}\right)^2} = \frac{1}{1 + \left(\frac{1}{\psi}\right)^2}$

where $\psi = \frac{M}{T}$

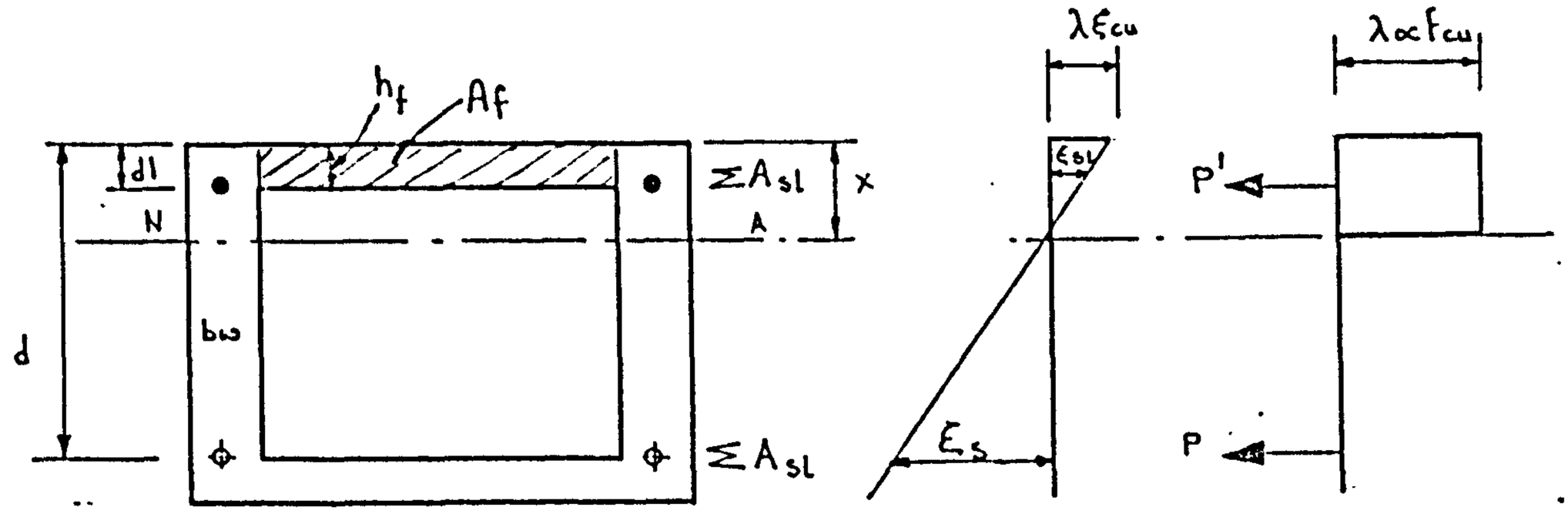

FIG. 5·9 Shear Compression Failure of box section

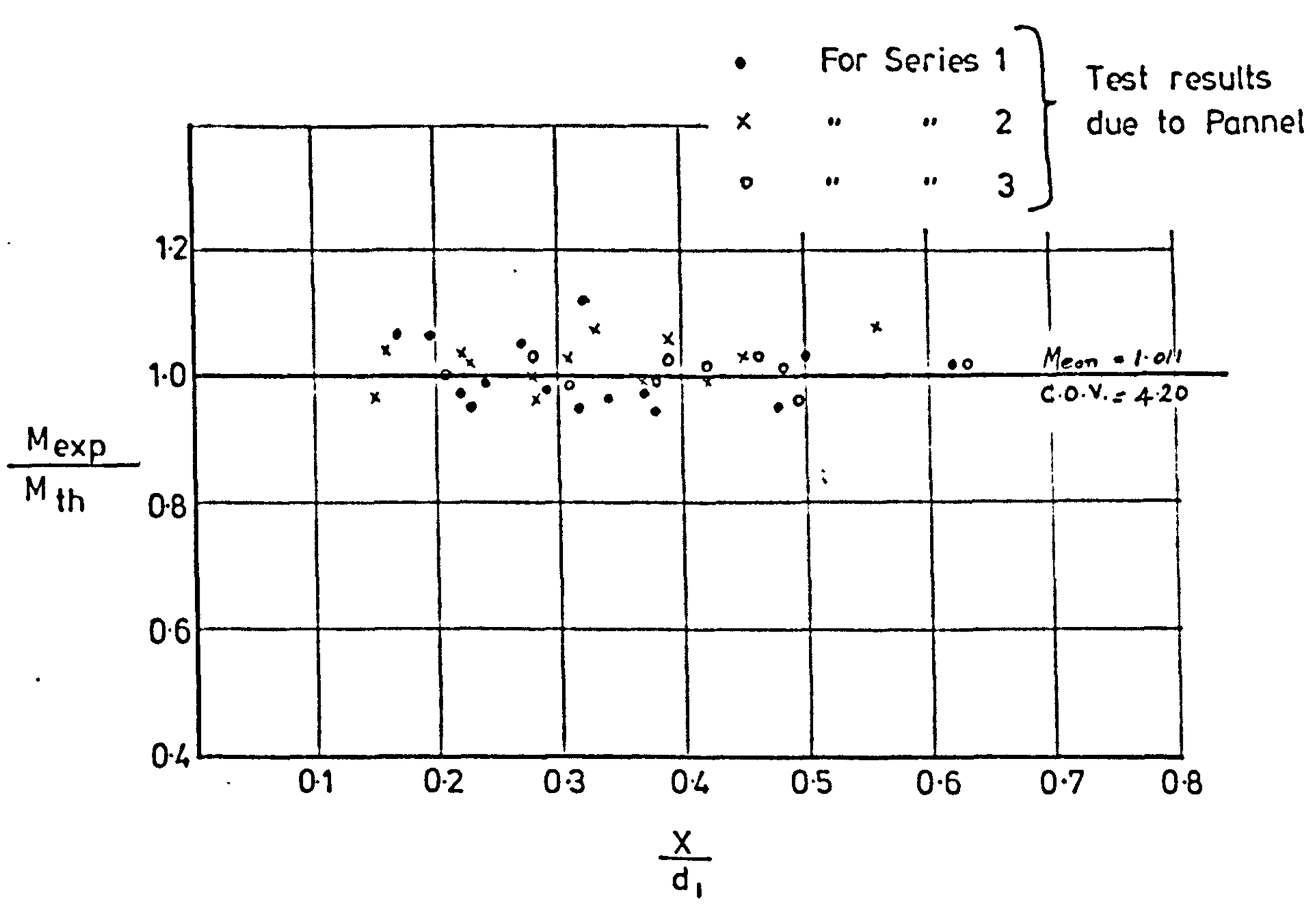

FIG 5·10 COMPARISON BETWEEN PREDICTION EQUATION (5·28) & TEST RESULTS OF UNBUNDED PRESTESSED CONCRETE BEAMS.

For other types of torsional resistance may be written as:

$$\lambda = \frac{1}{1 + \left(\frac{\alpha_\psi}{\psi}\right)^2} \qquad 5.38$$

where α_ψ is a factor which depends on the type of torsional resistance.

For box beams without lateral reinforcement and having $\frac{d}{h_f} = 17$, will have the following values:

$\alpha_\psi = 25$ if the torque is assumed to be resisted by the compression flange

$\alpha_\psi = 7$ if the torque is assumed to be resisted according to the St. Venant theory for open sections using the whole cross section

$\alpha_\psi = 2$ if the torque is assumed to be resisted by the compression flange and the bottom wires in differential bending or warping restraint.

The results of strain measurements taken on the compression flange from the tests reported in chapter 6 on box beams with and without lateral reinforcement indicate that the torsional stresses in the compression flange are due to the combined action of these modes of torsional resistance. However, the reduction in the flexural strength due to increase in the applied $\frac{M}{T}$ ratio on these beams indicates that the following values of may be assumed:

$\alpha_\psi = 1$ for beams with lateral reinforcement and

$\alpha_\psi = 2$ for beams without lateral reinforcement.

i.e. the additional shear stresses due to the

local twisting of the top flange has negligible effect on the strength of these beams.

5.7 Conclusions

1. It has been shown that reinforced and prestressed concrete beams subjected to bending, torsion and shear may fail in one of six partial yield modes of failure.

2. The prediction of a partial yield mode of failure may be represented by a simple shearing mode theory which ignores the effect of axial stresses in the compressive zone.

3. Over-reinforced failure occurs due to the failure of concrete under combined direct and shear stresses and may occur in various modes.

4. The discrepancies between measured diagonal compressive strains obtained from tests on box beams subjected to torsion and the prediction from the space truss theory have been traced back to the effect of the spring action of the concrete strut and to the positioning of the lateral reinforcement in the wall.

CHAPTER 6

EXPERIMENTAL INVESTIGATIONS INTO THE BEHAVIOUR AND STRENGTH OF PRESTRESSED BOX-BEAMS SUBJECTED TO BENDING, TORSION AND SHEAR

Summary

This chapter gives full details of an experimental investigation into the behaviour and strength of simply supported prestressed concrete box beams subjected to bending, torsion and shear. Twenty five box beams, 305 mm wide, 228 mm deep and having a total length of 3.81 m were tested in groups of five beams. Beams of series T contained varying amounts of lateral reinforcement and were subjected to pure torque. Beams of series 1 and 3 were subjected to combined bending and torque. Beams of series 2 and 4 were subjected to combined action of bending torsion and shear. Deflections and strains at various stages of testing were measured at selected points. The changes in prestressing force were also recorded. The effects of transverse reinforcement and the moment/torque ratio were the main variable parameters of this test programme.

6.1 Object and Scope of Tests

Very little test evidence on the strength of prestressed concrete rectangular beams under combined bending, torsion and shear were available at the start of this research programme in early 1970 and practically no information had been published on the strength of prestressed concrete box beams. This lack of information hampered the development of a rational theory for predicting the strength of this type of structural element, therefore, the object of the tests reported in this chapter was to study the behaviour and strength of prestressed concrete box beams and to produce the experimental evidence necessary for the development of a rational design method.

The test specimens were designed to represent a box beam bridge of single cell construction having 36 m span to a scale of approximately 1 : 10.

6.2 Details of Tests Specimens and Materials

6.2.1 General Discriptions of The Specimens.

Twenty Five post-tensioned concrete box beam specimens of 305 mm width, 228 mm depth and 3.81 m total length, having different volumes of transverse reinforcement were tested to failure. The general arrangement and reinforcement details of the specimens are shown in Fig. 6.1.

The practical problems of fabricating and handling small size box beams and their cost necessitated that each specimen be made of three segments. This was practical due to the fact that unbonded post tensioned concrete beams usually behave elastically up to failure except in the region of

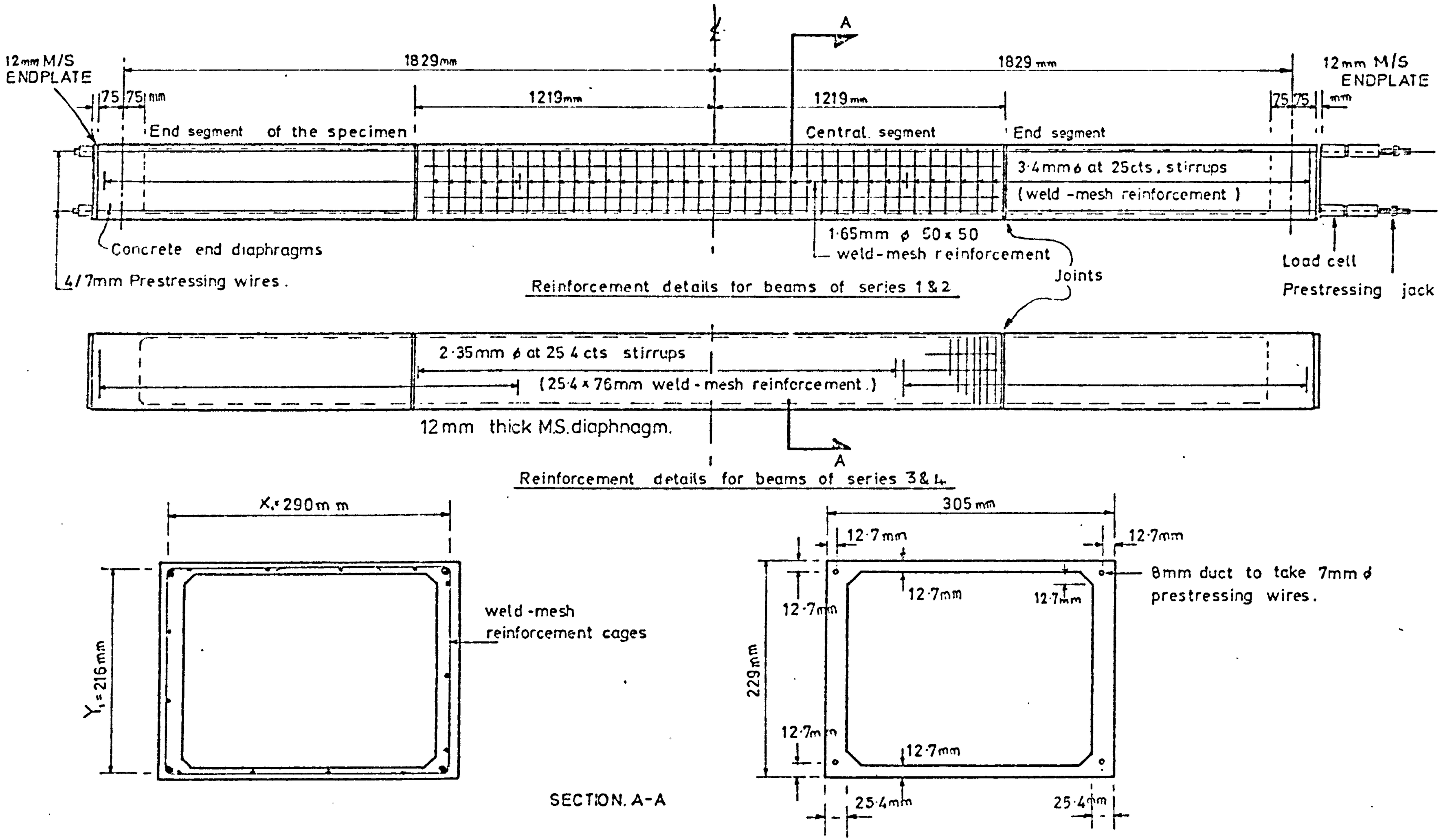

FIG 6.1 DETAILS OF TEST SPECIMENS

maximum moment. This arrangement also has the added advantage that it approximately represents the situation where concrete box beam bridges are constructed by the segmental method. The length of the central segment was made equal to half the span of the beam, and each end segment was made equal to a quarter of the span. High strength concrete was used and sufficient reinforcement was provided in the end segment to prevent cracking and failure of these segments so that they could be used throughout the tests programme.

The specimens were divided into five series as follows:

Series T : Subjected to pure torque and containing varying lateral reinforcement as follows:

T_o: contains 1.65 mm dia 50 x 50 mm steel mesh (un-prestressed)

T_1: 1.65 mm dia 50 x 50 mm steel mesh

T_2: 1.65 mm dia 25 x 25 mm steel mesh

T_3: 2.35 mm dia 25 x 75 steel mesh

T_4: 3.4 mm dia 25 x 75 mm steel mesh

Beams T_o, T_2, T_3 and T_4 were tested using 1.98 m total length.

Series 1: Contained 1.65 mm dia 50 x 50 mm square steel mesh and subjected to bending and torsion.

Series 2: Contained 1.65 mm dia 50 x 50 mm square steel mesh and subjected to bending, torsion and shear.

Series 3: Contained 2.3 mm dia 25 x 75 mm steel mesh and subjected to bending and torsion.

Series 4: Contained 2.3 mm dia 25 x 75 mm steel mesh and subjected to bending, torsion and shear.

The moment/torsion ratio was varied in series 1, 2, 3 and 4.

6.2.2 Properties of Materials

Concrete

Micro-concrete was used for all the specimens. Ordinary Portland Cement and river washed sand, from the Thames Valley as an aggregate were used for the concrete in the following proportions:

Aggregate/Cement ratio	3 : 1
Water/Cement ratio	0 . 5

The mix proportions were selected from the requirements of workability necessary for casting thin walled sections. The strength was equivalent to that of high strength concrete usually used in the construction of prestressed box girder bridges.

Concrete strengths were determined from 100 mm cubes and 150 mm x 300 mm cylinders cast with each specimen and tested at the same time as the box beams. The results of these control specimen are given in Table 6.1 and the relationship between the cube strength and the indirect tension strength obtained from the cylinders of this test investigation and those obtained from reference 6.1 are shown in Fig. 6.2. Further information was obtained by testing 150 mm x 300 mm cylinders in compression and monitoring the concrete strains. A typical stress/strain curve is shown in Fig. 6.3. The relationship between the modulus of elasticity and cube strength is shown in Fig. 6.2.

Reinforcement

The reinforcement used was B.R.C. weld mesh having 1.65 mm, 2.35 mm and 3.4 mm diameter respectively.

The properties of the reinforcement was determined from three tensile tests for each type. The results of these tests and the stress/strain relationship are given in Fig. 6.4. The prestressing tendons were 7 mm dia high tensile steel wires with a 0.2% proof stress of 1500 N/mm^2.

6.3 Fabrication of The Specimens

6.3.1 Formwork

The mould was designed so that the dimensions of the specimens could be maintained throughout the casting programme and so that any variation of the wall thicknesses of the box would be kept to a minimum. Acrow steel shutter units were sued to form the external mould with two rigid mild steel frames having the same shape and dimensions as the cross section of the beam as shown in plate 1. These frames were fixed by screws to the external mould. The inner core consisted of two 10 mm thick x 260 mm wide x 2 m long plywood sheets and two 6 mm x 114 mm wide x 2 m long plywood sheets. The 6 mm plywood was stiffened by gluing a further 6 mm thick strip along one edge of the sheet. The edges of the plysood sheets were machined accurately and arranged as shown in Fig. 6.5, in order to produce a simple method of dismanteling the mould. A polythene bag with a circumference equal to that of the specimen's internal circumference was made to enclose the inner core and form the outer face of the core. This bag provided a smooth and water tight arrangement for the inner core. This core was supported on two Acrow steel moulds forms held by two screw jacks as shown in Fig. 6.5.

One 8 mm dia duct was formed in each corner of the box using 8 mm dia plastic tubes which were held in position by steel wires having a diameter slightly less than the bore of the tube. These tubes were located in position by providing 8 mm dia holes in the end steel frames. The wires were stretched between the two ends of the external mould as shown in Fig. 6.5.

6.3.2 Reinforcement and Assembly of the Mould

The reinforcement cages were fabricated by bending a plain B.R.C. weld mesh sheet to the required dimentions and soldering the lapped joints.

The outer mould was coated with mould oil and then the cage was dropped in position followed by the plastic tubing. The wires which hold the plastic tubes were tensioned adequately by simple jacking arrangements in order to obtain reasonably straight ducts. The polythene bag was then inserted and the parts of the inner core were assembled. An external vibrator was attached to the top of the mould as shown in plate 2.

6.3.3 Casting and Curing

The Concrete was mixed in a Pan type mixer. One batch was required for each beam specimen and its control specimens, each batch being mixed for three minutes. A slump test was carried out to check the workability of each mix.

The concrete was placed in one of the vertical walls and vibrated until it appeared in the other wall. This procedure was necessary to prevent air pockets forming in the bottom flange. Casting of

the walls and top flange followed, the whole process lasted approximately one hour.

The inner formwork, the plastic tubes and the sides of the moulds were removed two days after casting. The specimen was then cured by being covered with wet canvas for six days, after which it was allowed to stand in a laboratory.

The end segments of the specimen were cast with 150 mm thick diaphragms at each end.

6.3.4 Instrumentation

The following measurements were usually observed at each loading stage.

a) Strain on the reinforcement: This was measured by E.R.S. gauges fixed to the reinforcement cage and waterproofed prior to casting.

b) Beam deflections and rotations: Deflections were taken at six points by 50 mm travel dial gauges located below the beam. Four additional dial gauges were used to measure the rotation of the supports as shown in Fig. 6.6.

c) Concrete strains: Longitudinal strains were measured at both webs and the top flange of each beam by means of a 200 mm Demec strain gauge at 49 positions as shown in Fig. 6.6. 100 mm Demec strain gauge Rosette arrays were positioned on both webs and the top flange as shown in Fig. 6.6.

d) Applied load and torque were measured by means of 50 kN capacity proving rings.

6.3.5 Assembly and Final Condition of Test Specimen

The thickness of each specimen at twelve points of the central section were measured using the device shown in Fig. 6.7. which was specially designed for this purpose. The average thickness of the webs and flanges and the coefficient of variations are given in Table 6.1.

The central andtwo ends segments were placed on a test bed as shown in Fig. 6.8. and the four 7 mm dia wires were inserted in position. After applying an adhesive to both ends of segments they were pulled together by lightly stressing the prestressing wires. These wires were greased in the locality of the joints to prevent them bonding at the joint.

Polybond adhesive mixed with plaster was used for beams subjected to a low value of torque, but an epoxy resin of high bond strength was found necessary for beams which were subjected to a high value of torque. Corro-Proof Epoxy Cement manufactured by Corrosion Technical Services Ltd. was used for this purpose. This adhesive was made of resin, hardener and filler. The first two were mixed with a 1 : 2 ratio and the filler was added to obtain the desired workability.

When Polybond adhesive was used the end segments were retrieved after each test with little effort, in contrast the epoxy resin joint had to be cut by an abrasive disk cutter. This procedure was found to be difficult and was subsequently modified by placing 6 mm thick mild steel diaphragms at these joints which proved to be satisfactory.

Demec gauge studs were fixed by means of Durofix to the central segment of the beams as shown in Fig. 6.6.

The beams were painted with Ceiling White to facilitate the observation of cracks. The Demec studs were protected by plastic tape during the painting.

The specimens were left on the test bed for a period of at least 24 hours to allow the adhesive to harden and reach adequate strength before the final prestressing force was applied.

6.4 Test Rig and Loading Arrangement

The test rig consisted of two 5 m long steel channel and two 6 mm thick x 400 mm wide and 5 m long top and bottom cover plates forming a torsionally stiff testing bed as shown in Fig. 6.9. and plates 3 and 4. Two close frames made of H.R. Steel section were used as reaction frames.

The bending moment was applied by means of 50 kN capacity hydraulic jacks fixed to these reaction frames and positioned at third points of the span for the beams subjected to bending and torsion as shown in plate 3. A single point load was applied at the centre of the beam from the beams subjected to bending, torsion and shear. The hydraulic jacks were connected to a four way manifold which in turn was connected to a hydraulic pump and to another 50 kN capacity dummy jack reacting against a 50 kN capacity proving ring as shown in Fig. 6.9. All the jacks used were of identical type

The applied load was spread to the webs of the beam by means of a 50 x 75 X 350 mm mild steel bar

and 25 mm diameter steel ball arrangement to prevent any rotational restraint.

The torque was applied through torsion arms fastened to the top of the beam by means of a saddle arrangement made of four 12.7 mm dia threaded rods, two 50 x 20 x 100 mm mild steel plates and one 20 x 100 x 400 mild steel plate each end as shown in Fig. 6.9 and 6.10. A downward vertical pull was applied by high tensile steel wire at an arm of 500 mm from the centre of the section. The wire was connected to another R.H. Section fixed to the bottom of the test bed and the force was applied by means of threaded screw arrangements which accommodated the wire through a central hole. Small thrust ballbearing and a rocker was used at the end of the wires to maintain the applied force in vertical direction and to reduce frictional restraint. The force in the wire was measured by a proving ring inserted between the torsion arms as shown in Fig. 6.9.

The beam was simply supported at each end using the bearing arrangements shown in Fig. 6.10. This bearing was designed to secure free rotation about the central axis of the beam and free longitudinal movements. The free rotation about the longitudinal axis was achieved by introducing the cylinderical bearing whose centre coincided with axis of the beam.

The beams were post-tensioned by four 7 mm diameter prestressing wires using the screw jacks shown in Fig. 6.10. The prestressing forces were measured by means of load cells which had been designed to carry 70 kN force, details are shown in

Fig 6.10. On each load cell four E.R.S. gauges were fixed around the external surface to measure the longitudinal strain and four E.R.S. gauges were fixed around the external surface to act as a dummy. These strain gauges were connected in series and with B.P.A. transducer meter to measure the strain. These load cells were calibrated in the 100 kN compression machine. The calibration test was repeated at least four times and the average of the calibrations was used. A straight line relationship was obtained between load and strain readings for these calibration tests. The calibration tests were repeated during the test programme.

Prestressing jacks, the load cells and the bearing arrangements were all specially designed for this test programme and were manufactured by the technical staff of the Department of Civil Engineering.

6.5 Test Procedure

6.5.1 Prestressing

Each beam was post-tensioned just prior to testing by four 7 mm dia prestressing wires using the equipment described earlier. A set of initial demec readings were taken before prestressing and then while the prestressing forces were applied gradually in a sequence which insured no cracking of the beam. The prestressing wires were stressed from one end only. The surface strains of the concrete were also read and recorded at the end of prestressing operation.

All the beams were stressed to give a uniform

prestress of 6.9 N/mm^2. An additional prestressing force was applied to counteract the self weight of the specimens. The prestressing force recorded by the load cells for the top wires and the bottom wires immediately after the prestressing operations and the longitudinal strains are given in table 6.2.

6.5.2 Test to Failure

Pure Torsion Tests

The torsional moment was increased in stages, in about 10 increments up to failure. Readings of the dial gauges, strains, changes in prestressing forces etc. were recorded at each stage. The torque causing initial cracking, maximum strength and mode of failure was noted carefully and recorded as given in table 6.3. Cracks were marked directly on beams and recorded at the end of each test.

Combined Bending and Torsion Tests

Each beam of this series was tested over a 3.6 m span. The bending loads were applied at the third points of the span. The moment and torque were applied simultaneously according to a predetermined ratio. The loads were applied in about 10 increments up to failure. After each increment, the load was held constant for ten to fifteen minutes while deflections, strains, change in prestressing force and crack developments were recorded.

Torsion, Bending and Shear Tests

Beams in this series were tested over a 3.6 m span. The bending moment was applied by a central point load and the procedure was identical to that for beams subjected to bending and torsion mentioned above.

The torque, moment and shear causing failure and the mode of failure are given in Table 6.3.

TABLE 6.1. Concrete properties and measured wall thickness at the central section of the specimen

Beam No.	Age at test (days)	100mm cube strength at test		Indirect tensile strength at test N/mm^2	Measured wall thickness at ℄ of beam					
					Top Flange		Bottom Flange		Webs	
		mean N/mm^2	C.O.V.		mean mm	C.O.V.	mean mm	C.O.V.	mean	C.O.V
To	40	51	4.5	3.55	12.83	1.47	13.44	1.37	25.2	3.33
T_1	40	59	4.0	3.40	-	-	-	-	-	-
T_2	37	45.5	4.9	3.10	-	-	-	-	-	-
T_3	50	64.0	4.0	3.20	14.05	0.86	14.97	2.36	25.57	0.72
T_4	39	48	5.4	3.70	14.78	4.25	13.84	2.63	24.7	3.4
B11	23	42.8	3.3	2.3	-	-	-	-	-	-
B12	40	44.0	5.1	3.88	11.09	2.1	14.98	3.67	24.6	4.38
B13	56	53.0	3.8	3.90	-	-	-	-	-	-
B14	50	44.9	4.5	2.80	12.36	1.27	14.87	4.95	25.41	1.42
B15	47	44.7	13.2	3.4	-	-	-	-	-	-
B21	72	55.8	5.5	4.1	12.41	3.85	12.27	1.76	49.82	1.77
B22	72	50.4	7.2	4.4	13.2	1.37	13.52	4.19	25.41	4.4
B23	72	54.3	5.0	3.0	17.64	1.2	14.56	1.65	24.8	2.78
B24	40	48.1	3.3	2.7	-	-	-	-	-	-
B25	41	44.2	6.4	3.6	14.91	7.2	14.81	1.62	25.1	2.8
B31	42	55.2	2	4.0	12.7	0	16.09	3.69	25.3	1.27
B32	31	47.8	5.4	4.4	12.26	4.09	16.0	2.6	24.8	0.98
B33	55	51	11.6	3.0	12.01	4.40	16.23	2.04	24.9	9.75
B34	60	51.9	9.6	2.7	17.06	6.02	15.57	1.55	24.8	2.25
B35	64	68.7	5.6	3.6	15.32	6.81	15.70	3.65	24.7	2.47
B41	32	53.8	0	2.7	12.7	0	13.97	0.8	24.1	1.11
B42	26	53.2	3.9	4.1	14.72	1.44	12.98	3.46	25.97	1.77
B43	40	53.6	5.2	3.3	14.56	1.65	13.12	3.25	53.1	3.66
B44	40	43.4	3.8	4.0	11.97	3.5	13.97	2.5	24.9	3.97
B45	39	53.5	1.5	4.6	12.7	0	13.71	2.67	24.91	4.75
Average					13.12	9.0	14.44	7.72	25.1	1.94

TABLE 6.2. Prestressing Forces and Average measured Longitudinal strains

Beam No.	Initial Prestressing Forces recorded by Load Cells			Average measured Longitudinal strain due to prestressing x 10 - 6			
				At the section		Overall	Average
	Top kN	Bottom kN	Total kN	Top Flange	Bottom Flange	Top Flange	Bottom Flange
To	0	0	0	0	0	0	0
T_1	60	66	126	214	235.2	-	-
T_2	60	66	*	134	172	133	181
T_3	60	63	123	219	180	218	221
T_4	59	64	123	193	726	201	207
B11	62	74	136	-	-	-	-
B12	64	70	134	234	245	215	250
B13	67	69	136	221	187	227	195
B14	64	71	135	253	240	256	232
B15	65	70	135	186	264	208	240
B21	59	65	124	221	163	216	174
B22	59	63	122	236	187	225	192
B23	59	65	124	284	192	224	197
B24	59	65	124	214	202	231	208
B25	59	65	124	214	226	214	227
B31	59	66	125	198	197	201	182
B32	59	66	125	256	211	266	214
B33	59	65	*	380	187	347	171
B34	58	63	121	250	187	246	201
B35	58	63	121	246	206	247	199
B41	59	65	124	246	211	246	215
B42	58	64	122	227	230	236	223
B43	59	65	124	160	211	176	220
B44	59	65	124	224	178	218	181
B45	59	65	124	243	192	242	209

* Cell mal-function

TABLE 6.3. Principal test results

Beam No.	Cracking Moments		Maximum Moment Capacity		Max. Shear Force kN	Type of Failure
	Torsion kN.m	Bending kN.m	Torsion kN.m	Bending kN.m		
To	4.05	0	4.05	0	0	Cracking of the beam
T_1	8.60	0	8.60	0	0	Cracking of the beam
T_2	6.10	0	10.10	0	0	Rupture of Stirrups
T_3	8.13	0	11.4	0	0	Edge spalling
T_4	8.20	0	13.03	0	0	Edge spalling
B11	0	13.4	0	19.5	0	Crushing of top flange
B12	1.52	12.0	2.5	20.0	0	" " " "
B13	2.64	12.0	3.51	14.82	0	" " " "
B14	4.25	8.5	4.81	9.71	0	" " " "
B15	5.49	5.49	6.58	7.29	0	Cleavage failure of top flange
B21	0	10.97	0	16	8.75	Crushing of top flange
B22	1.37	10.97	1.82	14.60	8.0	" " " "
B23	2.28	9.14	2.48	12.80	7.0	" " " "
B24	4.8	9.6	5.5	10.97	6.0	" " " "
B25	5.5	5.44	5.43	5.50	3.0	Cleavage failure of top flange
B31	0	10.97	0	19.26	0	Crushing of top flange
B32	1.27	11.82	2.4	19.20	0	" " " "
B33	2.74	10.97	5.30	21.35	0	" " " "
B34	4.00	8.28	8.05	17.0	0	" " " "
B35	6.33	6.33	9.75	9.75	0	Edge spalling
B41	0	10.05	0	16.5	9.0	Crushing of top flange
B42	1.26	10.05	1.99	15.9	8.7	" " " "
B43	2.74	10.97	4.34	17.4	9.5	" " " "
B44	4.34	8.68	7.20	15.03	8.25	" " " "
B45	6.22	6.22	10.5	11.15	6.1	Edge spalling

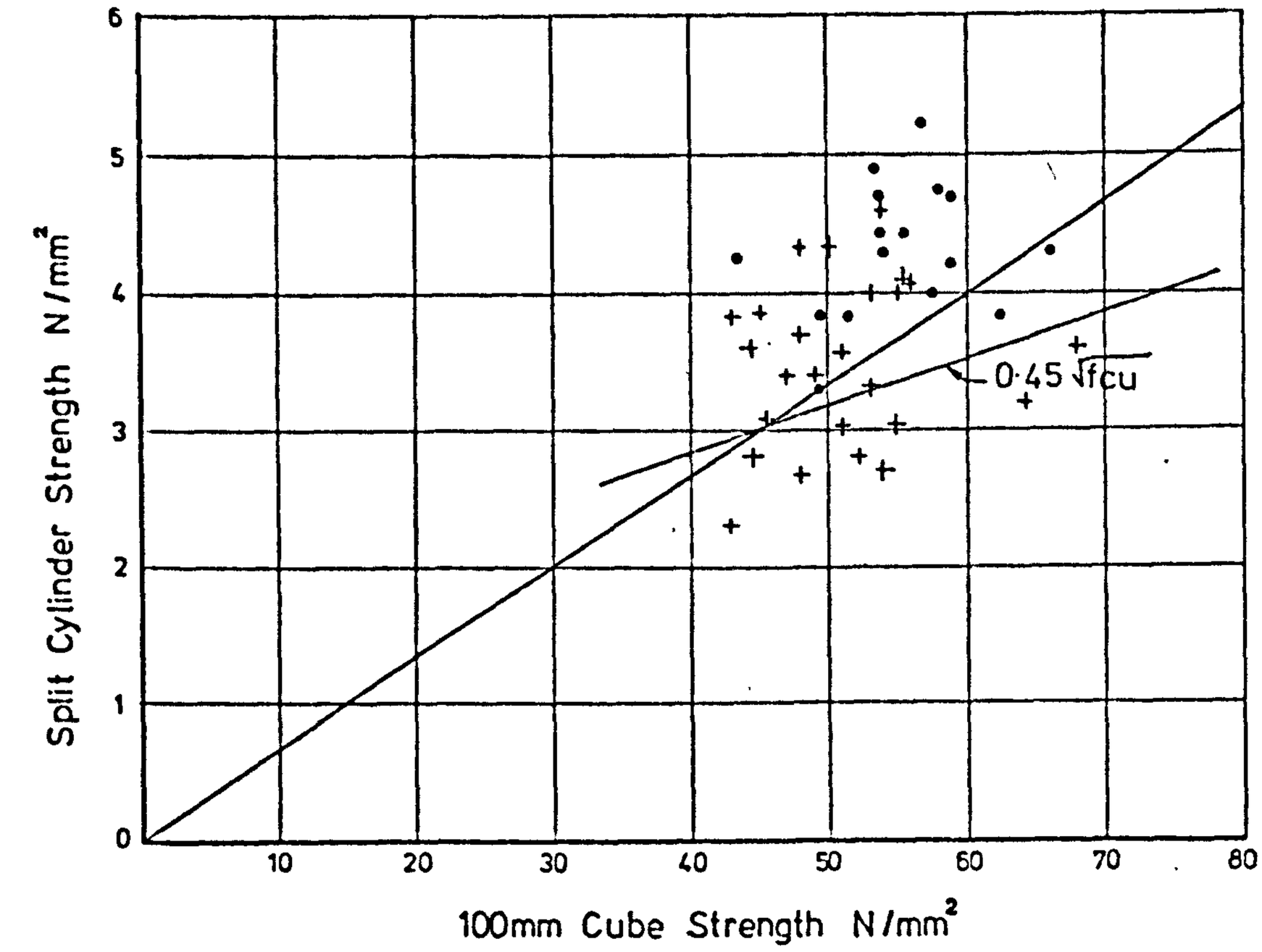

(+) From This Investigation (300 × 150 Cylinder)

(•) From Results Of Ref. 6.1 (200 × 100 Cylinder)

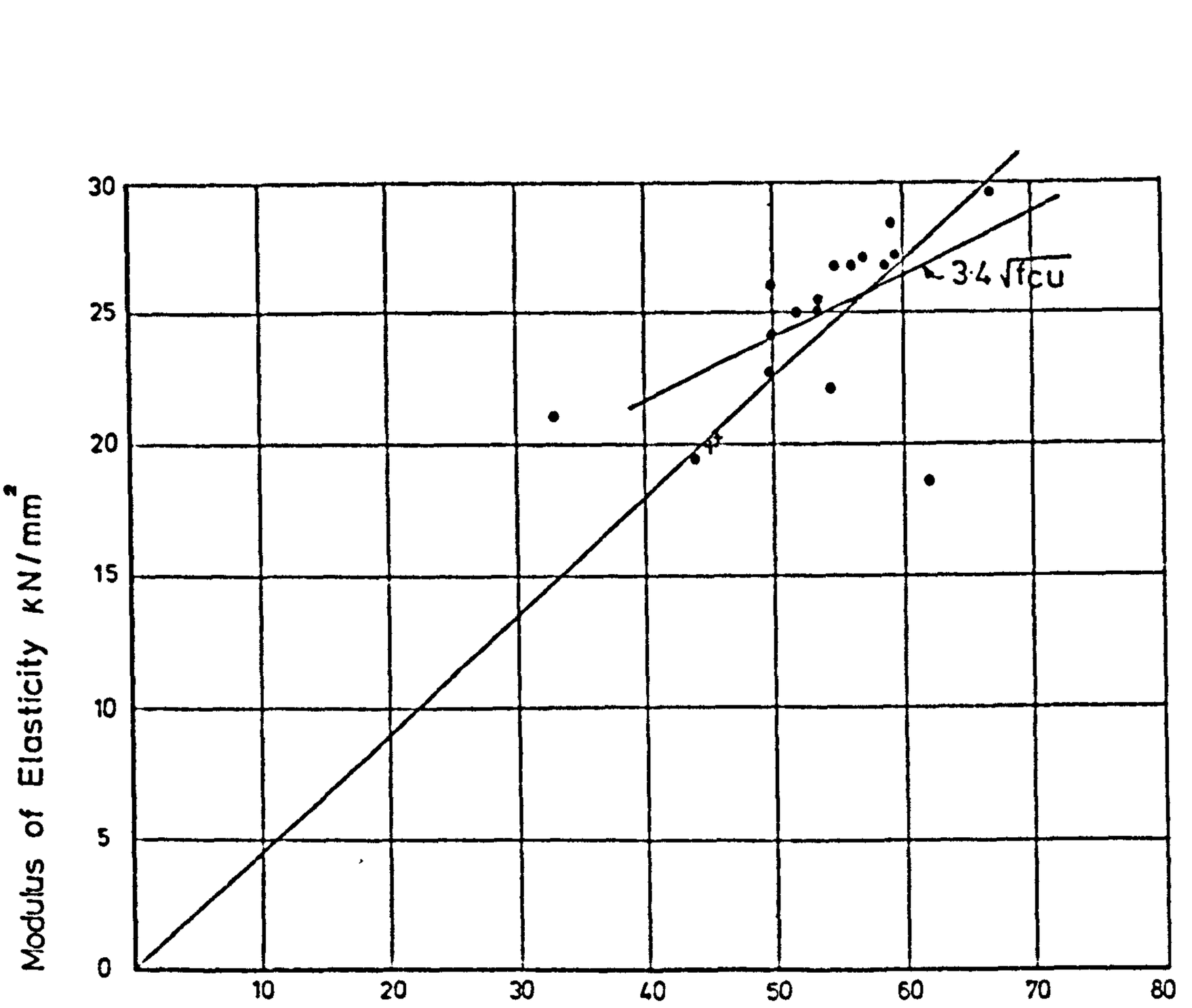

FIG.62 Relationship Between Cube Strength, Split Cylinder and Modulus Of Elasticity For Micro-Concrete.

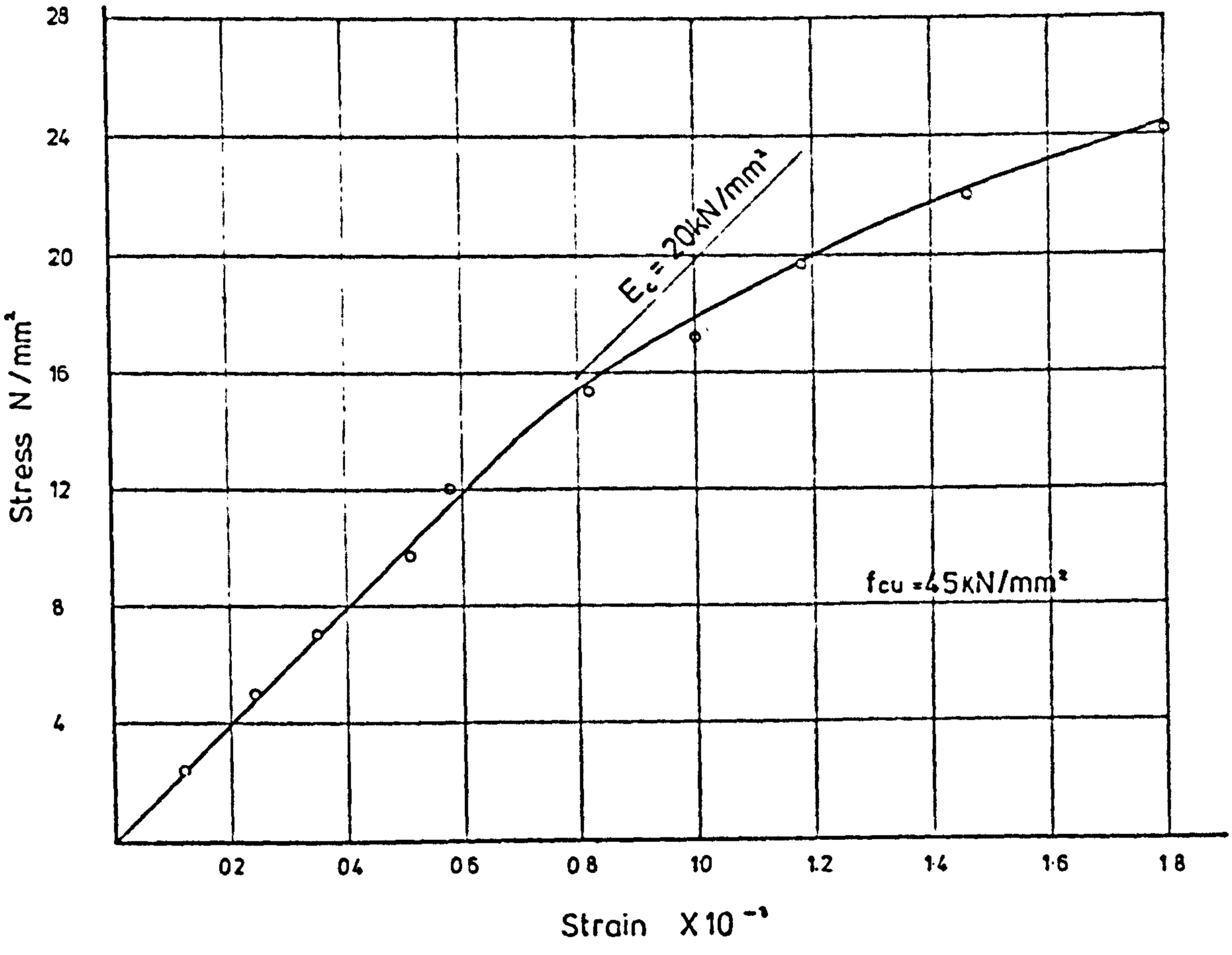

FIG.6.3 Typical stress-strain curve for micro-concrete in compression

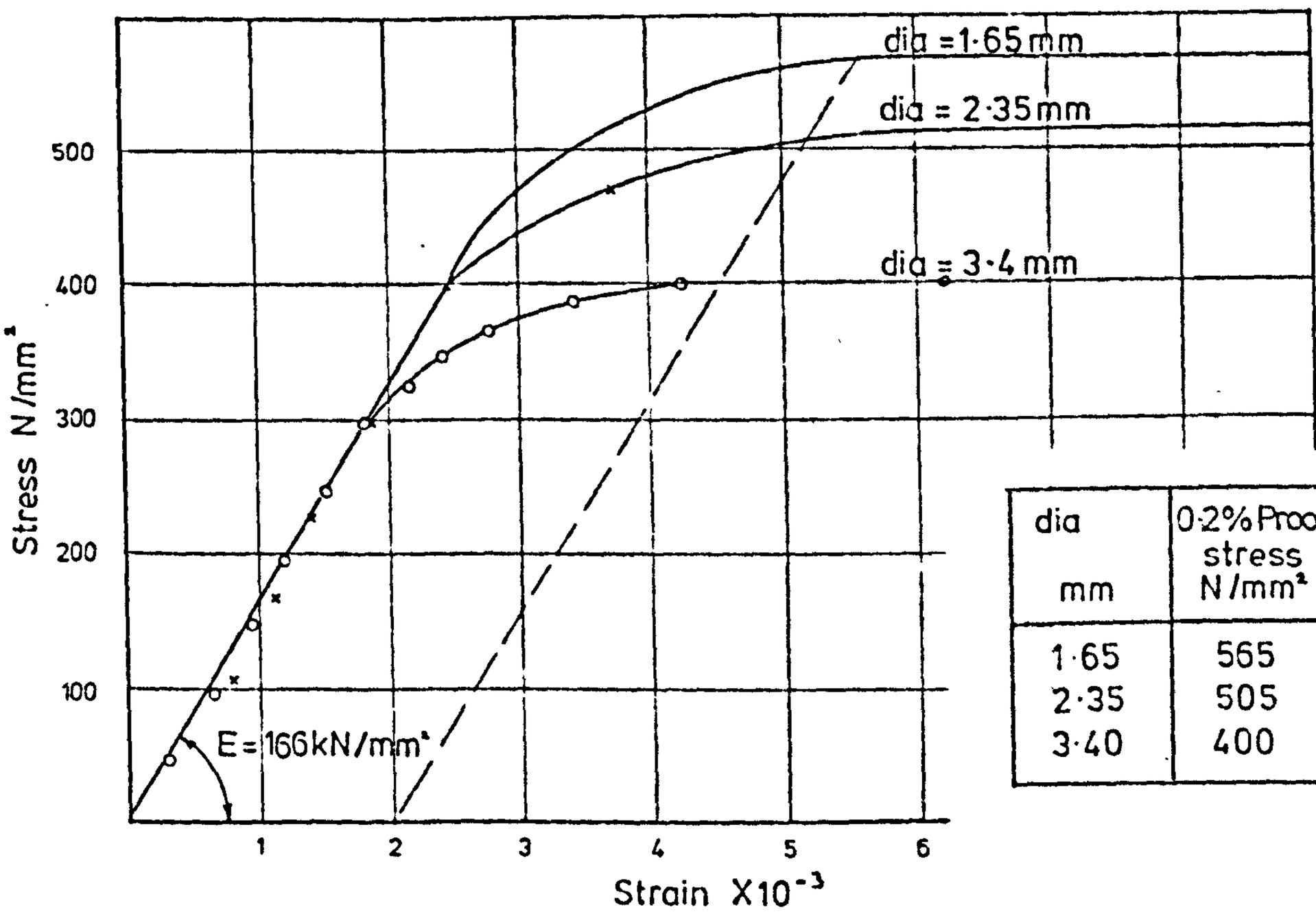

dia mm	0·2% Proof stress N/mm²	Ultimate stress N/mm²
1·65	565	570
2·35	505	520
3·40	400	410

FIG.6.4 Stress - strain curves for welded-mesh reinforcement.

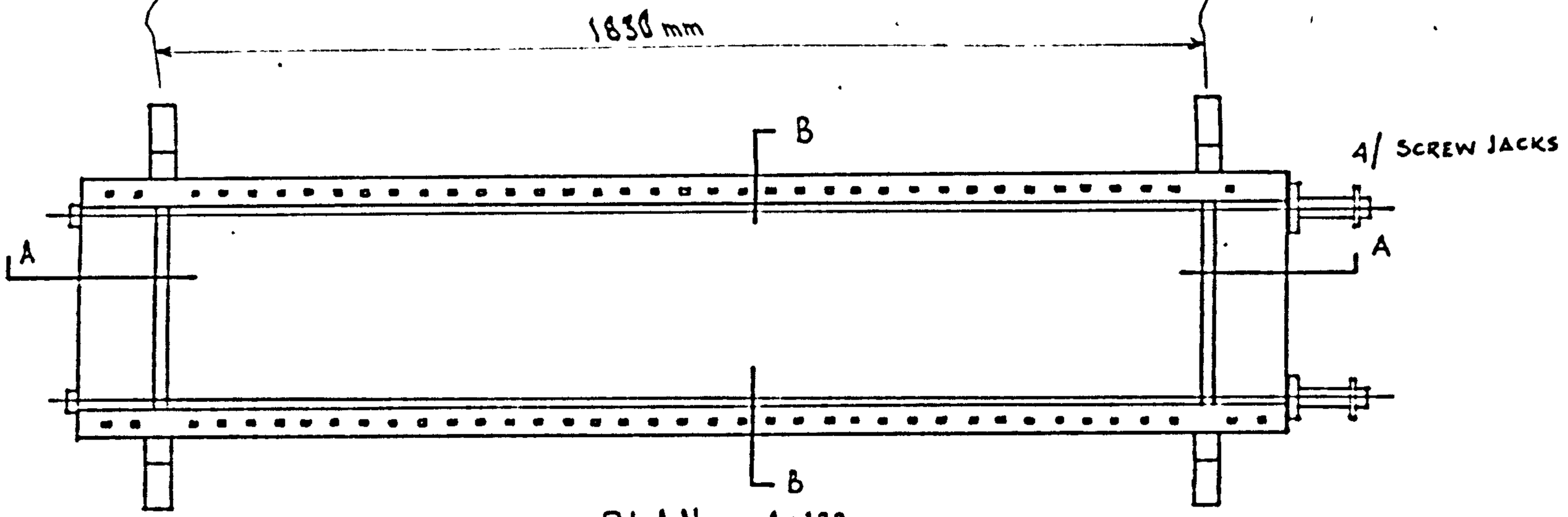

PLAN. 1:100

EXTERNAL FORMWORK ONLY

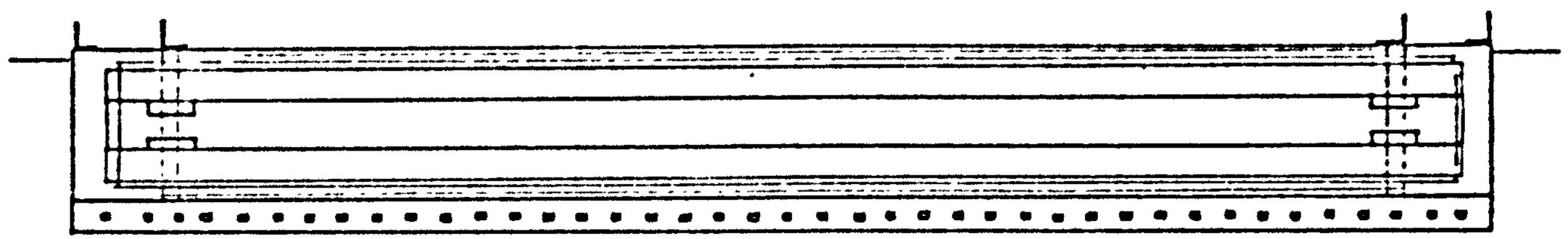

SECTION A-A 1:100

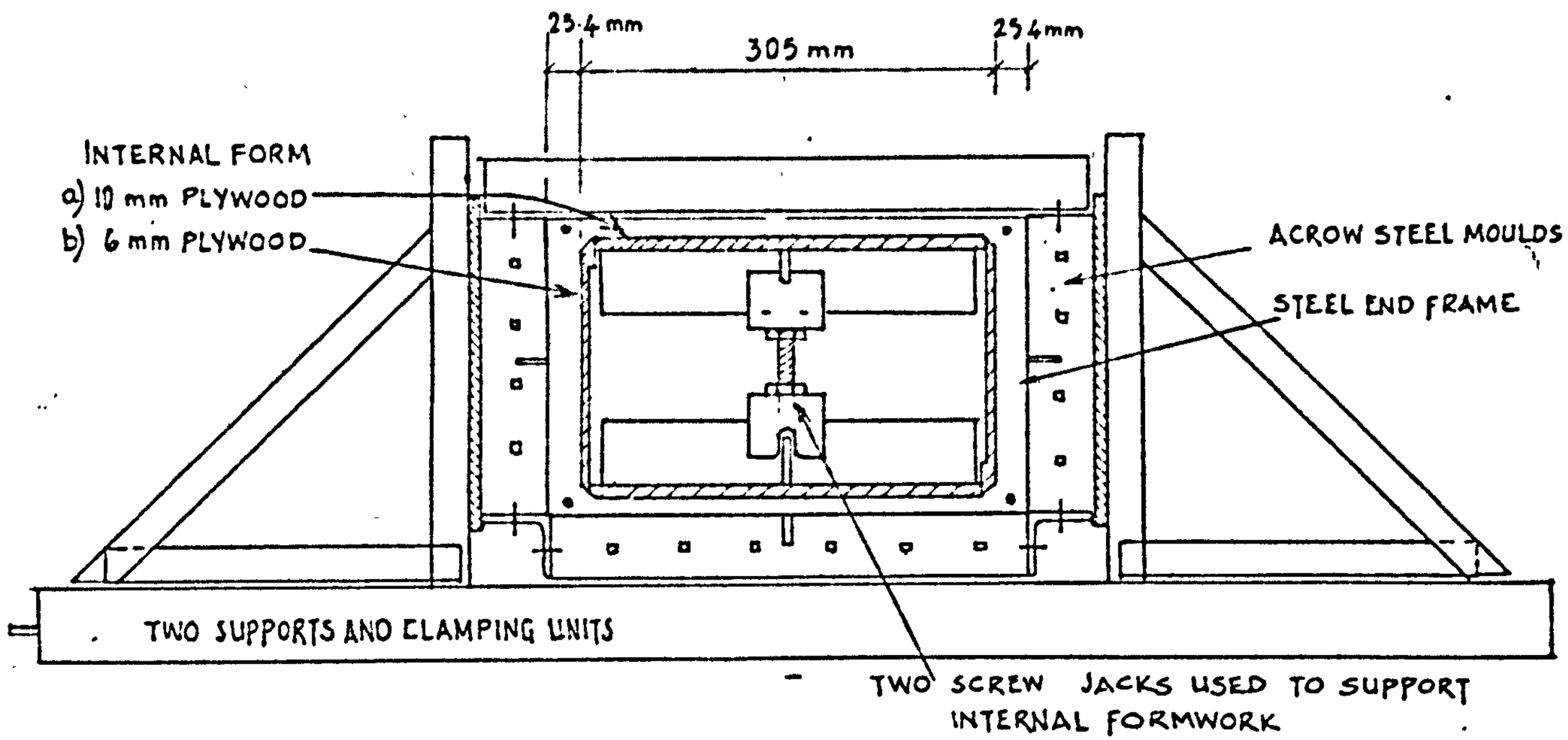

SECTION B-B 1:50

Fig.6.5. Steel form use for casting central segment of box beam.

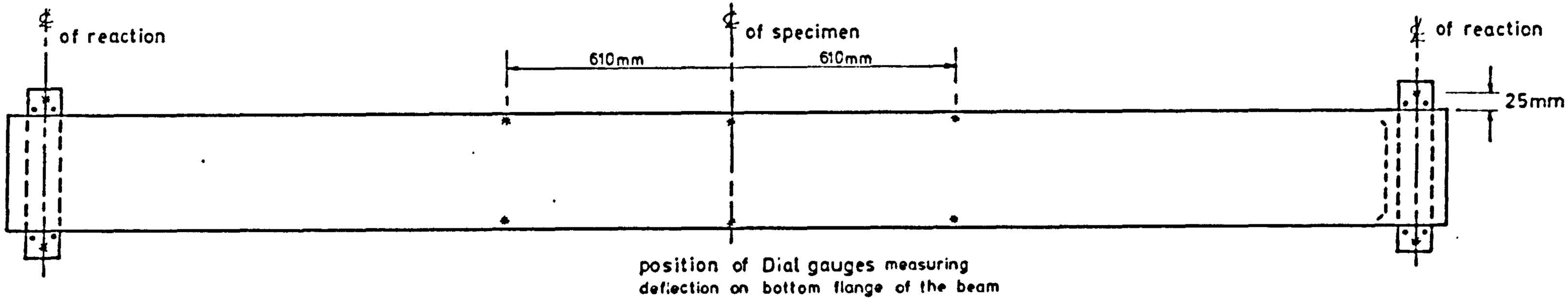

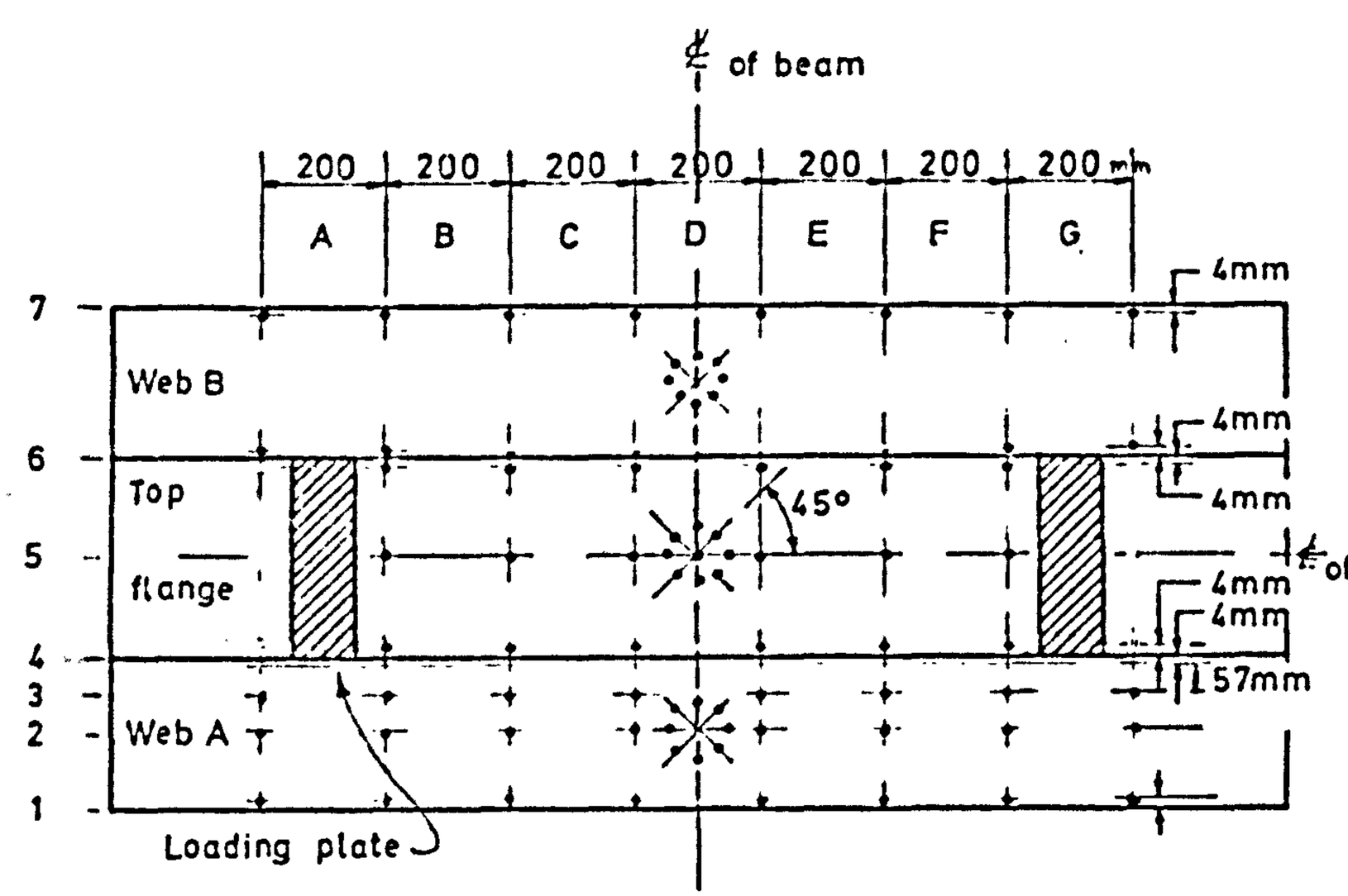

position of 200mm & 100 Demec gauges for series 1 & 3

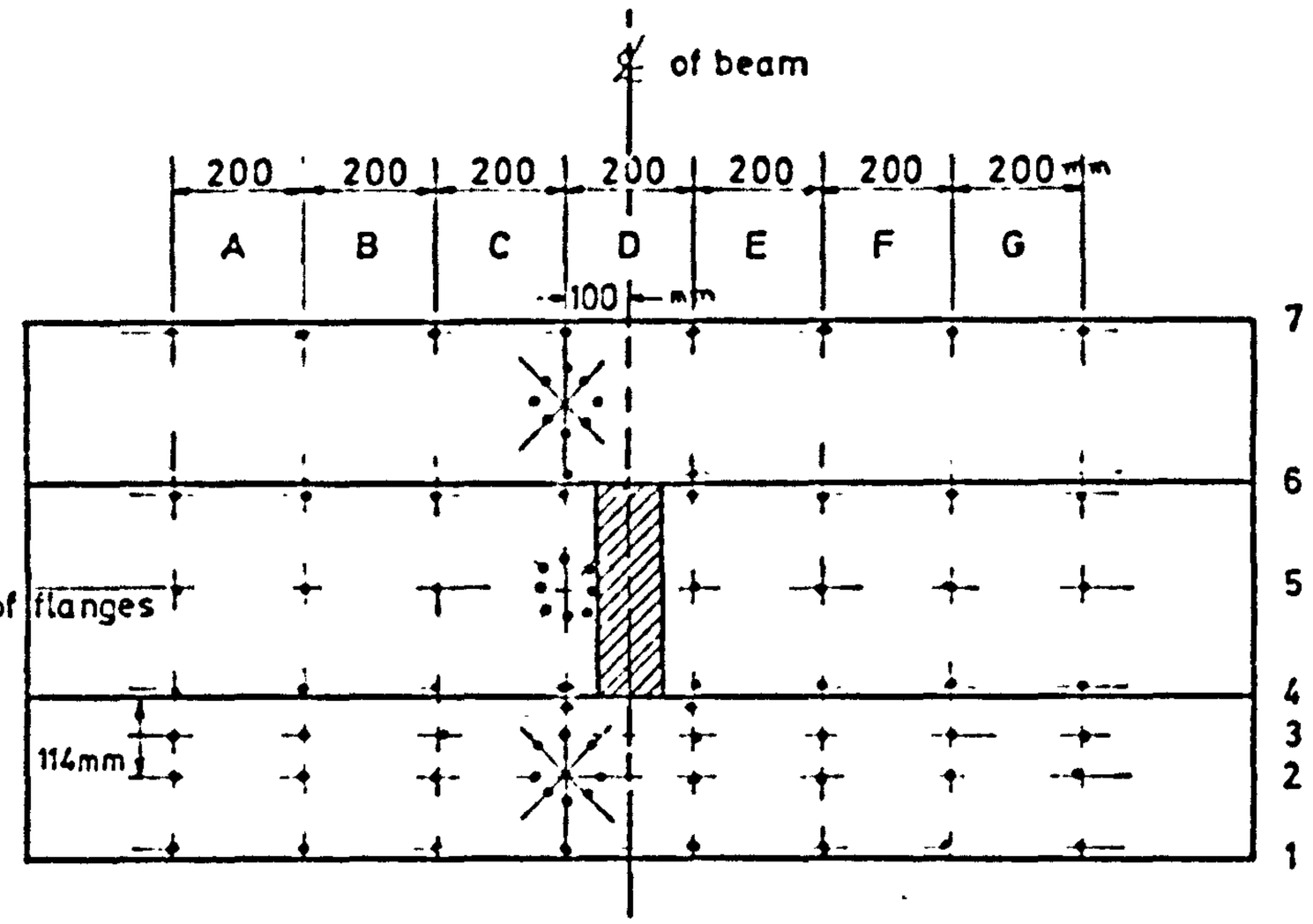

position of 200mm & 100 Demec gauges for series 2 & 4

FIG. 6.6 POSITION OF DEMEC & DIAL GAUGES.

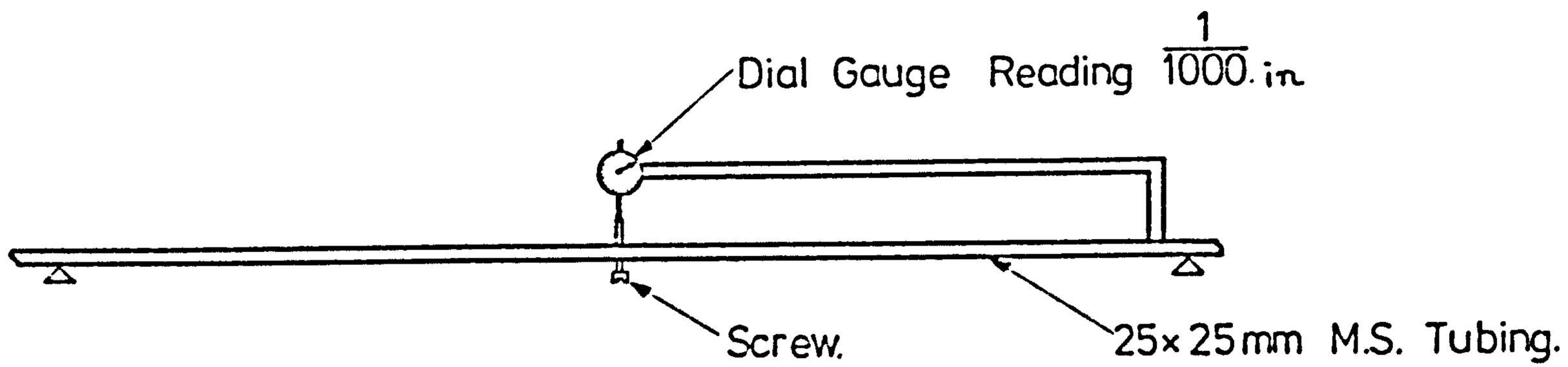

FIG 6·7 Device used for measurements of walls thickness.

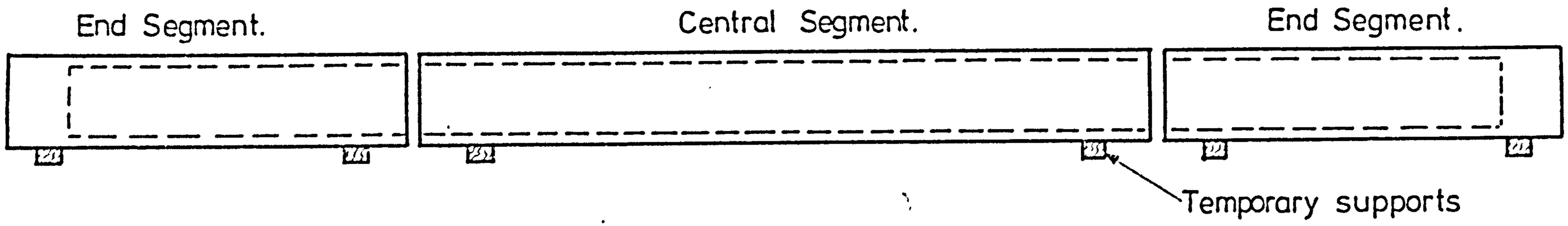

FIG 6·8 Supports arrangement before Prestressing.

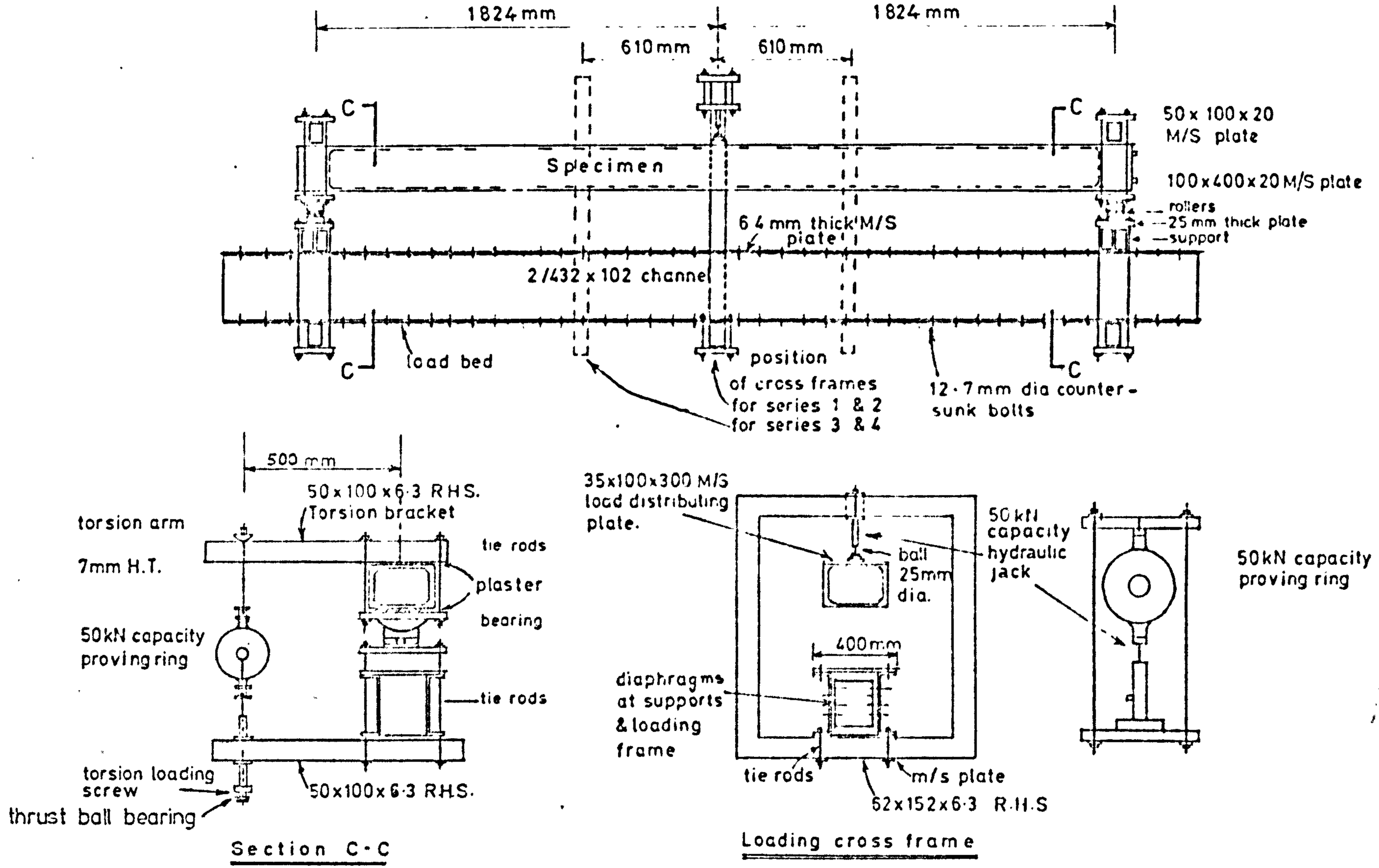

Fig.6.9 TEST RIG AND LOADING ARRANGEMENT

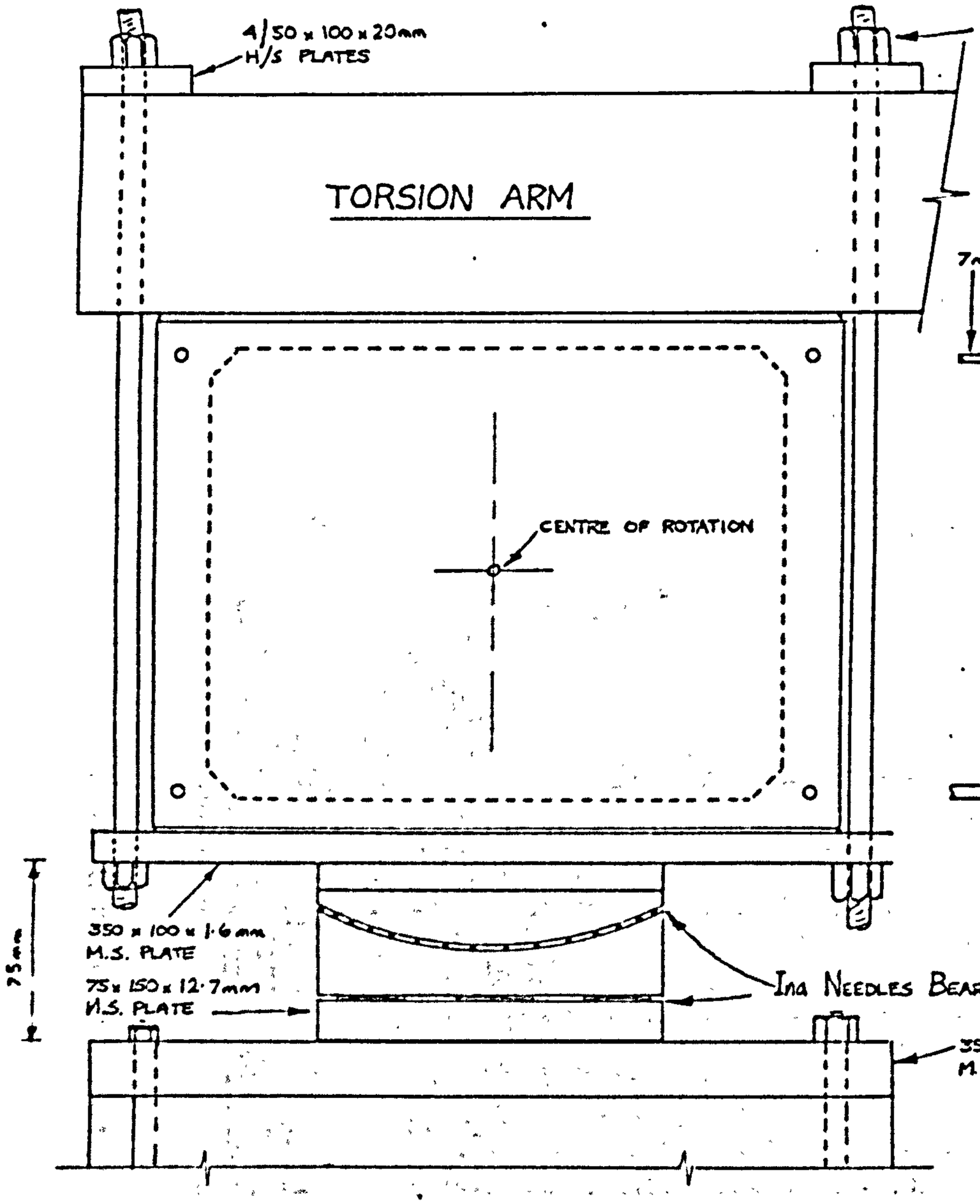

SECTION A-A

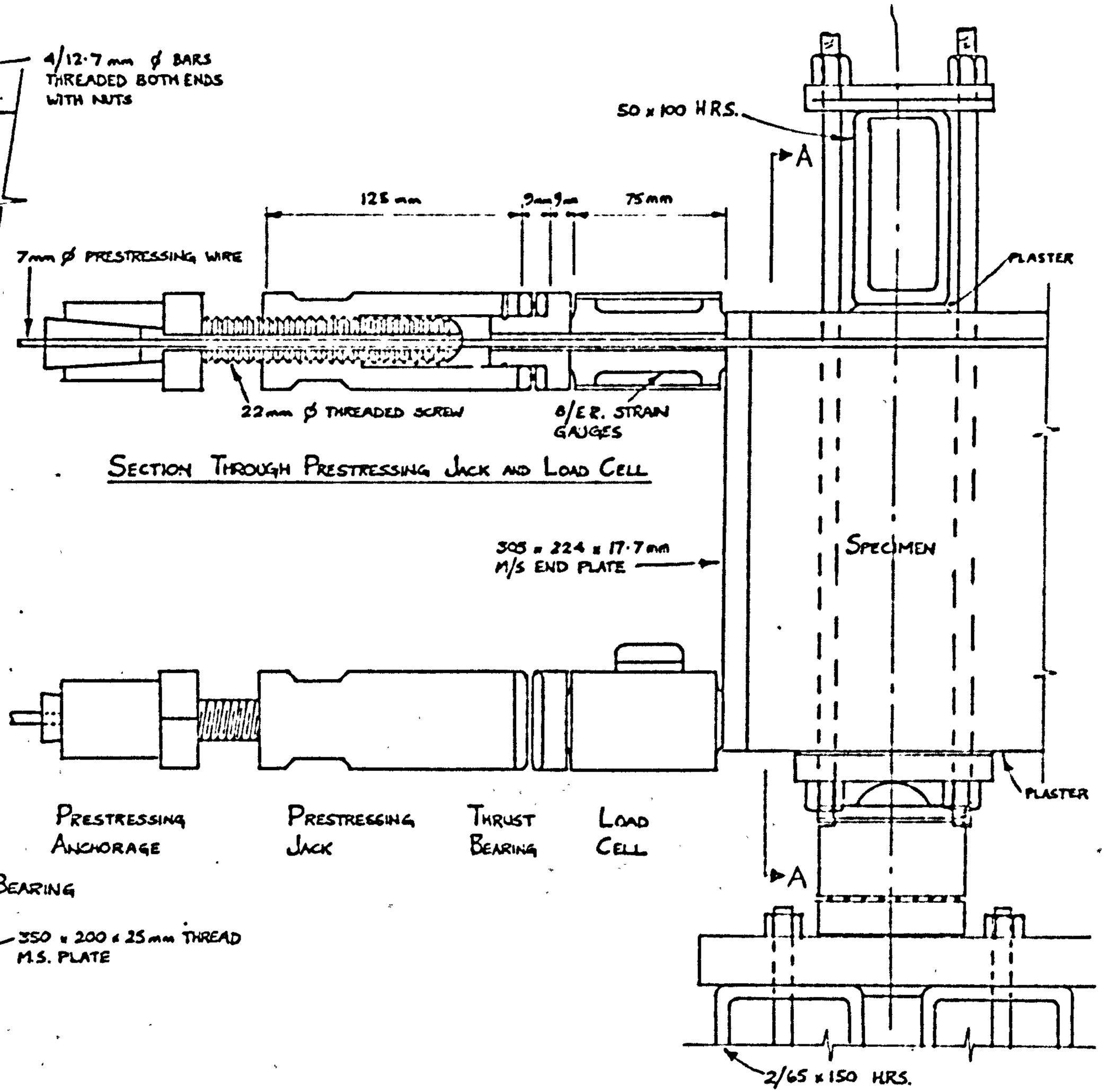

SECTION THROUGH PRESTRESSING JACK AND LOAD CELL

FIG 6.10 SUPPORT AND PRESTRESSING ARRANGEMENT

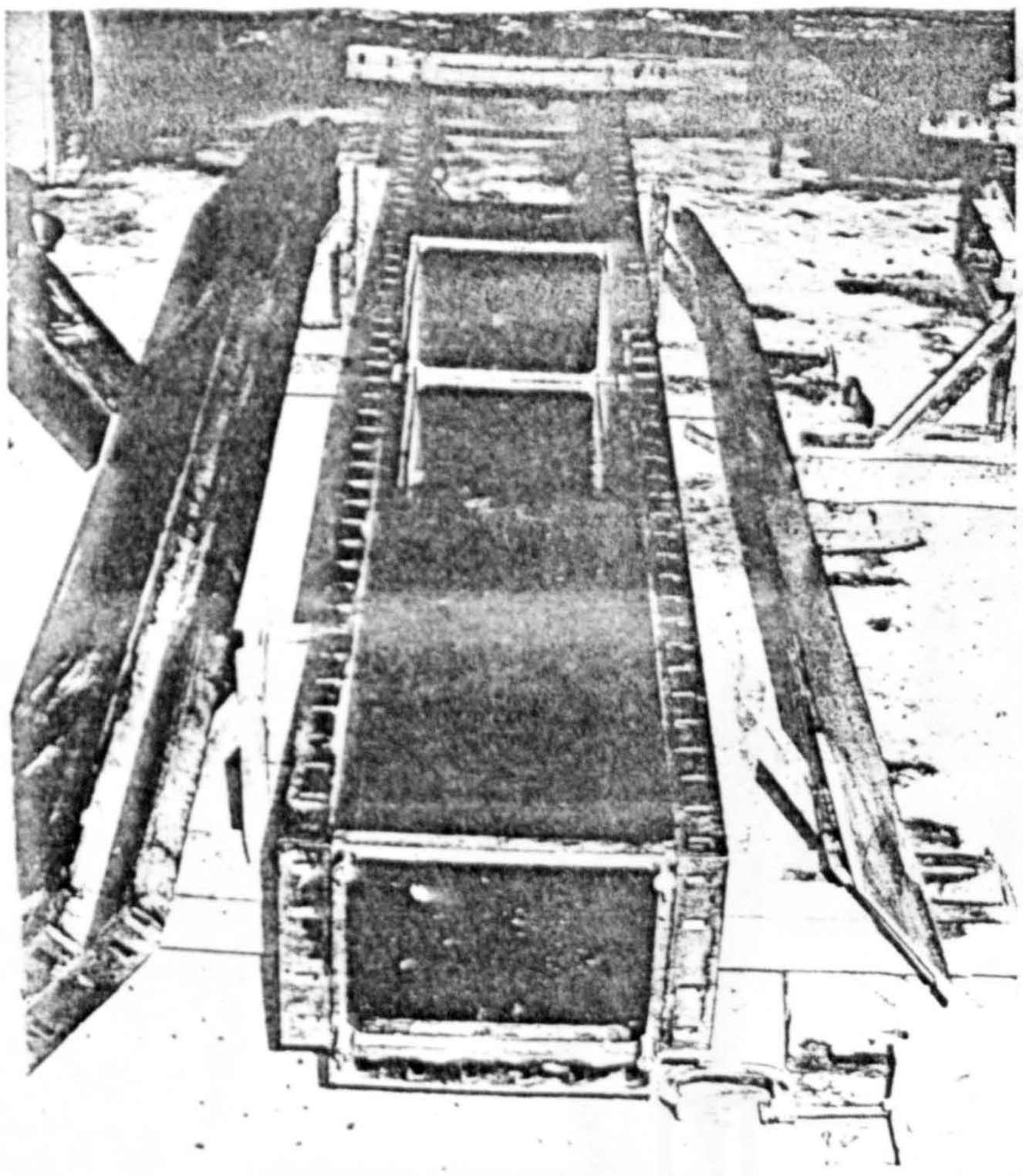

Plate 1. Steel Forms used for Casting Central Segment of Box Beam.

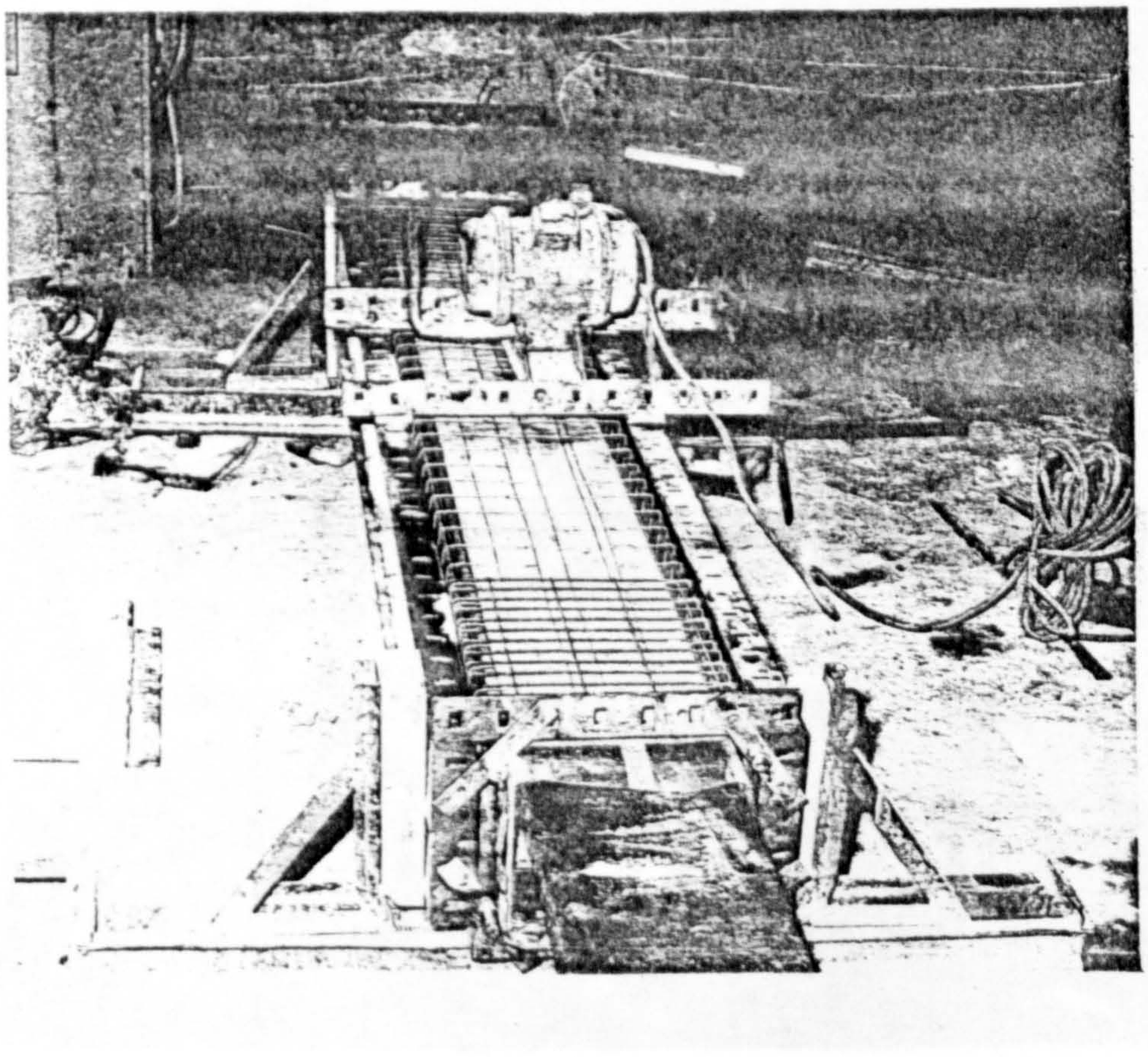

Plate 2. Formwork in Final Condition before Casting.

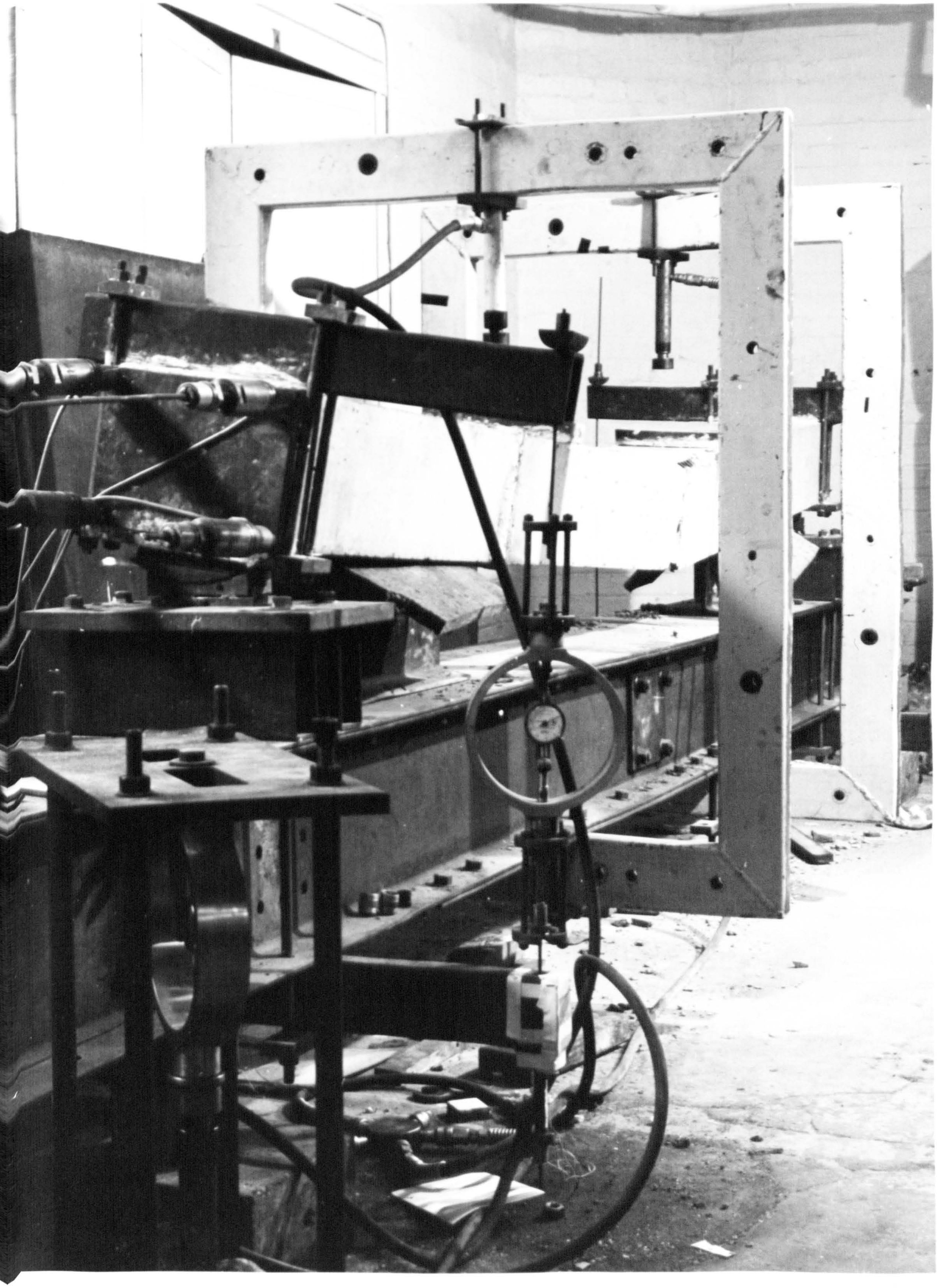

Plate 3 Test Arrangement used for Beams of Series 1 & 4

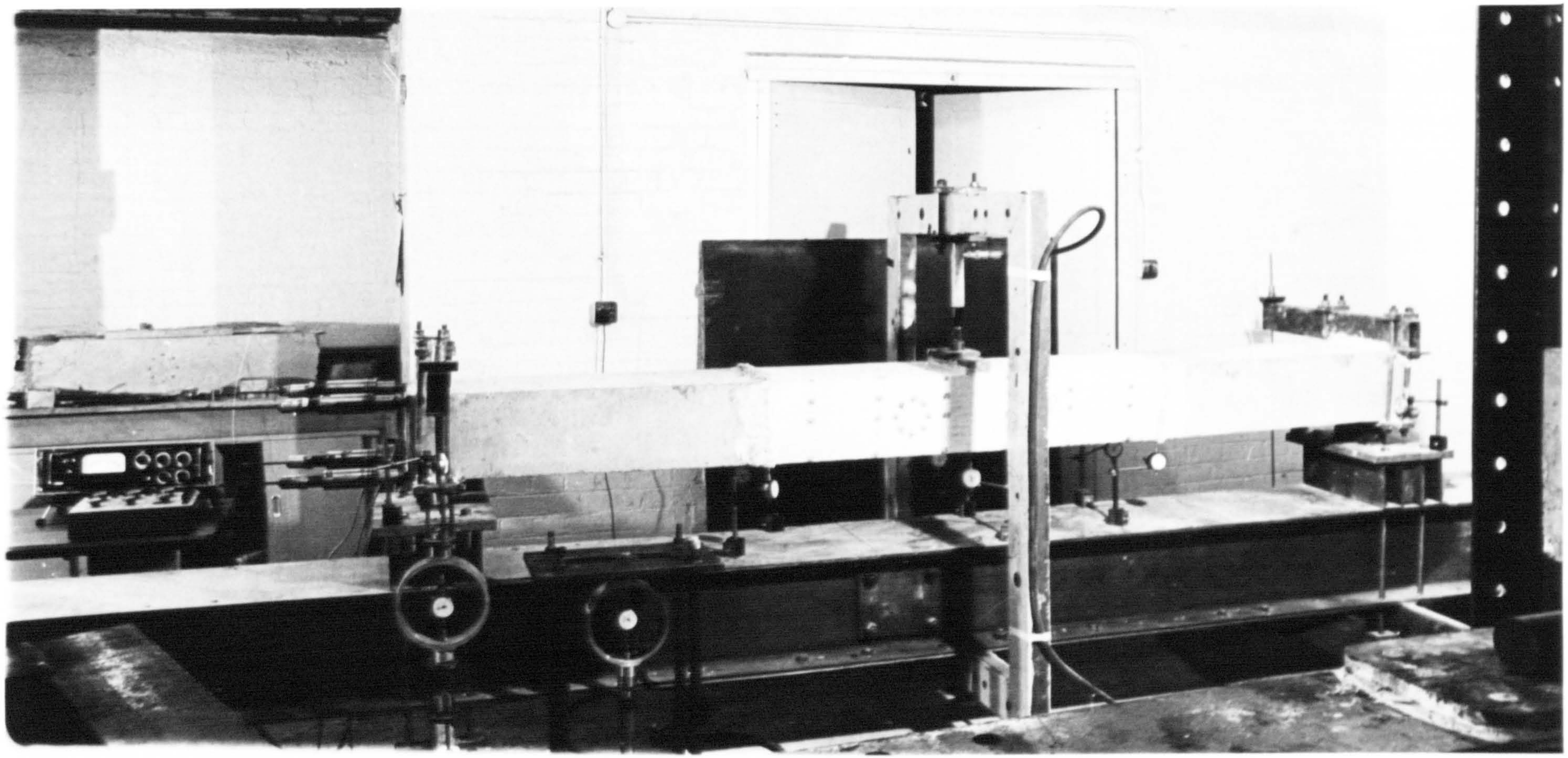

Plate 4 Test Arrangement used for Beams of series 2 & 4.

6.6 Behaviour of Beams Under Test

6.6.1 Prestressing

The longitudinal strains measured at the central section and those obtained from averaging all the Demec readings taken on the top and bottom flanges due to prestressings are given in Table 6.2. These values appear to be consistently lower than 345×10^{-6} obtained by taking the applied prestress as 6.9 N/mm^2 and E = 20 kN/mm^2. This discrepancy may be attributed to one or more of the following reasons:

I - Frictional losses at the joint

II - Creep of the adhesive used at the joints

III - Error in estimating the E value

V - Cross sectional dimensions were consistently greater than the nominal dimension of the specimen

VI - Error arising from load cells due to some disturbances that may have occurred during the prestressing operation.

Some of these factors may be considered when estimating the effective prestress and the other factors may be treated by considering 15% losses in the prestressing force to those values given in Table 6.2. This procedure appears to provide a reasonable estimate of the effective prestress of the beam.

6.6.2 Test to Failure - Beam Subjected to Pure Torsion

a) General Observations, Cracking and Failure

For all prestressed specimens inclined cracks making an angle approximately 30 to 35 degree with the longitudinal axis of the beam were initiated

at the bottom and top flange and were propagated to the web. This angle was approximately 45 degree for the beam with no prestress (T_o).

For beam T_o and T_1, the maximum torque correspondended to the torque which caused the appearance of the first crack and was followed by a sudden drop in the applied torque to almost half the maximum torque for beam T_1. The reinforcement of the cage which intersected the crack ruptured at this stage. Subsequently the beam sustained considerable increase in twist and crack width as shown in plate 5, with little or no change in the applied torque recorded until it failed as shown in plate 5.

Beam T_2 continued to carry a further increase in torque beyond the torque which caused first cracking. After the formation of the first crack more cracks developed extending from one end of the beam to another forming a spiral as shown in Fig. 6.11. This increase in torque continued until the reinforcement of the cage ruptured causing a sudden drop in the applied torque to a value equal to half the torque which caused the first cracking. The behaviour of this beam at this stage is identical to that of beam T_1.

For these three beams there was a marked change in the position of the centre of rotation after the maximum torque was reached. Rotation took place about one of the flanges with the two portions of the beam on either side of this major crack rotating relative to each other.

Beams T_3 and T_4 which contained a larger

volume of lateral reinforcement than beam T_1 and T_2 behaved in similar manner to beam T_2 during the formation of crack as shown in Fig. 6.12 but they failed suddenly due to spalling of the concrete which occurred at one corner of the box spreading along their entire length as shown in plates 6 and 7. After a drop in torque to between 60 and 70% of the maximum value the beams started to carry increases in torque until finally the tests were stopped when it was not possible to apply any further twist. This corner spalling caused a fundamental change in the equilibrium of the internal forces at this spalled edge, for example the stirrups at this corner as shown in plate 6 and 7 are subjected to considerable shear displacement along the spalled edge. Further increase in torque caused a longitudinal splitting crack in the web and flange which are only linked by the stirrups. This provided further evidence that the shear transmitted between the web and the flange at this stage was entirely by the dowel action of the stirrups as shown in plate 6.

b) Angle of Twist

In Fig. 6.13 the angle of twist per meter length is plotted against torque. It can be seen that the torque/rotation characteristic is reasonably linear up to cracking. The change in the slope which is seen prior to cracking is due to a change in the stiffness of the test bed which was found to occur at a certain torque as a result of slip between the main components of the test bed.

The remainder of the curves indicate that a considerable reduction in the torsional stiffness occurs after cracking and provides further evidence for the discussion given in the previous section.

c) Strain In Reinforcement and Forces in The Prestressing Wires

The relationship between the strains in the reinforcement as measured by the E.R.S. gauges on the stirrups and the torque for beams T_3 and T_4 are plotted on Fig. 6.14 and 6.15 respectively.

It can be seen that before diagonal cracking occurred the reinforcement strains were quite small but they increased rapidly after cracking and a few strains reached the yield strains at maximum torque.

No changes in the force in the prestressing wires were recorded up to cracking and the percentage increase in the prestressing forces which were recorded between the maximum and cracking torque for beams T_2, T_3 and T_4 were between 15% and 20%.

d) Deformation of Concrete

Strain measurements indicated that the diagonal compressive strains measured at the top flange and the webs increase linearly with torque up to cracking. Beyond this stage the diagonal compressive strain increased at a higher rate. However, the strains which occur at maximum torque were only 15 to 40% of the maximum strain usually sustained by concrete in compression (0.0035). These results

therefore exclude the possibility of diagonal compression failure.

Measurements of longitudinal strains indicated that the beams T_2, T_3, and T_4 suffered longitudinal extension after cracking which suggests that torque in cracked P.C. beam is resisted by the space truss action.

The strain readings and the change in the prestressing force for this series are not reproduced here.

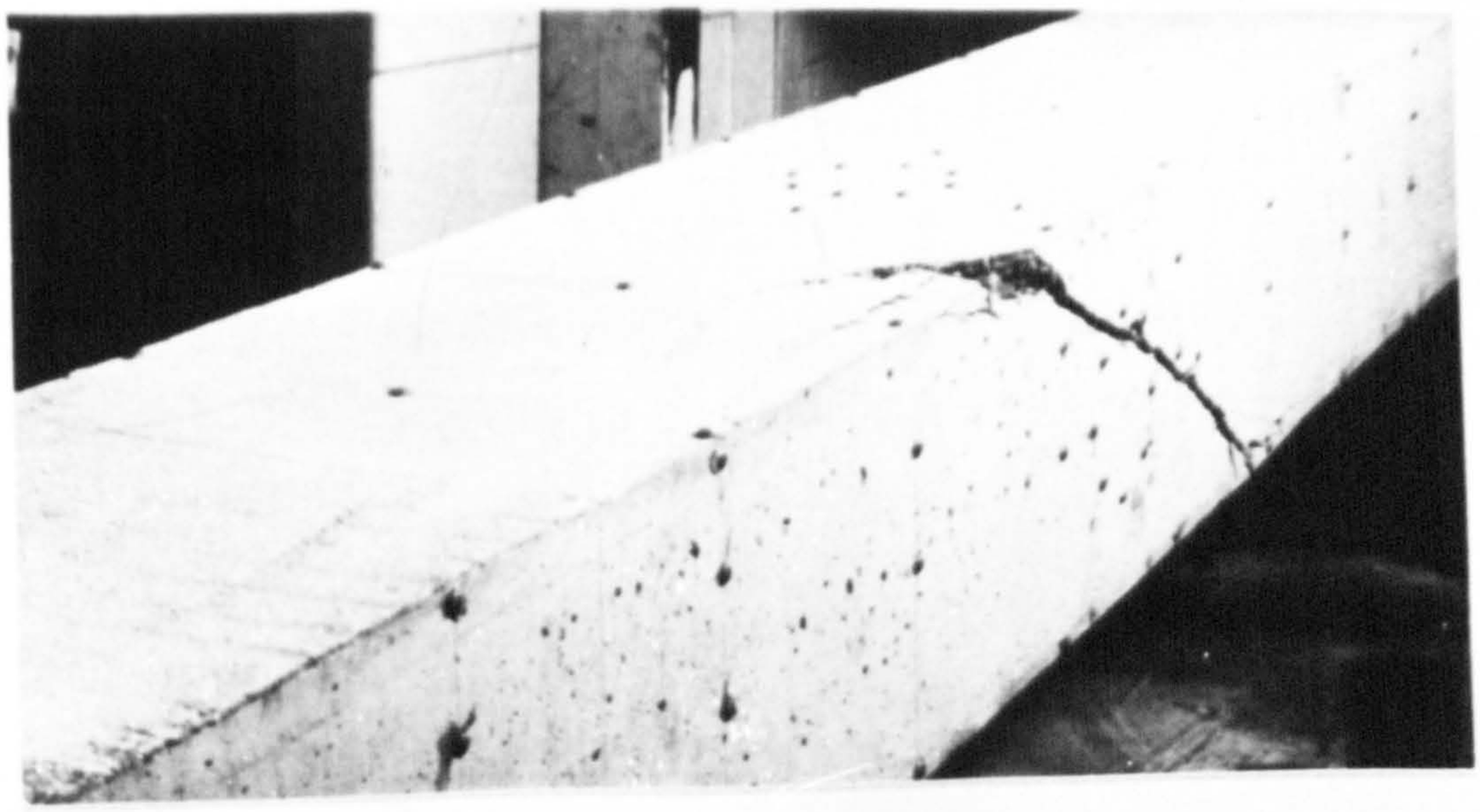

After cracking

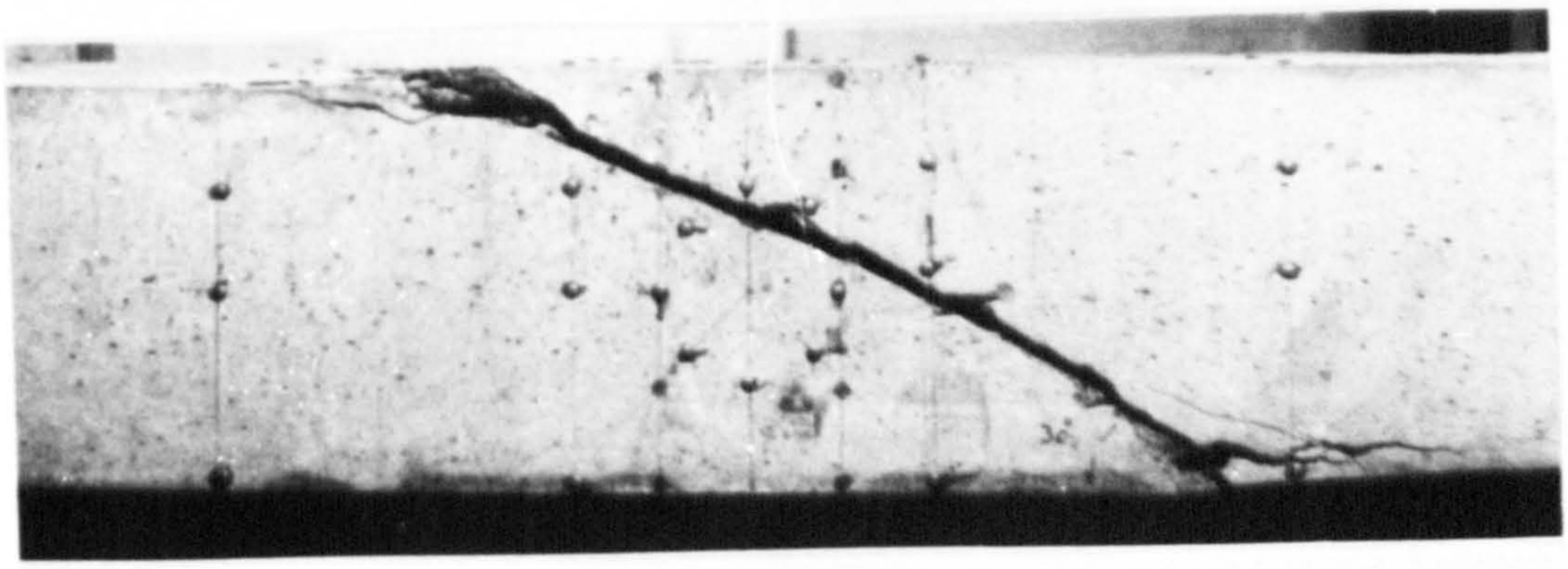

Before failure

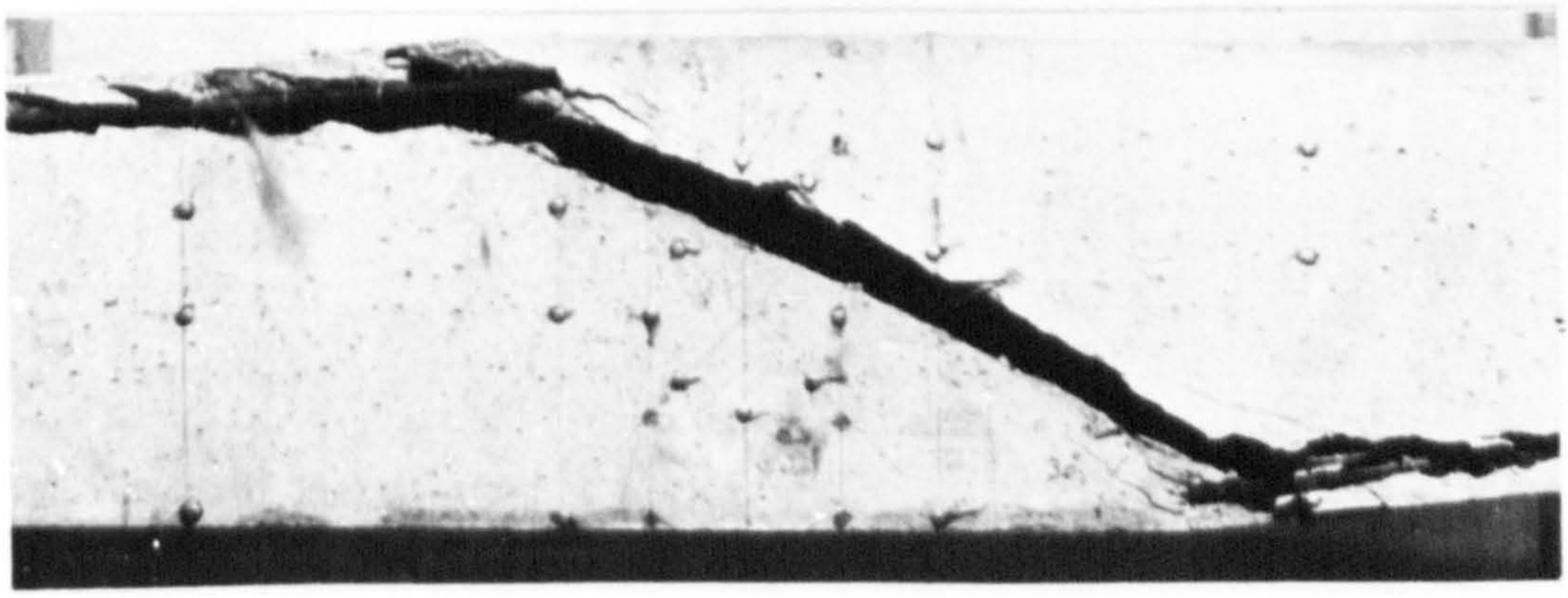

Before failure

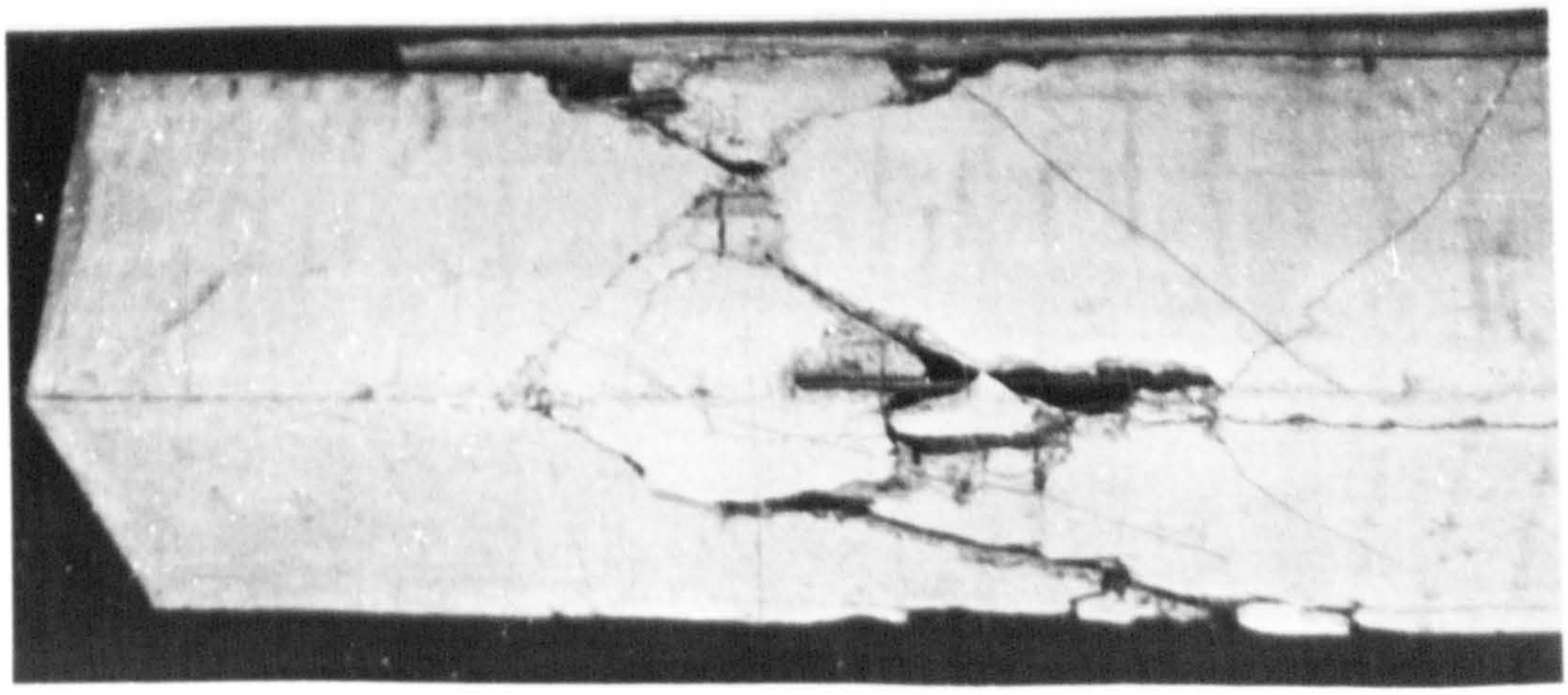

After failure

Plate 5 Crack patterns after cracking, before failure and after failure for beam T_1

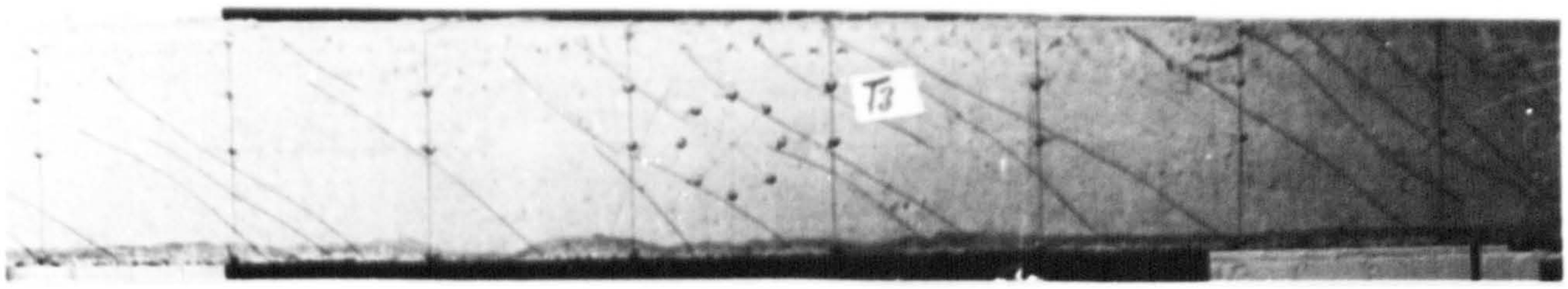

At maximum torque

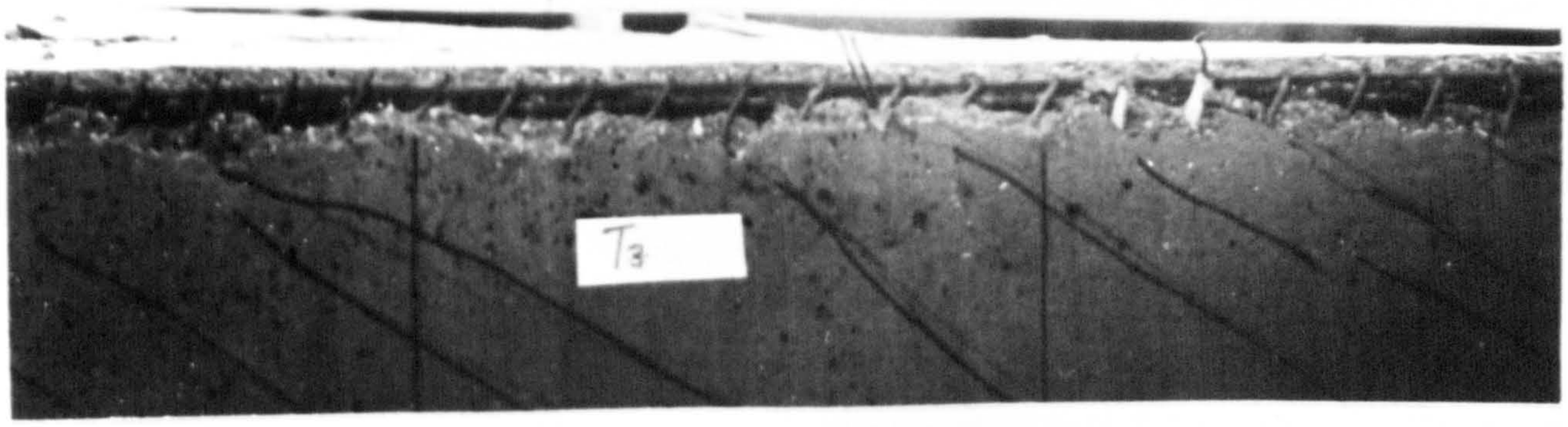

After maximum torque

Plate 6 Crack patterns at failure for beam T_3

Plate 7 Crack patterns after failure for beam T_4

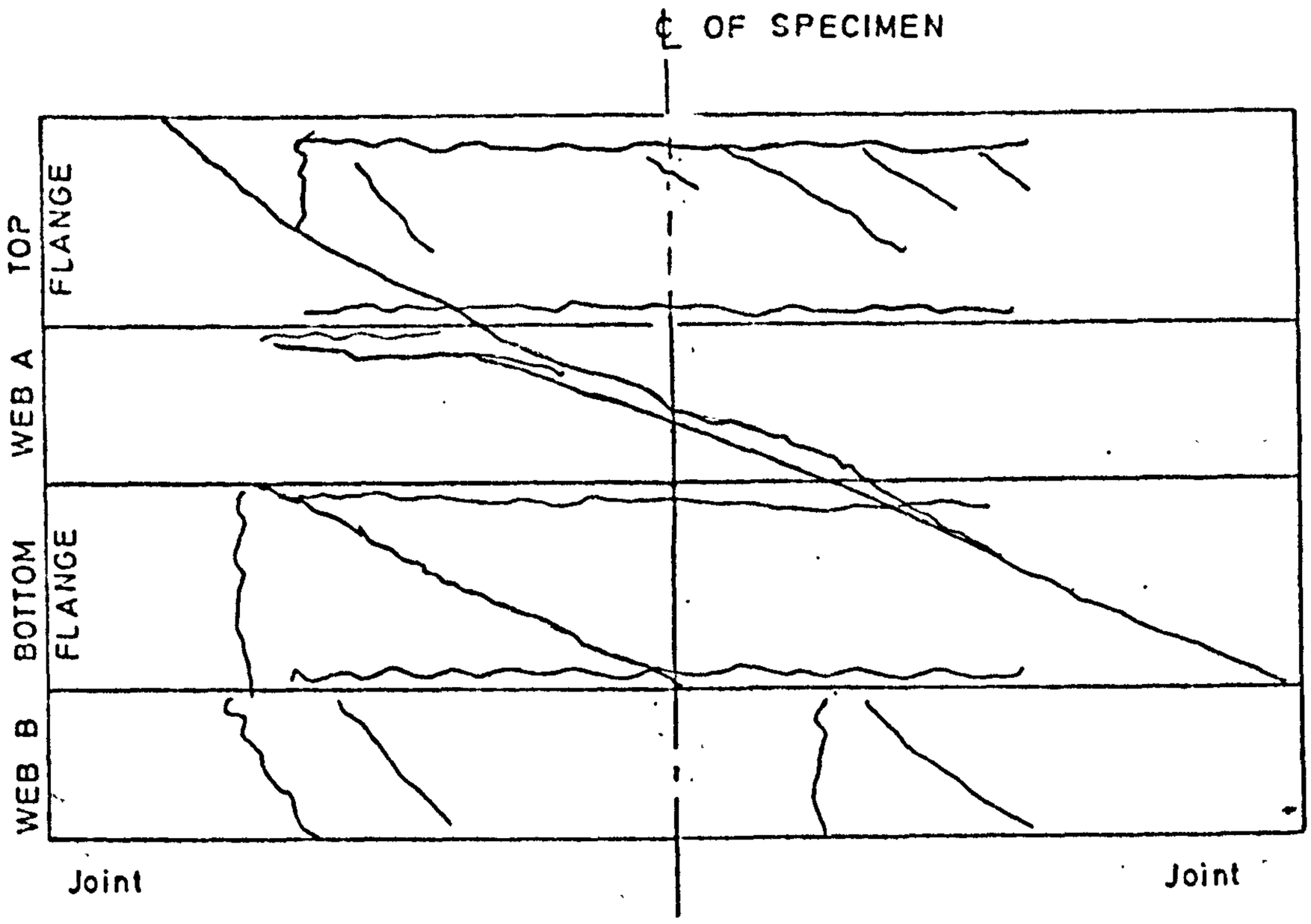

SPECIMEN No T1 $\frac{M}{T} = 0$

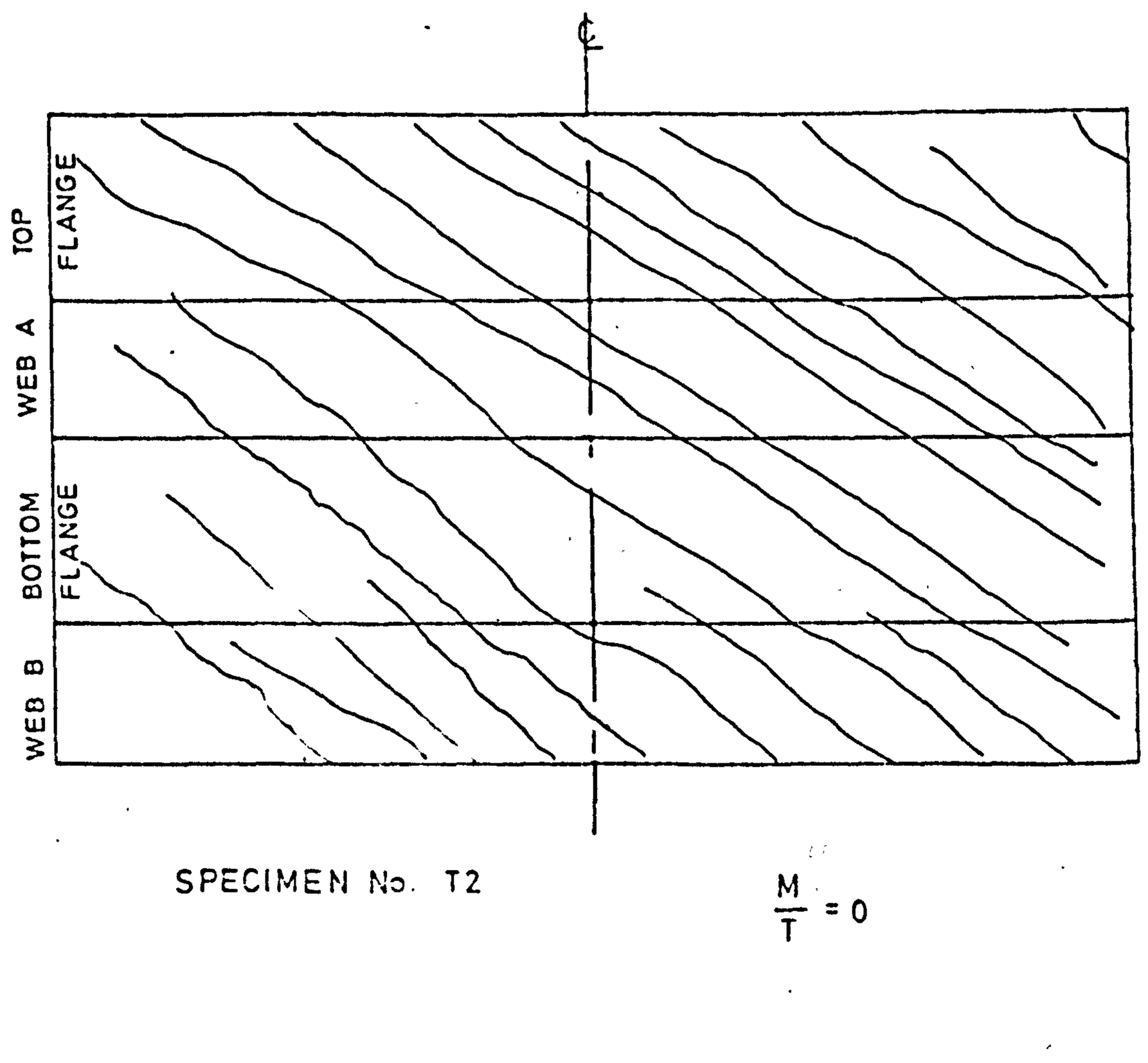

SPECIMEN No. T2 $\frac{M}{T} = 0$

FIG. 6.11 CRACK PATTERNS FOR No T1 AND T2

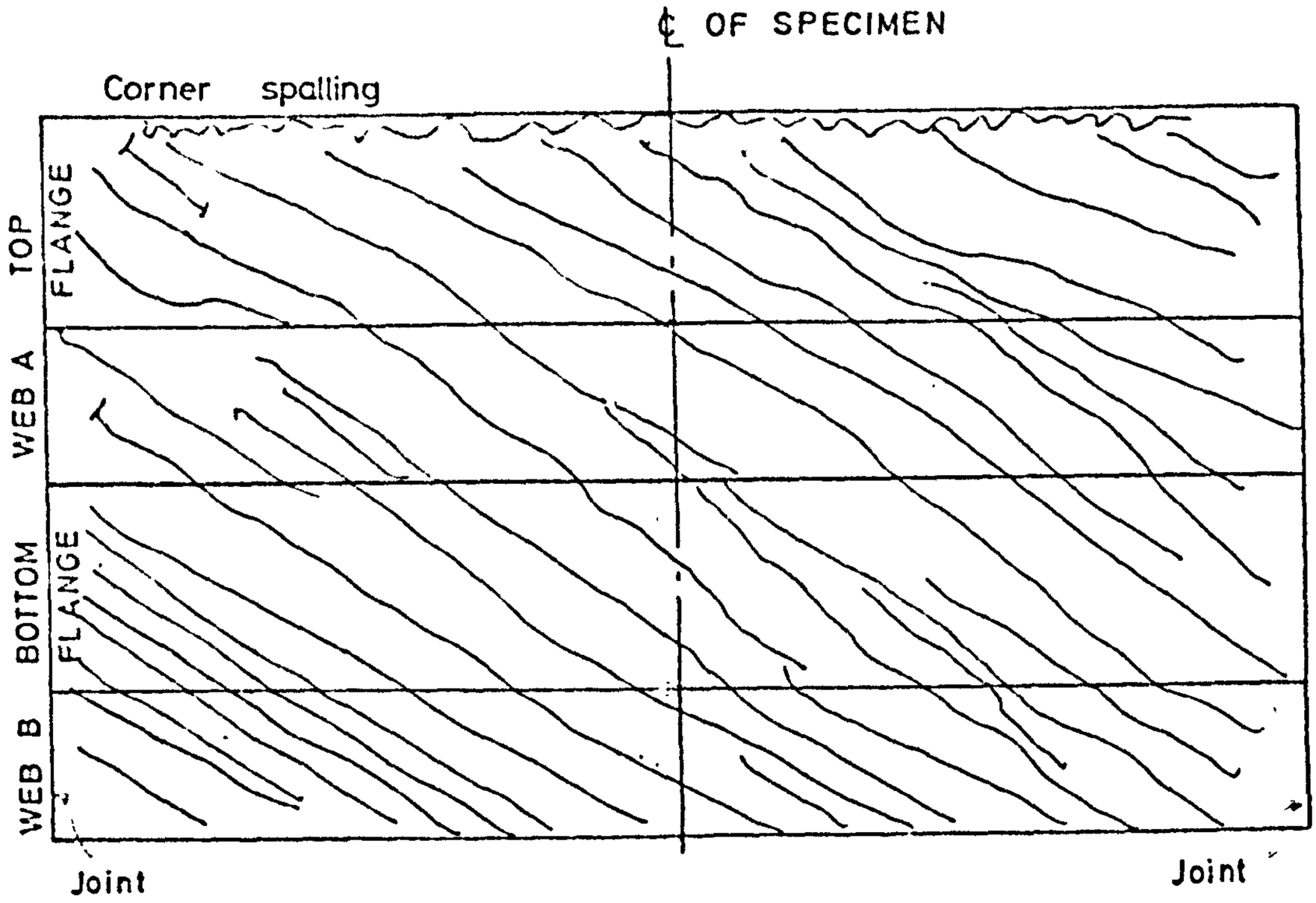

SPECIMEN No T3 $\frac{M}{T} = 0$

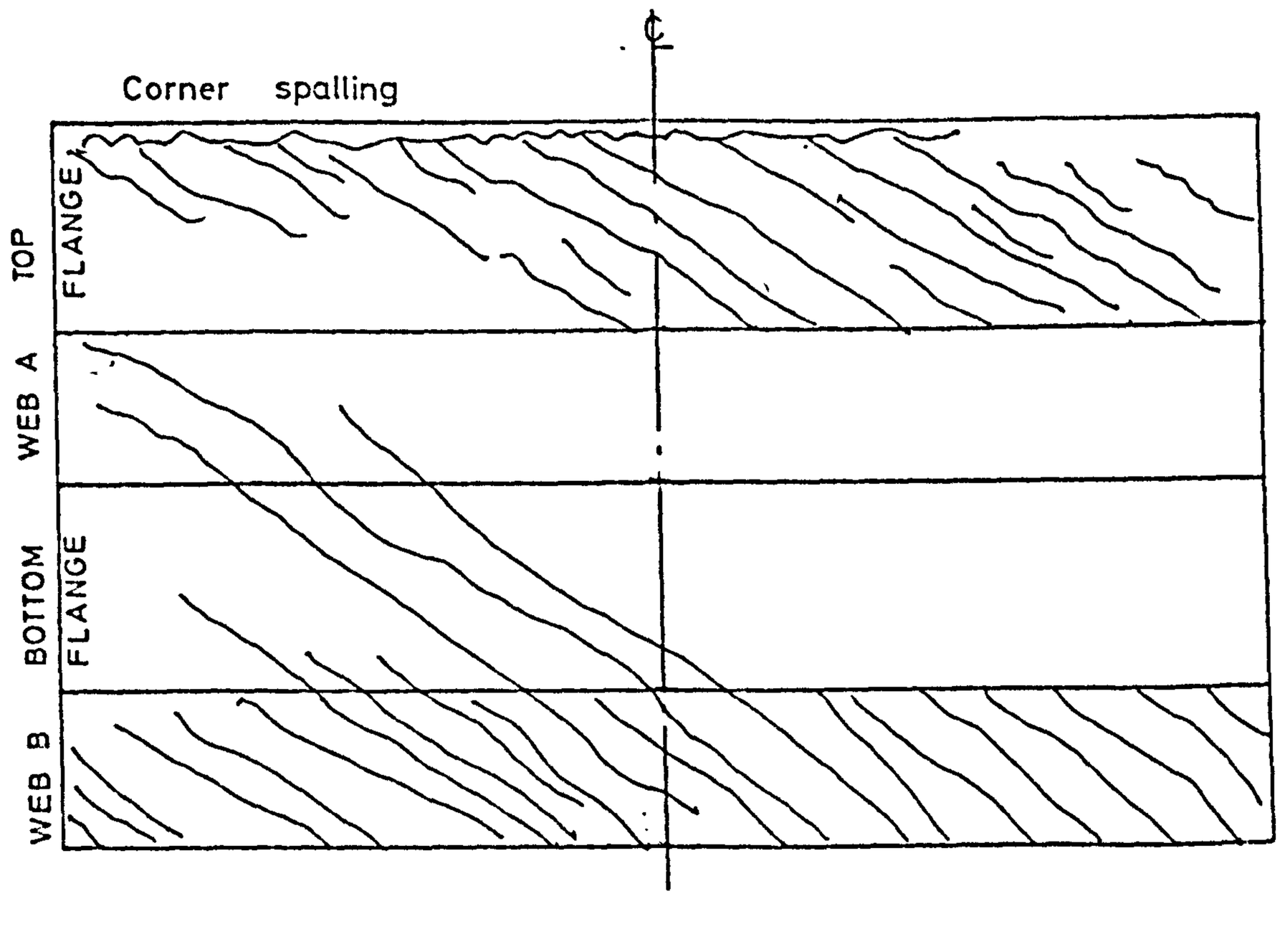

SPECIMEN No. T4 $\frac{M}{T} = 0$

FIG. 6.12 CRACK PATTERNS FOR No T3 AND T4

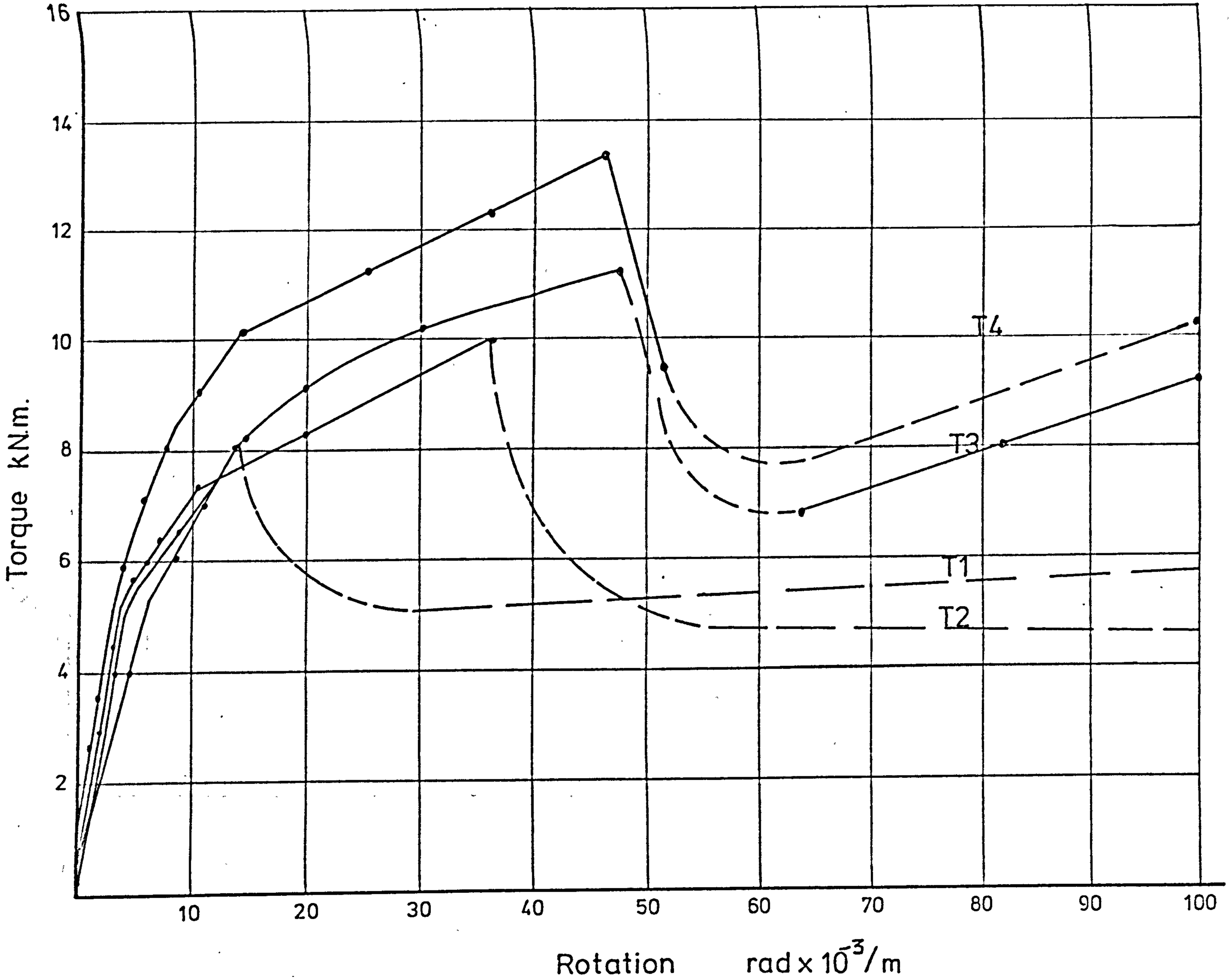

Fig 6.13. Torque - Rotation Curves For Specimen T1 to T4

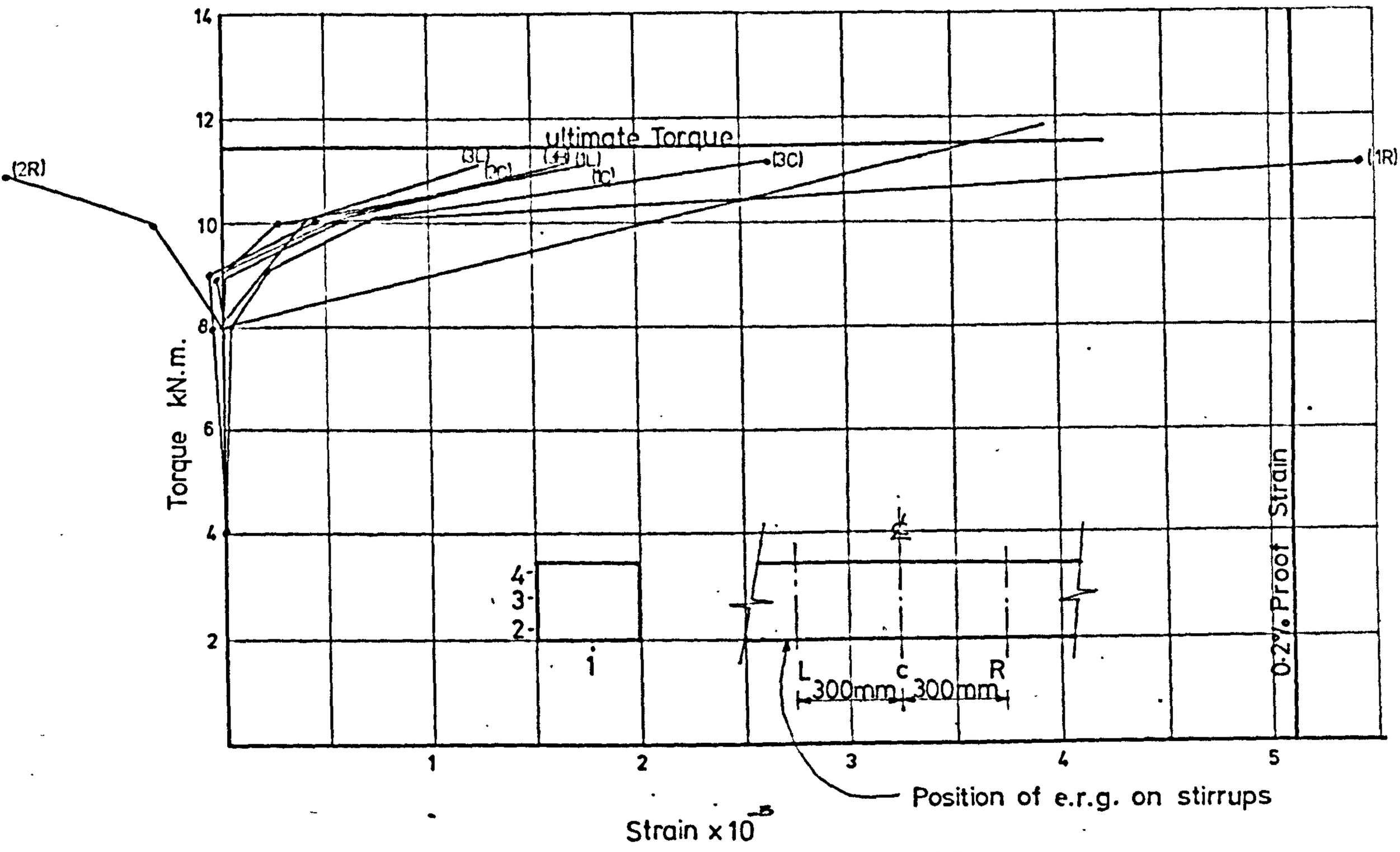

Fig 6.14. Torque Versus Stirrups Strain For Specimen T3

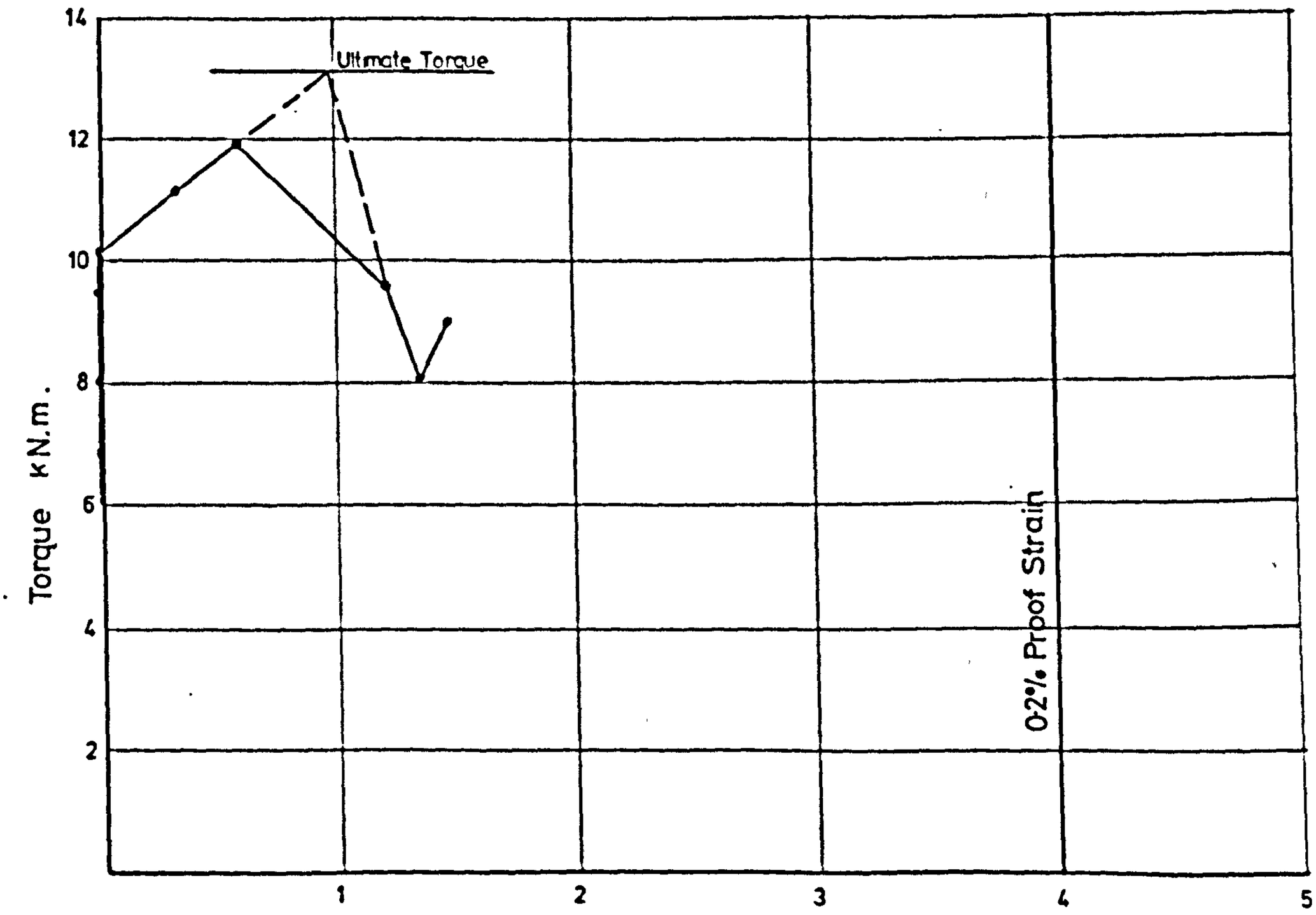

Fig 6.15. Torque Versus Stirrups Strain For Specimen T4

6.6.3 Test to Failure - Beam Subjected to Bending and Torsion Series 1

a) General Observations, Cracking and Failure.

For the beams of this series cracks were initiated at the bottom flange and propagated suddenly to the webs. The inclination of these cracks to the longitudinal axis varies in accordance with theapplied moment torque ratio as shown in Fig. 6.16 and 6.17. With increase in the moment one of these cracks opened up and propagated upwards. The reinforcement of the cage which crosses this crack ruptured resulting in the formation of a major crack and a further increase in crack widths as shown in plates 8 and 9. The beams of this series behaved after the rupture of the reinforcement as if they were without lateral reinforcement. Afterward, the portions of the beam on each side of this major crack rotate relative to each other about the top compression flange. This ratation brings into action dowel forces that occur between the bottom prestressing wires and the surrounding concrete which was evident from the spalling of the concrete in these zones as shown in plates 8 and 9.

Finally the concrete in the compression zone crushed explosively as shown in plates 8, 9 and 10 precipitating failure.

The ratio of ultimate bending moment capacity to the moment which caused cracking decreased with increase in the applied torque.

Beam B15 which was subjected to equal values of moment and torque, exhibited a

cleavage failure of the compression flange accompanied by spalling of one of the corners of the beam as shown in plate 11. This mode of failure as shown in plate 11 suggests the presence of a bi-moment in the top flange which was evidenced from the tendency of the top flange to bend laterally. This bi-moment could be the main restraining internal force resisting the applied torque in this category of beams.

b) Deflections and Rotations

Central deflections were obtained by averaging the readings of the two dial guages located at the central section. They are plotted against applied loads for all beams of this series in Fig. 6.18.

Rotations were obtained from the deflection readings of the dial gauges which were located at mid span and under the load. The rotations between the central section and the sections under the load (averaged and reduced to a rotation per meter length) are plotted against torque in Fig. 6.19.

These results indicate that the beams behaved almost linearly up to cracking and the simple theory of bending and torsion may be adequately used for predicting the deformation behaviour of these beams in the uncracked stage. In the cracked stage both torsional and bending stiffnesses are reduced. In general it appears that the flexural stiffness descreases with increase in the torque to bending moment ratio.

It was not possible to record the deflection at ultimate load for all the beams because of the large deformations occuring and the sudden nature of failure required that dial gauges were removed in order to prevent them being damaged.

c) Forces in Prestressing Wires

No significant changes in the prestressing forces were recorded until the appearance of the first crack beyond which the force in the bottom wires began to increase while the force in the top wires decreased as the applied load increased, as shown in Fig. 6.20. It can be seen that in no case did the force in the wires reach their ultimate characteristic strength as the beams reached their ultimate load carrying capacity. It can also be noticed that the maximum force occuring at failure in the bottom wires decreased with increase in the applied torque.

The strains on the lateral reinforcement were not measured since it was expected that they would rupture and not contribute significantly to the strength of the beams.

d) Deformation of Concrete

The results of the strain rosettes taken on the top flange are plotted against the moment in Fig. 6.21.

The relationship between the longitudinal compressive strains measured on the top flange and the applied moments are shown in Fig. 6.22. The longitudinal strains across five sections of the beams are presented for various loading stages in Fig. 6.23 to 6.24.

It can be seen that the maximum concrete strains at failure show wide variations depending on the ratio of bending and torsional moment. These results also indicate that the strain distribution across a section of the box beams is influenced by the presence of a major crack. Although the assumption of plane sections before bending remaining plane after bending does not seem to be valid for sections in the vicinity of a major crack, it does appear to apply to the average strain distribution measured over the entire length of the zone.

The depth of the neutral axis at failure appears to increase with an increase in applied torque.

6.6.4 Test to Failure - Beams Subjected to Bending, Torsion and Shear Series 2

In general the beams of this series exhibited similar characteristics to those of series 1. The presence of shear appeared to reduce the ultimate carrying capacity of the beam by 10% to 20% compared to the corresponding beams of series 1. Also fewer cracks were formed at the bottom of the specimens, as shown in Fig. 6.25 and 6.26, compared with the corresponding beams of series 1. Beam B21 to B24 failed as a result of crushing of the top flange as shown in plate 12 whereas beam 25 failed by cleavage fracture of the top flange accompanied with longitudinal corner spalling as shown in plate 12.

Deflection and rotation results are also given in Fig. 6.18 and 6.19 respectively. The force measurements in the prestressing wires are given in Fig. 6.20. The results obtained from the strain

measurements at the top flange are shown in Fig. 6.21 and 6.22 and the results of the experimental strain distribution at various stages of loading and sectionsare shown in Fig. 6.27 to 6.28.

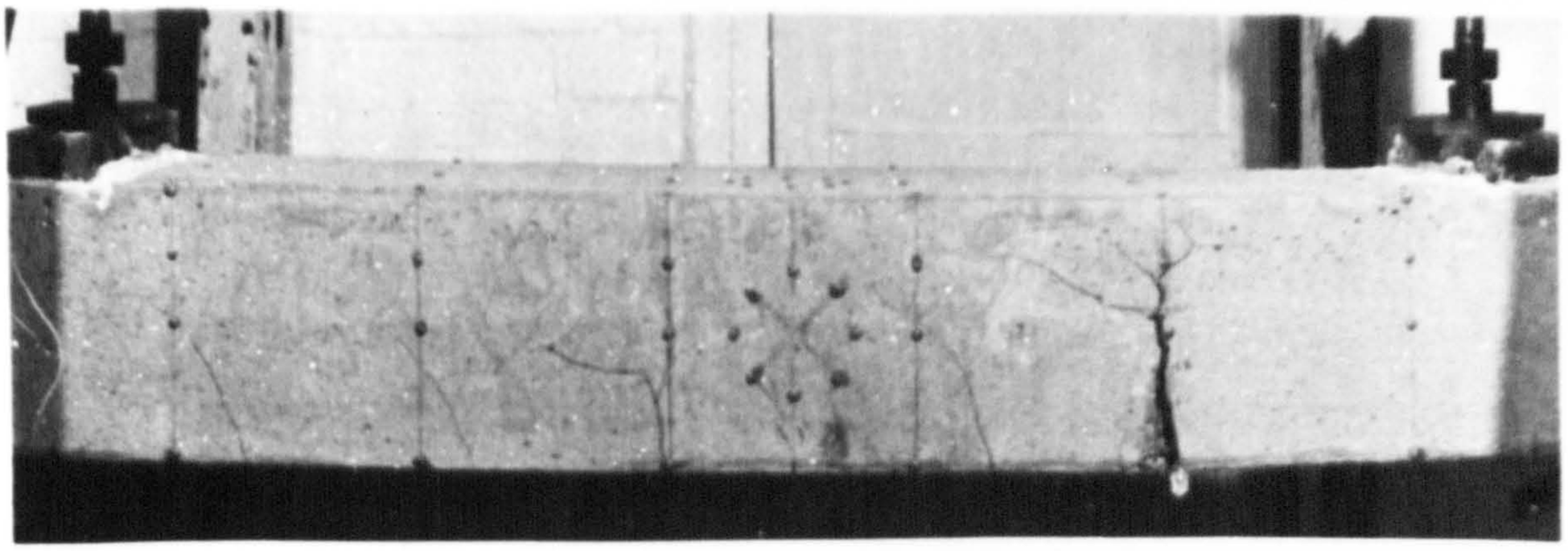

During test

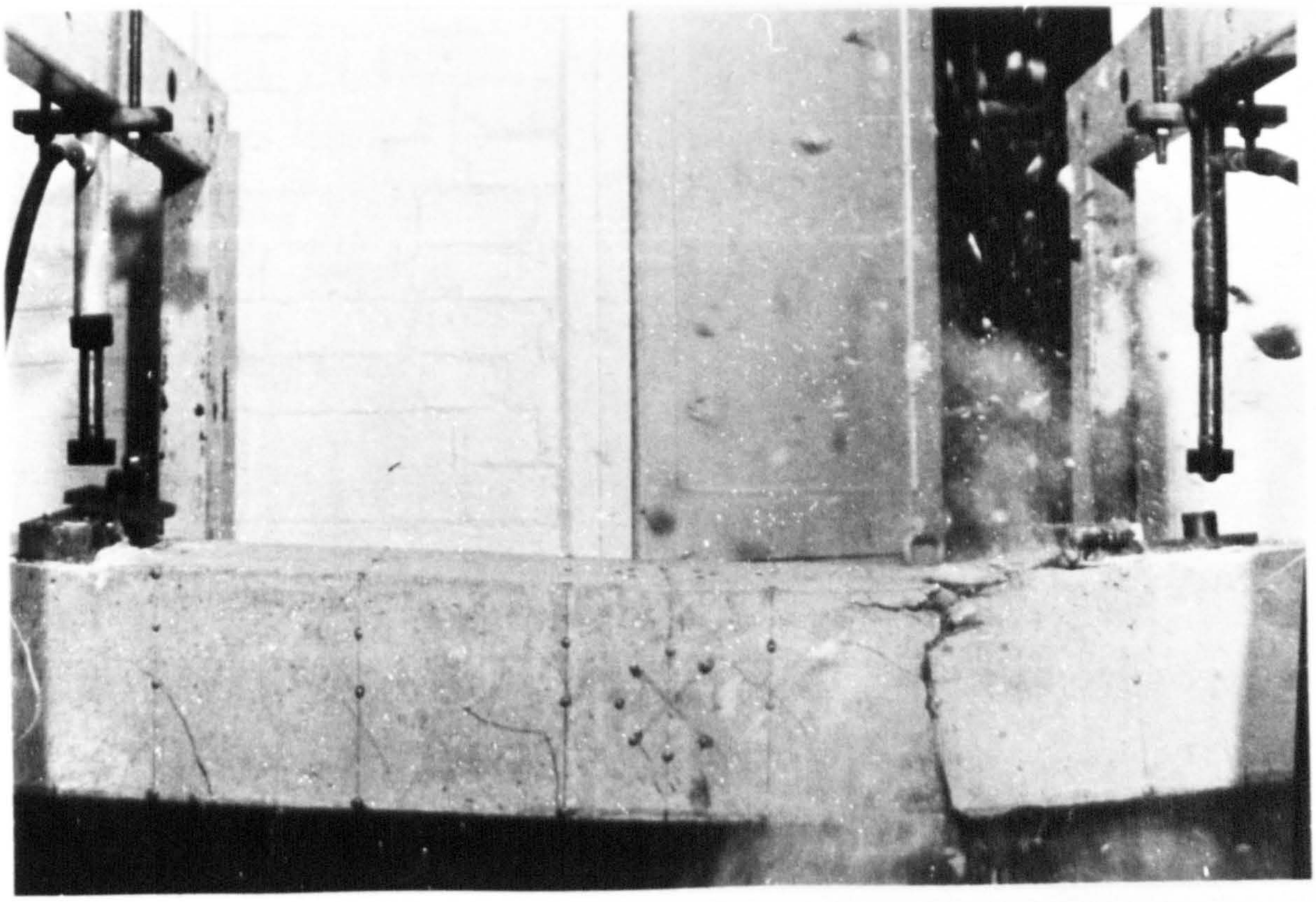

At failure

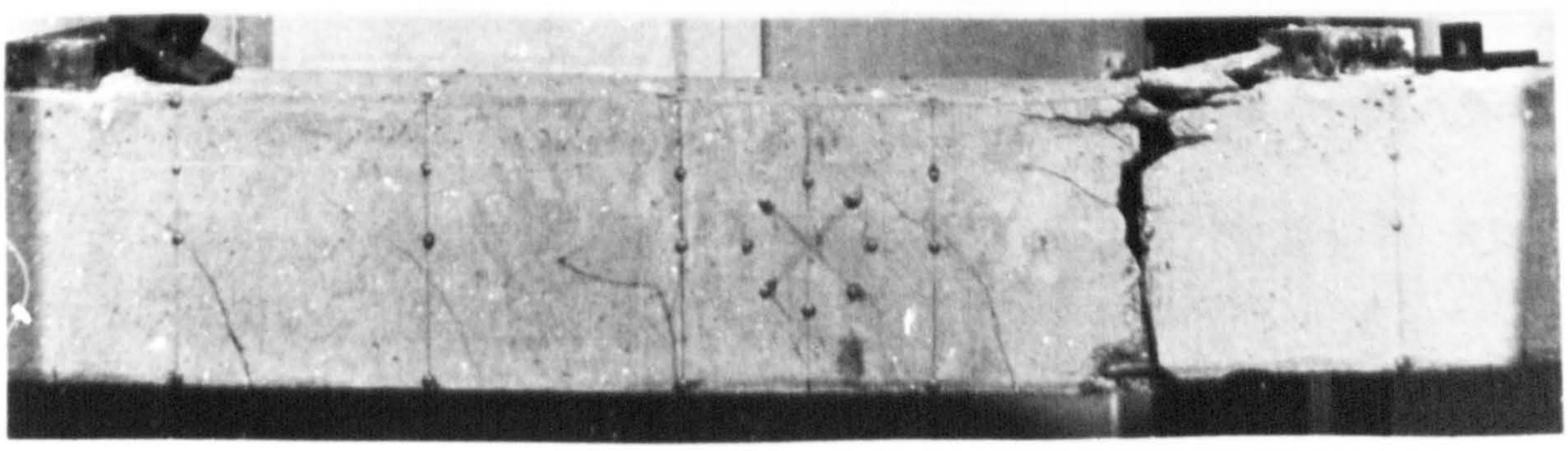

After failure

Plate 8 Cracks development during test, at failure and crack patterns after failure for Beam B12

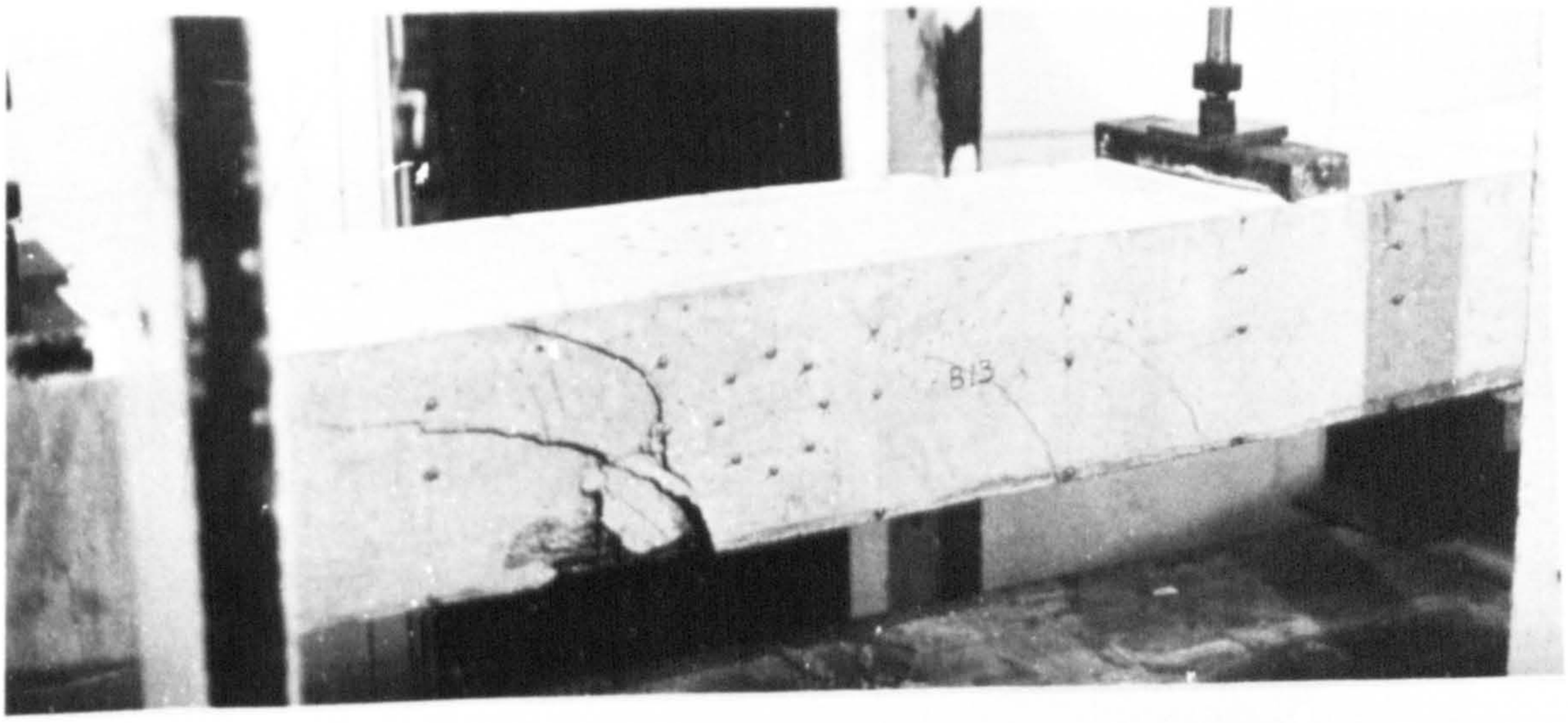

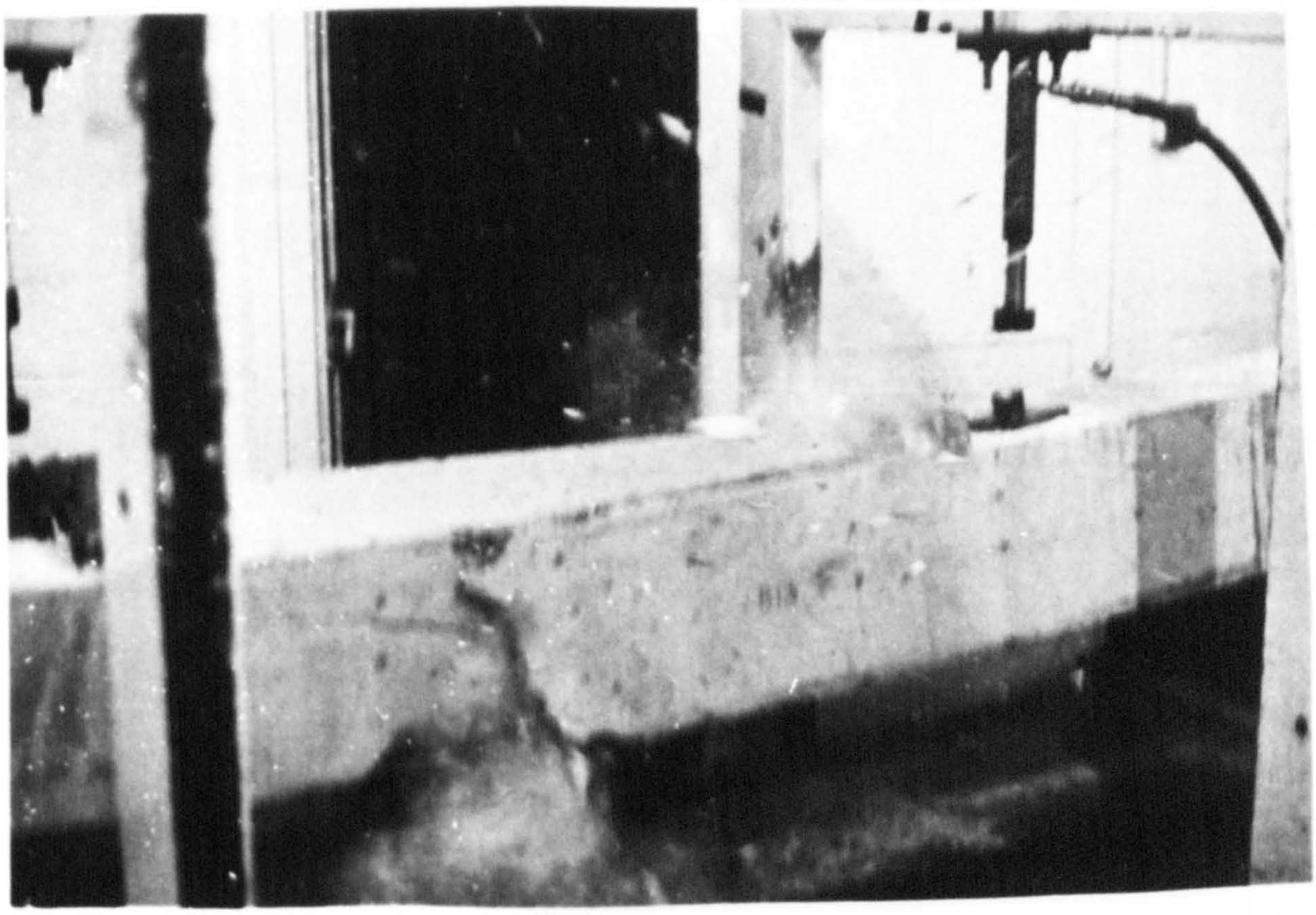

At failure

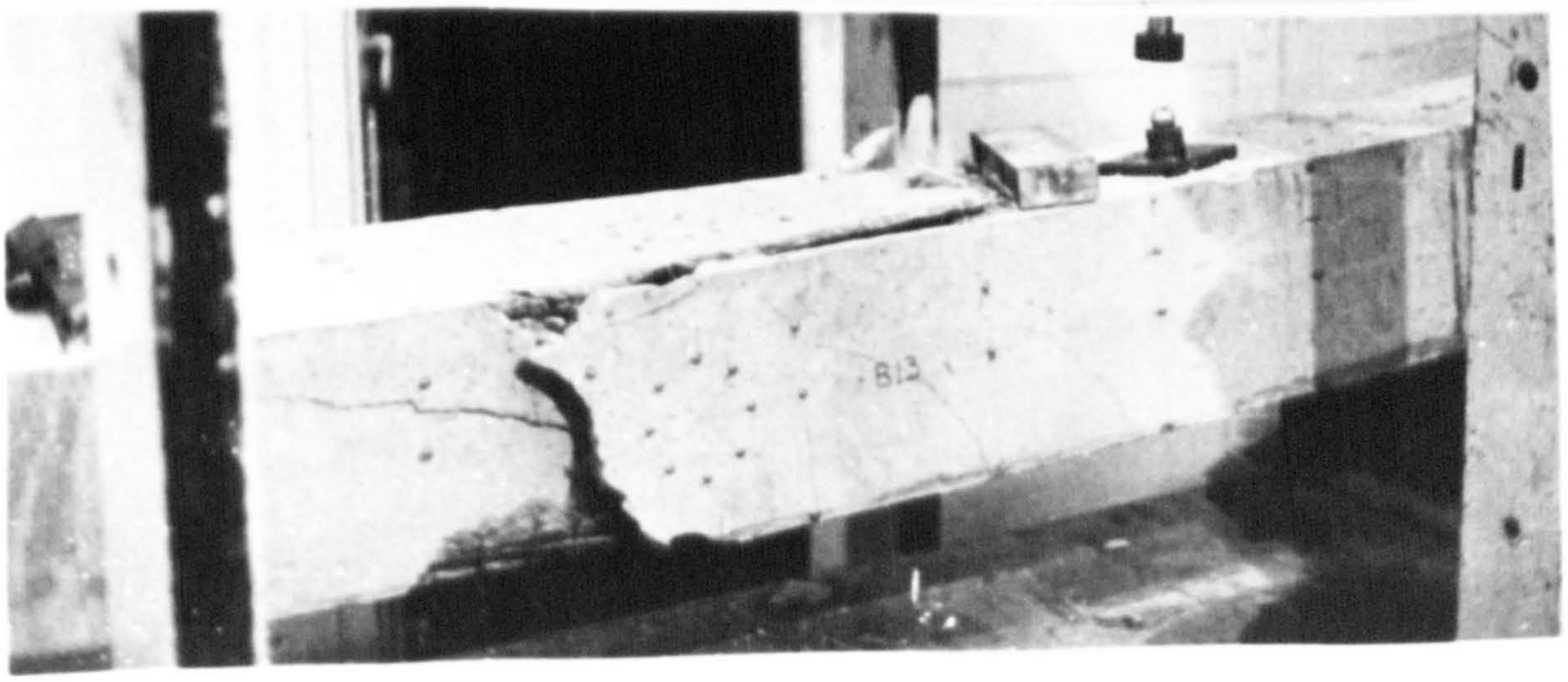

After failure

Plate 9 Cracks development during test, at failure and crack patterns after failure for Beam B13

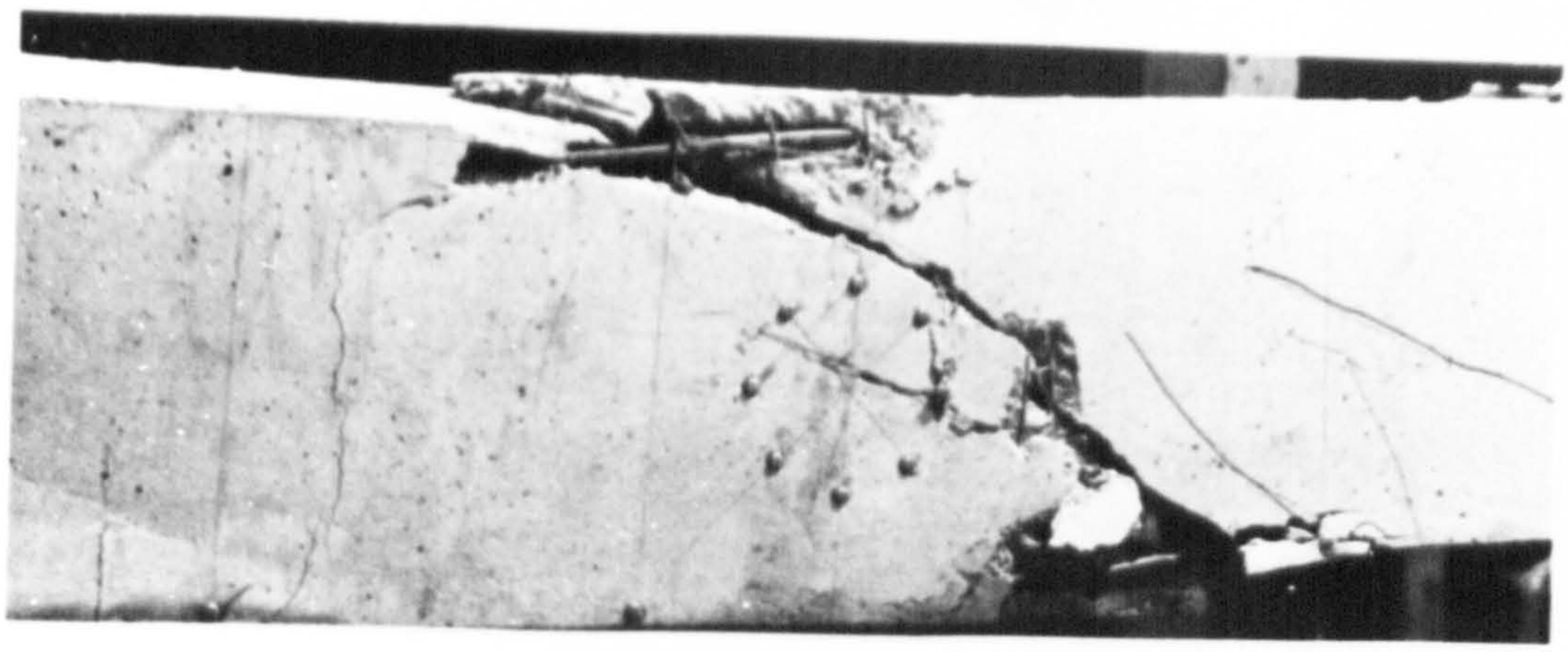

Plate 10 Crack patterns after failure for beam B14

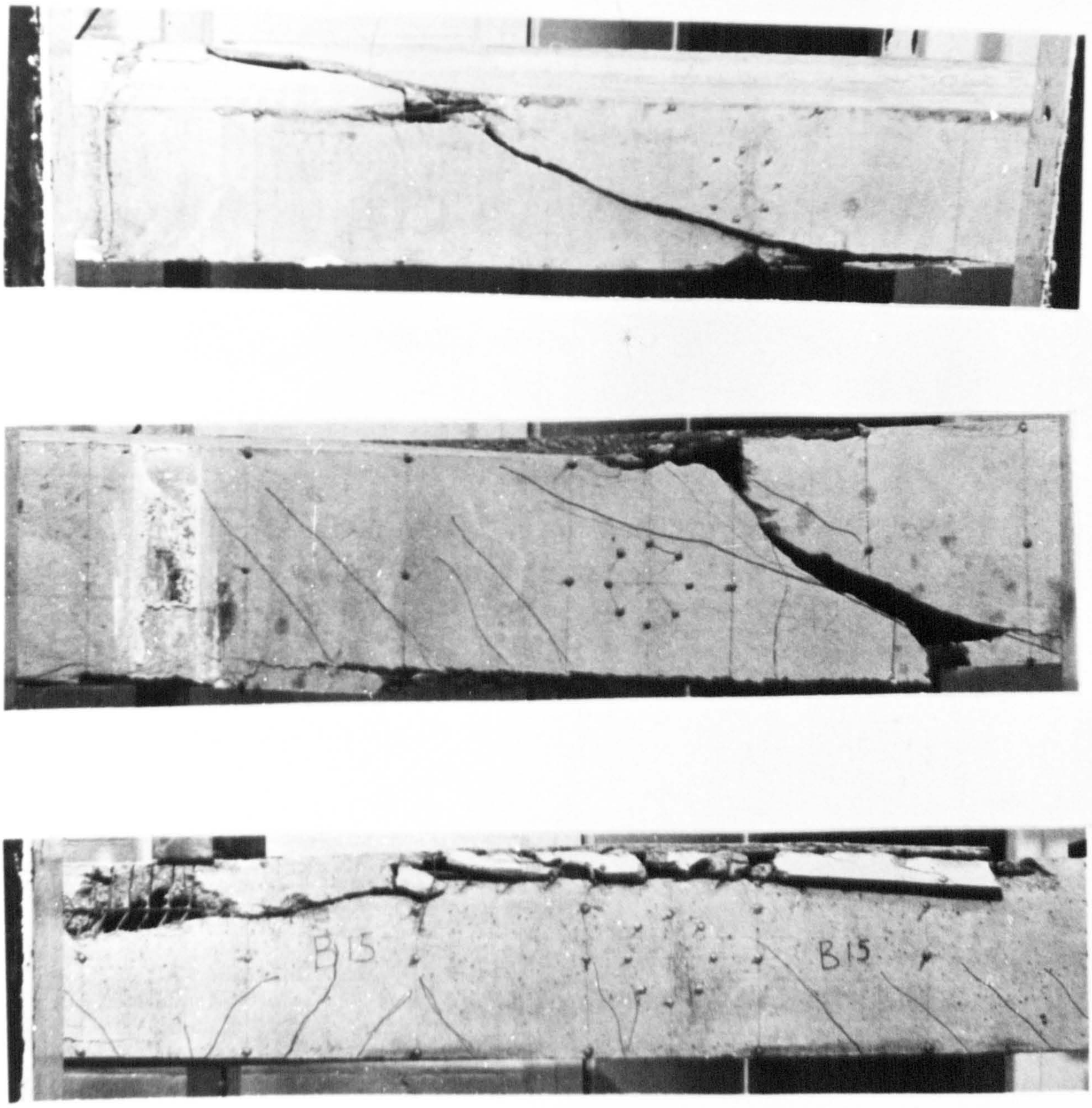

Plate 11 Crack patterns after failure for beam B15

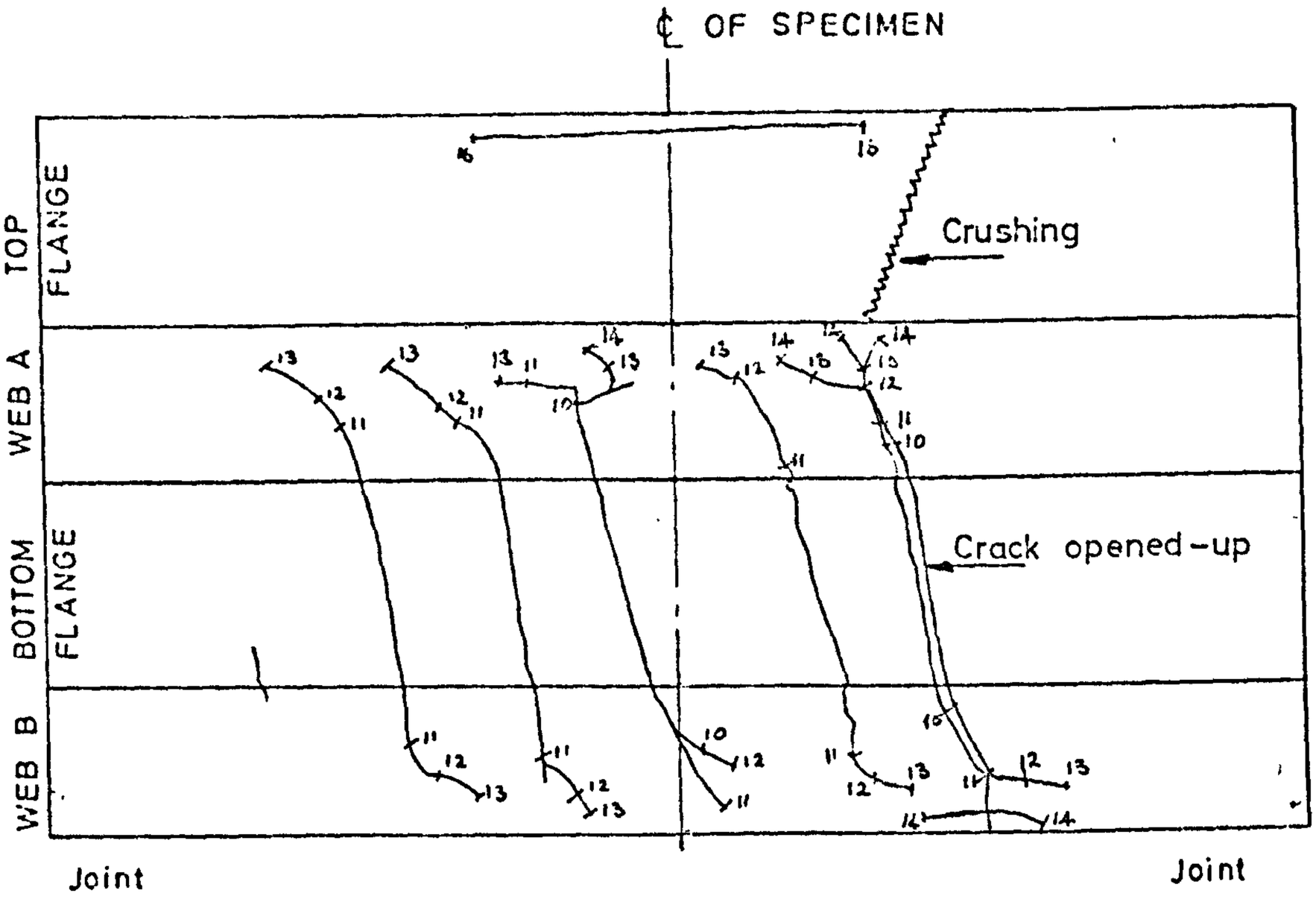

SPECIMEN No B12 $\frac{M}{T} = 8$

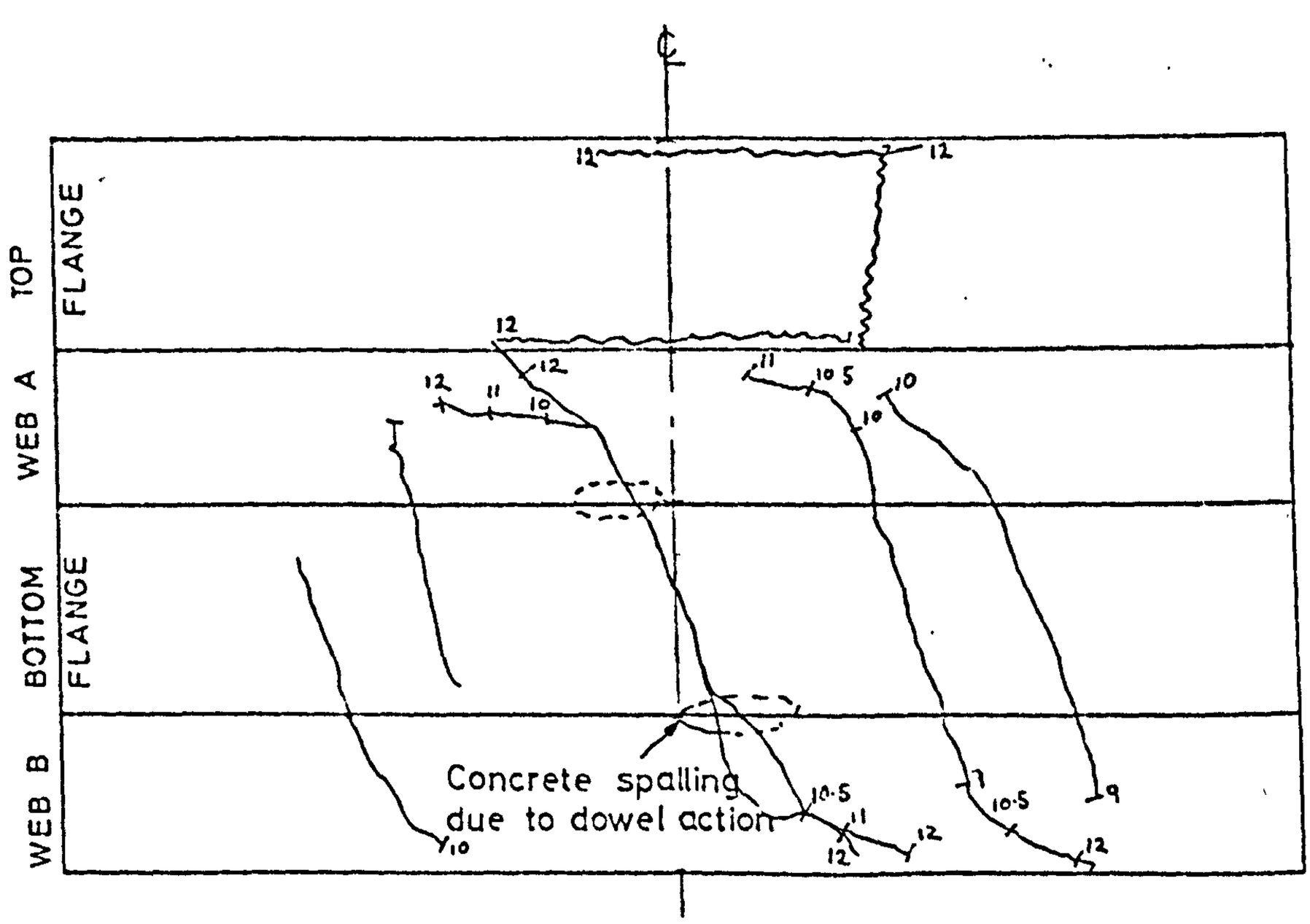

SPECIMEN No. B 13 $\frac{M}{T} = 4$

FIG.6.16. CRACK PATTERNS FOR No B12 AND B13

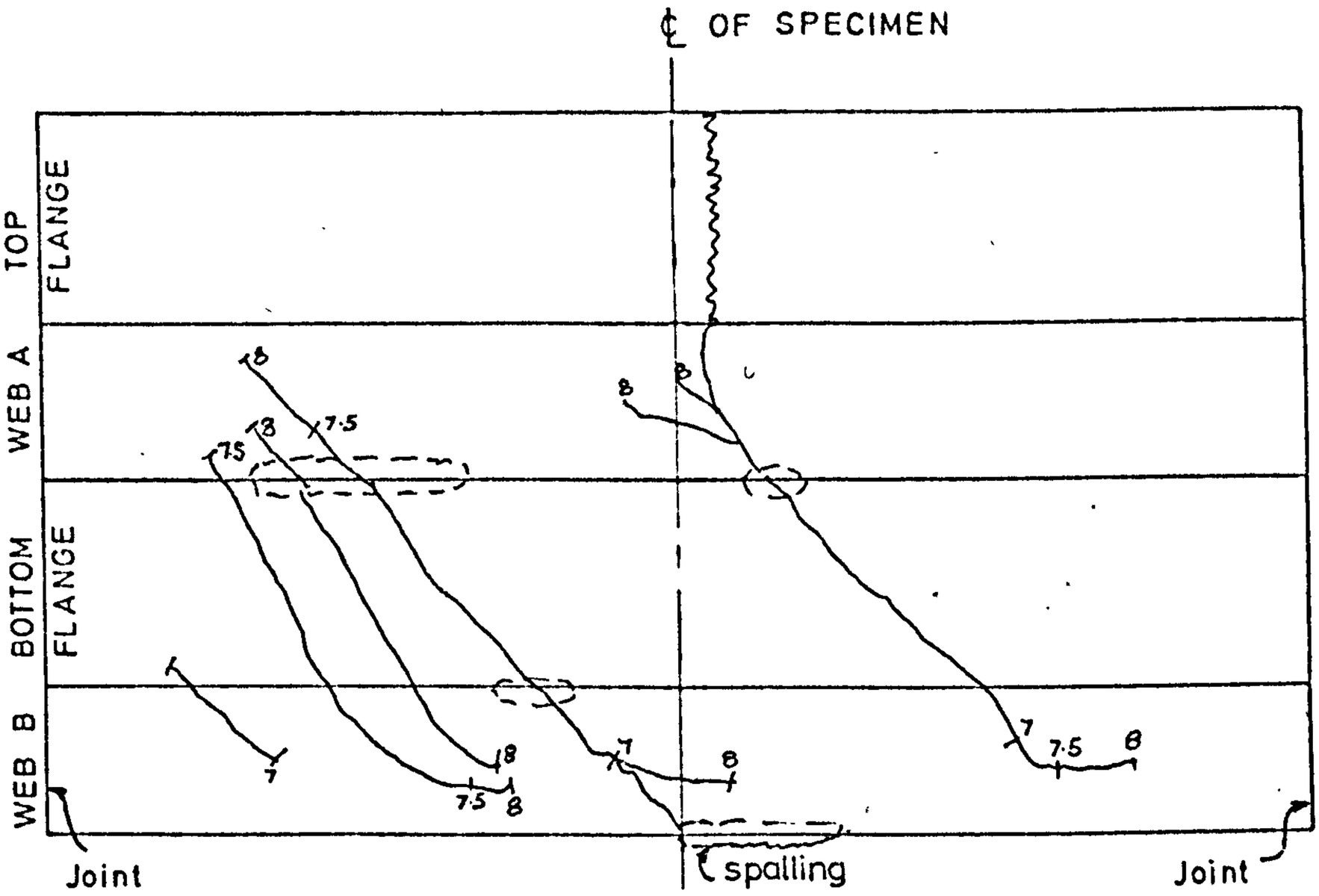

SPECIMEN No B14

$\frac{M}{T} = 2$

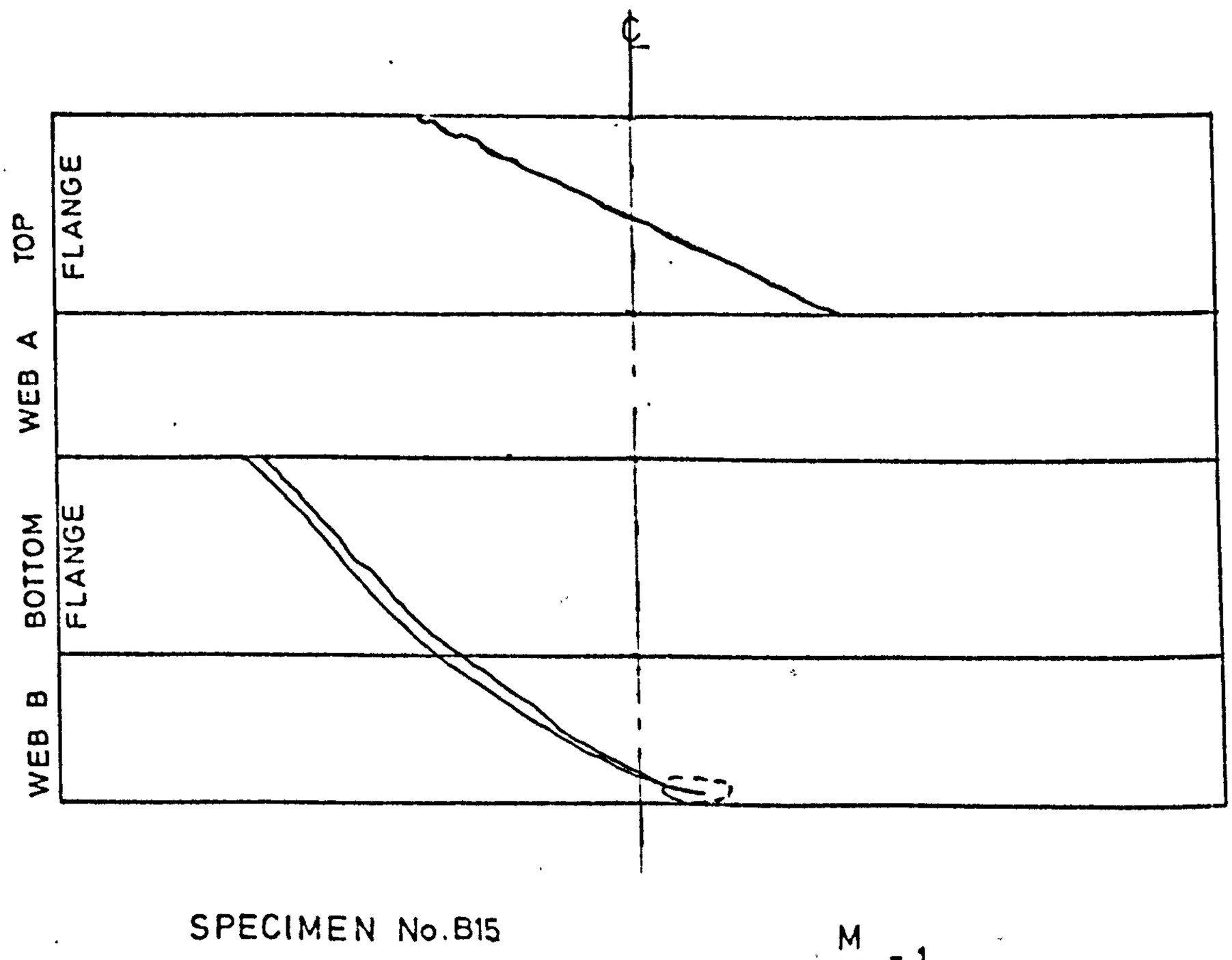

SPECIMEN No.B15

$\frac{M}{T} = 1$

FIG.617 CRACK PATTERNS FOR No B14 AND B15

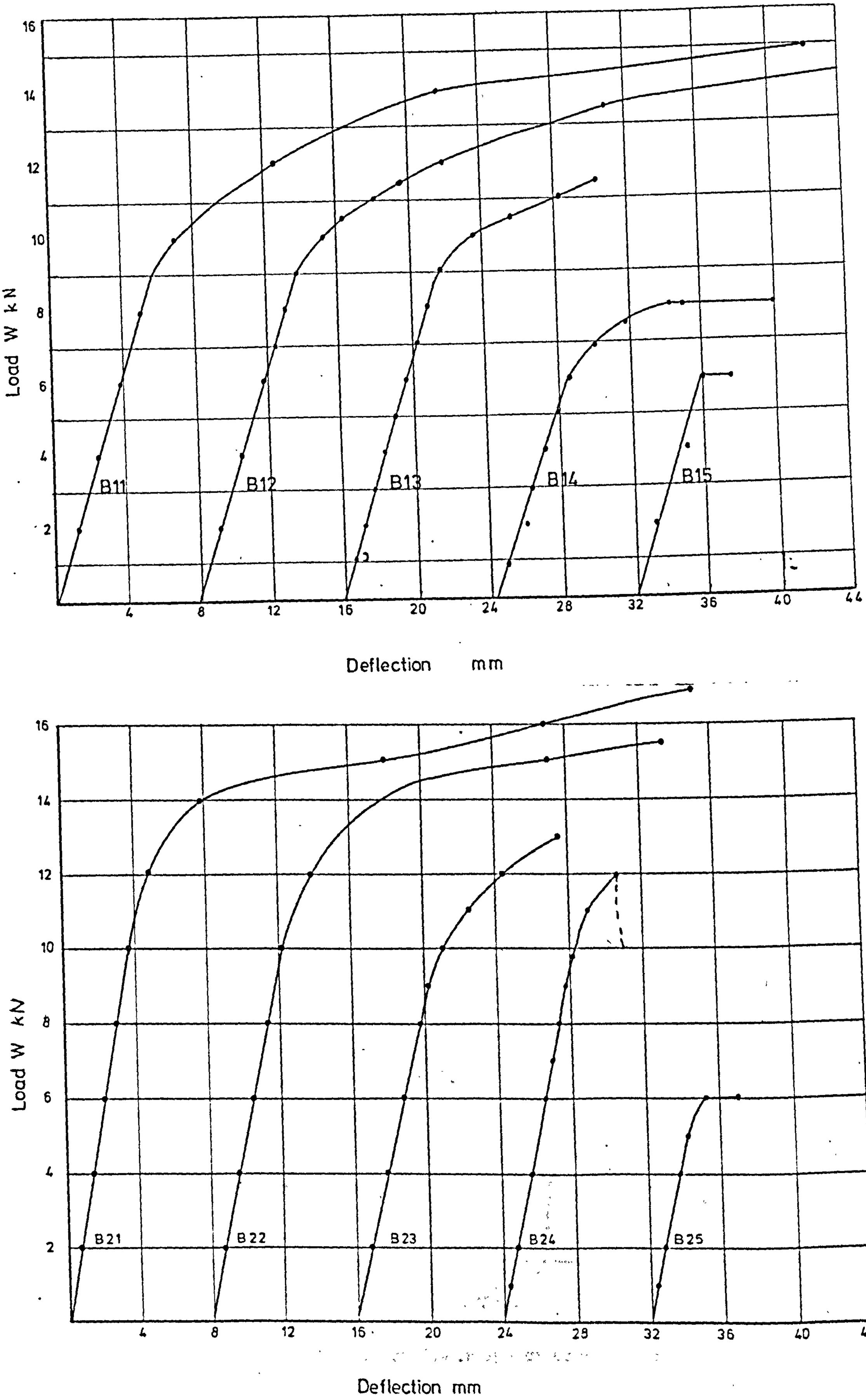

FIG. 6.18. Load Versus Central Deflection

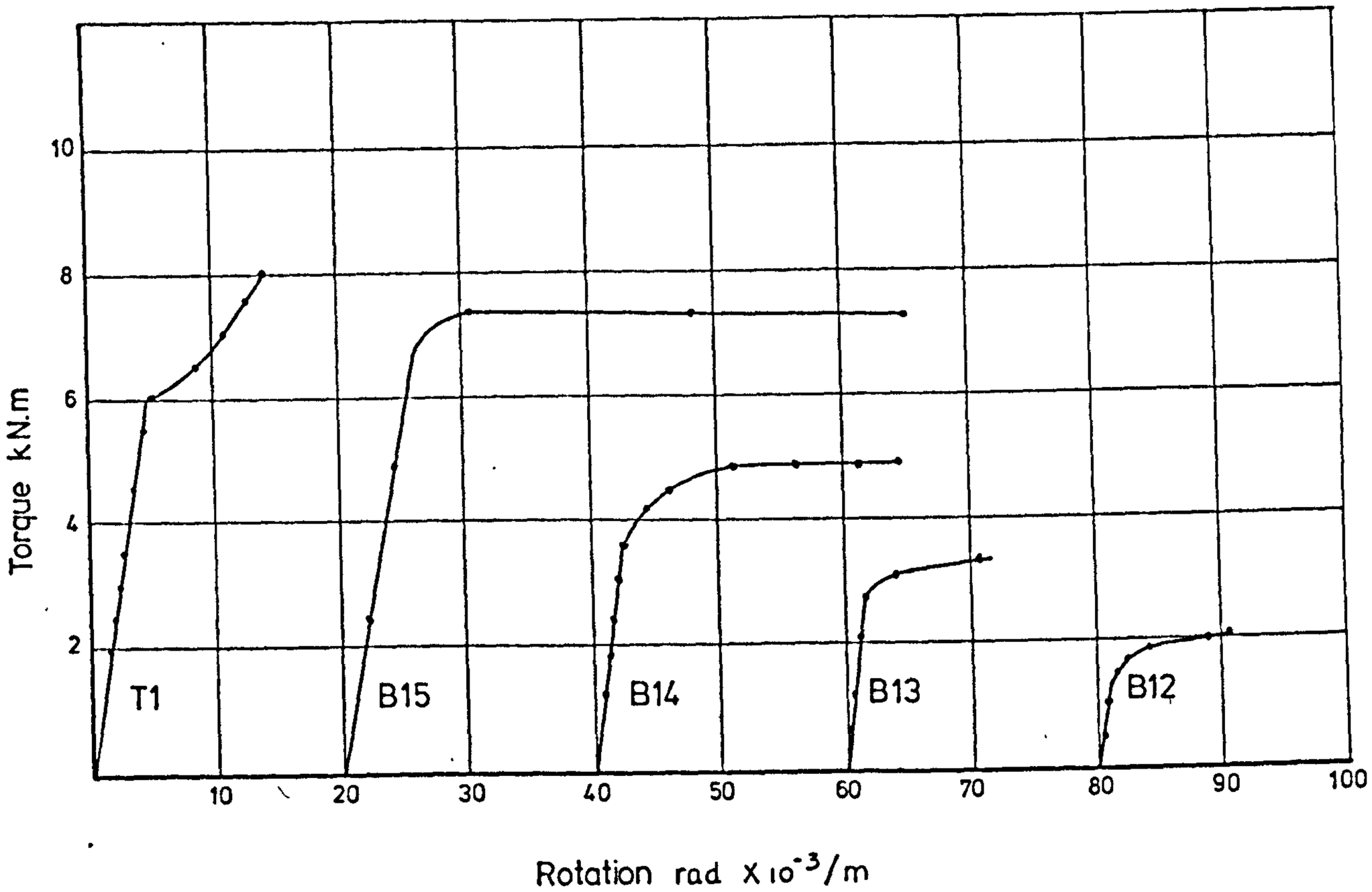

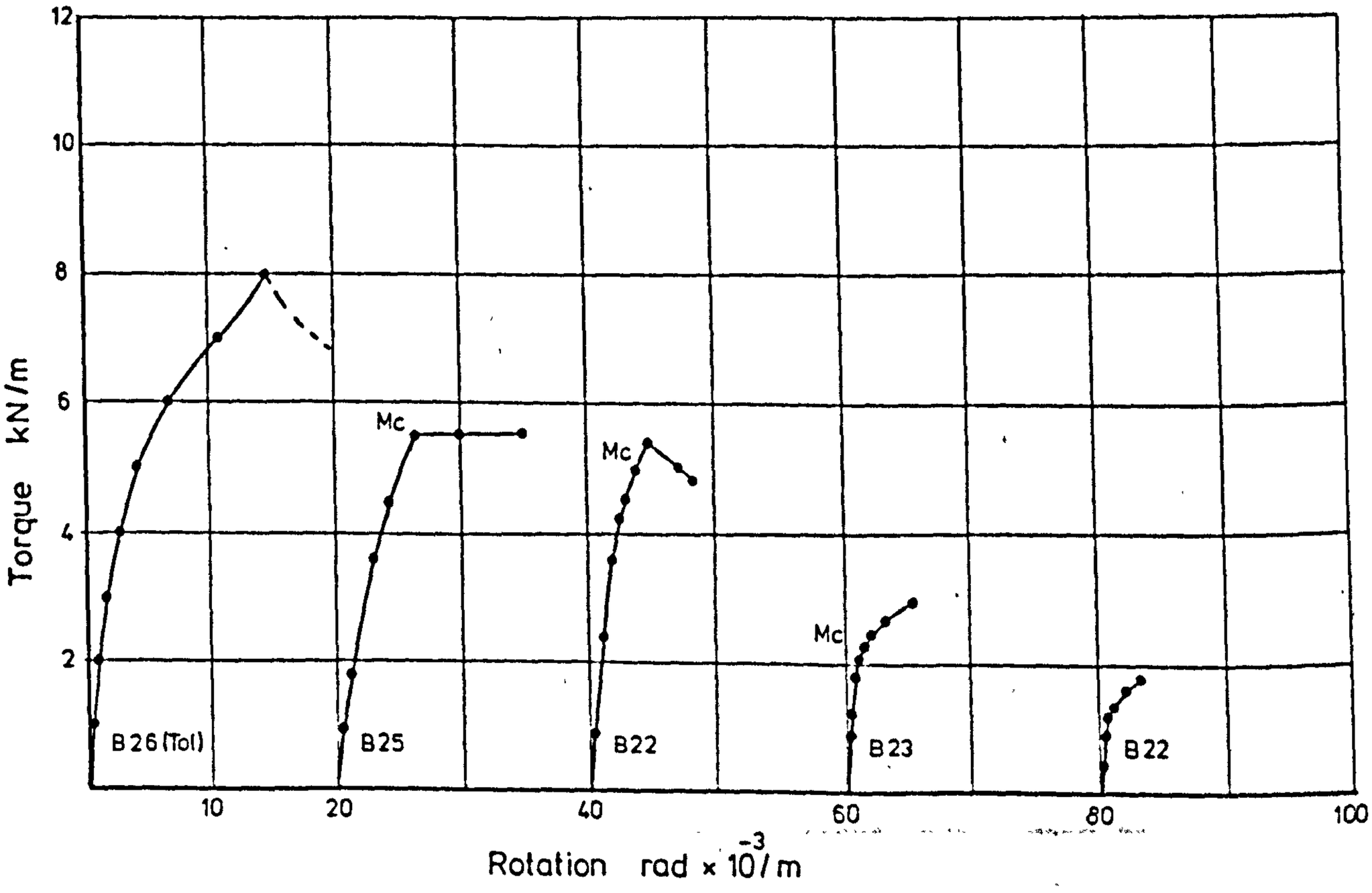

FIG.619 Torque-Rotation Curves For Specimens of series 1 and 2

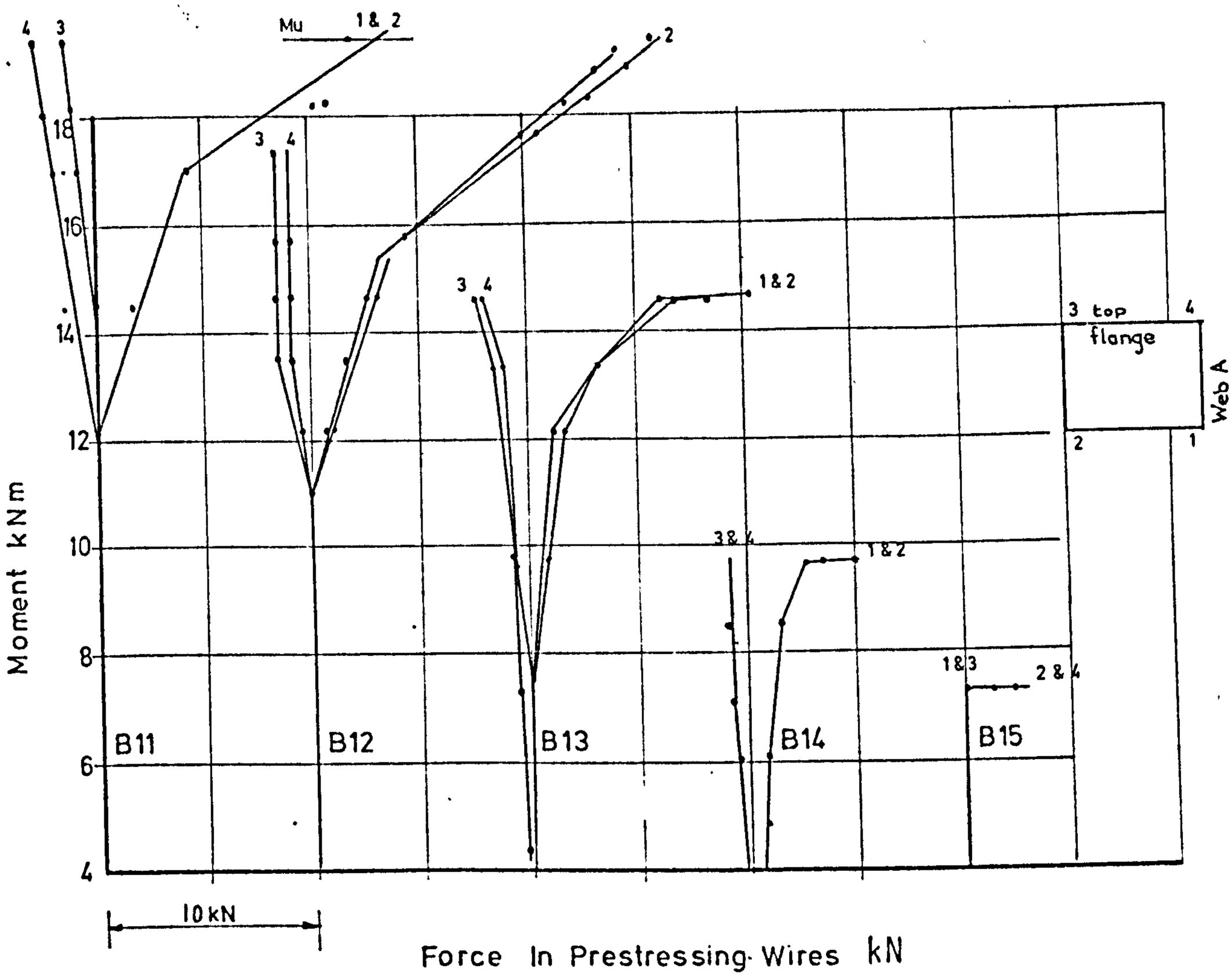

FOR INITIAL PRESTRESSING FORCE
SEE. TABLE 6.2.

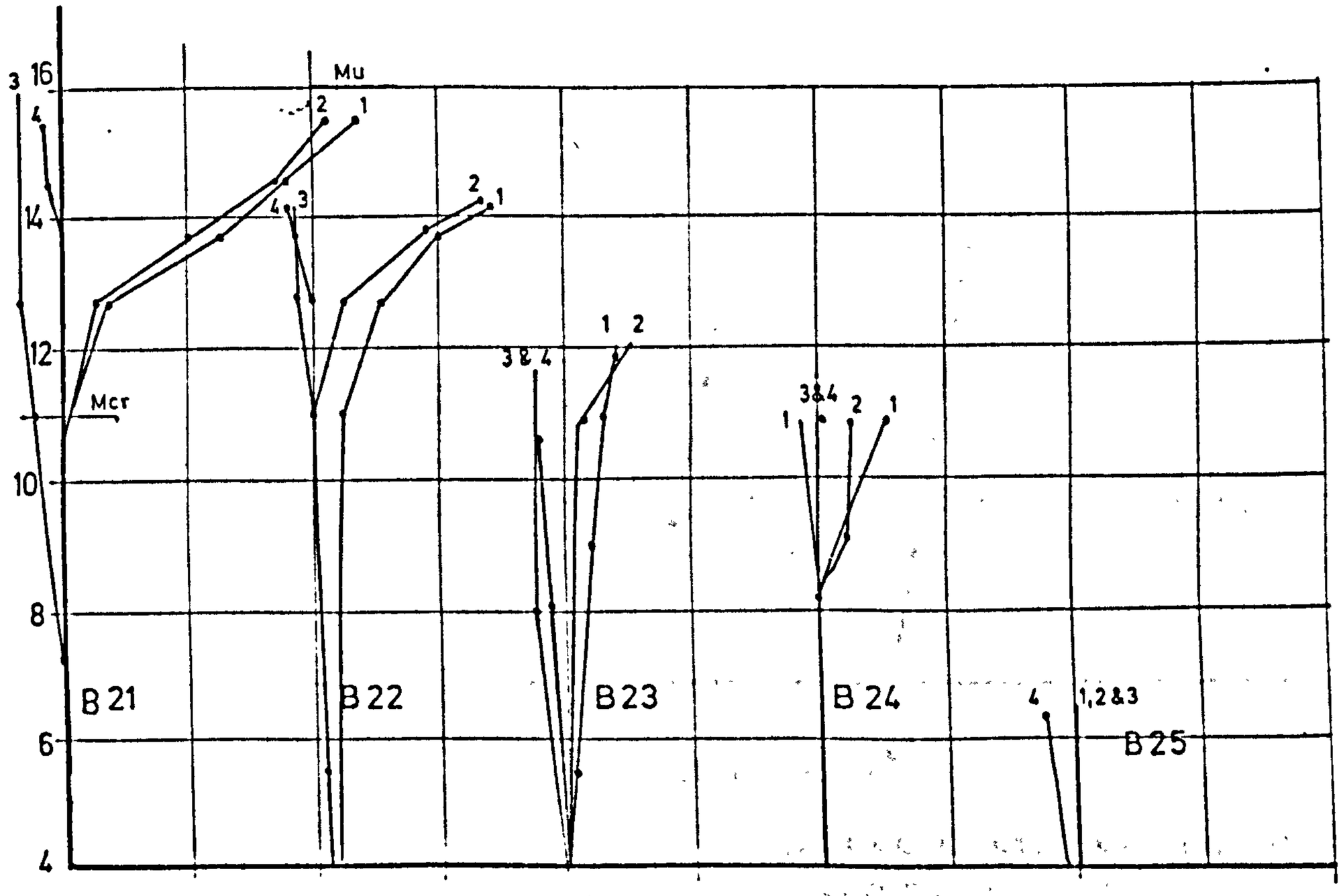

FIG. 6.20 MOMENT-VERSUS CHANGE IN PRESTRESSING FORCE IN WIRES

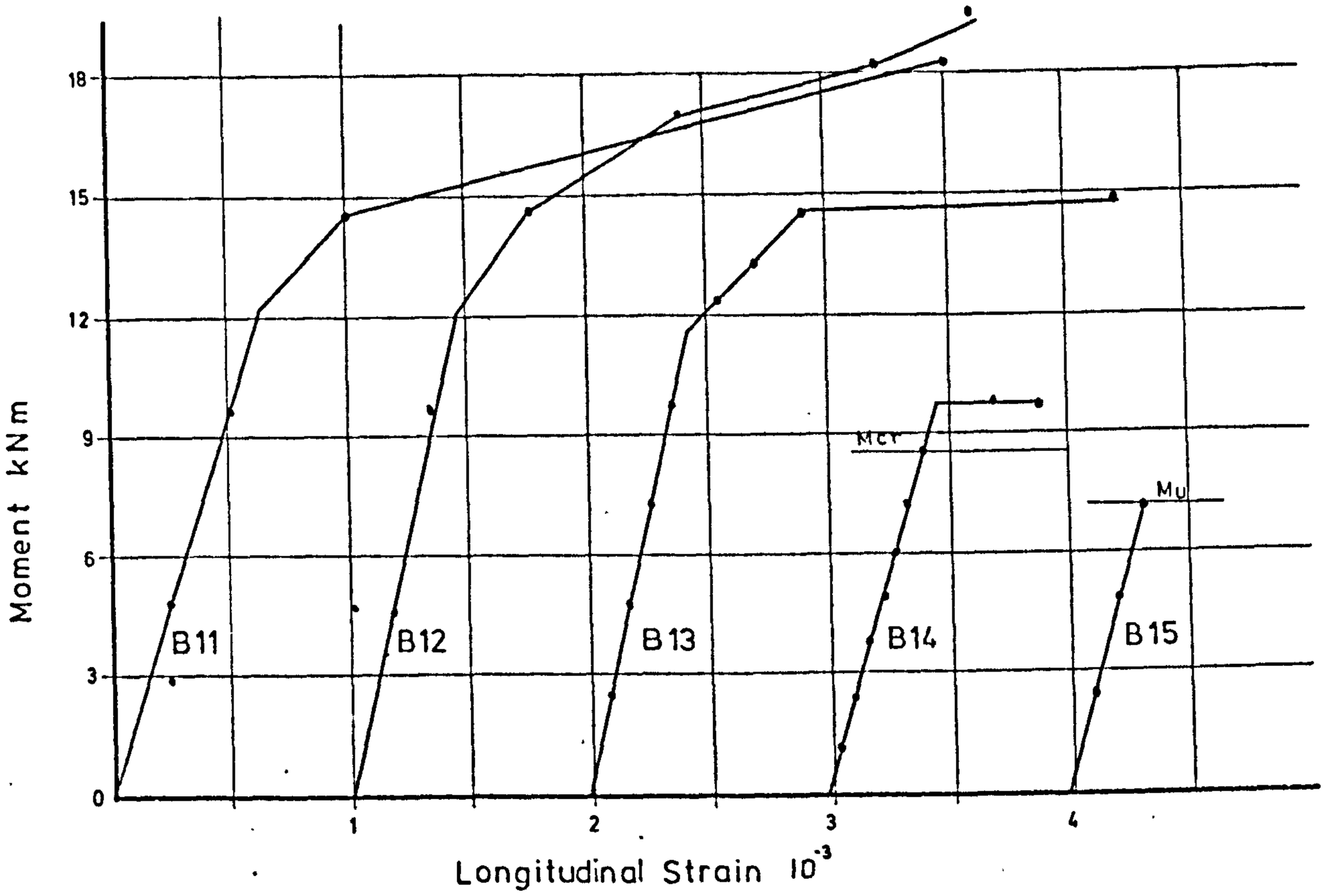

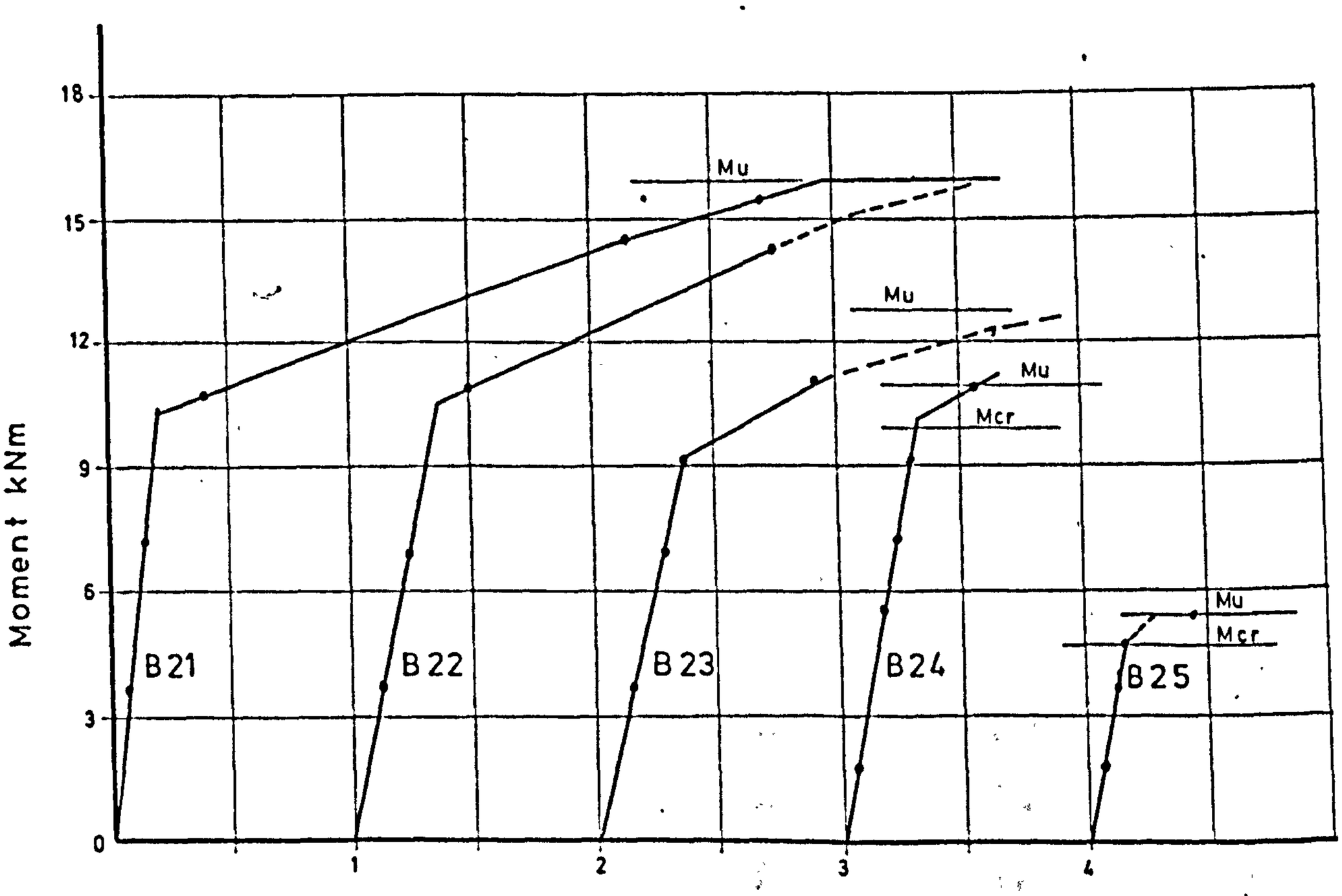

FIG6.21. MOMENT - LONGITUDINAL COMPRESSIVE STRAINS FOR THE TOP FLANGE OF THE SPECIMENS OF SERIES 1 and 2

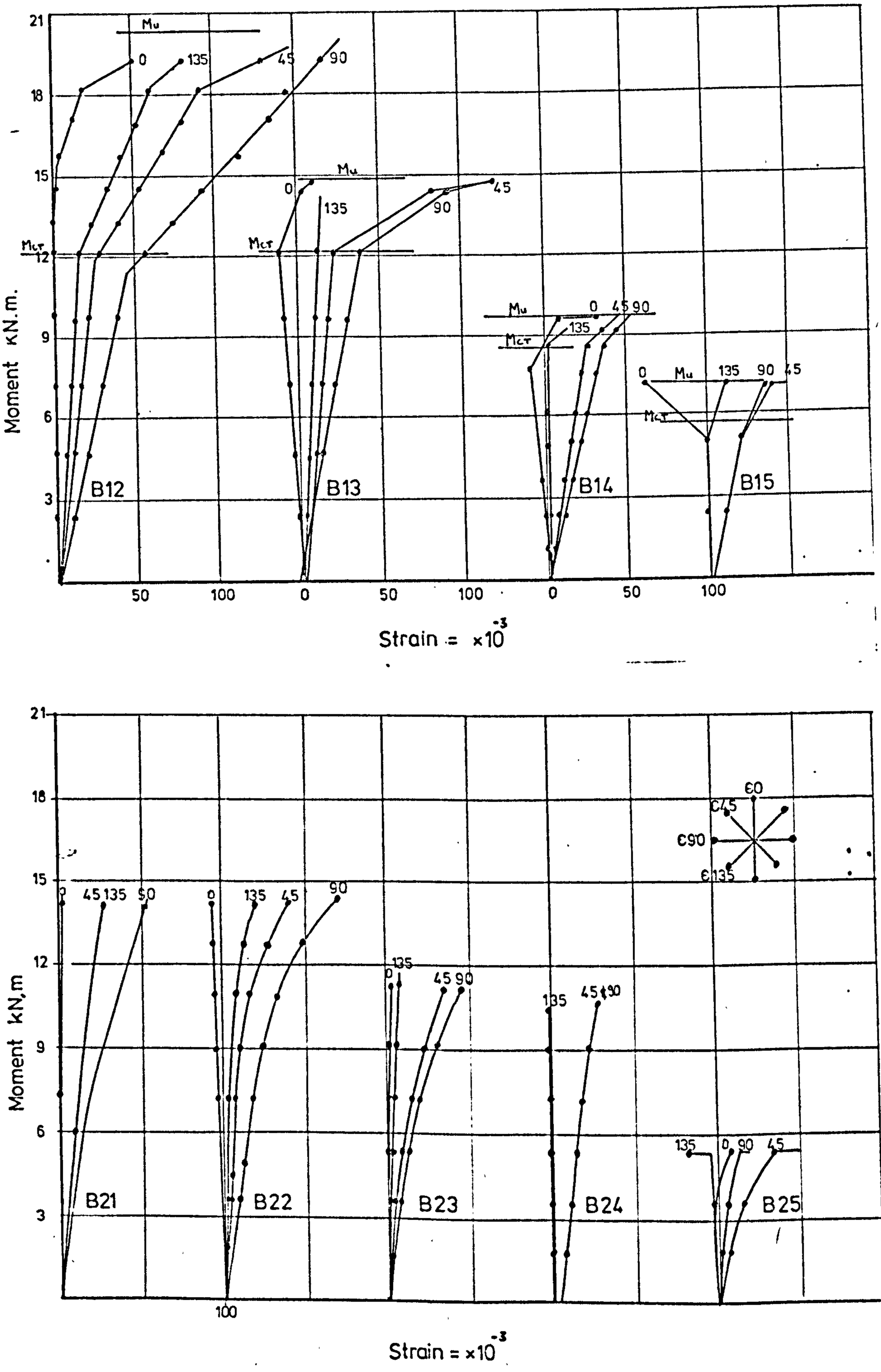

FIG 6.22 Moment - Strain Rosette On Top Flange For Specimens of Series 1 & 2

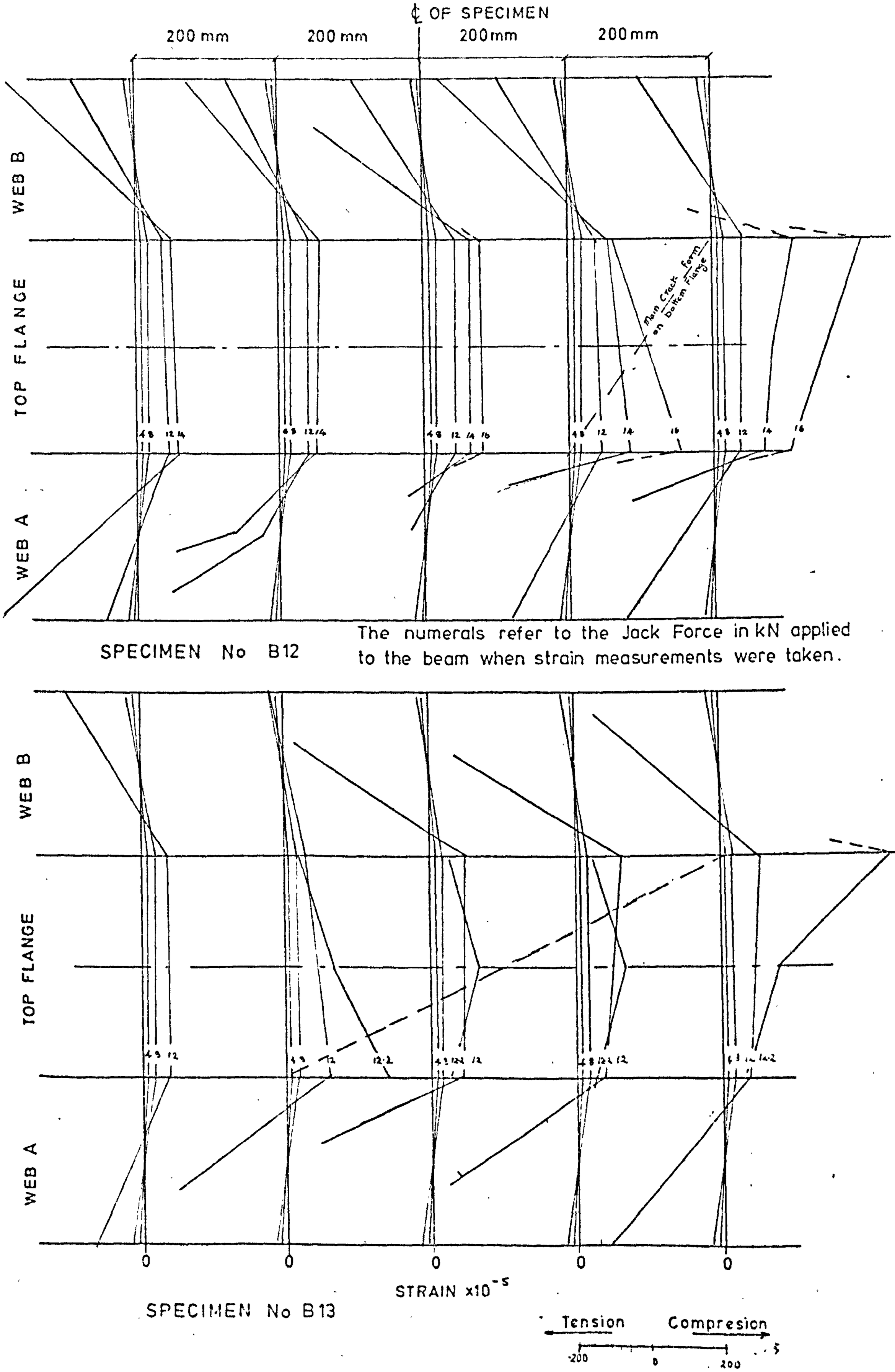

FIG 6.23 LONGITUDINAL STRAINS FOR SPECIMEN No B12 AND B13

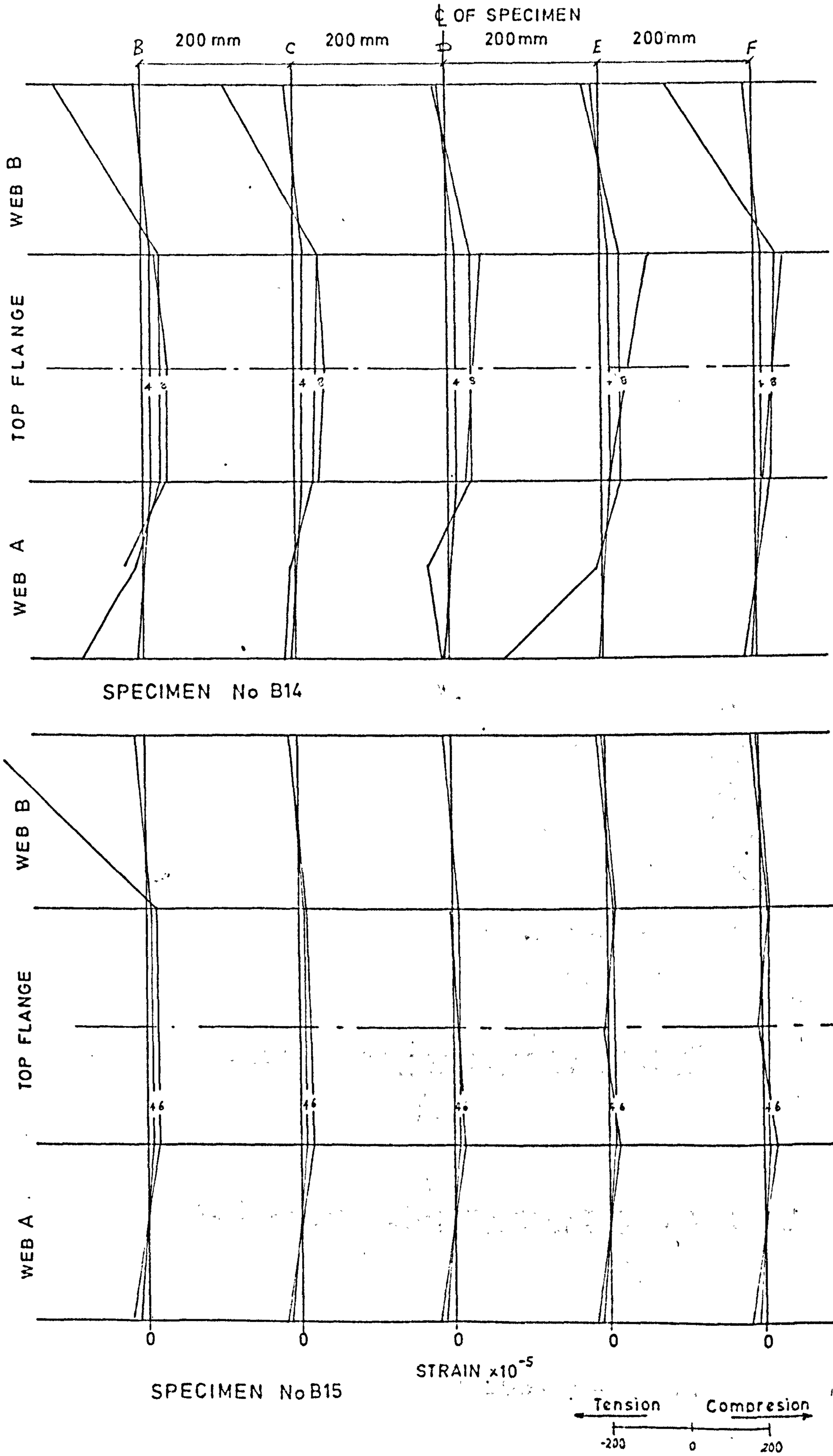

FIG.6 24 LONGITUDINAL STRAINS FOR SPECIMEN No B14 AND B15

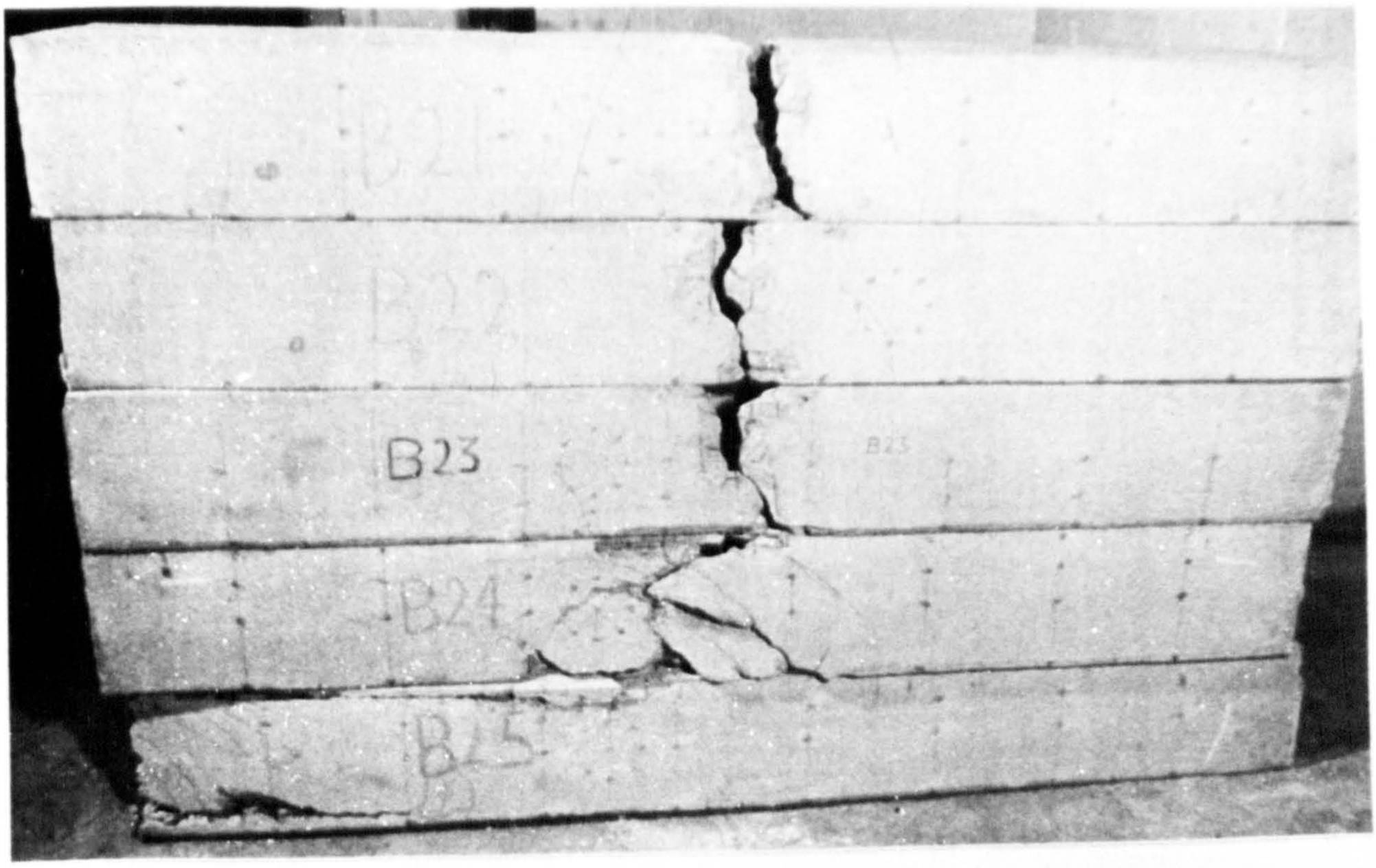

Webs A

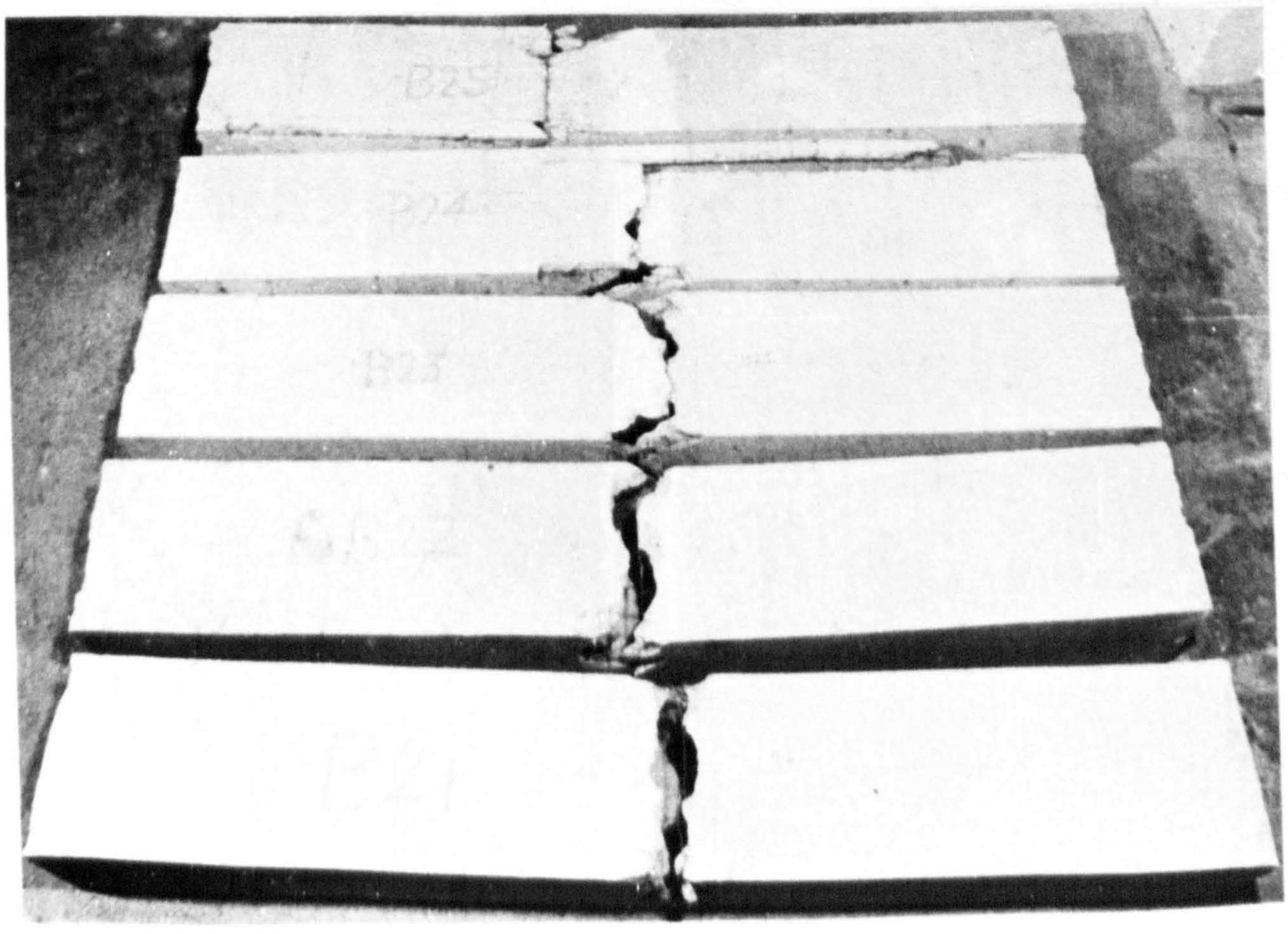

Top Flanges

Plate 12 Crack patterns after failure for beams of series 2

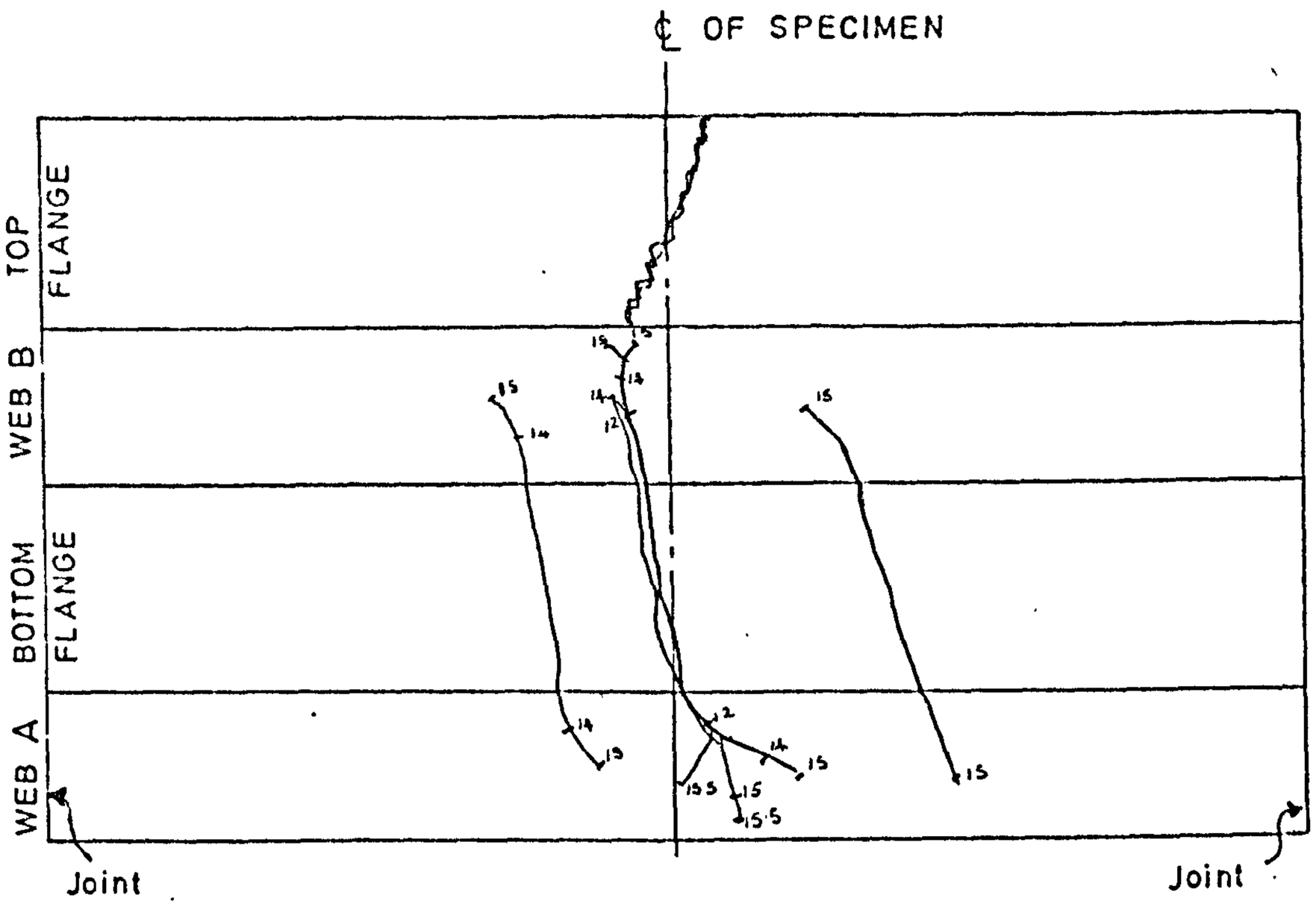

SPECIMEN No B22

$\frac{M}{T} = 8$

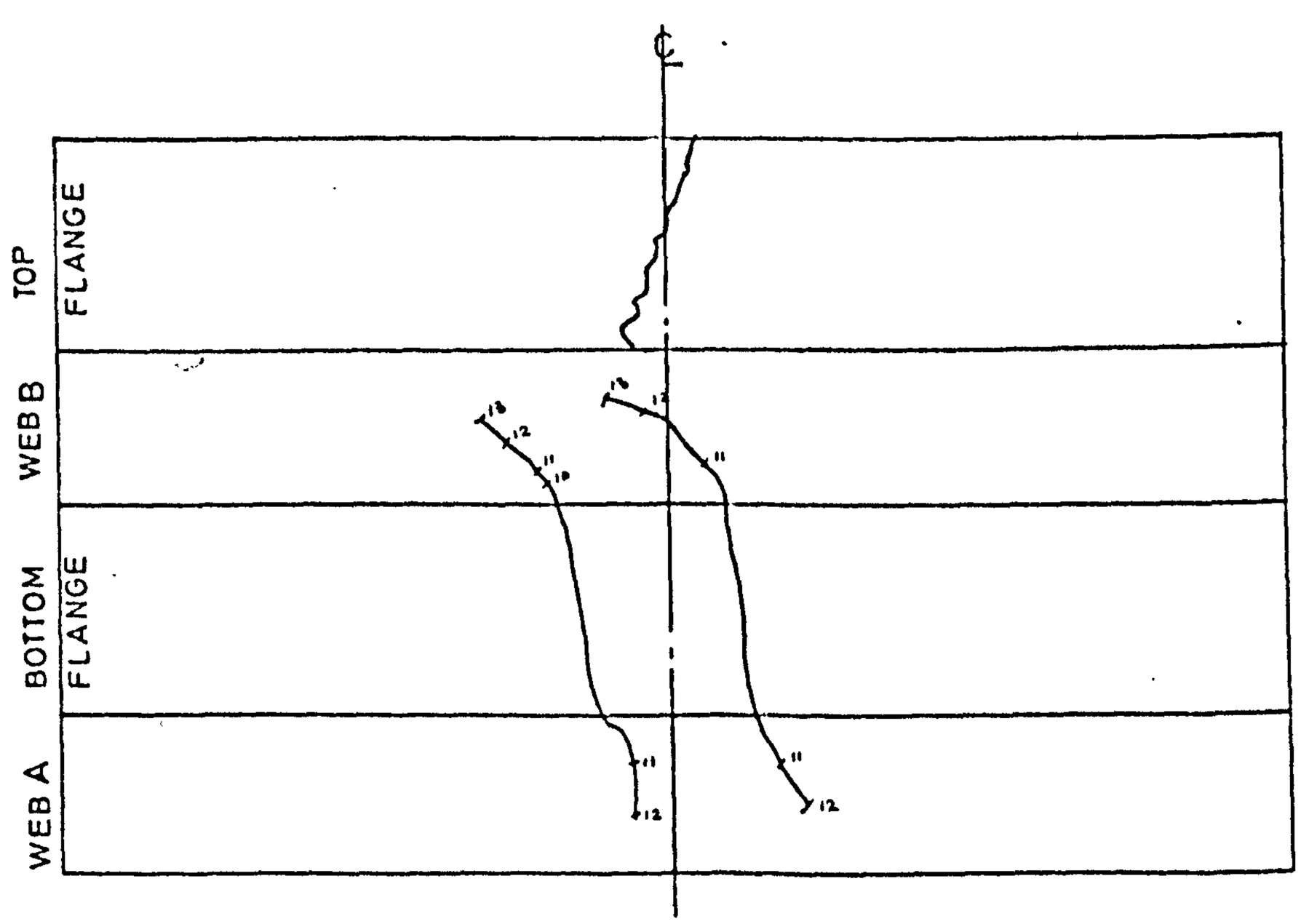

SPECIMEN No. B23

$\frac{M}{T} = 4$

FIG.6.25CRACK PATTERNS FOR No B22AND B23

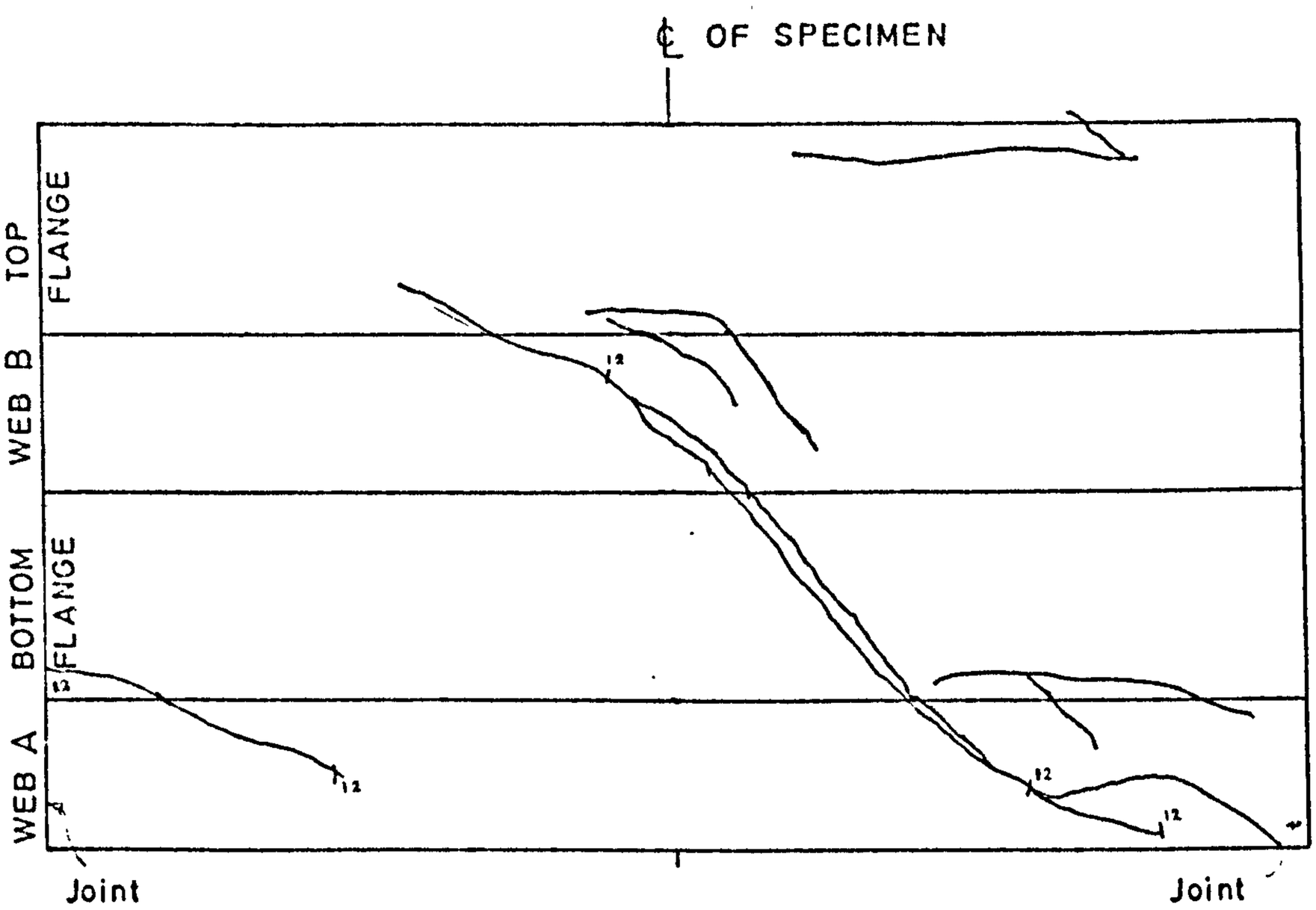

SPECIMEN No B24 $\frac{M}{T} = 2$

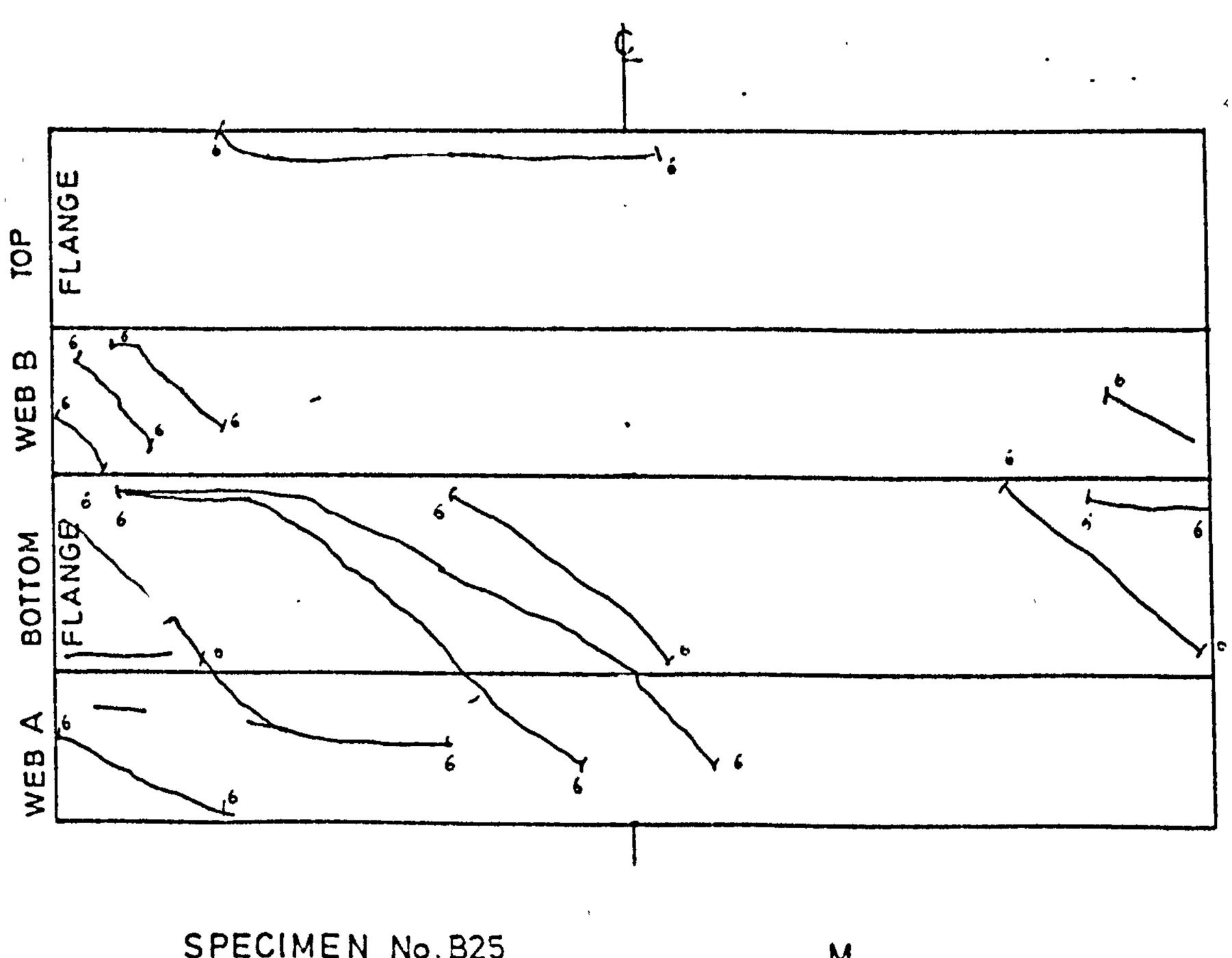

SPECIMEN No. B25 $\frac{M}{T} = 1$

FIG. 626 CRACK PATTERNS FOR No B24 AND B25

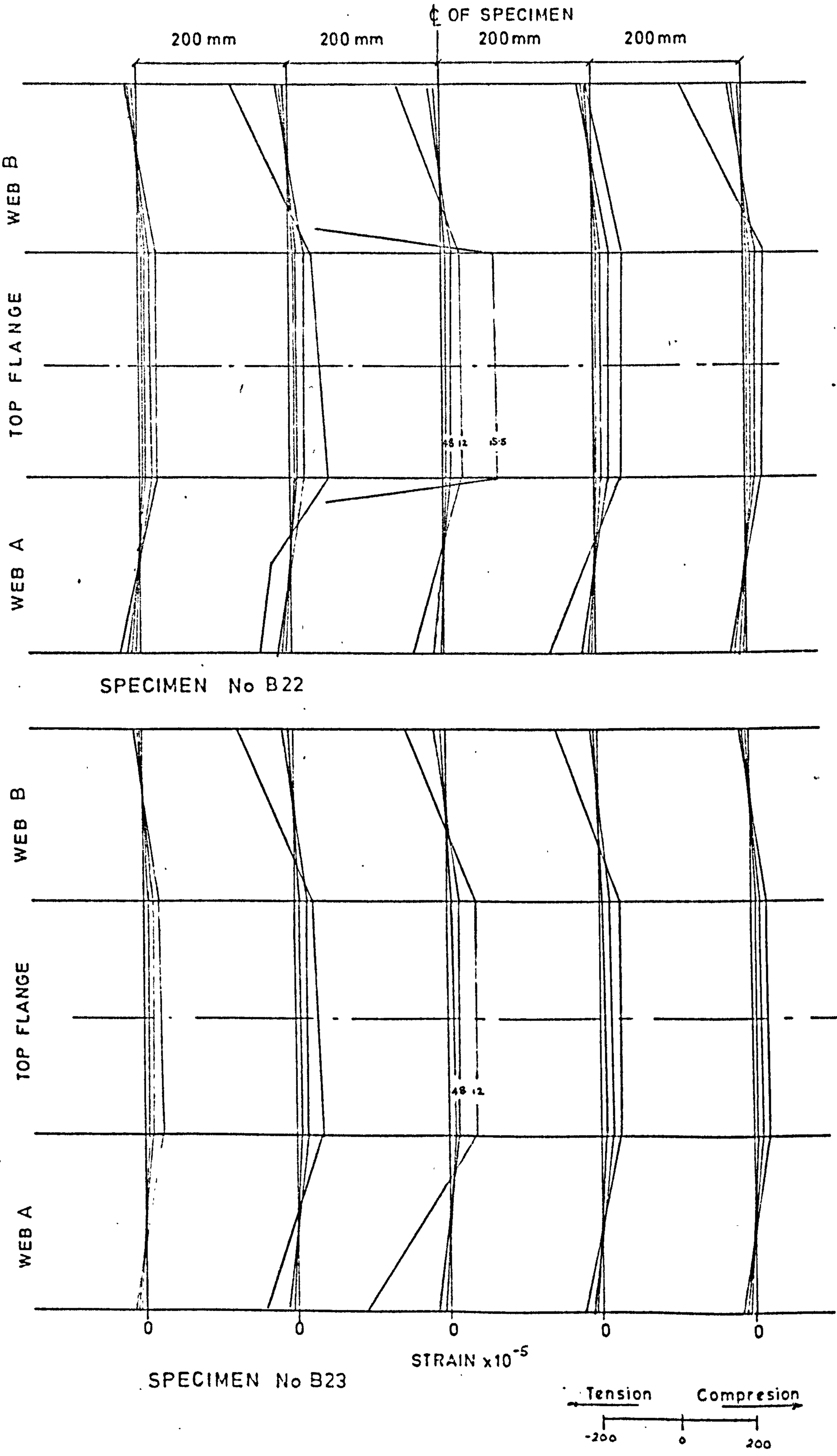

FIG.6.27 LONGITUDINAL STRAINS FOR SPECIMEN NoB22 AND B23

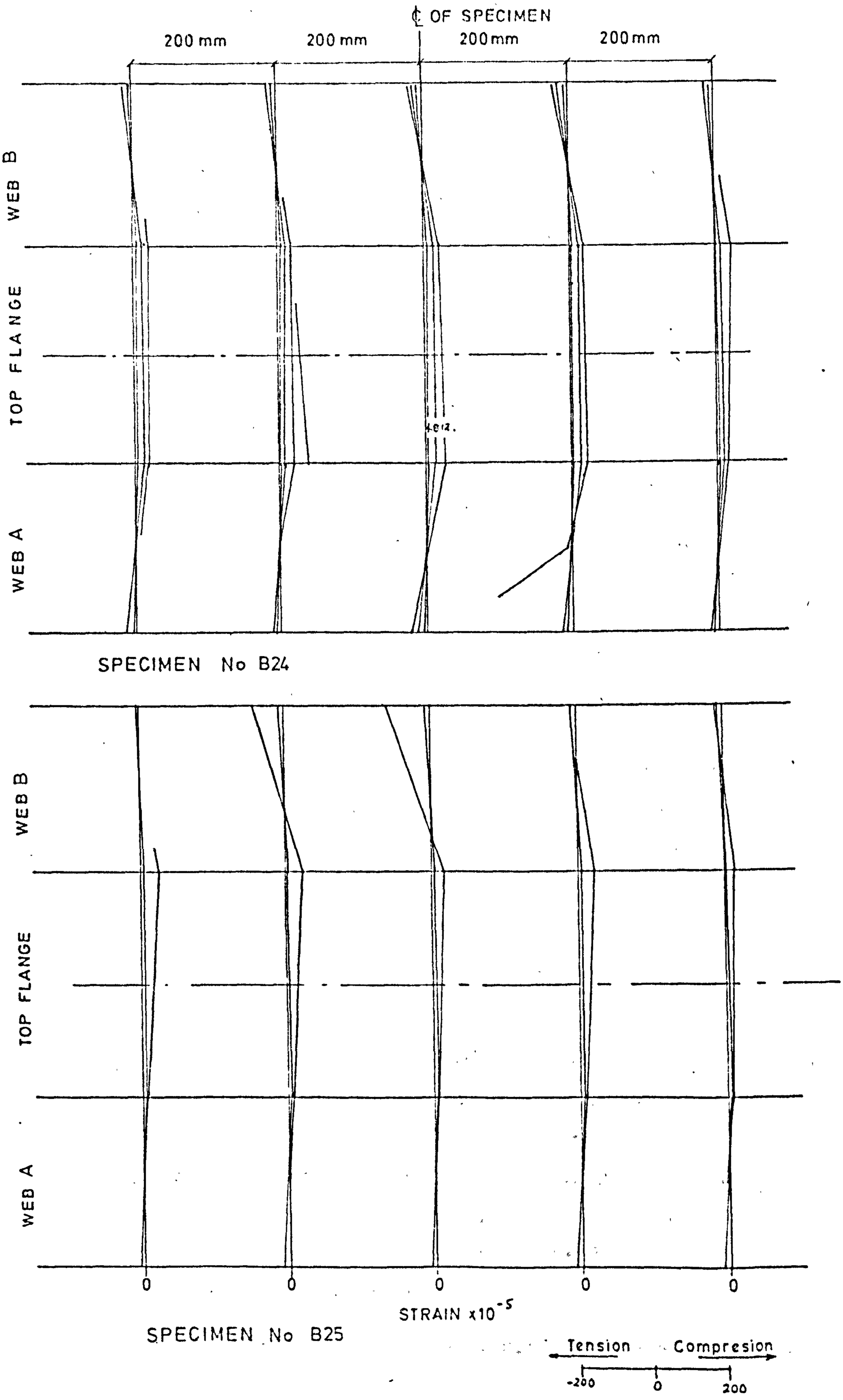

FIG 6.28 LONGITUDINAL STRAINS FOR SPECIMEN No B24 AND B25

6.6.5 Tests to Failure - Beams Subjected to Bending and Torsion Series 3

a) General Observations, Cracking and Failure

The addition of web reinforcement in the form of a cage, in the beams of this series resulted in an increase in the load carrying capacity for the beams subjected to high torsional moment, it also reduced the crack widths but resulted in more cracks which were evenly distributed along the length of the beam as shown in Fig. 6.29 to 6.31 and plates 13 to 15. Beams B32 to B34 failed by crushing of the concrete in the top flange. Simultaneously, both sides of the top flange at this failure zone suffered transverse displacements relative to each other indicating that failure was due to the combined action of compression and shear. Beam B35, on the other hand, reached its maximum load carrying capacity when one of the corners of the box spalled as shown in plate 15, resulting in a drop in the applied forces of 20 to 30% and finally the beam failed without reaching this maximum load by the cleavage failure of the compression flange.

Failure always occurred suddenly and explosively and sometimes took place while reading of dial and demec gauges was in progress. For beam B32 and B33 failure occurred under one of the loads and no significant spalling due to the dowel action of the bottom reinforcement took place.

In this series cracking occurred initially

in the bottom flange propagating immediately to the side webs and the axis of rotation appeared to shift towards the top compression flange.

b) Deflections and Rotations

The torque/rotation curves and the load/deflection curves are given in Fig. 6.32 and 6.33 respectively. From these results it can be seen that the presence of lateral reinforcement has no significant effect on the pre-crack stage and the beams exhibited similar characteristics to those in series 1. The addition of lateral reinforcement however, appeared to significantly improve the torsional stiffness of the beams in the post-cracking stage. In addition this reinforcement considerably improved the ductility of the beams.

c) Strains in Reinforcement and Forces in Prestressing Wire

E.R.S. gauges were fixed to beam B32 and B33, the results of the strains readings obtained are plotted against torque in Fig. 6.34. These results demonstrate again that the reinforcement does not contribute to the torsional strength prior to cracking but starts to play a major role in resisting torque after cracking. The maximum strains recorded, were in general below the yield strains. This must be attributed in part to the fact that the electrical strain gauges did not always cross a cracked section and that the major crack did not cross the steel

at the position of the gauges.

No strain measurements were recorded for beams B34 and B35 since it was assumed that the trend in the strain could be deduced from The results of strain readings taken on beam B33 and T_3.

The relationship between the applied load and the forces in the prestressing wires are shown in Fig. 6.35. These results indicate that the forces in the bottom wires of beams B31 to B34 almost reached their ultimate characteristic strength as the beams reached their ultimate carrying capacity. In contrast, the forces in the bottom wires for beam B35 did not increase appreciably at failure of the beam.

d) Deformation of Concrete

The results of the strain rosette readings taken by Demec gauge for the beams of this series are shown in Fig. 36 to Fig. 38. The strain readings taken from the Rosette on the top flange showed that all the strains are in compression except for beam 35, for which diagonal tensile strains were recorded.

The results of the longitudinal compressive strains measured on the top flange and shown in Fig. 6.38 indicate that the maximum compressive strains occuring at failure decreased with increase in the applied torque.

The results of the strain distribution for various loadings and sections shown in Fig. 6.38 and 6.39 indicate that the presence of reinforcement in the form of cages

influenced these distributions and they approximate very closely to the assumptions of plane sections before bending remaining plane after bending.

6.6.6 Test to Failure Beams Subjected to Bending, Torsion and Shear Series 4

The experimental results obtained from this series were similar in many respects to those obtained from series 3.

Cracks were initiated at the bottom flange and propagated first to the web in which the torsional and shear stresses were additive as shown in Fig 6.41 to 6.43.

The mode of failure was crushing of the top flange under the load for beam B42 to B44 as shown in plate 16. Beam 45 however, reached its maximum load carrying capacity when one of its edges spalled as shown in plate 17.

The rotations and deflections are shown in Fig. 6.32 and 6.33.

No strain readings on the reinforcement were taken for this series. The forces in the prestressing wires at various stages of loading are shown in Fig. 6.35.

The top flange strain readings are given in Fig. 6.36 and 6.37. The distribution of longitudinal strains are given in Fig. 6.44 and 6.45.

6.6.7 Additional Test On Beams Subjected to Bending, Torsion and Shear

It was possible to cut four pieces of 1.22m length from some of the specimens of series 3 and 4 and retest them. These tests were similar to beams B41, B42, B43 and B44 in all respects but tested over a span of 3.05m. The results of these tests indicated no reduction in the strength of the beams and in some cases they sustained larger torsional moments at failure. These beams were fully instrumented and readings were taken for all the strains, deflections, rotations etc. Most of these beams were cracked but these cracks closed during prestressing. The results of these beams are not included in this chapter since the concrete strengths were not known at the time of testing.

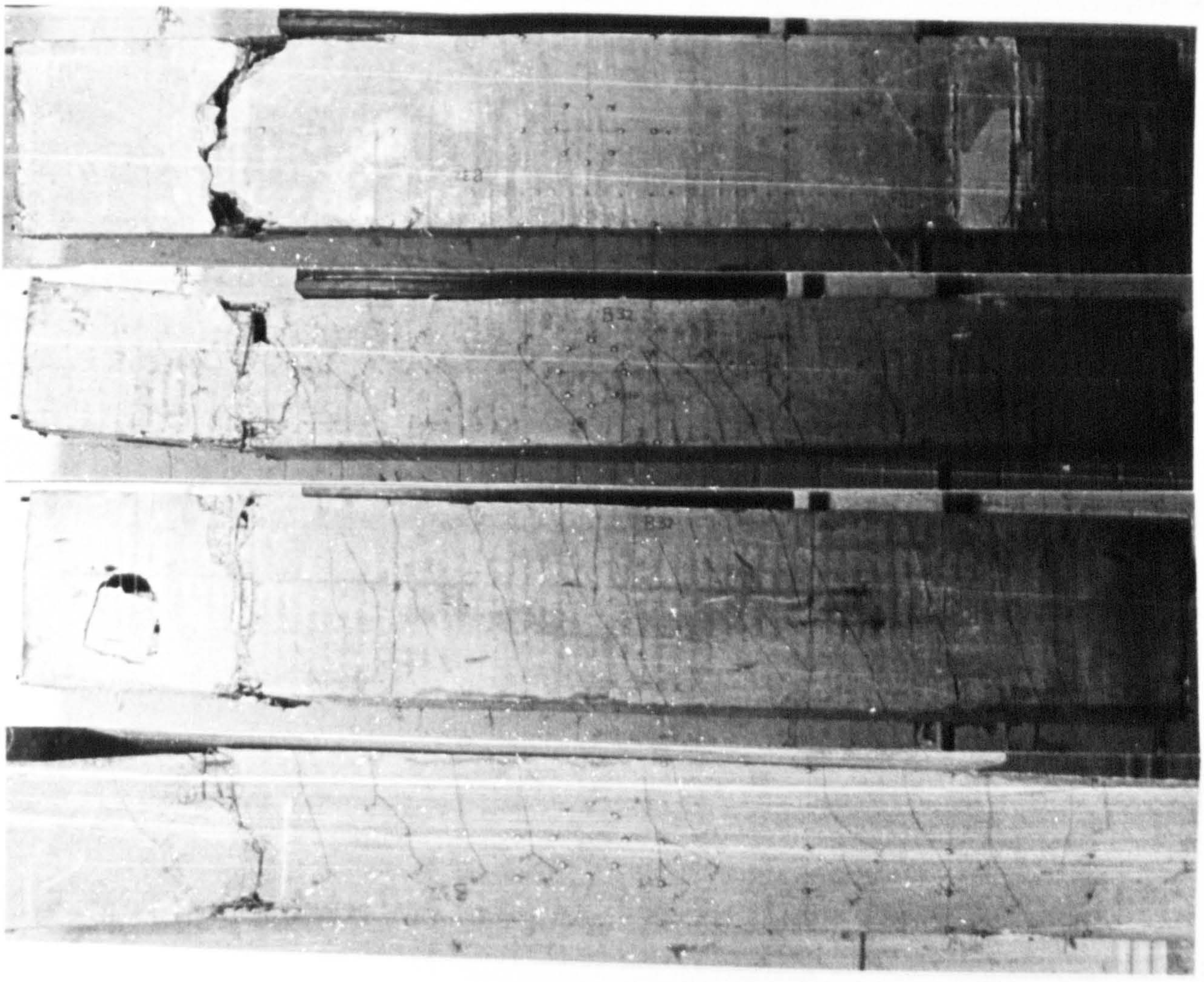

Plate 13 Crack patterns after failure for beam B32

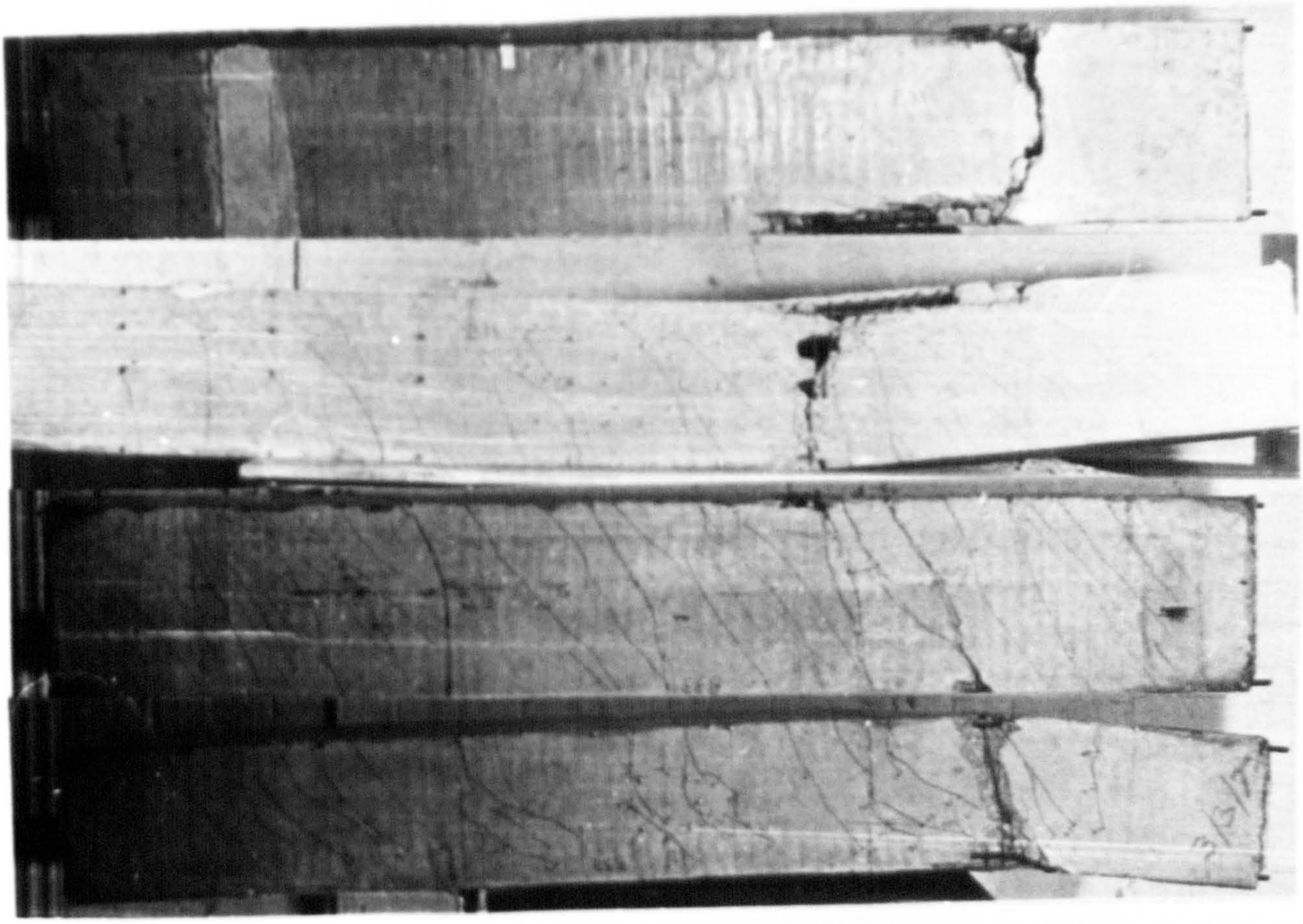

Plate 14 Crack patterns after failure for beam B33

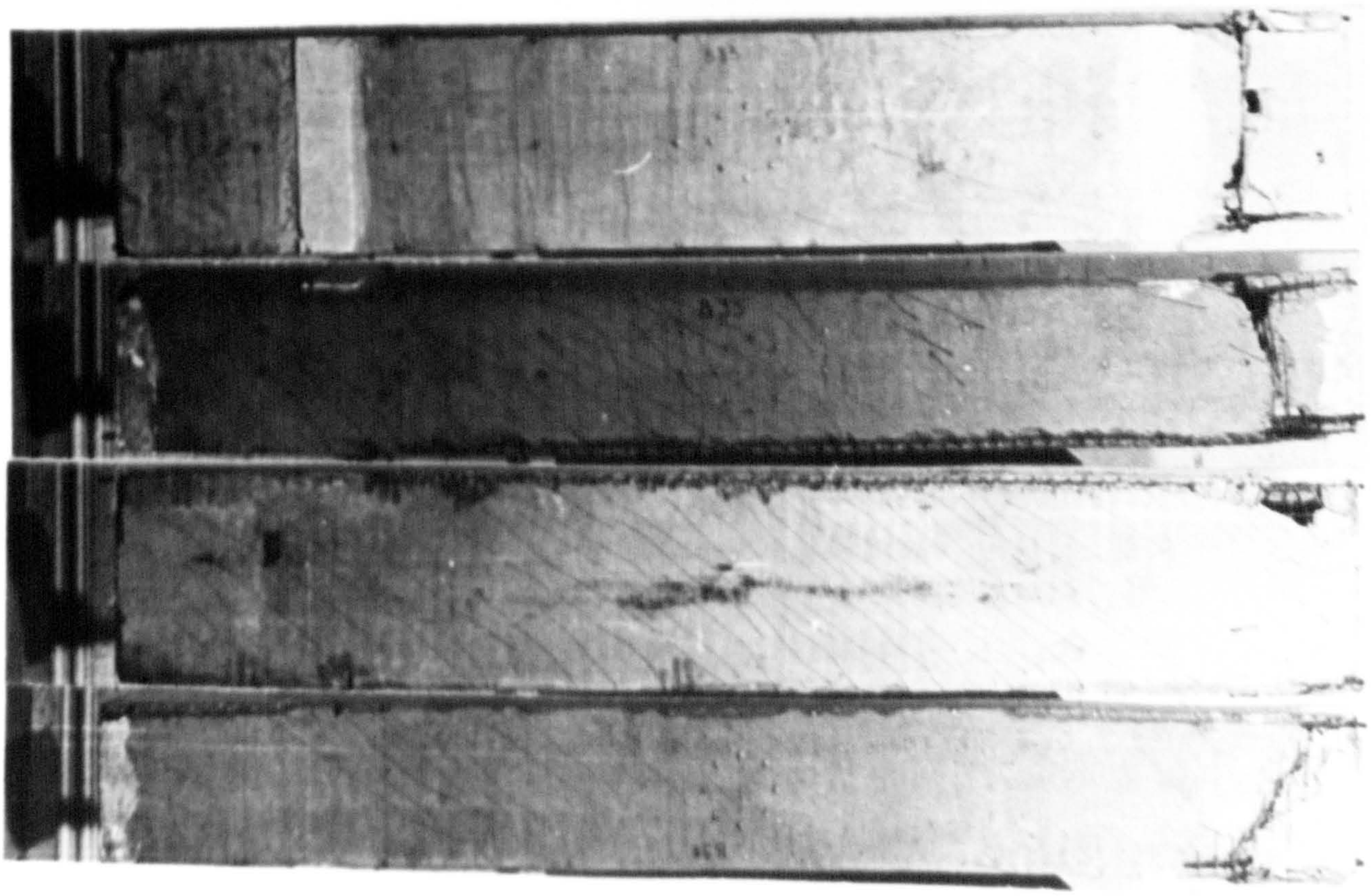

Plate 15 Crack patterns after failure for beam B35

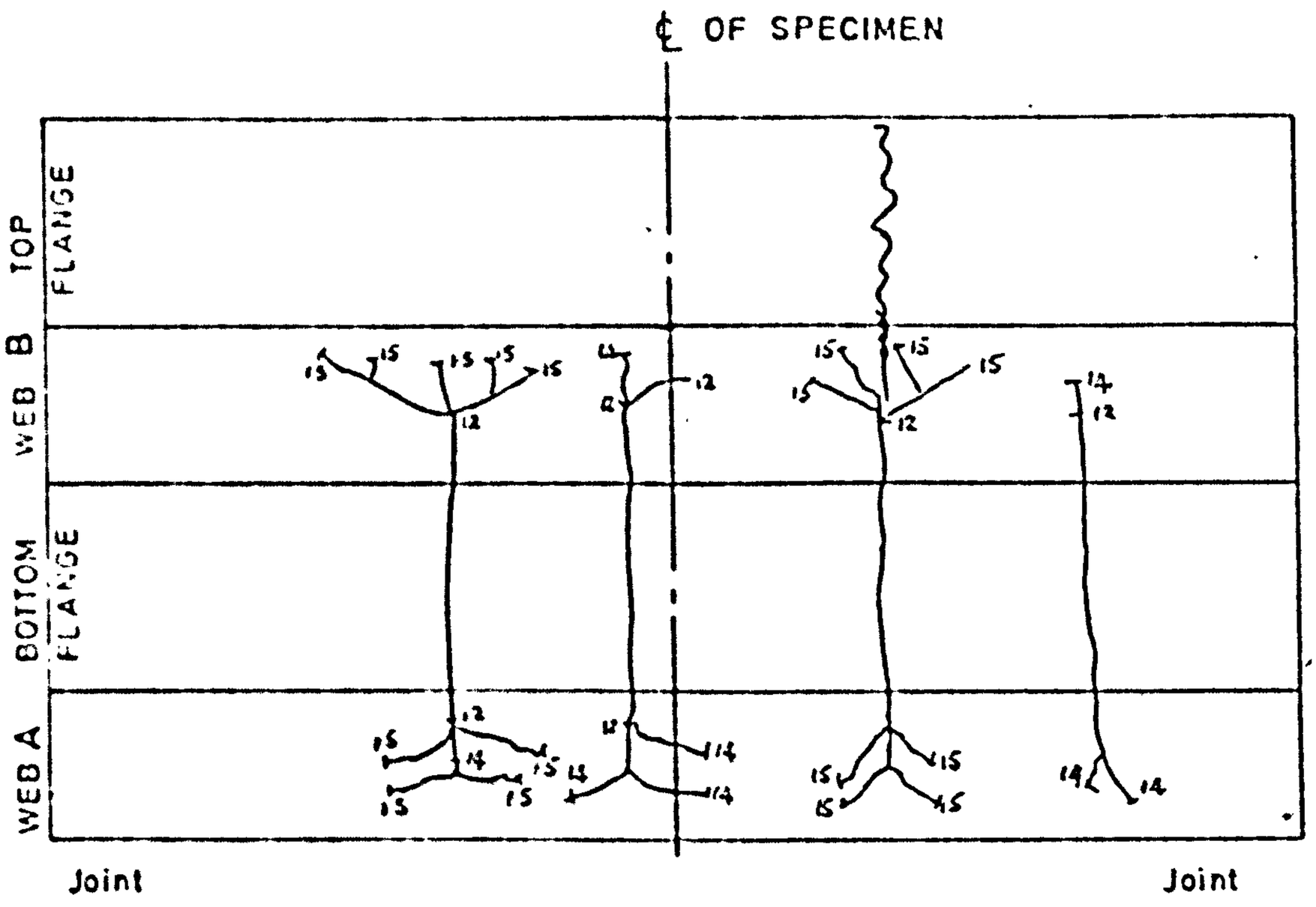

SPECIMEN No B11

$\frac{M}{T} = \infty$

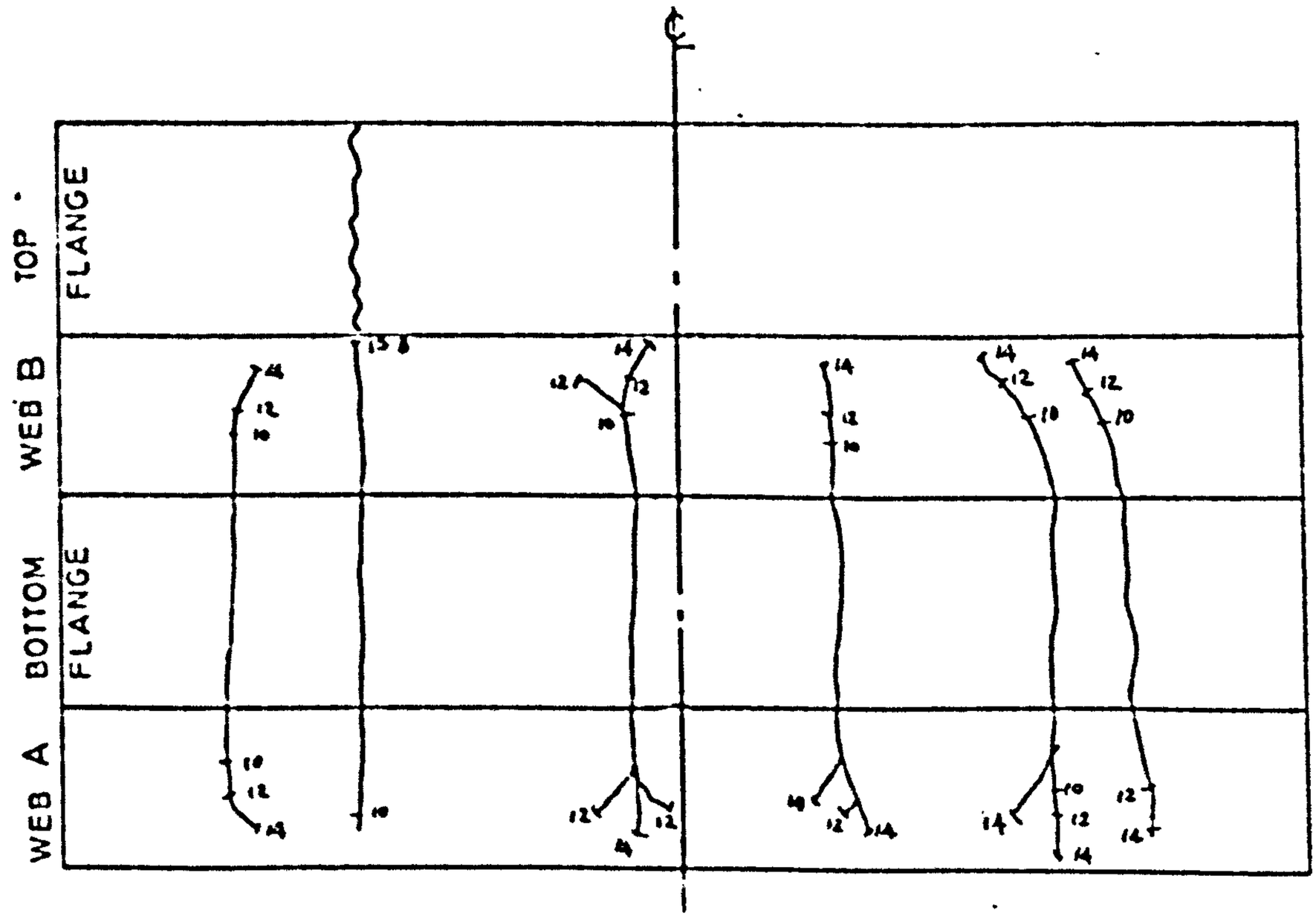

SPECIMEN No B31

$\frac{M}{T} = \infty$

FIG 6.29 CRACK PATTERNS FOR No B11 AND B31

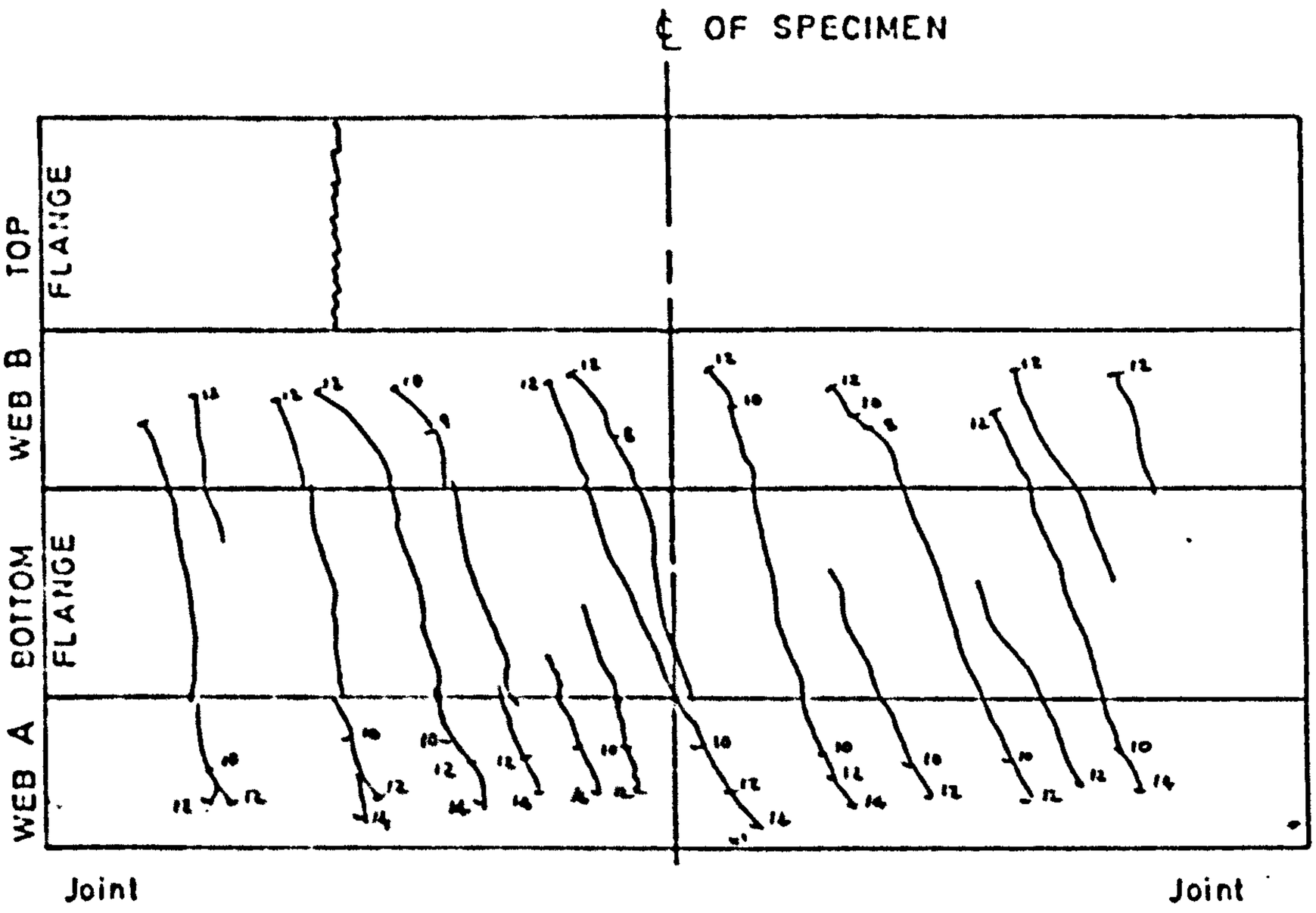

SPECIMEN No B32

$\frac{M}{T} = 8$

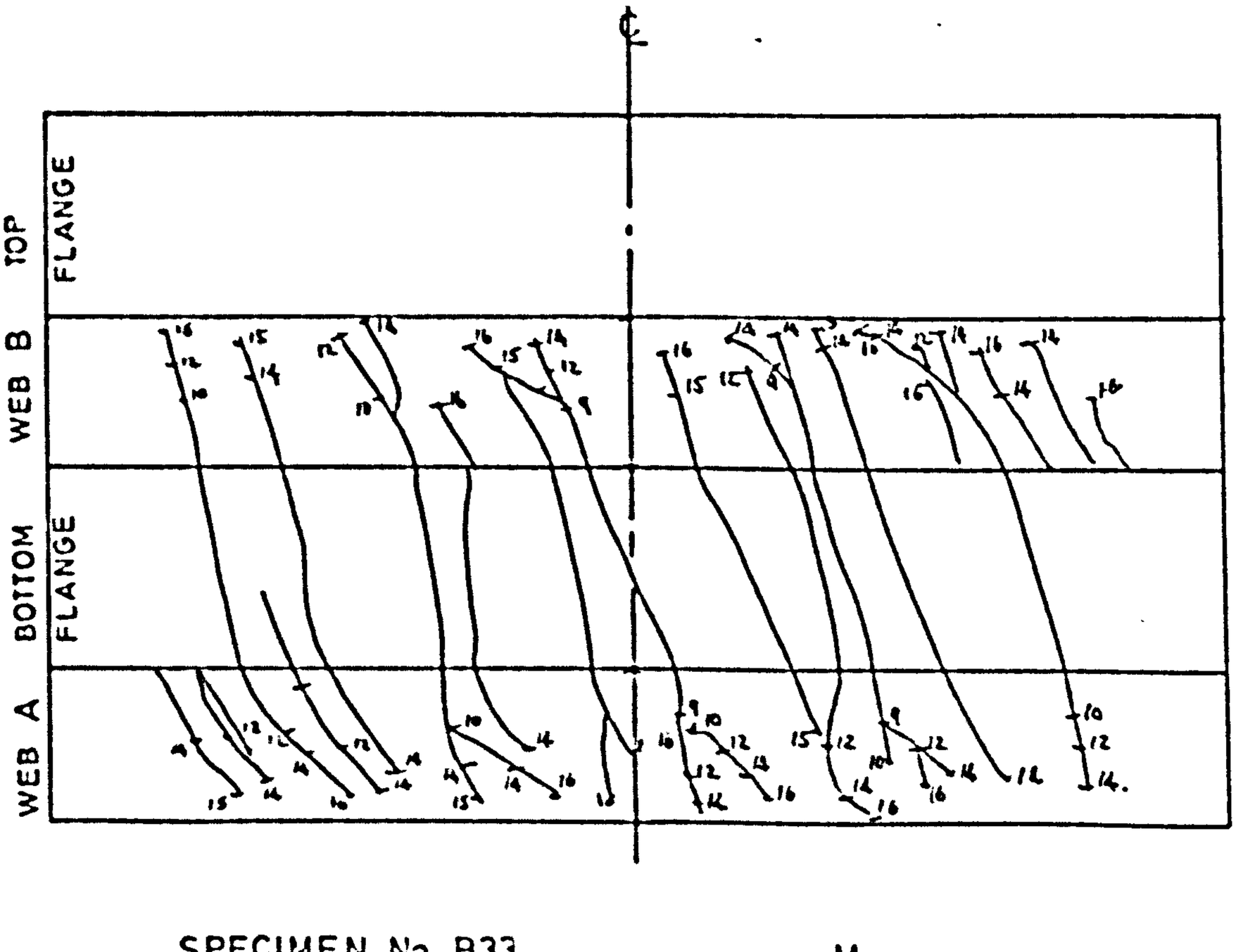

SPECIMEN No. B33

$\frac{M}{T} = 4$

FIG.6.30 CRACK PATTERNS FOR No B32 AND B33

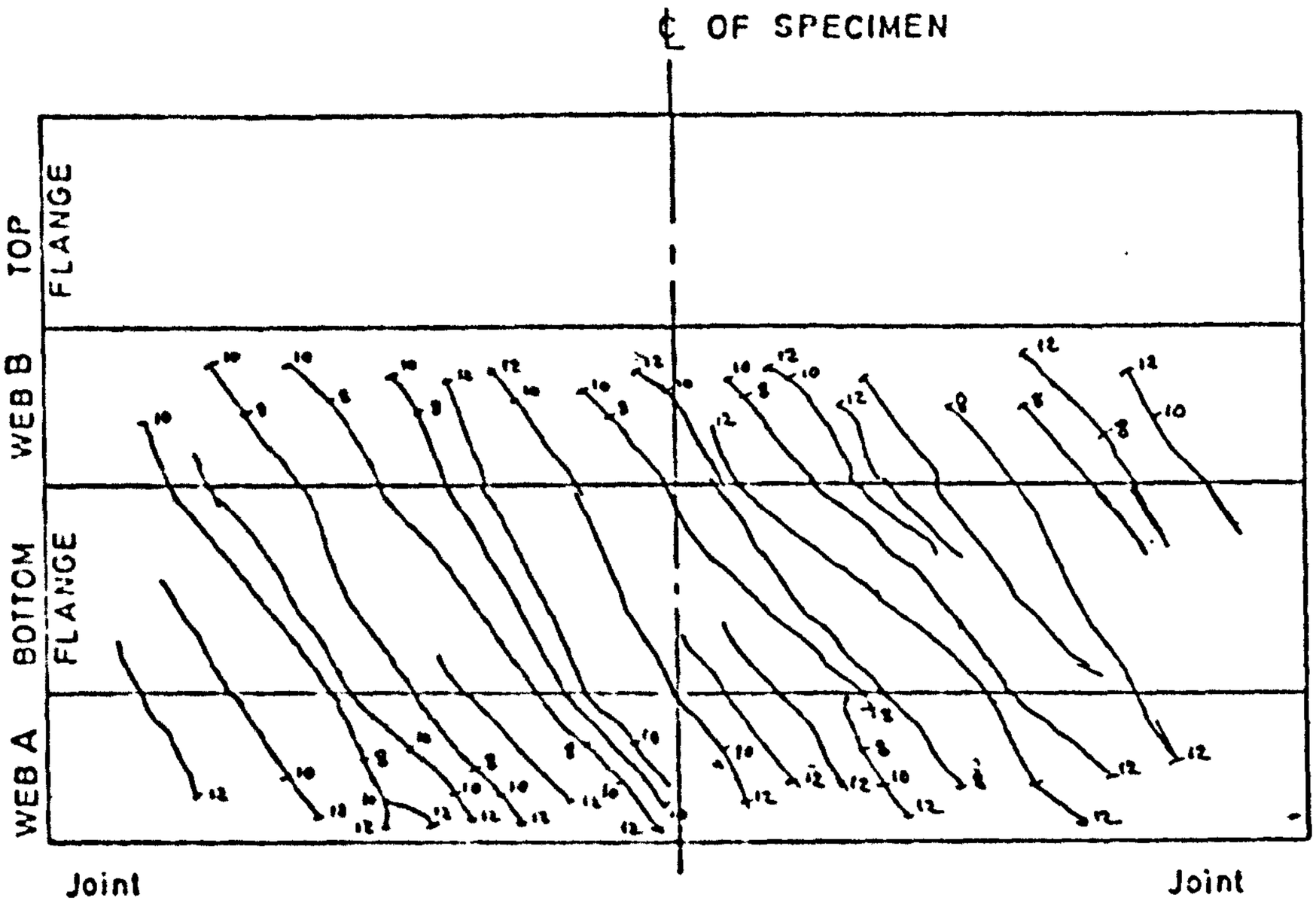

SPECIMEN No B34

$\frac{M}{T} = 2$

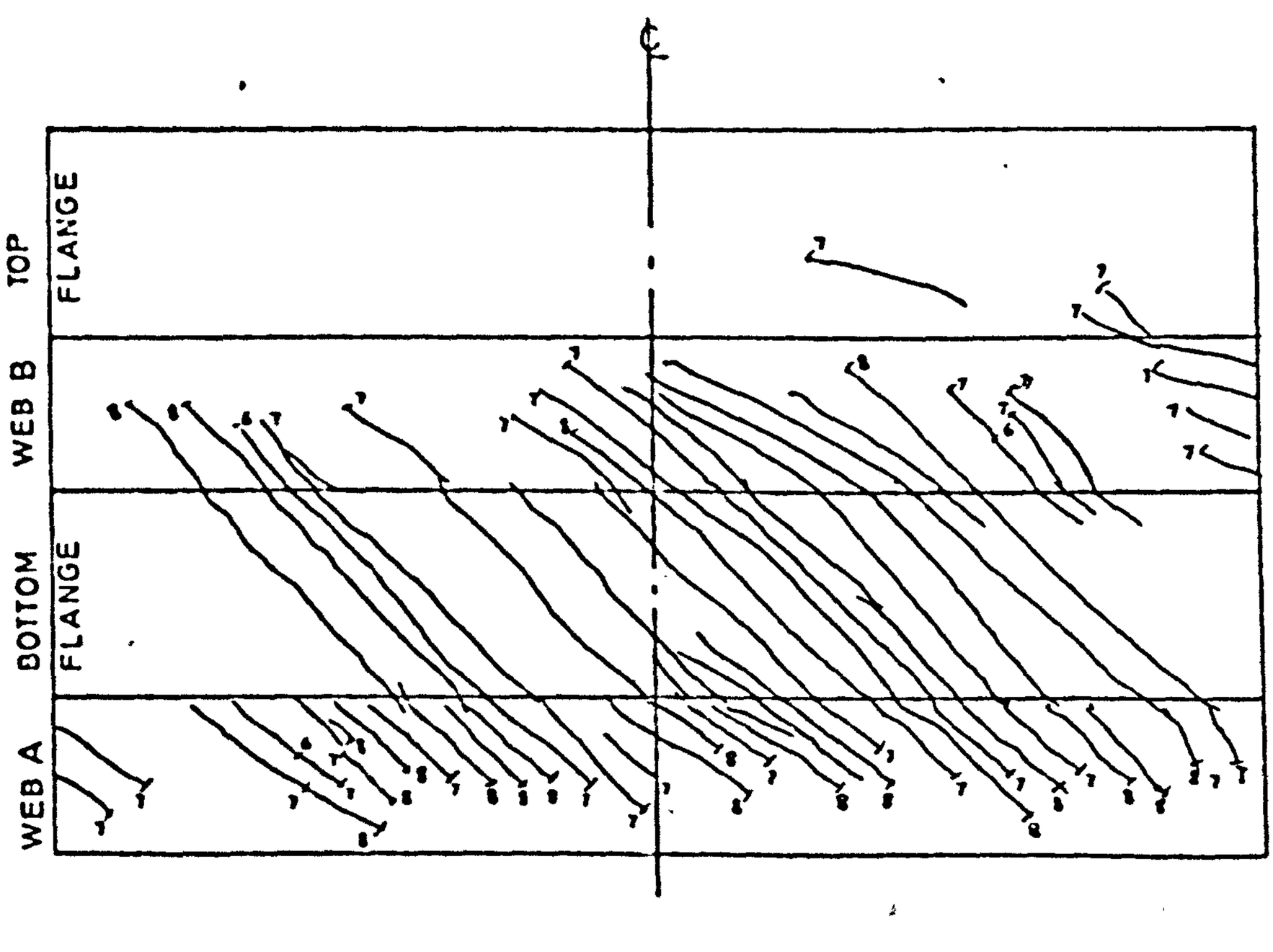

SPECIMEN No.B35

$\frac{M}{T} = 1$

FIG.6 31 CRACK PATTERNS FOR NoB34 AND B35

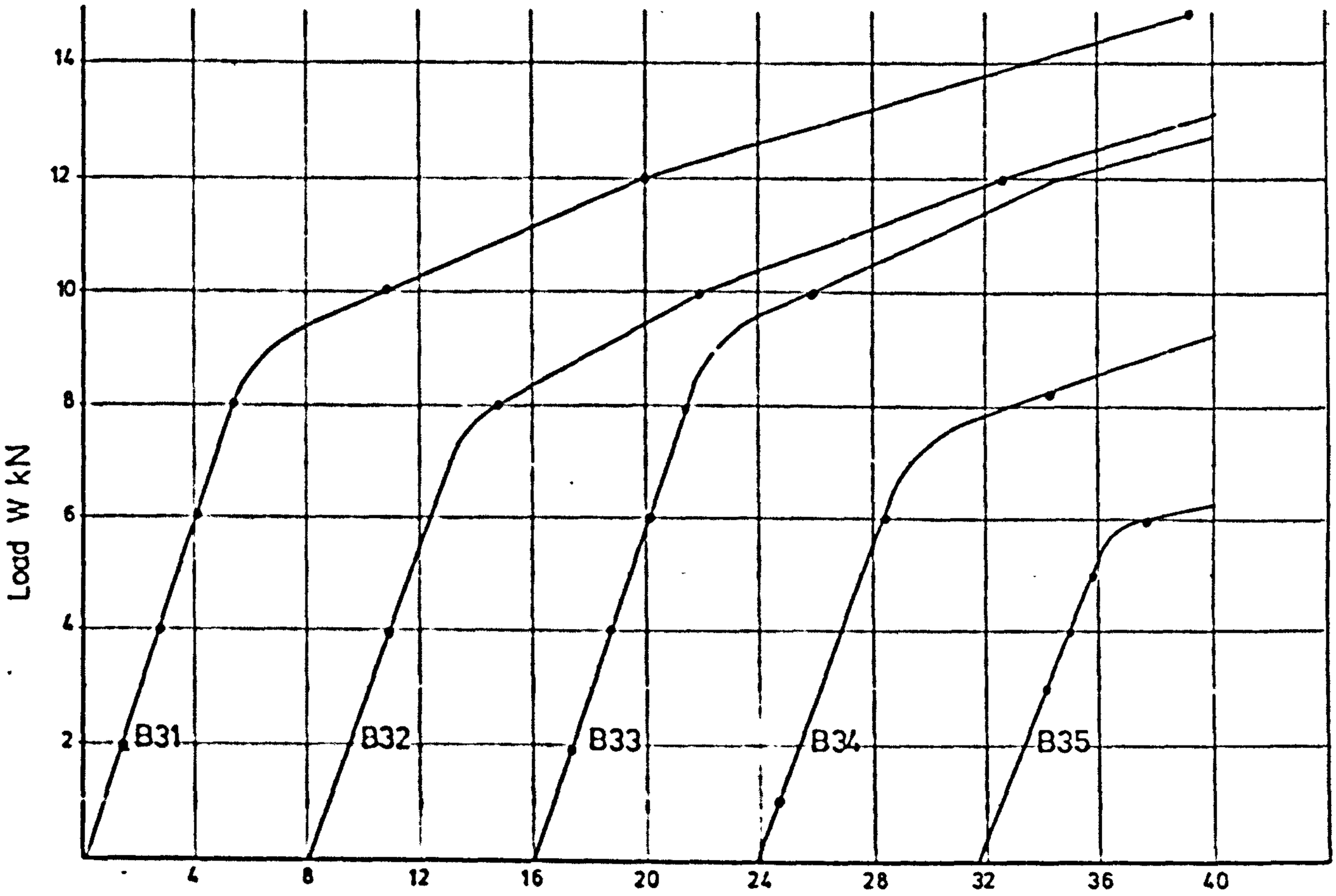

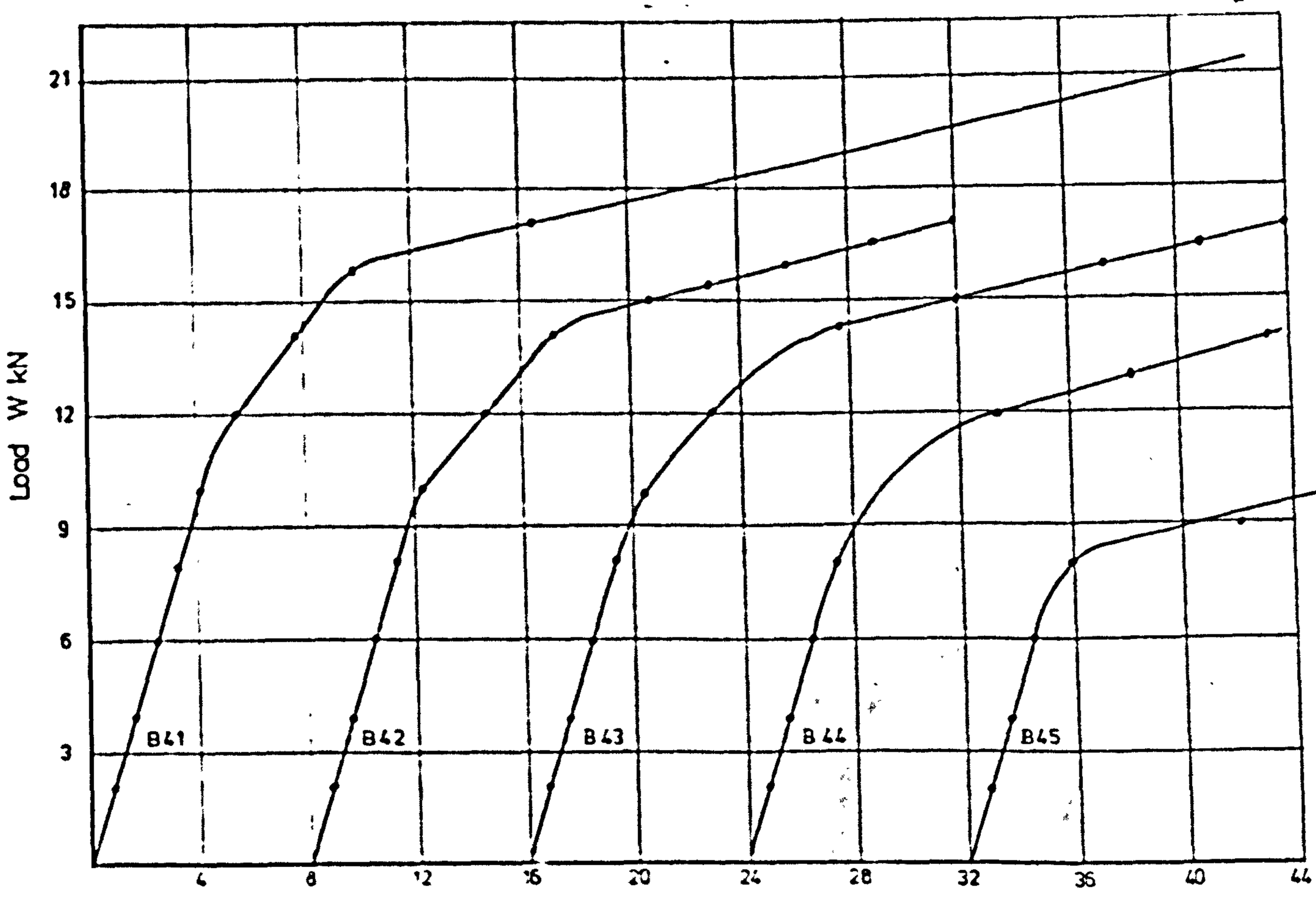

FIG.6.32 Load Central Deflection For Specimens of Series 3& 4

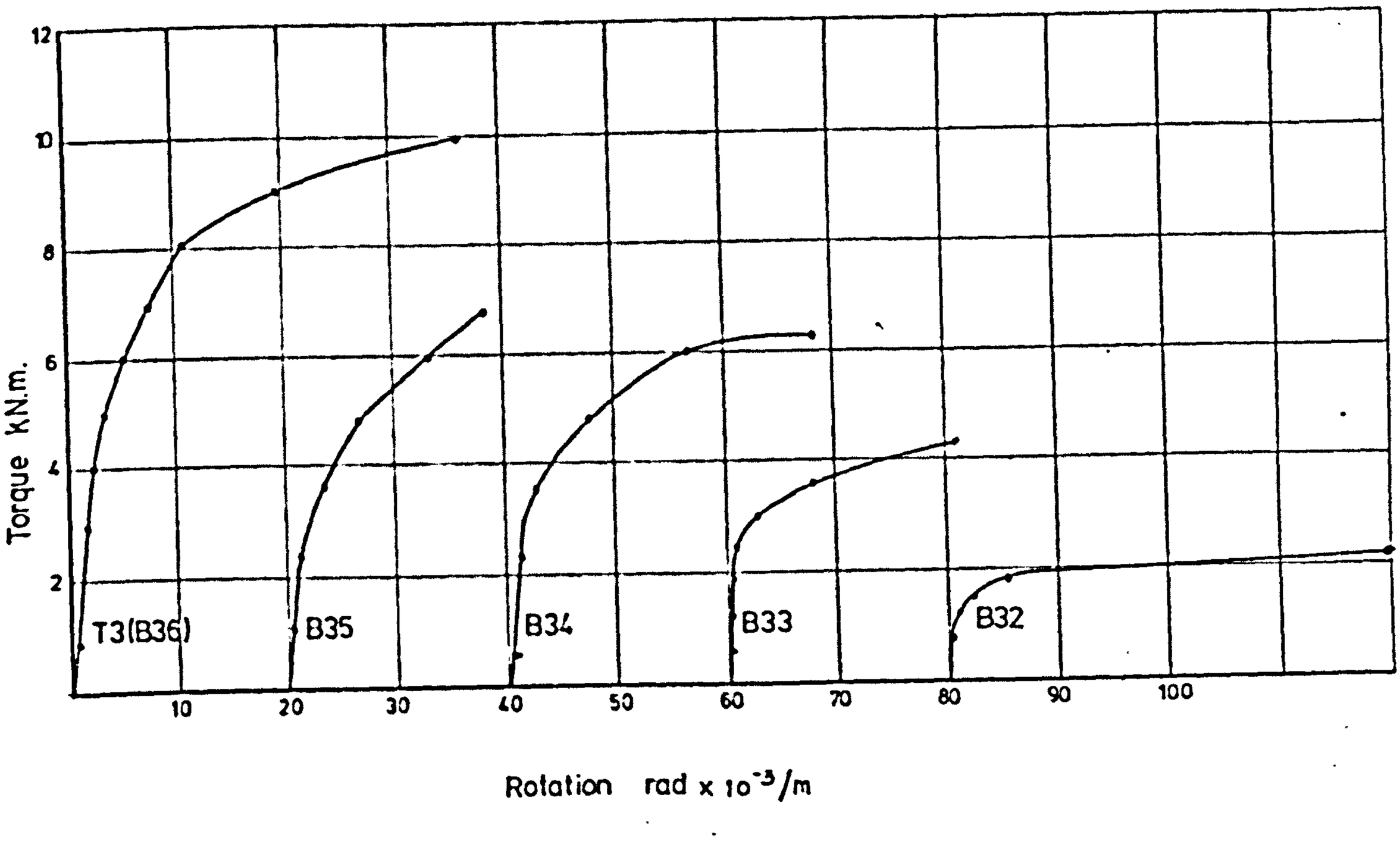

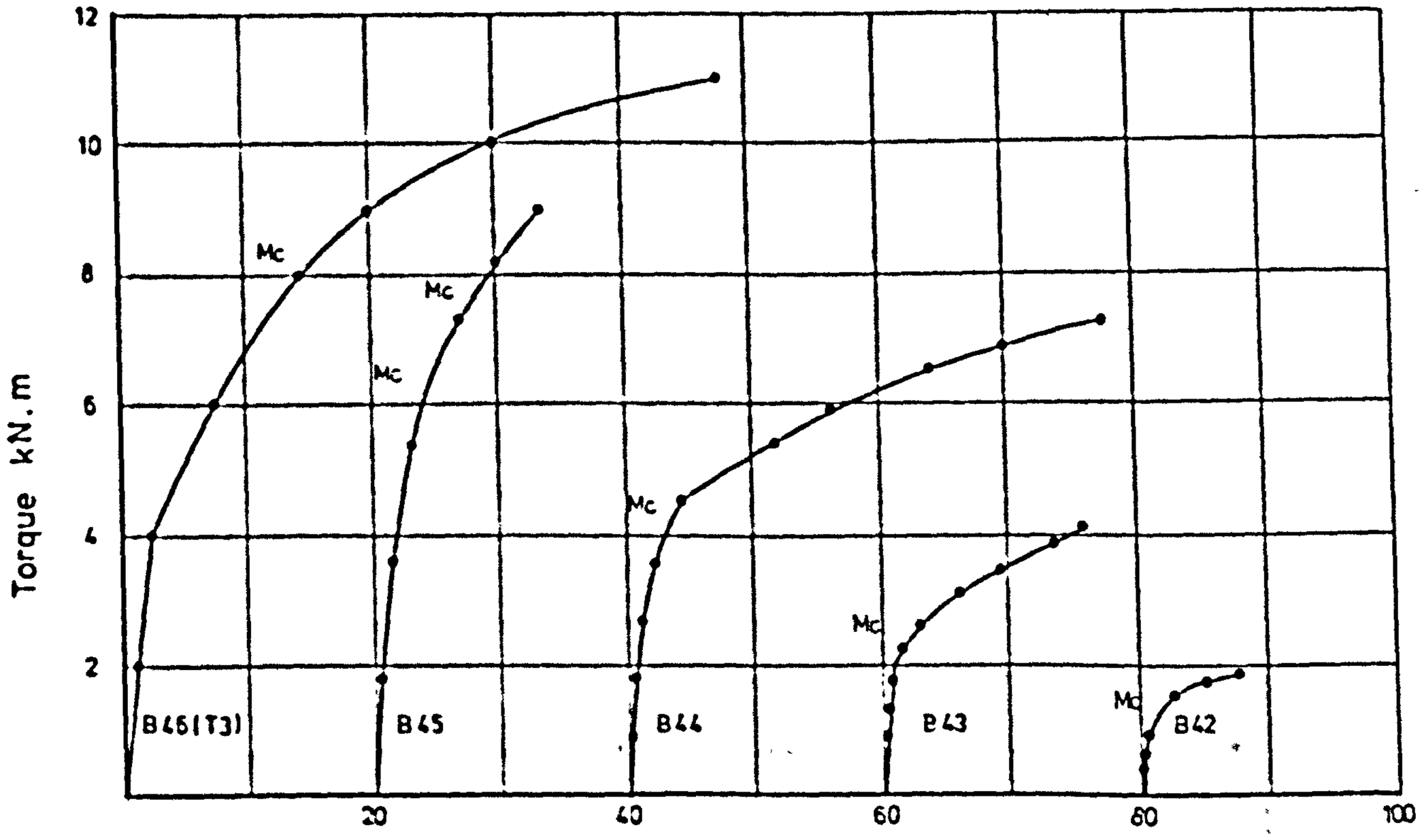

FIG.6.33Torque Rotation Curves For Specimens of Series 3 & 4

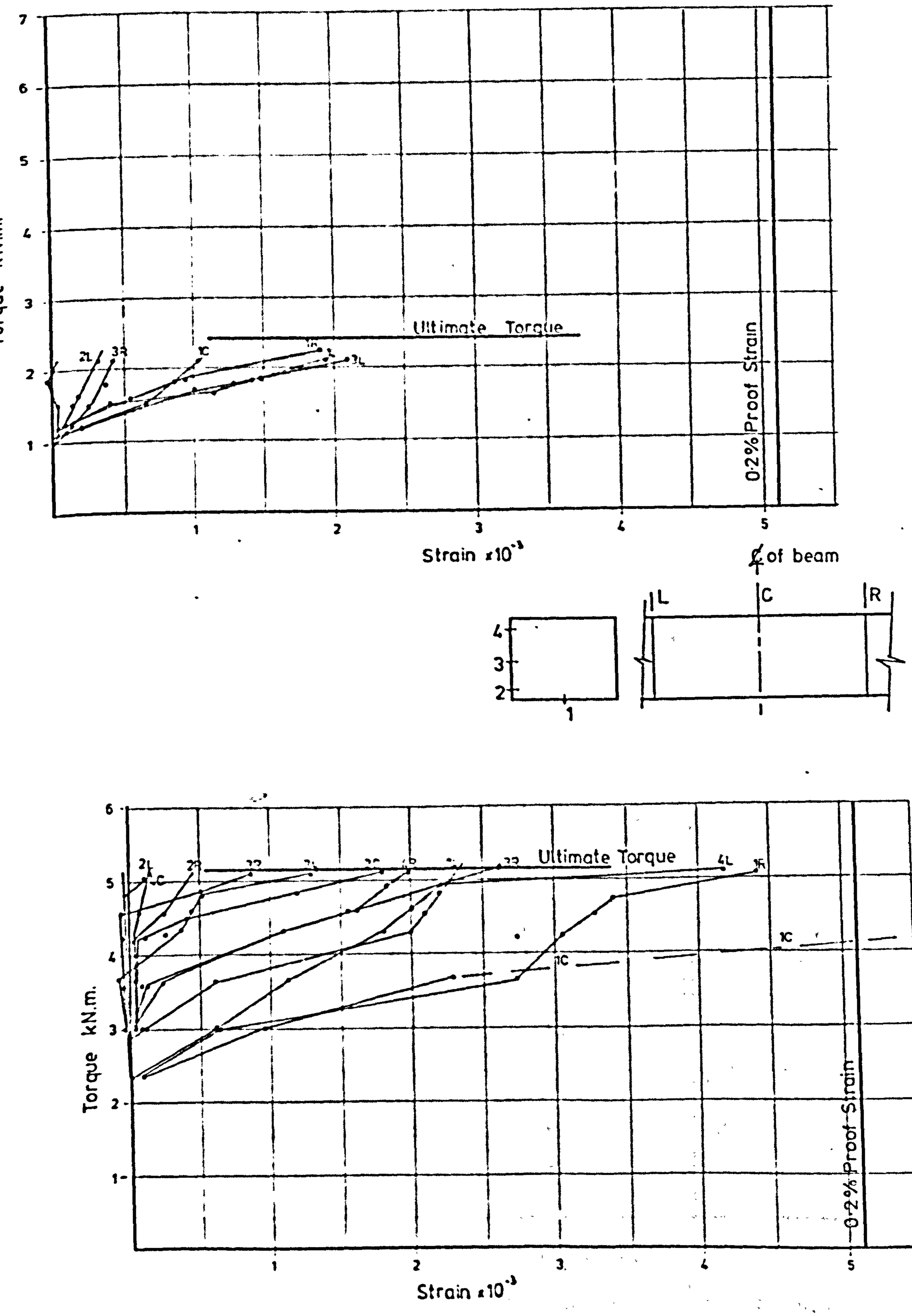

FIG 6.34 Torque Versus Stirrups Strain For Specimen B32 & B 33.

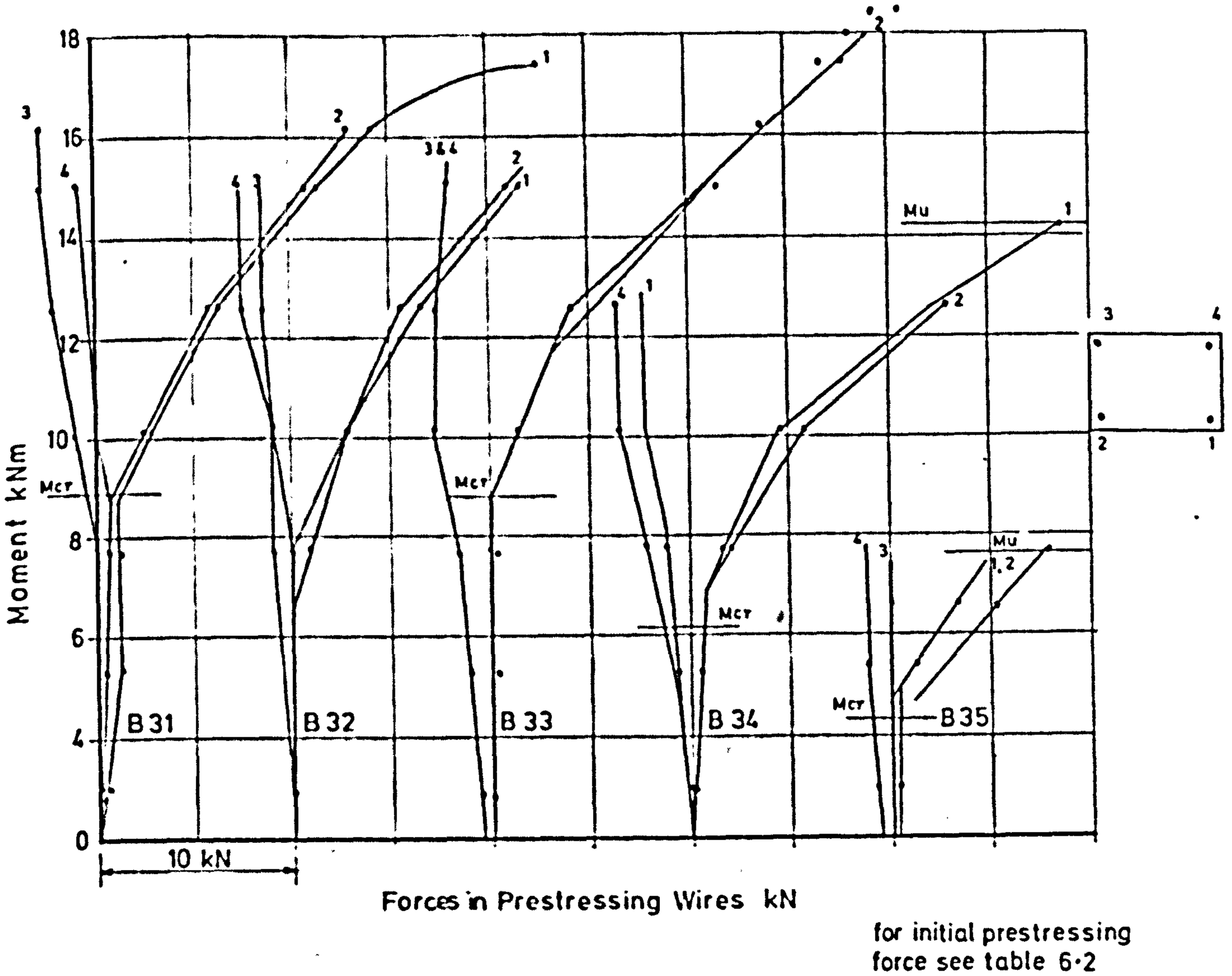

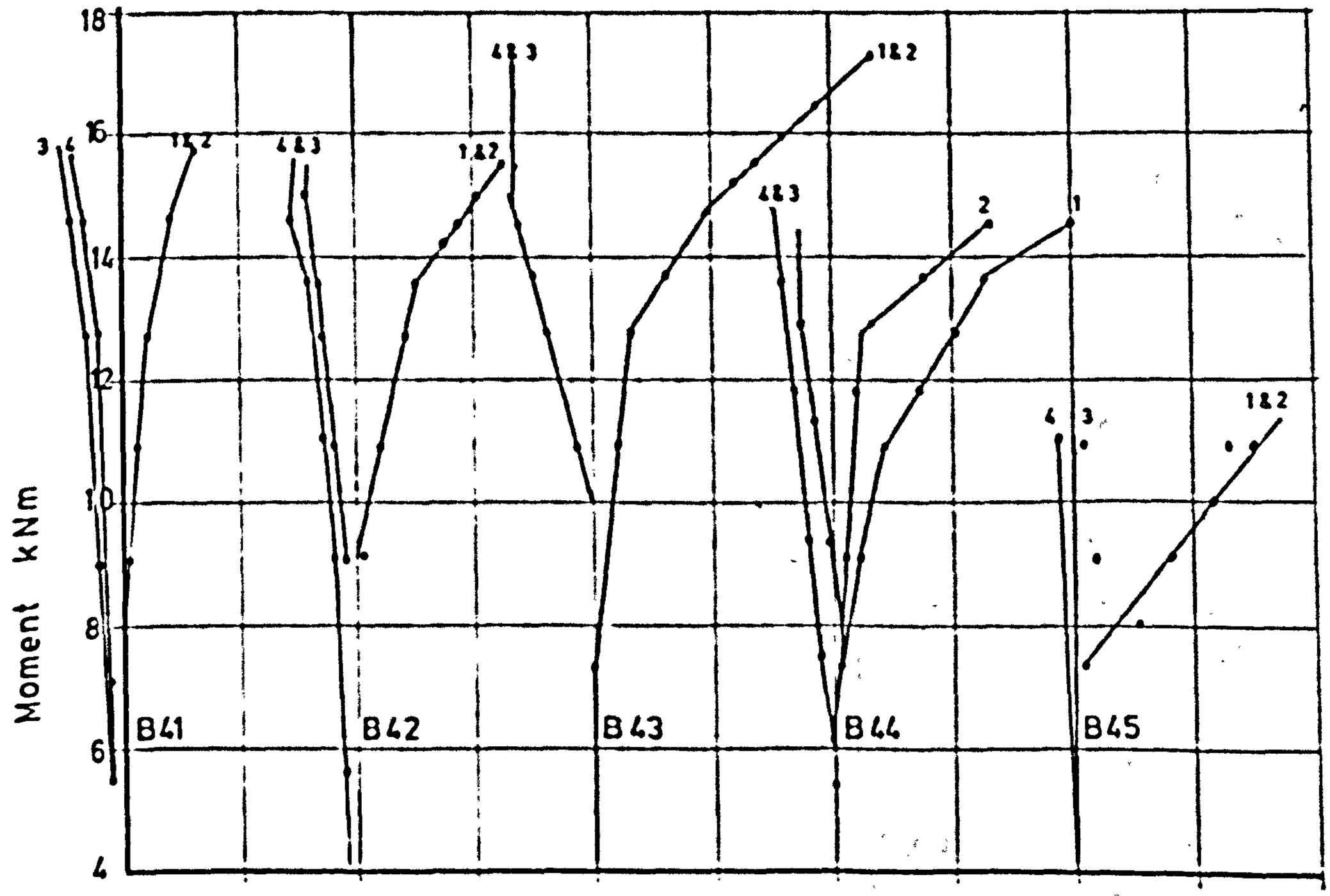

FIG 6·35 MOMENT - VERSUS CHANGE IN PRESTRESSING FORCE IN WIRES

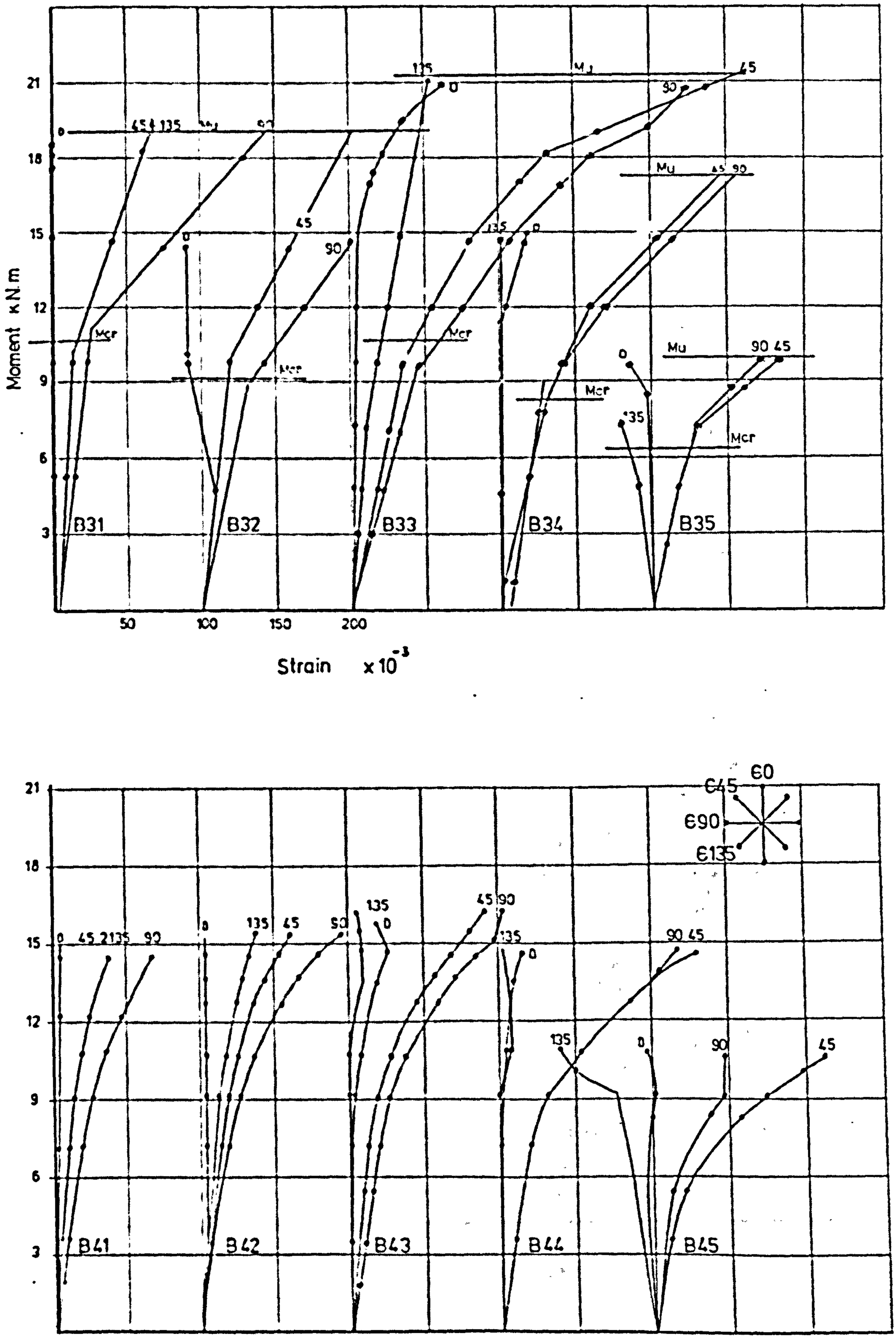

FIG.6.35 Moment - Strain Rosette on Top Flange For Specimens of Series 3 & 4

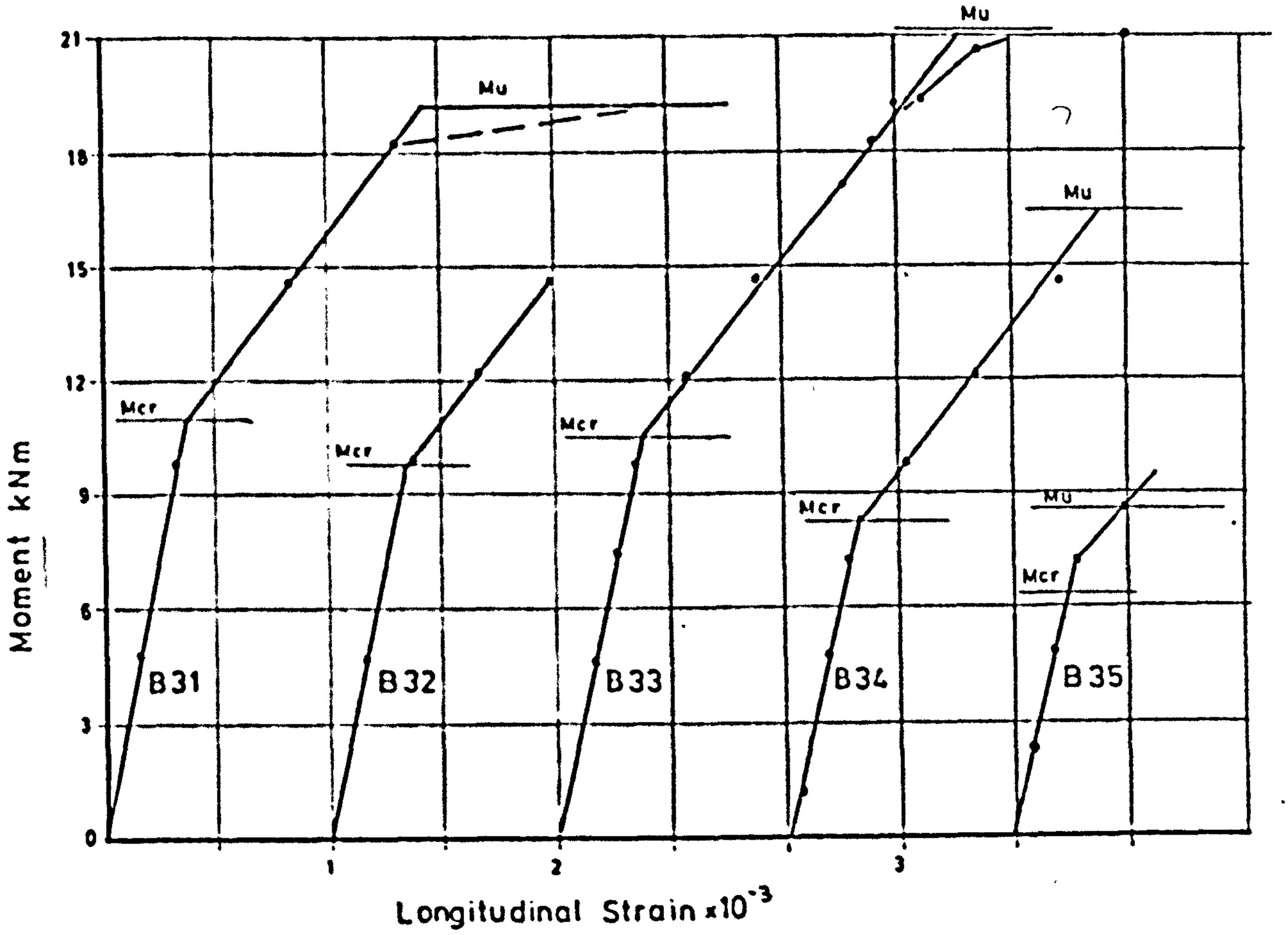

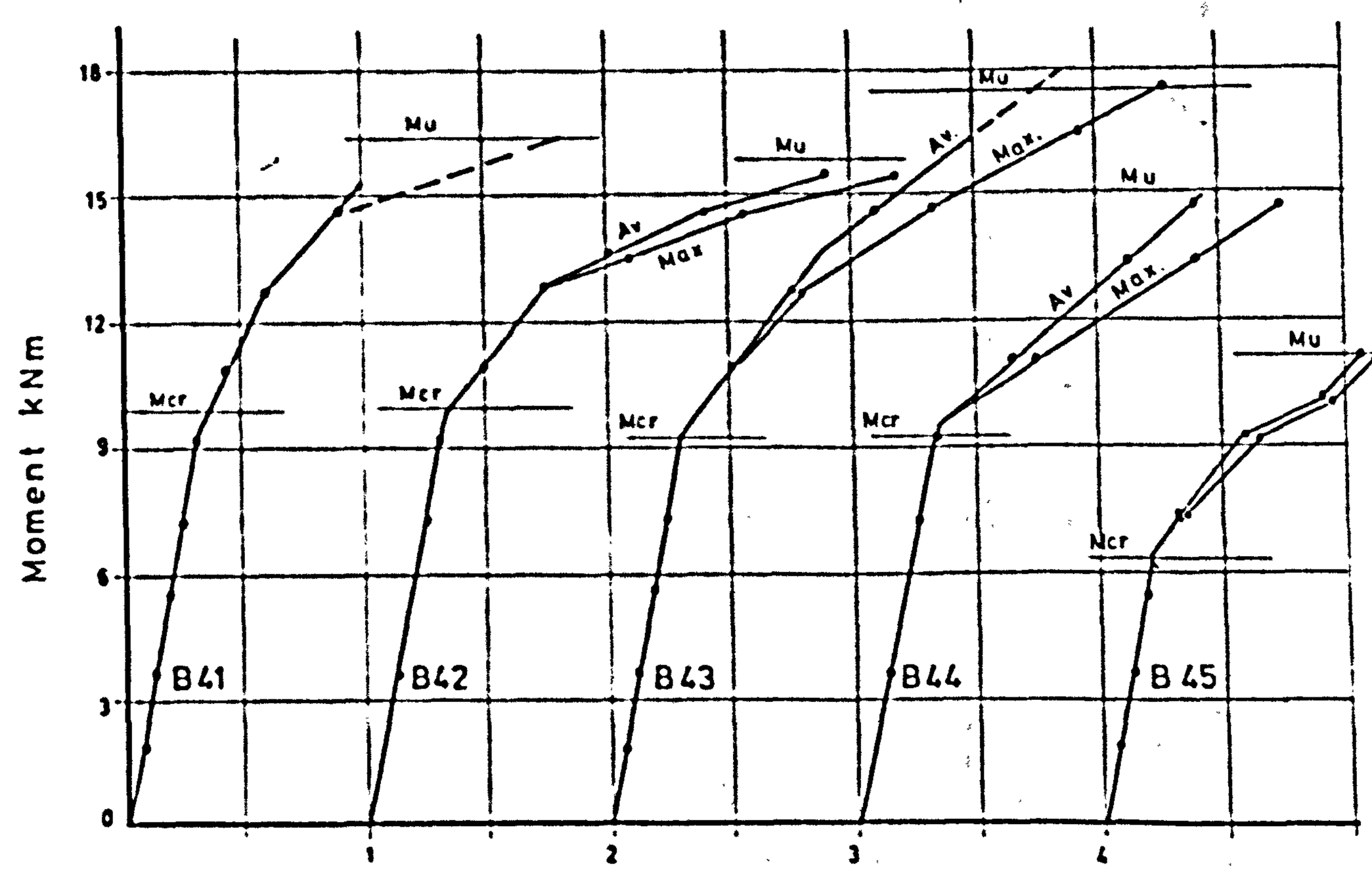

FIG 6.37 MOMENT - LONGITUDINAL COMPRESSIVE STRAINS FOR THE TOP FLANGE OF THE SPECIMEN OF SERIES 3 and 4

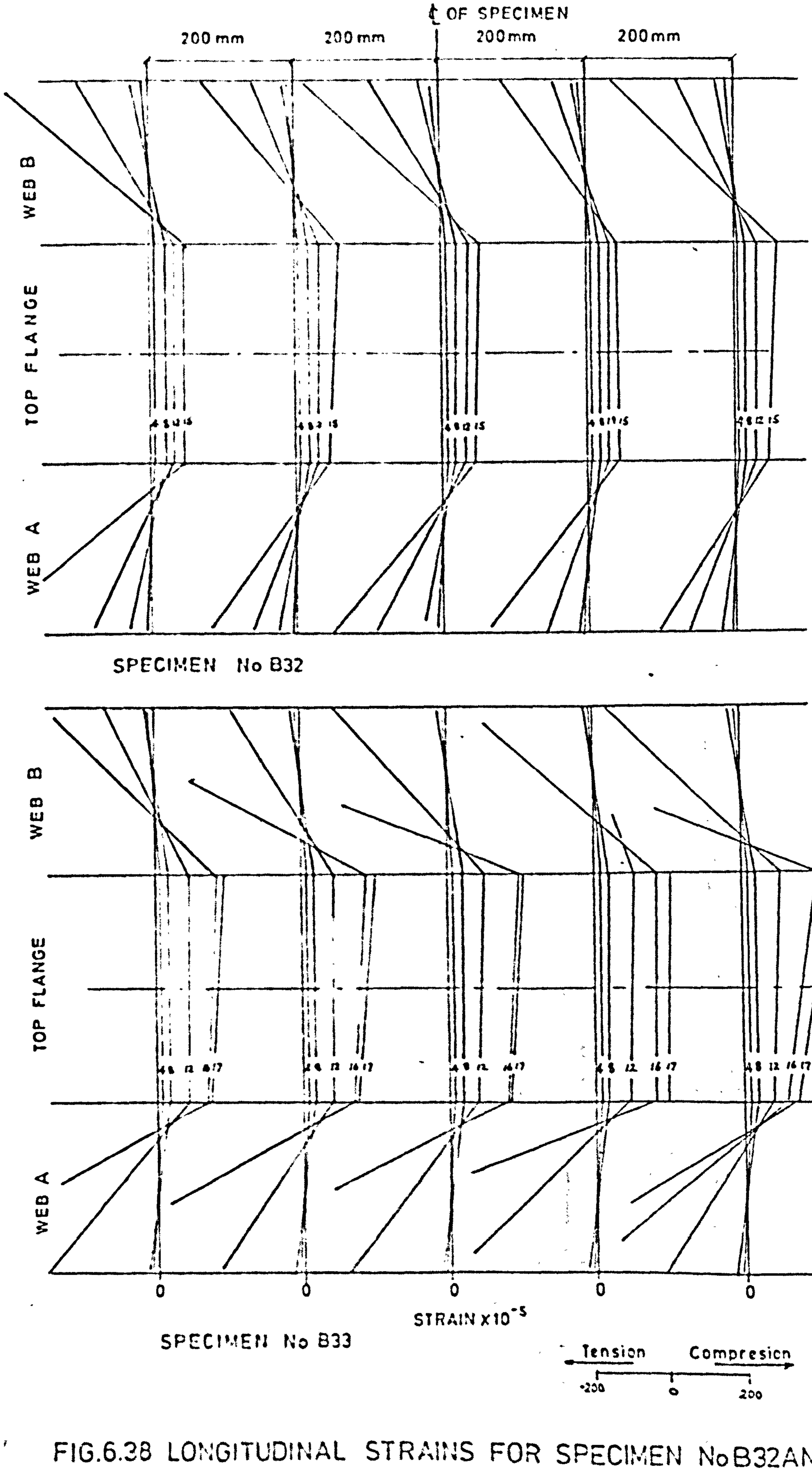

FIG.6.38 LONGITUDINAL STRAINS FOR SPECIMEN NoB32AND B33

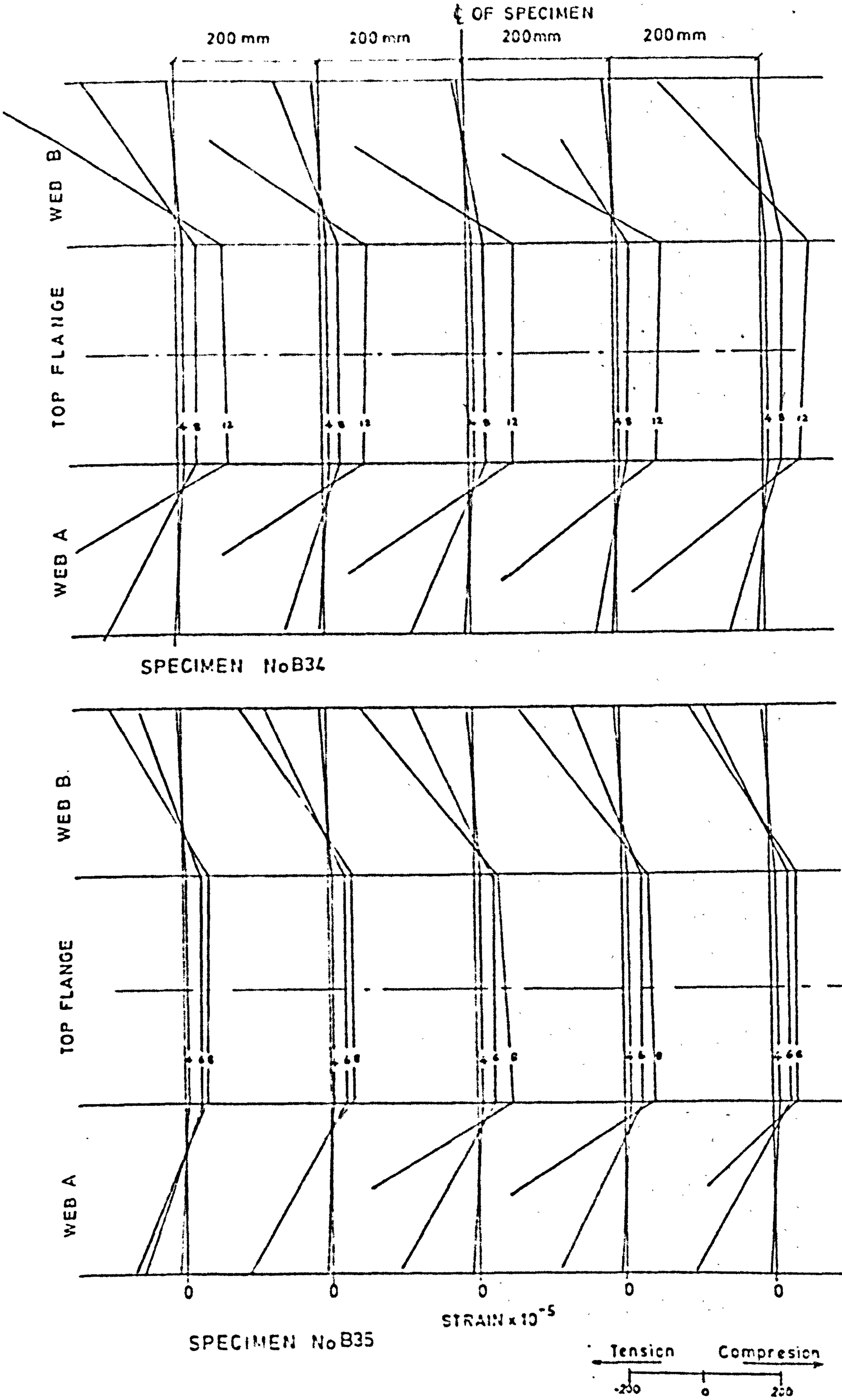

FIG. 6.39 LONGITUDINAL STRAINS FOR SPECIMEN NoB34 AND B35

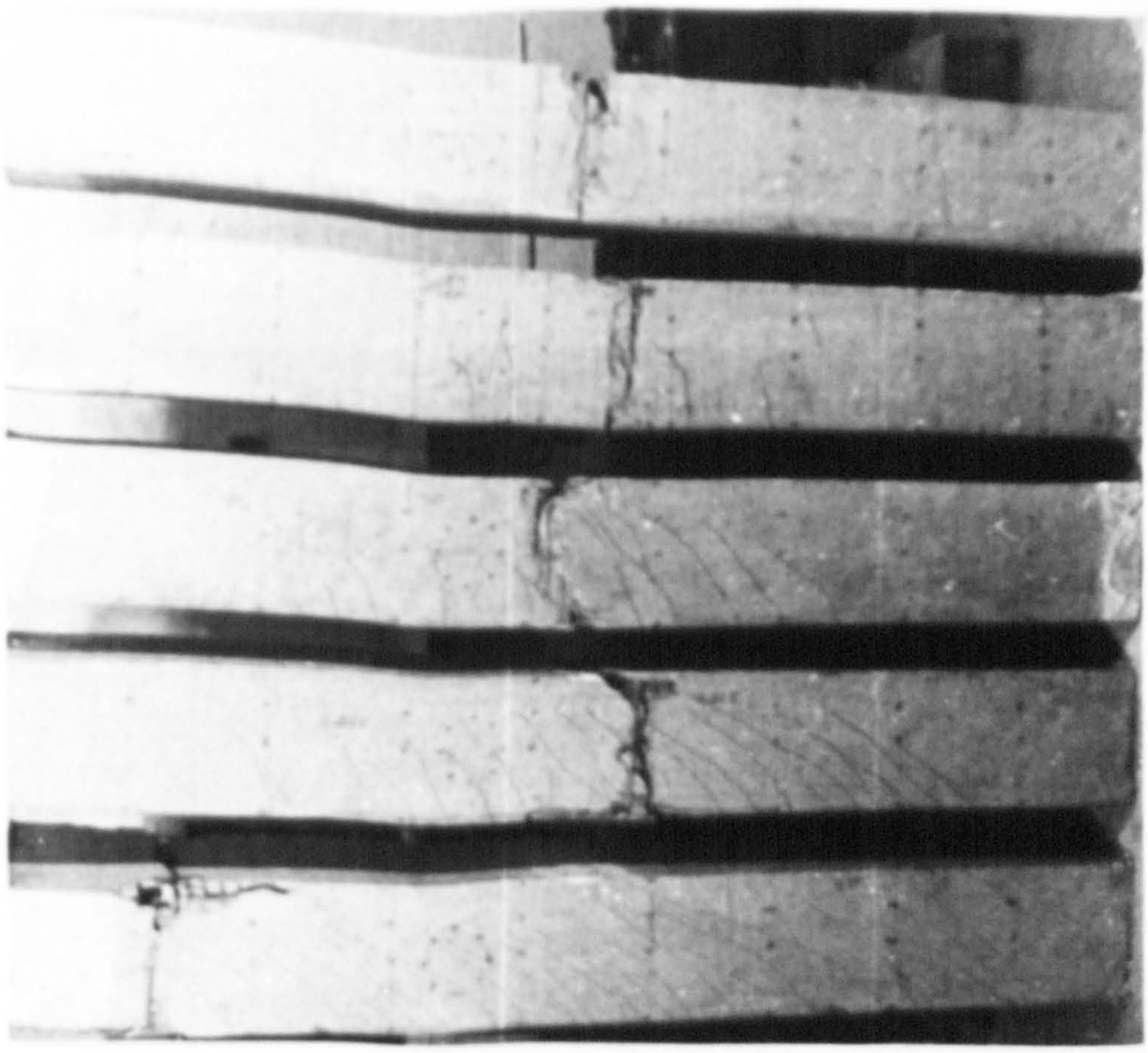

Webs

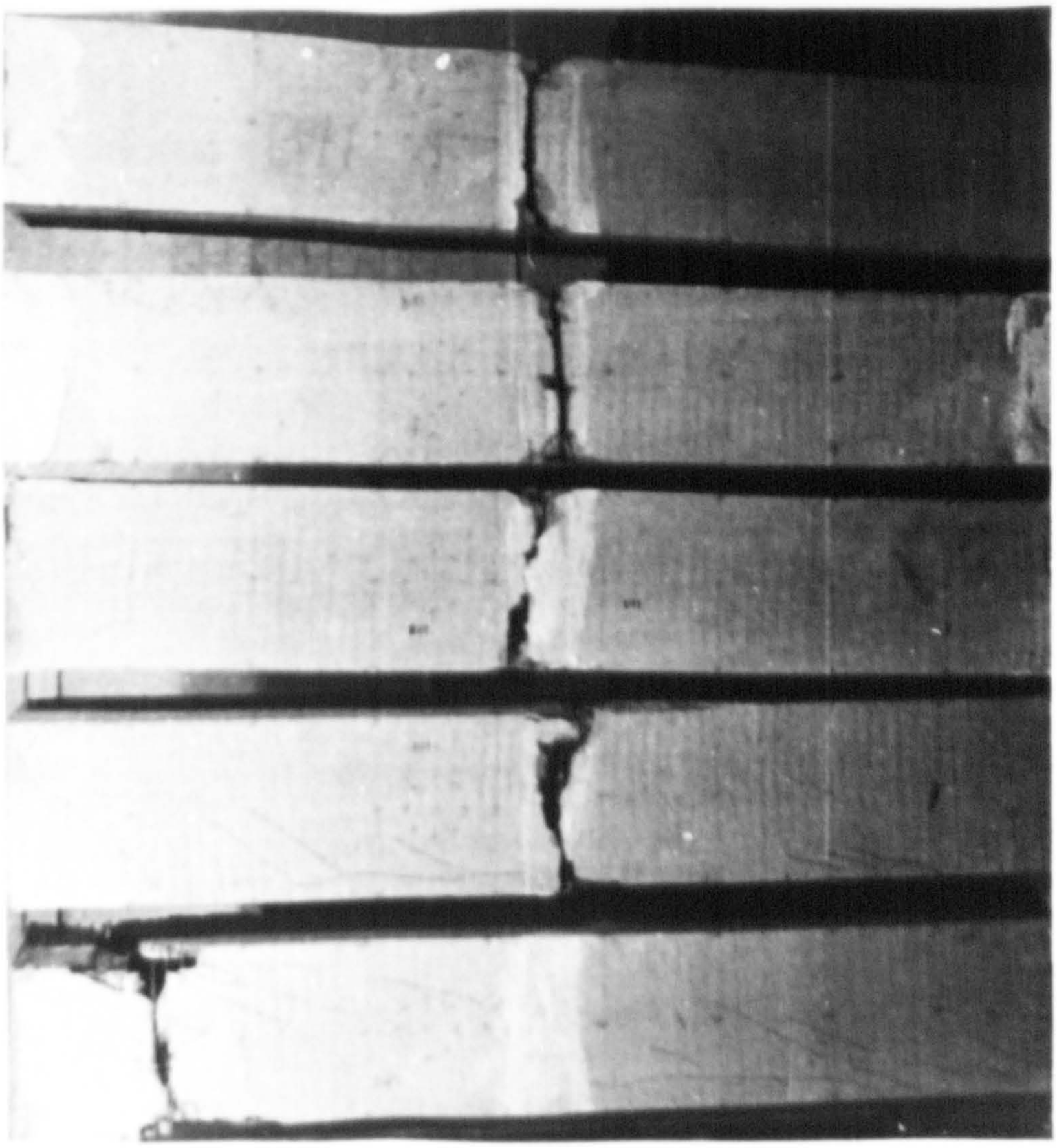

Top Flanges

Plate 16 Crack patterns after failure for beams of series 4

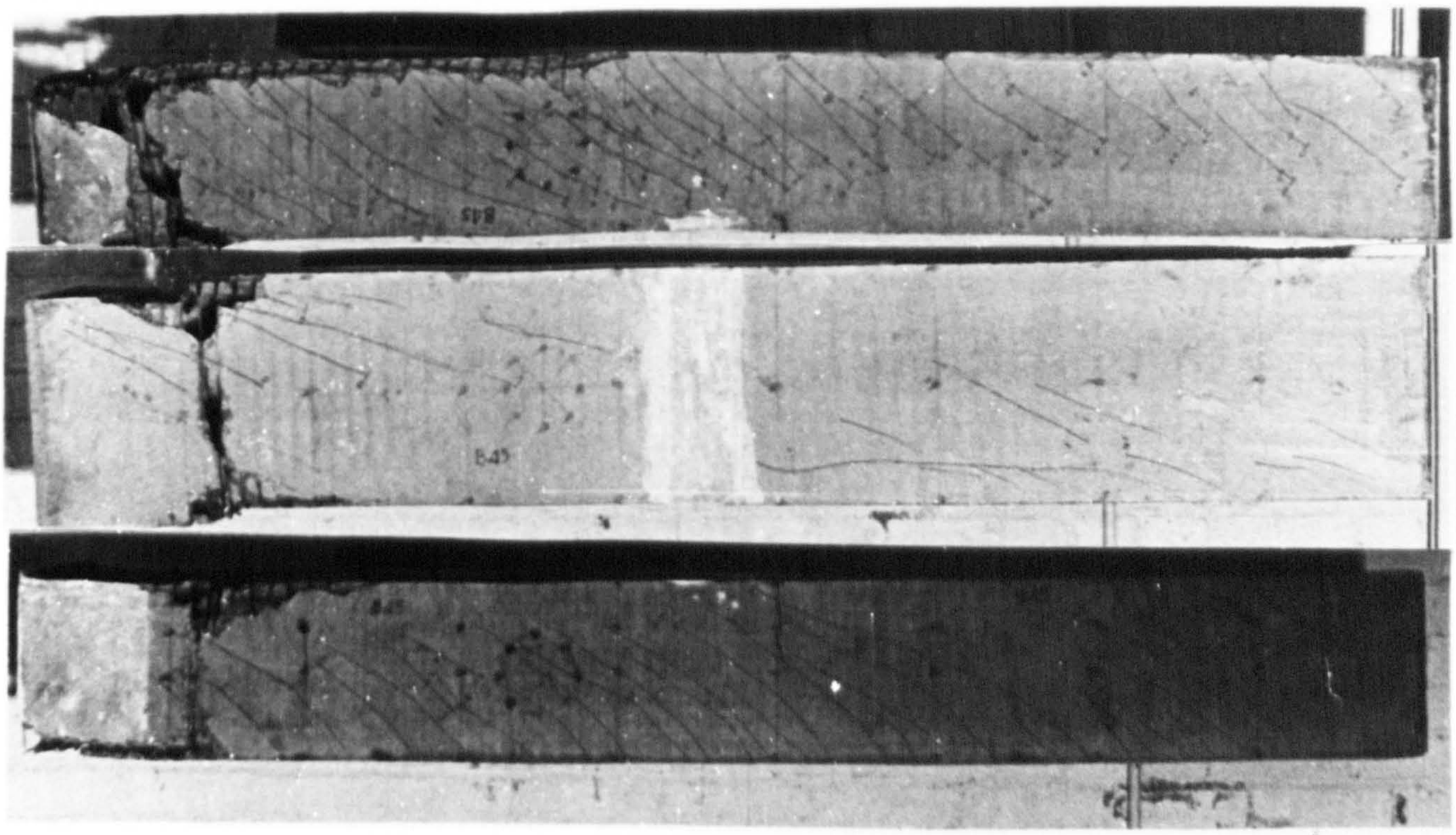

Plate 17 Crack patterns after failure for beam B45

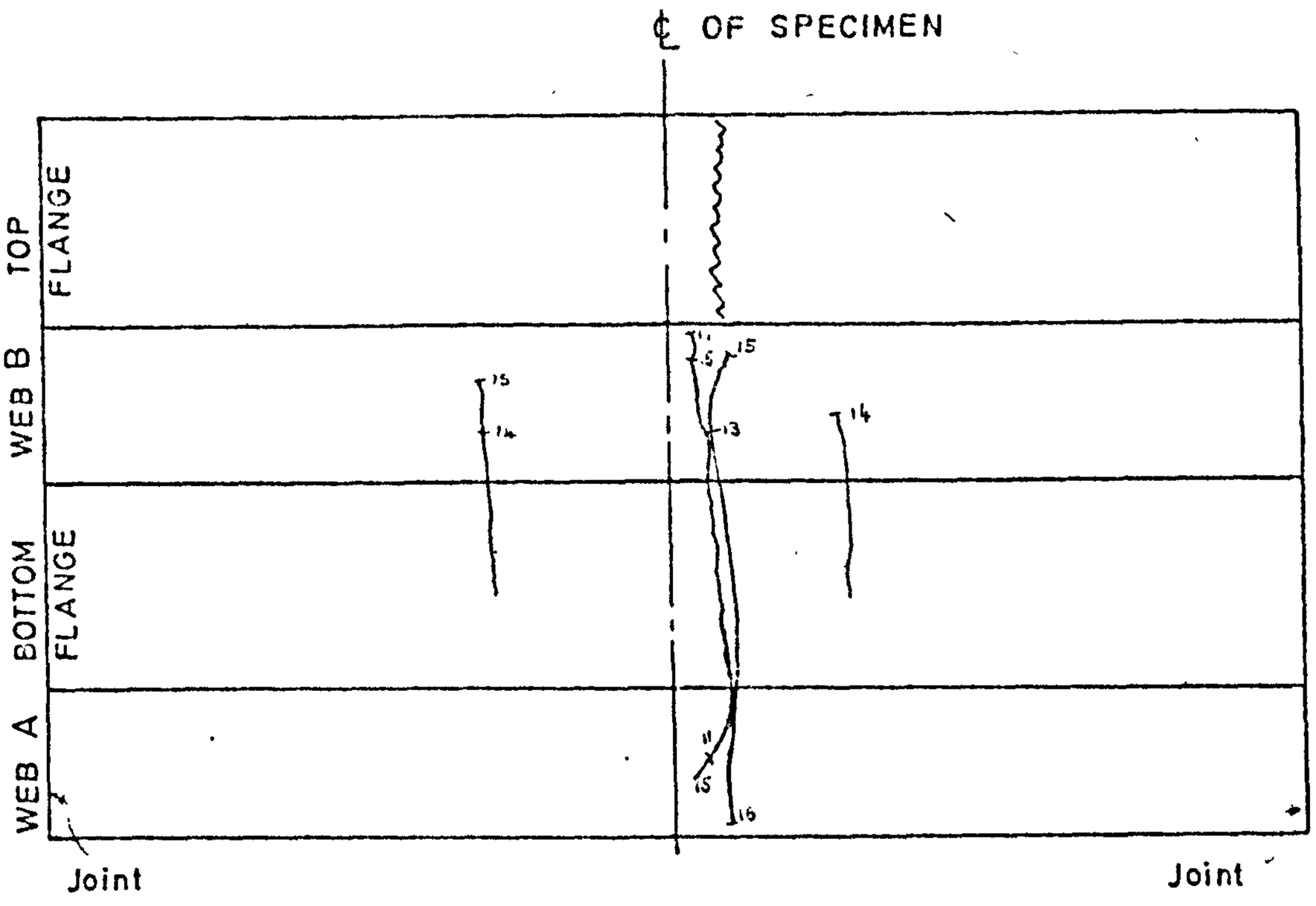

SPECIMEN No B21

$\frac{M}{T} = \infty$

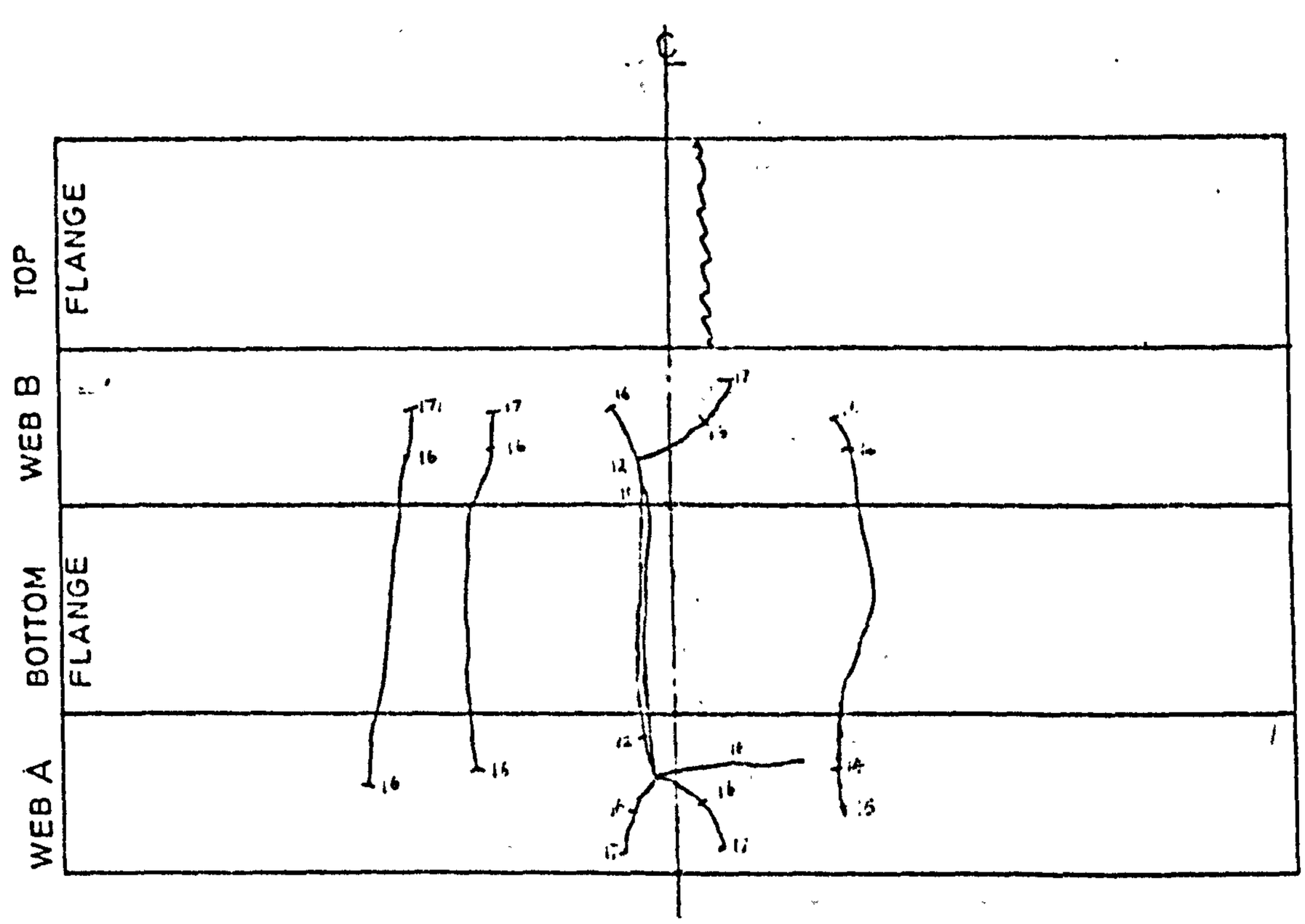

SPECIMEN No. B41

$\frac{M}{T} = \infty$

FIG.6.41 CRACK PATTERNS FOR No B21 AND B41

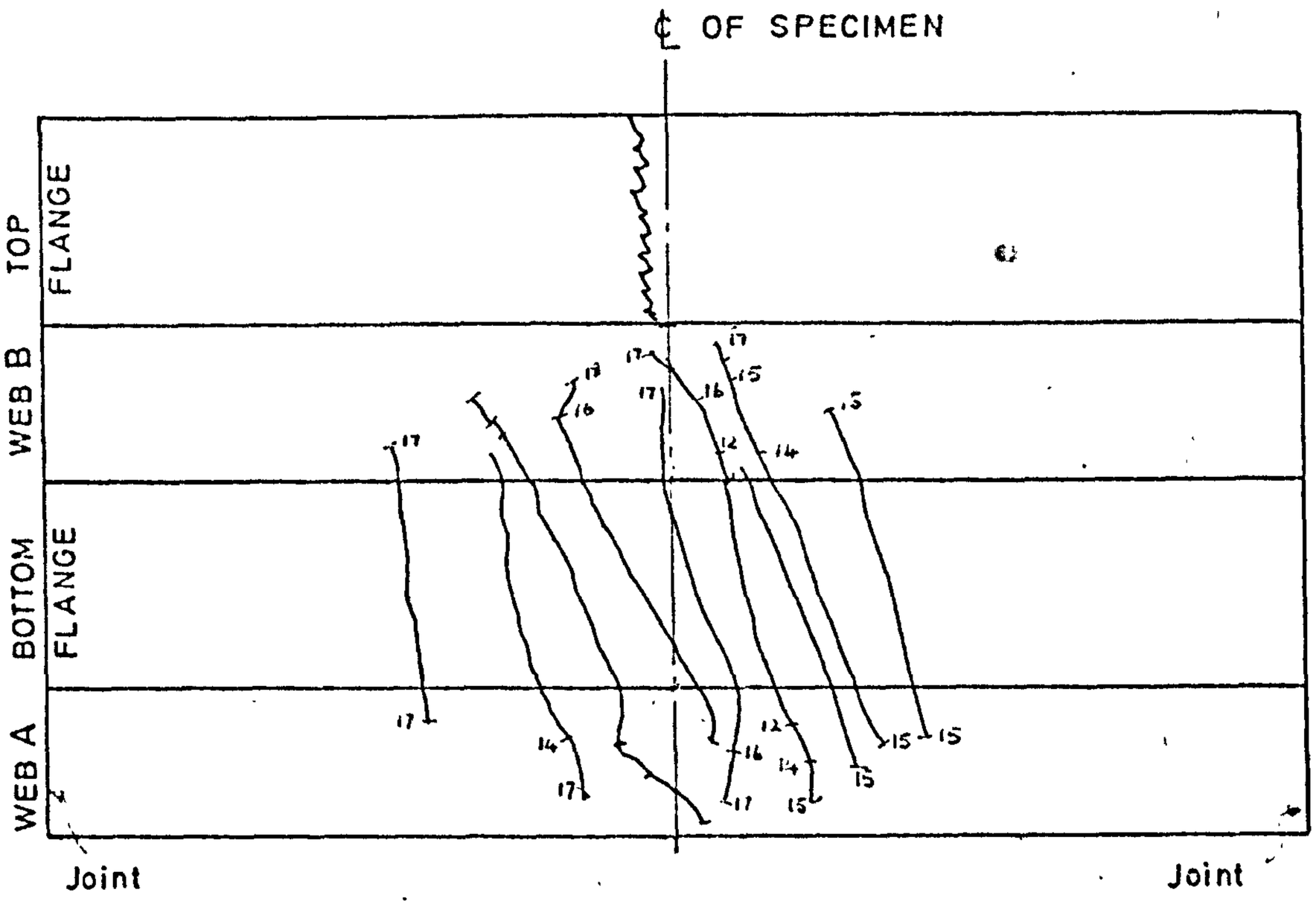

SPECIMEN No B42

$\frac{M}{T} = 8$

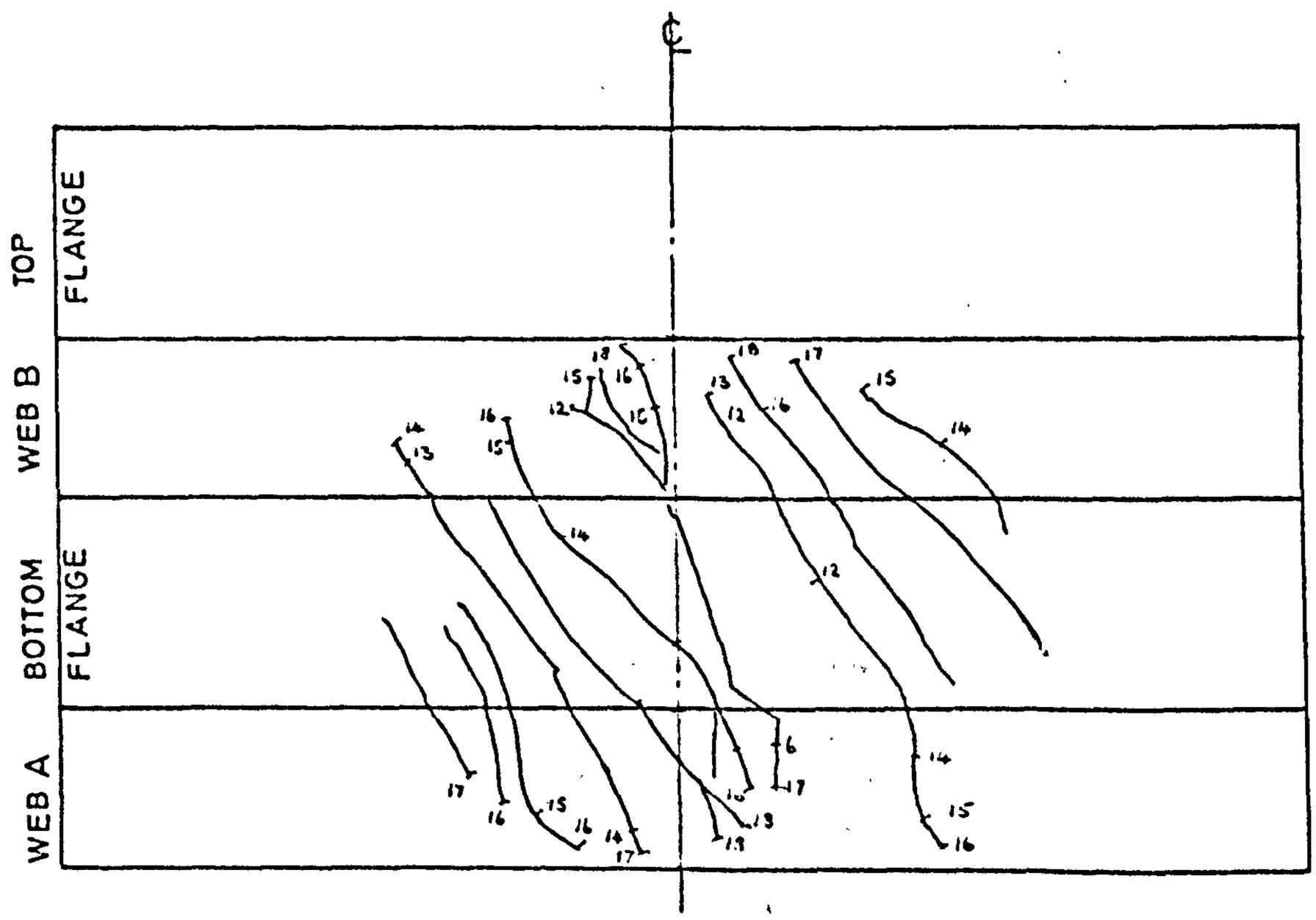

SPECIMEN No.B43

$\frac{M}{T} = 4$

FIG.6.42 CRACK PATTERNS FOR No B42 AND B43

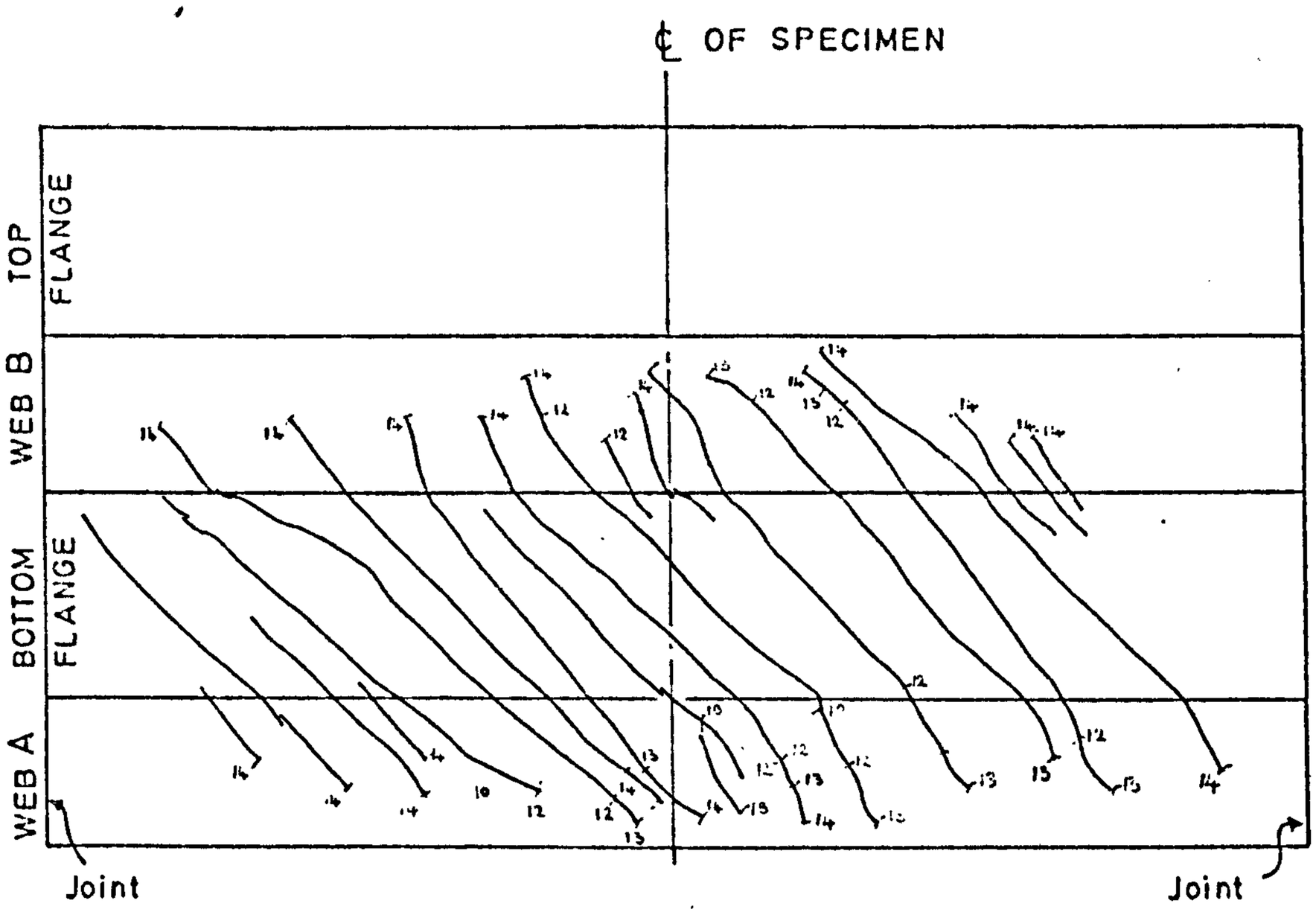

SPECIMEN No B44

$\frac{M}{T} = 2$

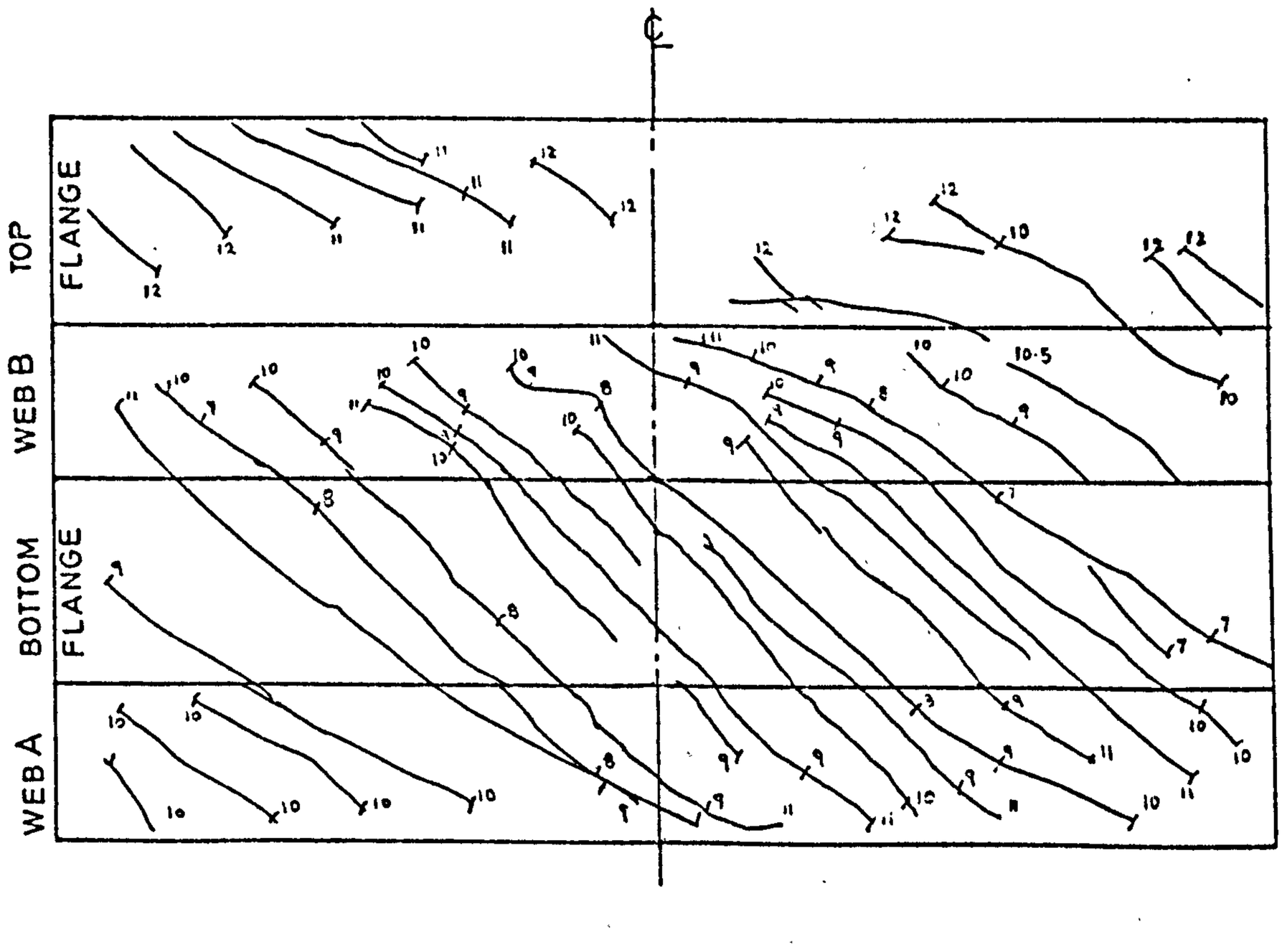

SPECIMEN No.B45

$\frac{M}{T} = 1$

FIG.6.43 CRACK PATTERNS FOR NoB44 AND B45

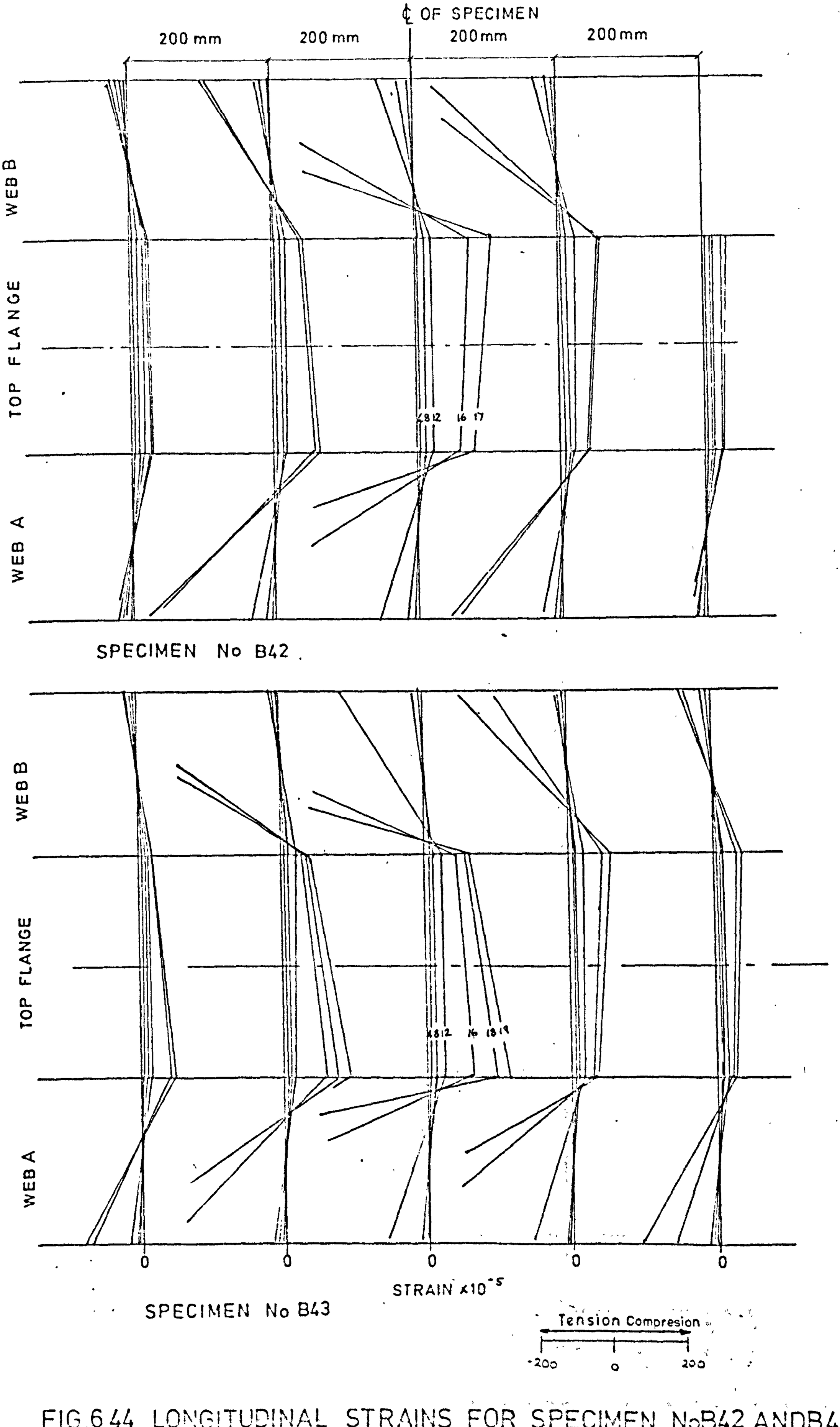

FIG.6 44 LONGITUDINAL STRAINS FOR SPECIMEN NoB42 ANDB43

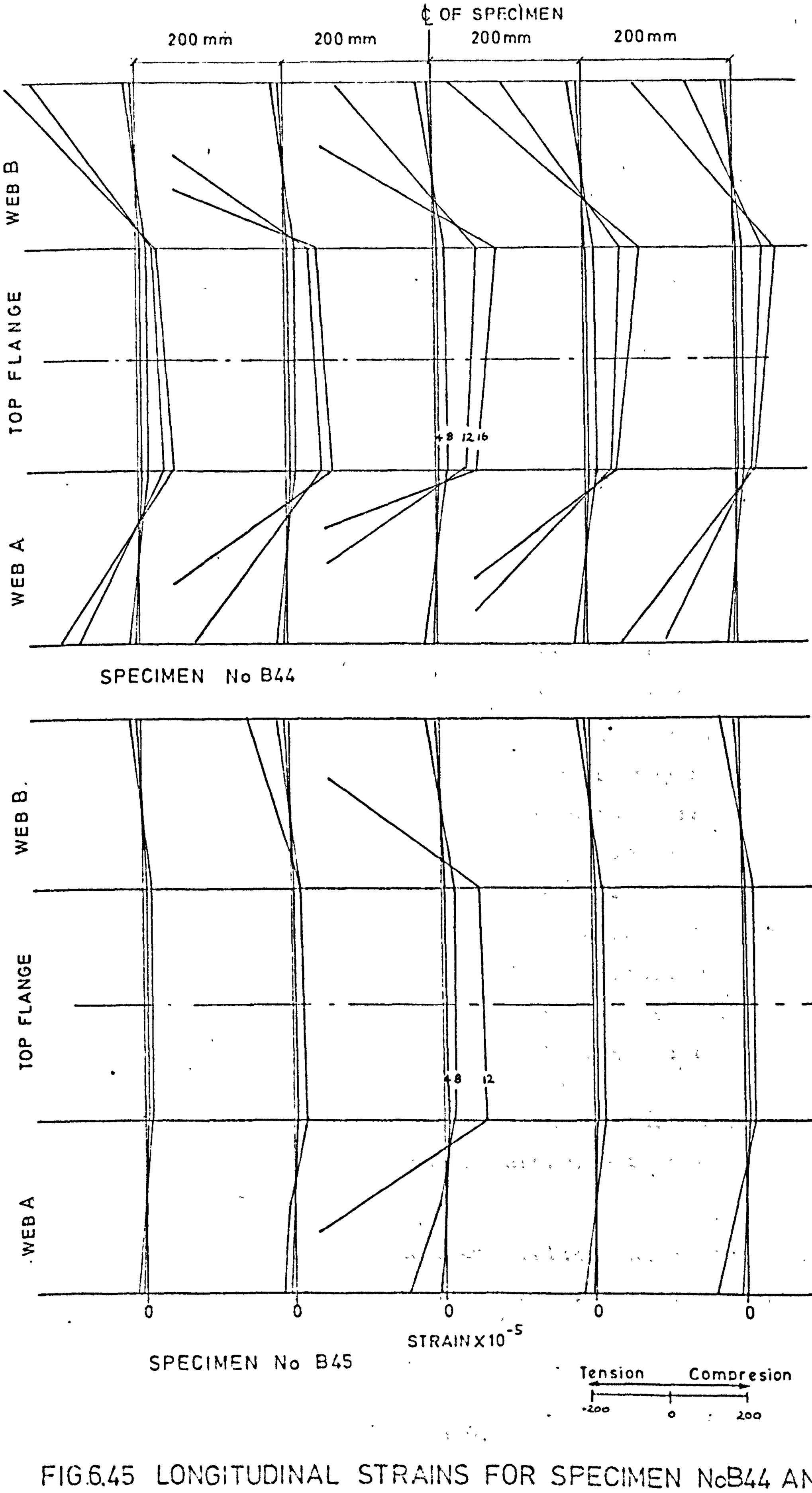

FIG.6.45 LONGITUDINAL STRAINS FOR SPECIMEN NoB44 AND B45

6.7 Discussion of The Results

Any rational method for predicting the ultimate carrying capacity of reinforced and prestressed concrete structural members must consider the following conditions:

a) Equilibrium of forces
b) A law of strain compatibility.
c) A rule of maximum strains for concrete at failure
d) Accurate failure criterion.

These are discussed in the light of the experimental evidence of this investigation as follows:

6.7.1 Equilibrium of Forces

This investigation demonstrated that torque can be transmitted through different load paths at various stages and conditions of the specimens. Many of the internal forces however, may be relatively small and can be ignored. In certain circumstances some of the internal forces may assume a secondary role in resisting the applied torque but they could precipitate local failure which in turn could cause a complete change in the equilibrium conditions of the elements which could then lead to failure. These alternative paths could be summarized as follows:

1. Shear flow in the closed and uncracked box or through the lateral reinforcement in the cracked stage.

2. Shear flow in the open section which may occur after cracking if no transverse reinforcement is present.

3. Dowel action of the longitudinal reinforcement.

4. Differential bending of the flanges and the web after longitudinal cracks have occurred forming an internal bi-moment.

5. Dowel action of the transverse reinforcement, particularly after longitudinal cracks or corner spalling has occurred.

6. Aggregate interlock. The results of these experiments show however, for unbonded pre-stressed concrete beams subjected to high value of that cracks open up considerably as failure is approached. Therefore the interlock forces are negligible. This method of transfer of shear may contribute significantly to the resistance of torque in beams where bond between longitudinal reinforcement and the concrete is fully operative.

7. Resistance of uncracked concrete between adjacent cracks. In beams subjected to pure torsion, the concrete between cracks forms continuous helices from one end of the beam to the other which resists the applied torque.

The multiplicity of load paths in beams subjected to torque is the main reason for the lack of general agreement on how torque is resisted in reinforced concrete and prestressed concrete members and for the absence of a general method for predicting ultimate strength of members when they are subjected to torque.

If the strength of specimen T_1 and T_2 is assessed after cracking of specimen T_1 and rupture of reinforcement of specimen T_2, then it would be

found that new equilibrium condition is established at this loading stage where the applied torque is resisted by the differential bending of the flanges. This conclusion is reached after assessing the strength of the cracked concrete and the dowel action which was found to be small compared with the actual strength of the beams.

In order to determine the manner in which the torque is resisted in the test beams, the numerical average of the diagonal strains measured on the top flange rosettes are plotted against torque for all the beams as shown in Fig. 6.46 and 6.47. Theoretical strain values obtained from the assumption that torque is resisted by:

a) closed section,
b) differential bending of the top flange,
c) open section
d) top flange

are also plotted on the graph. It can be noticed that the measured strain readings closely follow those values obtained from the closed box assumption up to cracking. The strain rate can be seen to increase rapidly after cracking when it approaches the value obtained from the differential bending theory for beams of series 1 and 2. The rate of increase in strain after cracking is seen to be less rapid for beams of series 3 and 4 than for series 1 and 2.

It can be shown that the prediction of torsional strength for these beams based on the torsional resistance of the compression flange will be considerably underestimated.

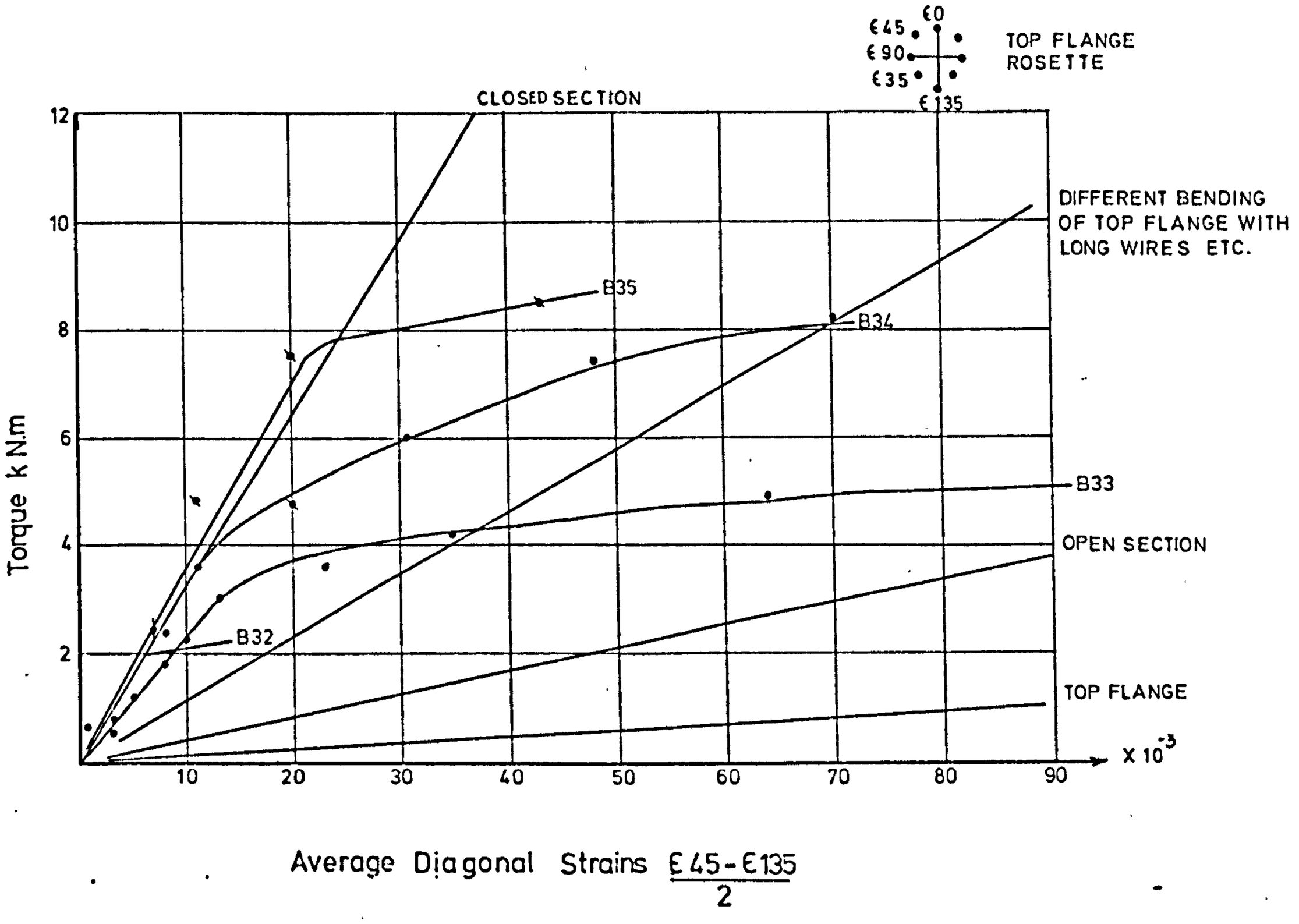

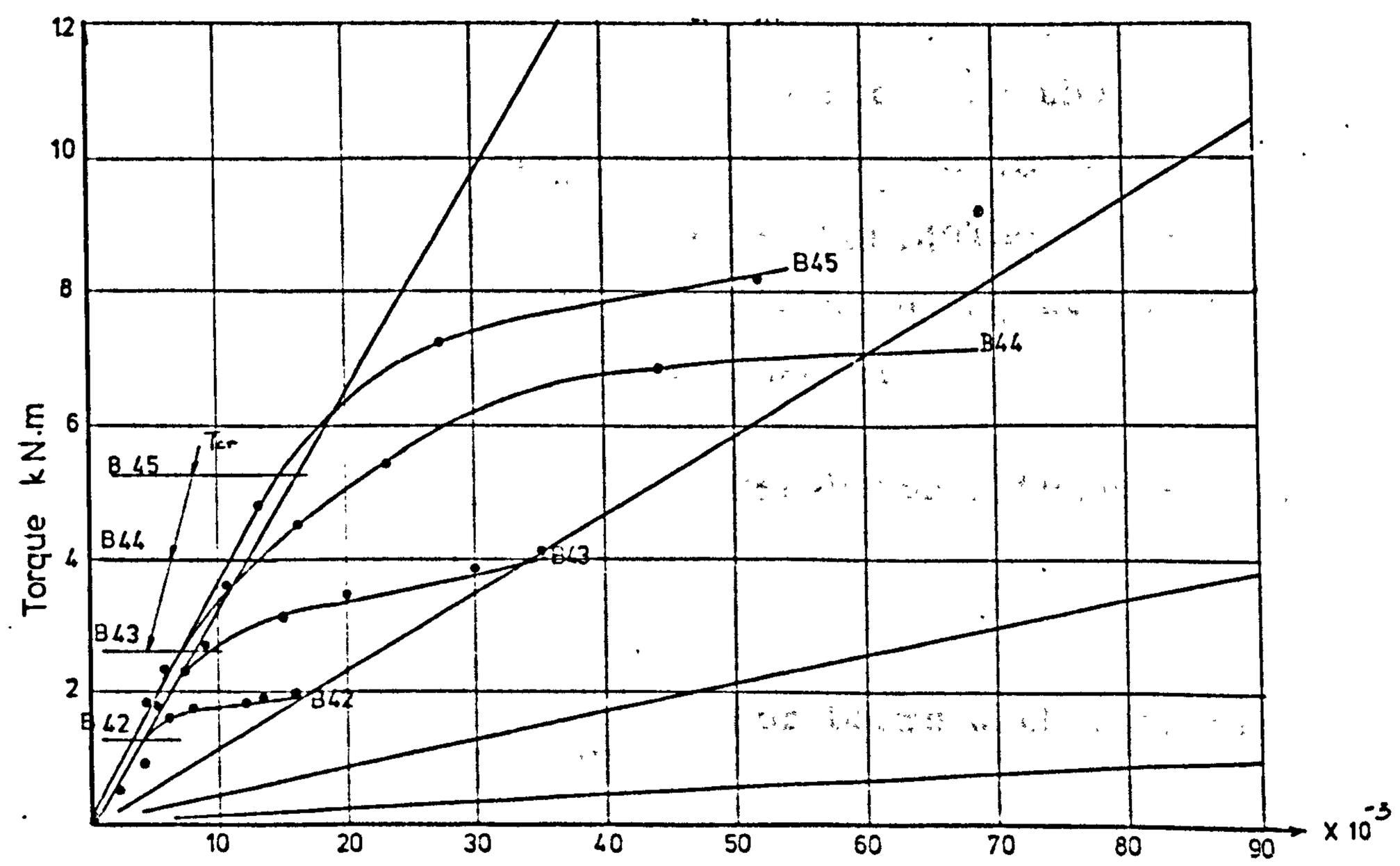

FIG.6.47. TORQUE - AVERAGE DIAGONAL STRAINS MEASURED ON TOP FLANGE FOR SPECIMENS OF SERIES 3 and 4.

6.7.2 Strain Compatibility

The results obtained from the comprehensive longitudinal strain readings agree in general with the assumptions that plane sections before bending remain plane after bending except in the case of beams without lateral reinforcement where the strain readings deviate from this assumption in the locality of major cracks. This phenomena could be more important in a fully bonded beam than in the case of unbonded reinforcement where the force in the tensioned wires remain almost constant over the length of the beam where major cracking occurs, therefore, this assumption can be generally applied for unbonded prestressed concrete beams subjected to a large ratio of $M/_T$.

6.7.3 Maximum Compressive Longitudinal Strain

The maximum compressive strains occuring at failure are found to decrease with a decrease in the value of the $M/_T$ ratio, they are also influenced by the presence or otherwise of lateral reinforcement. The strain results obtained from these investigations are plotted against the $T/_m$ ratio for beams of series 1, 2, 3 and 4 in Fig.6.48&6.49These results indicate that the maximum strain occuring at failure have the following relationship:

$$\epsilon'_u = \frac{\epsilon_{cu}}{1 + (\frac{T}{m})\ 2} \qquad \text{For beams without stirrups}$$

$$\epsilon_u = \frac{\epsilon_{cu}}{1 + (\frac{2T}{m})\ 2} \qquad \text{For beams with stirrups}$$

where ϵ_{cu} is the maximum compressive strain occuring

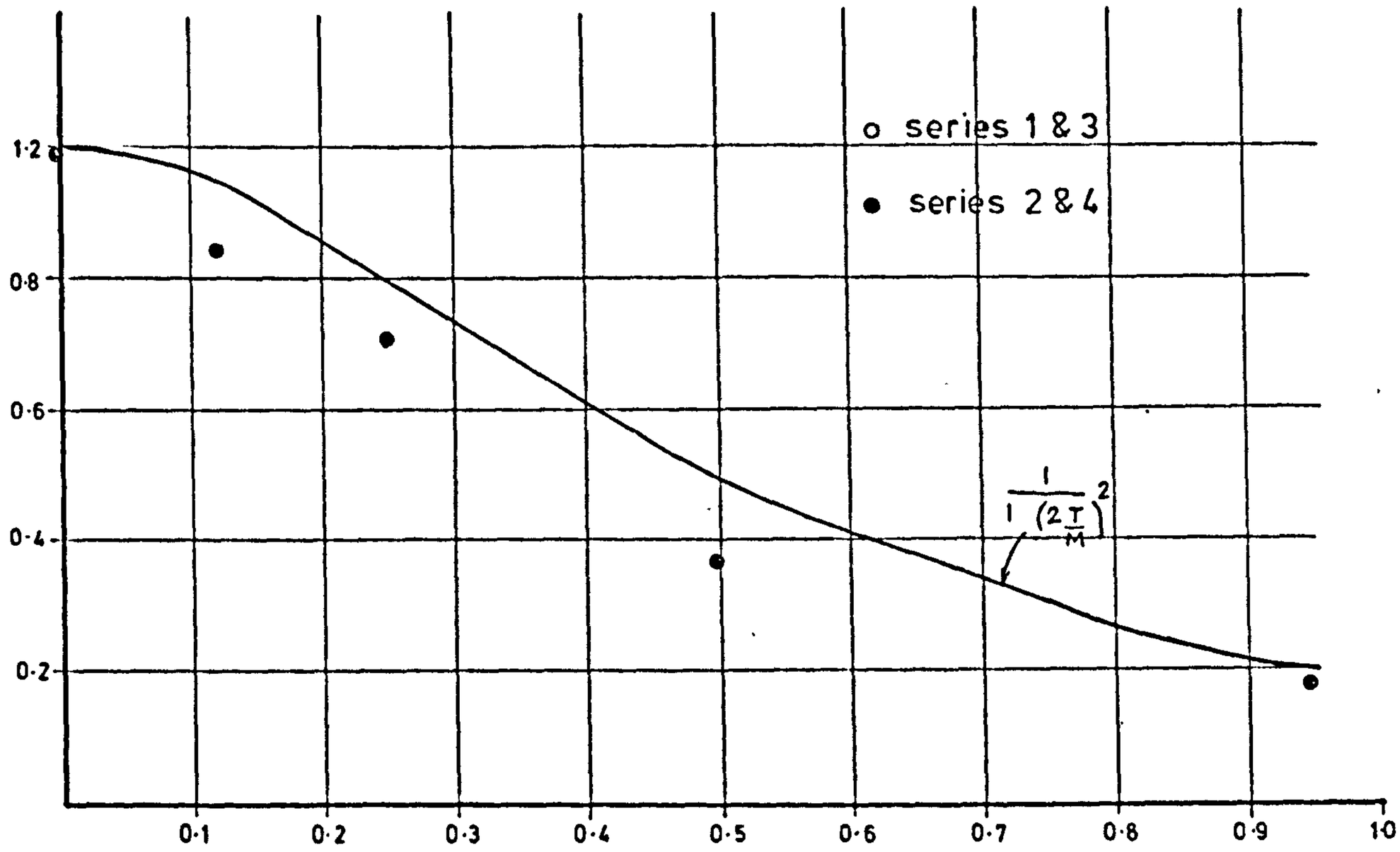

FIG.6.48 RATIO OF MAXIMUM EXTREME LOGITUDINAL FIBRE STRAIN AGAINST T/M RATIO FOR SERIES 1 & 2

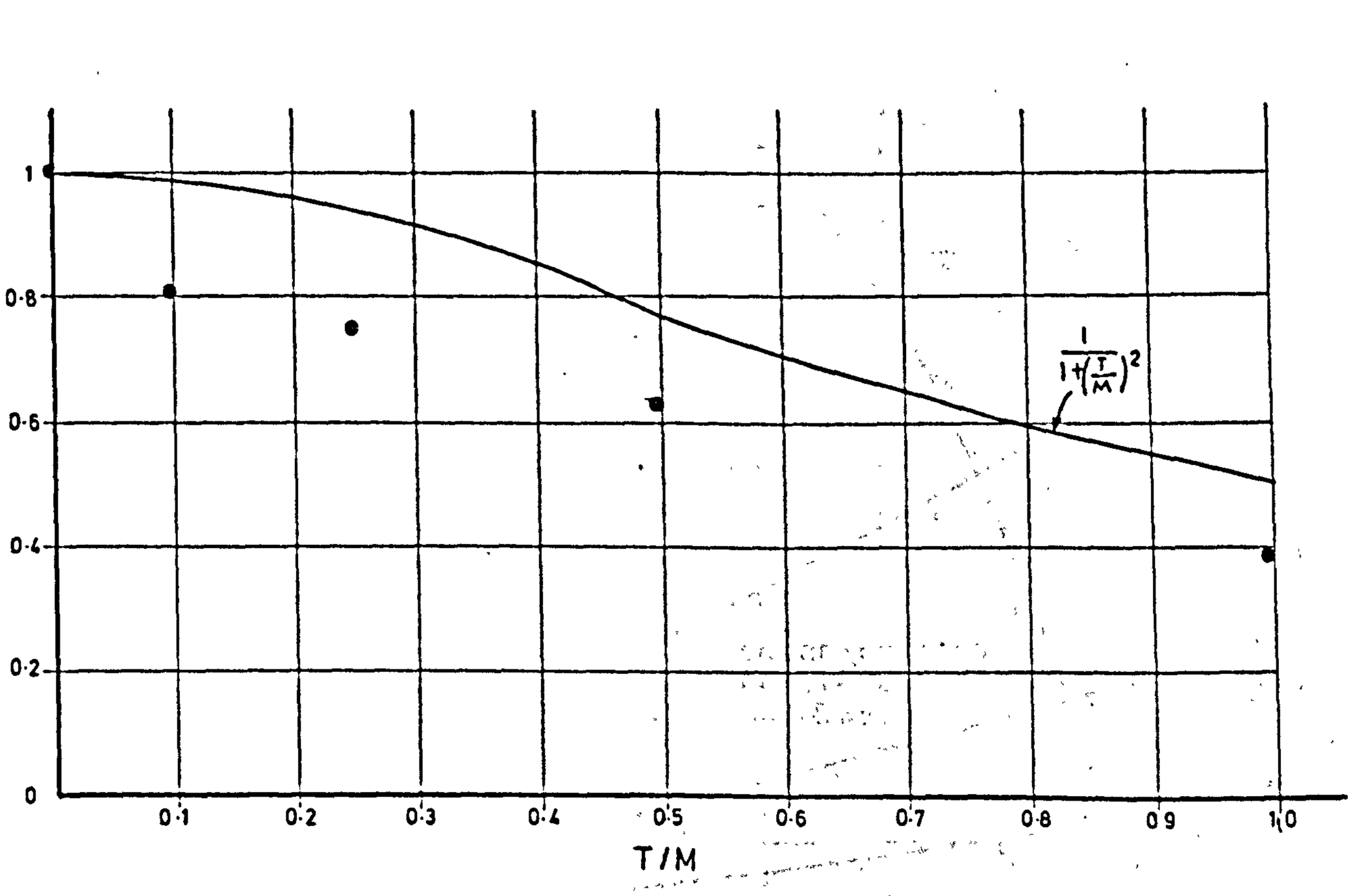

FIG.6.49 RATIO OF MAXIMUM EXTREME LONGITUDINAL COMPRESSION STRAIN AGAINST T/M RATIO FOR SERIES 3 & 4

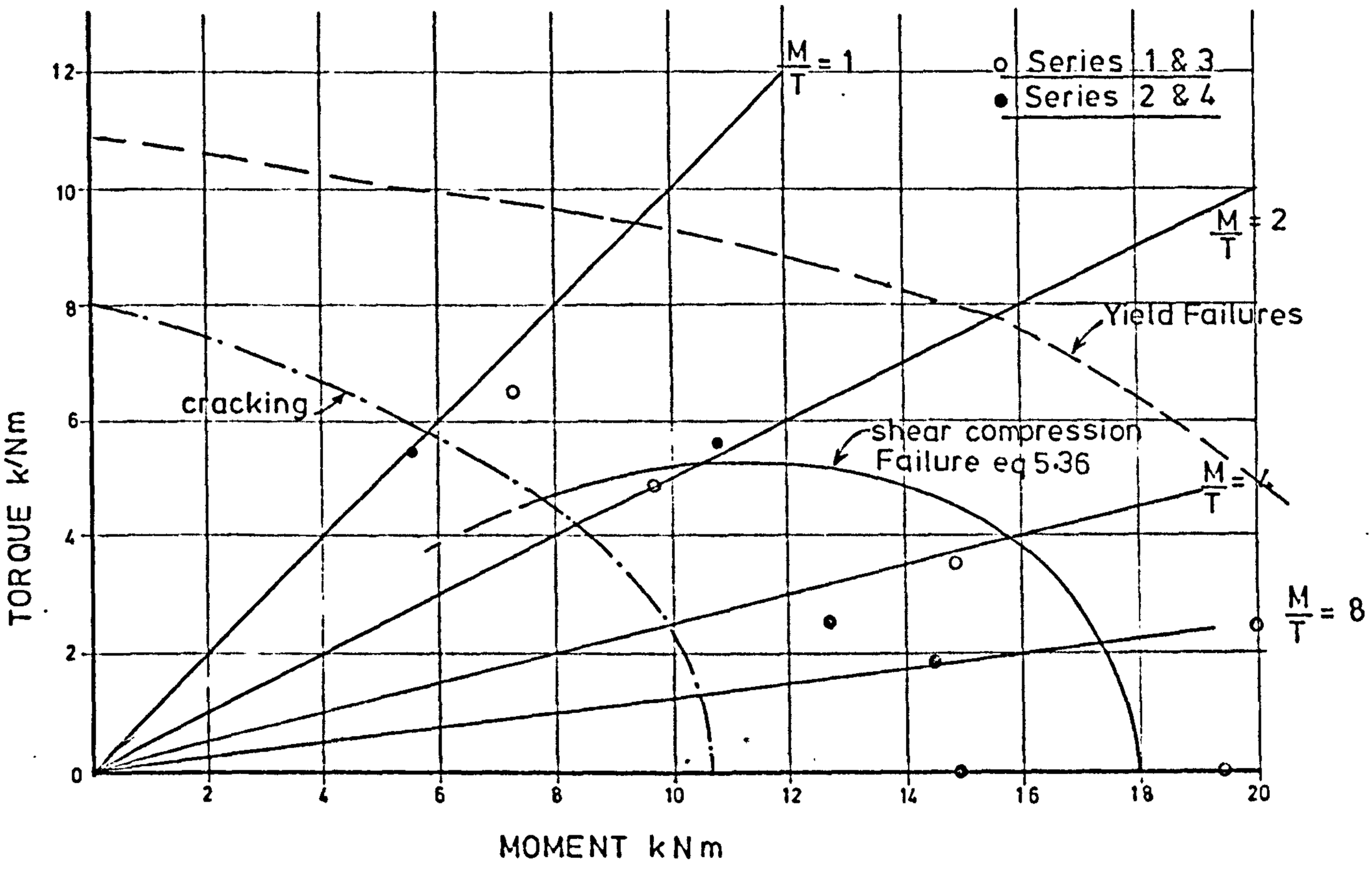

FIG.6.50. BENDING - TORSION INTERACTION DIAGRAM FOR SERIES 1 & 2

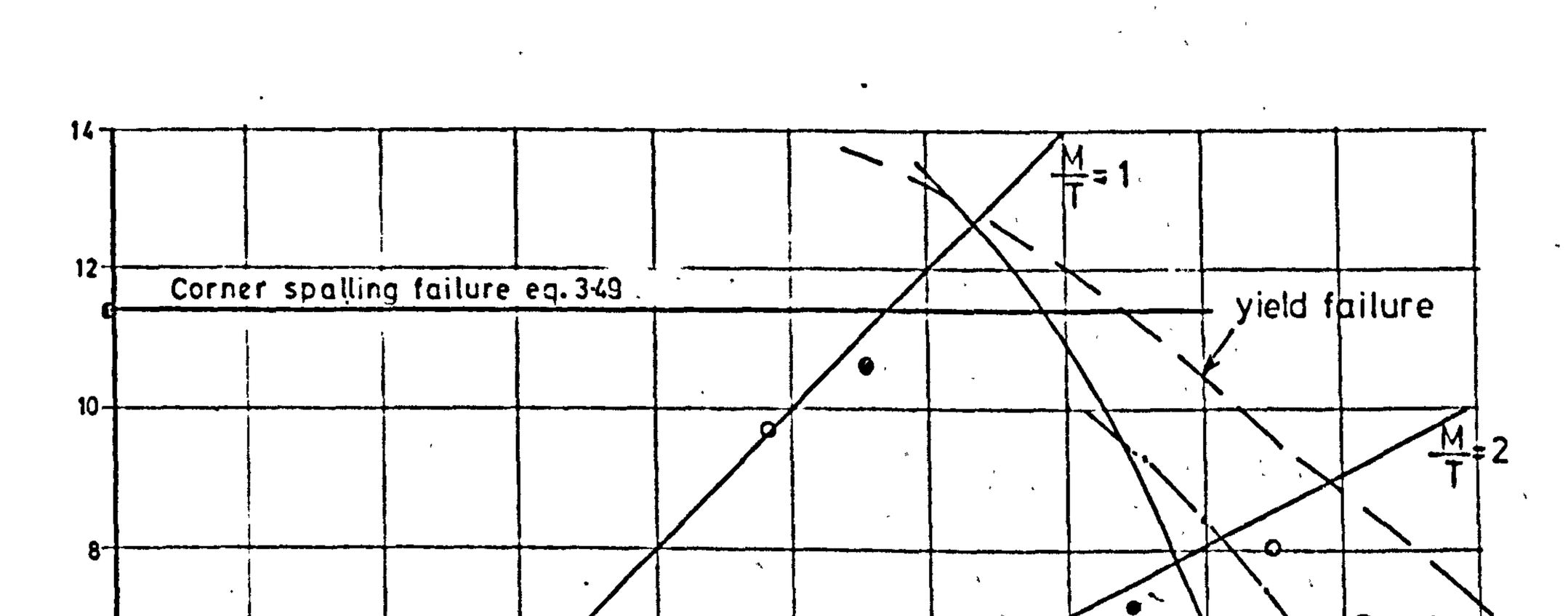

Fig6.51. BENDING - TORISION INTERACTION DIAGRAM FOR SERIES 3 & 4

at the upper most fibre for beams subjected to bending only.

6.7.4 Failure Criterion

The results of this investigation show that beams subjected to bending and torsion on bending, torsion and shear may fail in one of two modes: cleavage failure occuring in beams subjected to low value of $M/_T$. Typical failure of this mode is shown in plate 18, or a crushing type of failure as shown in plate 19 which is associated with beams sustaining a high value of $M/_T$. Therefore, a dual failure criterion is required for any general and rational theory.

6.8 Correlation With Theoretical Results

The Theoretical and experimental results for cracking and ultimate moments for the test specimens subjected to pure torsion, combined bending and torsion and combined bending, torsion and shear are summarized in Table 6.4. The cracking moments were computed by the elastic torsion theory proposed in chapter 2 and using $f_t = 0.45\sqrt{f_{cu}}$ and 15% prestress losses. The ultimate strengths were computed on the basis of the theories given in chapter 4 and 5.

The ultimate load carrying capacities of the tested beams are presented in the interaction diagrame shown in Fig. 6.50 and 6.51. The full lines represent the theoretical interaction curve for loading in torsion and bending and failing by the shear compression mode. The broken lines represent the theoretical interaction curves based on the assumption that all the reinforcement attains full axial yield strength. This comparison clearly

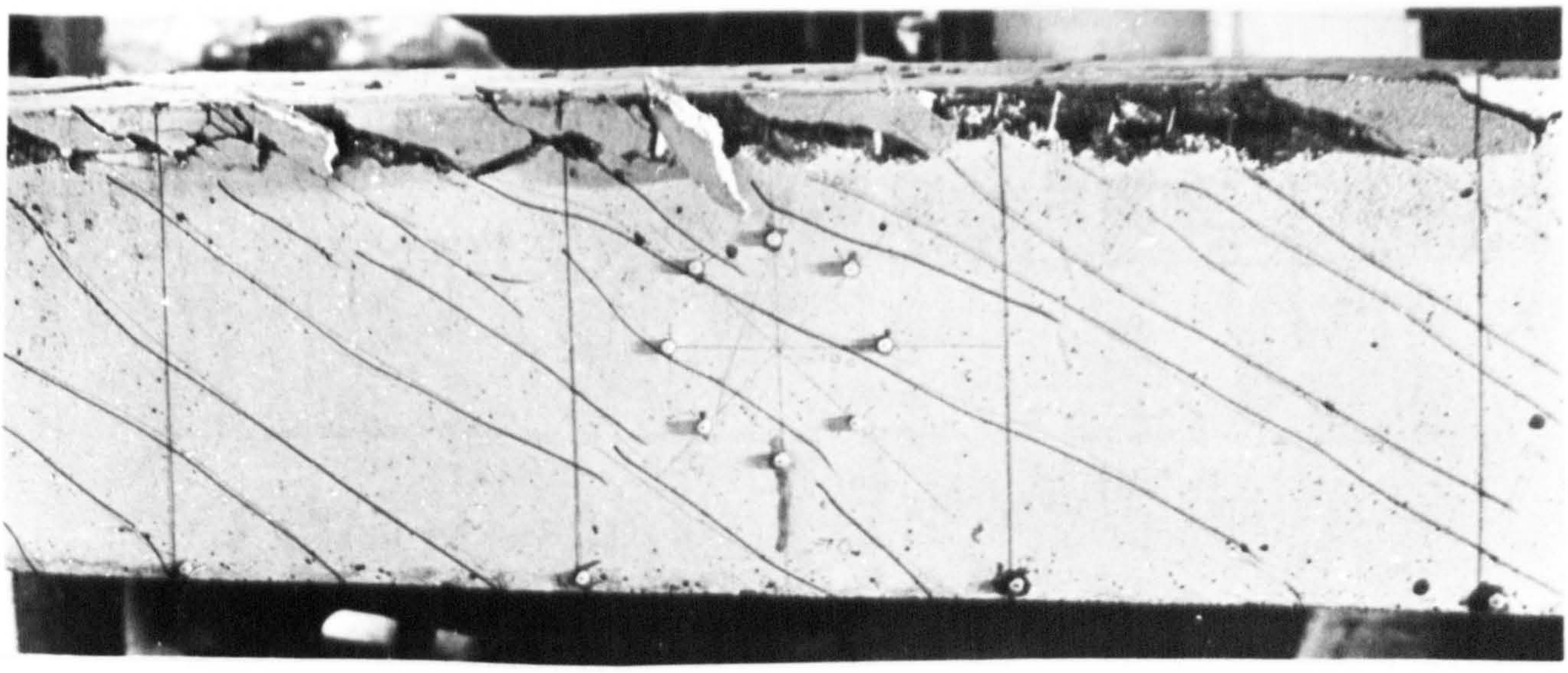

Plate 18 Typical edge spalling failure associated with beams subjected to pure torque or to a low value of $\frac{M}{T}$

Plate 19 Typical shear-compression failure associated with beams subjected to high value of $\frac{M}{T}$

TABLE 6.4. Comparison of Theoretical Predictions with Test Results

Beam No.	Cracking Torque kNm			Ultimate Moments kNm					
	T exp	T th	$\frac{Texp}{Tth}$	Tex	Tth	$\frac{Texp}{Tth}$	Mexp	M_{th}	$\frac{Mexp}{M_{th}}$
To	4.03	4.76	0.85	4.05	4.76	0.85	-	-	-
T_1	8.60	8.19	1.05	8.60	8.19	1.05	-	-	-
T_2	6.10	7.50	0.81	10.10	9.60	1.05	-	-	-
T_3	8.13	9.48	0.86	11.11	13.01	0.88	-	-	-
T_4	8.20	8.46	0.97	13.03	13.4	0.97	-	-	-
B11	0			0			19.50	17.78	1.09
B12	1.52	1.31	1.16	2.50	2.08	1.20	20.00	16.62	1.21
B13	2.64	2.43	1.09	3.51	4.13	0.85	14.82	17.44	0.85
B14	4.25	4.25	1.00	4.81	6.00	0.75	9.71	17.73	0.80
B15	5.49	5.55	0.99	6.58	5.55	1.18	7.29	6.15	1.16
B21	0			0			16.00	18.32	0.87
B22	1.37	1.31	1.05	1.82	2.15	0.85	14.60	17.76	0.84
B23	2.28	2.52	0.91	2.48	3.25	0.77	12.80	16.65	1.07
B24	4.80	4.14	1.16	5.50	6.20	0.89	10.97	17.49	0.84
B25	5.50	5.89	0.93	5.43	5.89	0.92	5.50	5.96	0.92
B31	0			0			19.26	17.89	1.06
B32	1.21	1.20	1.06	2.40	2.16	1.11	19.20	17.39	1.11
B33	2.74	2.39	1.15	5.30	4.33	1.22	21.35	17.35	1.22
B34	4.00	3.99	1.00	8.05	7.91	1.02	17.00	16.69	1.02
B35	6.30	6.53	0.96	9.75	10.80	0.90	9.75	10.80	0.92
B41	0						16.5	17.86	0.97
B42	1.26	1.21	1.04	1.99	2.26	0.88	15.90	18.15	0.87
B43	2.74	2.33	1.18	4.34	4.53	0.96	17.40	18.13	0.95
B44	4.34	4.04	1.07	7.20	7.80	0.92	15.03	16.46	0.91
B45	6.22	5.80	1.07	11.00	11.80	0.93	11.15	11.96	0.93
Mean			1.02			0.96			0.98
C.O.V.			10.16%			13.62%			12.80

demonstrates that the tested beams failed in a shear compression mode before yielding of longitudinal reinforcement was reached.

Table 6.4 also includes the ratio of the experimental cracking torque to the theoretical cracking torque. This ratio has a mean value of 1.02 and coefficient of variation of 10.16%. The ratio of the experimental strength of the theoretical strength for these results has an average value of $\frac{M_{exp}}{M_{th}} = 0.98$ and a coefficient of variation of 12.8%

6.9 Conclusions

From the test results and observations made in this investigation, the following conclusions may be drawn:

1. Inclination of initial cracks and the cracking torque are functions of the magnitude of the prestress and the moment to torque ratio.

2. With decrease in moment/torque ratio, the margin between ultimate and cracking strength decreases. This margin can be increased appreciably at low values of moment/torque ratio by the use of closely spaced sitrrup reinforcement.

3. For the box beams containing stirrups and subjected to combined bending and torque, two distinct types of failure occur depending on the magnitude of moment/torque ratio. With high values of $M/_T$ bending type (shear compression) failures occur. These failures tend to be violent and explosive resulting in the formation of considerable debris due

to crushing of concrete. With low values of $M/_T$ cleavage failures due to spalling of one of the corners of the box occur. This mode of failure is sudden.

4. For box beams without stirrups and subjected to combined bending and torque, three distinct modes of failure are possible:
   a) Crushing failure at the top flange associated with beams subjected to high values of $M/_T$,
   b) Torsional type of failure where the ultimate strength corresponds to the formation of the first crack and
   c) Transitional mode of failure where failure occurs as a result of cleavage fracture of the top flange.

5. The presence of shear in combined loading reduces the ultimate carrying capacity of the beam by the order of 10% compared to beams loaded in torsion and bending only.

6. For beams subjected to combined bending, torsion and shear, the ultimate torsional capacity appears to increase with a decrease in the length of test span.

7. The use of stirrups can significantly improve the ductility of the beam.

8. Cracking causes substantial reductions in torsional stiffness particularly for beams without lateral reinforcement.

9. The maximum compressive strains at the extreme fibres occuring at failure decrease with a decrease in the moment torque ratio and are influenced by the presence or otherwise of

lateral reinforcement.

10. The strain distribution across any section follows approximately the Bernoulli law when lateral reinforcement is present and deviate appreciably for beams without lateral reinforcement.

11. The proposed theories predicted the strength and carcking of the test beams with a good degree of accuracy.

CHAPTER 7

BEHAVIOUR AND STRENGTH OF DOWELS IN CONCRETE

Summary

Theoretical and experimental studies on the behaviour and strength of dowels are presented.

The dowel problem has been classified in this study into two categories according to the boundary conditions.

Rational theories for dowel behaviour and dowel strength are developed.

The effect of various parameters influencing dowel strength are examined.

The results of 76 dowel test are reported.

The methods of analysis used show a satisfactory agreement with all the experimental results on dowel which are available in literature and from the results of this test programme.

7.1 Introduction

The use of stud shear connectors in order to obtain a complete composite action between steel and concrete structural components is only one example where shear is transmitted primarily by dowel action. Although the contribution of the dowel action of the reinforcement to the resistance of shear in reinforced concrete and prestressed concrete structures, is recognised, it has been ignored by many research workers studying the strength of reinforced and prestressed concrete beams subjected to shear and torsion. The reason has probably been the lack of information on this subject. However, a few research workers (7.1 to 7.4) studying the behaviour of reinforced concrete beams subjected to shear and bending have in recent years provided some information on the contribution of dowelresistance. Different testing techniques have been devised in each case to assess the behaviour and strength of dowel action and various empirical expressions have been suggested. It can be said that the previous work on dowel action is fragmentated, incomplete and of little use for applications to problems other than those studied by the various investigators.

In order to examine the effect of dowel forces in the reinforcement on the strength of concrete beams subjected to torsion, bending and shear, a thorough understanding of dowel action is needed. The aim of this chapter is to provide a comprehensive study of this problem.

The solution may be simplified by classifying

the boundary conditions regarding the position of supports as shown in Fig. 7.1, into two categories:

1. Where the distance between the dowel force and the vertical reaction shown in Fig. 7.1 is zero.
2. Where the distance between the dowel force and the vertical reaction shown in Fig. 7.1 is infinity.

7.2 Dowel of Category 1

This dowel category represents the dowel action which is induced by the transverse reinforcement of reinforced and prestressed concrete beams subject to pure torsion.

7.2.1 Elastic Analysis

If we consider the bar embedded in the concrete block shown in Fig. 7.1 to be equivalent to a beam that is supported by elastic foundations (Fig. 7.2) such that when the beam is deflected, the intensity of the continuously distributed reaction at every point is directly proportional to the deflection. Under such conditions the reaction per unit length can be expressed by kw, in which w is the deflection and k is the modulus of the foundation. Consideration of equilibrium of an unloaded portion of the beam leads to the following classical beam on elastic foundation equation:

$$\frac{d^4w}{dx^4} - \frac{kw}{EI} = 0 \qquad 7.1$$

where EI is the flexural rigidity of the beam. The solution of this equation for various loading

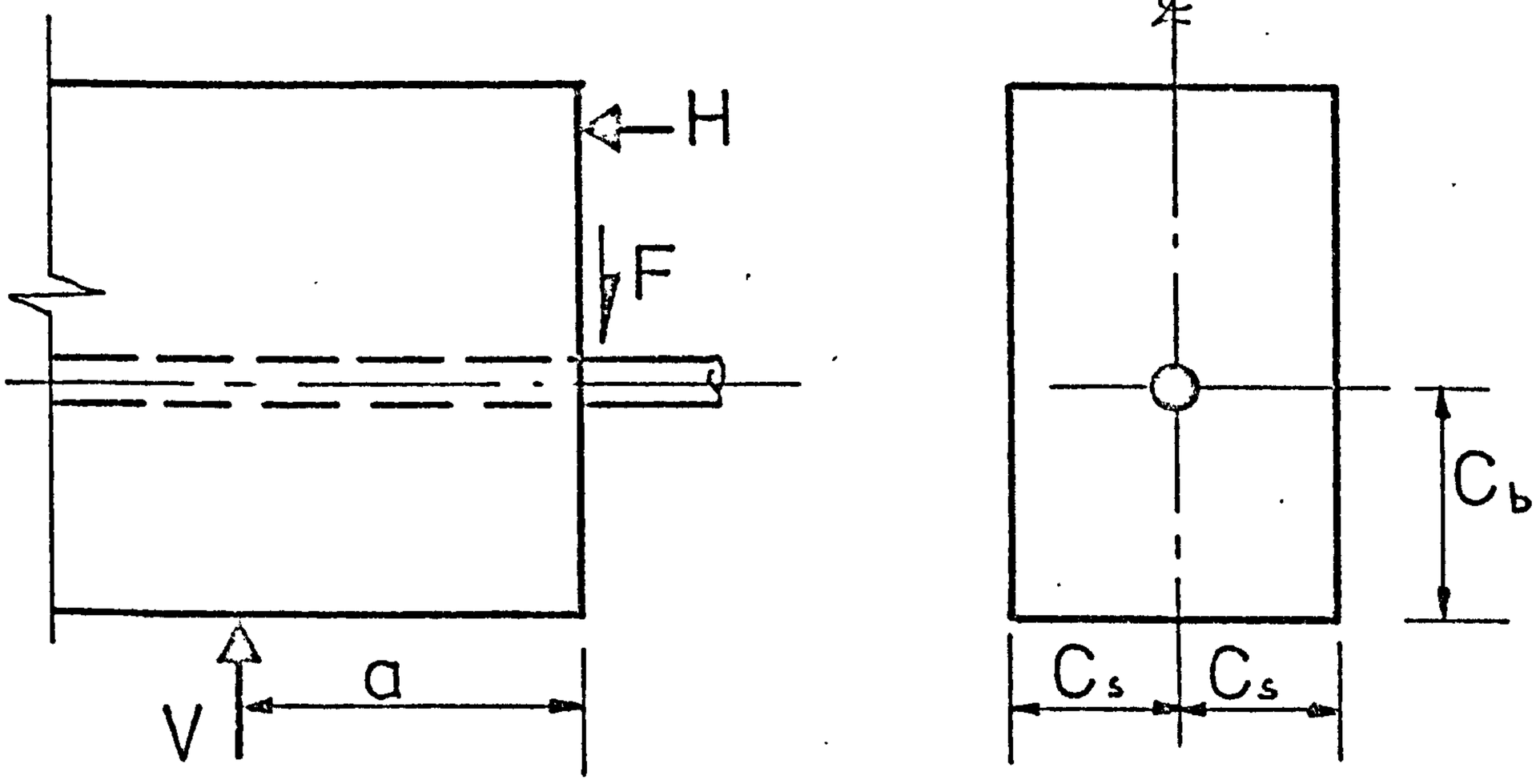

Fig. 7.1 Typical concrete block with dowel.

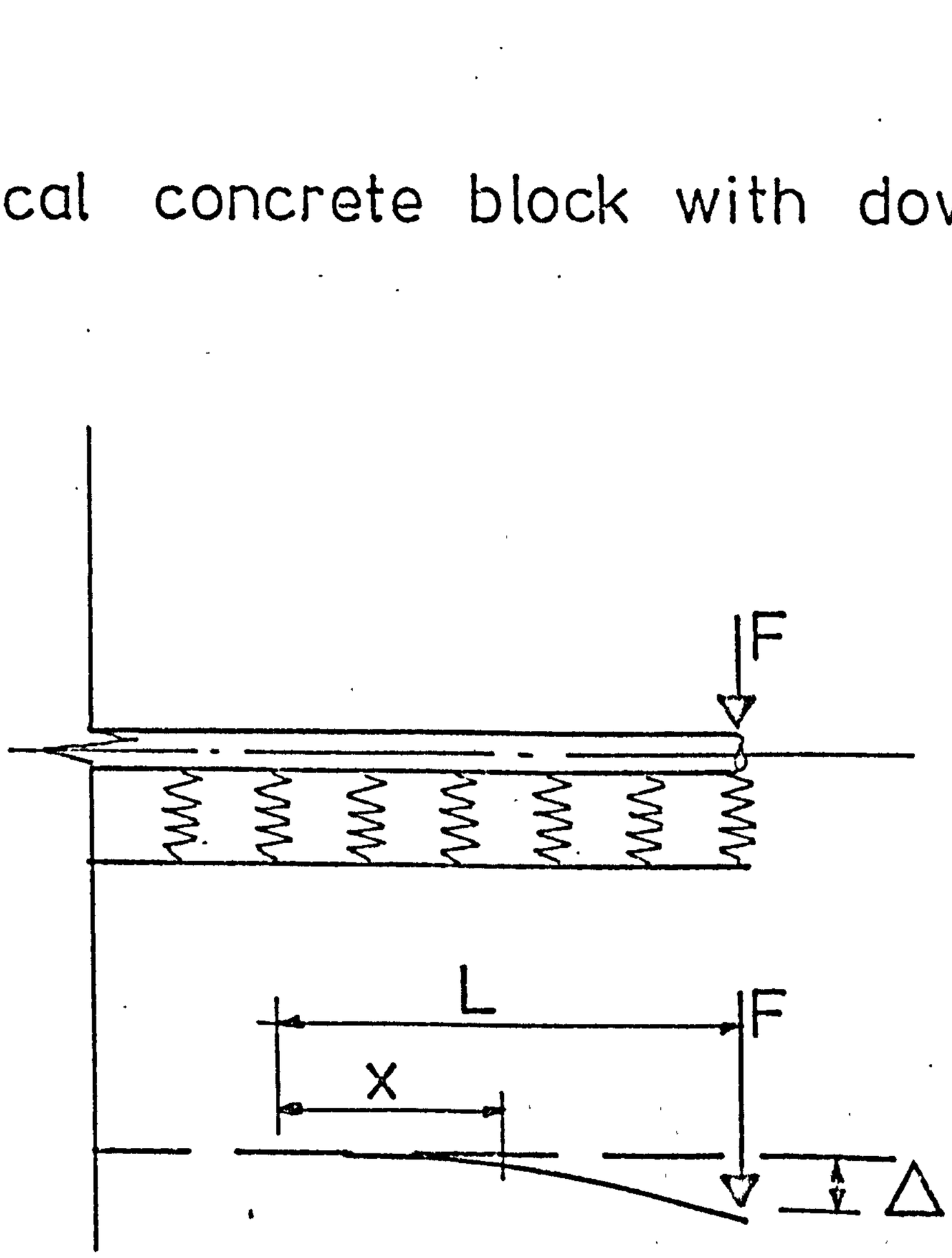

Fig. 7.2 Mathematical model for dowel of category 1

and boundary conditions may be found in a text book on the subject of beam bearings on elastic foundation by Hatanyi (7.5) with a complete discussion on the application and limitation of this method. However, despite the simplicity of this method, equation 7.1 usually yields solutions that are rather cumbersome. Therefore, an alternative treatment of the problem is followed.

In addition to the assumption made above it is assumed that at some distance (L) from the point of application of the load, the bar will remain undeflected. Actually the bar does not become abruptly fixed, but oscillates about the unloaded line. The amplitude of even the first wave after the initial crossing of the unloaded line is small compared with the maximum deflection which occurs under the load and it is thus satisfactory to consider the bar fixed at some definite point.

Assuming that the deflected shape of the beam and its elastic foundation is represented by the following equation:

$$w = a_o + a_1 x + a_2 x^2 + a_3 x^3 \qquad 7.2$$

where a_o to a_3 are constants to be determined from the boundary condition of this problem which are:

at $x = 0$, $w = 0$; $\frac{dw}{dx} = 0$

$x = L$, $\frac{d^2w}{dx^2} = 0$, $w =$

where is the maximum deflection under the load.
If the above boundary conditions are introduced equation 7.2 becomes:

$$w = \frac{\Delta}{2}\left[3 \left(\frac{x}{L_d}\right)^2 - \left(\frac{x}{L_d}\right)^3 \right] \qquad 7.3$$

The total internal en rgy for the beam and its foundation is given by

$$U = \frac{EI}{2} \int_0^L (w\ ")^2\ d\ x + \frac{k}{2} \int_0^L w^2 dx \qquad 7.4$$

where EI and k are as defined previously.
Now substituting equation 7.3 into equation 7.4, the total internal strain energy equation becomes:

$$U = \frac{3}{2}\frac{EI}{L_d^3} \Delta^2 + \frac{33}{28}\ kL\ \Delta^2 \qquad 7.5$$

but the external work done by the dowel force F is $w = \frac{F_d \Delta}{2}$

Equating the internal and external energy,

$$F_d = 3\ \frac{EI}{L_d^3}\ \Delta + \frac{33}{140}\ kL_d \Delta \qquad 7.6$$

To find L so that the energy is a minimum $\frac{dF}{dL} = 0$

$$\frac{dF_d}{dL_d} = -\ 9\ \frac{EI\Delta}{L_d^4} + \frac{33}{140}\ k\Delta = 0$$

$$\therefore L_d = \sqrt[4]{\frac{420}{11}\ \frac{EI}{k}} \qquad 7.7$$

Substituting equation 7.7 into equation 7.6

$$= \frac{35}{11}\ \frac{F_d}{kL_d}$$

or

$$= \frac{L_d^3\ F_d}{12\ EI} \qquad 7.8$$

The pressure at any point may be found from wk

$$P = wk = \frac{35}{22}\left[3\left(\frac{x}{L_d}\right)^2 - \left(\frac{x}{L_d}\right)^3\right]\frac{F_d}{L_d}$$

and the maximum pressure is given by:

$$P_{max} = k = \frac{35}{11}\frac{F_d}{L_d} \qquad 7.9$$

It can be shown that the maximum moment acting on the beam will occur approximately at $\frac{L}{2}$ from the load and is equal to

$$M = 0.2\ F_d\ L_d \qquad 7.10$$

7.2.1 Evaluation of k_c

The bearing characteristics of concrete blocks subjected to concentrated loads has been studied for the purpose of this investigation. A typical load/deflection relationship is given in Fig. 7.3. It can be seen that the load/deflection relationship is reasonably linear. The modulus of the foundation per unit area (k_o) was found to be affected slightly by the shape, size of the loading areas and the position of the concentrated load on the concrete block. However, k_o was found to have a value varying from $\frac{E_c}{50}$ to $\frac{E_c}{100}$ kN/mm^3, therefore, an average value of $\frac{E_c}{75}$ is suggested.

The modulus of the foundation per unit length k is therefore

$$k = k_o \varnothing$$

where $\varnothing$ is the diameter of the dowel

substituting $k_c = \frac{E_c}{75}\varnothing$ and $I = \frac{\varnothing^4}{20}$ in equation 7.7 we get:

$$L_d = 3.5 \sqrt[4]{\alpha_e}\ \phi^{3/4} \qquad 7.11$$

where e is the modular ratio $\frac{Es}{E_c}$, and for

$$\alpha_e = 10\ ,\ L \simeq 6\ \phi^{3/4} \qquad 7.12$$

7.2.2 Comparison With Test Results

In a recent investigation on the behaviour of dowel action, Dulacsha (7.8) measured the slip (maximum deflection) in series of specially designed specimens and gave the following empirical expression for the slip:

$$= \frac{3F_d}{\phi_d 10^6} \sqrt{\frac{1}{f_{cu}} \tan\left(\frac{F_d}{F_u}\ \frac{\pi}{2}\right)}$$

where F is the dowel force in lb, f_u is the ultimate dowel force, f_{cu} is the concrete cube strength in kips/in^2 and is the slip in inches. This expression is plotted in Fig. 7.4 for one of the test results. Also shown are the theoretical results obtained from equation 7.8.

The theory seems to predict deflection with reasonable accuracy up to 50% of the ultimate dowel force. It can be shown that this will correspond to the dowel force causing initial yield in the dowel.

7.2.3 Ultimate Strength

A dowel embedded in concrete reaches ultimate strength as a result of the bar and for the concrete bearing strength reaching their limiting strength. Therefore, different modes of failure are expected. The can be classified as follows:

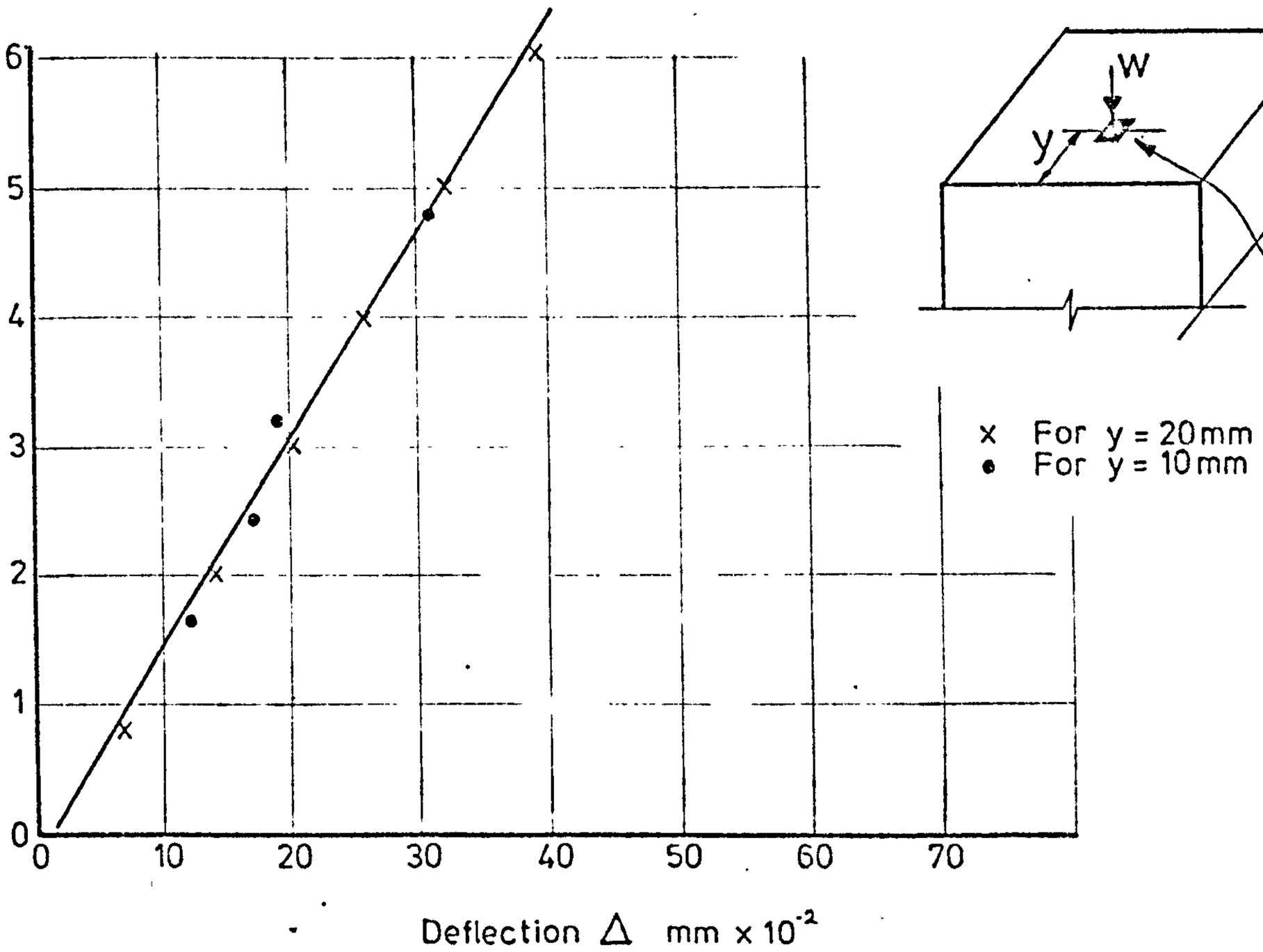

Fig. 7.3 Typical Load / Settlement relationship for concrete .

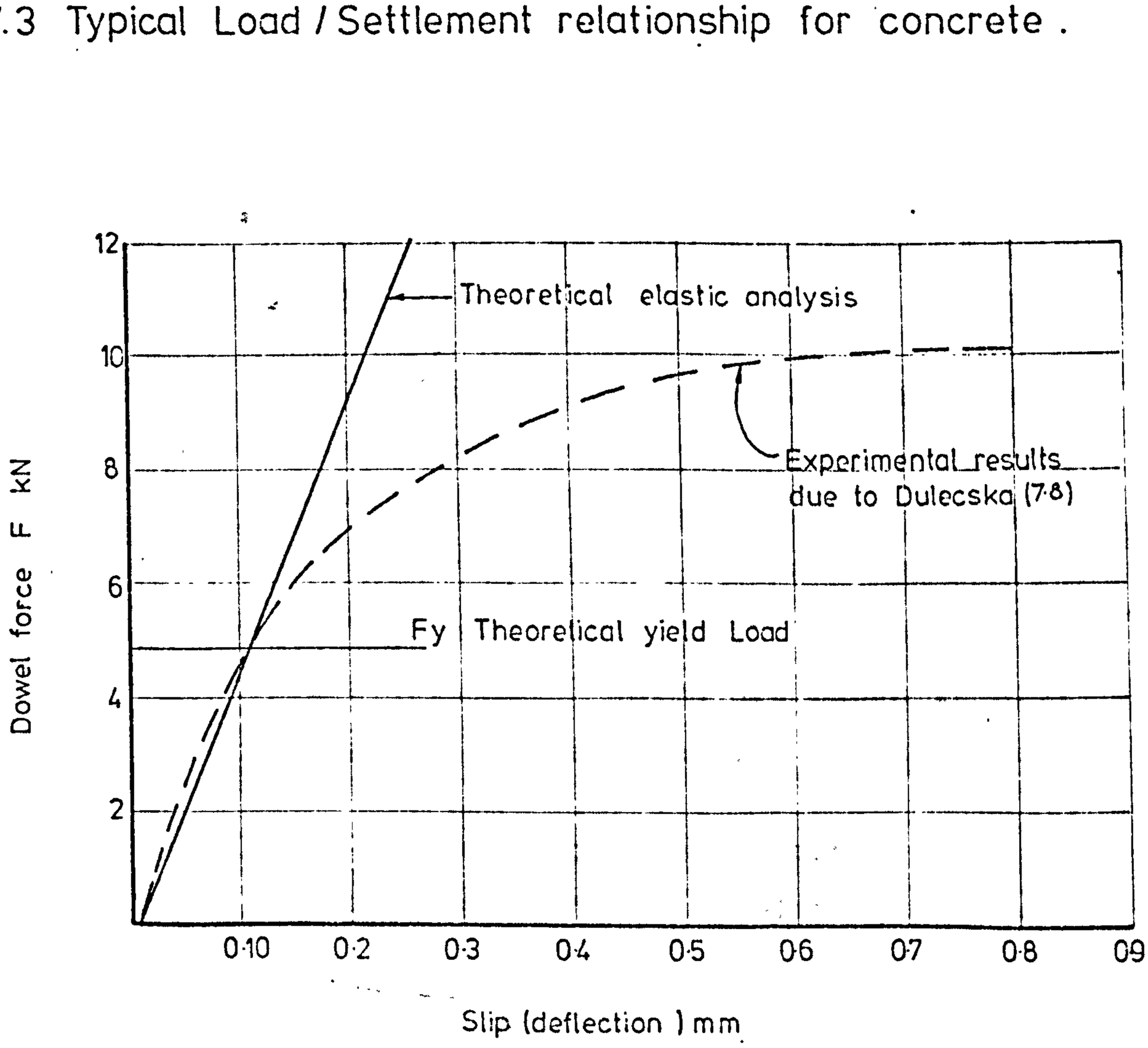

Fig. 7.4 Comparison of dowel Theory with test results .

Elastic Mode

This failure occurs as a result of the concrete bearing stresses reaching the ultimate value, before the steel stresses reach the yield value.

Plastic Mode

In this mode, failure takes place when the bearing stresses reaches the ultimate value after the formation of a plastic hinge in the dowel.

Elastic-Plastic Mode

In this mode, failure takes place when the bearing stresses reach the ultimate value after the yielding of the dowel has started and before the formation of full plastic hinge in the dowel.

However, it is expedient at this stage to examine the bearing strength of concrete before considering these modes of failure further.

7.3 Bearing Strength of Concrete

Due to the lack of research information on bearing strengths of concrete relevant to this problem, it was found necessary to carry out such tests. These tests consisted of a number of concrete blocks subjected to concentrated loads, the details of which are shown in Fig. 7.5. The following factors have been investigated:

a. Size and shape of loading area.
b. Position of loading in relation to the concrete block.

c. Stress (bearing) distribution.

d. Cover to width ratio.

e. Size of specimen.

f. Lateral restraint.

The results and conclusions of this investigation are summarised below.

In order to examine the effect of the above variables on the bearing strength, the variation due to concrete strength was removed by the use of the parameter $\frac{f_{cb}}{\sqrt{f_{cu}}}$ which was suggested by Hawkins (7.6) who found that the ultimate bearing strength f_{cb} is proportional to the $\sqrt{f_{cu}}$.

1. The relationship between the parameter $\frac{f_{cb}}{\sqrt{f}}$ and the cover (C_s)/width of loading area (ϕ) is shown in Fig. 7.6. Cover is defined as the distance from the central line of the loading area to the face of concrete. For small values of $\frac{C_s}{\phi}$, the bearing strength is seen to increase linearly with C_s/ϕ.

2. The ratio $f_{cb}/\sqrt{f_{cu}}$ has an upper limit which depends on the shape of loading area, and the stress distribution above which it will remain constant.

3. For the unsymmetrical cover condition and with a square loading area, the upper limit occured at $C/\phi = 2$ whereas for the symmetrical cover condition using a square loaded area, the upper limit was found to occur at $C_s/\phi = 3$.

4. Two modes of failure were observed, splitting and shearing (crushing). Shearing failure

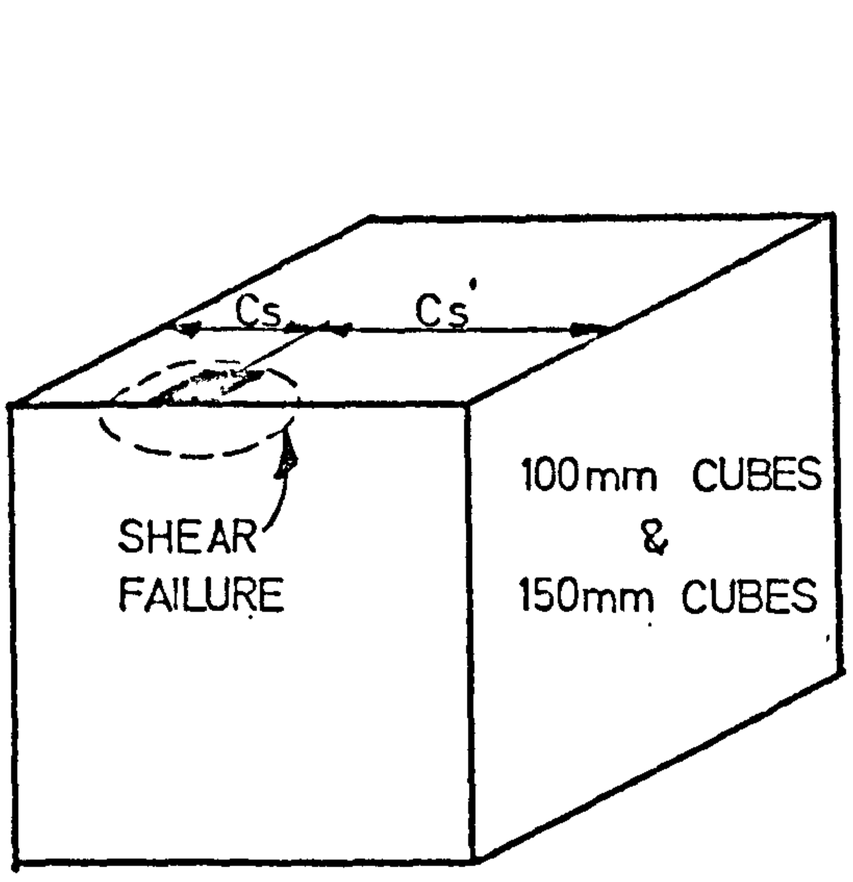

SPECIMENS WITH Cs < Cs'

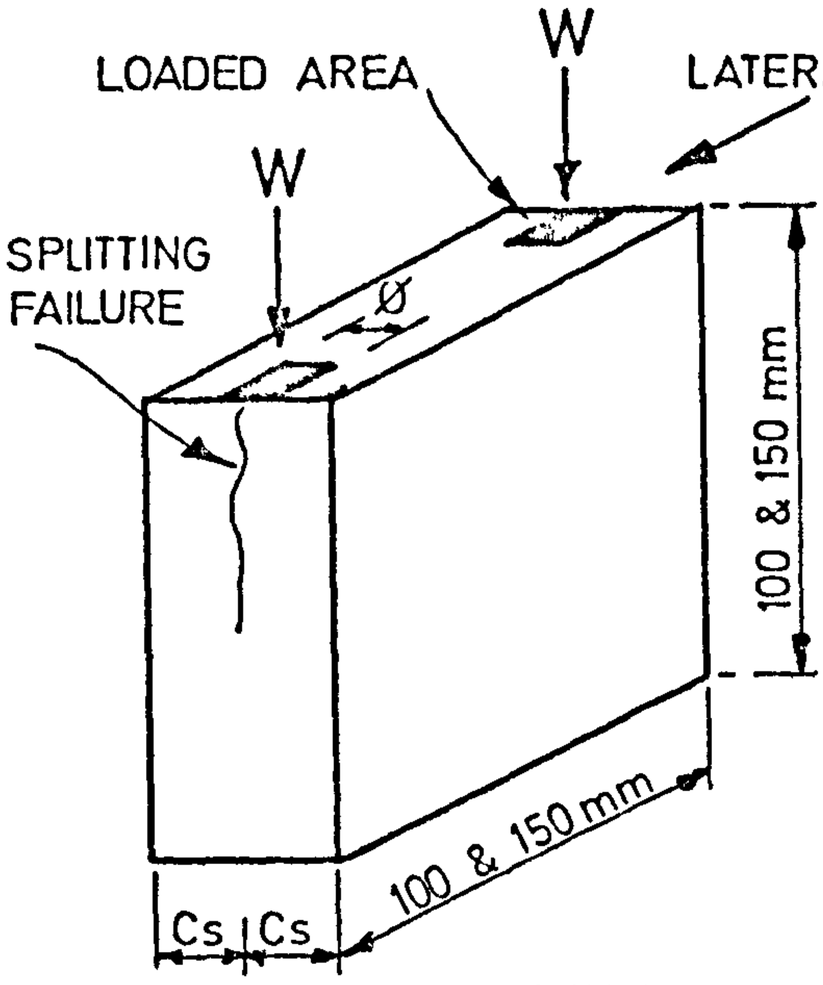

SPECIMEN WITH EQUAL Cs

Size of Loaded Area mm	Cs mm
5 × 5	2·5
	5·0
5 ×10	7·50
	10·0
10 ×10	15
	20
10 ×20	30
	40
10 × 30	50
	60
15 ×15	75

FIG 7·5 Details of concrete block used for the bearing strength tests

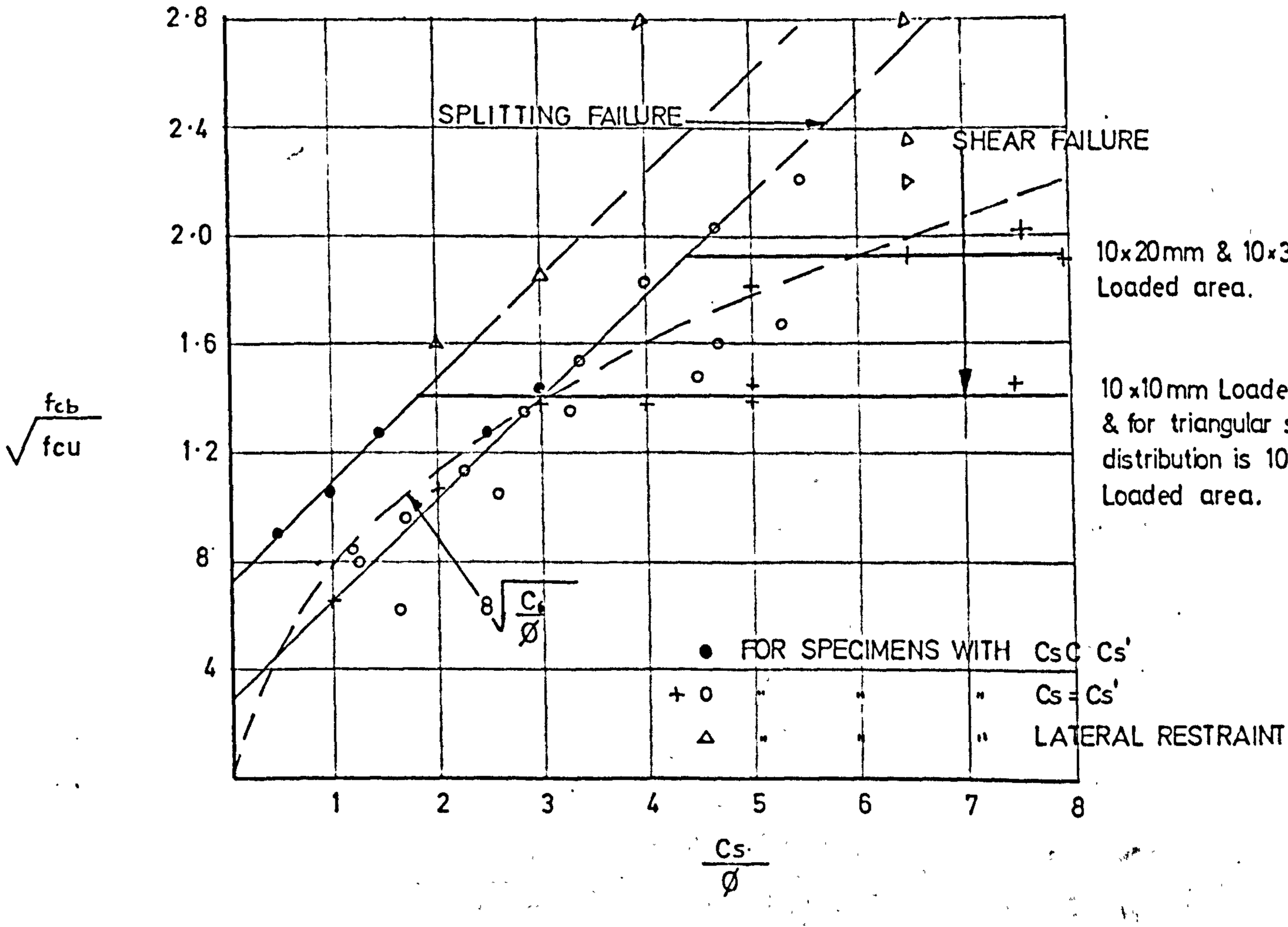

FIG 7·6 Relationships between concrete bearing strength and side cover

was always associated with C/ϕ equal or greater than the upper limit stated above, otherwise failure occured as a result of vertical splitting.

5. When the length of the loaded area was equal to or greater than twice the width; bearing strength continued to increase linearly with C_s/ϕ with an upper limit of $C_s/\phi = 4.5$. Failure was by splitting up to $C_s/\phi = 4.5$ above which failure mode changed to a shearing or crushing.

6. When bearing failure was due to vertical splitting, the bearing strength was appreciably higher for the unsymmetrical cover conditions - than the symmetrical cover condition as shown in Fig. 7.6.

7. The bearing failure characteristics for the case of triangular stress distribution using a rectangular loading area were similar to those obtained from the square and uniformly stressed cases.

8. When a lateral restraint was provided as shown in Fig. 7.5, the bearing strength was unaffected when failure was initiated by splitting. For the cases where C_s/ϕ were above the upper limit stated before, failure was started as for the unrestrained cases, but the specimen continued to sustain further increases in load until failure occured by splitting.

9. The bearing strength was found to depend on the position of loading in relation to the trowelled face of the specimen. The bearing

strength was found to be 20% less when loading was applied near the trowelled face than the opposite face. The bearing strengths given in Fig. 7.6 are based on the averages between the results obtained from the trowelled face and the opposite face. This variation agrees with Coles (7.7) findings which show that when a cube is cut in two halves and each half tested in compression, the half containing the trowelled face was approximately 20% less than the opposite face.

10. Scatters in bearing strength were found to be higher than the compression cube test and to increase as the loading area decreased.

11. There were no significant differences between the bearing strength results obtained from the 100 x 100 mm blocks and those obtained from 150 x 150 mm blocks.

12. The bearing strength may be found from the following expressions:

$$f_{cb} = 8 \sqrt{f_{cu} \frac{C_s}{\phi}} \qquad 7.13$$

7.4 Ultimate Strength of Dowel - Category 1

7.4.1 Elastic Mode of Failure

As stated earlier, this mode of failure would occur when the maximum bearing stress induced by the dowel reaches the ultimate bearing strength of concrete prior to the yielding of reinforcement.

If it is assumed that the load displacement relationship is to remain linear up to failure then from equations 7.9 and 7.12 is obtained:

$$F_e = 1.85 \ \phi^{\frac{7}{4}} \ f_{cb} \qquad 7.14$$

where ϕ is the diameter of the dowel and f_{cb} is the maximum bearing strength obtained from Fig. 7.6 or equation 7.13.

For equation 7.14 to be valid, the maximum stress in the dowel must be equal or less than the yield stress. Therefore, an upper limit to equation 7.14 may be found by determining the dowel force that would cause yielding (Fy). From equation 7.10 we get:

$$\frac{f_y \ \phi^3}{10} = 0.2 \ F_y \ L_d$$

rearranging and substituting L_d

$$F_y \simeq \phi^{\frac{9}{4}} \ f_y \qquad 7.15$$

where f_y is the yield stress of the dowel.

7.4.2 Plastic Mode of Failure

For this mode of failure to occur a full plastic hinge develops in the dowel and the final failure is reached when the maximum bearing stress induced by the dowel reaches the maximum bearing strength for the concrete. At this stage of loading, the deformation of the bar and the bearing stress distribution underneath it are highly indeterminant .

Dulacsha (7.8) and Tharmaratnam (7.9) developed a theoretical expression for this mode of failure based on the assumption that the bearing pressure underneath the dowel are uniformly distributed. The dowel strength

according to these expressions is a function of the diameter of the dowel and the material strength. These assumptions can be seen to be incorrect since the bearing stress below the dowel would vary along the dowel and the bearing strength of concrete is influenced by other factors as was shown previously.

The plastic dowel strength may be assessed with reasonable accuracy if it is assumed that the plastic hinge develops at a distance x + e from the dowel force as shown in Fig. 7.7 and the bearing pressure under the bar is assumed to vary from a maximum value q at point 1 to zero at the plastic hinge as indicated in Fig. 7.7.

Taking moments about the plastic hinge:

$$M_p = F_{dp}\ (x + e) - \frac{5 f_{cb} \varnothing\ x^2}{12} \qquad 7.16$$

where M_p is the plastic moment of resistance of the dowel which is $= \frac{\varnothing^3\ fy}{6}$.

By invoking the theorems of plastic collapse, the dowel force may be obtained by differentiating equation 7.16 with respect to x and equating it to zero.

or $\frac{dM}{dx} = 0$ equation gives:

$$x = \frac{6}{5} \quad \frac{F_{dp}}{\varnothing\ f_{cb}} \qquad 7.17$$

Substituting for x and M into equation 16 and rearranging equation 16:

$$F_{dp} = \frac{5}{6}\ \varnothing^2 f_{cb} \left[\sqrt{\frac{2}{5}\ f \frac{fy}{f_{cb}} + \left(\frac{e}{\varnothing}\right)^2} - \left(\frac{e}{\varnothing} \right) \right] \qquad 7.18$$

The second term under the square root sign in equation 17 can be shown to be very small compared to the first term under the square root sign and hence equation 7.18 may be simplified to

$$F_{dp} = \frac{5}{6} \phi^2 f_{cb} \left[\sqrt{\frac{2}{5} \frac{f_y}{f_{cb}}} - \left(\frac{e}{\phi} \right) \right] \qquad 7.18a$$

and if e = 0

$$F_{dp} = 0.53 \phi^2 f_{cb} \sqrt{\frac{f_y}{f_{cb}}} \qquad 7.18b$$

$$\simeq \frac{A}{2} \; fy \sqrt{\frac{f_{cb}}{f_y}} \qquad 7.18c$$

The position of a plastic hinge may be found by substituting equation 7.18b into equation 7.17 as follows:

$$x = 0.64 \sqrt{\frac{f_y}{f_{cb}}}$$

and for $\frac{f_y}{f_{cb}} = 3$; $x \simeq 1.1 \phi$

7.4.3 Effect of Axial Load on the Plastic Mode of Failure.

The presence of axial force in a beam is known to reduce its plastic moment of resistance, hence, for a beam of a circular section subjected to an axial load (F) the plastic moment of resistance may be obtained approximately from:

$$M = M_p \left[1 - \left(\frac{F}{F_{dp}} \right)^2 \right]$$

where M_p is the full plastic moment of resistance of the section and F_{dp} is the full axial yield capacity of the section.

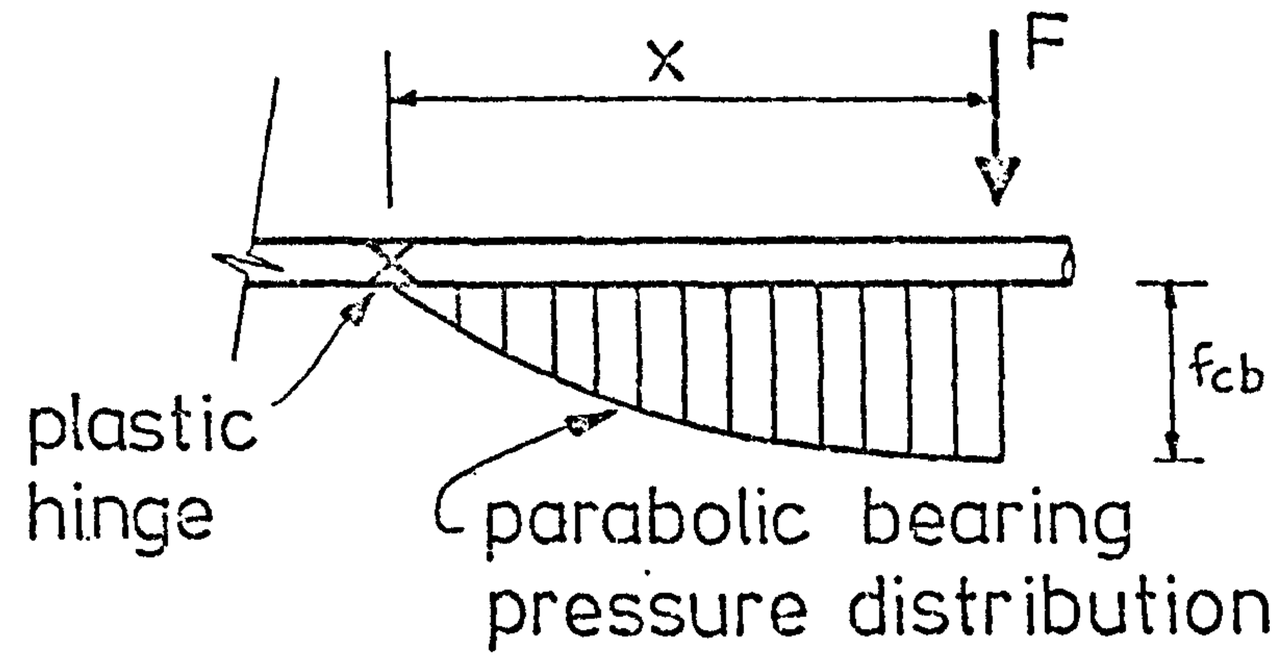

Fig:7.7 Assumed bearing pressure distribution for plastic failure of dowel.

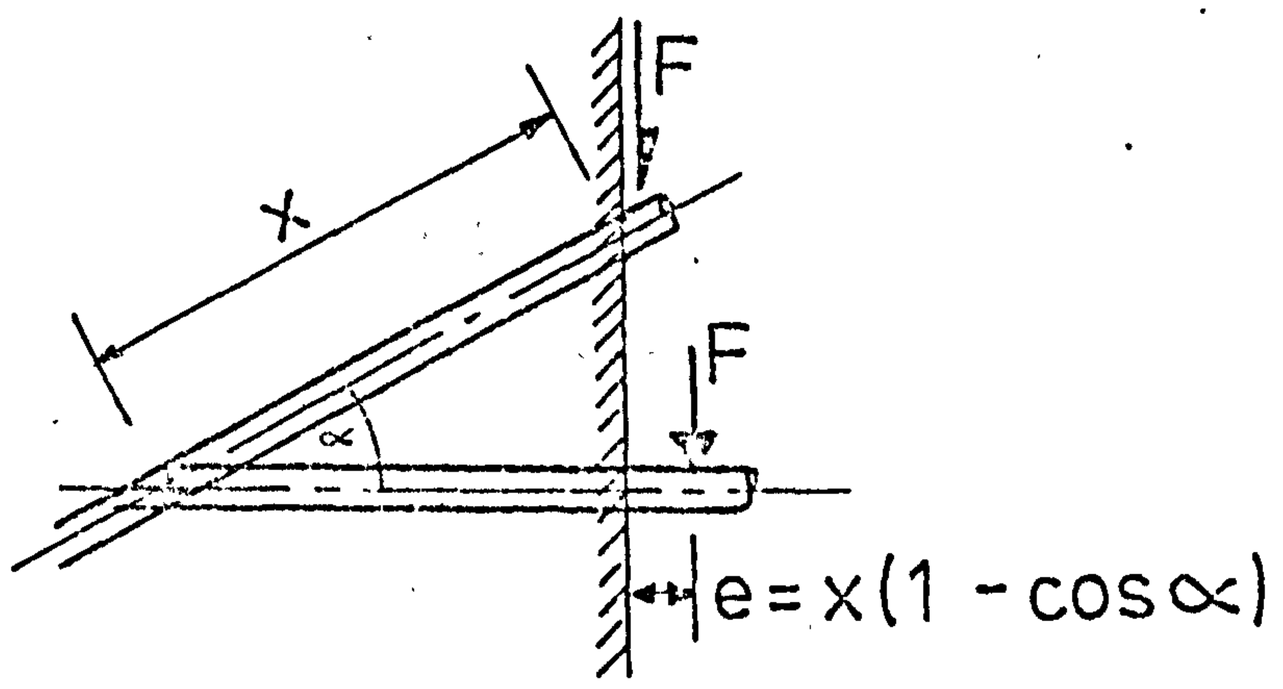

Fig. 7.8 Increase in eccentricity for inclined dowel.

For the case where e is zero, equation 2.18 may be written as:

$$F_{dp}^{\ 2} = \frac{5}{3} f_{cb} \phi \, Mp$$

and for the case where the bar is subjected to axial load, the dowel force will be:

$$F_{d}^{\ 2} = \frac{5}{3} f_{cb} \phi \, M \qquad 7.19$$

Combining the above equations and rearranging in the following non-dimensional equation:

$$\left(\frac{F_d}{F_{dp}}\right)^2 + \left(\frac{F}{F_p}\right)^2 = 1 \qquad 7.20$$

7.4.4 Effect of Bar Inclination on the Plastic Mode of Failure.

The ultimate dowel strength for the inclined dowel shown in Fig. 7.8 can also be predicted from equation 7.18 with the following modification. As a result of the hinge formation and the crushing of the concrete, the bar will rotate and take an almost horizontal position before failure takes place.

If the position of the applied dowel force is to remain unchanged, then as a result of this angular rotation of the bar, the dowel force will have an eccentricity e. If the initial distance between the dowel force and the plastic hinge x is assumed to be $\frac{6}{5}\phi$ and if the dowel is assumed to rotate by an angle α prior to failure, then the eccentricity of the dowel force becomes:

$$e = \frac{6}{5} \phi \ (1 - \cos \alpha) \qquad 7.21$$

Substituting equation 7.21 into equation 7.18 and taking $\frac{f_y}{f_{cb}} = 3.6$:

$$F_{dp} = \phi^2 f_{cb} \cos\alpha$$

Comparing this expression with equation 7.18b it is seen that the dowel strength would be reduced by a factor = Cos α due to the effect of bar inclination. Therefore, equation 7.18b may be modified to account for this effect which gives:

$$F_{dp} = 0.53 \cdot \phi^2 f_{cb} \sqrt{\frac{f_y}{f_{cb}}} \cos\alpha \qquad 7.22$$

7.5 Comparison of Proposed Dowel Strength Theories with Test Results

Plum (7.10) has investigated experimentally the strength of dowel using the specimen shown in Fig. 7.9. The effect of side covers (C_s), the diameter of the bar and the effect of concrete strength have been examined. The theoretical dowel strength has been taken as the smaller value obtained from equation 7.14 and 7.18. The maximum bearing strength was taken from Fig. 7.6. The mean ratio F(exp)/F(th) is 1.17 and the coefficient of variation 14.8 percent. The scatter of F(exp)/F(th) from unity is well within the scatter found in the investigation of the bearing strength of concrete. These scatters are also consistant with results obtained from tests on shear connectors reported by Menzies (7.11).

Dulacsha (7.8) carried out tests on specially designed specimens shown in Fig. 7.9. In this investigation the inclination of the dowel, the diameter of the dowel and the concrete strength

were considered. A summary of comparison between the theoretical prediction and the experimental dowel strength are given in Table 7.1, and Fig. 7.10. The mean of the F(exp)/F(th) is 1.18 and the coefficient of variation is 14.3 percent.

It can be seen that the proposed theory predicts the dowel strength satisfactorily and considers the various important parameters that are known to affect the dowel strength. However, the discrepancy between the theoretical and experimental results may be attributed to the variation between the assumed and the actual bearing and yield stresses of the materials.

In these tests the value of the bottom cover (C_b) was kept constant and the ratio of $C_b/\emptyset$ was relatively high, therefore, further experimental work was needed in order to examine these effects and provide further information about the subject.

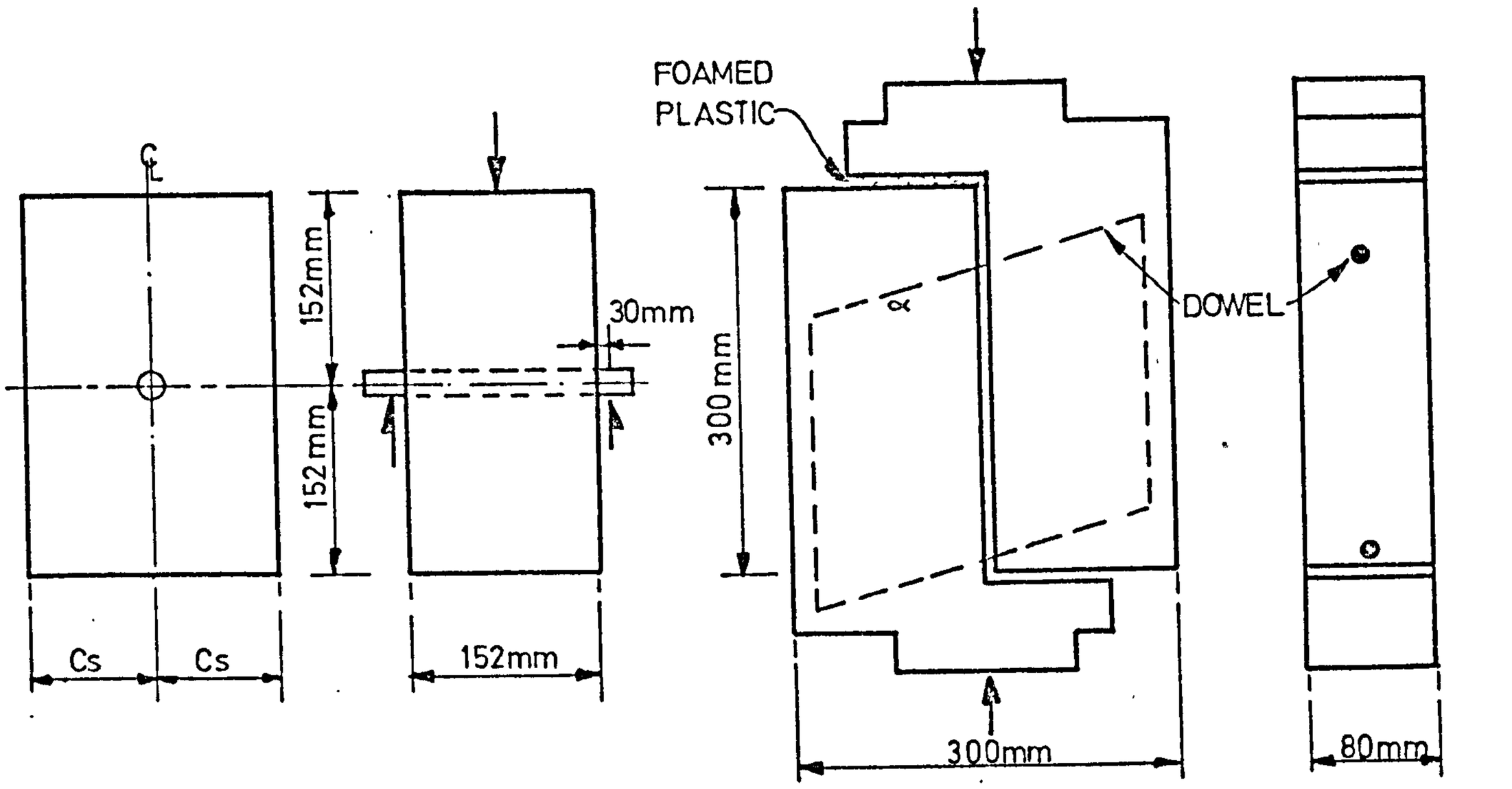

DOWEL TEST ARRANGEMENT DUE TO PLUM

DOWEL TEST ARRANGEMENT DUE TO DULACSHA

FIG 7·9 Details of dowel test specimen due to Plum & Dulacsha

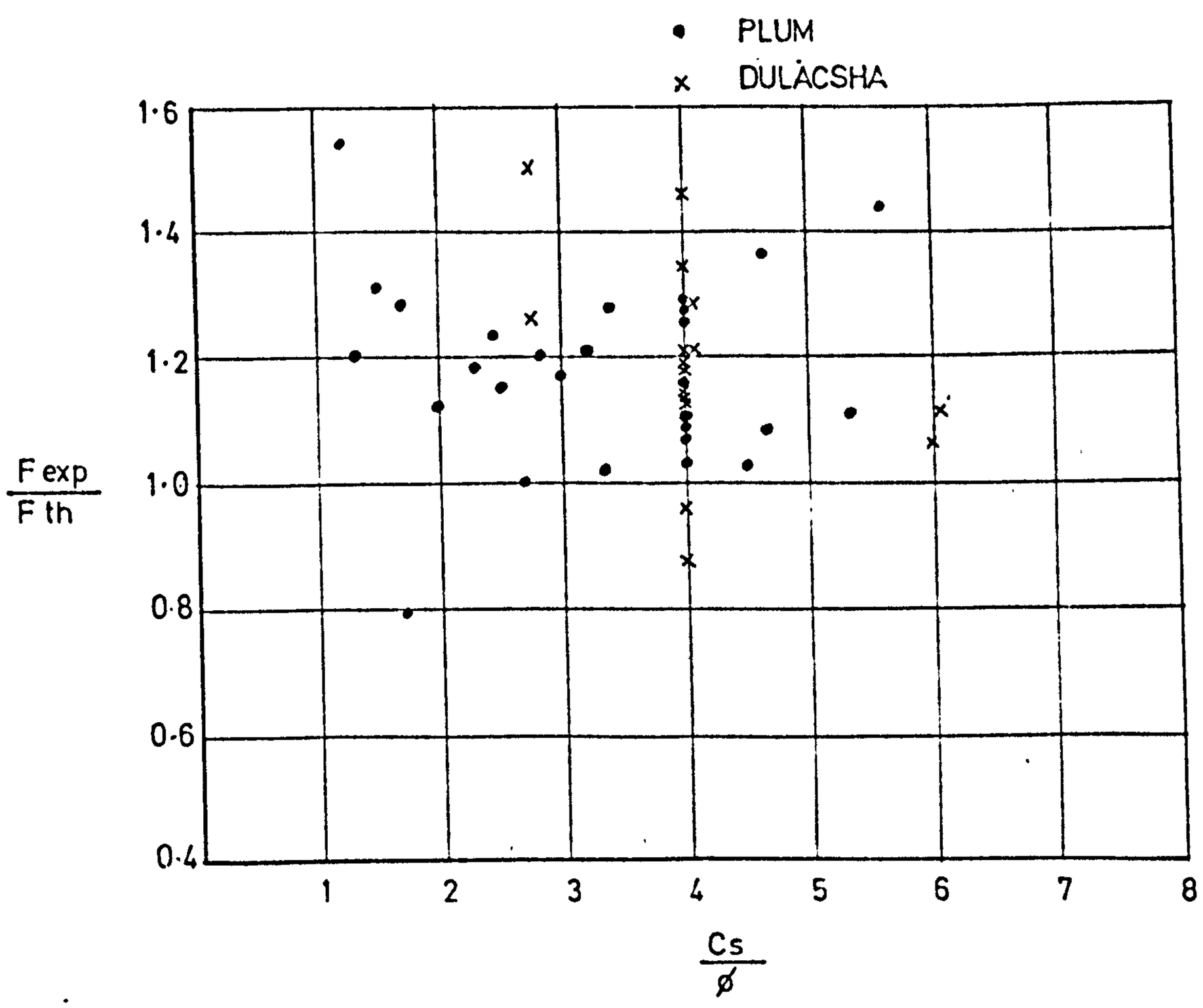

FIG 7 10 Comparison between theoretical prediction and test results.

TABLE 7.1 Comparison between experimental and theoretical Prediction for dowel of Category 1

Investigator	Ref	Mode of Failure	Number of Specimen	Mean $\frac{F\ exp}{F\ th}$	Coefficient of Variation
Plam	7.10	E	18	1.15	14.69
		P	12	1.20	15.07
Dulacsha	7.8	E	4	1.24	19.0
		P	11	1.16	11.22
Total		E	22	1.16	15.9
		P	23	1.18	13.56
		E & P	45	1.17	14.8

E = Elastic mode of failure

P = Plastic mode of failure

7.6 Dowel Tests

In order to examine the effect of C_b/ϕ and provide further test evidence on dowel strength, a series of specimens were tested. The effect of covers C_s and C_b and the dowel diameter were investigated.

The details of the specimens and property of materials are summarised in Fig. 7.11 and Table 7.2. The concrete mix used for fabricating these specimens was the same as the mix used for the bearing strength test. The specimens were tested in an Amesler Universal testing machine as indicated in Fig. 7.11 and the ultimate dowel strength is summarised in Table 7.2.

The mean ratio of F (exp)/F (th) is 0.95 and the coefficient of variation is 10.9 percent. In calculating the theoretical dowel strength no adjustment was made for the effect of C_b/ϕ. The ratio F (exp)/F (th) is plotted against C_b/ϕ in Fig. 7.12. These results clearly indicate that C_b/ϕ has no apparent affect on the dowel strength in this experiment.

It is interesting to compare these findings with those obtained on bearing strengths by Hyland and Chen (7.12) who found that the bearing strength of concrete is independant of C_b/ϕ provided that C_b/ϕ is greater than 2.

TABLE 7.2 Details of dowel test and Comparison between experimental results with theoretical Prediction

Specimen No.	$2C_b$ mm	ϕ mm	$\frac{C_b}{\phi}$	$\frac{C_s}{\phi}$	f_y N/mm^2	f_{cu} N/mm^2	f_{cb}* N/mm^2	Mode of Failure	F (exp) kN	F (th) kN	$\frac{Fd(exp)}{Fd(th)}$
1A	73	6	6.1	5.3	280	28	116	P	3.25	3.31	0.98
1B	73	6	6.1	5.3	280	23	105	P	3.50	3.27	1.07
1C	89	6	7.5	5.3	280	23	105	P	3.10	3.27	0.95
2A	73	10	3.7	3.1	265	28	75	P	7.36	7.50	0.98
2B	73	10	3.7	3.1	265	23	68	E	5.83	7.10	0.82
2C	89	10	4.4	3.1	265	23	68	E	7.48	7.10	1.05
3A	73	16	2.3	2.0	315	28	53	E	12.1	12.50	0.97
3B	73	16	2.3	2.0	315	23	48	E	8.0	11.30	0.71
3C	89	16	2.8	2.0	315	23	48	E	9.85	11.30	0.87
4A	73	20	1.8	1.6	280	28	43	E	13.93	15.1	0.92
4B	73	20	1.8	1.6	280	23	39	E	12.90	13.6	0.95
4C	89	20	2.2	1.6	280	23	39	E	15.35	13.6	1.13
Plastic Mode : mean F exp/F_{th}											0.93
Coefficient of variation											13.10
Elastic Mode : mean F exp/F_{th}											4.00
Coefficient of variation											3.1
Total : mean F exp/F_{th}											0.95
Coefficient of variation											10.9

* From Fig. 7.6

P = Plastic

E = Elastic

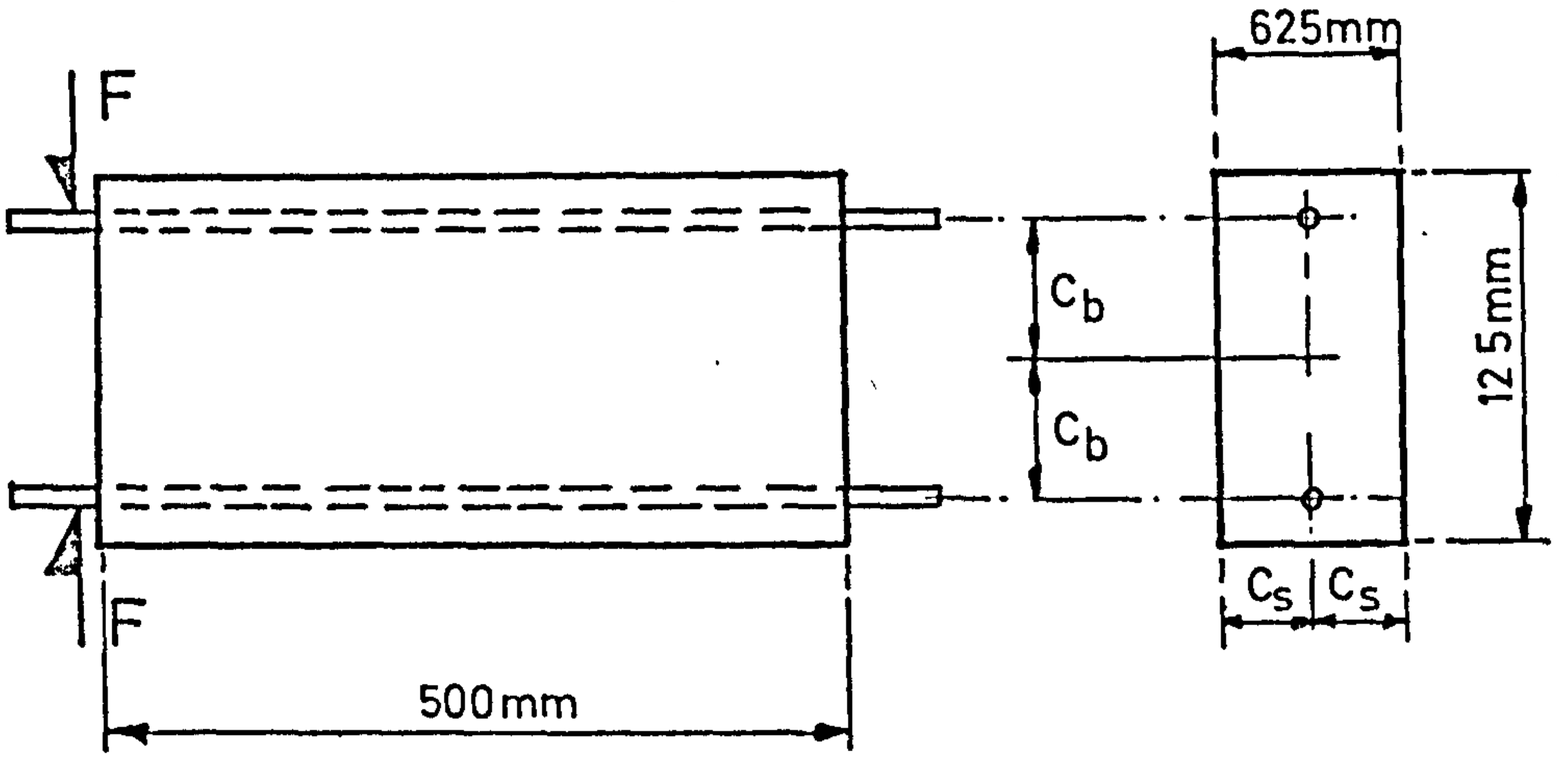

FIG 7.11 Details of dowel test specimen

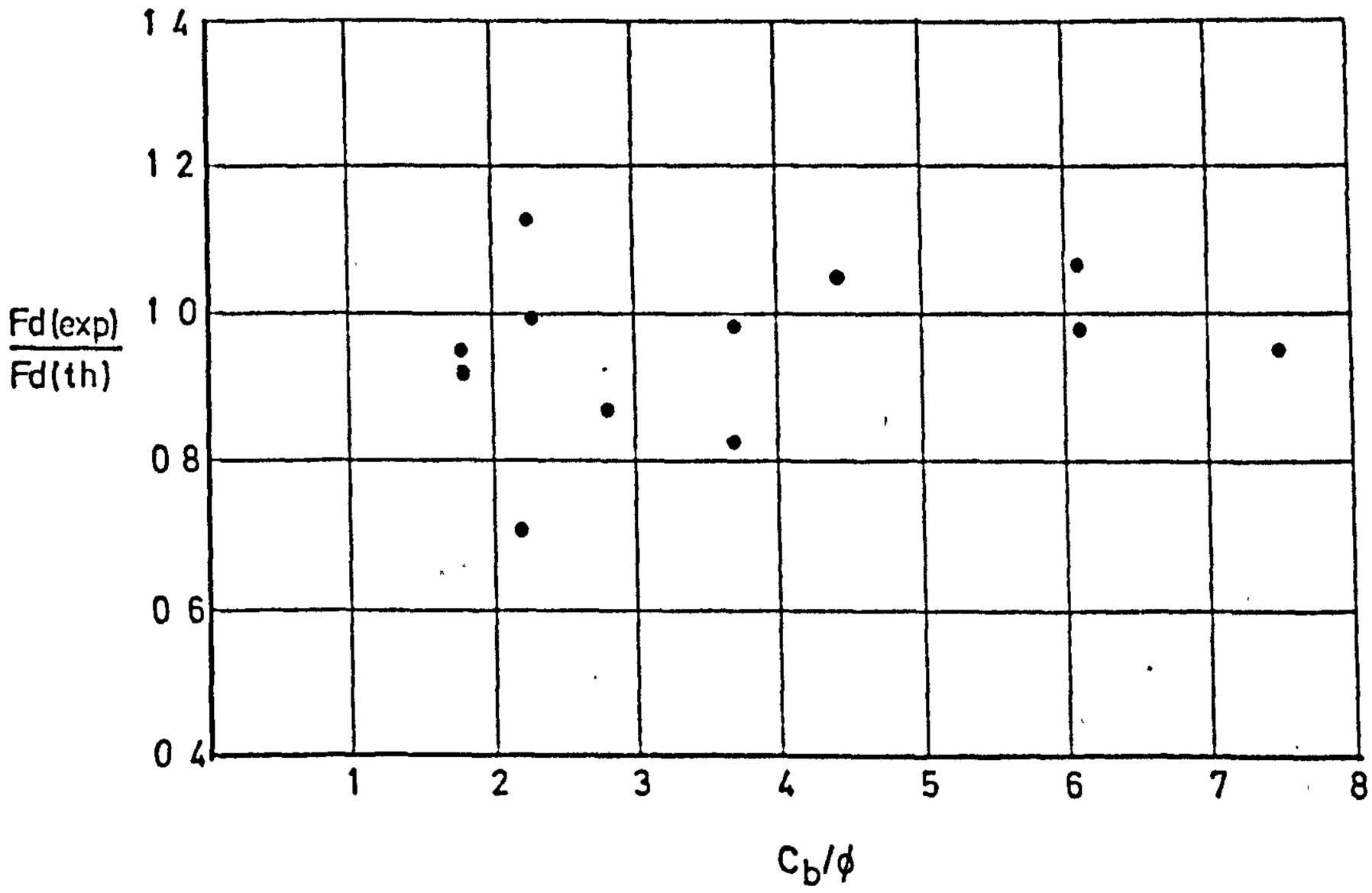

FIG 7.12 Comparison between theoretical predictions and test results

7.7 Dowel of Category 2

This dowel category represents the dowel action which is induced by the longitudinal reinforcement for beams subjected to bending and shear, torsion and other combinations.

A change in the position of the vertical support which was considered earlier would result in fundamental changes in the stress path in the vicinity of the bar, such that, tensile and shear stresses are induced in the concrete surrounding the bar.

If the vertical support is placed outside the length L_d which has been defined in the previous analysis to be the distance from the zero deflection of the dowel to the free end, then it can be assumed that the local stresses produced by the vertical reaction would not influence the stress distribution induced by the dowel force.

These tensile stresses due to the dowel forces could cause spalling of concrete surrounding the bar.

Jones (7.1) was the first to propose a method for predicting the ultimate strength of this type of dowel which is based on the assumption that the reinforcement and the concrete below it (acting compositely) was equivalent to a beam supported on elastic foundation as shown in Fig. 7.13. This foundation was intended to reproduce the action imposed by the concrete above the reinforcement. From the solution of the classical beam on elastic foundation problem, and his experimental results, he produced the following relationship for the dowel strength

$$F_{du} = 0.7\ f_t \sqrt{Z\ I\ b_e}^{\frac{3}{4}}$$

where f_t is the tensile strength of concrete, b_e is the effective width resisting these stresses at the level of reinforcement, I, the moment of inertia of the equivalent beam and Z is the lever arm.

In deriving this equation a number of erroneous assumptions and approximations were made, such as the composite action of the reinforcement and the concrete below it.

Krefeld and Thurston (7.2) carried out nine tests on especially designed specimens aimed at determining the contribution of the longitudinal tensile reinforcement of a reinforced concrete beam to the resistance of applied shear force. They have proposed two expressions for predicting dowel strength. The first was based on a similar mathematical model used by Jones and the following empirical expression:

$$F_{du} = b \sqrt{f'_c} \left[1 - 3 \left(1 + \frac{180P}{\sqrt{f'_c}} \right) C_b + H \right] \sqrt{\frac{1}{\frac{a}{H}}}$$

where a is the distance from the support point to the crack and H is the depth of the specimen.

Fenwick (7.3) carried out tests on a number of specimens using two testing techniques. The first was intended to model the conditions existing between the cracks of a reinforced concrete beam subjected to bending and shear (short dowel) and the second testing technique was intended to model the conditions at the end of a reinforced concrete beam (long dowel). He also developed an expression for the ultimate strength of dowels based on beam

elastic foundations, but he assumed that this beam consisted of the reinforcement and part of the surrounding concrete. The flexural rigidity of the beam elastic foundation EI was taken as:

$$EI = C' E_s I_s$$

where C' is a constant depending on many factors. Substituting the equivalent flexural rigidity of the beam in the solution of the beam elastic foundation problem, the following expression was obtained.

$$F_{du} = \frac{b_e f_r}{2} \sqrt{\frac{4 C' E_s I_s}{k'}}$$

where C' and k' are to be obtained from test results. This treatment to the problem appears to suffer from the same short comings as the solution given earlier by Jones.

Fenwick also gave the following empirical expression for short dowel

$$F_{du} = C'' f_r b S_r$$

where C" is a constant depending on the position of the bar in the mould and Sr is the length of the specimen.

This brief review of the previous theoretical investigations clearly demonstrate the limitation of the various expressions that have been suggested for assessing the dowel strength. They were either based on an erroneous mathematical model or based on a limited number of test results, hence, there is a need for a rational theory that can consider the actual behaviour of the dowel as closely as possible.

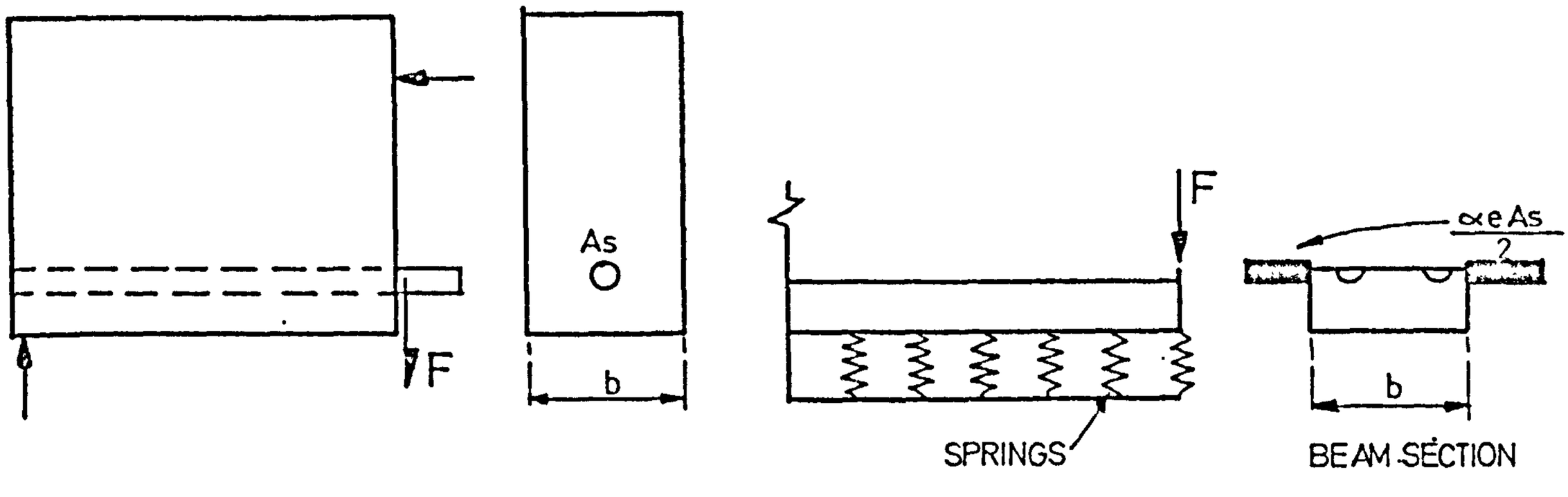

DOWEL OF CATEGORY 2

MATHEMATICAL MODEL OF
DOWEL ACTION DUE TO JONES

FIG 7·13 Mathematical model used by Jones for dowel of category 2

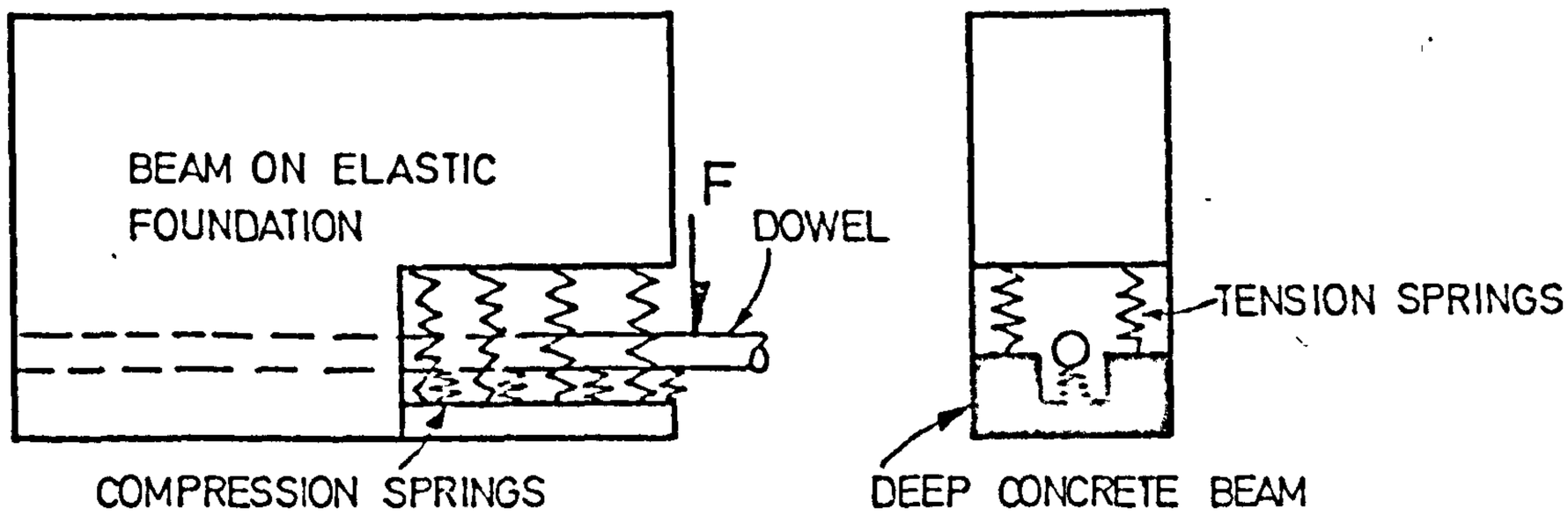

ON ELASTIC FOUNDATIONS

FIG 7·14 Proposed mathematical model for dowel of category 2

7.7.1 Elastic Analysis

A solution to this problem may be obtained if a dowel is considered to be equivalent to a beam supported on elastic foundation or a series of springs. If it is assumed that these springs are supported by a concrete beam which consist of the concrete below the dowel and in turn, this beam is supported by a series of tensile springs which represent the contribution of the concrete above the dowel as shown in Fig. 7.14, then, this mathematical model is considered in this analysis to represent the behaviour of dowels of this category. If it is assumed that the deflection of the dowel and the compression springs which are supporting the dowel to take the following form.

$$W_1 = \frac{\Delta_1}{2}\left[3\left(\frac{x}{L_d}\right)^2 - \left(\frac{x}{L_d}\right)^3\right] \qquad 7.23$$

where Δ_1 is the vertical deflection of the bar at the free end.

The deflection of a deep concrete beam is mainly due to shear deformations and the deflection due to flexural deformation is extremely small and hence may be ignored.

If it is assumed that the average vertical displacement (due to shear) of this concrete deep beam is represented by the following expression:

$$W_2 = \frac{\Delta_2}{2}\left[3\left(\frac{x}{L_d}\right)^2 - \left(\frac{x}{L_d}\right)^3\right] \qquad 7.24$$

where Δ_2 is the average deflection of this concrete beam at the free end. If it is further assumed that the shear deformation of this concrete beam is to vary linearly from a maximum (γ_c) at the level of

the dowel to zero at the sofit of the beam such that

$$\gamma_y = \gamma_c \left(1 - \frac{y}{C_b}\right) \qquad 7.25$$

where γ_c is the shear deformation of the concrete beam at the level of the dowel, C_b is the cover to the dowel measured from the bottom of the beam and y is the distance measured from the bottom of the beam to the point under consideration.

In order to find a solution to this statically indeterminant problem, the principle of minimum total Potential Energy is employed.

Now, the total internal strain energy stored in the structure is

$$U_{total} = U_b + U_c + U_t + U_s \qquad 7.26$$

where U_b is the flexural strain energy in a dowel

U_c is the strain energy stored in the concrete below the dowel (compression spring)

U_t is the tensile strain energy stored in the concrete above the dowel (tension spring)

U_s is the strain energy stored in the concrete deep beam.

The strain energy may be expressed in term of deflection as follows:

$$U_b = \frac{E_s I_s}{2} \int_o^{L_d} (W_1")^2 \, dx$$

where Es Is is the flexural rigidity of the dowel

$$W_1" = \frac{d^2 W_1}{dx^2}$$

$$U_c = \frac{k_c}{2} \int_o^{L_d} (W_1 - W_2)^2 \, dx$$

where k_c is the stiffness of the springs per linear length of the dowel.

$$U_t = \frac{k_t}{2} \int (W_2)^2 \, dx$$

where k_t is the stiffness of the springs per linear length of the dowel

$$U_s = \frac{Gb}{2} \int_0^{L_d} \int_0^{C_b} \gamma_y^2 \, dy \, dx$$

where G is the shear modulus of concrete and b is the width of concrete beam. Equation 26 may be written as follows:

$$U_{total} = \frac{E_s I_s}{2} \int_0^{L_d} (W_1")^2 dx + \frac{k_c}{2} \int_0^{L_d} (W_1 - W_2)^2 dx + \frac{k_t}{2} \int_0^{L_d} (W_2)^2 dx + \frac{Gb}{2} \int_0^{L_d} \int_0^{C_b} \gamma_y \, dy \, dx \qquad 7.26a$$

substituting equations 23 to 26 and their derivatives into equation 7.26a carrying out the integration, equation becomes

$$U_{total} = \frac{3}{2} \frac{E_s I_s}{L^3} \Delta_1^2 + \frac{33}{280} k_c L_d (\Delta_1 - \Delta_2)^2 + \frac{33}{280} k_t L_d \Delta_2^2 + \frac{G b}{5} \frac{C_b \Delta_2^2}{L_d^2}$$

The loss in the potentail energy of the dowel force is $V = - F_d \Delta_1$

Using the theorum of stationary total potential

$\frac{\partial (U + V)}{\partial \Delta_i} = 0$, the following equations are obtained

$$\frac{\partial (U + V)}{\partial \Delta_1} = \frac{3 E_s I_s}{L_d^3} \Delta_1 \quad \frac{33}{140} k_c L_d (\Delta_1 - \Delta_2) - F_d = 0$$

$$\frac{\partial (U+V)}{\partial \Delta} = \frac{33}{140} k_c L_d(-\Delta_1 + \Delta_2) + \frac{33}{140} k_t L_d \Delta_2 + \frac{2}{5} \frac{G b C_b}{L} \Delta_2 = 0$$

equations 7.27 have the following solution

$$\frac{F_d}{\Delta_2} = \frac{33}{140} k_t L_d + \frac{2}{5} \frac{G b C_b}{L_d} + \frac{3 E_s I_s}{L_d^3} \left(1 + \frac{k_t}{k_c}\right) + \frac{56}{11} \frac{E_s I_s}{k_c} \frac{G b C_b}{L_d^5} \qquad 7.28$$

$$\Delta_1 = \left[1 + \frac{k_t}{k_c} + \frac{56}{33} \frac{G b C_b}{k_c L_d^2}\right] \Delta_2 \qquad 7.29$$

Again L_d remains to be determined and may be found by minimising equation 7.28 by setting $\frac{dF}{dL} = 0$. This may be done either algebracally by differentiating equation 28 which lead to a complex transdental equation or can be obtained numerically by trying few values of L and finding the minimum value of F.

If we take as before $k_c = \phi\, k_o$, and if we assume that $k_t = b_e\, k_o$, where b_e is the effective concrete resisting tension which is $C_s - \phi$ and if we take $G = \frac{E_c}{2.5}$, $k_o = \frac{E_c}{75}$, $I_s = \frac{\phi^4}{20}$ and $\alpha_e = \frac{E_s}{E_c}$ then equation 28 becomes:

$$\frac{F_d}{\Delta_2} = \left[A + \frac{B}{L_{d(min)}^2} + \frac{C}{L_{d(min)}^4} + \frac{D}{L_{d(min)}^6}\right] k_o\, b_e L_{d(min)} \qquad 7.30$$

where $A = \frac{33}{140}$

$$B = \frac{2}{5} \frac{G}{k_t} b\, C_b = 12 \frac{b C_b}{b_e}$$

$$C = \frac{3 E_s I_s}{k_t} \left(1 + \frac{k_t}{k_c}\right) = 11.25 \left(1 + \frac{b_e}{\phi}\right) \frac{\phi^4}{b_e}$$

$$D = \frac{56}{11} \frac{E_s I_s}{k_c k_t} G\, b C_b = 48\, \alpha_e\, \phi^3\, B$$

However, the deflection of the concrete beam Δ_2 is small compared with Δ_1 and hence the deflection of a dowel of this category may be determined from the method given for category 1.

7.7.2 Ultimate Strength

The ultimate strength of a dowel of this category may be obtained if it is assumed that this structure would behave elastically until the maximum vertical stress at the level of the dowel reaches the tensile strength of concrete i.e.

$$k_t = k_o b_e = f_t b_e$$

substituting these values into equation 7.30 we get:

$$F_{du} = \left[\frac{33.}{140} + \frac{12\ b\ C_b}{L^2_{d\,min}\ b_e} + \frac{11.25}{L^4_{d\,min}} \left(1 + \frac{b_e}{\phi}\right) x \frac{\phi^4}{b_e} + \frac{576}{L^6_{d\,min}} \propto_e \frac{b^{C_b}}{b_e} \phi^3 \right] \lambda$$

$$f_t\ b_e L_{d\,min}$$

Solution of this equation for wide range of problems indicates that the contribution of the third and fourth terms in the bracket which contain the effect of ϕ are usually small compared with the first and second terms. Such that 100% increase in the dowel diameter would produce approximately 10 percent increase in dowel strength. Therefore, equation 7.31 may be considerably simplified by putting $\phi = 0$ as follows:

$$\frac{F_{du}}{f_t\ b_e} = k_\phi \left[\frac{33\ L_{d\,min}}{140} + \frac{12\ b\ C_b}{b_e\ L_{min}} \right] \qquad 7.32$$

where k_ϕ is a coefficient allowing for the simplification of equation 7.31.

$L_d$min may be found by putting $\frac{d\ F_{du}}{dL} = 0$, we get:

$$L_{d\,min} = 7.2 \sqrt{\frac{b}{b_e} x\ C_b} \qquad 7.33$$

Substituting equation 7.33 into equation 7.32 we get:

$$F_{dU} = 3.4k_{\phi}\sqrt{\frac{b}{b_e}\,c_b}\qquad b_e\, f_t \qquad 7.34$$

Available test data suggest that k_{ϕ} may take the following form:

$$k_{\phi} = \left(1 + \frac{\phi^2}{b\, c_b}\right)$$

It is seen that dowel strength is a function of many parameters. These will be considered in detail in the following section.

7.7.3 Factors Influencing Dowel Strength (Category 2)

It is impractical to include the effect of all the factors that are know to influence dowel strength into any simple theoretical or empirical expressions. Therefore, a detailed study of the importance or otherwise of these factors is necessary in order to determine the accuracy and limitations of the proposed theory.

1. Concrete Strength

Equation 7.34 indicate that the dowel strength is directly proportional to the tensile strength of the concrete, hence, the accuracy of this theory depends on the accuracy of prediction of tensile strength of concrete which has been discussed in chapter two. For this problem, the relation $f_t = 0.4\sqrt{f_{cu}}$ appears to give a reasonable estimate of the tensile strength of concrete.

Fenwick found that there is a considerable

difference in the strength of dowel located in top and in the bottom position in the mould during casting. He attributed these differences to the phenomenon of water gain which leads to a weaker concrete strength near the trowelled face than the concrete in the bottom of the mould. His experimental results indicated that the average strength of a dowel located near the trowelled face is only 58% of that obtained from dowels located in the bottom of the mould. Hence unless the position of the dowel is known, when predicting its strength, considerable scatter in the results will be expected.

2. Side covers or effective width of the beam.

The proposed theory and available experimental results (7.1 to 7.4) suggests that the dowel strength is directly proportional to the effective width of the beam. However, these test results were carried out over very narrow range of width of test specimens and do not provide sufficient information on the effect and limitation of this factor such that there must be a limit on the width of specimens above which an increase in the side covers will not produce an increase in dowel strength. Hence further experimental research on the effect of this factor is needed.

3. Diameter of the dowel ϕ

As shown earlier, a considerable simplification can be made by ignoring the terms containing $\phi^{\frac{s}{}}$ in equation 7.31. This simplifying assumption requires further experimental verification.

4. Bond strength

In deriving equation 7.31 to 7.34, the effect of bond or adhesion between the dowel and the surrounding concrete has been implicitly ignored. This has been based on test results reported by Fenwick who found that the bond characteristic of a dowel has a negligible effect on the dowel strength.

5. Distance to the vertical support (a)

Although an infinite distance to the support has been assumed in deriving the proposed theory, this theory may also be used for the case where (a) has a finite value. The stresses caused by the dowel force are usually similar in nature to the stress concentration that would occur in the vicinity of the support i.e. these stresses are localised and decay rapidly, becomes negligible at a distance L_{min} from the point of application of the dowel force, hence, a minimum distance of $2L_{min}$ for (a) may be taken as a limit to the application of this theory.

The effect of (a) on the dowel strength has been studied experimentally by Krefeld (7.2) who found that the dowel strength increases with a decrease in (a) even for (a) greater than $2L_{min}$. This finding has been contested by Taylor (7.4) who found from tests on model specimens scaled down from the Krefeld specimens that (a) has insignificant effect on dowel strength. Therefore, further experimental work is needed to verify the assumption made above and clarify the confusion existing between Krefeld and Taylor claims.

6. Method of tests

There is no standard method used for determining the dowel strength and all the published results on dowel strength are based on different testing technique by researchers studying the shear strength of reinforced concrete beam. Krefeld (7.2) devised a method which simulates the dowel action in a longitudinal reinforcement in reinforced concrete beam. This method reproduces the conditions which exist in a reinforced concrete beam in relation to the presence of axial force in the reinforcements and rotational displacement that take place at a crack section. On the other hand, simple testing techniques have been suggested by Fenwick which do not reproduce these conditions.

In order to make use of the available test data it is necessary to determine whether a testing technique has any influence on the dowel strength. Therefore further experimental work is needed in this area.

7. Dowel length

Fenwick found that dowel length is proportional to dowel length up to a certain limit above which it has no effect on dowel strength. This limiting dowel length may be taken as $2L_{min}$ and the dowel strength of a short dowel may be determined from equation 7.34 by multiplying by a reduction factor equivalent to the ratio of the length of the dowel over $2L_{min}$.

7.8 Experimental Work on Dowels of Category 2

The aim of this work is to provide further experimental information on dowel strength in order to verify the validity of the proposed theory and to establish its limitation.

The experimental work presented in this chapter may be divided into three parts:

1. Tests on specimens of narrow width.
2. Tests on specimens of wide width.
3. Tests on specimens under torsion.

All the specimens were cast in steel mould using 3 : 1 sand/cement mortar having 0.7 W/C ratio. Three 100 mm cubes were made with each set.

7.8.1 Tests on specimens of narrow width.

In this group 7 sets of specimens were manufactured and tested. The influence of the following factors were investigated:

a. the diameter of the dowel $\emptyset$,
b. bottom cover C_b,
c. bond characteristics of reinforcement and
d. initial prestressing of the dowel.

In examining the effect of items a, b and c, the test arrangement given in Fig. 7.15 was employed. This method was used by Fenwick. In contrast, the effect of prestressing of the dowel was examined using the test arrangement shown in Fig. 7.16 which was originally suggested by Krefeld. The testing technique shown in Fig. 7.15 and 7.16 are referred to as method type A and B respectively. Further details of these specimens, concrete strength and

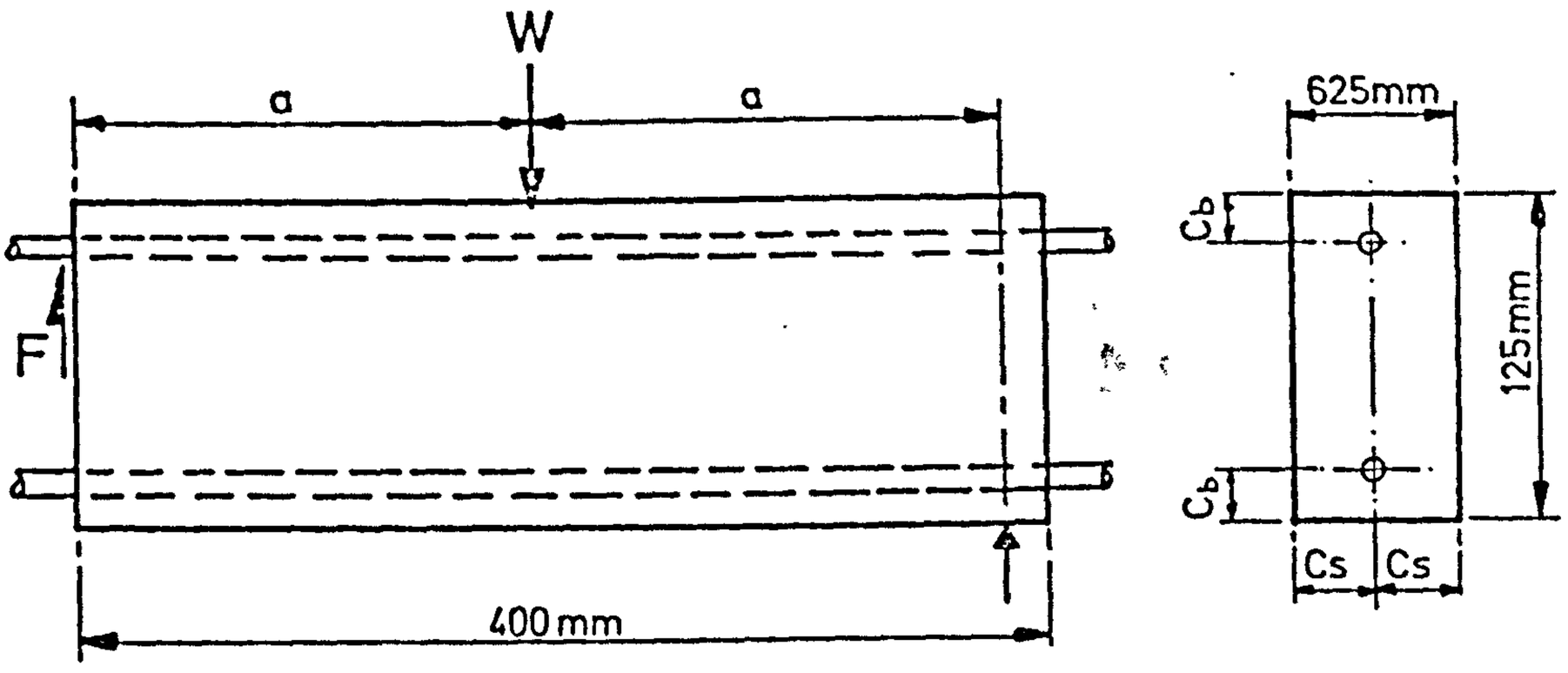

FIG 7·15 Dowel test specimen 1 to 24 Method A

FOR OTHER DETAILS SEE TABLE 7·3

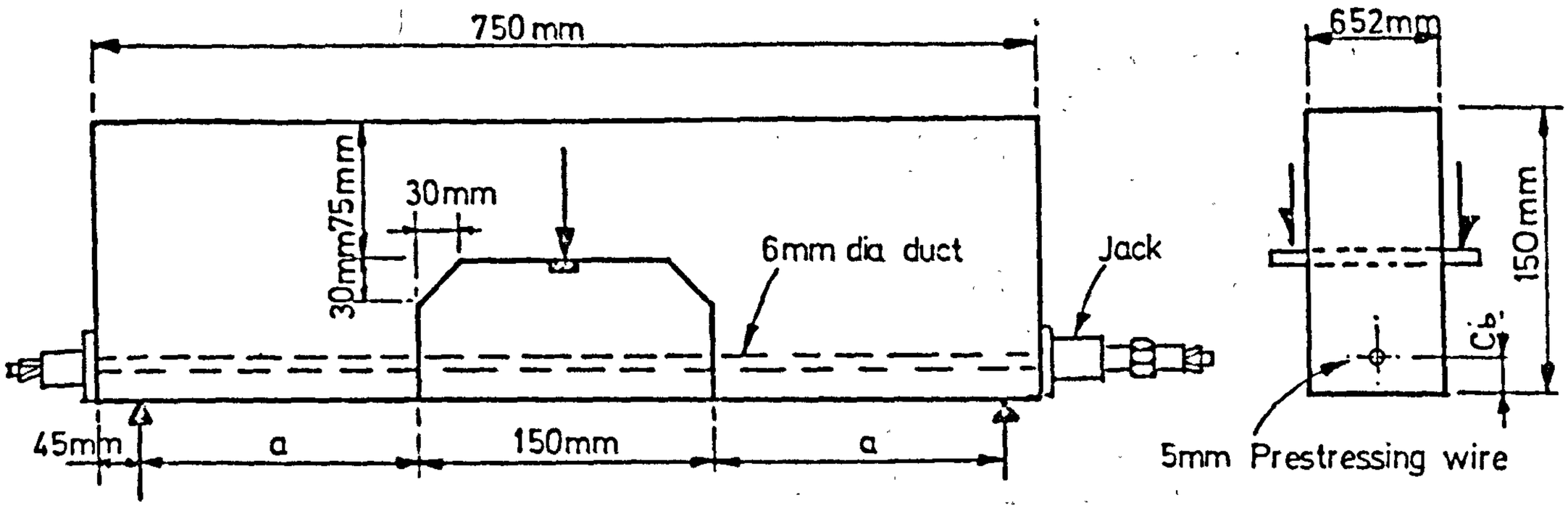

FIG 7·16 Dowel test specimen 25 to 28 Method B

TABLE 7.3 Details of specimens and test results for specimens of narrow width $b < b_l$

Spec. No.	Size mm	a mm	C_b mm	be mm	Bar size and bond	fcu N/mm^2	F_{bu} exp kN	F_{bu} th Eq7.31 kN	$\frac{F_{bu}\ exp}{F_{bu}\ th\ eq\ 7.31}$	F_{bu} th Eq7.35 kN	$\frac{F_{bu}\ exp}{F_{bu}\ th\ Eq7.35}$
1.	62.5 X 125	175	18	56.5	6M	22.5	1.24	1.71	0.73	1.67	0.74
2.			"	52.5	10M		1.51	1.76	0.65	1.71	0.88
3.			"	46.5	16M		1.36	1.96	0.70	1.80	0.76
4.			"	42.5	20M		1.83	2.06	0.89	1.91	0.96
5.	62.5 X 125	175	26	56.5	6M	23.0	2.16	2.02	1.07	2.01	1.07
6.			"	52.5	10M		1.60	2.08	0.77	2.02	0.79
7.			"	46.5	16M		2.10	2.2	0.95	2.07	1.01
8.			"	42.5	20M		2.54	2.73	0.93	2.14	1.18
9.	62.5 X 125	120	63	56.5	6M	23.0	3.9				
10.			"	52.5	10M		5.7	1.91			
11.			"	46.5	16M		6.12	2.18			
12.			"	42.5	20M		6.02	2.14			
13.	62.5 X 125	175	26	56.5	6M	28.3	2.71	2.19	1.24	2.22	1.22
14.			"	52.5	10M		3.33	2.26	1.47	2.23	1.49
15.			"	46.5	16M		2.57	2.38	1.08	2.29	1.12
16.			"	42.5	20M		2.50	2.45	1.02	2.37	1.05
17.	62.5 X 125	175	26	56.5	6HD	28.3	1.83	2.19	0.84	2.23	0.82
18.			"	52.5	10HD		2.19	2.26	0.97	2.23	0.98
19.			"	46.5	16HD		2.47	2.38	1.04	2.29	1.08
20.			"	42.5	20HD		2.78	2.45	1.13	2.37	1.17
21.	62.5 X 125	175	26	56.5	6M	26.0	2.08	2.18	0.95	2.23	0.93
22.			"	52.0	10M		1.96	2.25	0.87	2.23	0.88
23.			"	46.5	16M		1.92	2.37	0.81	2.29	0.84
24.			"	42.5	20M		2.52	2.44	1.03	2.37	1.06
25.	62.5 X 150	205	26	56.5	5PS	37	2.58	2.57	1.00	2.93	0.86
26.			"	"	"		2.83	2.57	1.10	2.93	0.96
27.			"	"	"		2.90	2.57	1.13	2.93	0.99
28.			"	"	"		2.46	2.57	0.96	2.93	0.84

M Mild Steel

HD High yield

dowel strength are given in Table 7.3.

In table 7.3, specimens 1 to 16 were designed to examine the effect of diameter and the effect of bottom cover. The effect of yield strength of a dowel was examined by testing specimen 17 to 20 which were identical in detail to specimens 13 to 16 but dowel of high tensile yield strength was used. The effect of bond characteristics of a dowel was examined by testing specimens 21 to 24 which were identical in detail to specimens but were cast dowel greased to eliminate bond strength. Examination of these results indicates that yield strength of a dowel and the bond strength has no apparent effect on a dowel strength confirming assumption made earlier. Specimens 25 to 28 were tested with different initial prestressing force from zero prestressing force for specimen 25 to 75% of the characteristic strength of the prestressing wire as prestressing force in specimen 28. These results also show that the axial force in the wire has no significant effect on dowel strength.

The results given in Table 7.3 are average values obtained from 4 test results, for each specimen 2 of which were obtained from dowel cast near the trowel face and the other two were obtained from dowel cast near the bottom of the mould. Specimens 9 to 12 were tested with distance (a) being less $2L_{min}$.

7.8.2 Tests on specimens of wide width

In this group 5 sets of specimens were manufactured and tested. Again each set consisted of 4 specimens. The influence of the following

parameters was investigated:

a. width of the specimen,
b. the side covers C_{s1} and C_{s2} of the specimen,
c. the bottom cover C_b
d. method of test.

The detail and the varied parameters of these specimens are shown in figure 7.17. Table 7.4 gives detail of specimens, concrete cube strength and the experimental dowel strength of these specimens.

The outer portion of these specimens was cast first in a 150 x 150 x 750 steel mould, an 8 mm duct was formed in each corner using plastic tubing which was held in position by steel wires stretched between the ends of the mould and located to provide the desired covers as shown in fig. 7.17. The specimens were stripped 24 hours later and the central portions were filled with concrete. Before filling the central portion, a thin sheet of polystyrine was used to separate the 2 portions of the specimen. 24 hours later the complete specimen was stored in a curing tank for 7 days, then taken out and stored in the laboratory for another week before testing. Prior to testing, 7 mm dia prestressing wires were inserted in the ducts and their ends were firmly secured to both ends of the specimens by prestressing anchorages. These wires were slightly stressed by means of mecahnical jacks placed between the end of the specimen and the anchorage.

Each specimen was tested according to method b where the load was applied in small increments up to failure. The specimen was then tested using method b. The results are given in table 7.4.

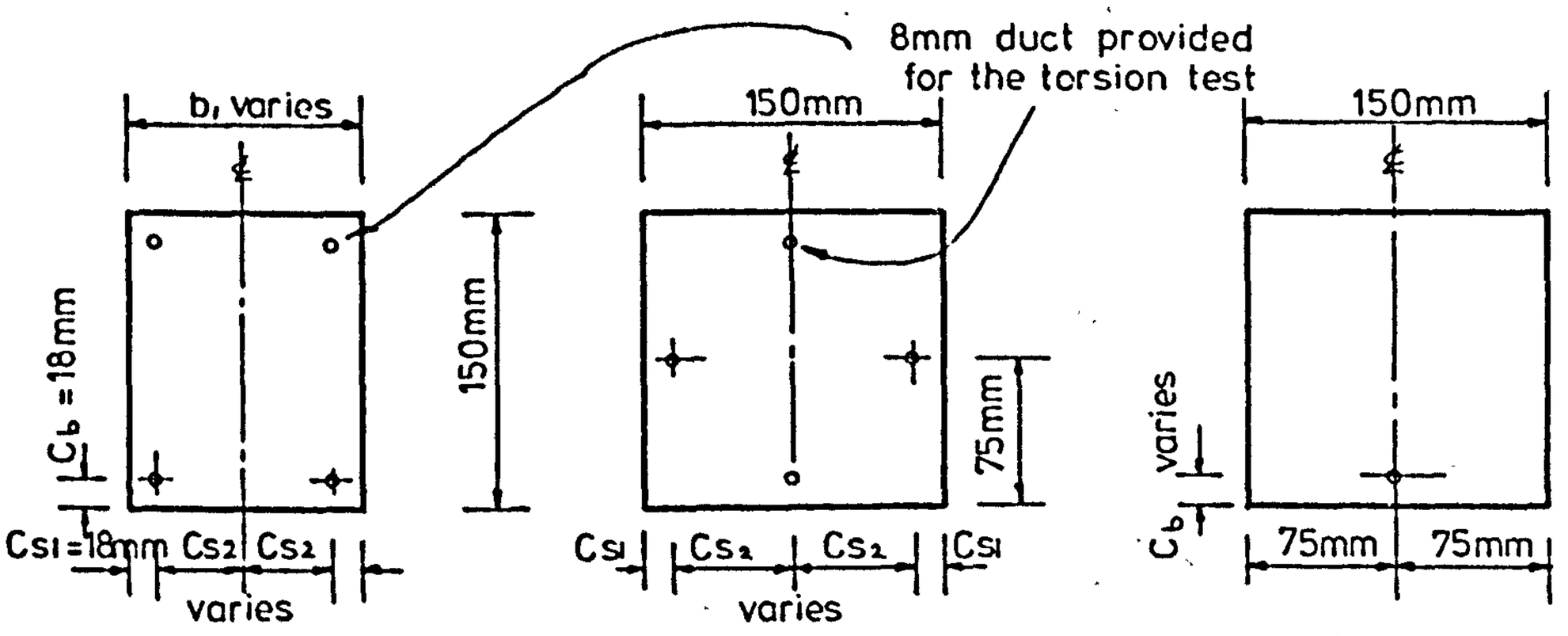

Specimen 1-4 Specimen 5-8 Specimen 9-12

FOR DETAILS SEE TABLE 7.4.

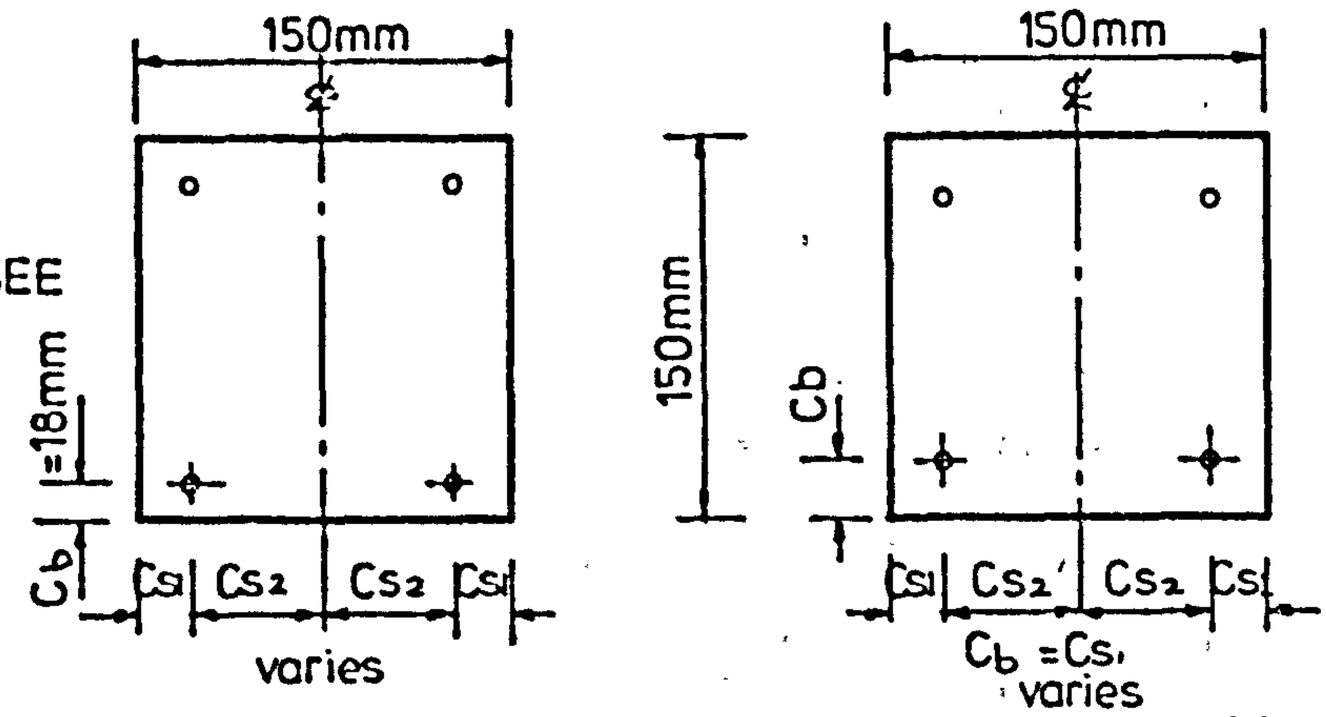

Specimen 13—16 Specimen 17-20

Fig.7.17 Cross sectional detail for specimens used in the wide width specimen torsion tests .

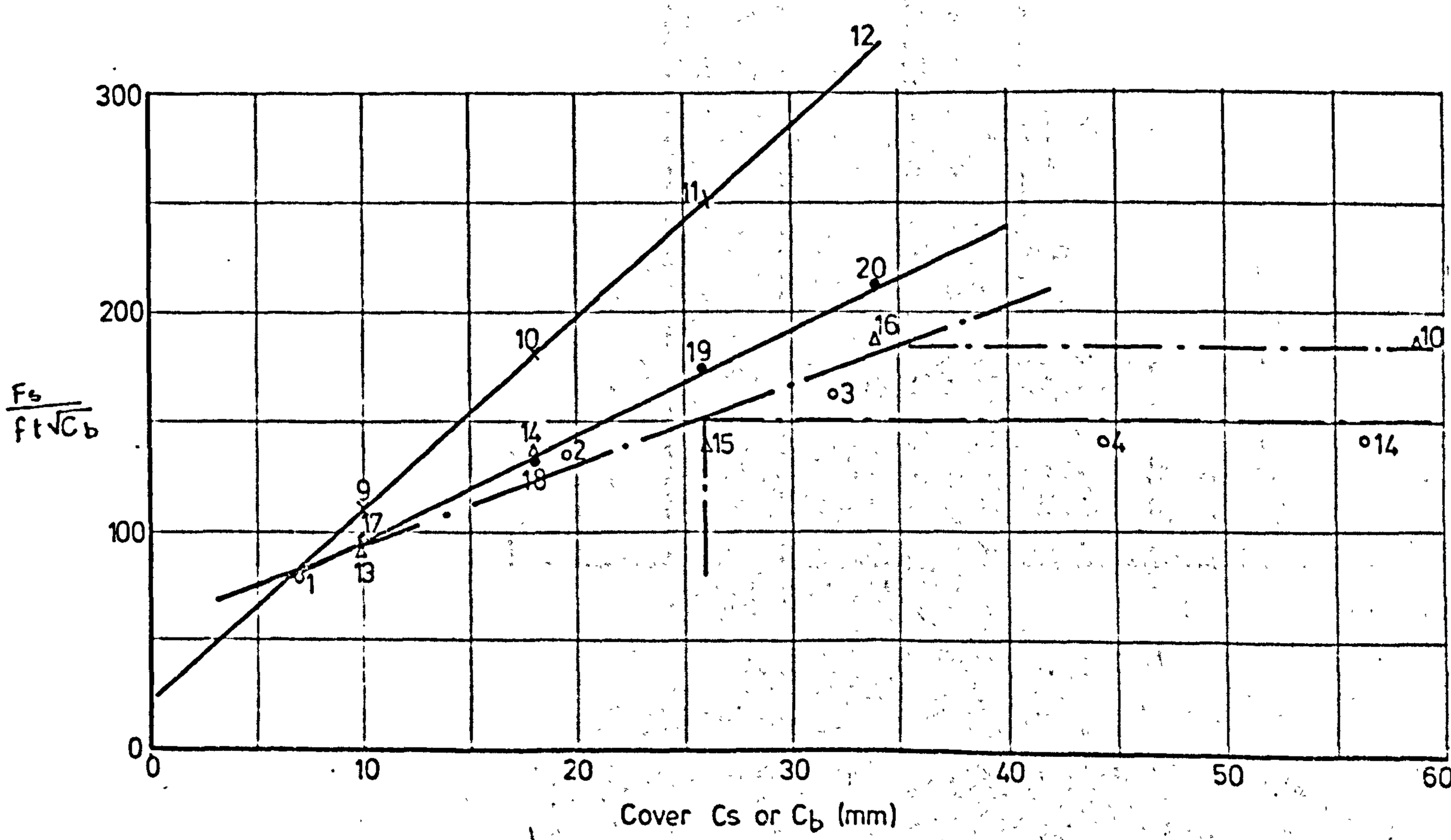

Fig 7.18 Effect of covers on dowel strength .

TABLE 7.4 Details of Specimens and test results for specimens of wide width $b > b_t$

Beam No.	Size mm	bar No. & dia mm	C_s mm	C_b mm	b_e mm	f_{cu_2} N/mm^2	F_{du} Method B	F_{du} (exp) Method A	kN Average	F_{du} th kN	$\frac{F_{du}\ exp}{F_{du}\ th}$
1	50 x 150	2/7	18	18	17	26.32	0.51	0.83	0.67	0.65	1.03
2	75 x 150	"	"	"	29.5	23.70	0.98	1.26	1.12	1.04	1.08
3.	100 x 150	"	"	"	"	27.50	1.50	1.35	1.43	1.32	1.08
4.	125 x 150	"	"	"	"	31.57	1.35	1.39	1.37	1.44	0.95
5.		2/7	10	75	67	25.70	-	4.6		4.22	
6.	150 x 150	"	18	"	"	27.10	-	5.4		4.17	
7.		"	26	"	"	23.00	-	6.0		4.01	
8.		"	34	"	"	22.30	-	5.2		4.0	
9.		1/7	75	10	"	25.70	0.63	0.85	0.74	0.65	1.14
10.	150 x 150	"	"	18	"	27.10	2.20	1.60	1.97	1.60	1.23
11.		"	"	26	"	23.00	-	2.70	2.70	2.52	1.07
12.		"	"	34	"	22.30	-	3.8	3.80	3.72	1.02
13.		2/7	10	18	"	27.50	0.9	0.7	0.8	1.07	0.75
14.	150 x 150	"	18	"	"	25.50	1.2	1.14	1.17	1.25	0.94
15.		"	26	"	"	23.90	1.1	1.19	1.15	1.45	0.79
16.		"	34	"	"	26.70	1.5	1.78	1.64	1.56	1.05
17.		2/7	10	10	"	29.0	0.7	0.59	0.65	0.58	0.89
18.	150 x 150	"	18	18	"	29.5	1.38	1.17	1.27	1.37	0.93
19.		"	26	26	"	32.90	1.95	2.12	2.18	2.61	0.84
20.		"	34	34	"	31.80	2.73	2.80	2.77	3.21	0.87

The results of these investigations are plotted in figure 7.18 as a ratio $\frac{F_{du}}{f_t\sqrt{C_b}}$ against the varied parameter C_s or C_b. These results confirm that the dowel strength increases with increasing covers up to a limiting value beyond which any increase in the side cover or width would not produce an increase in dowel strength. This limiting width is seen to be influenced by the bottom cover. Therefore, this limiting side cover or width may be expressed in terms of the ratio of the side cover to the bottom cover (C_s/C_b). This ratio was found to be 1.4 for specimen 1 to 4 and 1.9 for specimen 13 to 16. Hence a suitable average limit of C_s/C_b may be taken as 1.5 for all cases. These results indicate that the limiting width for wide specimens should be taken as the lesser of the following:

$$b_1 = C_{s1} + C_{s2} = b$$

$$\text{or } b_1 = 1.5\ C_b + C_{s1} \qquad 7.35$$

$$\text{or } b_1 = 1.5\ C_b + C_{s2}$$

$$\text{or } b_1 = 3\ C_b$$

from which the effective width can be taken as $b_1 = b_e - \emptyset$. Where C_{s1} and C_{s2} are side cover one and two measured to the centre line of the dowel.

7.8.3 Tests on specimens under torsion

Simultaneously with each specimen made for the group 7.8.2 another specimen having identical cross-sectional detail was cast. The property of concrete and detail of each specimen can be found in table 7.4 such that specimen 1 in table 7.4 and specimen T1 in table 7.5 are cast sim-

ultaneously.

Before testing, each specimen was sown into 2 halves as shown in figure 7.19. The 2 halves were then assembled into one specimen using 7 mm prestressing wires and the end details shown in figure 7.18. The specimen was then tested under pure torsion where the dowel was the main media for transmitting the torque between two halves of the specimen. The specimen was loaded in about 10 increments of loading where the rotation between the 2 halves of the specimen was recorded.

The cross-sectional detail of these specimens are such that the centre of rotation coincided with the centre of specimen cross-section. Consequently, the applied torque can be assumed to be resisted equally by the corner dowel where the maximum dowel force developed in each of the corner wires is $F_d = \frac{T}{4r}$ where r is the distance between the centre of the rotation and the dowel. The direction of this dowel force is perpendicular to the line joining the centre of rotation and the dowel. This dowel force may be resolved into 2 components Fsx and Fsy parallel to the short and long side of the specimen cross-section respectively. The relationship between these components of dowel force and the applied torque may be written:

$$F_{dx} = \frac{T}{2Y_{"}\left[1 + \left(\frac{X_{"}}{Y_{"}}\right)^2\right]} \qquad 7.36$$

and $F_{dy} = F_{dx}\left(\frac{X_{"}}{Y_{"}}\right)$

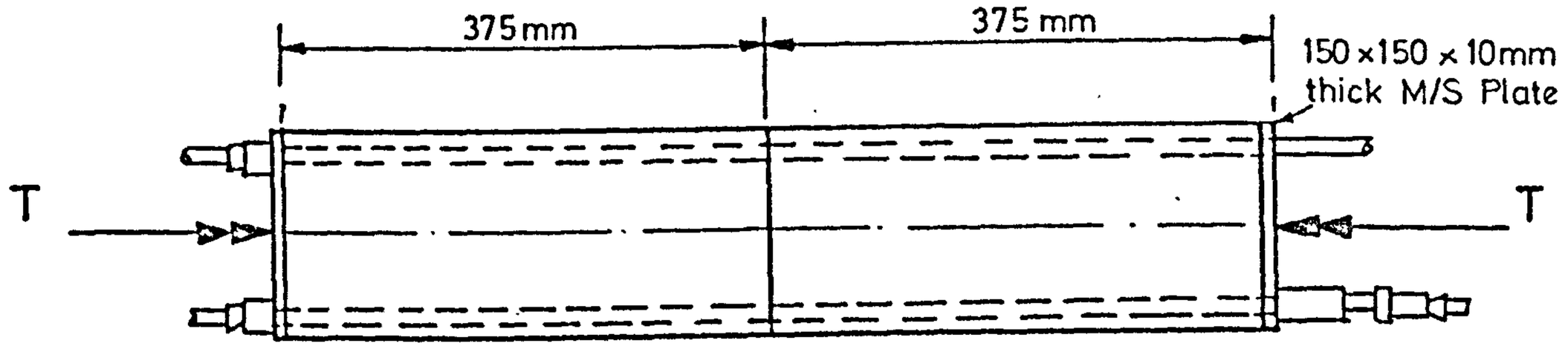

FIG 7·19 Dowel test under pure torsion

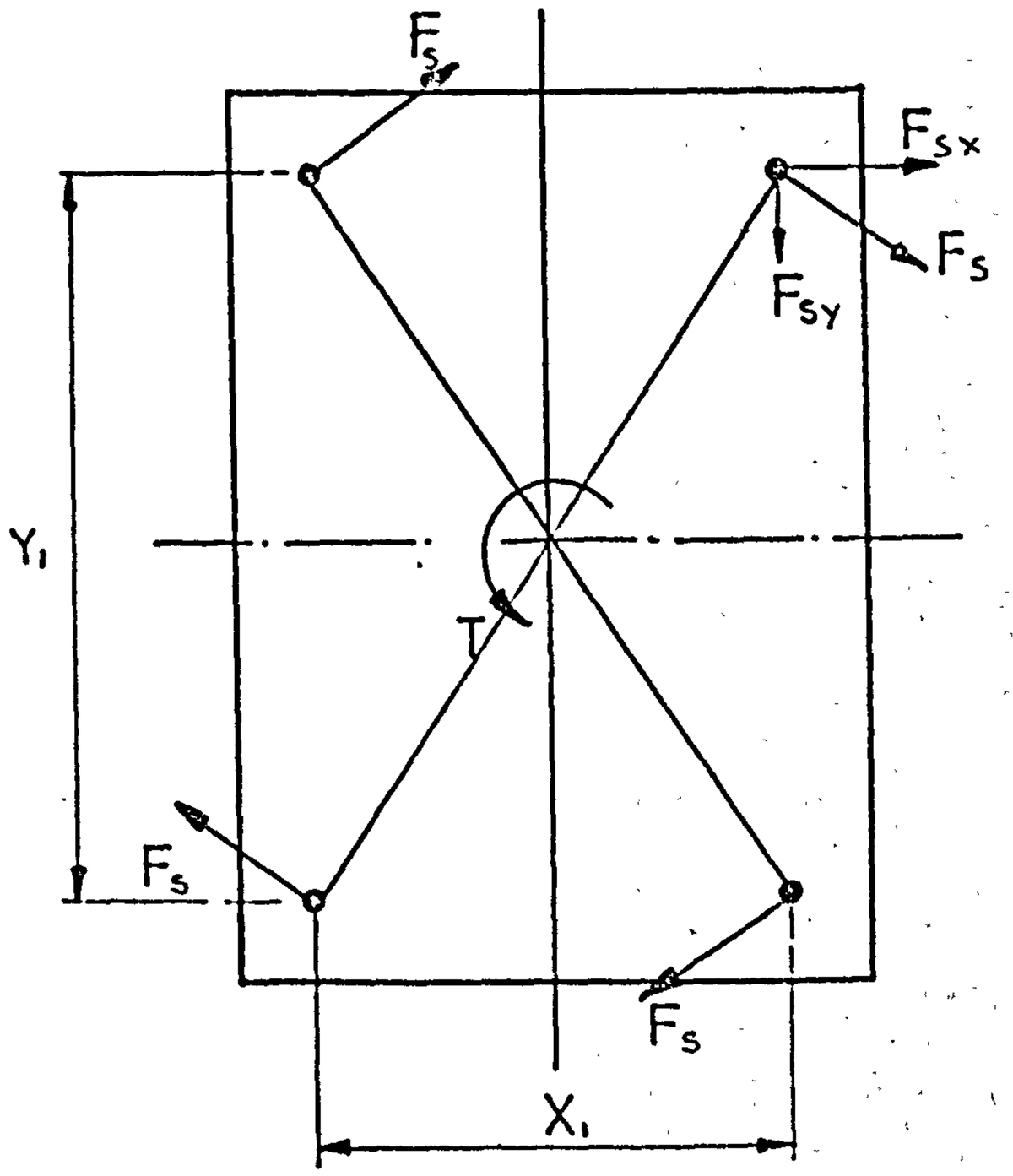

FIG 7·20 Dowel forces in specimen under pure torsion

TABLE 7.5 Test results for specimens subjected to pure torsion

Beam No.	r mm	T_u kN mm	F_{du}(exp) kN	$F_{dux\ exp}$ kN	$F_{duy\ exp}$ kN	$F_{dux\ th}$ kN	$F_{duy\ th}$ kN	$\frac{F_{du\ exp}}{F_{du\ th}}$
T1	57.4	168	0.73	0.73	(0.09)	0.65	0.65	1.12
T2	60.3	280	1.16	1.09	(0.35)	1.04	1.04	1.05
T3	65.3	480	1.84	1.59	(0.89)	1.32	1.32	1.20
T4	72.3	600	2.04	1.64	(1.28)	1.44	1.44	1.14
T5	65.0	360	1.38	1.38	1.38	3.13*	-	
T6	57.0	650	2.46	2.46	2.46	4.30*	-	
T7	49.0	1180	6.02	6.02	6.02	4.85*	-	
T8	41.0	900	5.50	5.50	5.50	5.8 *	-	
T13	86.5	480	1.20	0.92	(1.04)	0.76	(1.07)	1.21
T14	80.5	610	1.90	1.34	1.34	1.29	1.29	1.04
T15	75.0	360	1.20	(0.91)	0.73	(1.76)	1.45	1.54
T16	70.0	650	2.30	(1.88)	1.35	(2.44)	1.56	0.87
T17	92.0	430	1.17	0.82	0.82	0.58	0.58	1.42
T18	80.5	627	1.95	1.37	1.37	1.37	1.37	1.00
T19	69.5	1080	3.88	2.75	2.75	2.61	2.61	1.04
T20	58.0	1208	5.51	3.68	3.88	3.21	3.21	1.12

The values without parentheses represent the critical dowel forces.

* These obtained assuming this dowel is the type of category No. 1

where X_n and Y_n are the smaller and larger dimension between the centre of the dowel as shown in figure 7.20. One of these components will produce a stress field similar to thedowel of category 1 and the other will produce stress field similar to those induced in dowel of category 2.

Since the dowel resistance of category 2 is small compared to that of category 1, failure will always be initiated for a dowel located at the corner of the specimen by that component of dowel force which produces stress field similar to that of a dowel of category 2. Assuming that the stresses produced by the other component of the dowel force has a negligible effect on dowel failure then the dowel strength may be predicted by the proposed theory.

7.9 Comparison Of Theoretical Prediction With Test Results for Dowel Of Category 2

7.9.1 Specimens of Narrow Width

The proposed dowel strength theory has been compared with the test results of this investigation and those available in technical literature. The theoretical dowel strength for tests have been calculated using equation 7.31 and the simplified method of equation 7.34 and they are given in Table 7.3 with a summary of results given in Table 7.6.

These comparisons indicate that the position of the dowel in the mould and the casting procedure has a pronounced effect on the dowel strength. Hence accurate prediction of dowel strength can not be achieved unless the condition of casting and the

local strength of concrete are known.

Comparison of the mean value of $F_{du}(exp)/F_{du}(th)$ for Krefeld and Fenwick results reveal that the testing technique has negligible effect on dowel strength. In other words the axial force in the dowel and the relative rotation which are developed in the dowel by Krefeld testing technique has no or little effect on dowel strength of this category. As a consequence to the considerable variation between dowel strength obtained from an identical specimen and the effect of the position of a dowel which cannot likely predetermine the use of refined dowel theory is not justified. Comparison between the theoretical prediction from equations 7.31 and 7.34 suggest that the prediction of equation 7.34 is almost as accurate as the prediction of equation 7.31 and hence equation 7.34 is to be recommended for its simplicity.

This investigation also indicates that the position of the support (a) and the length of a dowel (S_r) do not effect the dowel strength provided that they are greater than 2L min. For beams tested with (a) less than 2L min exhibit an increase in dowel strength than for specimen with a = 2L min. Therefore, a limit must be imposed on a and S_r S_r = 2L min for the use of the proposed theory.

This comparison indicates that the proposed theory considers the effect of various parameters accurately and confirms all the assumptions and simplifications which have been used.

TABLE 7.6 Comparison between theoretical and experimental dowel strength For $b < b_l$

Investigator	Ref	Position of dowel in the mould	Test arrangement	Number of specimen	F_{du} exp/F_{du} th Equation 7.31		F_{du} exp/F_{du} th Equation 7.34	
					mean	Coefficient of variation %	mean	Coefficient of variation %
Fenwick	7.3	BF	A	14	1.52	12.2		
		TF	&	9	0.89	17.4		
		Average	C	23	1.27	27.5	1.2	27.6
Krefeld and Thurston	7.2	BF	B	9	1.65	20	1.98	17.1
Taylor	7.4	$\frac{BF + TF}{2}$	B	34	1.19	8.4	1.18	11.5
This investigation		$\frac{BF + TF}{2}$	A & B	24	0.98	17.0	0.99	17.0
Total				90	1.2	25	1.21	29.4

BF = Bottom of the mould

TF = Trowelled faced of the specimen

7.9.2 Specimens of Wide Width

The dowel strength for the wide specimens given in section 7.8.2 has been computed using equation 7.34 and the rules of the limiting width given in equation 7.35. These results are listed in Table 7.4 and a summary of comparison with test results is given in Table 7.7. The average value for $F_{du}(exp)/F_{du}(th)$ is 0.96 and the coefficient of variation is 16.5 percent. This comparison is based on the average test results obtained in each case from testing techniques A and B. The results of specimens 5 to 8 were excluded from this comparison because (a) was less than 2L min.

The proposed theory has also been compared with tests carried out by Gergely (7.13) with specimen can be classified according tothe rules given in equation 7.35 as wide specimens. For these results, the average value $F_{du}(exp)/F_{du}(th)$ is 1.03 and the coefficient of variation is 23 percent. However, if the actual width is used in the computation of dowel strength instead of the proposed effective width, the theory overestimates the dowel strength appreciably and yield higher coefficient of variation for the $F_{du}(exp)/F_{du}(th)$. Johnson and Zia (7.14) compared their theoretical prediction (which are based on the mathematical model due to Jones) with these test results. The ratio $F_{du}(exp)/F_{du}(th)$ for this comparison of 1.06 and coefficient of variation of 32 percent. Therefore, the proposed theory gives better agreement with test results than any existing theories.

TABLE 7.7 Comparison between theoretical and experimental dowel strength For $b > b_\ell$

Investigator	Ref	Position of dowel in the mould	Test arrangement	Number of specimen	$\frac{F_{du}\ exp}{F_{du}\ th}$ mean	Coefficient of variation %
Gergely	7.13	-	A	16	1.03	23
This Investigation		$\frac{BF + TF}{2}$	A	16	1.0	30
		"	B	14	0.96	30
		"	A + B	16	0.98	16.5
			T	12	1.06	30

7.9.3 Specimens Subjected to Pure Torsion

Equations 7.34, 7.35 and 7.36 were used to predict the dowel strength for the specimens under pure torsion. These results are given in Table 7.5 and 7.7. The average value of $F_{du}(exp)/F_{du}(th)$ is 1.06 and coefficient of variation is 30 percent. The results of specimens 5 to 8 have been excluded from this comparison since the stress distribution induced by the dowel and the mode of failure are similar to those produced by dowel of category 1. These results confirm once again that the testing technique has little influence on dowel strength.

7.10 Conclusions

Based on the results of this investigation, the following conclusions may be drawn:

1. The classification of the dowel problem into two main categories considerably simplify dowel analysis.

2. Comparison of the proposed theories with all

test data available in the technical literature and those reported in this chapter indicate that the dowel strength can be predicted with reasonable accuracy.

3. It has been found that dowel strength of category 1 increases with increase in diameter of the dowel, the concrete strength and the side cover. For this category there is a limit to the side cover above which an increase in the cover would not increase the dowel strength.

4. Dowel strength of category 2 has been found to increase with increase in the side cover, bottom cover, concrete strength and to a lesser degree with the dowel diameter. For this category a limit has been found to the side cover where any additional increase in the side cover would not produce any increase in the dowel strength. This limit on the side cover was found to be a function of the bottom cover.

5. The testing technique has little influence on dowel strength.

6. The proposed theory can be used to assess the dowel action of the longitudinal and transverse reinforcement subjected to shear and or torsion.

CHAPTER 8

8.1 Conclusions

As a summing up, it can be concluded that:

1. The degree of accuracy of predicting the cracking strength of reinforced and prestressed concrete beams depends primarily on the accuracy of estimating the tensile strength of concrete.

2. The cracking strength of reinforced and prestressed concrete beams is influenced by the size and shape of the member.

3. For reinforced and prestressed concrete beams with web reinforcement, space truss action is the primary mechanism for resisting applied torque.

4. The contribution of dowel action and aggregate interlock in resisting applied torque depends on the mode of failure and for beams failing by yielding of all reinforcement, the contribution of dowel action is almost negligible whereas for beams without web reinforcement, the resistance of torque by dowel action of the longitudinal reinforcement may account for up to 20 percent of the applied torque.

5. Although the dowel resistance to shear and torsion in general is small, the dowel forces may be sufficient to cause dowel failure.

6. For reinforced and prestressed concrete beams with web reinforcement, the resistance of torque by aggregate interlock depends on the ratio of the volume of longitudinal to transverse reinforcement, the ratio of applied moment to torque and the bond characteristics of the longitudinal reinforcement.

7. Reinforced and prestressed concrete beams subjected to bending, torsion and shear may fail in one of 12 modes of failure.

8. Expressions for predicting the strength of reinforced and prestressed concrete beams subjected to combined bending, torsion and shear have been derived. In general these expressions were obtained from consideration of the equilibrium conditions and gave a coefficient of variation for the ratio of the experimental to predicted strength of the order of 10 to 15 percent which is an acceptable accuracy for reinforced concrete members.

9. It has been found that the effect of applied shear force and shear lag on the strength of unbonded prestressed concrete box beam is negligible. This may be due to the fact that shear unbonded prestressed concrete beams behave as a shallow tied arch rather than a beam.

10. For unbonded beams the contribution of aggregate interlock in resisting torsion

decreases as the M/T ratio increases and for beams subjected to M/T greater than 2, this contribution is completely destroyed.

11. The contribution of the uncracked part of the concrete to the resistance of torque in reinforced and prestressed concrete beams by St. Venant torsion is small.

12. Yield theories which are based on the inclination of the compressive field underestimate test results by an order of 5 percent whereas yield theories which are based on the inclination of a crack calculated from the directions of the principal tensile stresses prior to cracking over estimated the torsional strength by the order of 5 percent.

13. Prestressed concrete box-beams may fail prematurely by corner spalling, hence reducing the maximum torsional strength appreciably.

14. The majority of the failures that have been investigated (modes 2 and 3) can be avoided by provision of an appropriate volume of longitudinal reinforcement at the top of the beam. In addition an unsymmetrical arrangement of longitudinal reinforcement would produce a more efficient use of material.

15. For beams containing both longitudinal and transverse reinforcement, the interaction diagrams between bending, torsion and shear failure depend on many parameters and therefore diagrams which have been obtained

empirically must be considered with caution.

16. Partial yield failures may be attributed to the failure of aggregate interlock.

8.2 Suggestions For Further Research

1. Further research is needed on the resistance of shear stresses by aggregate interlock under various loading conditions.

2. There is a need for more detailed study of the mechanism of transfer of torsion in reinforced and prestressed concrete beams failing by yield, partial yield and over-reinforced modes.

3. Research information on the contribution to the resistance to torsion of warping restraint in the cracked stage and ultimate load condition for reinforced and prestressed concrete beams.

4. The strength of beams with other cross sections such as trapezoidal and multi-cells box girders is needed.

5. The effect on the strength of box beams of transverse forces on the walls of the box beams (such as those occuring in the deck of a bridge) acting in addition to the forces considered in this investigation.

6. The effect of distortion of a cross section due to non-uniform torsion on the strength of these box girders is needed.

7. Research is required into the behaviour of concrete cores in multi-storey structures,

the cores (box beams) usually contain holes and they are subjected to axial load in addition to bending torsion and shear.

8. The effect of the shear lag on the strength of box beams has not been fully understood.

9. Research aimed at determining the changes in the shear centre and other torsional properties of box girders as cracking occurs is needed.

10. Although eccentric loading applied to the deck of a box girder bridge appears to induce an "equilibrium torsion", in reality the applied torsion depends on the change in stiffness occuring after cracking and hence the torsion applied to any section cannot be estimated from the condition of equilibrium alone. This problem may be solved by a development of a finite element programme with an element stiffness changing as cracking and plasticity progress up to failure.

11. Research is needed to quantify the plasticity of various modes of failure. This is particularly important for analysing the redistribution of forces in continuous structures.

12. Further research is needed on the effect of shrinkage, creep and temperature stresses on cracking strength.

References - Chapter 1

1.1 Swann R.A. A feature survey of concrete box spine-beam bridges. Cement and concrete association. Technical report 42.469 June 1972.

1.2 Vlasov V.Z. Thin-walled elastic beams. English translation of the 2nd Russian edition by U.S. Department of Commerce. OTS 61-11400, 1961.

1.3 Maisel B.I. Review of literature related to the analysis and design of thin-walled beams. Cement and concrete association. Technical report TRA 440, July, 1970.

1.4 Mitwally M.H. A theoretical and experimental investigation of box girder bridges. Ph.D thesis - The City University U.K. September 1974.

1.5 Morsch E. Schub - und Scherfestigkeit des Betons. Schweigerische Baugeitung (Zurich), Vol. 44, No. 25, 24 Dec 1904 and No. 26, 31 Dec 1904.

1.6 Rausch E. Berechnung des Eisenbetons gegen Verdrehung (Torsion) and Abscheren. Dissertation yur Erlangungder Wurde eines Doktor-Ingenieurs der Technischen Hochschule yu Berlin, Julius Springen, Berlin 1929.

1.7 Nylander H. Torsion and Torsional restraint of concrete structures. Statens Kommitte for Byggnads for skning, Meddelanden, nr 3 Stockholm 1945.

1.8 Cowan H.J. The strength of plain, reinforced and prestressed concrete under the action of combined stresses with particular reference to the combined bending and torsion of rectangular sections. Magazine of concrete research Vol. 5, No. 14, Dec. 1953.

1.9 Lessig N.N. Theoretical and experimental investigation of reinforced concrete element subjected to combined bending and torsion. "Theory of design and construction of reinforced concrete structures (Moscow) 1958.

1.10 Fisher G.P. et al Torsion of Structural Concrete ACI special publications Sp-18, 1968.

1.11 Lampert P. and Thurlimann B. Ultimate strength and design of reinforced concrete beams in torsion and bending. Publications of International Association for bridge and structural engineering Vol. 31-I, 1971.

1.12 Goode C.D. and Helmy M.A. Ultimate strength of reinforced concrete beam in combined bending and torsion. Torsion of structural concrete A.C.I. special publications Sp-18, 1968.

1.13 Collins M.P. et al — Reinforced concrete in torsion UNICIV Report No. 31, March 1968. University of New South Wales, Australia.

1.14 Evans R.H. and Sarkar S. — A method of ultimate strength design of reinforced concrete beam in combined bending and torsion. Structural Engineer, Col. 43, No. 10, October, 1965.

1.15 Evans R.H. and Khalil M.G.A. — The behaviour and strength of prestressed concrete rectangular beam subjected to combined bending and torsion. Structural Engineer Vol. 48 No. 2 Feb. 1970.

1.16 Zia P. — What do we know about torsion in concrete members? A.S.C.E. Journal of the Structural Division June 1970.

1.17 Lampert P. and Collins M.P. — Torsion, bending and confusion. An attempt to establish the facts. ACI Journal, August 1972.

References - Chapter 2

2.1. Bach & Graf — Deutsche Ausschus fur Eisonbeton Vol. VXI.

2.2. Cowan H.J. — An elastic theory for the torsional strength of rectangular reinforced concrete beams. Mag. of Conc. Research 1950 Vol. 2, N. 4.

2.3. Cowan H.J. — The strength of plain, reinforced and prestressed concrete under the action of combined stresses, with particular reference to the combined bending and torsion of rectangular section. Mag of Conc. Research 1953 Vol. 5 No. 12.

2.4. Humphreys R. — Torsional Properties of prestressed concrete: The structural Engineer, June 1957.

2.5. Zia P. — Torsional strength of prestressed concrete members. Journal of Am Conc. Inst. April 1961.

2.6. Evans R.H. & Khalil M.G. — The behaviour and strength of Prestressed concrete and rectangular beams subjected to combined bending and torsion. The Structural Engineer Feb. 1970. No. 2 Vol. 48.

2.7. Collins M.P., Walsh P.F., and Hall A.S. — Reinforced concrete in torsion UNI CIV report No. 31 March 1968.

2.8. Gausel E. — Ultimate strength of prestressed I beams under combined torsion, bending and shear. A.C.I. Journal Sept. 1970.

2.9. Marshall W.T. and Tembe N.R. — Experiments on Plain and Reinforced Concrete in Torsion. The Structural Engineers Nov. 1941.

2.10. Marshall W.T — The torsional resistance of plastic materials with special reference to concrete. Conc. & Constr. Eng. Vol. 39 No. 4 April 1944.

2.11. Marshall W.T. — Torsion in concrete and CP 110 1971. The structural Engineer March 1974 No. 3 Vol. 52.

2.12. Navaratnarajah V. — A new approach to the ultimate strength of concrete in Pure torsion A.C.I. Journal Feb 1968.

2.13. Hsu T.C. — Torsion of Structural Concrete, plain concrete and rectangular sections. A.C.I. Special Publication No. SP. 18-8 1966.

2.14. Hsu T.C. — Torsion of structural concrete. A summary on pure torsion.

2.15. Hsu T.C. — Torsion of structural concrete-Uniformerly prestressed rectangular members without Web reinforcement. Journal of the Prestressed Concrete Inst. Vol. 13 No. 2 April 1968.

2.16. Hsu T.C. — Torsion of Structural Concrete - Behaviour of Reinforced Concrete Rectangular Member. A.C.I. Special Publication No. SP. 18-8.

2.17. Martin L.H. — Bending and torsion of plain concrete members Build Sc. Vol. 6 1971.

2.18. Martin L.H. and Wainwright P.J. — Torsion and bending of prestressed concrete beams. A.S.C.E. Journal of the structural DIV. No. 1973.

2.19. Gonnerman, H.F. and Shomon E.C. — A study of method of loading in flexural list of concrete. Portland Cement Association. Report of the Director of Research series 209 Nov. 1928.

2.20. Reagal. F.V. and Willis, T.F. — The effect of the dimensions of the test specimens on the flexural strength of concrete. Public Roads. Vol. 12 No. 2 April 1931

2.21. Wright P.J.F. — The effect of the method of test on the flexural strength of concrete. Mag of Concrete Research. No. 11. Oct. 1952.

2.22. Komlos K. — Comments on the long-term strength of plain concrete. Mag. of Conc. Research. Vol. 22. No. 73. Dec. 1970.

2.23. Johnston, C.D. and Ward, M.P. — Discussion on ref. 22. Mag. of Conc. Research. Vol. 23 No. 77 Dec. 1971.

2.24. Evans R.H. and Sarkar — A method of ultimate strength of reinforced concrete beams in combined bending and torsion. The Struct. Eng. Vol. 43 No. 10 Oct. 1965.

2.25. Fairbairn, D.R. and Davis S.R. — Combined bending and torsion in reinforced Concrete beams. The Structural Engineer No. 4 Vol. 47 April 1969.

2.26. Iyenar K.T.S. and Rangan B.V. — Factors influencing the strength of reinforced concrete beams under combined bending and torsion. Mag. of Concrete Research Vol. 21 No. 67 June 1969.

2.27. Navaratnarajah V. — A New Approach to the Ultimate Strength of Concrete in Pure Torsion A.C.I. Journal Feb. 1963.

2.28. Goode S.D. and Helmy M.A. — Bending and torsion of reinforced concrete beams. Mag. of Conc. Research Vol. 20 No. 64 Sep 1968

2.29. Okada K. et al — Experimental studies on the strength of rectangular reinforced and Prestressed Concrete Beams under Combined Flexure and torsion. Trons of J.S.C.E. No. 131 July 1966.

2.30. Mitchell D., Lampert P. and Collins M.P. — The Effects of stirrup spacing and Longitudinal Restraint on the Behaviour of Reinforced Concrete Beams subjected to pure torsion. University of Toronto. Publication 71-27 Oct. 1971.

2.31. Lampert P. and Thurlimann B. — Torsion Tests on Reinforced Concrete Beams. Report No. 6506-2. Institute for Structural Engineering, Swiss Federal Institute of Technology, June 1968.

2.32. Nylander H. — Torsion and Torsional restraint of concrete structures. Statens Kommitte for Bygnadsforskning No. 3 1945.

2.33. Ranja Rao H.V.S. and Zia P. — Rectangular Prestressed Beams in Torsion and Bending. Journal of the Structural Division. A.S.C.E. Vol. 99 No. STI Proc. Paper 9501, Jan 1973.

2.34. Henry R.L. and Zia P. — Prestressed Beams in Torsion, Bending and Shear. Journal of the structural Division. A.S.C.I. Vol. No. 99 STS Proc. Paper 10560 May 1974.

References - Chapter 3

3.1. Marsch, E. — Schub-und Scher Festigkeit des Betons Sch weizerische Bauzeitung (Zurich) Vol 44. No. 25 24 Dec 1904 and No. 26 31 Dec 1904.

3.2. Rausch — Berechung des Eisenbetons gegen Verdrehurg und Abscheren (Design of reinforced concrete for torsion and shear). Dissertation Submitted to the Technological University of Berlin 1929.

3.3. Zia, P. — What do we know about torsion in concrete members. Journal of the structural division ASCE Vol 96. No. ST6 June 1970.

3.4. Zia, P. — Torsional strength of prestressed concrete members. Proceeding of the A.C.I. Vol 32 No. 10 April 1961.

3.5. Hsu, T.C. — Torsion of Structural Concrete behaviour of reinforced concrete rectangular members. Torsion of Structural concrete A.C.I. special publication No. SP.18.10.

3.6. Hsu, T.C. — Ultimate torque of reinforced rectangular beams. Journal of the structural division ASCE Vol. 94 No. ST3 Feb 1968.

3.7. Hsu, T.C. and Kemp, E.L. — Background and practical application of tentative design criteria for torsion. A.C.I. Journal Jan. 1969.

3.8. Turner and Davis, V.C. — Plain and reinforced concrete in torsion. Selected engineering paper No. 165 Inst. of Civil Eng. 1934.

3.9. Marshall, W.T. and Tembe, N.R. — Experiments on plain and reinforced concrete in torsion. Structural engineer (London) V. 19, 1941.

3.10. Iyengar, K.T.S.P. and Rangan B.V. — Strength and stiffness of reinforced concrete beams under combined bending and torsion. Torsion of Structural concrete. A.C.I. special publication paper S.P. 18-15. March 1966.

3.11. Pandit, G.S. — Ultimate torque of rectangular reinforced concrete beams. Journal of the Structural Division A.S.C.E. Vol. 96 No. ST9 Sept. 1970.

3.12. Anderson P. — Rectangular concrete section under torsion A.C.I. Journal V. 9 Sept-Oct 1937.

3.13. Cowan H.J. — The strength of plain reinforced and prestressed concrete under the action of combined stresses with particular reference to the combined bending and torsion of rectangular sections. Magazine of concrete research (London) V. 5 No. 14 Dec 1953.

3.14. Lessig, N.N. Theoretical and experimental investigation of reinforced concrete beams subjected to combined bending and torsion. Moscow 1950. This reference is quoted from ref. 15.

3.15. Gvozdev, A.A. and Lessig, N.N. and Rulle, L.K. Research on reinforced concrete beams under combined bending and torsion in the Soviet Union. Torsion of struct. concrete. A.C.I. special publication No. 18-11 1968.

3.16. Mattock, A.H. How to design for torsion. Torsion of structural concrete. A.C.I. special publication No. SP 18-10.

3.17. Lampert, P. Torsion and bending in reinforced and prestressed concrete members. Proceedings Institution of Civil Engineers (London) Vol. 50 Dec 1971.

3.18. Lampert, P. and Thurlimann, B. Ultimate strength and design of reinforced concrete beams in torsion and bending. Publications International Association for Bridge and Structural Engineering V.31-I. 1971.

3.19. Lampert P. and Collins, M. Torsion, bending and confusion, an attempt to establish the facts. A.C.I. Journal Aug. 1972.

3.20. Lampert, P. Postcracking stiffness of

reinforced concrete beams in torsion and bending A.C.I. special publication Paper S.P. 35-12. 1971.

3.21. Lampert, P., Luchinger, P. and Thurlimann — Torsion tests on reinforced and prestressed concrete (Torsionversuche on Stahl- und spannbeton balken) Bericht No. 6506-4 Institute fur Baustatik E.T.H. Zurich.

3.22. Lampert, P. and Thurlimann B. — Torsion test on reinforced concrete beams. (Torsionsavesuche on Stahlbetonblken). Zurich Institute fur Baustatik E.T.H. Zurich June 1968 Report 6506-2.

3.23. Swann, R.A. — The effect of size on the torsional strength of rectangular reinforced concrete beam. Cement and concrete Association. Technical report No. 42 453. March, 1971.

3.24. Swann, R.A. — Experimental basis for a design method for rectangular reinforced concrete beams in torsion. Cement and Concrete Assoc. 1970. Technical report 42 452.

3.25. Victor, D.J. and Muthukrishnan — Effect of stirrups on ultimate torque of reinforced concrete beams A.C.I. Journal April 1973.

3.26. Gausel, E. — Ultimate strength of Prestressed I-beams under combined torsion, bending and shear. Journal of A.C.I. Vol. 67 No. 9 Sept 1970.

3.27. Bishara, A. Prestressed concrete beams under combined torsion, bending and shear. A.C.I. Journal July 1969.

3.28. Kuyt, B. A theoretical investigation of ultimate torque as calculated by truss theory and by the Russian ultimate equilibrium method. Mag. of concrete research. Vol 23, No. 77. Dec 1971.

3.29. Karlsson, I. Torsional stiffness of reinforced concrete member subjected to pure torsion. Mag. of concrete research Vol. 24. No. 80. Sept. 1971.

3.30. Elfgren, L. Reinforced concrete beams loaded in combined torsion, bending and shear. A study of the ultimate load-carrying capacity. PhD thesis submitted to the Chalmers University of Technology, Sweden, 1971.

3.31. Yudin, V.K. Determination of the load-carrying capacity of rectangular reinforced concrete elements subjected to combined torsion and bending. Beton i Zhelezohetr. No. 6 Moscow, USSR June 1962.

3.32. Collins, M.P.
Walsh, P.F.
Archer, F.E.
and Holl, A.S. Reinforced concrete in torsion UNICIN report No. 31 March 1968 University of New South Wales, Australia.

3.33. Mitchell, D.
Lampert, P.
and Collins, M.
The effect of stirrup spacing and longitudinal restraint on the behaviour of reinforced concrete beams subjected to pure torsion. University of Toronto. Dept. of Civil Eng. Publication 71-72.

3.34. Fretheim, I.B.
Flexure-torsion interaction behaviour of reinforced concrete beams. Dept. of Civil Eng. University of Colorado, M.S thesis, 1970 (Summary of the results are given in ref 33).

3.35. Gesund, H. and Boston, L.A.
Ultimate strength in combined bending and torsion of concrete beams containing only longitudinal reinforcement A.C.I. Journal Vol. 61. No. 11 Nov. 1964.

3.36. Gesund, H.
Schuette, E.J.
Buchanan, G.R.
and Gray, G.A.
Ultimate strength in combined bending and torsion of concrete containing both longitudinal and transverse reinforcement A.C.I. Journal Vol. 61 No. 12 Dec 1964.

3.37. Martin, L.H.
The ultimate strength in bending and torsion of concrete of reinforced concrete members. PhD thesis University of Aston Birmingham 1972.

3.38. Martin, L.H.
and Wainwright P.J.
Torsion and bending of prestressed concrete beams. Journal of the structural division. A.S.C.E. Vol. 99 No. ST11 Nov. 1973.

3.39. Timoshenko, S. Strength of materials Vol. II McGrow-Hill.

3.40. Rajagopalan, K.S. and Ferguson, P.M. Partially over-reinforced concrete beam, under pure torsion. A.C.I. Journal Oct. 1971.

3.41. Fenwick, R.C. Shear strength of reinforced concrete beam. PhD thesis University of Canterbury, Christchurch , New Zealand 1966.

3.42. Taylor, H.P.J. Investigation of the forces carried across cracks in reinforced concrete beams in shear by interlock of aggregate London, Cement & Concrete Association, 1970. Technical report 42. 447.

3.43. Stewart F. Reinforced and prestressed concrete beams subjected to pure torsion. BSc Final year project, 1973. Dept. of Civil and Struct. Eng. Polytechnic of the South Bank.

3.44 Ernst, G. Ultimate torsional properties of rectangular reinforced concrete beams. A.C.I. Journal Vol. 29 No. 4 Oct. 1957.

3.45. McMullen, A.E. and Worworuk, J. Concrete beams in bending, torsion and shear. Journal of the structural division A.S.C.E. Vol. 96 No. ST5 proc paper 7270 May, 1970.

3.46. Evans, R.H. and Sarkar — A method of ultimate strength design of reinforced concrete beams in combined bending and torsion The Structural Engineer Vol. 43 No. 10 Oct, 1965.

3.47. Mutkerjee, P.R. and Warwaruk, J. — Torsion, bending and shear in prestressed concrete. Journal of the Struct. Division A.S.L.E. Vol. 97 No. ST4 Proc Paper 8041. April 1971

3.48. GangaRao, H.V.S. and Zia, P. — Rectangular Prestressed beams in torsion and bending, journal of the Structural Division, A.S.C.E. Vol. 99 No ST1 Proc Paper 9501, Jan 1973.

3.49. Evans, R.H. and Khalil, M.C.A. — The behaviour and strength of prestressed concrete rectangular beams subjected to combined bending and torsion. Structural Engineer Vol. 48 No. 2 Feb. 1970.

3.50. Okada, K. Nishibayashi, S. and Abe, T. — Experimental studies of the strength of rectangular reinforced and prestressed concrete beams under combined flexure and torsion. Transection of the Japanese Society of Civil Eng. No 121 July, 1966

3.51. Superfesky, M.J. — Torsional behaviour of prestressed concrete rectangular beams. MSc thesis West Virginia Univ. at Margan town. 1968.

References - Chapter 4

4.1. Lessig, N.N., "Theoretical and experimental Investigation of Reinforced Concrete Elements subjected to combined bending and torsion." Theory of design and construction of reinforced concrete structures (Moscow) 1958.

4.2. Lessig, N.N., "Determination of Load-Carrying Capacity of reinforced Concrete Elements with Rectangular Cross-section under Simultaneous action of Flexure and Torsion", Beton i Zhelezabeton (Moscow) No. 3, 1959.

4.3. Lessig, N.N., "Determination of the Load-Bearing Capacity of Reinforced Concrete Elements with Rectangular Cross-section Subjected to Flexure with Trosion", Institute Betona i Zhelezabetona, Trudy, Moscow No. 5, 1959.

4.4. Guozden, A.A. Lessig, N.N. and Rulle, L.K. Research on Reinforced Concrete Beams Under Combined Bending and Torsion in the Soviet Union. Torsion of Struct. Concrete A.C.I. special publication No. 18-11, 1968.

4.5. Collins, M.P. Walsh, P.F. Archer, F.E. and Hall, A.S. Reinforced Concrete in Torsion UNICIV Report No. 31 March, 1968 University of New South Wales, Australia.

4.6. Yudin, U.K. — Determination of the Load-Carrying Capacity of rectangular Reinforced Concrete Elements Subjected to Combined Torsion and Bending, Beton i Zhelezabeton, No. 6, (Moscow) June 1962.

4.7. Gesund, H. Schuette I.J. Buchanan, G.R. and Gray, G.I. — Ultimate strength in combined Bending and Torsion of concrete containing both longitudinal and transverse Reinforcement A.C.O. Journal Vol. 61, No. 12 Dec. 1964.

4.8. Evans, R.H. and Sarkar — A method of Ultimate strength design of Reinforced Concrete Beams in Combined Bending and Torsion. The Structural Engineer, Vol 43 No. 10 Oct. 1965

4.9. Evans, R.H. and Khalil M.G.A. — The Behaviour and strength of prestressed concrete Rectangular Beams subjected to Combined Bending and Torsion, Structural Engineer Vol. 48 No. 2 Feb. 1970.

4.10. Fairbairn, D.R. and Davis, S.R. — Combined bending and Torsion in reinforced concrete beams. The Struct. Eng. No. 4, Vol. 47, April, 1969.

4.11. Lampert, P. and Thurlimann, B. — Ultimate strength and Design of Reinforced Concrete Beams in Torsion and Bending. Publications International Association for Bridge and Structural Engineering V. 31-1, 1971.

4.12. Lampert, P. — Torsion and Bending in reinforced and prestressed Concrete Member. Proceedings Institution of Civil Engineers (London) Vol. 50 Dec. 1971

4.13. Lampert, P. and Collins M. — Torsion, Bending and Confusion. An attempt to establish the facts. ACI Journal, Aug. 1972.

4.14. Martin, L.H. — The ultimate strength in Bending and Torsion of Reinforced Concrete Members. PhD thesis, University of Aston, Birmingham.

4.15. Elfgren, L. — Reinforced Concrete Beams Loaded in Combined Torsion, Bending and Shear. A study of the ultimate load-carrying capacity. PhD thesis submitted to the Chalmers University of Technology (1971) Sweden.

4.16. Kuyt, B. — A method for Ultimate Strength design of rectangular reinforced concrete beams in combined torsion, bending and shear. Mag. of Concrete Research, Vol. 24 No. 78 March 1972.

4.17. Rangan, B.V. and Hall, A.S. — Strength of rectangular Prestressed Concrete Beams in Combined Torsion, Bending and Shear. A.C.I. Journal, April, 1973.

4.18. Zia, P. Torsion theories for concrete members. Torsion of Structural concrete A.C.I. special publication SP - 18, 1968.

4.19. Jackson, N. and Estanero, R. The plastic flow law for reinforced concrete beams under combined flexure and torsion. Mag. of concrete research, Vol. 23, No. 77 Dec, 1971.

4.20. Lyalin, I.M. Experimental Studies of the behavious of reinforced concrete beams with rectangular cross-section subjected to the combined action of transverse force, flexural and torsional moment. Trudy, No. 5 concrete and reinforced concrete Instit. (Moscow) 1959, p.p 54-77.

4.21. Goade, C.D. and Helmy, M.A. Bending and Torsion of Reinforced concrete beams. Mag. of Concrete Research. Vol. 20 No. 64 Sept. 1968.

4.22. Iyengar, K.T.S.R. and Rangan, B.V. Factors influencing the strength of reinforced concrete beams under combined bending and torsion. Mag. of Concrete Research Vol. 21, No. 67 June 1969.

4.23. Iyengar, K.T.S.R. and Rangan, B.V. Strength and stiffness of reinforced concrete beams under combined bending and torsion. Torsion of Structural Concrete. American concrete Institute,

1967, A.C.I. Special publication No. 18 pp 403-440.

4.24. Chinenkov, U.V. — Study of the behaviour of reinforced concrete elements in combined flexure and torsion. Beton i Zhelezabeton Vol. 5 1959 p.p. 29-53. English translation by Margaret Corbin-Skokie, Portland Cement Association. Foreign literature study No. 370.

4.25. Pandit, G.S. and Warwaruk, J. — Reinforced Concrete beams in combined bending and torsion - part 2, Experiments, Torsion of Structural Concrete special publication No. 18, American Concrete Institute, 1968.

4.26. McMullen, A.E. and Warwaruk, J. — Concrete beams in bending, torsion and shear. Journal of the Struct division A.S.C.E. Vol. 96 No. T5 Proc. paper 7270 May 1970.

4.27. Okada, K. Nishibayashi, S. and Abet, T. — Experimental Studies of the Strength of rectangular reinforced and prestressed concrete beams under combined flexure and torsion. Transactions of the Japanese Society of Civil Eng. No. 121 July, 1966.

4.28. Mukherjee, P.R. and Warwaruk J. — Torsion, Bending and Shear in prestressed concrete. Journal of the Structural Division, ASCE Vol. 97 No. ST4 Proc. paper 8041 April, 1971.

4.29. GangaRao, H.V.S. and Zia, P. Rectangular prestressed beams in torsion and bending. Journal of the Structural division, A.S.C.E. Vol. 99 No. ST1 Proc. paper 9501 Jan. 1973.

4.30. Henry, R.L. and Zia, P. Prestressed beams in torsion, bending, and shear. Journal of the struct division ASCE Vol. 100 No. ST5, May, 1974.

4.31. Swann, R.A. and Williams, A. Combined loading tests on model prestressed concrete box beams reinforced with steel mesh. Cement and Concrete Association. Technical report 42 485 Oct. 1973.

References - Chapter 5

5.1	The Institution of Structural Engineers	"The Shear Strength of Reinforced concrete Beams" A report by the Shear Study Group 1969
5.2	Goode, C.D. and Helmy, M.A.	"Ultimate Strength of Reinforced Concrete Beams in Combined Bending and Torsion" Torsion of Structural Concrete ACI publication SP-18 1968.
5.3	Goode, C.D. and Helmy, M.A.	"Design of rectangular beams subjected to combined bending and torsion" Concrete, July 1967.
5.4	Helmy, M.A.	"The Strength of reinforced Concrete rectangular beams in combined bending and torsion" Ph.D Thesis. University of Manchester, 1966.
5.5	Collins, M.P. Walsh, P.F. Archer, F.E. and Hall, A.S.	"Reinforced Concrete in Torsion" UNICIV Report No. 31, March 1968. University of New South Wales, Australia.
5.6	Regan, P.E.	"Shear in reinforced concrete beams". Magazine of Concrete Research, Vol 21, No. 66, March 1969.
5.7	Regan, P.E. and Placas, A.	"Limit-state design for shear in rectangular and T beams". Magazine of Concrete Research, Vol. 22, No. 73, December 1970.

5.8 Regan, P.E. "Behaviour of reinforced and prestressed concrete subjected to shear forces" Proceedings of the Institute of Civil Eng. Supplement (xvii). Paper 7415. 1971.

5.9 Regan, P.E. and Yu, C.W. "Limit-state design of structural concrete". Chatto and Windus, London 1973.

5.10 Walther, I.R. "Calculation of the shear strength of reinforced and prestressed concrete beams by the shear failure theory". C & CA Library. Translation No. 110. 1964.

5.11 Bjuggren, U. "Skjuvbo" j brott. Nordisk Betong 1962. See ref 5.1.

5.12 Sheikh, M.A. de Paiva, H.A.R. and Neville, A.M. "Calculation of flexure-shear strength of prestressed concrete beams". Journal of the prestressed concrete Institute. Vol. 13. No. 1 Feb. 1968.

5.13 Sheikh, M.A. de Paiva, H.A.R. and Neville, A.M. "Flexure shear strength of reinforced concrete deep beams". The structural Eng. August 1971 No. 8. Vol. 49.

5.14 Pandit, G.S. and Warwaruk, J. "Reinforced Concrete Beams in Combined Bending and Torsion". Torsion of Structural Concrete. ACI SP-18. 1968.

5.15 Iyengar, K.T.S.R. and Rangan, B.V. "Strength and Stiffness of reinforced concrete beams under combined bending and torsion". Torsion of Structural Concrete ACI publication SP-18. 1968

5.16 Evans, R.H. and Khalil, M.G.A. "The Behaviour and Strength of Prestressed Concrete and rectangular beams subjected to combined bending and torsion". The Structural Eng. Feb. 1970. No. 2, Vol 48.

5.17 Martin L.H. and Wainwright P.J. "Torsion and bending of prestressed concrete beams". Journal of the Structural Division A.S.C.E. Vol 99 No. ST11 Nov. 1973.

5.18 Femwick R.C. "Shear strength of reinforced concrete beam." Ph.D Thesis University of Canterbury, Christchurch, New Zealand 1966.

5.19 Taylor H.P.J. "Investigation of the forces carried across cracks in reinforced concrete beams in shear by interlock aggregate." London Cement and Concrete Association. 1920. Tech. report No. 42 447.

5.20 Cowan H.J. "The strength of plain reinforced and prestressed concrete under the action of combined stresses with particular reference to

the combined bending and torsion of rectangular sections". Mag. of Concrete Research (London) V. 5 No.14 December 1953.

5.21 Cowan, H.J. "The ultimate strength of prestressed concrete beams". The Struct. Eng. Vol. 33, No. 7, July 1955. pp 197-212.

5.22 Kemp, E.L. "Behaviour of concrete members subjected to torsion and combined torsion, bending and shear torsion of structural concrete." ACI publication No. SP-18.

5.23 Zia P. and Cardenas R. "Combined bending and torsion of reinforced plaster model beams Torsion of structural concrete. ACI publication No. SP-18.

5.24 Klus, J.P. "Ultimate strength of reinforced concrete beams in combined torsion and shear." ACI Journal, March 1968.

5.25 Mitchell, D. Lampert, P. and Collins, M. "The effect of stirrup spacing and longitudinal restraint on the behaviour of reinforced concrete beams subjected to pure torsion" University of toronto. Dep. Civil Eng. Pub 71-22.

5.26 Lampert, P. and Thurlimann, B. "Ultimate strength and design of reinforced concrete beams in torsion and bending". Publication International Association for Bridge and Struct. Eng. V.31-I, 1971.

5.27 Baker, A.L.L. "A plastic theory of design for ordinary reinforced prestressed concrete including moment redistribution in continuous members". Mag. of Concrete Research. Vol. 1 No. 2. June 1949.

5.28 Pannel, F.N. "The ultimate moment of resistance of unbonded pre-stressed concrete beams" Mag. of concrete Research Vol. 21, No. 66, March 1969.

6.1 Swann, R.A. and Williams, A. Combined loading tests on model prestressed concrete box beams reinforced with steel mesh. Cement and Concrete Association. Technical report 42 485 Oct. 1973.

References - Chapter 7

7.1 Jones, R. "The Ultimate Strength of Reinforced Concrete Beams in Shear". Magazine of concrete Research Vol. 8 No. 23, August, 1956.

7.2 Krefeld, W.J. and Thurston, C.W. "Contribution of longitudinal Steel to Shear Resistance of Reinforced Concrete Beams". Journal of the A.C.I. Proceeding Vol. 63, No. 3 March, 1966.

7.3 Fenwick, R.C. "Shear Strength of Reinforced Concrete Beams". PhD Thesis, University of Canterbury, Christchurch, New Zealand, 1966.

7.4 Taylor, H.P. "Investigation of the Dowel Shear Forces Carried by the Tensile Steel in Reinforced Concrete." Technical Report TRA 431 Cement and Concrete Association 1969.

7.5 Hetenyi, M. "Beam on Elastic Foundation" The University of Michigan Press.

7.6 Hawkins "The Bearing Strength of Concrete for Strip Loadings". Magazine of Concrete Research Vol. 22 No. 71 June 1970.

7.8 Dulacsha, H. "Dowel Action of Reinforcement Crossing cracks in Concrete". A.C I. Journal, December, 1972.

7.9 Tharmaratnam, K. "Structural Behaviour of External Horizontal Joints in Large Panel Buildings". PhD Thesis, University of London, 1972.

7.10 Plum, D.R. "Strength of Studs in Composite Construction". Proceeding A.C.I., 1972.

7.11 Menzies, J.B. "CP117 and *Shear Connectors in* Steel Composite Beams". The Structural Engineer, March, 1971. No. 3 Vol. 49.

7.12 Hyland, M.W. and Chen, W.F. "Bearing Capacity of Concrete Blocks". A.C.I. Journal March, 1970.

7.13 Gergely, P. "Splitting Crack Along The Main Reinforcement in Concrete Members". Research Paper. Dept. of Struct. Eng., Cornell University, New York, 1969.

7.14 Johnston, D.W. and Zia, P. "Analysis of Dowel Action". Proceeding of the A.S.C.E. Struct. Division, May, 1971.